

Bulletin de la  
**Commission  
Géologique**  
de Finlande

N:o 222

Suomen Geologisen Seuran julkaisuja  
Meddelanden från Geologiska Sällskapet  
i Finland  
Comptes Rendus de la Société Géologique  
de Finlande

XXXVIII



Geologinen tutkimuslaitos • Otaniemi 1966

CORRECTION to p. 286 in Comptes Rendus de la Société géologique de Finlande N:o XXXVIII (1966) and in Bulletin de la Commission géologique de Finlande N:o 222.

TABLE 1.

CaO-contents (determined by J. Siivola) and the corresponding An-contents of the maxima and minima in the CaK $\alpha$  intensity diagram in Fig. 3.

	CaO-content %	Calculated An-content %
Core of the plagioclase .....	9.7	48.1
I maximum .....	9.9	49.1
I minimum .....	6.7	33.2
II maximum .....	10.1	50.1
II minimum .....	7.0	34.7
III maximum .....	10.0	49.6
(standard) .....	(12.8)	(63.5)

SUOMEN GEOLOGISEN SEURAN JULKAISUJA  
MEDDELANDEN FRÅN GEOLOGISKA SÄLLSKAPET  
I FINLAND  
COMPTES RENDUS DE LA SOCIÉTÉ GÉOLOGIQUE  
DE FINLANDE

XXXVIII

Editor

MAUNO LEHIJÄRVI

*Geological Survey of Finland  
Otaniemi, Finland*

Editorial Committee

VLADI MARMO

*Geological Survey of Finland*

MARTTI SAKSELA

*Institute of Geology and Mineralogy  
University of Helsinki*

ESA HYYPPÄ

*Geological Survey of Finland*

JUHANI SEITSAARI

*Institute of Geology  
University of Oulu*

VALTO VELTHEIM, *ex officio*

*Geological Society of Finland*

Published yearly by The Geological Society of Finland  
Helsinki 1966

---

SISÄLLYSLUETTELO — CONTENTS

	Sivu—Page
KIRJOITUKSIA — PAPERS	
RISTO AARIO, Kieselgur in fluvioglazialen Ablagerungen in Haapajärvi in Ostbottnien . . . . .	3
Th. G. SAHAMA, Polygonal Growth of Beryl . . . . .	31
OLEG v. KNORRING, Th. G. SAHAMA and ESKO SAARI, A Note on the Properties of Manganoantalite . . . . .	47
ATSO VORMA, Rozenite — Iron Sulphate Tetrahydrate — as Fissure Coatings in the Black Schist at Mulo, Pyhäselkä, in Eastern Finland . . . . .	51
VLADI MARMO, Monzonitic Hornblende Granite NW of Tebo, Central Sierra Leone . . . . .	55
ATSO VORMA, PEKKA KALLIO and KAUKO MERILÄINEN, Molybdenite-3R from Inari, Finnish Lapland . . . . .	67

*(Contents continued)*

	Sivu—Page
VLADI MARMO, On the Petrological Classification of Granites .....	69
KARL MÖLDER, Über die Entstehung des inneren Salpausselkä zwischen Jaala und Saimaa ....	75
AHTI SIMONEN, Orbicular Rock in Kuru, Finland .....	93
ANTTI SAVOLAHTI and RAIMO KUJANSUU, Some Features of the Salmenkylä Gabbro in Kangasniemi Commune, Finland .....	109
HEIKKI PAPUNEN, Framboidal Texture of the Pyritic Layer found in a Peat Bog in SE-Finland	117
RISTO TYNNI and JAAKKO SIIVOLA, On the Precambrian Microfossil Flora in the Siltstone of Muhos, Finland .....	127
Th. G. SAHAMA, ESKO SAARI and KAI HYTÖNEN, Relationship between Götzenite and Rosenbuschite .....	135
KAI HYTÖNEN and AULIS HEIKKINEN, Alkali Amphibole of Otanmäki, Finland .....	145
PENTTI RASTAS and VLADI MARMO, On a Peculiar Breccia at Hirvijärvi, Virrat, Central Finland	157
VLADI MARMO and JAAKKO SIIVOLA, On the Barium-Content of Some Granites of Finland ...	169
ANTTI SAVOLAHTI, The Differentiation of Gabbro-Anorthosite Intrusions and the Formation of Anorthosites .....	173
ANTTI SAVOLAHTI and REINO MARJONEN, On the Petrography of the Metamorphic Schist Belt of Hautajärvi, Kiuruvesi Commune, Finland .....	199
T. A. HÄKLI and P. KEROLA, A Computer Program for Boulder Train Analysis .....	219
K. VIRKKALA, Radiocarbon Ages of the Råbacka Bog, Southern Finland .....	237
ATSO VORMA, PENTTI OJANPERÄ, VÄINÖ HOFFRÉN, JAAKKO SIIVOLA and ARVO LÖFGREN, On the Rare Earth Minerals from Pyörönmaa Pegmatite in Kangasala, SW Finland .....	241
K. J. NEUVONEN, Paleomagnetism of the Dike Systems in Finland. II. Remanent Magnetization of Dolerites in Vaasa Archipelago .....	275
MAUNU HÄRME and JAAKKO SIIVOLA, Plagioclase Zoning in a Gabbroic Dike from Alatornio, Northern Finland .....	283
O. VAASJOKI and KAUKO PUUSTINEN, On the Titaniferous Ore Oxides in Some Subsilicic Dikes and Sills .....	289
O. VAASJOKI, On the Faults and Diabasic Formations in Herajoki Region, Karelia, East Finland	303
HEIKKI V. TUOMINEN, Structural Control of Composition in the Orijärvi Granodiorite .....	311
A. HORRELL CLARK, The Mineralogy and Geochemistry of the Ylöjärvi Cu-W Deposit, Southwest Finland: Mackinawite-Pyrrhotite-Troilite Assemblages .....	331
ANTTI SAVOLAHTI, On Rocks Containing Garnet, Hypersthene, Cordierite and Gedrite in the Kiuruvesi Region, Finland. Part I: Juurikkajärvi .....	343
HEIKKI V. TUOMINEN, On Synkinematic Svecofennian Plutonism .....	387
JÄSENLUETTELO — 30. 4. 1966 — MEMBERSHIP LIST .....	395

This bulletin is the journal of the Geological Society of Finland. It contains articles on geology and related scientific subjects.

Manuscripts for publication should be sent to the Editor before March 1st. The papers should be in English, German or French. References to other publications should be in accordance with the forms used in this issue. The headings should generally be restricted to three classes. The articles should be brief and should be preceded by a short Abstract (Zusammenfassung, Résumé). The illustrations, in black and white, should be kept separate from the text. The author's name and the figure number to be on each illustration.

The contributors may have 100 reprints without covers free of charge. Additional author's reprints can be supplied at printer's rates if ordered in advance of publication.

# KIESELGUR IN FLUVIOGLAZIALEN ABLAGE- RUNGEN IN HAAPAJÄRVI IN OSTBOTNIEN

VON  
RISTO AARIO

*Institut für Geologie und Paläontologie, Universität Helsinki*

## ZUSAMMENFASSUNG

Die in Haapajärvi getroffene Kieselgur besteht aus Planktonarten und ist in einer verhältnismässig kühlen Interglazial- oder Interstadialzeit entstanden. Der in diesem Gebiet festgestellte Vorstoss des Inlandeises spät in der Finiglazialzeit ist jünger als die Kieselgur auch in ihrer heutigen sekundären Lage.

## INHALT

	Seite
Vorkommen und Lagerung .....	3
Fundstellen .....	3
Lagerung .....	7
Orientierung .....	10
Mikrofossilien .....	12
Diatomeen .....	12
Pollen .....	17
Zur chronologischen Einstufung .....	20
Schriftenverzeichnis .....	29

## VORKOMMEN UND LAGERUNG

### Fundstellen

Bei meinen 1960 in Haapajärvi durchgeführten Untersuchungen des nördlichen Abflusses des Päijänne beobachtete ich in den Wandungen einer gerade begonnenen Sandgrube am Ostufer des Mustolanjärvi 5 km südsüdöstlich von Haapajärvi (Abb. 1) reine Kieselgur, unter Bänder-ton. Bei den weiteren Untersuchungen dieses Vorkommens fand ich Kieselgur auch in der Sandgrube von Karjalahdenranta, 1 km nordnordwestlich vom obigen Ort. Ausserdem machte mich Dozent Virkkala während der Untersuchungen auf das Vorkommen von Kieselgur auch in der Sand-

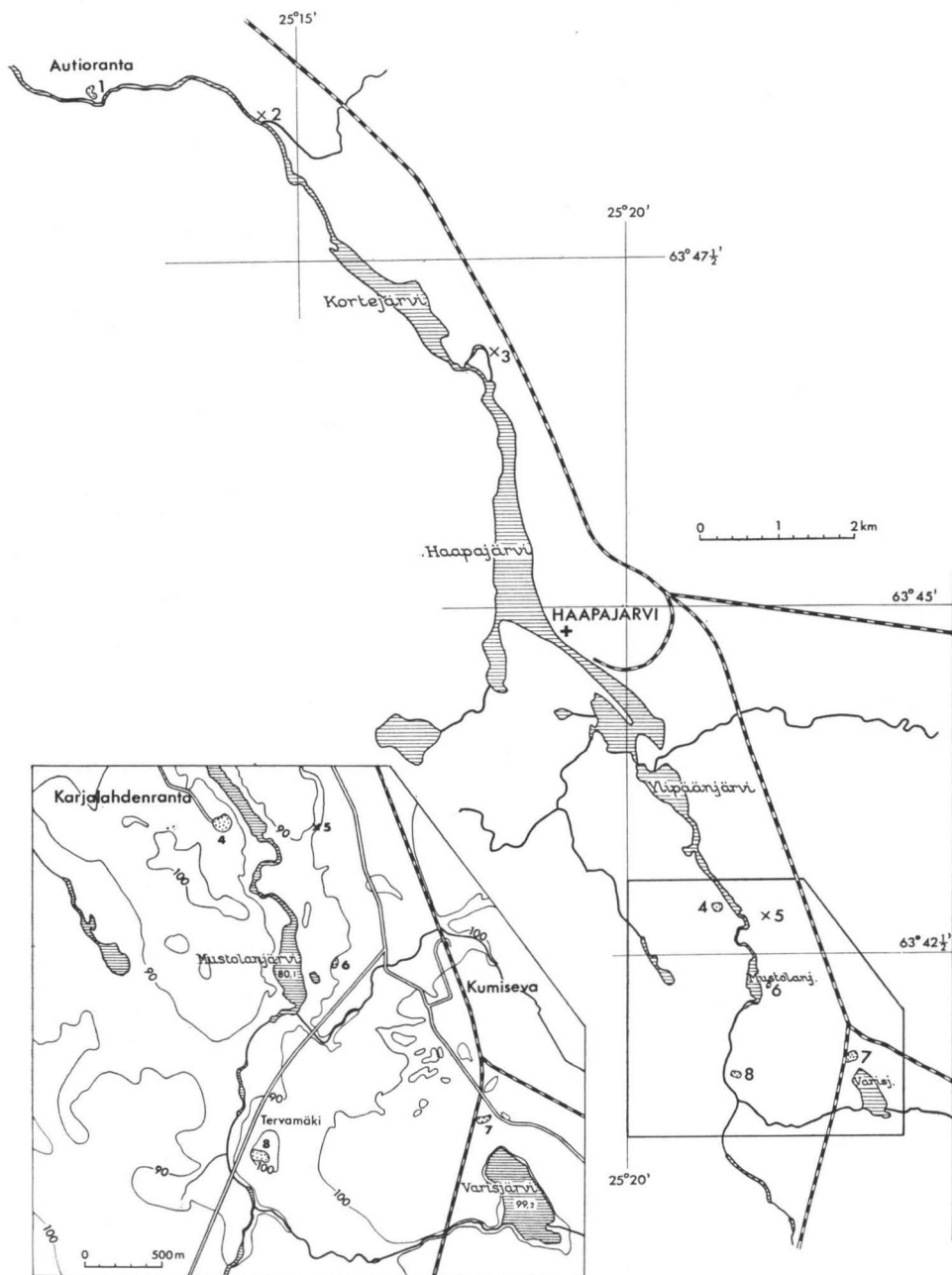


ABB. 1. Untersuchungsstellen. 1. Autioranta, 2. Kuusanjoki, 3. Siponkoski, 4. Karjalahdenranta, 5. Kangasniemi, 6. Mustolanjärvi, 7. Varis, 8. Tervämäki.



ABB. 2. Gefalteter und gebrochener Bändertone am Ostrand der Sandgrube von Karjalahdenranta. Auch im Sand Störungen. Die schwarze Linie zeigt die Grenze zwischen Sand und Ton an.

grube des Hofes Varis aufmerksam, etwa 3 km südöstlich der Sandgrube am Mustolanjärvi. In anderen Sand- und Kiesgruben der Umgebung von Haapajärvi fand sich keine Kieselgur, obgleich ich im Laufe von drei Jahren in einigen von ihnen an den durch die Entnahme von Sand und Kies immer neu entstehenden Schnitten Beobachtungen anstellte.

Der obere Rand der Sandgrube von Karjalahdenranta liegt etwa 94 m, der von Mustola 91 m und der der Varis'schen etwa 105 m über dem Meeresspiegel. Der Höhenunterschied beträgt also 14 m. Alle drei Vorkommen liegen in der nordwestlichen Fortsetzung des Oszuges von Pitkäkangas, aber keins von ihnen hebt sich morphologisch als Os aus der Landschaft heraus, obgleich die Mächtigkeit des fluvioglazialen Materials in ihnen oft sogar über 10 m geht.

Auch in der Struktur sind sich alle drei Fundstellen der Diatomeenerde ähnlich. Da das fluvioglaziale Material als verhältnismässig ebene Bildung auftritt, gibt es keine von der Neigung der Oshänge abhängige grosszügige Neigung der Schichten. Selbst in den verschiedenen Teilen der Aufschlüsse finden sich in der Schichtenfolge keine grossen Abweichungen. An allen drei Stellen liegt über den Sandschichten, wenigstens zum Teil, eine Tonschicht. In Karjalahdenranta und Mustola sind sie in den unteren Teilen warvig, während die oberen Teile nahezu homogen sind, dem Typus nach postglazial. In der Varis'schen Sandgrube fehlt der Bändertone jedoch und auch homogener Ton tritt in den östlichen hohen Teilen des Schnittes nicht auf.

In der Sandgrube von Mustolanjärvi sowie im nordwestlichen Teil der Sandgrube von Karjalahdenranta geht der Sand mit vorwiegender Kreuzschichtung erst in Sandwarven (oft mit Rippelschichtung) und dann in den ungestörten Bändertone über. In den östlichen und südöstlichen Teilen der Sandgrube von Karjalahdenranta treten in den unteren Teilen des warvigen Tones dagegen reichlich Störungen auf (Abb. 2), so wie auch in dem darunterliegenden Sand. Sogar Tonstücke mit völlig aufrechtstehenden Warven sind hier keine Seltenheit.

In der Sandablagerung unter dem Ton liegt zuoberst meistens eine Schicht Mittelsand, der feiner ist als weiter unten (Tabelle 1, Proben K2, K7, V8, V9 und V11). In dem ungestörten Nordwestteil der Sandgrube von Karjalahdenranta tritt in der Übergangszone zwischen diesem Sand und dem darüberliegenden warvigen Teil eine etwa 3 cm starke Kiesschicht auf. Im oberen Sand tritt in der Fallwinkel der Schichten sowie in der Fallrichtung verhältnismässig viel Variation auf. Die Kreuzschichtung ist allgemein, die Diagonalschichtung seltener.

Unter der Schicht von Mittelsand liegt im allgemeinen gröberer, gleichmässiger Sand (Tabelle 1, Proben K1, K3, K4, K5, K6 und V10), der das Hauptmaterial in allen drei Sandgruben ist. Im östlichen und südöstlichen Teil der Sandgrube Karjalahdenranta liegt diese Sandschicht direkt unter der gestörten Tonschicht und der obenerwähnte feinere Sand ist bis auf wenige Reste verschwunden. Den obersten Teilen des groben Sandes ist wenigstens örtlich eine Regelmässigkeit in der Fallwinkel (ca. 30°) sowie in der Fallrichtung (SO) der kleinen Schichtungen eigen. Diagonalschichtung kommt häufig vor. Weiter unten gibt es in der Neigung der Schichten etwas mehr Variationen, aber das Material ist in der Hauptsache das gleiche.

In der Varis'schen Sandgrube gibt es ausser der obigen Reihe von Schichten einen Rücken in NW-SO-Richtung, der aus sehr grobem Material besteht, in dem reichlich über 20 cm, ja sogar über 1 m grosse Geschiebe vorkommen. Diese Bildung reicht am Nordrand der Grube bis an die Oberfläche, sinkt aber nach Süden hin steil ab unter den oben beschriebenen groben Sand.

Nach der obigen Beschreibung sind alle drei Vorkommen in den wesentlichsten Zügen ihrer Schichtenfolge ziemlich gleichartig und offensichtlich auch unter ähnlichen Umständen entstanden. Trotz des grossen Höhenunterschiedes und der grossen Entfernung der Vorkommen voneinander (über 3 km) müssen diese offensichtlich als gleiche Bildung betrachtet werden.

Der in der Varis'schen Sandgrube auftretende, reichlich Geschiebe enthaltende Rücken entspricht der frühesten Phase der betrachteten Schichtenfolge, des wahrscheinlich im Inneren oder in einer Spalte des Inlandeises stark fliessenden Schmelzwasserstromes. Der diagonalschichtige grobe Sand darüber hat sich im wesentlich langsamer, laminar fliessenden Wasser (Illies 1949, S. 98) vor dem Rande des Eises abgelagert oder unter ihm, falls der Rand des Eises geschwommen hat. Auch die letzterwähnte Möglichkeit ist da, denn der Eisrand muss dünn gewesen sein, und es handelt sich um ein präglaziales Flusstal, das deutlich tiefer liegt als seine Umgebung. Jedenfalls hat sich das Material dabei frei ausbreiten können, ohne eine besondere Osform zu bilden, obgleich es genug Material gab (vgl. Sauramo 1927, S. 36). Das Auftreten von warvigem Ton über dem fluvioglazialen Sand in der Schichtenfolge zeigt, dass das Fehlen der Osform hier ursprünglich ist, und nicht auf die Ebnung der Küstenagenzien bei der Hebung des Landes zurückzuführen ist. Das wird auch bestätigt durch die Ähnlichkeit der Schichtenfolgen an den verschiedenen Stellen.

Die obere Schicht mit feinerem Sand vertritt offensichtlich eine grössere Entfernung von der Mündung des Schmelzwasserstromes. Weniger klar ist jedoch,

warum das Material in dieser Schicht in der Korngrösse sowie in Fallrichtung und -winkel der kleinen Schichten mehr als im unteren gröberen Sand wechselt, was auf eine veränderlichere Strömung hinzuweisen scheint. Ist doch auch die Kreuzschichtung in dieser Schicht verbreitet. Da darüber warziger Ton liegt, kann die Unterschiedlichkeit nicht von flachem Wasser herrühren. Wenn sich der weiter unten liegende gröbere Sand unter den Randteilen des Eises abgelagert hat, wie oben ausgeführt wurde, könnte die Veränderung der Struktur zum Unregelmässigen hin durch die Nähe des Eisrandes erklärt werden. Die unter dem Bändertone in Karjaladenranta anzutreffende dünne Schicht von gut gerundetem Kies würde sich auf diese Weise auch leicht erklären. Als zweite Erklärung für die Veränderlichkeit der oberen feineren Sandschicht liesse sich anführen, dass diese verhältnismässig dünne Schicht (im allgemeinen weniger als ein Meter) langsam entstanden ist. So hat sie mehr Veränderungen »registrieren« können als die darunter liegenden Schichten aus grobem Sand.

### Lagerung

Kieselgur tritt in verschiedener Korngrösse in sekundärer Lage zusammen mit Osmaterial auf. In einem Fall begegnete Diatomeenerde in Form von kleinen Körnern auch in den Sommerzonen der unteren Warven einer Bändertonschicht. In postglazialen Ton und in dem aus groben Geschieben bestehenden Rücken des Varis'schen Schnittes wurde sie nicht gefunden.

Die Form der kleinen Kieselgurkörner ist im allgemeinen unbestimmt, und sie zerfallen leicht bei der Berührung. Die grösseren, über 1 cm langen Körner sind dagegen meistens ziemlich fest, und sie sind deutlich abgerundet in der Art der entsprechend grossen Kieskörner. Die abgeplatteten Formen sind jedoch etwas allgemeiner als in dem gewöhnlichen, aus dem Stein gebildeten Kies, wie es natürlich ist im geschichteten Material (Abb. 3).

Nach meinen Versuchen sind die Kieselgurkörner in ihrem jetzigen Zustand selbst in stehendem Wasser nicht beständig, aber in gefrorenem Zustand sind sie haltbarer. Es ist auch offensichtlich, dass das Diatomeenmaterial in gefrorenem Zustand mit den Schmelzwässern mitgeführt wurde, wobei sich seine Stücke wie fluvioglazialer Kies abschleifen. Diatomeenmasse, die zum Teil durch dieses Abschleifen frei wurde, zum Teil durch Schmelzen zerfiel, kommt reichlich im Sand als nur mit dem Mikroskop unterscheidbares Material vor. Die starke Neigung zum Zerfallen macht es unwahrscheinlich, dass die Kieselgur mit den Schmelzwässern weit von ihrem primären Ablagerungsort mitgeführt worden ist.

Die Grösse der Kieselgurkörner steht in einer gewissen Korrelation zur Korngrösse des entsprechenden Sandes. In grobem Sand, den die Siebanalysen K1, K3, K5, K6 und V10 (Tabelle 1) vertreten, schwankt die Grösse der Kieselgurkörner nach den durchgeführten Messungen im allgemeinen zwischen 2 Millimetern und 2 Zentimetern, wobei die häufigste Korngrösse in den verschiedenen Vorkommen

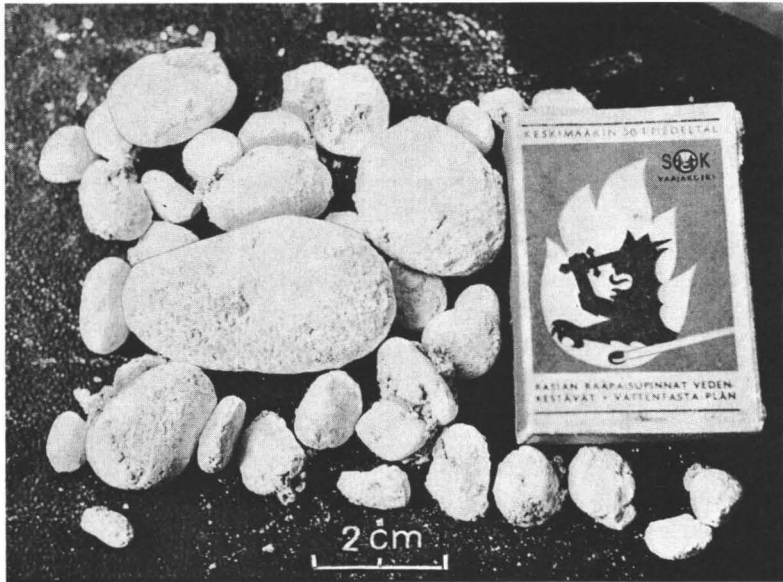


ABB. 3. Die grössten Kieselgurkörner aus dem unter dem warvigen Ton liegenden Sand, Karjalahdenranta. Die länglichen Formen herrschen vor.

etwas über oder etwas unter einem Zentimeter liegt. In Mittelsand (Analysen K2, K4, K7, V8, V9 und V11) liegt die Grösse der Kieselgurkörner im allgemeinen unter 2 mm, während die häufigste Grösse etwa 1 mm beträgt. Die durchschnittliche Sinkgeschwindigkeit der grösseren Kieselgurkörner ist etwas grösser gewesen als die der kleineren, was ihr Vorkommen mit dem groben Sand verbunden hat. Die Korngrösse der Diatomeenerde ist immer wesentlich grösser als die des gleichzeitig abgelagerten Sandes, entsprechend dem kleineren spezifischen Gewicht der gefrorenen Kieselgur.

TABELLE 1

Die Verteilung der Kieselgur enthaltenden Sandproben auf die Korngrösseklassen. Die Zahlen sind Gewichtprozente. K = Karjalahdenranta, V = Varis.

Korngrösse mm	K 1	K 2	K 3	K 4	K 5	K 6	K 7	V 8	V 9	V 10	V 11
>6 ..	0.1	—	0.1	—	0.0	—	—	1.7	—	0.8	0.8
6—2 ..	1.7	0.1	0.5	0.0	0.4	0.5	0.1	10.8	0.1	5.0	0.6
2.0—0.6 ..	91.3	10.0	94.6	16.0	66.1	83.9	12.5	36.9	4.1	50.1	6.5
0.6—0.2 ..	5.8	60.6	3.0	80.1	27.8	13.8	77.6	42.2	79.5	37.9	72.7
0.2—0.06 ..	0.9	28.1	1.3	3.5	5.4	1.6	9.7	7.9	14.4	5.6	16.3
<0.06 ..	0.1	1.2	0.5	0.4	0.3	0.2	0.2	0.4	1.9	0.6	3.2
Tiefe m	1.5	0.8	3.5	8.0	9.0	4.0	1.5	3.0	3.0	3.5	3.0



ABB. 4. Eine aus Kieselgurkörnern gebildete Linse, Varis. Sowohl die Linsen als auch die dünnen Kieselgurschichten folgen jeweils der Richtung der Sandschichten.

Die einzelnen Körner treten im allgemeinen zusammengeballt zu dünneren linsenförmigen Kieselgurklumpen oder 1—3 mm starken Schichten auf. Die horizontale Ausdehnung sowohl der dünnen Schichten als der Linsen beschränkt sich im allgemeinen auf einige Zentimeter bis etwa zwanzig Zentimeter. Die dünnen Kieselgurschichten und die Linsen folgen den Schichten des Sandes. Abb. 4 vertritt einen recht typischen Fall, wenn reichlich Diatomeenerde da ist. Die Körner haben sich zusammen mit dem Sand abgelagert.

Da die Körner der Diatomeenerde und die daraus geformten Linsen in grobem Sand grösser sind, entfällt der quantitative Hauptteil des Kieselgurvorkommens auf diese Schicht, obgleich Kieselgur am häufigsten in der sofort unter dem Ton gelegenen, in bezug auf die Neigung der Schichten und die Korngrösse etwas unhomogenen Sandschicht vorkommt, wo der Mittelsand vorherrscht. Dennoch sind auch die in grobem Sand gelegenen Vorkommen nicht sehr gross. Diatomeenerdelinsen, deren Stärke grösser ist als 2 cm und deren Breite 15 cm überschreitet, sind verhältnismässig selten. Dennoch hat man auch Linsen gefunden, deren Stärke über 5 cm betrug. Meistens hat man diese direkt an der oberen Grenze von grobem Sand gefunden.

Tiefer in grobem Sand nimmt das Vorkommen von Diatomeenerde ab, aber in Karjalahdenranta hat man sie noch in über 8 m Tiefe gefunden, vom unteren Rand des Tones gerechnet.

### Orientierung

Zur Ermittlung der Fließrichtung der die Kieselgurkörner befördernden Strömungen wurde an drei Vorkommen der Kieselgur eine Richtungsanalyse durchgeführt, und zwar an zwei von Karjalahdenranta (Abb. 5, 1—2) und an einem von Varis (Abb. 5, 3). In beiden Richtungsrosen für Karjalahdenranta ist die NW-SE-Richtung stark vorherrschend. Auch in der Richtungsrose von Varis ist dieselbe Richtung im allgemeinen bevorzugt, aber das Orientierungsmaximum trifft die N-S-Richtung. Die Unterschiede zwischen den verschiedenen Richtungen sind auch in diesem Fall kleiner als in den beiden anderen. Die Richtungsrose 11 bezieht sich auf die dünne Kies-Schicht mit einem Beischlag von Kieselgurkörnern dicht unter den Sandwarven unter dem Bänderton. Auch hier herrscht die NW-SE-Richtung vor. Da die zur Verfügung stehenden Kieselgurvorkommen klein waren, konnte die Orientierung an nur je 100—200 Körnern bestimmt werden. Aus diesem Grund musste man sich in den Diagrammen mit einer verhältnismässig spärlichen Gruppierung der Richtungen begnügen.

Auch an den Sandschichten, die Kieselgur enthalten, wurden Richtungsanalysen durchgeführt, und zwar aus Lackfilmproben (Voigt 1949) mit etwa 50-facher Vergrößerung nach einem von Prof. Dr. H. Reinhard (Greifswald) mir mündlich empfohlenen Verfahren. In jeder Analyse wurde die Richtung von 500 Sandkörnern bestimmt. Die Richtungsrose 7 (Abb. 5) an grobem Sand bezieht sich auf dieselbe Schicht des groben Sandes, an der die Richtungsanalyse 2 für die Kieselgurkörner gemacht wurde. Die Übereinstimmung ist vollkommen. Auch die Analyse 6 an grobem Sand aus der Nähe der Analyse 7 zeigt die Vorherrschaft der NW-SE-Richtung. In den Richtungsrosen 4—5 und 8—9, betreffend die Schicht des Mittelsandes, kommt auch die N-S-Richtung stark zum Vorschein. In zwei von 4 Richtungsrosen ist diese sogar die stärkste und auch in beiden anderen recht stark.

In den Geschieben des aus einem groben Steinmaterial bestehenden Osrückens bei Varis ist auch die NW-SE-Richtung deutlich dominierend. (Abb. 5, 10).

Die Strömungsrichtung wurde auch makroskopisch direkt aus den Schichten mit Hilfe der stärksten Fallrichtung bestimmt, deren Azimuth meistens etwa 150—155 Grad betrug. In unserem Fall stimmen also die mit Hilfe der Fallrichtung bestimmten Strömungsrichtungen gut mit den vorherrschenden Richtungen der Sand-, Kies- und Kieselgurkörner überein. In seinem Lehrbuch »Sequence in layered rocks« stellt Shrock eine ähnliche Übereinstimmung in gewissen rezenten und älteren Stromablagerungen dar, aber nach G. Lundqvist (1948) lagern sich die Sandkörner senkrecht zur Strömungsrichtung. Der Unterschied mag auf den Verschiedenheiten in der Strömungsgeschwindigkeit beruhen.

Soweit man aus den oben dargestellten, vorläufig noch knappen Beobachtungen Schlussfolgerung ziehen kann, scheint die Strömung bei der Ablagerung der Hauptmasse des Sandes aus Nordwesten und Nordnordwesten gekommen zu sein, aber in der letzten Phase, in der sich die Schicht des Mittelsandes bildete, kam noch eine

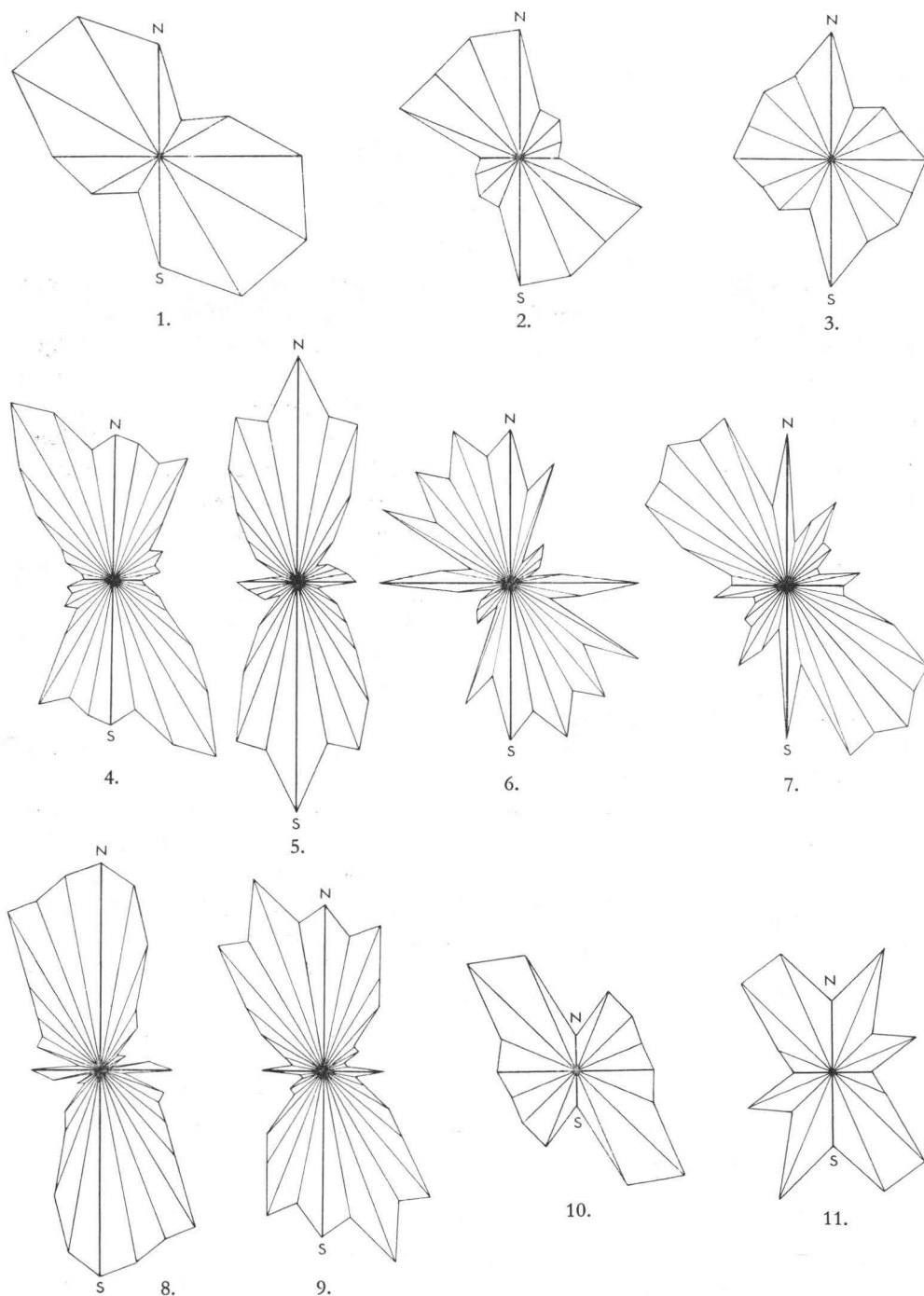


Abb. 5. Richtungsrosen für fluvioglaziale Ablagerungen an Fundstellen von Kieselgur. 1. Kieselgur, Karjalahdenranta W (Tiefe 1 m), 2. Kieselgur, Karjalahdenranta NW (Tiefe 3.5 m), 3. Kieselgur, Varis W (Tiefe 3 m), 4. Mittelsand, Karjalahdenranta W (Tiefe 0.8 m), 5. Mittelsand, Karjalahdenranta W (Tiefe 1.0 m), 6. Grobsand, Karjalahdenranta W (Tiefe 1.2 m), 7. Grobsand, Karjalahdenranta NW (Tiefe 3.5 m), 8. Mittelsand, Varis W (Tiefe 3 m), 9. Mittelsand, Varis W (Tiefe 3 m), 10. grosse Geschiebe, Varis N (Tiefe 1—1 ½ m), 11. Kies-Schicht an der Grenze von Ton und Sand, Karjalahdenranta NW (Tiefe 2 ½ m).

recht starke nördliche Strömung dazu. Sowohl die nordwestlichen als nördlichen Strömungen haben Kieselgur mitgebracht.

## MIKROFOSSILIEN

### Diatomeen

Diatomeenanalysen wurden von allen drei Vorkommen sowohl an mehreren einzelnen Kieselgurkörnern (auch verschiedenen Teilen der Körner) als auch an den senkrechten Schnitten der Sandgruben (Tabellen 2 und 3) vorgenommen. Wegen der Gleichartigkeit des Artenbestandes in den einzelnen Körnern und Schichtenfolgen der verschiedenen Vorkommen beschränke ich mich darauf, nur die Analysenergebnisse eines Untersuchungsobjektes, des von Karjalahdenranta, darzustellen.

In den einzelnen Körnern (Tab. 2) ist mit Ausnahme von Probe 5 in allen *Melosira islandica* die vorherrschende Art, zusammen mit ihrer Subspezies *helvetica*, und sie machen im allgemeinen über 80 % aller Diatomeen aus. Ein Teil der *M. islandica* liesse sich noch als *M. islandica* var. *vänerensis* (A-Cleve) aussondern, aber die Bestimmung ist in zu vielen Fällen wegen der Zerbröcklung der Individuen und wegen ihrer Erscheinungsform als Dauersporen unsicher. So habe ich in der Tabelle diese Variation mit der Hauptform der *M. islandica* zusammen gerechnet.

Von anderen Diatomeen erscheinen nennenswerte Mengen nur von *Coscinodiscus lacustris*, *Stephanodiscus astraea* und *Stephanodiscus hantzschii*; die letztgenannte macht in Probe 5 von allen unbeschädigten Diatomeen 55 % aus. Die genannte Probe dürfte zu einer im Alter etwas abweichenden Phase der Primärablagerung von Kieselgur gehören.

Alle genannten Arten, wie auch der grösste Teil der anderen in Kieselgurkörnern angetroffenen Arten, gehören zum Plankton des süssen Wassers und zumindest *M. islandica* ist eine Art kühlen Wassers (u. a. Cleve-Euler 1912). Eine Ausnahme stellt die nur in Probe 2 vorkommende *Thalassiosira kryophila* dar, die eine Meeresart ist. Die Kieselgur von Haapajärvi unterscheidet sich also in ihrem Artenbestand und hinsichtlich ihrer Bildungsumstände in starkem Masse von allen früher in Finnland gefundenen Vorkommen von Kieselgur (K. Mölder, mündl. Mitt.).

Da die Kieselgur zu ihrer jetzigen Lagerstätte eine kleine Strecke aus Richtung Nordwesten gekommen ist (S. 8—10), wo das Gelände ohne Hindernisse recht gleichmässig zum Bottnischen Meerbusen abfällt, muss das Becken, in dem sich ein so reines Diatomeenplankton abgelagert hat, zu irgendeiner Binnenseeperiode des Baltikums gehört haben. Die Bildung von reiner Kieselgur wiederum setzt voraus, dass sich vom Inlandeis kommender Schlamm nicht in nennenswertem Masse im Becken abgelagert hat und dass auch das vom Festland stammende minerogene Material das Kieselgurvorkommen nicht erreicht hat.

Besonders interessant ist die Erscheinungsform der *Melosira islandica* und ihrer Subspezies: von allen unbeschädigten Individuen umfassen über 90 % ihre

TABELLE 2

Diatomeen in einzelnen Kieselgurkörnern von Karjalahdenranta. Die Zahlen sind Prozente und beziehen sich auf die unversehrten Exemplare.

	1	2	3	4	5	6	7
<i>Coscinodiscus lacustris</i> Grun. ....	14	14	21	9	2	11	7
<i>C. lacustris</i> fragm. ....		16	15	5			2
<i>Cyclotella kützgingiana</i> var. <i>radiosa</i> Fricke .				2			1
<i>C. ocellata</i> Pant. ....					2		1
<i>Melosira ambigua</i> (Grun.) Müll. ....		1	1	1	4	1	1
<i>M. arenaria</i> fragm. ....				1			
<i>M. distans</i> (Ehr.) Kütz. ....	1				2	1	
<i>M. granulata</i> (Ehr.) Ralfs ....			1	1	4	1	1
<i>M. islandica</i> O. Müll. ....	7	9	6	3	1	16	5
<i>M. islandica</i> , Dauersporen ....	67	47	62	82	19	61	75
<i>M. islandica</i> fragm. ....	150	507	322	56	57	209	145
<i>M. islandica</i> ssp. <i>helvetica</i> O. Müll. ....	1	5			3	2	1
<i>M. islandica</i> ssp. <i>helvetica</i> , Dauersporen ..		3					
<i>M. islandica</i> ssp. <i>helvetica</i> fragm. ....	1	5	1	1			
<i>M. spp.</i> fragm. ....		9	6	1			
<i>Stephanodiscus astraea</i> (Ehr.) Grun. ....	7	5	7			6	7
<i>S. astraea</i> fragm. ....	10	10	12	5		7	6
<i>S. hantzschii</i> Grun. ....		11			55	1	1
<i>Thalassiosira kryophila</i> (Grun.) Joergensen		1					
<i>Achnanthes exigua</i> fragm. ....			1				
<i>Achnanthes linearis</i> (W. Sm.) Grun. ....	1						
<i>Cymbella sinuata</i> Greg. ....	1						
<i>Epitbemia</i> sp. fragm. ....		3				1	
<i>Fragilaria brevistriata</i> Grun. ....			1				
<i>F. construens</i> var. <i>binodis</i> (Ehr.) Grun. ...					3		
<i>F. construens</i> var. <i>venter</i> (Ehr.) Grun. ....				1			
<i>F. pinnata</i> Ehr. ....		1			2		
<i>F. pinnata</i> var. <i>lancettula</i> (Schum.) Hust.		3					
<i>F. virescens</i> Ralfs ....			1	1			
<i>F. sp.</i> ....					3		
<i>Opephora martyi</i> Hërib. ....	1						
<i>Tabellaria fenestrata</i> fragm. ....			1				
Zahl der untersuchten Diatomeen .....	261	652	459	169	157	317	253

Dauersporen (Abb. 6)! Auch unvollständige Teile der *Melosira*, die in der Tabelle als besondere Gruppe verzeichnet sind, stammen ihrer Struktur nach hauptsächlich von Dauersporen.

Viele niedrigere Pflanzenarten bilden Dauersporen, wenn die Umstände für die normalen Lebenstätigkeiten zu ungünstig werden. Mit Hilfe der Dauersporen »überwintert« die Pflanze über eine ungünstige Periode. Für die Bildungsvoraussetzungen von Dauersporen der *Melosira* habe ich jedoch keine Darstellung gefunden. Es lässt sich jedoch kaum bezweifeln, dass die Dauersporen auch bei dieser dem Überbestehen ungünstiger Perioden dienen. Nach Cleve-Euler (1912) bildet die *Melosira islandica* ssp. *helvetica* in 0—6° warmem Wasser Auxosporen, mit deren Hilfe sich bekanntlich die Grösse der Diatomeenindividuen in gewissen Grenzen hält; bei

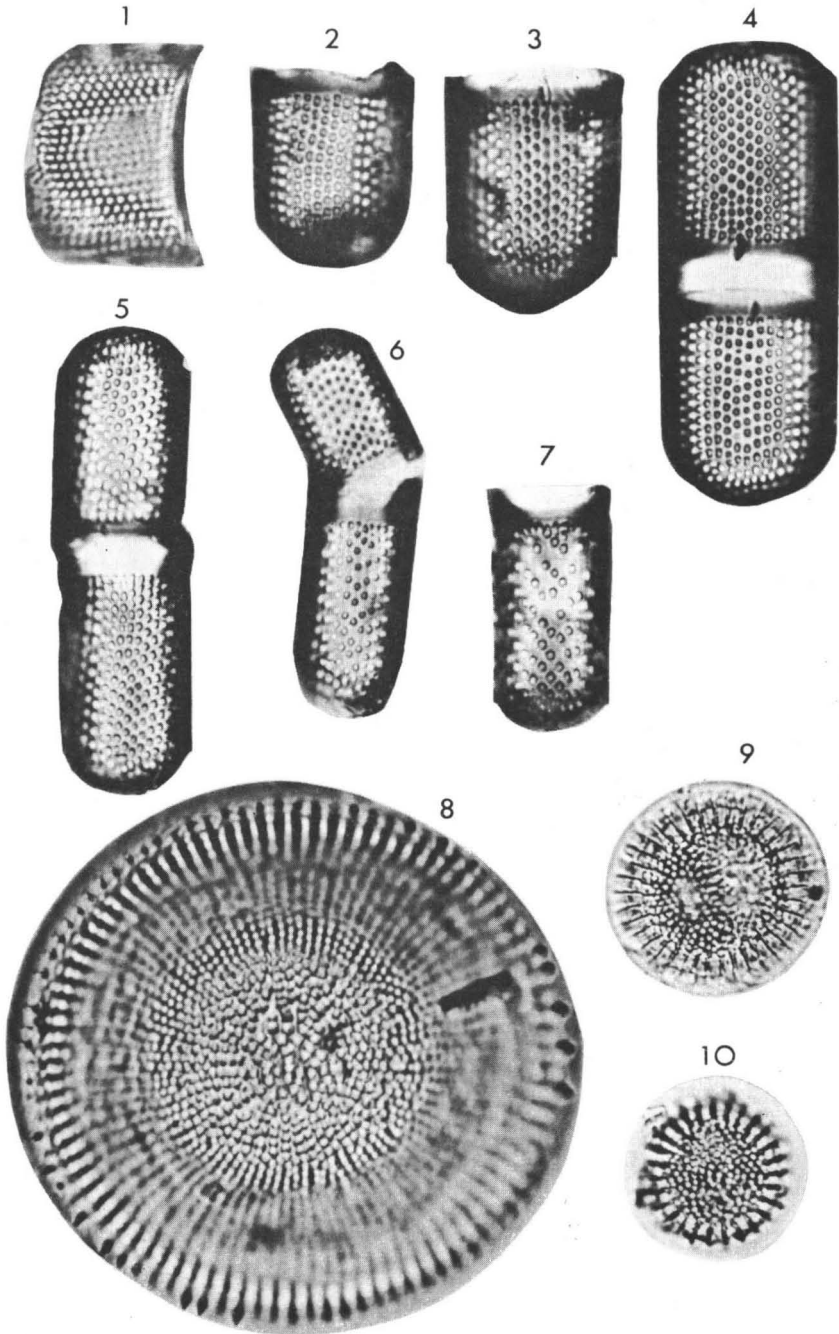


ABB. 6 Die häufigsten in der Kieselgur auftretenden Diatomeenarten. 1—7 Doppelwandige und an den Ende gerundete Dauersporen und Dauersporenhälften der *Melosira*-Arten. 1. *Melosira islandica* ssp. *helvetica*, 2—7 *Melosira islandica*, 8. *Stephanodiscus astraea*, 9—10 *Coscinodiscus lacustris* (etwa 1500 fach vergr., Photo E. Halme).

TABELLE 3

Diatomeen in der Lagerfolge am westlichen Rand der Sandgrube von Karjalahdenranta. Die Lage der Proben in der Schichtenfolge in Abb. 7. Die Zahlen geben die Anzahl der Exemplare an.

	1	2	4	5	6	8	10	11	12	14	16
<i>Coscinodiscus lacustris</i> Grun. ....				2	2	4	1			3	
<i>C. lacustris</i> fragm. ....						3				2	1
<i>C. sp.</i> fragm. ....				1	1						5
<i>Melosira ambigua</i> (Grun.) Müll. ....						1	1				1
<i>M. arenaria</i> Moore ....				1	3						
<i>M. arenaria</i> fragm. ....			1			1				1	
<i>M. islandica</i> O. Müll. ....			2	4			1			2	1
<i>M. islandica</i> , Dauersporen ....	3	68	40	39	45	46	40			14	4
<i>M. islandica</i> fragm. ....	1	15	34	42	23	20	36			8	10
<i>M. islandica</i> ssp. <i>helvetica</i> O. Müll. ....					2	4				1	5
<i>M. islandica</i> ssp. <i>helvetica</i> , Dauersporen ...			2	3	6	14	6	8			3
<i>M. islandica</i> ssp. <i>helvetica</i> fragm. ....				2	3	7	6	6		1	12
<i>M. spp.</i> fragm. ....							2	2		2	1
<i>Stephanodiscus astraea</i> (Ehr.) Grun. ....			1				3			2	
<i>S. astraea</i> fragm. ....		1	1		3	2	3			4	1
<i>S. hantzschii</i> Grun. ....				1							
<i>Epithemia turgida</i> (Ehr.) Kütz.) ....							1				
<i>E. sp.</i> fragm. ....							1				1
<i>Eunotia</i> sp. ....			1								
<i>Fragilaria</i> sp. ....				1							
<i>Gomphonema</i> sp. fragm. ....											1
<i>Grammatophora oceanica</i> (Ehr.) Grun. ....				1							
<i>Navicula rhynchocephala</i> Kütz. ....				1							
<i>N. sp.</i> fragm. ....			1								
<i>Neidium</i> sp. fragm. ....						1					
<i>Nitzschia stagnorum</i> Rabh. ....			1								
<i>Pinnularia hyppäei</i> fragm. ....			1								
<i>P. sp.</i> fragm. ....											1
<i>Rhabdonema minutum</i> Kütz. ....				1							
<i>Synedra tabulata</i> (Ag.) Kütz. ....					1						1
<i>S. tabulata</i> var. <i>acuminata</i> Grun. ....				1							
<i>S. sp.</i> ....			1								
<i>Tabellaria fenestrata</i> fragm. ....											1
Zahl der untersuchten Diatomeen .....	4	89	90	100	100	100	100	—	—	40	49

Temperaturen darüber verläuft die Lebenstätigkeit normal. Auch Dauersporen bilden sich in reichlichem Masse kaum in solchem Wasser, das wärmer als jenes ist. Dagegen könnte ein langes Verweilen der Jahreshöchsttemperatur in den Grenzen der genannten Temperaturwerte die ganze Lebenstätigkeit in den Zustand von Dauersporen überführen, wobei sich diese als Kieselgur ablageren können. Dieses Problem muss jedoch noch weiter geklärt werden.

Die Tabelle 3 stellt die Diatomeenanalysen einer Schichtenfolge von Karjalahdenranta dar. Die Beschaffenheit des Materials in verschiedenen Tiefen geht aus der Abbildung 7 hervor, sowie die Entnahmestellen der Proben an der rechten Seite. Die Numerierung der Proben ist dieselbe wie für die später dargestellten Pollenanalysen.

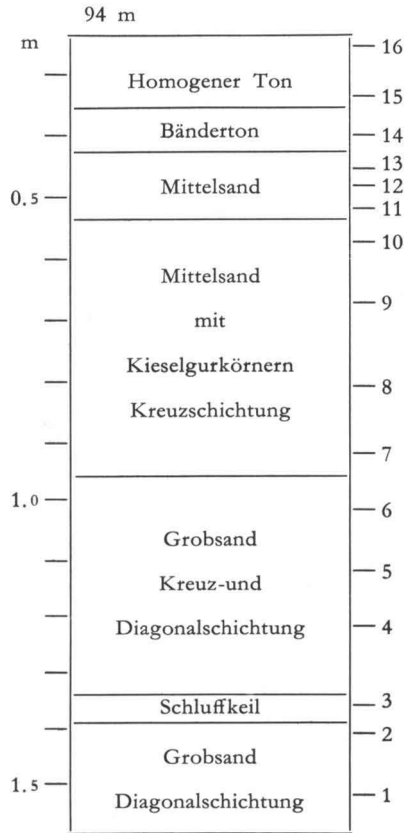


ABB. 7. Entnahmestellen der Proben für Diatomeen- und Pollenanalysen in Karjalahdenranta (Tab. 3 und 5).

Die Proben 8 und 10 bestanden aus Sand vermisch mit Kieselgur und enthielten die gleichen Kieselalgen wie die an einzelnen Kieselgurkörnern vorgenommenen Analysen. In den Proben 5 und 6 gab es auch reichlich Kieselalgen, obwohl Kieselgur im Probensand makroskopisch nicht festgestellt werden konnte. In den oberen und unteren Teilen des geprüften Schnittes gab es weniger Diatomeen, in den Proben 11 und 12 fehlen sie sogar ganz. Doch Kieselgur kommt auch makroskopisch feststellbar noch bedeutend unterhalb der untersten untersuchten Probe (1) vor, woraus hervorgeht, dass die Kieselgur sich ziemlich unregelmässig abgelagert hat.

Aus der Vorkommensart der Diatomeen geht hervor, dass ihr primäres Vorkommen erst in der Randzone des Eises starker Erosion unterlag und das lose Material sich bald ablagerte, nach einem kurzen Wege. Aus zerfallenen Körnern stammende Dauersporen sind jedoch im Wasser auch noch viel später aufgetreten, so dass sie

sowohl im Bänderton als auch in dem darüberliegenden homogenen Ton begegnen. Ungeklärt bleibt, ob sie direkt aus den weiterhin der Erosion unterliegenden Primärablagerungen stammen oder aus den aufs neue abgetragenen Sekundärablagerungen.

Die in dem kieselgurhaltigen Sand auftretenden unbeschädigten Diatomeenindividuen des Salz- und Brackwassers, wie *Grammatophora oceanica*, *Rhabdonema minutum* sowie *Synedra tabulata* und ihre Variation *acuminata*, die in den entsprechenden, aus reinem Kieselgur gemachten Proben nicht begegnen, weisen darauf hin, dass die sekundäre Ablagerung der Kieselgurkörner in salzigem Wasser (Yoldia?) erfolgt ist. Der Anteil der Salzwasserarten ist jedoch klein im Vergleich zu der sekundären Diatomeenmasse. Im übrigen gibt es in den Sandproben der untersuchten Schichtenfolge einen gleichartigen Artenbestand wie in den entsprechenden Kieselgurkörnern. Die Dauersporen der *Melosira islandica* sind auch in ihnen vorherrschend.

### Pollen

Die Pollenanalyse der Kieselgur ist von zwei Proben aus Mustola, zwei aus Karjalahdenranta und neun aus der Varis'schen Grube durchgeführt worden. Da die Körner von ihrer ursprünglichen Stelle anderswohin transportiert worden sind, hat der Ort ihrer Entnahme für deren Pollenbestand keine Bedeutung. Da andererseits zwischen der Pollenfrequenz und dem Pollenbestand eine gewisse Korrelation zu herrschen scheint, sind die Proben in Tabelle 4 nach der Pollenfrequenz geordnet. Die Entnahmestelle ist durch einen der Probennummer vorangestellten Buchstaben gekennzeichnet.

Die Proben gliedern sich in bezug auf die Pollenfrequenz und den Pollenbestand in drei Gruppen. Zu der ersten gehören die, in denen je Präparat weniger als fünf Pollenkörner da sind.

In den beiden Proben von Karjalahdenranta fand sich kein Pollen, in der ärmsten Probe aus der Varis'schen Grube fanden sich 4 *Chenopodiaceae*-Pollen, aber kein einziges Baumpollenkorn. Insgesamt wurden in den über 20 Präparaten aus den sechs Proben dieser Gruppe zwölf Baumpollenkörner gefunden, alle Birke. Das völlige Fehlen anderer Baumarten erklärt sich natürlich hauptsächlich aus der geringen Anzahl der gefundenen Pollenkörner, aber andererseits zeigt es, dass deren prozentualer Anteil auf jeden Fall sehr niedrig gewesen wäre. Die Menge sowohl der NBP als auch der Sporen ist  $\frac{3}{4}$  von der Menge der Birkenpollen, also vergleichsweise gross, soweit man einer auf so kleinem Material beruhenden Zahl Bedeutung beimessen kann.

Zu der zweiten Gruppe gehören M 1, V 5 und V 6, in denen die Pollenmenge je Präparat 5—20 beträgt. Sogar die am wenigsten *Betula* enthaltende Probe hat davon 80 %, die anderen über 90 %. Insgesamt wurden in den zwölf untersuchten Präparaten aus den Proben dieser Gruppe 147 Baumpollenkörner gefunden, davon 4 % *Alnus*, 88 % *Betula*, 7 % *Pinus* und 1  $\frac{1}{2}$  % *Tilia*. Fichte gab es nicht. Der Anteil

TABELLE 4

Die Pollen der Kieselgurkörner. K = Karjalahdenranta, V = Varis, M = Mustolanjärvi.

	K 1	K 2	V 1	V 2	V 3	V 4	M 1	V 5	V 6	V 7	V 8	M 2	V 9
<i>Alnus</i> .....							1	4	1	2	4	2	6
<i>Betula</i> .....				3	3	6	20	47	62	64	82	47	66
<i>Picea</i> .....									6	5	3		4
<i>Pinus</i> .....								7	3	27	10	50	23
<i>Tilia</i> .....								1	1				
<i>Ulmus</i> .....												1	1
<i>Corylus</i> .....								1		1			
<i>Juniperus</i> .....						1		1	1				
<i>Salix</i> .....									1	1			
<i>Ericales</i> .....							1	5	5	5	9	1	3
<i>Cyperaceae</i> .....				1								1	
<i>Gramineae</i> .....					1	1						2	4
<i>Caryophyllaceae</i> .....										1			
<i>Chenopodiaceae</i> .....			4									1	
<i>Drosera</i> .....											1		
<i>Plantago</i> .....							1						
<i>Rosaceae</i> .....													1
<i>Rumex</i> .....						1							
<i>Varia</i> .....							2	1	1	1	1	3	1
<i>Potamogeton</i> .....							1						
<i>Typha latif.</i> .....						1					1		
<i>Equisetum</i> .....											3		
<i>Lycopodium</i> .....				1		5	9	17	5	3	14	6	6
<i>Polypodiaceae</i> .....				1			1	6		1	3	1	7
<i>Selaginella</i> .....													1
<i>Sphagnum</i> .....				1		1	8	7	5	13	12	1	6
Zahl der Präparate .....	4	4	4	4	4	4	4	4	4	3	3	3	2

von *Betula* ist also auch in dieser Gruppe hoch. Die NBP-Menge macht 13 % aus, davon 8 Erikazeen. Sporen gab es 43 % (*Lycopodium* 25 %, *Sphagnum* 14 %).

Zur dritten Gruppe gehören die Proben M 2 sowie V 7—9. In jeder von diesen liessen sich 100 Pollenkörner in 2 oder 3 Präparaten zählen. In einer von diesen beträgt der Anteil von *Betula* noch 82 %, in den anderen 46—66 %, durchschnittlich 65 %. Die prozentualen Anteile der anderen Bäume sind: *Alnus* 3 ½ %, *Picea* 4 ½ %, *Pinus* 27 % und *Ulmus* ½ %.

Die Fichte erscheint recht gleichmässig in allen Proben. Die NBP-Menge macht 9 % aus, davon die Hälfte Erikazeen. Sporen gibt es 52 %, davon 20 % *Lycopodium* und 22 % *Sphagnum*. Der Anteil von *Lycopodium* ist also niedriger als in der vorigen Gruppe, der von *Sphagnum* höher.

Aufgrund des oben beschriebenen geringen Materials ist es nicht möglich, weitgehende Schlussfolgerungen zu ziehen, aber es lässt sich wohl nicht bezweifeln, dass die letzte Gruppe deutlich günstigere Umstände vertritt als die beiden vorhergehenden. Schwieriger ist es, die Gruppen im Vergleich mit den heutigen Vegetationszonen einzuordnen. Dabei muss beachtet werden, dass diese aus Planktonarten entstandene Diatomeenerde verhältnismässig weit von der Küste

TABELLE 5

Pollenanalysen aus Schichtenfolgen von Mustolanjärvi und Karjalahdenranta. Die oberste Ziffernreihe für Karjalahdenranta zeigt die Entnahmestellen der Proben (Abb. 7).

Tiefe m.	Mustolanjärvi (91 m)										Karjalahdenranta (94 m)					
	Sand		Bänderton							Ton	Sand					Ton
	3.7	3.3	3.1	2.8	2.7	1.6	1.1	0.4	0.3	0.2	4 1.2	6 1.0	7 0.9	9 0.7	12 0.5	16 0.3
<i>Alnus</i> .....		12	4		4	4		2	2	1	1					
<i>Betula</i> .....		64	31	3	4	17	2	1	3		2			1	2	
<i>Picea</i> .....		3	3			1							1		5	
<i>Pinus</i> .....	1	20	4	1	1	23	2	1	2	3	1	3			7	2
<i>Corylus</i> .....		1														
<i>Salix</i> .....			1													
<i>Ericales</i> .....		1		1		1										
<i>Cyperaceae</i> .....										1						
<i>Gramineae</i> .....		7	6						2						1	
<i>Artemisia</i> .....		1														
<i>Chenopodiaceae</i> .....					1	4										
<i>Compositae</i> .....										1						
<i>Cruciferae</i> .....						1										
<i>Plantago</i> .....				1	1											
<i>Rosaceae</i> .....												1			1	
<i>Saxifragaceae</i> .....												1				
<i>Varia</i> .....		1	1				1	1								
<i>Equisetum</i> .....					1											
<i>Lycopodium</i> .....		7	9		9	3	3	1		2	1					
<i>Polypodiaceae</i> .....		16	13		4	10		4	3	5						
<i>Sphagnum</i> .....			2	1		1										1
Zahl der Präparate .....	4	4	4	4	4	4	4	4	4	4	2	4	2	2	4	2

entstanden ist, und nicht viel Sekundärpollen enthält. Dagegen ist beim Fehlen einer nahegelegenen örtlichen Pollenquelle die Wirkung des Fernfluges gross. Danach scheint es, dass die beiden erstgenannten Gruppen ein Stadium vertreten, in dem weite umgebende Gebiete kahl waren oder von spärlichen Birkenwäldungen bedeckt. Während der Entstehung der zur letztgenannten Gruppe gehörenden Diatomeenerde sind die Nadelwälder deutlich näher gewesen, möglicherweise kann es sogar in den nächstgelegenen Küstengebieten Nadelbäume gegeben haben. Zusammenhängende Nadelwälder kann es in der näheren Umgebung kaum gegeben haben, weil in der langsam abgelagerten Diatomeenerde der Anteil der Pollen auch in dieser Gruppe gering ist und die Menge der NBP und Sporen im Vergleich zu den Baumpollen gross ist. Auf jeden Fall zeigt die Unterschiedlichkeit der Pollenzusammensetzung, dass die Ablagerung der Diatomeenerde so lange angedauert hat, dass in dieser Zeit im Pflanzenkleid eine beachtliche Veränderung hat stattfinden können.

Von derselben, Diatomeenerde enthaltenden Schichtenfolge in Karjalahdenranta (Abb. 7), von der die Diatomeen untersucht wurden, sind auch Pollenanalysen 1—16 durchgeführt worden. Die Schichtenfolge, besonders der Sand, erwies sich als besonders pollenarm. In 13 aus Sand angefertigten Präparaten fanden sich

insgesamt 13 Baumpollenkörner. Das ist auch natürlich, weil sich der grobe Sand vergleichsweise schnell abgelagert hat, vielleicht zum Teil auch unter dem Eis. Zum grössten Teil muss der Pollen aus älteren Ablagerungen stammen, u.a. aus der Diatomeenerde. Der grosse Nadelholzanteil zeigt jedoch, dass die Diatomeenerde dabei von geringerer Bedeutung ist. Die von dem Mittelsand der Schichtenfolge von Mustolanjärvi (Tab. 5) durchgeführte Analyse hat dagegen ein ziemlich gleichartiges Bild ergeben wie die dritte Gruppe der Diatomeenerdeproben. Das braucht jedoch nicht zu bedeuten, dass der Pollen der Diatomeenerde dort wirklich der Hauptteil ist, sondern der grösste Teil des Pollens kann primär sein und demnach den zur Zeit der Entstehung der Schicht herrschenden Umständen entsprechen.

Sowohl aus der Schichtenfolge von Karjalahdenranta als auch aus der von Mustolanjärvi ist ausserdem eine Pollenanalyse von dem über Sand und Diatomeenerde liegenden Bänderton sowie von der untersten Probe des darüberliegenden homogenen Tones durchgeführt worden (Tab. 5). Wie im allgemeinen, dürfte auch in diesem Falle der Anteil von Sekundärpollen beträchtlich sein, aber der grösste Teil des Pollens vertritt wohl die Pflanzendecke zur Zeit der Entstehung der Schicht. Darauf deutet der grosse Anteil von *Betula* und von Sporen hin sowie die verhältnismässig grosse NBP-Zahl. Wenn auch der Pollenbestand stark an den Pollen der dritten Gruppe der Diatomeenproben erinnert, vertritt er demnach die Pflanzendecke einer ganz verschiedenen Periode. Beachtenswert ist, dass im grossen und ganzen genommen der Anteil der Birke in der Schichtenfolge nach oben hin abnimmt, was sich vielleicht als Näherkommen der Kiefernwälder auslegen lässt.

#### ZUR CHRONOLOGISCHEN EINSTUFUNG

Um das Alter der Diatomeenerde zu bestimmen, ist versucht worden, die Entstehung der spätglazialen Ablagerungen des Gebietes und deren Altersverhältnisse zu klären. In diesem Sinne mussten ausser den Fundstellen von Diatomeenerde einige andere Aufschlüsse untersucht werden. Die Klärung der Altersverhältnisse wurde dadurch erleichtert, dass Sauramo im Geologischen Institut mehrere aus der näheren Umgebung entnommene Probserien von Bänderton hinterlegt hat, die er in seine Warvenchronologie eingearbeitet hat.

In Karjalahdenranta wurden die warvigen Tone sowohl in dem südöstlichen Teil der Grube untersucht (Karjalahdenranta I, Abb. 8), wo der Ton diskordant über dem diagonalschichtigen Sand liegt (S. 3), als auch in dem störungsfrei scheinenden Nordwestteil (Karjalahdenranta II). Ganz nahe gelegen, konnektieren sich die Tone ausserordentlich gut, und das nicht nur in bezug auf die Mächtigkeit der Warve, sondern auch auf die anderen dabei verwendeten Züge (Sauramo 1923, S. 12—13), wie die Mikrostruktur der einzelnen Warven und ihre anderen speziellen Eigenschaften. Die Konnexion zeigt, dass an dem gestörten Ostrand der Grube an dieser Stelle etwa 60 unterste Warven fehlen. Da auch die Schicht Mittelsandes unter

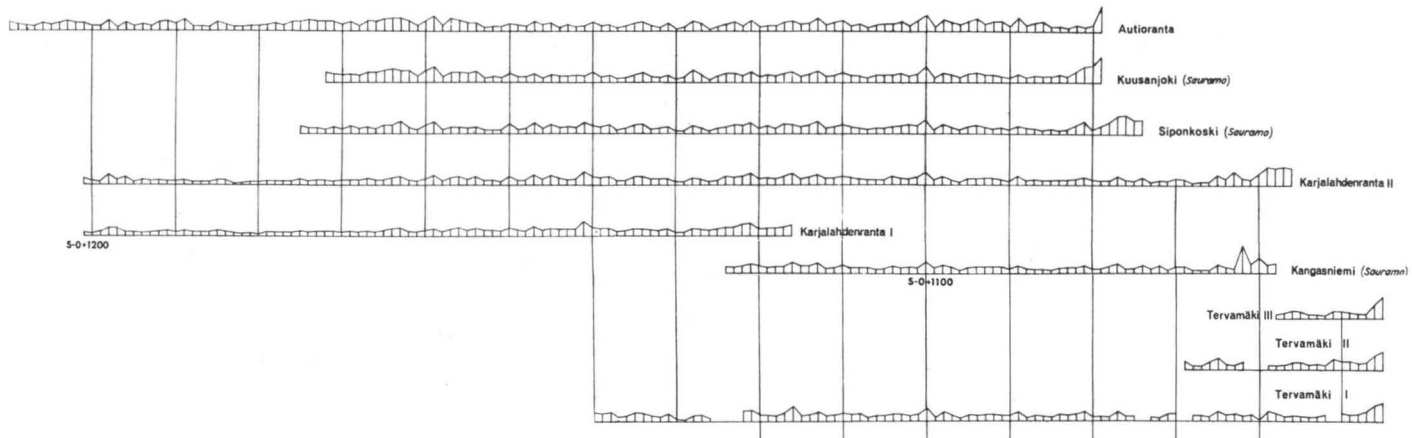


ABB. 8. Zuordnung warviger Tone. S—0 = Sauramos 0-Jahr, in dem das Eis vom zweiten Salpausselkä zurückzuweichen begann.

dem Bänderton im südöstlichen Teil der Grube fehlt und der Ton direkt an groben Sand grenzt, ist die Störung ganz beachtlich.

Der Ton von Karjalahdenranta konnektiert sich zuverlässig auch mit Diagrammen und Tonproben, die Sauramo von dem Gebiet zeigt. Die zur Konnexion verwendeten Diagramme habe ich aus darstellungstechnischen Gründen auf der Grundlage der Museumsproben und der Ursprungsbezeichnungen Sauramos neu gezeichnet. Das nächstliegende Diagramm von Sauramo liegt von Karjalahdenranta nur etwa 400 m nach Osten (Kangasniemi), die anderen Diagramme stammen aus der Gegend nordwestlich vom Kirchdorf Haapajärvi (Siponkoski, Kuusanjoki) (Sauramo 1927, S. 42, 1929, S. 42).

Bei den im Museum aufbewahrten Proben aus Kangasniemi fehlen einige untere Warven, so dass auch in den daraus angefertigten Diagrammen die ersten Jahre nach der Befreiung vom Eise fehlen. Der unterste Teil des Diagrammes II von Karjalahdenranta umfassen auch die ersten Warven.

Die Nebeneinanderstellung mit Sauramos Warvenchronologie (Sauramo 1918, 1923, 1927) zeigt, dass Karjalahdenranta etwa 1035 Jahre nach dem O-Jahr Sauramos, d.h. nach Abschluss der zweiten Salpausselkäperiode, vom Eis befreit worden ist. Die unter dem Bänderton im fluvioglazialen Sand befindliche Kieselgur ist also schon an ihrer sekundären Stelle älter.

Ausführliche Analysen des Tones im Kieselgurvorkommen Mustolanjärvi wurden als nicht notwendig erachtet, weil schon aufgrund einzelner Probestücke festgestellt werden konnte, dass die Tonwarven denen von Karjalahdenranta entsprechen.

Die warvigen Tone von Karjalahdenranta wurden auch mit den Tonserien aus einem Sandgrubenschnitt etwa 200 m nördlich von Autiorannankoski konnektiert, sowie mit Sauramos Proben aus Kuusanjoki und Siponkoski (Abb. 1 und Abb. 8). Zuunterst in der Schichtenfolge von Autioranta ist fluvioglazialer Sand und Kies. Darüber liegt an mehreren Stellen eine gut ein Meter mächtige Moränenschicht, die bedeckt wird von den bei der Konnexion verwendeten störungsfreien Tonen. Die Schichtenfolge erinnert an den von Sauramo (1927, S. 22) aus Pyhäsalmi beschriebenen Sandgrubenschnitt, wo er einen entsprechenden Vorstoss von Moräne über das Osmaterial als durch ein wahrscheinlich kurzes Vorrücken des Eises verursacht erklärt, wofür es in den Osen Finnlands reichlich Beispiele gibt. Dennoch betrachtete er die interglaziale Herkunft des unter der Moräne befindlichen Osmaterials als nicht unmöglich, welche Auslegung (oder die Auslegung als interstadial) einige andere Geologen für die entsprechenden Bildungen in Finnland als wahrscheinlicher betrachten (Mölder 1949, Aurola 1949).

Das Vorkommen von fluvioglazialen Material in Autioranta erinnert auch in der Hinsicht an die Vorkommen von Karjalahdenranta, Mustola und Varis, dass es sich landschaftlich nicht aus dem ganz ebenen Gelände abhebt. Kieselgur hat sich trotz Nachforschungen darin nicht gefunden.

Die Konnexion des über der Moräne liegenden Tones sowohl mit den Probenserien Sauramos als auch mit den Tönen von Karjalahdenranta hat mit Sicherheit durchgeführt werden können. Nur eine Warve sowohl in den Proben von Autioranta als auch in denen Sauramos aus Kuusanjoki weicht in ihrer relativen Mächtigkeit von den anderen Probenserien ab. Die Warve 0 + 1 140 bildet darin eine kleine Spitze, während die entsprechende Spitze in den weiter südlich befindlichen Proben bei Warve 0 + 1 141 liegt. Aufgrund der anderen in diesen Warven vorkommenden Eigenschaften müssen sie jedoch in der vom Diagramm gezeigten Weise konnektiert werden. Die Schwankungen der Dicke sind auch garnicht immer so konstant wie viele andere kennzeichnende Züge der einzelnen Warven (Sauramo 1923, S. 11—12).

Die untersten groben Warven von Autioranta haben sich offensichtlich recht bald nach dem Eisrückgang gebildet und sie zeigen zusammen mit den Probenserien von Sauramo, dass die Ablagerung hier deutlich später als in Karjalahdenranta und Kangasniemi begonnen hat (*ibid.* S. 41).

Die Sandgrube von Tervämäki liegt etwa 1.5 km westlich der Varis'schen Grube, in einer Höhe von etwa 110 m. In ihrer Form und teilweise auch in ihrer Struktur unterscheidet sich das Objekt von den früheren, indem es sich, wenn auch sanft ansteigend, über seine Umgebung erhebt. Wie auch in Autioranta, liegt über den fluvioglazialen Sandschichten zum grossen Teil eine Moränendecke, an mehreren Stellen sogar zwei gesonderte Moränendecken. Deren untere ist fest gepackt, oft gefaltete Stauchmoräne. Die obere hat eine waagerechte Lamellenstruktur. Abb. 9 zeigt die Struktur des Südrandes der Grube im Herbst 1964. Das von Westen vorstossende Eis hat einen ganzen Osteil (ganz rechts im Bild) verschoben und den Südostteil des Oses gefaltet. Ein Teil des Osmaterials hat sich mit dem Moränenmaterial vermischt, ein Teil erscheint in der Moräne in Form von Klumpen, wie auch die da und dort vorkommenden 10—20 Warven umfassenden Bändertonklumpen. Im südöstlichen Teil schiebt sich (ganz links im Bild) ein hauptsächlich aus Osmaterial gebildeter Keil zwischen das Moränenmaterial. Der als Ganzes verschobene Osteil und die als Klumpen auftretenden Stücke des Osmaterials waren offensichtlich während des Vorstosses tief gefroren.

Im Sommer 1965, als dieselbe Sandgrube einer genaueren Prüfung unterzogen wurde, war die Falte durch die Entnahme von Kies und Sand zerstört, aber an den Rändern der Grube liess sich noch warviger Ton unter der Moräne feststellen. In den grössten unbeschädigt erhaltenen Klumpen von Bänderton konnte man sogar über 120 Warven zählen, von denen allerdings ein Teil gestört war. Es handelt sich also um einen recht beachtlichen Eisvorstoss nach einem langen Zwischenraum.

Für die Konnektierung des Bändertones wurden drei Proben genommen (Abb. 8. Tervämäki I, II und III). Das Material in den Klumpen war brüchig, so dass es nicht immer möglich war, die Proben so zu nehmen, dass sie an ihren Enden teilweise einander decken. Da an den Enden der Proben sich leicht die äussersten Warven lösten, blieben in einzelnen Fällen zwischen den Proben kleine Lücken. Von den

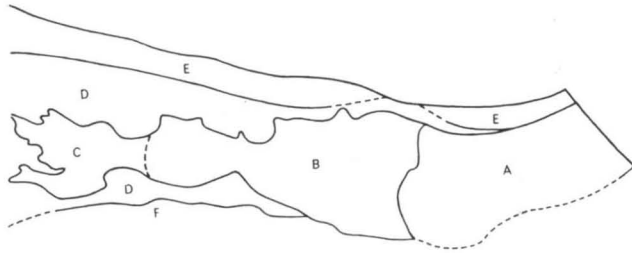
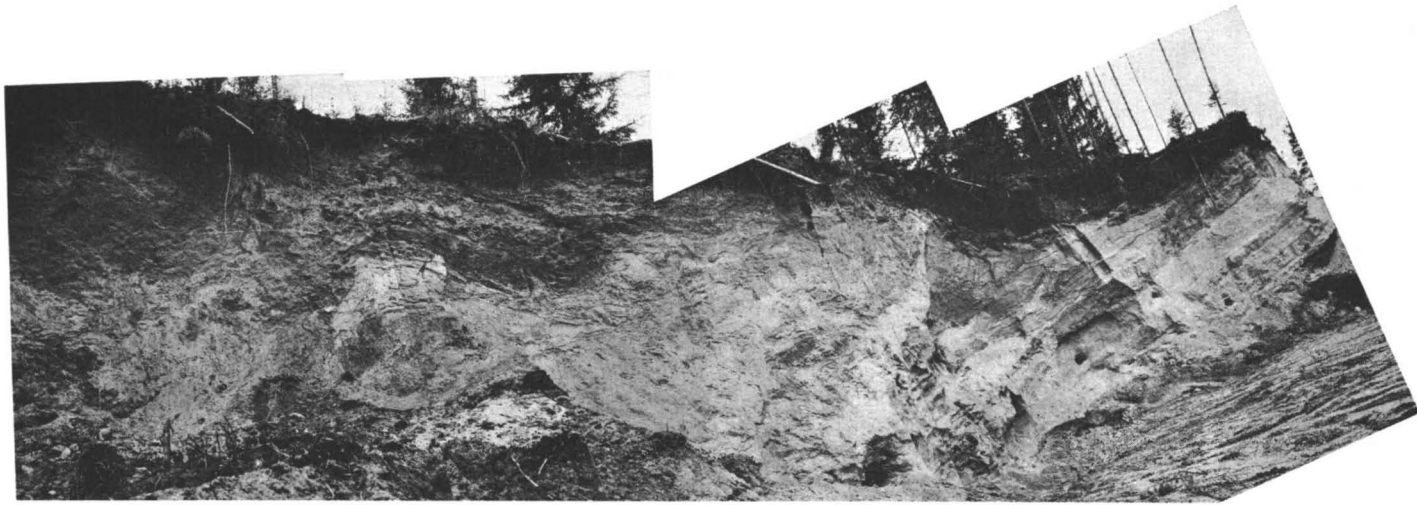


ABB. 9. Stauchmoräne in Tervämäki. A. Als Ganzes verschobener Teil eines Oses. B. Gefaltetes und vermishtes Osmaterial, mit Stücken von Bänder-ton, C. Sortiertes Material vermischt mit Moräne, D. Faltige Moräne, E. Deckmoräne, F. Herabgerutschter Schutt.

jüngsten, an die Moräne angrenzenden Teil des Tones konnte keine Analyse gemacht werden, weil dort reichlich Brüche und Faltungen erfolgt waren.

Die unter der Moräne liegende lange Serie von warvigem Ton (Tervämäki 1) konnektiert sich ausgezeichnet sowohl mit den etwa 1 km entfernten Bändertonen von Karjalahdenranta als auch mit den Proben Sauramos aus Kangasniemi. Auch alle kleinen kennzeichnenden Züge der einzelnen Warven stimmen mit den entsprechenden Zügen der anderen Probenserien überein.

Da sich in den jüngsten, in die Moräne übergehenden Teilen eines in die Analyse einbezogenen Tonklumpen ausser den im Diagramm dargestellten noch wenigstens 30 unbestimmte Warven zählen liessen, würde deren jüngste Warve wenigstens dem Jahre 0 + 1 170 in Sauramos Chronologie entsprechen. Damals hatte sich das Eis nach Sauramo (1927, S. 37) schon nordwestlich vom Kirchdorf Nivala zurückgezogen, von wo es also nocheinmal zurückgestossen war.

Das beobachtete Vorrücken des Eisrandes hat trotz seiner grossen Ausdehnung überraschend wenig Spuren in den Schichtenfolgen des Gebietes hinterlassen. In den von Sauramo untersuchten warvigen Tönen nordwestlich von Tervämäki sieht man es nicht, auch nicht in dem vom Verfasser geprüften Teil der Schichtenfolge von Autioranta, wo man jedoch eine andere, ältere Vorrückungsphase des Inlandeises erkennt. In Karjalahdenranta hat der Vorstoss des Eises Spuren in der Schichtenfolge nur in den östlichen und südöstlichen Teilen der Sandgrube hinterlassen (S. 3) (Karjalahdenranta 1).

Die verhältnismässig begrenzte Wirkung des Eisvorstosses dürfte sich daraus erklären, dass der Eisrand in der fraglichen Zeit schon ziemlich dünn war und ausserdem wahrscheinlich noch zum Teil von tiefem Wasser getragen. In den tiefsten Teilen des Geländes hat das Eis den Grund vielleicht garnicht berührt. In der Ebene schob sich das Eis über das Gebiet, ohne nennenswerte Störungen zu verursachen, aber als es auf das höhere Hindernis in Tervämäki traf, verursachte es eine starke Stauchung der Schichten. Die Richtung der Faltung scheint ausserdem darauf hinzuweisen, dass der Vorstoss des Eises in dieser Phase aus Westen<sup>1)</sup> gekommen ist, wo das Gelände höher ist als im Nordwesten in Richtung des Flusstales. Eine Richtungsanalyse der Moräne ist jedoch zunächst noch nicht durchgeführt worden. Es scheint auf jeden Fall eigenartig, dass die besagte Vorrückungsphase keine deutlichen Spuren in den Warven der Bändertone in der Umgebung hinterlassen hat.

Nach Sauramos Warvenchronologie hat sich das Eis aus diesem Gebiet etwa im Jahre 0 + 1 050 (1927, S. 46) zurückgezogen. In die gleiche Chronologie eingeordnet, hat das festgestellte vorübergehende Vorrücken des Eises wie oben erwähnt nach dem Jahre 0 + 1 170 stattgefunden, wonach erst das Eis endgültig aus dem Gebiet zurückwich.

<sup>1)</sup> Die in demselben Gebiet von Hyypä (1948) und Okko (1949) festgestellte starke westliche Bewegungsrichtung dürfte eine längere Periode vertreten und ist wohl nicht gleichen Alters wie die gleichgerichtete Stauchung von Tervämäki.

Und wie steht es mit der Möglichkeit, den unter der Moräne befindlichen warvigen Ton als interglazial oder interstadial zu erklären? Dann wäre offensichtlich Sauramos ganze Serie P (ibid. S. 45) roter Tone aus West-Finnland interglazial oder interstadial, weil deren innere Konnexion, wenigstens was die verwendeten Teile betrifft, als ausserordentlich sorgfältig und zuverlässig durchgeführt gelten muss. Das scheint nicht möglich, insbesondere weil diese Serie an mehreren Stellen auch mit Binnenfinnland konnektiert ist, und Störungen in den Schichtenfolgen nicht beobachtet worden sind (u.a. Sauramo 1927, S. 23). Da nun aber in Sauramos Chronologie die im Untersuchungsgebiet festgestellte recht bedeutende Eisvorstossphase fehlt, zeigt das, dass die besagte Chronologie noch viel durch örtliche Detailforschung vorzunehmende Nachprüfung verlangt.

Dagegen ist es wahrscheinlich, dass ein Teil des anderen Materials der Stauchmoräne von Tervamäki aus der vorangegangenen Vereisungsperiode vor der letzten bedeutenden Interstadial- oder Interglazialzeit stammt. Die rechts in Abb. 9 (S. 22) zu sehende Schichtenfolge hat sich als Ganzes nur in tief gefrorenem Zustand verschieben können. Wenn sie sich erst um das Jahr 0 + 1 050 im Wasser vor dem Eis abgelagert hätte, hätte sie kaum, von tiefem Wasser bedeckt, vor dem erneuten Vorrücken des Inlandeises gründlich frieren können. Wenn sie dagegen vor der letzten Vereisung entstanden war, hat sie beim Vorrücken des Eises schon gefroren sein können.

Die Kieselgur ist in Sauramos Chronologie um 0 + 1 050 in ihre heutige Lage gekommen. Wenn nach E. Nilsson (1964) Sauramos 0-Jahr dem Jahr 10 378 v.h. entspricht, wäre die sekundäre Ablagerung der Kieselgur etwa im Jahre 9 300 v.h. erfolgt. Die primäre Ablagerung der Kieselgur ist davor geschehen.

Es erhebt sich die Frage, wann vor diesem Zeitpunkt die Umstände für die Bildung von Kieselgur geeignet waren? Da die Kieselgur ganz rein ist, war die Voraussetzung ihrer Ablagerung das Fehlen des Inlandeises in der betreffenden Zeit. Aus dem Umfang des Gebiets mit heutigen sekundären Kieselgurvorkommen und aus der Häufigkeit von Kieselgur zu schliessen, ist das Primärvorkommen gross gewesen, was wiederum eine lange Bildungszeit voraussetzt. Die Zeit war lang genug für die in den Ablagerungsumständen erfolgten Änderungen, die durch die in einzelnen Kieselgurkörnern vorhandenen verschiedenen Mikrofossilien veranschaulicht werden. Aus dem Obigen geht hervor, dass sich die Kieselgur an ihrer primären Stelle entweder in der Interstadial- oder Interglazialzeit abgelagert haben muss.

In Finnland sind zahlreiche unter Moränen gelegene Wassersedimente bekannt, unter Osmaterial liegender Ton oder übereinander liegende Moränendecken, die nach der Ansicht einiger Forscher entweder die Interstadial- oder die Interglazialzeit ausdrücken (u.a. Brander 1937 a, b, 1938, 1941; Mölder 1949; Aurola 1949; Kauranne-Tynni 1961). Nicht alle haben jedoch deren Zuweisung als unbestritten betrachtet. So lässt sich nach Hyypä (1937, 1939) nicht mit Sicherheit feststellen, dass die in Südostfinnland gefundenen, inmitten des Osmaterials auftretenden Tonstücke die

Interglazial- oder Interstadialzeit vertreten. Als unbestrittener Interglazial- oder Interstadialfund muss jedoch der von Korpela entdeckte, unter Moräne liegende Torf betrachtet werden, für den sich bei der  $C^{14}$  Bestimmung ein Alter von über 35 000 Jahren ergab (Korpela 1962, a, b).

Korpelas Fund enthält eine gleichartige Pollenflora wie die Kieselgur von Haapajärvi, und es ist möglich, dass die beiden von derselben Phase stammen.

Wegen seiner Lage verdient in diesem Zusammenhang auch der von Okko (1953) veröffentlichte Fund eines Mammutzahnes in dem Oszug von Pitkäkangas Beachtung, nur etwa 4 km südöstlich der Varis'schen Sandgrube. Der den Zahn umgebende Sand hatte sich dort in salzigem Wasser abgelagert, wie wahrscheinlich auch die von mir untersuchten Kieselgurkörner an ihrer sekundären Stelle (S. 15). Auch in der Pollenflora entspricht er den Ablagerungsorten meiner Funde. Es wäre demnach natürlich, dass diese auch in ihrer Lage gleichartigen Funde aus der gleichen Periode stammen.

In verschiedenen Teilen Schwedens, auch ziemlich nahe Haapajärvi, sind mehrere offensichtlich zur gleichen eisfreien Phase gehörenden Funde gemacht worden: (Grip 1949; J. Lundqvist 1955, 1958; Fromm 1960; G. Lundqvist 1951, 1955, 1957, 1960; Munthe 1890, 1904, 1946; Sandegren 1948; Asklund 1936; Kulling 1945; Thorslund 1939; Halden 1915; von Post 1918). Diese hat G. Lundqvist in Zusammenhang mit seinem Fund von Porsi besprochen (1960).

Alle diese Funde, sowie die von Haapajärvi und Rovaniemi, vertreten in ihrer Pollenflora eine ziemlich kalte Periode, aber in vielen anderen Hinsichten sind sie verschieden (G. Lundqvist 1960 S. 21). Sie scheinen zu verschiedenen Phasen des *Balticums* gehören. Die Süßwasserphase mit einem niedrigen Wasserstand vertritt der von Munthe (1890) dargestellte Fund, die Binnenseephase hohen Wassers die Kieselgur von Haapajärvi und die Phase hohen salzigen Wassers der Fund von Bollnäs (?) (Erikson 1912, Halden 1915). Wenn nun die genannten Funde wirklich zu verschiedenen Teilen der gleichen grösseren Periode gehören, was anzunehmen ist, muss diese ziemlich lang gewesen sein. Dafür sprechen auch, wie oben erwähnt, der offensichtlich grosse Umfang des ursprünglichen Kieselgurvorkommens und die Verschiedenheiten in seinem Mikrofossilienbestande.

Die Zuordnung der Funde zu den der letzten Vereisung vorangegangenen aus Europa bekannten eisfreien Perioden ist schwierig, weil von den Funden nur das Minimal-Alter bekannt ist. Vor allem kämen bei der Zuordnung die Göttweiger-Interstadialzeit oder die Eem-Interglazialzeit in Frage. Das genaue Alter dieser Phasen mit ihrer Dauer ist jedoch auch in Mitteleuropa noch unsicher (G. Lundqvist 1960, S. 22), ebenso wie zumindest der Charakter des Göttweigers, was die Zuordnung erschwert.

Inbezug auf ihre Länge würde die Periode anscheinend besser zum Eem passen, aber dagegen spricht, dass das Eem nach der herrschenden Ansicht wärmer ist als die heutige Zeit, während in Fennoskandien nur aus kühlen Phasen stammende Vorkommen begegnen. Allerdings könnte der als Sekundärpollen allgemein in alten

Sedimenten erscheinende Eichenmischwald (Iversen 1936; Heinonen 1957) einen Teil der untersuchten Phase vertreten, der wärmer als unsere Zeit war.

Die Phase lässt sich auch schwerlich als irgendeine bekannte Interstadialzeit betrachten. Die zeitlich lange Ausdehnung der Götterzeit so weit in den Norden scheint fraglich. Die Zuordnungsfrage muss also als noch offen betrachtet werden. Einige Forscher sind jedoch geneigt, diese Ablagerungen dem Eem zuzusprechen.

Ob die betrachteten Vorkommen als interglaziale oder als interstadiale Bildungen zu betrachten sind, hängt in erster Linie von der Definition dieser Begriffe ab. Wenn eine als interglazial anerkannte Phase mindestens so warm wie heute sein muss, was häufig als Kriterium gilt, lässt sich die betrachtete Phase aufgrund der bisher gefundenen Vorkommen nicht als interglazial bezeichnen (vgl. Hyypä 1937, 1939).

U.a. G. Lundqvist (1960, S. 22) hat jedoch den Interglazialbegriff auf alle die Perioden ausdehnen wollen, in denen das Inlandeis nachweisbar auch aus den zentralsten Teilen des Vereisungsgebietes verschwunden war. In Finnland tritt Okko ebenfalls für eine weniger enge Definition ein (1964, S. 251), was auch meiner Ansicht nach als konsequenter und richtiger zu betrachten ist. Man lässt die postglaziale Zeit spätestens mit dem Zeitpunkt beginnen, zu dem die Zweiteilung des letzten Restes von Inlandeis in dem Fjeldgebiet Fennoskandiens erfolgte oder, wie heute im allgemeinen, mit dem Ende der zweiten Salpausselkä-Phase. Dann muss ein ebenso grosses Abnehmen des Inlandeises und das entsprechende Klima auch für den Beginn der Interglazialzeit ausreichen, vorausgesetzt, dass es eine längere Phase vertritt.

*Manuskript eingegangen am 15. September, 1965*

## SCHRIFTENVERZEICHNIS

- ASKLUND, BROR (1936), Frösöns submoräna avlagringar. Preliminärt meddelande. Sveriges geol. unders. C 402.
- AUROLA, ERKKI (1949), Über die Verbreitung submoräner Sedimente als Widerspiegelung der Bewegung des Inlandeises. Bull. Comm. géol. Finlande 144.
- BRANDER, GUNNAR (1937 a), Ein Interglazialfund bei Rouhiala in Südostfinnland. Bull. Comm. géol. Finlande 118.
- »— (1937 b), Zur Deutung der intramoränen Tonablagerung an der Mga, unweit von Leningrad. Bull. Comm. géol. Finlande 119.
- »— (1938), Entgegnung auf Dr. E. Hyyppäs Kritik meiner Abhandlung: Ein Interglazialfund bei Rouhiala in Südostfinnland. Bull. Comm. géol. Finlande 123.
- »— (1941), Neue Beiträge zur Kenntnis der interglazialen Bildungen in Finnland. Bull. Comm. géol. Finlande 128.
- CLEVE-EULER, ASTRID (1912), Das Bacillariaceen-Plankton in Gewässern bei Stockholm II; Zur Morphologie und Biologie einer pleomorphen Melosira. Arch. f. Hydrobiol. u. Planktonkunde Bd. VII.
- ERIKSON, BERTIL (1912), En submorän fossilförande aflagring vid Bollnäs i Hälsingeland. Geol. Fören. Förh. 34.
- FROMM, ERIK (1960), An interglacial peat at Ale near Luleå, northern Sweden. Sveriges geol. unders. C 574.
- GRIP, E. (1949), Ett fynd av submoräna, växtförande avlagringar vid Boliden. Geol. Fören. Förh. 71.
- HALDEN, BERTIL (ERIKSON) (1915), Det interglaciala Bollnäsfyndets stratigrafi. Geol. Fören. Förh. 37.
- HEINONEN, LEO (1957), Studies on the Microfossils in the Tills of the North European Glaciation. Ann. Acad. Sci. Fennicae A, 52.
- HYYPÄ, ESA (1937), Bemerkungen über Branders Aufsatz »Ein Interglazialfund bei Rouhiala in Südostfinnland», und zwei neue Tonfunde auf der karelischen Landenge. Bull. Comm. géol. Finlande 119.
- »— (1939), Bemerkungen über Dr. Branders Entgegnung auf meine Kritik über seine Abhandlung »Ein Interglazialfund bei Rouhiala in Südostfinnland». Bull. Comm. géol. Finlande 119.
- »— (1948), Tracing the source of the pyrite stones from Vihanti on the basis of glacial geology. Bull. Comm. géol. Finlande 142.
- ILLIES, HENNING (1949), Die Schrägschichtung in fluviatilen und litoralen Sedimenten, ihre Ursachen, Messung und Auswertung. Mitt. Geol. Staatsinst. Hamburg 19.
- IVERSEN, JOHS. (1936), Sekundäres Pollen als Fehlerquelle. Danmarks geol. Unders. 4. Raekke 2,15.
- KAURANNE, K. und TYNNI, R. (1961), Malmipitoisen moreenikonglomeraatin ja moreenin ikäsuhteista siitepölyanalyysin ja geologisten rinnakkaistutkimusten valossa. Geotekn. julk. 66.
- KORPELA, KAUKO (1962 a), Interglasiaalista turvetta Rovaniemen seudulta. Edeltävä tiedonanto. Geologi 2.
- »— (1962 b), Voimalaitospaikkojen geologiset tutkimukset sekä niissä saavutettuja kvartääri- ja insinöörigeologisia tuloksia. Manuskript im Geol. Inst., Univ. Helsinki.
- KULLING, OSKAR (1945), Om fynd av mammoth vid Pilgrimstad i Jämtland. Sveriges geol. unders. C 743.

- LUNDQVIST, G. (1948), Blockens orientering i olika jordarter. Sveriges geol. unders. C 497.
- »— (1951), Beskrivning till Jordartskarta över Kopparbergs län. Sveriges geol. unders. Ca 21.
- »— (1955), Stocke i Öje. Ett säkert interglacialfynd. Geol. Fören. Förh. 77.
- »— (1957), C<sup>14</sup>-analyser i svensk kvartärgeologi. 1955—57. Sveriges geol. unders. C 557.
- »— (1960), The interglacial ooze at Pors i Lapland. Sveriges geol. unders. 575.
- LUNDQVIST, J. (1955), Interglacialfyndet vid Boliden. Geol. Fören. Förh. 77.
- »— (1958), Beskrivning till Jordartskarta över Värmlands län. Sveriges geol. unders. Ca 38.
- MUNTHE, H. (1890), Sedimentära fossilförande bildningar öfverlagrade av morän. Geol. Fören. Förh. 12.
- »— (1904), Om den submoräna Hernögyttjan och dess ålder. Geol. Fören. Förh. 26.
- »— (1946), Nya bidrag till kännedomen om Härnögyttjan. Sveriges geol. unders. C 481.
- MÖLDER, KARL (1949), Wassersedimente unter der Moräne in Süd-Pohjanmaa. Bull. Comm. géol. Finlande 144.
- NILSSON, ERIK (1964), Geochronological Investigations in Southern Sweden. Geol. Fören. Förh. 86.
- OKKO, VEIKKO (1949), Suomen geologinen yleiskartta. Lehti B 4, Kokkola. Maalajikartan selitys. Geologinen tutkimuslaitos.
- »— (1953), Haapajärven mammuttilöytö. Geologi 2.
- »— (1964), Maaperä. Rankama, K., Suomen geologia. Helsinki.
- VON POST (1918), Ett finiglacialt granfynd i Södra Värmland. Geol. Fören. Förh. 40.
- SANDEGREN, R. (1948), Interglacialfyndet i Långsele av N. Sundius och R. Sandegren med bidrag av T. Lagerberg, C. Lindroth och H. Persson. Sveriges geol. unders. C 495.
- SAURAMO, MATTI (1918), Geochronologische Studien über die spätglaziale Zeit in Südfinnland. Bull. Comm. géol. Finlande 50.
- »— (1923), Studies on the Quaternary Varve Sediments in Southern Finland. Bull. Comm. géol. Finlande 60.
- »— (1927), Suomen geologinen yleiskartta. Lehti C 4, Kajaani. Maalajikartan selitys. Suom. geol. toimik.
- »— (1929), The Quaternary Geology of Finland. Bull. Comm. géol. Finlande 86.
- SHROCK, ROBERT (1948), Sequence in layered rocks. New York.
- THORSLUND, PER (1939), Kvartärgeologiska iakttagelser inom östra Storsjöområdet i Jämtland. Sveriges geol. unders. C 429.
- VOIGT, ERHARD (1949), Die Anwendung der Lackfilm-Methode bei der Bergung geologischer und bodenkundlicher Profile. Mitt. Geol. Staatsinst. Hamburg 19.

## POLYGONAL GROWTH OF BERYL

BY

TH. G. SAHAMA

*University of Helsinki, Finland*

### ABSTRACT

A number of beryl crystals from different localities were studied under the polarizing microscope. Plates cut perpendicular to the  $c$ -axes of the crystals were used. The thickness of the plates ranged from 0.3 to ca. 5 mm.

The optical properties of beryl are often anomalous resulting in a small optic axial angle up to  $2V_a = \text{ca. } 20^\circ$ . Between crossed nicols the optically anomalous crystals exhibit a variety of crystallization textures that are described. A summary is schematically presented in Fig. 1. The growth hillocks found on crystal faces are illustrated. The crystallization textures are interpreted as originating from strain in the crystal that varies during the crystal growth.

### INTRODUCTION

Anomalous optical behavior resulting in a small optic axial angle is a very common phenomenon in many tetragonal, trigonal and hexagonal minerals. In beryl the biaxial optics is so common that such an anomaly can be regarded for the mineral a characteristic rule rather than an occasional exception. This is true especially for clear beryl crystals usually grown in more or less open wugs and often showing well developed crystal forms.

The optical anomaly found in beryl is known for the mineral since more than a hundred years. A good summary of the oldest literature is contained in 'Handbuch der Mineralogie' by Carl Hintze (2 Band, II, pp. 1274—1275, 1897). Later, following the views first expressed by E. Mallard in 1877 (Hintze, *op. cit.*), the biaxial optics and the polygonal texture microscopically found in sections perpendicular to the  $c$ -axis has been regarded as twinning much in the same way as is known for the structurally related low-cordierite (*cf.* A. N. Winchell and H. Winchell, 'Elements of Optical Mineralogy' and W. A. Deer, R. A. Howie and J. Zussman, 'Rock-Forming Minerals').

Because no recent general descriptions of the polygonal texture of beryl are available and because the interpretation of the optical anomalies found in the mineral seems to need reconsideration, some beryl crystals from various localities were studied with respect to their optical anomaly. The results of the study will be presented in this paper. A summary on the subject was presented in the fourth session of the International Mineralogical Association held in New Delhi in 1964 and a short abstract will be published in the papers of that session.

### BIAXIAL OPTICS FOUND IN BERYL

Optically uniaxial beryl is normally negative,  $\varepsilon$  being parallel to the crystallographic  $c$ -axis. In the notation of the anomalous biaxial optics the  $\alpha$ -direction is parallel to the  $c$ -axis of the crystal and the negative optic axial angle  $2V_\alpha$  ranges from  $0^\circ$  up to  $18^\circ$ — $20^\circ$ . In the beryl crystals studied by the author no deviation of the  $\alpha$ -direction from that of the crystallographic  $c$ -axis can be detected.

The optic axial angle in beryl is most conveniently measured from the interference figure on plates cut perpendicular to the  $c$ -axis. The plates must be polished on both sides and the crystals should preferably be free from inclusions. The measurements were made using the relationship  $\sin V = d/2nk$ , where  $d$  is the distance between the traces of the two optic axes in the interference figure expressed in readings of the micrometer eye piece,  $n$  is the approximate mean refractive index of beryl, and  $k$  is the Mallard constant to be separately determined with the apertometer for the microscope optics used.

If the beryl plate is thin, of the thickness of an ordinary thin section, the isogyres in the interference figure are broad and the small optic axial angle can not be measured, mostly not even qualitatively detected. If, however, the plate was left thick on grinding, then the isogyres are sharp. Even very small optic axial angles can be measured. As an example it may be mentioned that an optic axial angle of only  $2^\circ$  can easily be measured on a plate of, say, ca. 5 mm thick. On a thin plate such a crystal would look optically uniaxial.

The biaxial optics exhibited by the beryl plate results in the fact that the plate perpendicular to the  $c$ -axis shows a very weak interference color between crossed nicols. Assuming a maximum value found for the optic axial angle, *viz.*  $2V_\alpha = 20^\circ$ , the birefringence ( $\gamma - \beta$ ) shown by the plate of an optically anomalous crystal is calculated to amount to the order of 0.0002. This value, of course, represents a maximum. Mostly, the optic axial angle is considerably less than  $20^\circ$  and, accordingly, the value for ( $\gamma - \beta$ ) is well below the maximum mentioned, for example of the order of 0.000 05. Such a small birefringence can be detected only on thick plates. In practice, the beryl plates cut perpendicular to the  $c$ -axis and used in this study ranged in thickness from a few tenths of a millimeter to one millimeter or even more. The interference color produced is first order grey with varying brightness depending on the magnitude of  $2V_\alpha$ .

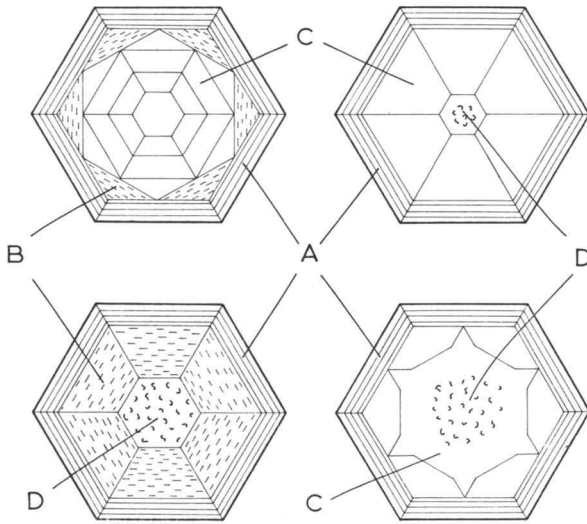


FIG. 1. Schematic summary of the crystallization textures found in beryl. A. Laminated margin. B. Lamellar intermediate zone. C. Polygonal intermediate zone. D. Irregular core pattern.

### CRYSTALLIZATION TEXTURE

The crystallization textures of beryl crystals are best studied on plates of sufficient thickness that have been cut perpendicular to the *c*-axis. Seen under the microscope between crossed nicols such a beryl plate rarely looks homogeneous. A schematical summary of the textures is presented in Fig. 1 and the nomenclature used to characterize the various zones of a crystal is given in the explanation of that figure. The four types of texture reproduced are idealized and the true pattern to be found in a particular beryl crystal can represent any combination of these types. Any of the zones marked *A—D* may be lacking.

Examples of actual textures found in the beryl crystals are illustrated in Plates I a—d and Plates II a—d. All the photographs contained in these two plates represent gemmy Brazilian crystals. The same kinds of textures have been found also in beryl crystals from other localities studied, including Nigeria, Mozambique, Southern Rhodesia etc.

Plate Ia illustrates a beryl plate consisting of regular polygons the boundaries of which are parallel to the traces of  $10\bar{1}0$  or  $11\bar{2}0$ . The texture exhibited represents a good example of what is called the 'polygonal texture' proper in this paper.

Quite often, however, no regular polygonal texture proper is seen but the entire crystal shows an irregularly extinguishing pattern illustrated in Plate I b and, photographed with higher power, in Plate Ic. Because this kind of texture, evidently a

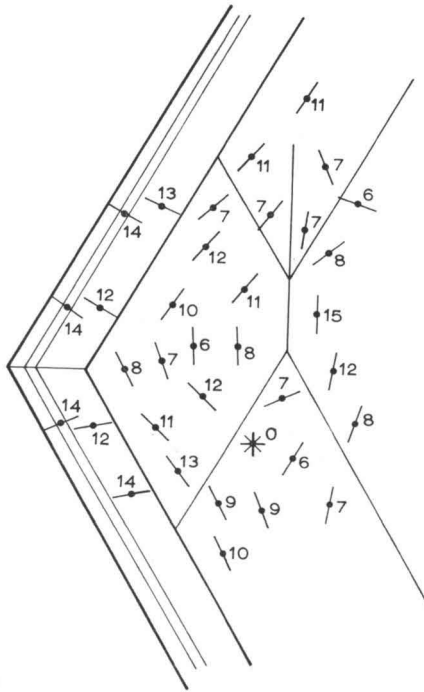


FIG. 2. Traces of optic axial planes and values for optic axial angles in a part of the crystal of Plate IIc.

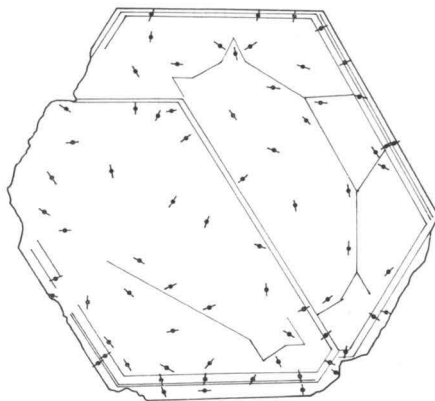


FIG. 3. Overall view of the traces of the optic axial planes in the composite crystal of Plate IIc.

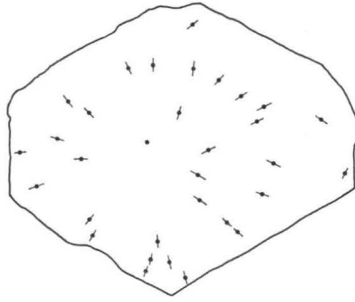


FIG. 4. Radial arrangement of the traces of the optic axial planes in a crystal.

strain pattern, occupies in many crystals only the core, it will be called the 'irregular core pattern'. As is schematically indicated in Fig. 1 (bottom left), the irregular core pattern may show hexagonal outlines and be surrounded by a 'lamellar intermediate zone' with six-sided hexagonal lamination (Plate I d). A detail of the lamination is illustrated in Plate II a and looks like plagioclase twinning. Single lamellae of the intermediate lamellar zone are not persistent throughout one of the six sectors. They extend only over a short distance and then they die out. Many crystals like that of Plate II b show an outermost 'laminated margin' in which single lamellae extend over the whole sector and the marginal texture looks like that of a polysynthetic twinning.

Plate II c presents another kind of crystallization texture schematically summarized in bottom right of Fig. 1. The core of the crystal, actually a composite of two individuals in parallel growth, shows the irregular strain pattern and the margin is very regularly laminated. The intermediate zone, between the core and the margin, exhibits a curious star-like polygonal texture with the sharp points of the stars perpendicular to the traces of the prism faces. A detail of such a star point is seen in Plate II d.

The extinction is more or less wavy in all parts of a beryl plate and the value to be found for  $2V_a$  varies considerably from one spot to another even inside one single polygon. Fig. 2 gives the traces of the optic axial planes and the values for the optic axial angles in a corner of the crystal of Plate II c. Fig. 3 gives an overall view of the traces of the optic axial planes in the same composite crystal. In the laminated margin of this composite crystal the optic axial planes tend to be mostly roughly perpendicular to the prism face, but exceptions to this rule will be found on some spots. The optic axial planes are irregular in the inside of the crystal. Fig. 4 illustrates the traces of the optic axial planes in another crystal. In this case, the optic axial planes are roughly radial.

The wavy extinction makes it understandable that the extinction directions on both sides of a polygonal boundary are not symmetrical with respect to that boundary.

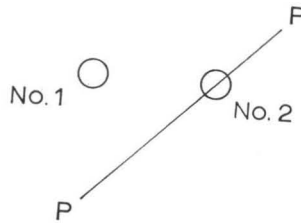


FIG. 5. P-P polygonal boundary.  
Nos 1 and 2 circular areas to be drilled out by diamond drill.

This statement holds true both for the boundaries in the polygonal intermediate zone (*C* in Fig. 1) and for the lamellar boundaries in the marginal parts of the crystal (*A* and *B* in Fig. 1). All boundaries will, however, disappear when turned in a position parallel to one of the nicols. The extinction directions and, on the other hand, the optical retardations are such that both sides of the boundary exhibit equal brightness in the interference color in that position. The contrast in interference color between both sides of the boundary is strongest when the boundary is in a diagonal position.

It can easily be demonstrated that the anomalous optical retardation produced by the beryl plate is caused by strain in the crystal. Fig. 5 illustrates the procedure. The line *P—P* represents a boundary in any of the zones *A*, *B*, or *C* in Fig. 1. With a diamond marker inserted in the microscope in place of the objective, a circle is marked inside a polygon (circle No. 1 in Fig. 5) or so that it crosses the boundary (circle No. 2 in Fig. 5). With a dental diamond drill illustrated in Fig. 6 the two circled areas of the beryl plate are drilled out. To prevent the beryl plate from breaking during drilling, the plate must be mounted on glass with Canada balsam and the drilling operation, with an ordinary drill press, must be made under water. Under the microscope the small circular area No. 1, after having been drilled out, looks entirely black between crossed nicols and gives an interference figure of a strictly uniaxial crystal. Evidently, the drilling out of the small circular plate means liberating it from the strain existing in the crystal. The optical anomaly thus disappears and the optical symmetry becomes normal for the hexagonal unstrained crystal. After drilling the plate No. 2 is also black between crossed nicols except in a very narrow zone on both sides of the boundary where it still remains weakly biaxial. The boundary represents a surface of discontinuity in the strain that can not entirely disappear on releasing the external strain. It seems that the polygonal boundary just represents a plane along which the strain distortions of both polygons coincide, the boundary thus being analogous to the plane of an epitaxial overgrowth.

The easy with which strain may open up the optic axial angle in beryl can be demonstrated under the microscope in the way described in detail by Bücking\*.

\* H. Bücking, Ueber den Einfluss eines messbaren Druckes auf doppeltbrechende Mineralien. *Zeitschr. f. Kryst.*, VII, p. 555, 1883.

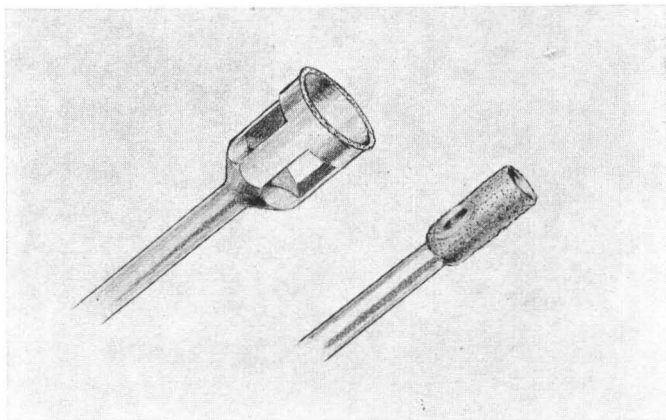


FIG. 6. Dental diamond drill. Drawn by Toini Mikkola.

When pressed in a direction perpendicular to the  $c$ -axis the optically uniaxial negative beryl plate develops an optic axial angle. On increasing pressure the optic axial plane starts rotating and tends to become perpendicular to the pressure direction. After releasing the pressure the interference figure returns back to the original.

The polygonal boundaries that produce the textures summarized in Fig. 1 are often quite sharp and evidently are parallel to the  $c$ -axis of the crystal. In many cases, however, the boundaries are more or less diffuse indicating that they are in an inclined position, not perpendicular to the beryl plate. In plates of considerable thickness, like those used in this study, the inclined position is easy to verify. All the observations

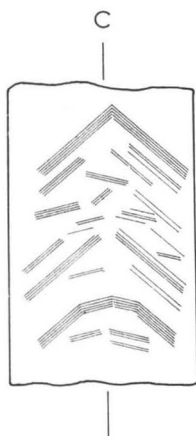


FIG. 7. Polygonal boundaries on a beryl plate parallel to the  $c$ -axis.

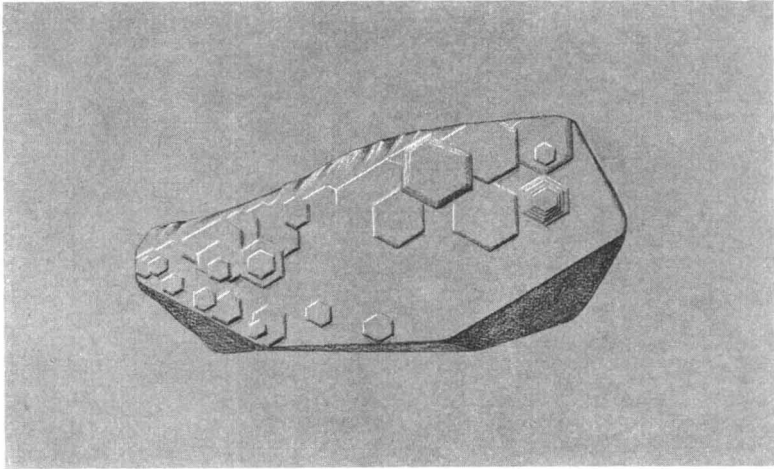


FIG. 8. Growth hillocks on the basal plane of a platy beryl crystal from Mozambique. Longest diameter of the crystal 8 cm. Drawn by Toini Mikkola.

described above have been made on sections perpendicular to the  $c$ -axis. When looked along the  $c$ -axis under the microscope, the crystal exhibits only weak interference color that is produced by the anomalously biaxial optics of the plate and the crystallization texture thus becomes visible. In principle, the texture should reveal itself also on plates parallel to the  $c$ -axis. On such plates, of course, the very small path differences between neighboring polygons that are caused by the optical anomalies will be drowned in the high retardation normally produced by the crystal. By using a rotating mica compensator and turning the analyzer very slightly off from its normal position the texture can be made visible. The  $c$ -axis of the beryl crystal must be almost parallel to one of the nicols. Because the texture is too faintly visible to be photographed, it is shown only in the schematic drawing of Fig. 7. In the particular section reproduced in the drawing there are several series of boundaries throughout the crystal. On the basis of this drawing it may be understood that a plate cut perpendicular to the  $c$ -axis will yield a polygonal pattern.

#### GROWTH HILLOCKS

Well formed faces of beryl crystals often show growth hillocks. Although not described in detail in more recent literature the occurrence and shape of such hillocks is well known to the mineralogist. Because, however, the development of the hillocks seems to be a regular phenomenon in crystal growth of natural beryl and because it seems to be of importance in interpreting the crystallization textures found, the hillocks may be briefly illustrated in this paper.

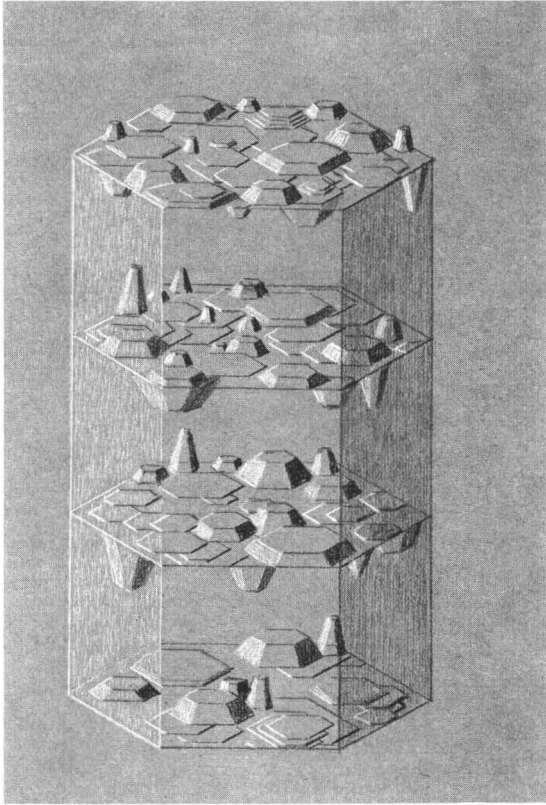


FIG. 9. Illustrating basal growth hillocks on four horizontal sections of a beryl prism. Drawn by Toini Mikkola.

The drawing of Fig. 8 indicates somewhat schematically a platy beryl crystal from Zambezia, Mozambique, with growth hillocks sticking out from the basal plane.

Photographs of growth hillocks on some Brazilian beryl crystals are presented in Plates III a—c. Plate III a shows six-sided growth hillocks rising up stepwise from the basal plane on the side and on top of each other. In some cases the hillocks are negative representing six-sided pits that extend down into the crystal. Plate III b presents a few growth hillocks on a pyramidal face. On some other pyramidal faces of the same crystal the growth hillocks are very numerous forming a continuous carpet that covers the entire face. The sharp ends of the hillocks point towards the trace of the  $c$ -axis of the crystal, WNW in the figure. Plate III c illustrates numerous growth hillocks on a prism face. The  $c$ -axis is almost N—S in the photograph.

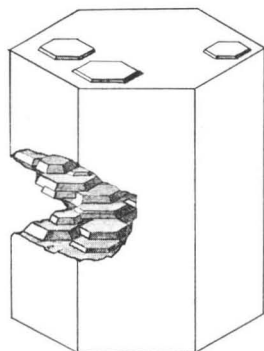


FIG. 10. Illustrating the way of packing of growth hillocks inside a beryl crystal. Drawn by Toini Mikkola.

### POLYGONAL GROWTH

It is evident that the growth hillocks are not to be found only on the present outer faces of the crystal but must have been formed at all stages of the crystal growth. Only the very last ones are seen on the faces of the present crystal and the earlier ones are now buried by material that was deposited later on the crystal face. Thus the crystal would look like the schematical drawing of Fig. 9 that illustrates the growth hillocks on four horizontal sections. If the rate of crystal growth is not constant on all spots of one single crystal face, then the whole crystal may be thought to consist of those hillocks much in the way presented in the hypothetical drawing of Fig. 10.

The crystal habit and, especially, the combination of pyramidal faces varies much for beryl. The variation is best illustrated by top views of crystals that are found in any compilation of crystal forms, like in the 'Atlas der Krystallformen' by Victor Goldschmidt, printed in Heidelberg in 1913. Evidently, the conditions that prevail in the environment in which a beryl crystal is grown are likely not to remain constant throughout the period of the crystal growth. This variation is reflected in the change of the strain conditions in the crystal. During crystallization each crystal face develops its own growth hillocks in which the strain differs from that of the base of the hillock. Depending on the rate of growth on different crystal faces, the crystallization textures summarized in Fig. 1 will result.

The texture presented for beryl in Fig. 10 is no mosaic proper, because the term mosaic would imply a slight displacement of the crystallographic axes in single polygons with respect to their neighbor polygons. Single crystal X-ray photographs do not indicate any such displacement in the beryl crystals studied. Precession and Laue photographs taken show uniform crystallographic axes throughout the crystal.

The polygonal texture in beryl represents a strain pattern, not caused by twinning of orthorhombic or other units of lower symmetry. Textures analogous to those in beryl were found also in minerals like tourmaline, scapolite, apatite, vesuvianite, calcite, corundum, quartz etc.

*Acknowledgments.* — The author is indebted to Mr. Esko Saari, M. A., for assistance in the laboratory, and to Mrs. Toini Mikkola for making several drawings.

*Manuscript received, September 15, 1965*

Explanation to Plate I.

Crystallization textures in Brazilian beryl crystals.  
Plates perpendicular to the c-axis.

- a. Example of well developed polygonal texture.  
Plate thickness 0.56 mm. Diameter of the plate 8 mm.
- b. Irregular core pattern occupying the entire crystal.  
Longest diameter of the plate 28 mm.
- c. Irregular core pattern. 80 x.
- d. Irregular core pattern in hexagonal outlines surrounded by lamellar intermediate zone. 40 x.

Explanation to Plate II.

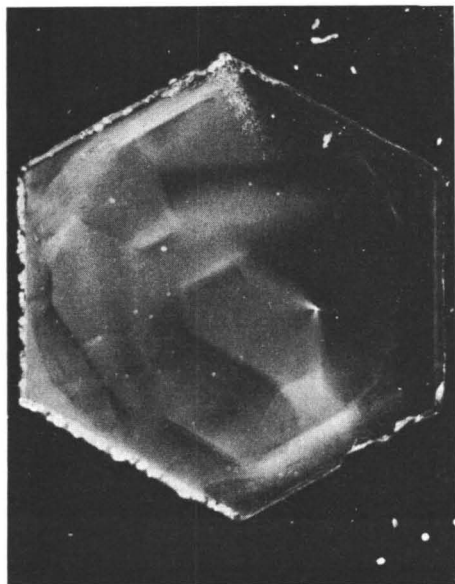
Crystallization textures in Brazilian beryl crystals.  
Plates perpendicular to the c-axis.

- a. Lamellar intermediate zone. 40 x.
- b. Laminated margin. Plate diameter 5 mm.
- c. Star-like polygonal texture in the intermediate zone.  
Two crystals in parallel growth. Plate diameter 14 mm.
- d. Detail of the star-like polygonal texture. 15 x.

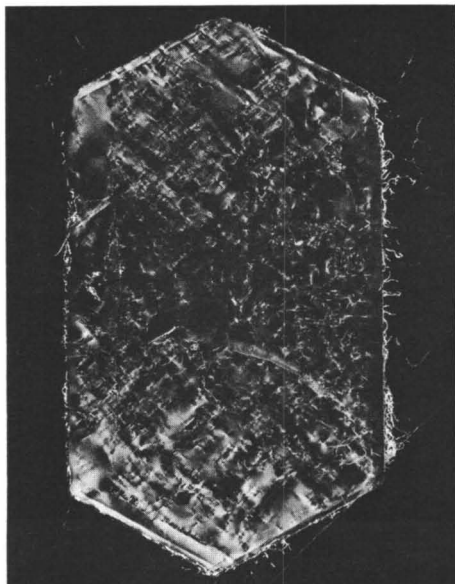
Explanation to Plate III.

Growth hillocks on Brazilian beryl crystals.

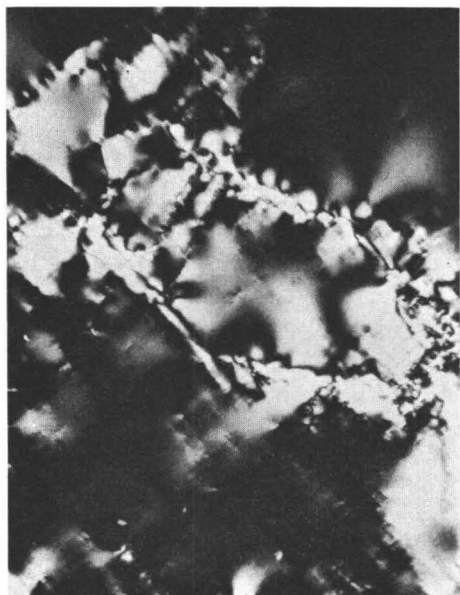
- a. Growth hillocks on basal plane. 20 x.
- b. Growth hillocks on a pyramidal face. 50 x.
- c. Growth hillocks on a prism face. 30 x.



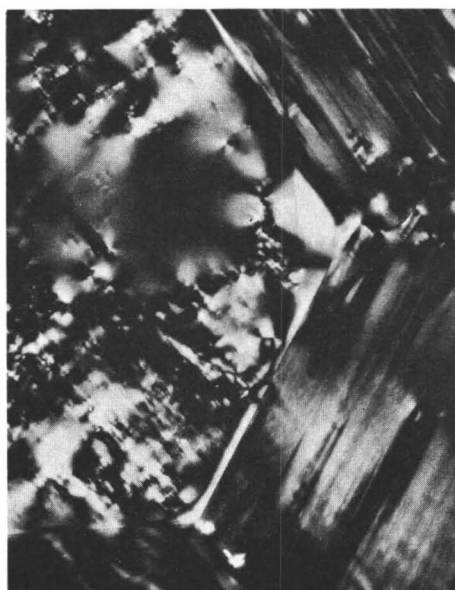
a.



b.



c.



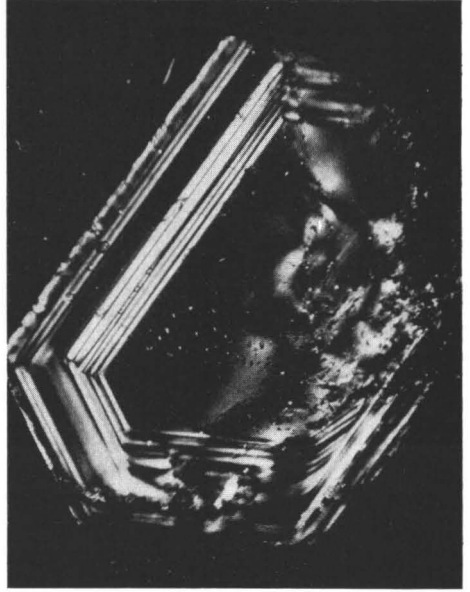
d.

*Th. G. Sabama: Polygonal Growth of Beryl.*

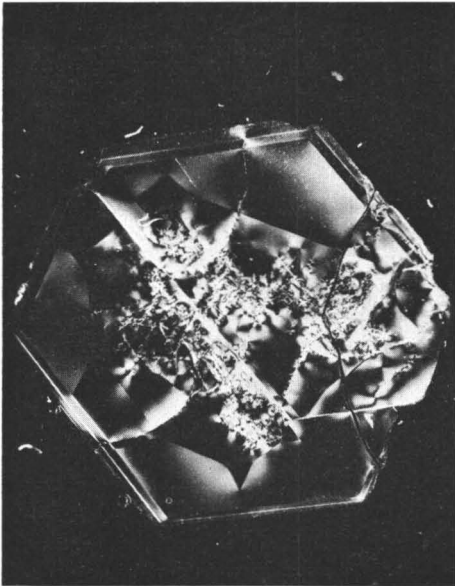
PLATE II



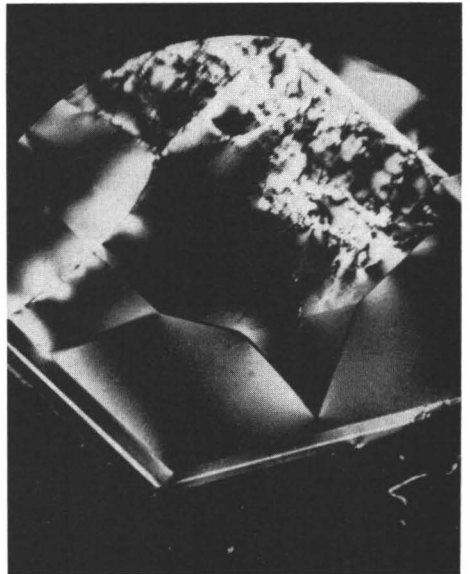
a.



b.

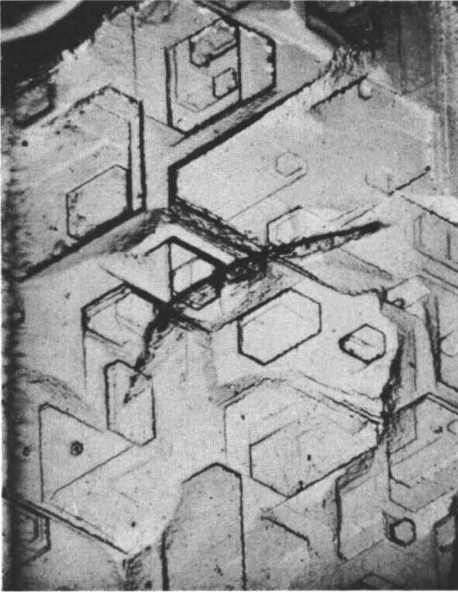


c.



d.

*Tb. G. Sabama: Polygonal Growth of Beryl.*



a.



b.



c.

*Th. G. Sabama: Polygonal Growth of Beryl.*



## A NOTE ON THE PROPERTIES OF MANGANOTANTALITE

BY

OLEG v. KNORRING,

*University of Leeds, England*

TH. G. SAHAMA and ESKO SAARI

*University of Helsinki, Finland*

Despite the fact that red transparent orthorhombic manganotantalite is known from a number of pegmatite localities, its properties are incompletely recorded in literature. To the knowledge of the authors, the manganotantalite that corresponds closest to the ideal formula  $\text{MnTa}_2\text{O}_6$  is still that from Sanarka, Russia, referred to in the seventh edition of Dana's System of Mineralogy. In that manganotantalite the atomic ratio Ta/Nb is 91/9 and Mn/Fe is 92/8.

In the Morrua Mine in Zambesia, Mozambique, tantalite and manganotantalite are commercially obtained from a large granite pegmatite. Among the types of manganotantalite occurring in that pegmatite, a red transparent variety is found the color of which is remarkably pale. Accordingly, the variety could be expected to be very poor in iron and to represent an exceptionally pure MnTa-oxide. The variety was subjected to a closer study that verified this expectation. For that reason, it seems justified to record the data for the mineral in this paper. For comparison, two other red transparent samples of manganotantalite from S. W. Africa and Uganda, respectively, were analyzed chemically and studied by x-ray methods.

For crystal structural reasons Laves, Bayer and Panagos (1963) proposed for the columbite-tantalite group a setting that differs from the conventional one. The notation suggested by these authors is used throughout this paper.

The red variety of the Morrua manganotantalite occurs mostly as small prismatic crystals up to about 1 cm long and may exceptionally reach a length of 4 cm. According to the setting used in this paper the prism axis is crystallographic *b*. Twinning on (012) is common.

Chemical compositions, unit cell contents and unit cell dimensions for all three manganotantalite specimens are compiled in Table 1. The unit cell contents given in

TABLE 1

New chemical analyses, calculated unit cell contents, and unit cell dimensions of manganotantalite. Analysts: J. R. Baldwin and Oleg v. Knorring

Locality	Morrua Mine, Zambezia, Mozambique.	Monrepos, Karibib, S. W. Africa	Jemubi River, Ankole, Uganda
Mode of occurrence	Pegmatite	Pegmatite	Placer
Ta <sub>2</sub> O <sub>5</sub> .....	82.64 %	81.44 %	74.05 %
Nb <sub>2</sub> O <sub>5</sub> .....	0.70	3.81	10.60
TiO <sub>2</sub> .....	0.10	0.07	0.03
FeO* .....	0.40	1.45	0.53
MnO .....	13.89	12.61	14.27
Infusible in KHSO <sub>4</sub> .....	1.00	0.18	0.18
Total	99.62**	99.56	99.66

## Unit cell contents

Ta .....	7.76	7.42	6.45
Nb .....	0.11	0.58	1.53
Ti .....	0.03	0.02	0.01
Fe .....	0.12	0.41	0.14
Mn .....	4.06	3.58	3.87
O .....	23.92	24.00	23.99

## Unit cell dimensions

a <sub>0</sub> *** .....	14.457 Å	14.433 Å	14.446 Å
b <sub>0</sub> **** .....	5.772	5.753	5.766
c <sub>0</sub> **** .....	5.098	5.091	5.096

\* Total iron.

\*\* Includes 0.72 Al<sub>2</sub>O<sub>3</sub> (probably from impurities), 0.14 H<sub>2</sub>O +, 0.03 H<sub>2</sub>O—.

\*\*\* ± 0.01 Å.

\*\*\*\* ± 0.004 Å.

the table are based on a total of 36 atoms per cell. The unit cell dimensions have been calculated from powder patterns recorded by Philips Norelco diffractometer using filtered copper radiation and internal silicon standard. The powder patterns (not reproduced here) agree with that given by Nickel, Rowland and McAdam (1963) for columbite-tantalite except for a shift of the lines towards slightly smaller  $2\theta$  angles. No doubling of the peak at  $d = 2.95\text{--}3.00$  was detected indicating that the minerals are orthorhombic. The following lines were selected for calculating the unit cell dimensions: 200, 310, 400, 311, 020, 002, 021, 600, 330, 621. The results listed in Table 1 represent a least square fit of these lines.

The data compiled in Table 1 reveal the fact that the Morrua manganotantalite corresponds best to the ideal composition of the mineral with Ta/Nb = 99/1 and Mn/Fe = 97/3. The unit cell dimensions listed make it evident that the incorporation of iron in the structure of manganotantalite affects the unit cell size more than the incorporation of niobium. This fact is in agreement with the unit cell data given by

Brandt (1943) for synthetic  $\text{MnTa}_2\text{O}_6$ ,  $\text{MnNb}_2\text{O}_6$  and  $\text{FeNb}_2\text{O}_6$ . In addition to the wet chemical analysis, qualitative tests made by using XRF technique on the Morrue mineral showed no Bi nor V and only traces of Sb, Sn and Zr.

Of the three manganotantalite samples available only the Morrue mineral was studied with single crystal X-ray methods. The unit cell dimensions measured from oscillation photographs about all three crystallographic axes agree with those listed in Table 1. The  $a$ -axis oscillation photograph reveals a well pronounced sub-cell with  $a_0/3$ . The extinctions found in a series of Weissenberg and precession photographs are consistent with the space group Pbcn. No indication of the existence of a monoclinic phase was detected in the single crystal photographs.

The specific gravity of the Morrue mineral was measured by suspending it in water. The measurement was made using seven clear crystals of a total weight of 2.8 g. The value  $7.98 \pm 0.02$  was obtained. The specific gravities calculated on the basis of the data in Table 1 are: Morrue 7.92, Monrepos 7.83, Jemubi River 7.52.

The optical properties were determined for the Morrue mineral. The optical orientation is  $a//\beta$ ,  $b//\alpha$ ,  $c//\gamma$ . Pleochroism very weak with absorption  $a \sim \beta > \gamma$ . The refractive indices (sodium light) were measured on two oriented prisms yielding:

$$\left. \begin{array}{l} \alpha = 2.14 \\ \beta = 2.15 \\ \gamma = 2.22 \end{array} \right\} \pm 0.01$$

The mineral is optically positive with a small optic axial angle and extremely strong dispersion. The following optic axial angles were measured from the interference figure:

$\lambda = 460 \text{ m}\mu$	$2V_\gamma = 34^\circ$
500	$30^\circ$
550	$24^\circ$
589	$23^\circ$
600	$22^\circ$
650	$19^\circ$
700	$17^\circ$

The authors are indebted to Mr. J. D. Cabral, of the Morrue Mine, to Mr. H. Henckert of Karibib, to Mr. T. K. A. Collins of Ngoma, Ankole, for the manganotantalite specimens and to Miss Joy R. Baldwin for chemical analyses.

*Manuscript received, September 15, 1965*

#### REFERENCES

- BRANDT, KARIN (1943) X-ray studies on  $ABO_4$  compounds of rutile type and  $AB_2O_6$  compounds of columbite type. *Arkiv Kemi Min. Geol.*, 17 A, No. 158.
- LAVES, F., BAYER, G. und PANAGOS, A. (1963) Strukturelle Beziehungen zwischen den Typen  $\alpha$ - $PbO_2$ ,  $FeWO_4$  (Wolframit) und  $FeNb_2O_6$  (Columbit), und über die Polymorphie des  $FeNbO_4$ . *Schweiz. Min. Petr. Mitt.*, Bd. 43, S. 217.
- NICKEL, E. H., ROWLAND, J. P. and Mc ADAM, R. C. (1963) Wodginite — a new tin-manganese tantalite from Wodgina, Australia, and Bernic Lake, Manitoba. *The Canadian Mineralogist*, vol. 7, p. 390.

ROZENITE — IRON SULPHATE TETRAHYD-  
RATE — AS FISSURE COATINGS IN THE  
BLACK SCHIST AT MULO, PYHÄSELKÄ,  
IN EASTERN FINLAND

**Mineralogical communication**

BY

ATSO VORMA

*Geological Survey of Finland, Otaniemi*

The black schists — sulphide-graphite schists — have long aroused the interest of Finnish geologists and recently a couple of comprehensive papers on this subject have been published (Marmo, 1960; Peltola, 1960). The supergene minerals in connection with the black schists and other sulphide bearing rocks have also received attention in Finland. Marmo (1953) described the supergene alteration of pyrrhotite in the sulphide bearing schists at Nokia and Saksela (1952) described the alteration phenomena in connection with the weathering of some Finnish sulphide ores, to mention but a few examples.

This note is concerned with a black schist — Mulo schist — exposure visited during numerous geological excursions some of which were international. The locality is a road cut on main road no. 6, about  $\frac{1}{2}$  km to the north of the junction of the Nüittylahti railway station 10 km to the south of the town of Joensuu in Eastern Finland. 1—2 m from the top of the exposure some almost horizontal fissures coated by fine grained white gypsum, yellow jarosite, goethite and white calcite are visible in the cutting. In places the fissures are coated by a botryoidal mass of white — yellowish white mineral which is soluble in water, the coating being from one two mm:s in thickness. According to X-ray diffraction data (Table 1) the mineral belongs to the rozenite-ilesite group. The partial chemical analysis by Mr. Pentti Ojanperä, Mag. Phil., gave FeO 23.0, Fe<sub>2</sub>O<sub>3</sub> 7.5, MnO 0.0, MgO 0.6, CaO 1.0, SO<sub>3</sub> 35.0, insoluble 6.7, H<sub>2</sub>O 26.6 % (the last one from difference). The high ferric iron is due to jarosite occurring as an impurity and identified by X-ray powder photographs.

TABLE 1.

X-ray powder data for the rozenites from Mulo, Pyhäselkä and from Manitoba.

Mulo, Pyhäselkä, Finland <sup>1)</sup>		<i>hkl</i> <sup>2)</sup>	Manitoba <sup>2)</sup>	
<i>I</i>	<i>d</i>		<i>I</i>	<i>a</i>
3	6.87	011, 020	5	6.85
8	5.46	110	9	5.46
1	5.16	021	1/2	5.17
1.5	4.76	101	1	4.73
10	4.50	111, 120	10	4.47
6	3.98	002	7	3.97
1	3.61	130	1	3.61
5	3.39	040	6	3.40
2	3.26	131	1	3.27
3	3.22	112	5	3.22
5	2.97 { 2.975 <sup>3)</sup> 2.945 2.904	032	4	2.985
		140	5	2.953
		210	1/2	2.906
2	2.77	141	1	2.770
1	2.73	220, 211	1	2.722
1/2	2.667	132	1/2	2.673
3	2.578	051, 221	4	2.569
1/2	2.468	150, 023	1/2	2.470
2	2.424	103	3	2.430
2	2.366	231, 142, 113, 202, 231	2 {	2.371
		142, 151, 151		2.360
		212		1/2
2	2.268	033, 123	1/2	2.286
		123, 060	3	2.266
1	2.240	052, 240, 222	1	2.236
1/2	2.175	061	1/2	2.179
1/2	2.145	241, 133	1/2	2.142
1/2	2.101	160, 232	1/2	2.112
1/2	2.047	161, 161	1/2	2.049
2	1.979	143, 062, 143, 213	2	1.969
1/2	1.954	213, 251, 242, 251	1	1.944
1	1.892	053, 223	2	1.890
1/2	1.817	162, 162	1	1.871
		233	1/2	1.819
1	1.800	153, 260, 252	2	1.798
1	1.757	261, 261	1	1.755
1	1.728	063	2	1.725

<sup>1)</sup> Debye-Scherrer method; FeK $\alpha$ -rad., camera dia. 5.73 cm. Intensities are by visual estimation.

<sup>2)</sup> J. L. Jambor and R. J. Traill, 1963.

<sup>3)</sup> These data recorded with the Norelco diffractometer using CuK $\alpha$ -radiation and proportional (Xe) counter with pulse height analyser.

Calcium is due to gypsum. The high FeO and low MnO and MgO show the mineral to be rozenite.

The name rozenite was given to the natural FeSO $_4$  · 4H $_2$ O by Kubisz (1960). Fleischer (1961) supposed the mineral to be siderotil the water content of which would

have been erroneous in the old determinations and proposed the name rozenite to be disregarded. Based on this the tetrahydrate from the Thames river gravel has been described as siderotil (Midgley, 1962). Jambor and Traill (1963) showed, however, that iron sulphate tetrahydrate and pentahydrate really occur as separate mineral species, the former being monoclinic rozenite ( $P2_1/n$ ,  $a = 5.97$ ,  $b = 13.64$ ,  $c = 7.98$  Å,  $\beta = 90^\circ 26'$ ) the latter triclinic siderotil ( $a = 6.26$ ,  $b = 10.63$ ,  $c = 6.06$  Å,  $\alpha = 92^\circ 08'$ ,  $\beta = 110^\circ 10'$ ,  $\gamma = 77^\circ 05'$ ).

Specimens from some other exposures of black schists and sulphide bearing gneisses have also been investigated by the author. Mention need only be made here of the weathering products of sulphide bearing mica gneiss at Lahnahti village in Joroinen, where pickeringite ( $\text{MgAl}_2(\text{SO}_4)_4 \cdot 22\text{H}_2\text{O}$ ) accumulates in small amounts as efflorescences in sheltered places, especially in the fissures of mica gneiss. The mineral was identified by X-ray powder photographs and by determining the major elements (Mg and Al) by optical spectroscopy (Mr. Arvo Löfgren, Mag. Phil.). In addition to Mg and Al, Cu is present in small amounts. The mineral is very poor in iron.

*Manuscript received, October 4, 1965*

#### REFERENCES

- FLEISCHER, M. (1961) New mineral names. *Am. Mineral.*, 46, 242.
- JAMBOR, J. L. and TRAILL, R. J. (1963) On rozenite and siderotil. *Can. Mineral.*, 7, 751—763.
- KUBISZ, J. (1960) Rozenite —  $\text{FeSO}_4 \cdot 4\text{H}_2\text{O}$  — a new mineral. *Bull. Acad. Polonaise, Sci. Ser. Sci. Geol. Geogr.* 8, 107—113.
- MARMO, VLADI (1953) Supergene alteration of pyrrhotite in the sulphide-bearing schists at Nokia, southern Finland. *Bull. Comm. géol. Finlande* 159, 109—122.
- »— (1960) On the sulphide and sulphide-graphite schists of Finland. *Bull. Comm. géol. Finlande* 190, 1—80.
- MIDGLEY, H. G. (1962) On the occurrence of siderotil in Thames river gravel. *Am. Mineral.*, 47, 404—409.
- PELTOLA, ESKO (1960) On the black schists in the Outokumpu region in eastern Finland. *Bull. Comm. géol. Finlande* 192, 1—107.
- SAKSELA, MARTTI (1952) Über die Verwitterung einiger Finnischer Kieserze. *Bull. Comm. géol. Finlande* 157, 27—40.



## MONZONITIC HORNBLLENDE GRANITE NW OF TEBO, CENTRAL SIERRA LEONE

BY

VLADI MARMO

*Geological Survey of Finland, Otaniemi*

### ABSTRACT

A boss of Ba-bearing monzonitic granite, 4 by 10 km in size, is described. It is considered to be postkinematic. The emplacement of this granite is definitely intrusive. The granite may be magmatic, but could equally well have been emplaced under hydrothermal conditions, at a temperature high enough to prevent the formation of homogeneously triclinic potash feldspar.

### CONTENTS

	Page
Introduction .....	55
The monzonitic granite boss .....	56
Petrography of the monzonitic granite .....	57
Description of minerals .....	58
The chemical composition of the boss .....	61
Discussion .....	62
References .....	66

### INTRODUCTION

In Central Sierra Leone the latekinematic granites are not very common. They are either albite-muscovite granites or albite-epidote granodiorites.

Essentially different in composition is the granite of a boss NW Tebo (Fig. 1) at first also believed to be latekinematic (Marmo, 1962). It occupies an area 4 by 10 kms, stretching SE by NW and discordantly penetrating the embracing synkinematic country rock of granodiorite composition. The reconsideration of this granite resulted in the conclusion that the boss is postkinematic.

Tebo is situated 15 km SE of a large schist belt, 130 km in length, composing the Sula Mountains and the Kangari Hills (*e.g.* Pollett, 1951; Marmo, 1962). The granite boss near Tebo will be discussed below.

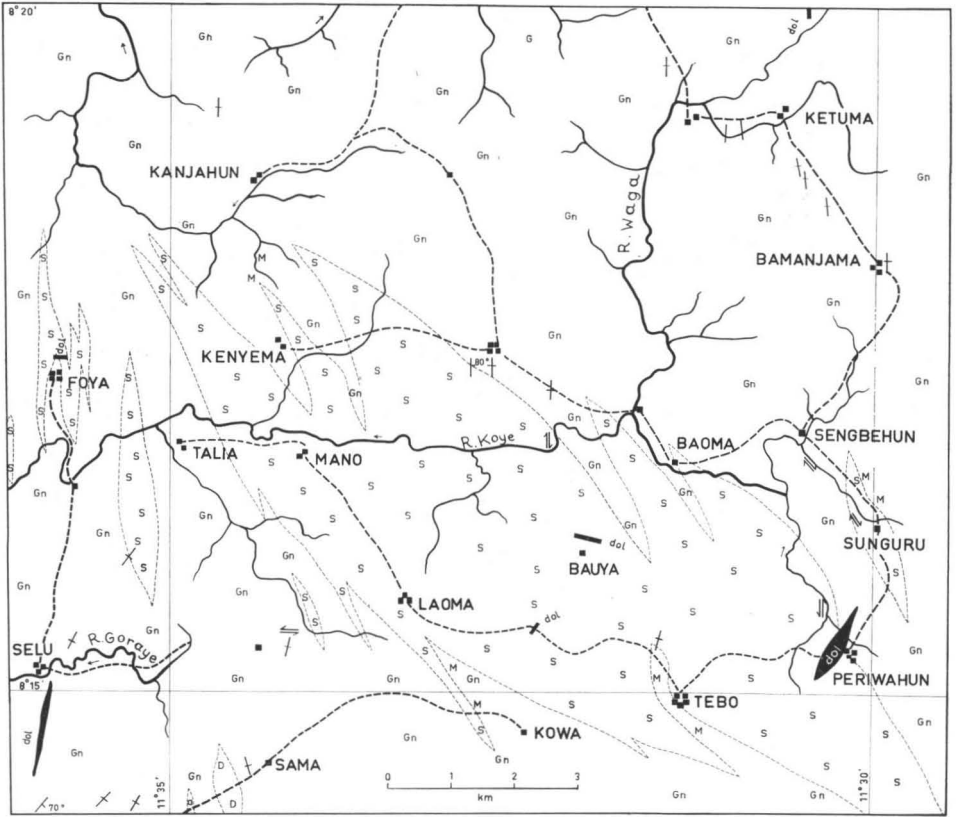


Fig. 1. Geological map of the area NW of Tebo. Gn = gneiss, granodiorite and granite; S = monzonitic granite; D = diorite; a = amphibolite; dol (black) = dolerite; M = strongly developed migmatite.

### THE MONZONITIC GRANITE BOSS

The country rock around the granite boss NW of Tebo consists of synkinematic granodiorites, granites and S-N stretching gneisses. In addition, there are narrow strips of granite similar to that composing the boss penetrating dike-like the synkinematic rocks around the boss itself (Fig. 1). Both the country rock and the granite have been penetrated at several places by dolerite dikes and veins which all seem to stretch SE by NW and have a vertical dip. The width of these dolerite dikes varies from a few centimeters to several meters. The largest dolerite dike detected so far occurs at Periwahun, where it is 30 m wide. At Selu, a 10 m wide dolerite dike has been met with. The dolerite consists mainly of pyroxene and ophitic plagioclase with varying amounts of magnetite.

On the petrographical basis (see below), this granite is named monzonitic granite. It is pink, massive, and only very occasionally orientated or sheared. It is medium-grained and spotted by greenish black laths of hornblende,  $\frac{1}{2}$  to  $1\frac{1}{2}$  cm, occasionally up to 3 cm in length.

The contacts of this granite are mostly masked by overburden, but, where they are visible, they are always sharp.

To the South of Kanjahun, between Kowa and Laoma, and near Sunguru, this granite forms migmatites with the country rock.

The synkinematic granodiorite and gneiss are usually coarse-grained containing portions of ader gneiss. Along the southwestern edge of the monzonitic granite, however, as well as between Kenyema and Baoma, the granodiorite is gray, medium-grained and conspicuously homogeneous.

The outcrops are ample in the interior of the boss, but sparse and rotten near the supposed contacts, and as far as can be judged by observations in the field, the monzonitic granite is definitely younger than the synkinematic granodiorite and gneiss, and it is intrusive. The mode of formation of the intrusion, however, is not indisputable, but will be discussed towards the end of the present paper.

During his field work in 1956, the present writer took this granite as being latekinematic (Marmo, 1962). Later on, however, the petrology of the rock with the potash feldspars of varying triclinicity, and many indications towards a higher temperature of formation than that usually found for latekinematic albite-microcline granites, led the writer to reconsider the kinematics of this boss. Thus it turned out, that the monzonitic granite is less disturbed than the typical latekinematic granites around the Sula Mountains (Wilson and Marmo, 1958). Furthermore, it is also petrologically less homogeneous, resembling with its extra constituents (BaO, SrO, Rb<sub>2</sub>O) rather the younger intrusive granites. It is also noteworthy that the large dolerite dykes associate with this granite in the same way as they often do with the postkinematic Alpine, and as at least in SW-Finland, with the rapakivi granites. Therefore it is very likely that the monzonitic granite of Tebo should be considered as a postkinematic intrusion.

## PETROGRAPHY OF THE MONZONITIC GRANITE

Megascopically, the rock of the monzonitic granite body is fairly homogeneous. Under the microscope, however, some compositional variations can be observed especially in the relative amounts of quartz and, to a lesser extent, the femic constituents. Hornblende is the main dark constituent, but, in some cases, it has a core of diopside. This observation led to the conclusion that at least part of the hornblende has been formed due to an autometamorphic uralitization of pyroxene. Epidote is sometimes present, but mostly it is absent. Biotite is an occasional and definitely unessential constituent of the rock.

TABLE 1.  
Modal composition of granite NW of Tebo

	Hornblende granite			Syenitic quartz monzonite 5119
	5104	5117	5117B	
Quartz .....	28.5	14.0	18.0	8.0
Microcline .....	48.0	49.0	52.0	45.0
Plagioclase .....	20.0	29.0	20.0	38.0
Hornblende and pyroxene .....	2.0	6.0	6.5	6.0
Biotite .....	—	0.5	0.5	—
Epidote .....	—	0.6	1.5	2.0
Apatite .....	0.5	0.2	0.4	0.5
Sphene .....	—	0.1	0.1	—
Magnetite or ilmenite .....	1.0	0.6	1.0	0.5
Total	100.0	100.0	100.0	100.0

In Table 1, the modal compositions of some specimens of the granite are given. In most cases, potash feldspar is more abundant than plagioclase. The specimen poorest in quartz (5119) has a mineral composition intermediate between that of quartz syenite and quartz monzonite. The varieties richest in potassium and quartz are definitely hornblende granites. 5 117, according to its modal composition and the definition of the text-book of Johannsen (1949) is an ademellite.

The rock is rich in potash feldspar, its plagioclase is mostly albite, but also, in some specimens examined, relatively rich in anorthite (An more than 30 %). There are also varieties of hornblende granite, adamellite and intermediates types with compositions between quartz syenite and quartz monzonite. The granitic rock of this postkinematic boss will be collectively classed with monzonitic granite, or, rather, monzonitic hornblende granite.

In general, the distribution of different varieties of this granite seems to be hap-hazard. There is, however, a definite trend for the marginal portions to be enriched in quartz. The varieties closest to the syenitic quartz monzonite composition, on the contrary, mainly occur in the central parts of the boss, between Laoma and Bauya.

#### DESCRIPTION OF MINERALS

Potash feldspar of syenitic granite of Tebo is mostly microcline but of varying triclinicities. There are two generations of this mineral. One is lithologically equivalent to the other major constituents of the rock, and is obviously more or less contemporaneous with plagioclase and quartz. The second, younger generation consists of true, highly triclinic microcline and occurs filling the interstices and fissures of other minerals.

The earlier generation of the potash feldspar tends to form minute insets, and it is almost always strongly perthitic. The plagioclase threads of the perthite are albite or oligoclase, and, judging by the refractive index, less anorthitic than the plagioclase of the main rock mass. Generally the perthitic plagioclase forms sub-parallel, curved or undulating strings and rods, but, sometimes also hexagonal patterns.

Usually this potash feldspar is well cross-hatched, and often it contains drops of quartz. The triclinicity of the potash feldspar varies markedly, however, and according to several x-ray determinations is between 0.0 and 0.85 without any maxima.

The interstitial microcline is very seldom perthitic and always well cross-twinned. This highly triclinic microcline may also occur replacing plagioclase.

The younger microcline is to be attributed tentatively to the potassium metasomatism which took place later than the general formation of the rock including that of the older potash feldspar.

Plagioclase is strongly saussuritized or sericitized, and often almost completely converted into pseudomorphs filled by extremely fine scales of sericite. Fresh plagioclase is rare, and occurs mainly, apart from the perthitic rods, as patches within the strongly sericitized plagioclase grains. Determinations made from such patches showed that this plagioclase contains mainly more than 30 % anorthite. The bulk of plagioclase seems, however, to be an albite with less than 10 % An.

The sericitization of plagioclase is obviously due to that same potassium metasomatism which also produced the interstitial microcline.

Amphibole and pyroxene are the main femic constituents of the monzonitic granite. Their total amounts, on an average, to 6—7 %. Aplitic varieties with less than 4 % dark constituents are exceptional, as are also the unusually dark varieties with more than 10 % femics.

Amphibole is strongly pleochroic green hornblende with an extinction angle of about 20°. It is regularly accompanied by small amounts of apatite, magnetite, ilmenite, and often also by sphene. Exceptionally latter may occur in abundance. In such cases it usually envelopes the grains of ilmenite (Fig. 2).

Especially between Laoma and Bauya, the hornblende often has a core of pyroxene, which is diopside augite ( $\epsilon A\gamma = 39^\circ$ ), uralitized along its margins.

Epidote is a common but not a frequent constituent. There is evidence that most, if not all, epidote has been formed at the expense of pyroxene and amphibole. It often occurs in the cracks of pyroxene or amphibole (Fig. 3). There are also especially interesting cases in which (Fig. 4) the epidote forms a reaction rim around grains of pyroxene, which are partially uralitized along the margins. In all the cases observed, this rim occurs between microcline and pyroxene or amphibole. Such a rim has never been seen around those grains which verge upon plagioclase or quartz. On the other hand, similar rims may also occur inside an amphibole grain. In such cases the rims are between strongly saussuritized or sericitized, entirely enclosed plagioclase grain and the enclosing amphibole (or pyroxene). But even then potash feldspar is also present, the whole plagioclase grain being filled with

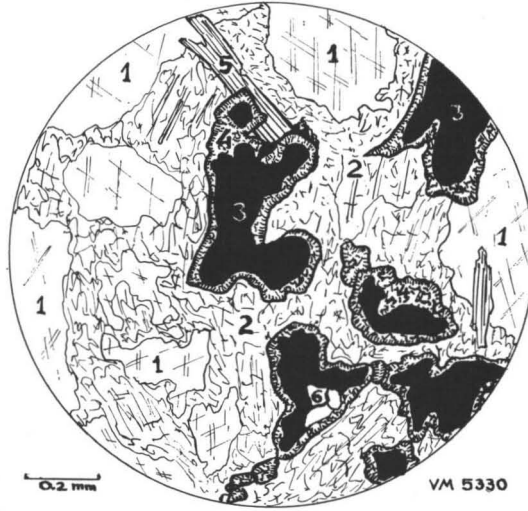


Fig. 2. Monzonitic granite. At Sunguru. Spene envelopes the ilmenite. 1 = microcline; 2 = sericitized plagioclase; 3 = ilmenite; 4 = sphene; 5 = biotite; 6 = quartz. N //.

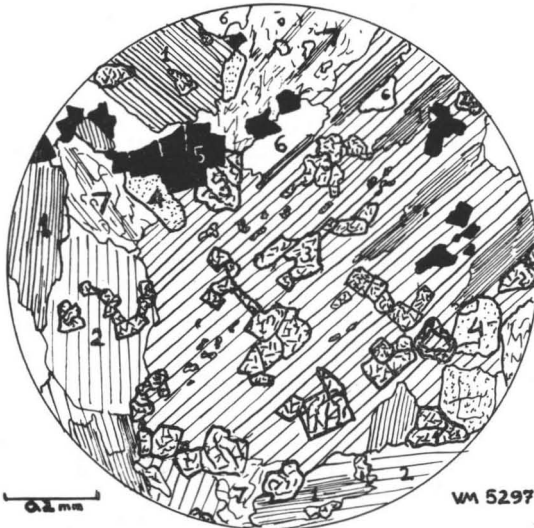


Fig. 3. Hornblende inset in the monzonitic granite. Between Foya and Kanjahun. 1 = olive green hornblende; 2 = pale hornblende; 3 = epidote; 4 = apatite; 5 = ilmenite; 6 = quartz; 7 = sericitized plagioclase. N //.



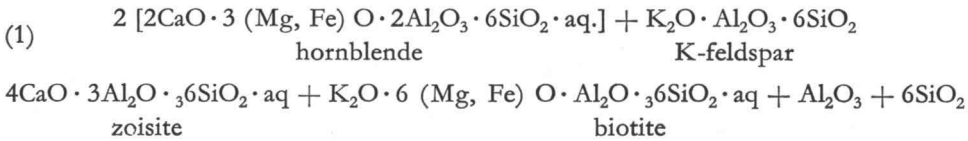
Fig. 4. Pyroxene-bearing monzonitic granite. W of Kowa. 1 = pyroxene; 2 = uralitic amphibole; 3 = epidote; 4 = microcline; 5 = plagioclase; 6 = quartz. N //.

TABLE 2.

Chemical composition of the quartz monzonite at Laoma. Analyst. A. Heikkinen (Geological Survey of Finland)

SiO <sub>2</sub> .....	64.23												
TiO <sub>2</sub> .....	0.62												
Al <sub>2</sub> O <sub>3</sub> .....	16.35												
Fe <sub>2</sub> O <sub>3</sub> .....	2.11												
FeO .....	1.16												
MnO .....	0.04												
MgO .....	0.92												
CaO .....	2.14												
BaO .....	0.47												
SrO .....	0.16												
Rb <sub>2</sub> O .....	0.01												
Na <sub>2</sub> O .....	3.87												
K <sub>2</sub> O .....	6.80												
P <sub>2</sub> O <sub>5</sub> .....	0.39												
CO <sub>2</sub> .....	0.00												
SO <sub>3</sub> .....	0.06												
H <sub>2</sub> O + .....	0.59												
H <sub>2</sub> O - .....	0.13												
Total 100.05													
		Mode:											
		Quartz .....	10.02										
		K-feldspar .....	40.03										
		Albite .....	32.49										
		Anorthite .....	5.46										
		Ba-Sr-feldspar .....	1.58										
		BaSO <sub>4</sub> .....	0.17										
		Amphibole .....	4.70	<table border="0" style="display: inline-table; vertical-align: middle;"> <tr> <td rowspan="4" style="font-size: 2em; vertical-align: middle;">}</td> <td>Al<sub>2</sub>O<sub>3</sub> .....</td> <td>0.2</td> </tr> <tr> <td>FeO .....</td> <td>0.4</td> </tr> <tr> <td>MgO .....</td> <td>2.3</td> </tr> <tr> <td>SiO<sub>2</sub> .....</td> <td>1.8</td> </tr> </table>	}	Al <sub>2</sub> O <sub>3</sub> .....	0.2	FeO .....	0.4	MgO .....	2.3	SiO <sub>2</sub> .....	1.8
}	Al <sub>2</sub> O <sub>3</sub> .....	0.2											
	FeO .....	0.4											
	MgO .....	2.3											
	SiO <sub>2</sub> .....	1.8											
		Apatite .....	1.01										
		Sphene .....	1.57										
		Magnetite .....	3.02										
			100.05										
		Microscopically: Plagioclase is albite with An <sub>6</sub> .											
		Trilicinity of K-feldspar: 0.0—0.85, no max.											

it. The plagioclase contains clear microcline grains and the sericitic mass is full of sub-microscopic patches of microcline. Consequently, this rim as well may be considered as having been formed on the boundary between microcline and amphibole. Thus, evidently, an epidotization of hornblende due to potash feldspar has taken place:



This reaction should produce biotite as well. Mica, however, does not occur in connection with these rims, which makes this equation less suitable for the explanation of the epidote rims.

### THE CHEMICAL COMPOSITION OF THE BOSS

The chemical analysis of Table 2 represents a fairly homogeneous portion of the rock near Laoma, from the southcentral part of the boss. This composition is close to quartz monzonite, but has some potassium in excess. Consequently it is close to the modal analysis 5 119 of Table 1. The trilicinity of the potash feldspar of this granite, as determined from the analysed sample and from the samples taken from the village of Tebo, is 0.0—0.85 without maxima. The plagioclase of the analysed sample contains An<sub>6</sub>.

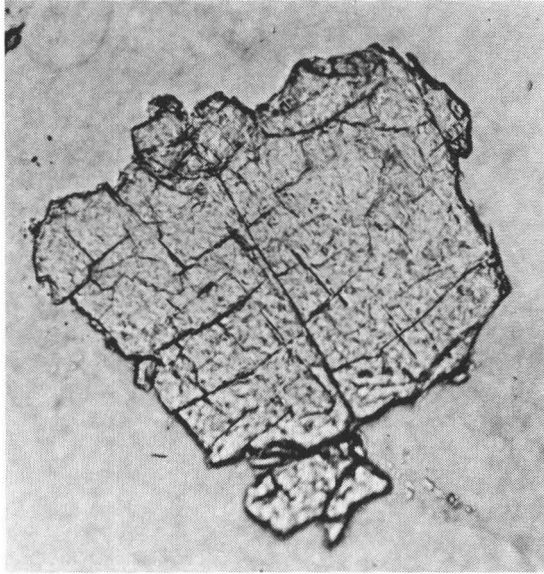


Fig. 5. Grain of baryte in granite N // . Magn. 200 x.

The most interesting feature of the analysed rock is the surprisingly high content of BaO (0.47 %), and also the amount of Sr is unusually high for a granite—that is, in as far as these elements have been determined for the granitic rocks. On the other hand, if BaO is present in a rock, it usually precipitates at such stage of the analysis that it is seldom overlooked. BaO is usually incorporated in the potash feldspar. Mr. J. Siivola (Geol. Survey of Finland) determined the barium content of the potash feldspar using a Geoscan microanalyser, obtaining approx. 0.1 % BaO. The rest, combined with 0.06 %  $\text{SO}_3$  of the chemical analysis, forms baryte. This mineral occurs in the rock forming minute grains, less than 0.1 mm in size (Fig. 5), and identifiable in a similar way. The identification and form of baryte grains is seen in Fig. 6. This is the first time the present writer has ever seen baryte in a granite. The BaO-content of granites has, however, been observed earlier, and especially in some Finnish postkinematic granites, but in those cases the BaO-contents are definitely lower than in the granite of Tebo.

#### DISCUSSION

The composition of the rock is such, that it corresponds well with Eskola's ideal granite (Eskola, 1955), except that it has a high lime- and a low quartz-content. The varieties poorest in albite are close to the composition of such a microcline — quartz mixture defined by Schairer (1954) as corresponding to the composition of the potash

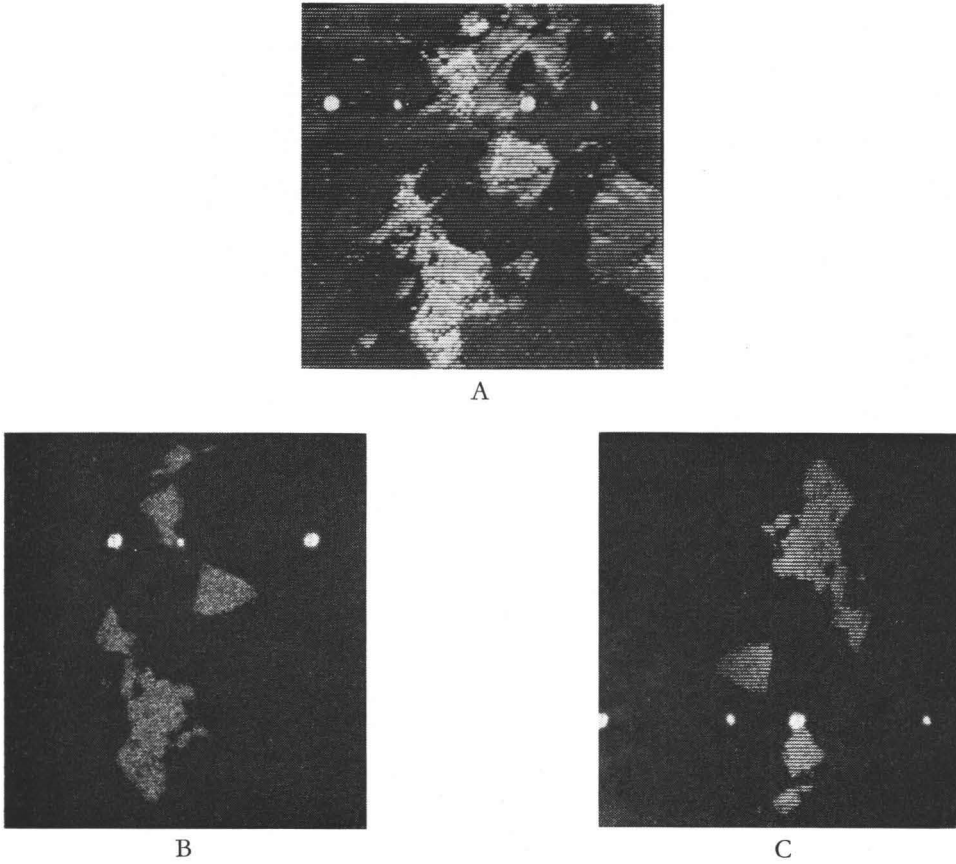


Fig. 6. Baryte grains in granite. Laoma-Tebo path. A: Electron image, x100. White areas are baryte. B: X-ray image, x100. Ba  $L\alpha$ , indicating the distribution of barium. C: X-ray image, x100. S  $K\alpha$  indicating the distribution of sulphur.

feldspar — silica eutectic, and also to the residual liquids of the dry quaternary system  $K_2O - MgO - Al_2O_3 - SiO_2$ , which liquids are of ideal granite composition. Schairer and Bowen (1955, p. 741) wrote: « — — — the residual liquids from crystallization in these systems closely approach the binary eutectic between potash feldspar and silica, with only small amounts of olivine, pyroxene or lime feldspar in the several ternary eutectics.»

The monzonitic granite at Tebo is undoubtedly »dry», which property is well portrayed in the presence of pyroxene and in the almost complete absence of micas. One could even say — allowing for the sometimes high anorthite content of the plagioclase — that those varieties of this granite which contain exceptionally much microcline are of almost ideal granite composition.

At present, the importance of the anorthite component of the plagioclase is not well understood. In the problem of the albitic latekinematic granites the difficulties arose with the abundance of albite, which makes the composition inconsistent with its magmatic origin from a melt, as was also pointed out by Tuttle (1952). In this monzonitic granite, however, the high anorthite-content could possibly make the co-crystallization of potash feldspar and plagioclase possible under magmatic conditions as well, providing the present albite is of secondary origin due to saussuritization. The magmatic possibility is also supported by the fact that the abundant and fine perthite obviously indicates the primarily crystallized potash feldspar as having been rich in albite.

Also the geological setting of the granite of Tebo is such that it suggests an intrusive origin of the body.

For the albitic latekinematic granites, the present author could not adopt the above mentioned explanation (Marmo, 1955—1956). But in the case under discussion such an explanation is quite plausible. Similarly the author is in full agreement, that also the true, orthoclase-bearing rapakivi-granites may be of magmatic origin.

Furthermore, the potash feldspar somewhat resembles that of rapakivi and alpine granites, in which all intermediate types between monoclinic and triclinic potash feldspar are present.

This feature is likewise quite common in the monzonitic granite at Tebo.

The homogeneity of the microcline of the latekinematic granites has led the present author to conclude that their potash feldspar has grown in triclinic form (Marmo, 1956), even if at the very initial stage of growths it might have been of monoclinic symmetry (Marmo, 1956b). This assumption is necessary to fulfill the requirements set out by Laves (1956) on a crystallographic basis for the formation of the cross-twinning typical of such microclines.

The present author also assumed (Marmo, 1956) that the requirement for the direct formation of microcline is slow growth at a temperature well below the triclinic-monoclinic transformation point.

In the case of the monzonitic granite at Tebo, there are signs certainly indicating that the potash feldspar could have been initially monoclinic.

As has been shown *e.g.* by Laves, both the exsolution of perthite and the formation of microcline, obviously follow each other. Thus, if in the primary crystallization an anorthite-rich plagioclase and albite-rich potash feldspar have been formed simultaneously, and then, due to prolonged heating at an appropriate temperature (Tuttle, 1952), exsolution has taken place, this could easily have been accompanied by a re-arrangement of the Si-Al framework of the potash feldspar. Under such conditions the triclinization of the latter could take place and preserve all the intermediate stages of the symmetries.

This conclusion is well consistent with the ideas presented by the present author in his earlier papers (*e.g.* 1956) in which he stated that the granite composition may be attained in different ways. There is a distinct difference between syn- and latekine-

matic granites. The potash feldspar of the former is almost exclusively of metasomatic origin — a point of view also held by Eskola (1956). In the latekinematic granites the mode of occurrence of potash feldspar is different and the plagioclase is mostly albitic, the fact which led the present author to abandon the wholly magmatic origin for these granites. In the monzonitic granite at Tebo, which also may be a latekinematic granite but probably is postkinematic, the feldspars are of such a composition and mode of occurrence, that these granites may well be of truly magmatic origin, as also the rapakivi, postulated by Eskola as being a perfect representative of the magmatic granites.

On the other hand, the same composition of a granite could also be attained were the emplacement to take place at a somewhat elevated temperature from solutions rich in water under hydrothermal conditions. Under such circumstances, the perfect triclinicity of potash feldspar would never have been attained, nor the complete separation of albitic components from the potash feldspar. The same would also be the result if the intrusion with consequent crystallization would have been too rapid to allow the formation of highly triclinic microcline throughout the whole rock mass.

In this connection attention may be drawn towards the facts, that the latekinematic granites investigated so far are always true albite-microcline granites, being emplaced at a comparatively low temperature (below 450°C), and they also often form migmatites. Consequently at the latekinematic stage of the orogenic evolution, the transport of potassic materials probably took place aided by water at a moderate temperature typical of the conditions of a regional metamorphism in general. Therefore the emplacement of the respective granites has lasted a long time and they have been able to attain the mineralogical composition typical of them. The postkinematic intrusion, on the contrary, seems to have taken place more rapidly and maybe also at a higher temperature, thus leading to a less perfect differentiation of feldspatic minerals. The elevated temperature may also be responsible for the fact, that the mineralogy of such granites seems to be more »dry» than that of latekinematic granites.

Thus also for the monzonitic granite of Tebo, the magmatic origin is not necessarily the only possible one. Rather the present writer is inclined to adopt the other alternative discussed above.

*Manuscript received, October 4, 1965*

## REFERENCES

- ESKOLA, PENTTI (1955) About the granite problem and some masters of the study of granite. Bull. Comm. géol. Finlande 168, p. 117.
- »— (1956) Postmagmatic potash metasomatism of granite. Bull. Comm. géol. Finlande 172, p. 85.
- LAVES, FRITZ (1956) Remarks on a paper by V. Marmo »On the microcline of the granite rocks of central Sierra Leone». Schweiz. Min. Petr. Mitt. 35 (1955), p. 296.
- MARMO, VLADI (1955) On the classification of the pre-Cambrian granites. Col. Geol. Min. Res. 5, p. 429.
- »— (1955a) On the microcline of the granitic rocks of central Sierra Leone. I. Schweiz. Min. Petr. Mitt. 35, p. 155.
- »— (1956) Reply on the remarks of Prof. F. Laves. Schweiz. Min. Petr. Mitt. 35 (1955), p. 299.
- »— (1956a) On the emplacement of granites. Am. Jour. Sci. 254, p. 479.
- »— (1962) Geology and mineral resources of the Kangari Hills schist belt. Geol. Surv. Sierra Leone, Bull. n:o 2.
- POLLETT, D. J. (1951) Geology and Mineral resources of Sierra Leone. Col. Geol. Min. Res. 2, p. 3.
- SCHAIRER, J. F. (1954) The system  $K_2O-MgO-Al_2O_4-SiO_2$  I. Results of quenching experiments of four joins in the tetrahedron cordierite-forsterite-leucite-silica, and on the join cordierite mullite-potash feldspar. Amer. Ceram. Soc. Jour. 37, p. 501.
- »— and BOWEN, N. L. (1955) The system  $K_2O-Al_2O_4-SiO_2$ . Am. Jour. Sci. 253, p. 681.
- TUTTLE, O. F. (1952) Origin of the contrasting mineralogy of extrusive and plutonic salic rocks. J. Geol. 60, p. 107.
- WILSON, N. W. and MARMO, VLADI (1958) Geology, geomorphology and mineral resources of the Sula Mountains. Geol. Surv. Sierra Leone, Bull. N:o 1.

## MOLYBDENITE-3R FROM INARI, FINNISH LAPLAND

### Mineralogical communication

BY

ATSO VORMA, PEKKA KALLIO AND KAUKO MERILÄINEN

*Geological Survey of Finland, Otaniemi*

The natural occurrence of the rhombohedral molybdenite has been reported so far from the quartz-feldspar porphyry at the Cone mine, Yellowknife, Northwest Territories, Canada (Traill, 1963), from the dolomite of the Binnatel, Ct. Valais, Switzerland (Greaser, 1964) and from the greisenized granite at the Minas da Panasquera, near Fundão, Beira Baixa, east-central Portugal (Clark, 1965). Takéuchi and Nowacki, 1964, described the crystal structure of molybdenite-3R and systematically deduced the other possible polytypes with simple structures. Their result gave one rhombohedral, two hexagonal and one trigonal structures, which were designated 3R, 2H<sub>1</sub> (the ordinary hexagonal molybdenite), 2H<sub>2</sub> and 2T respectively. The rhombohedral polytype can be identified by determining the *d*-spacings from x-ray powder photographs while other three polytypes can be effectively identified by comparing intensities of certain reflections.

About 170 specimens containing molybdenite and originating from different parts of Finland were systematically investigated to detect whether any of the new polytypes were present. X-ray powder photographs (Debye-Scherrer camera) and diffractometer charts (Norelco diffractometer) were made of the fine ground mineral powder. Glass powder was mixed with the material for diffractometer runs. The *d*-values were checked to detect the rhombohedral polytype. Only one specimen (No. 52/AT/56) proved to contain rhombohedral molybdenite in addition to the hexagonal one. Intensity comparison showed all the other specimens to contain exclusively the 2H<sub>1</sub> polytype. Weissenberg and Buerger precession photographs of two different crystals showed the rhombohedral molybdenite (No. 52/AT/56) to have  $a_b = 3.16 \text{ \AA}$  and  $c_b = 18.32 \text{ \AA}$  and space group *R3m*. All the single crystal pho-

tographs revealed two sets of reciprocal lattice points; the orientation of the lattices deviates only  $2^{\circ}$ – $3^{\circ}$  from the exact (0001)-twinning position. The intensity of the reciprocal lattice points of the one set were stronger than that of the corresponding points of the other.

The molybdenite specimen no. 52/AT/56 (from the eastern edge of the valley of the river Vaijoki, about 1 km SSW from the fork of the rivers Lemmenjoki and Vaijoki, Inari, Lapland) was collected from the western margin of the granulite complex of Lapland (Meriläinen, 1965), from a small quartz-plagioclase rich dike. The rock is gneissose, fine grained (grain size from one to two millimeters) and, in appearance, resembles mica gneiss rather than an acid dike rock. The mineralogical composition is: quartz, plagioclase ( $An_{35}$ ), chlorite, biotite and muscovite. Rutile, zircon and opaques occur as accessories. The plagioclase is strongly sericitized.

The molybdenite bearing dike is surrounded by hornblende gneiss, which consists of hornblende, plagioclase ( $An_{40}$ ), quartz, biotite, chlorite and cummingtonite. Megascopically the rock is strongly foliated and striped by thin quartz-feldspar veinlets. Biotite, chlorite and the greatest part of the opaques occur in thin movement shears. The colour of hornblende is brownish-green, that of biotite brownish-red.

The molybdenite bearing dike rock, as well as its country rock, is surrounded by garnet gneisses belonging to the granulite complex. However, on account of their mineralogical composition neither of them belongs to the rocks of the granulite facies. Both are, however, strongly foliated and *e.g.*, the quartz grains in the hornblende gneiss resemble in places the platy quartz in the garnet gneisses of the granulite complex.

*Acknowledgements* — The authors are thankful to the geologist at the Geological Survey of Finland and at the Otanmäki Co. for providing the samples investigated during this study. We are also thankful to Mr. Kari Vuorio for assisting us in the laboratory work.

*Manuscript received, November 20, 1965*

## REFERENCES

- CLARK, A. HORRELL (1964) Rhombohedral molybdenite from the Minas da Panasqueira, Beira Baixa, Portugal. *Mineral. Mag.*, vol. 35, pp. 69–71.
- GREASER, STEFAN (1964) Über Funde der neuen rhomboedrischen  $MoS_2$ -Modifikation (Molybdänit-3R) und von Tungstenit in den Alpen. *Schweiz. Min. Petr. Mitt.*, B. 44, H. 1, S. 121–128.
- MERILÄINEN, KAUKO (1965) Suomen geologinen yleiskartta C 8–9, Inari—Utsjoki. The General Geological Map of Finland, 1:400 000.
- TRAILL, R. J. (1963) A rhombohedral polytype of molybdenite. *Can. Mineral.*, vol. 7, part 3, pp. 524–526.
- TAKÉUCHI, Y. and NOWACKI, W. (1964) Detailed crystal structure of rhombodral  $MoS_2$  and systematic deduction of possible polytypes of molybdenite. *Schweiz. Min. Petr. Mitt.*, B. 44, H. 1, S. 105–120.

## ON THE PETROLOGICAL CLASSIFICATION OF GRANITES

BY

VLADI MARMO

*Geological Survey of Finland, Otaniemi*

Until now, the generally used classification of granites has been based on their position in orogenic (tectonic or kinematic) evolution. Thus there are syn-, late- and post-tectonic, -kinematic or -orogenic granites around the globe. Such classifications have been very satisfactory as long as definition of a »granite» has been very broad. The question was rather one of granite-looking acid plutonic rocks. The situation somewhat changed when petrological aspects were more carefully considered. It was found, that if the rocks of true granite composition are considered, there will be comparatively few actual granites among the synkinematic (or -tectonic, or -orogenic) rocks, but very many among the late-, and especially among the postkinematic rocks. The trend of modern petrology is to term only those rocks granite which are potash-rich or at least definitely approaching the true granite composition.

Such a classification is very satisfactory for general geological purposes and it may well justify its place, despite the fact that there are certain serious limitations in it. We may be unanimous about the conceptions, *e.g.*, syn-, late- and postkinematic, but their interpretation in the field may be sometimes very difficult and uncertain, especially in the case of the latekinematic rocks, where there often seem to be diverging opinions.

On the other hand, several authors have observed (see *e.g.* Marmo, 1962), that there are many petrological characteristics which are typical of different granite groups. These characteristics are often decidedly different for different granites; they are easily ascertainable, and they should not be neglected or omitted if one is to venture to discuss the mode of origin of granites. Thus, for instance, as early as in the Thirties Wahl (1936) had pointed out petrological differences between his syn- and serorogenic granites.

Classification on a petrographic basis has, however, also been used — either independently or simultaneously with tectonic classifications. Definitions like biotite

granite, muscovite granite, two-mica granite, hornblende granite, etc. have been widely used. In such cases, the main reason for petrological classification is to enable the synorogenic granites to be distinguished from each other and to establish subgroups for them. This is, of course, sometimes necessary and useful, but does not resolve the actual and essential questions connected with the granite problem. On the contrary the differences in the feldspars and their modifications are of more importance as are also certain minor constituents which often seem to play an important role among the post-kinematic granites. Furthermore, the feldspars reflect the grouping of granites on a tectonic or kinematic base with certain known exceptions:

1. *Synkinematic granites*. The potash feldspar is mainly microcline of high triclinicity, and it occurs mostly as infilling of interstices of other minerals, or replacing plagioclase. Thus it is usually younger than the other constituents of the rock. It may also occur forming porphyroblasts, which are mostly microcline, but there are also some known instances (Marmo, Hytönen, and Vormaa, 1963) where the porphyroblasts are of potash feldspar with inferior and variable triclinicity (0.0—0.8). Plagioclase of these granites is almost always oligoclase, typically with 25 to 30 per cent An. Among the dark constituents biotite prevails over muscovite (or is the sole mica), hornblende being present in certain varieties.

2. *Latekinematic granites*. Potash feldspar is predominantly highly triclinic and well cross-hatched microcline, orthoclase being met with only very occasionally; in Finland, for instance, only one such case is known. In most cases so far examined, potash feldspar is hardly younger than the other constituents of the rock. Perthite is, in general, uncommon, but among these rocks, varieties containing highly perthitic, but still distinctly triclinic microcline, are also known. Plagioclase is characteristically albite with 2 to 10 % An, or less commonly acid oligoclase with 10 to 15 % An. Muscovite is much more common than biotite in latekinematic granites. Varieties rich in epidote also occur, this mineral being uncommon in the synkinematic granites.

3. *Postkinematic granites*. Potash feldspar occurs usually as at least two separate generations. The older one is mainly orthoclase of very varying triclinicity (with cross-hatched patches of microcline), but mostly of monoclinic symmetry. The younger generation is represented by thin veinlets, often infillings of interstices, composed of well cross-hatched and perfectly triclinic microcline. This younger generation, however, is only of small importance, if compared with the older orthoclase generation. Plagioclase is mostly oligoclase with 20 to 30 % An, being only occasionally albitic. Furthermore, the orthoclase potash feldspar of this group is always strongly perthitic. Among these granites there is a special group to be distinguished, in which the single feldspar is anorthoclase, oligoclase being almost absent (for instance the so-called »Younger granites» of Nigeria). In addition, minerals of accessory elements are common constituents in such granites.

In this connection it must still be stressed, that the kind and mode of feldspars is not at all suitable for determining the tectonic group of a granite. In most cases, however, they seem to be parallel features.

The feldspars may have a very important bearing on the origin of granites. Thus the potash feldspar of the synkinematic granites, occurring as a comparatively late constituent infilling the interstices and replacing plagioclase, is most certainly of metasomatic origin. The microcline of late-kinematic granites has been formed at a somewhat lower temperature, and the temperatures of formation of such granites have been determined, in several cases, as being between 350° and 500°C. The lowest temperatures have been obtained for microcline-albite granites.

Orthoclase and microcline of inferior triclinicity correspond usually to somewhat elevated temperatures. Such feldspars are mostly typical of postkinematic granites (plagioclase has a composition of oligoclase), for which — in the case rapakivi for instance — the temperature of crystallization has been found to approach 700°C. The occurrence of single K-Na-feldspar (anorthoclase) seems to indicate the highest temperatures of formation, and such granites may well represent conditions close to the magmatic ones, or even be of magmatic origin, as is the case in Northern Nigeria where such granites grade over, through granite porphyry, into rhyolite within a comparatively short distance.

Thus, if the genetical questions of the granites are discussed, much more use may be made of a petrological rather than of a tectonic or kinematic classification of granites.

Certainly such a classification on a petrological basis may be made in different ways and in each case adjusted to the purpose of classification. Geologist who is mainly concerned with the prospecting of ores often associated with granite — as are the ores of molybdenum, tin, niobium etc. — needs other characteristics and more localized classification than does a petrologist studying granites in general. Such a geologist may also benefit from kinematic grouping. He probably would avoid prospecting within synkinematic granites, and if tin or porphyry ores are concerned, would be more interested in postkinematic rocks. But still the petrological classification is of more importance to him. Experience has taught him that the granites accompanying molybdenum ores are usually richer in potassium and silica than are otherwise similar granites elsewhere; the prospectors for tin in Nigeria know that cassiterite occurs there in the greisenized portions of biotite granite but hardly at all in connection with riebeckite granites of the same area — Jos Plateau. Also columbite associates with similar granite, but not pyrochlore which prefers the riebeckite — bearing varieties, and so on.

Black (1965) has reached, on a petrological basis, the conclusion, that in Niger and Northern Nigeria, the so called »Younger granites» have been differentiated along two trends: the one which is richer in alumina having produced biotite granite and the other which is poor in alumina having led to the formation of aegirine-amphibole granite. In both cases the potash feldspar is similar: mostly anorthoclase.

Similar trends among such granites may be found also in other postkinematic localities with riebeckite or aegirine granites.

A classification of granites on a petrological basis involves a negative aspect, too: each petrologist is making it on his own way, and the result will be that, depending

upon his exactness in the petrological study of granites, he may attain very different and incompatible groups in different areas. On the other hand, such a classification may also have the benefit of flexibility providing agreement can be reached as to which basic petrological groups are to be used. These groups may then be subdivided into any amount of sub-groups to meet the needs of particular local problems concerned. In the opinion of the writer, the basic groups should be such as to facilitate the understanding of the genetic problems of granites, at the same time being clear and easy to use. Therefore, in the following proposal the feldspars are used as the basis of such a classification. Groups below can then be enlarged and subdivided using additional indications of other — major or minor — constituents, structural or tectonic features, etc.

1. *One-feldspar granites*, containing predominantly only one feldspar which is highly perthitic, may be anorthoclase (*e.g.* the «Younger granites» of Nigeria).

2. *Orthoclase granites* which contain mainly orthoclase and oligoclase. Microcline is present as patches of variable triclinicity together with orthoclase and often inside it or as younger thin veinlets in which it is of good triclinicity. The potash feldspar is usually strongly perthitic (*e.g.* rapakivi and most Alpine postkinematic granites).

3. *Microcline-oligoclase granites* in which the potash feldspar is microcline but mostly extensively perthitic, and often of varying triclinicity. Such granites are not very common, but they do occur among the latekinematic granites of Finland (*e.g.* granite of Otanmäki), too; usually, however, they are postkinematic (*e.g.* Tebo granite, Sierra Leone).

4. *Microcline-albite granites* which are mostly aplitic, potash feldspar is highly triclinic, well cross-hatched, seldom perthitic microcline. Albite is associating plagioclase. (*e.g.* latekinematic granites, often forming migmatites).

5. *Granitized microcline-oligoclase granites* which are of varying composition mostly grading from granodiorite to granite. Microcline of these granites is younger than other mineral constituents of the rock, plagioclase is oligoclase (*e.g.* most synkinematic granites).

If there are porphyric or porphyroblastic textures, they can be indicated under such names as »porphyroblastic microcline-oligoclase granite», »porphyritic one-feldspar granite» etc.

Epidote is sometimes characteristic of the microcline-albite granites especially, (*e.g.* unakites and helsinkites). The rock can then be indicated as, for instance »microcline-albite-epidote granite». In the same way the presence of aegirine, riebeckite, pyrochlore etc. can be indicated in the rock name.

The writer has the feeling, that using petrological classifications, the descriptions of granites from various parts of the globe be more easily comparable with each other, and, also, as far as generalizations are concerned, such names will lead to fewer discrepancies than do the rock names used at present. Tonalite, adamellite and granite have been used by various authors for the same rock type. One can hardly

compare by descriptions, for instance, the granites of Hanko or Stockholm without visiting them first; or »granites» of Korhoogo, Ivory Coast, with those of Southern Finland, which, according to descriptions are rather similar, but in the field are different. Granite petrology is very important, but it can hardly be settled before definitions and nomenclature are sufficiently clear and adopted by various authors in the same way.

*Manuscript received, January 3, 1966*

#### REFERENCES

- BLACK, RUSSELL (1965) Sur la signification pétrogénétique de la découverte d'anorthosites associées aux complexes annulaires subvolcaniques du Niger. C. R. Acad. Sc. Paris, vol. 260, pp. 5 829—32.
- MARMO, VLADI (1962) On granites. Bull. Comm. géol. Finlande 201.
- MARMO, VLADI, HYTÖNEN, KAI and VORMA, ATSO (1963) On the occurrence of potash feldspars of inferior triclinicity within the Precambrian rocks in Finland. Bull. Comm. géol. Finlande 212, p. 51.
- WAHL, WALTER W. (1936) The granites of the Finnish part of the Svecofennian Archaean mountain chain. Bull. Comm. géol. Finlande 115, p. 489.



# ÜBER DIE ENTSTEHUNG DES INNEREN SALPAUSSELKÄ ZWISCHEN JAALA UND SAIMAA

VON  
KARL MÖLDER

*Geologische Forschungsanstalt, Otaniemi, Finnland*

## ZUSAMMENFASSUNG

Es wird die Entstehung des Zweiten Salpausselkä zwischen dem Kirchdorf Jaala und dem See Saimaa behandelt. Der Verfasser kommt zu den Ergebnissen, dass die Ose, die dieselbe Richtung wie Salpausselä haben, während dieser Zeit entstanden sind, wenn das Landeis recht dünn war und an den beiden Seiten des Salpausselkä lagte. Am Ende der Abschmelzung dieses Landeises war die Landeisbewegung von West nach Ost. Später hat das Landeis von NW nach SE bewegt. Erst nachdem haben die späteren Wasserstadien das Aussehen des Salpausselkä deutlich geändert und die Tiefungen zwischen den Osen im Salpausselkä erfüllt.

## INHALTSVERZEICHNIS

	Seite
Einleitung .....	76
Die Oberflächenformen des Zweiten Salpausselkä zwischen dem Kirchdorf Jaala und der Eisenbahnstation Selänpää .....	80
Anttilankangas .....	82
Der Salpausselkä zwischen Hevosoja und Tuohikotti .....	83
Kallinkangas .....	84
Järvi Taipale .....	84
Siilinkangas .....	85
Der Salpausselkä zwischen Siilinkangas und Savitaipale .....	86
Der Salpausselkä zwischen Savitaipale und Saimaa .....	87
Über die Entstehung der Ose im Salpausselkä .....	88
Die Bewegung des Landeises .....	90
Literaturverzeichnis .....	92

## EINLEITUNG

Seit mitte des vorigen Jahrhunderts haben Geologen in Finnland dem Äusseren und Inneren Salpausselkä Aufmerksamkeit zugewandt. Schon im Jahre 1876 schrieb Wiik in der Erläuterung zum Finnischen Atlas, dass beide Salpausselkä Moränenbildungen seien. Erst im Jahre 1889 veröffentlichte Sederholm die erste Untersuchung über die Bildungen der Eiszeit im inneren Finnland, und er äussert die Meinung, dass beide Salpausselkä eine Randmoräne des Landeises seien. Er schreibt: »Von diesen beiden Höhenzügen ist es schon lange von Wiik nachgewiesen, dass sie, gleichwie ihre Fortsetzungen gegen SW, der sogenannte Lojoås und dessen nördliche Parallelkämme, als Endmoränen betrachtet werden müssen. Später ist durch De Geer die wahrscheinliche Zusammengehörigkeit mit den schwedischen Endmoränen in der Gegend von Wener-See und die norwegischen Raén im Kristiania-Fjord und längs der Ostküste Norwegens dargethan.»

Im folgenden Jahre erschien von Frosterus (1890) eine kleine Untersuchung, in der er ein Querprofil durch den Ersten oder Äusseren Salpausselkä aus der Stadt Kouvola darstellt. Dieser Querschnitt ist ganz eigenartig, denn heutzutage sind an dieser Stelle ähnliche Ablagerungen nicht mehr zu finden. Es ist möglich, dass die Buchstaben S und N in der Abbildung verwechselt worden sind. An der Südseite des Salpausselkä kommen dicke Uferablagerungen vor, die aber in dem von Frosterus wiedergegebenen Querprofil fehlen.

Im Jahre 1890 unternahm W. Ramsay eine Reise nach Ostfinnland, wo er die Fortsetzung der beiden Salpausselkä untersuchte. Über die Ergebnisse dieser Reise veröffentlichte er im Jahre 1891 die Untersuchung: »Über den Salpausselkä im östlichen Finnland.« Aus dieser Untersuchung geht hervor, dass zwischen Lappeenranta und Joensuu Schrammen vorkommen, die von West nach Ost gerichtet sind. Ausser diesen Richtungen gibt es auch Schrammen, die von Nordwest nach Südost gerichtet sind. Er konnte zwei Landeisbewegungsrichtungen feststellen, von denen die ältere von Westen nach Osten und jüngere südlich gerichtet gewesen ist. Über den Jaamankangas schreibt er: »Die breite Sand- und Grusablagerung Jaamankangas auf der Südseite des Sees Höytiäinen ist auch eine Endmoräne.« Nach seinen Beobachtungen kommt er zu den Schlussfolgerungen, dass der Salpausselkä und auch die innere Randmoräne bis nach Joensuu reichen und von da knieförmig nach Osten abbiegen.

Im Sommer 1891 machte Rosberg (1892) eine Exkursion nach Finnisch- und Russisch-Karelien, um die Fortsetzung der beiden Salpausselkä in diesem Gebiet festzustellen. Von der Stadt Joensuu aus verfolgte er nach NE die beiden, etwas zerstückelten Parallelmoränen bis 63°15' n. Br., wo der Erste oder Äussere Salpausselkä nicht mehr kenntlich war. Der Innere Salpausselkä liess sich bis 66° n. Br. verfolgen. Er konnte während dieser Reise auch zwei verschiedene Schrammensysteme unterscheiden, von denen die west-östliche weniger deutlich war. Wie aus seiner Karte zu ersichtlich, sind diese Bildungen, die er als Salpausselkä ansieht,

sehr zerstückelt und erinnern nach der Beschreibung im Text mehr an Ose als an Randbildungen oder Endmoränen. Russische Geologen haben in letzter Zeit diese Gegenden eingehend untersucht und zu der Überzeugung gekommen, dass diese von Rosberg als Salpausselkä angegebene Endmoränen gewöhnliche Ose sind.

In seiner Arbeit schreibt Berghell (1893), dass bei der Stadt Lappeenranta der Salpausselkä als mächtiger Sandwall auftritt, wo an mehreren Stellen auf Randmoräne eine ca. 1 m mächtige Grundmoräne lagert. Spätere Untersuchungen haben aber erwiesen, dass diese von Berghell angenommenen Grundmoränen eigentlich Randbildungen sind.

Im Jahre 1899 veröffentlichte Rosberg eine neue Untersuchung über Oberflächenbildungen in Karelrien mit besonderer Berücksichtigung der Endmoräne. Auf dieser Untersuchungsreise begab er sich bis zum Weissen Meer und fand auch einige Endmoränen. Diese Endmoränen haben aber mit den eigentlichen Endmoränen nichts zu tun, und spätere Untersuchungen haben bestätigt, dass alle diese Bildungen Ose sind.

Erst 21 Jahre später veröffentlichte Leiviskä (1920) seine umfangreiche und ausführliche Untersuchung über die beiden Salpausselkä, in der er sogar 434 Querprofile aus der Oberfläche der beiden Salpausselkä darstellt. In dieser Arbeit gibt er 27 Detailkarten von verschiedenen Stellen der Salpausselkä und eine Karte über die Verbreitung der Randmoräne in Finland. Diese Untersuchung hat der Verfasser im Verlaufe von 10 Jahren durchgeführt, und da er Geograph gewesen ist, gibt die Untersuchung viel Neues in diesem Sinne.

Es ist schade, dass er in dieser Arbeit für geologische Fragen so wenig Raum vorgesehen hat, insgesamt nur sieben Seiten. Auf der Seite 240 schreibt er: »In den mehreren hundert verschiedenartigen Aufschlüssen, die ich den verschiedenen Teilen des Salpausselkä gesehen und studiert habe, war überall fast ohne Ausnahme ein deutlich geschichtetes Schuttmaterial zu beobachten, aus dem man also den Schluss ziehen kann, dass das Baumaterial des Salpausselkä in Osmaterial besteht.« Über die Entstehung des Salpausselkä schreibt Leiviskä auf Seite 341 folgendes: »Kurz, man gewinnt überall in beiden Salpausselkä die bestimmte Vorstellung, dass der Salpausselkä einen selbständigen Rücken bildet, welcher keineswegs ein »Anhängsel von Längsäsen«, sondern viel mächtiger ist als die anschliessenden Längsäse, welche, wie erwähnt, bis auf einzelne Ausnahmen im Vergleich mit ihm oft so undeutend sind, dass man über den oberen Teil des Proximalabhanges wandernd den anschliessenden Längsäse kaum bemerkt.« Auf Seite 343 schreibt er: »Nach allem Vorstehenden dürfte ich mit ausreichenden Gründen behaupten können, dass die Bodenstromtheorie von de Geer u. a. auf den Bau und die Formgestaltung des Salpausselkä keine Anwendung findet oder, mit anderen Worten, dass der Salpausselkä nicht durch subglaziale Bodenströme ausgebildet worden sein kann.«

Obleich Leiviskä die beiden Salpausselkä eingehend untersuchte, konnte er dennoch die Entstehung der Salpausselkä nicht richtig deuten und musste zu Fehlschlüssen kommen. Mit grosser Mühe versuchte er zu bestätigen, wie diese Rand- oder

Endmoränen entstanden waren, und zum Beweise seiner Ansichten gab er Beispiele aus Grönland, wo noch jetzt ähnliche Randbildungen entstehen.

Im Jahre 1921 veröffentlichte Ramsay eine Untersuchung, in der er schreibt, dass beide Salpausselkä als Ablagerungen am Rande des Inlandeises während der skandiglazialen Epoche entstanden seien. Er sagt, dass beide Salpausselkä aus äusseren und inneren Reihen von Querosen beständen. In dieser Arbeit beweist er ebensowenig wie in der früheren Untersuchung, warum diese beiden Querosreihen Endmoränen darstellen und bei längerem Stillstand in Eisrandlage entstanden wären.

Im Jahre 1927 veröffentlicht Metzger eine Untersuchung über den Salpausselkä bei Lohja. Er gibt ein Querprofil durch die obersten Schichten der Bildung an und kommt zu dem Resultat, dass der Salpausselkä den Aufbau eines Deltas erkennen lässt. Es ist gewiss schade, dass dieser Querschnitt nicht genügend tief in den Salpausselkä einschneidet, so dass er keinen Einblick in alle tiefer liegenden Ablagerungen gewährt.

In demselben Jahre gab Leiviskä dem Metzger eine Erwiderung und betont, dass dieser unrichtige Schlüsse gezogen habe. Zur Unterstützung seiner Auffassung stellt er noch ein Querprofil durch den Lohjanharju dar und zeigt, dass man es hier nicht mit einem Delta zu tun habe. Zum Schluss schreibt er: »Die Profile von Lohja, wie auch die anderen Profile des Salpausselkä beweisen, dass der Salpausselkä einfach eine im Meere abgelagerte Randmoräne ist, die in ihren westlichen Teilen vollständig subaquatisch entstanden ist, während in den mittleren und besonders in den östlichen Teilen kleinere oder grössere Hügel- und Rückenpartien bei der Bildung der Moräne aus dem Meere emporragten.»

Brenner und Tanner (1930) untersuchten einen Eisenbahnschnitt der Strecke Lahti—Heinola und kamen zu dem Ergebnis, dass der Äusserste Salpausselkä keine Deltabildung sei und ein grösserer Schmelzwasserstrom an Stelle nicht gemündet haben könne. Nach den Verfassern ist das Material des Salpausselkä seiner Ablagerungsstelle auf verschiedene Weise verfrachtet und während des Abschmelzens des Landeises subaquatisch abgelagert worden.

1933 veröffentlichte Tanner durch den Inneren Salpausselkä geführten Querschnitt bei Vierumäki, der wegen des Eisenbahnbaus angelegt worden war. Wie aus Fig. 5 ersichtlich ist, liegt glazifluvialer Schotter auf dem Felsgrund und lagern auf dem Distalhang Sandschichten, die schräg nach Süden fallen. Diese Sandablagerungen sind alte uferbildungen, die erst dann entstanden sind, nachdem das Wasser südlich bis zum Innersten Salpausselkä gereicht hatte. Der obengenannte Querschnitt durch den Zweiten Salpausselkä ist deutlich einfacher als die Querschnitte durch den Ersten Salpausselkä bei Lohja, Lahti und Kouvola.

In seiner Untersuchung stellt Leiviskä (1951) noch Väärämäenselkä, Jyväskylänharju und Jaamankangas als Randmoränen dar und vergleicht sie mit den beiden Salpausselkä. Er kommt zu dem Schluss, dass alle obengenannten Bildungen gleicherweise entstanden sind und deshalb auch Randmoränen oder Endmoränen wären.

Zur Bestätigung seiner Auffassung bringt er Beispiele von Island, wo er ähnliche Bildungen gefunden hat.

Im Jahre 1958 veröffentlichte V. Okko eine Untersuchung über den Inneren Salpausselkä bei Jylisjärvi. Aus der beigelegten Karte geht deutlich hervor, dass in dieser Gegend einzelne Osbildungen in der Richtung der Salpausselkä vorkommen. Neben obengenannten Osen treten auch Moränenrücken auf, die man Jahresmoränen nennt. Er kommt zu dem Schluss, dass die Umgebung von Jylisjärvi schon während der jüngeren Dryaszeit vom Landeis befreit gewesen sei und dass Salpausselkä an dieser Stelle während der Allerödzeit habe entstehen können, m. a. W. 9 000—10 000 Jahre vor unserer Zeit.

In seiner Untersuchung zur Frage des inneren Baus des Zweiten Salpausselkä in Finnland beschreibt Sauramo (1931) einen Querschnitt von Vierumäki. Er gibt das Material auf dem Grundfels als Moräne an. Tanner (1933) stellt in seiner Untersuchung dasselbe Material als glazifluvialen Schotter dar. Über diese Moräne schreibt Sauramo auf der Seite 304: »Indessen besteht der ganze mittlere und nördliche Teil nicht ausschliesslich aus Moräne, sondern er enthält ebenfalls Sand und Kies, und zwar in fragmentarischen, so gut wie waagerechten Schichten, deren Dicke im allgemeinen zwischen 0.25 und 1 m variiert. Mancherorts gibt es auch mehrere, von Moränenlagen abgetrennte Sandschichten übereinander.«

Nach dem Tode Sauramos erschien im Jahre 1958 seine Untersuchung über die Geschichte der Ostsee, worin der Verfasser der Beschreibung der beiden Salpausselkä beträchtlichen Raum zukommen lässt. Grösstenteils stellt er schon früher veröffentlichte Untersuchungen nochmals dar. Obgleich Sauramo im Text auch Untersuchungen zitiert, in denen abweichende Resultaten vorkommen, schreibt er kein Wort darüber, warum diese Autoren abweichende Ergebnisse erreicht haben. Auf Seite 91 schreibt Sauramo: »Im Kirchspiel Jaala löst sich die Randbildung in mehrere parallele Moränenrücken auf, die keine Zeugnisse für unseren Zweck bieten. Erst in einer Entfernung von etwa 30 km, bei der Eisenbahnstation Selänpää, setzt eine neue Plateaurihe mit dem 10 km langen und stellenweise nahezu 3 km breiten Schotterfeld von Anttilankangas (Heide von Anttila) ein. Es mag als Ideal einer südfinnischen fluvioglazialen Marginalbildungen gelten. Im N ein charakteristischer Proximalhang, der Eiskontakt der Randmoräne mit dem ehemaligen Inlandeis; an der einstigen Meerseite wiederum ein nach S lobenförmig vorspringendes Delta der Schmelzwässer.«

Im Jahre 1960 veröffentlichte der Verfasser dieser Untersuchung eine kleinere Arbeit, in dem er die Meinung aussagte, dass Innere Salpausselkä zwischen dem Kirchdorf Jaala und des Sees Saimaa keine Rand- oder Endmoräne ist. Zweite Salpausselkä enthält in dieser Strecke schon über 40 Ose, die dieselbe Richtung wie Salpausselkä haben. Auch hat das Landeis während dieser Zeit, als die obengenannte Ose entstanden, von Westen nach Osten bewegt. Erst danach, als die Landeisbewegung von N nach S bewegte, wurde dünne Moränenablagerungen auf die Nordseite der Salpausselkä aufgelagert.

DIE OBERFLÄCHENFORMEN DES INNEREN SALPAUSSELKÄ  
ZWISCHEN DEM KIRCHDORF JAALA UND DER  
EISENBAHNSTATION SELÄNPÄÄ

Östlich des Kirchdorfes Jaala teilt der Zweite oder Innere Salpausselkä sich in mehrere parallele Ose, die länger oder kürzer sind (Abb. 1). Nicht weit von dem Kirchdorf nach Osten fangen zwei Ose an, die an der Westseite des Sees Vähä Kortejärvi enden. Diese beiden Bildungen sind nach den Oberflächenformen typische Ose, deren beide Seiten schräg abfallen und Hänge von 25—30° bilden. Eine zweite Serie von Osen fängt etwas weiter nach Osten an; die von diesen nördlicher liegende endet am Westufer des Sees Sonnanjärvi und die beiden südlicher liegenden schon früher. Auch diese drei Ose sind gut ausgebildet, und auf den Hängen ist keine Zerstörung, wie sie das Landeis während seiner Bewegung hinterlässt, wahrzunehmen.

Am Nord- und auch am Süden des Sees Sonnanjärvi finden sich wieder gut ausgebildete Ose, die aber nicht so lang sind wie der Os südlich des Sees Vähä Kortejärvi. Weiter ostwärts von den obengenannten Osen kommen wieder drei parallele Ose vor; der erste am Süden des Sees Suolajärvi, der zweite westlich des Sees Saarijärvi und der dritte SE des Sees Kamponjärvi oder Kamponen. Auch diese parallel verlaufenden Ose sind gut ausgebildet, und Zerstörungen durch Inlaneis sind nicht zu erkennen.

Vom Süden des Sees Saarijärvi dehnt sich ein mehrere km langer Os bis zu der Eisenbahn im Dorfe Selänpää aus. Nördlich von dem obengenannten Os kommen noch mehrere Osrücken vor, die alle von Westen nach Osten verlaufen (Abb. 1). Viele kurze Ose kommen ferner auf der Landenge zwischen den Seen Niskajärvi und Vuohijärvi vor. Auch diese Ose haben west-östliche Richtung. Leiviskä (1920) hat alle obengenannten Osbildungen zwischen Jaala und Selänpää eingehend beschrieben und stellt auch viele Querprofile durch die Oberfläche dar. Auf Seite 150 schreibt er: »Östlich von Jaala kommen wir in eine Landschaft, die reich an Parallelbildungen ist und uns Gelegenheit gibt, die Beziehungen zwischen den Formen des Untergrundes und zwischen den Osrücken zu erkennen.« Darauf folgt eine genaue Beschreibung dieser Osbildungen, und er kommt zu dem Schluss, dass alle obengenannten Bildungen Ose seien, zwischen denen häufig Sandablagerungen vorkämen. Sauramo (1958) schreibt über diese Ose, dass sie keine Zeugnisse für seine Zwecke seien, und lässt diese Bildungen ganz ausser acht.

Die Beschreibungen und Profile der Ose zwischen dem Kirchdorf Jaala und dem Dorf Selänpää, die Leiviskä (1920) in seiner Untersuchung darstellt, sind richtig gearbeitet und spiegeln gut die Oberflächenformen wieder. Wie aus Profil 351 zu ersehen (Leiviskä 1920), kommen östlich des Kirchdorfes nebeneinander drei parallele Osrücken vor (Abb. 1). Zwischen diesen Osen liegen Feinsandschichten, die recht hoch auf die seitlichen Hängen der Ose hinaufreichen. Da die Sandschichten die Zwischenräume zwischen den Osen ausfüllen, sind diese jetzt viel niedriger, als

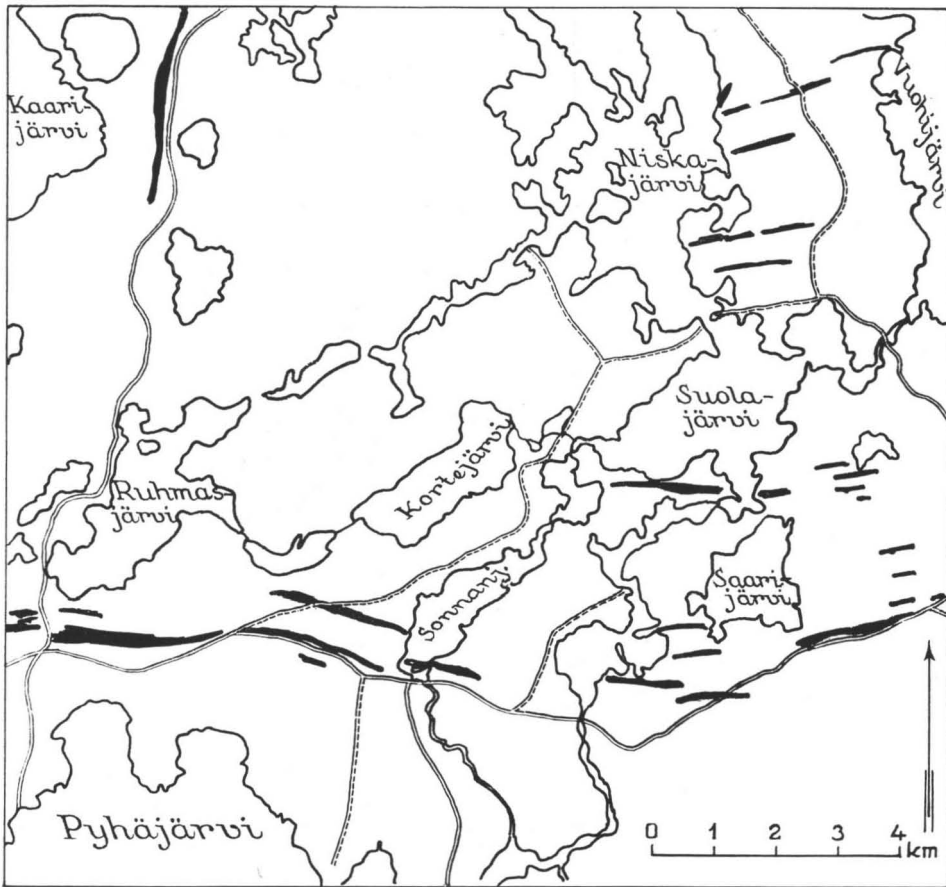


Abb. 1. Der Zweite Salpausselkä zwischen Jaala und Selänpää. Die schwarzen Striche sind die Ose.

sie nach der Entstehung waren. Leiviskä (*op. cit.* p. 150) schreibt über diese Ose folgendes: »Wenn man sich von dem Kirchdorf Jaala auf der Landstrasse nach E begibt, öffnet sich im S weite angebaute Tongebiete, während im N auf den jenseits des Weges ansteigenden Hügelabhängen hier und da das Felsengerüst sichtbar ist. Nachdem wir ein paar Kilometer gewandert sind, stossen wir nördlich von der Strasse auf einen ein paar hundert Meter langen, ca. 16 m über seine Umgebung hinausragenden länglichen Åshügel. Mit diesem beginnt ein unbedeutender, langsam nach E sich erhebender und breiter anschwellender Rücken (Karte XXV), der nach einiger Zeit südlicher von der Landstrasse einen anderen bescheidenen Rücken zum Begleiter erhält, während sich zugleich auch nördlich von ihm, durch eine sandige ebene Fläche getrennt, ein dritter, ganz unbedeutender parallelrücken ausbildet. Wie das Profil 351 zeigt, gehören jedoch alle drei zusammen.»

Zusammenfassend kann gesagt werden, dass alle obengeschilderten Bildungen zwischen dem Kirchdorf Jaala und dem Dorf Selänpää gut ausgebildete Ose sind. Es lassen sich keine Spuren auffinden, die bestätigten, dass das Inlandeis an dieser Stelle länger gestanden hätte. Während jener Zeit, als die genannten Ose entstanden sind, konnte sich das Inlandeis recht wenig nur in den Osrichtungen bewegen; wäre es von Norden nach Süden gewandert, dann hätte es die Ose zerstört. Abb. 3.

### ANTTILANKANGAS

Östlich von dem Dorfe Selänpää breitet sich das Plateau Anttilankangas aus (Abb. 2), das nach Sauramo (op. cit., p. 91) für seine Zwecke wichtig war. Er schreibt sogar, dass diese Heide Anttilankangas das Ideal einer südfinnischen fluvioglazialen Marginalbildung wäre.

An dieser Stelle, wo die Landstrasse über die Eisenbahnlinie führt, liegt am Südrande des Plateaus ein Os, dessen Richtung westöstlich ist, der aber nicht auf die Oberfläche des Anttilankangas steigt. Auf dem Südhang des Oses finden sich alte Uferablagerungen, die in dünnen Schichten die Oberfläche des Oses bedecken. Die Richtung des Oses ist west-östlich, und auf der Oberfläche lässt sich die höchste Stelle ca. 100 m verfolgen. Wahrscheinlich ist dieser Os noch länger, aber später entstandene Uferablagerungen bedecken die Oberfläche des Oses.

Von der obengenannten Stelle ca. 400 m nordwärts setzt sich der Os von der Westseite über die Eisenbahnlinie nach Osten fort. Am Rande des Plateaus ist der Os als steiniger Kamm zu sehen und verschwindet weiter ostwärts in der Oberfläche des Plateaus. Ungefähr 400 m weiter nach Osten erscheint der Os wieder als niedriger Rücken auf der Oberfläche des Plateaus und ist zum Teil 0.5 m hoch. Ostwärts steigt dieser Rücken immer höher. Er ist in der von Leiviskä dargestellten Karte XXV am Nordrand des Plateaus zu sehen.

Beinahe in der Mitte des Plateaus kommt noch ein Os vor, der aber nicht so deutlich auf die Oberfläche des Plateaus steigt. Während Bauarbeiten konnte Verfasser der vorliegenden Untersuchung diesen Os feststellen. Das Osmaterial reichte tief in das Plateau hin ein. Bisher haben drei Ose dem Plateau Anttilankangas festgestellt werden können, die alle parallel von Westen nach Osten verlaufen. Es ist möglich, dass dieses Plateau noch mehrere Ose birgt, die aber nur dann festgestellt werden können, wenn Kiesgruben an den entsprechenden Stellen vorhanden wären.

Nach Sauramo (1958, p. 91) wäre die Heide Anttilankangas ein typisches Delta, das am Inlandeisrand entstanden wäre. Die gründlichen Untersuchungen des Verfassers haben ergeben, dass die Heide Anttilankangas kein Delta ist. Am Proximalrand liegen wohl grössere oder kleinere Gruben, die während Abschmelzens des Inlandeisrandes mit Toteisblöcken erfüllt waren. In den Deltabildungen sind nie Ose zu finden, wie im Heide Anttilankangas der Fall ist, denn während der Entstehung des Deltas fliesst das Wasser vom Eisrand ab, und es ist unmöglich, dass unter solchen

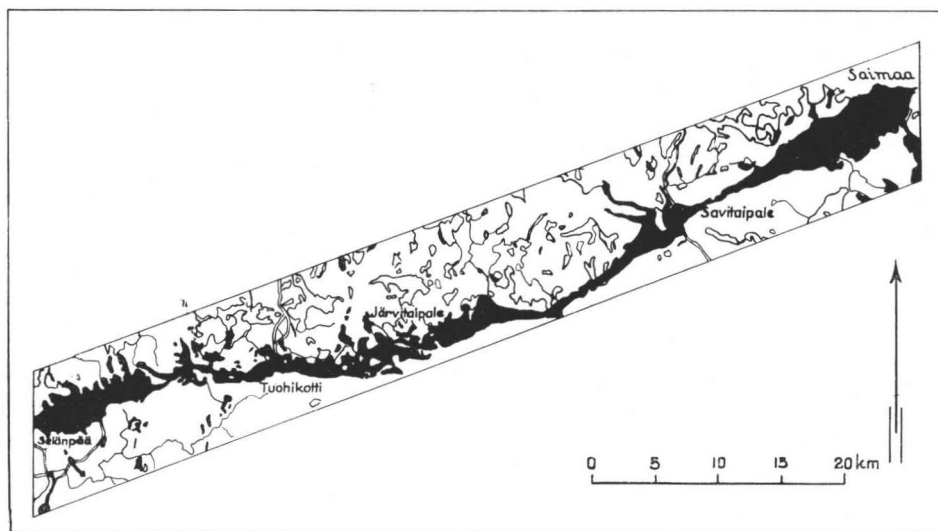


Abb. 2. Innere Salpausselkä zwischen Selänpää und Saimaa.

Verhältnissen in einem Delta Ose entstehen können, wie jetzt ihrer drei im Plateau Anttilankangas vorkommen.

Am Distalrand finden sich derartige vom Toteis hinterlassene Gruben nicht, weil südlich des Inneren Salpausselkä grössere Wasseransammlungen waren, die auch die Heide Anttilankangas zum grössten Teil bedeckten, und in der Uferregion erfüllten Uferablagerungen alle Unebenheiten ausgeglichen hat. Am Distalrand des Plateaus waren keine Spuren eines Deltas zu finden. Man muss zu dem Ergebnis kommen, dass die Zwischenräume zwischen den parallel laufenden Osen, die von Westen nach Osten liegen, nach deren Entstehung von dem Wasser mit Grus und Sand erfüllt worden sind und dass die Heide Anttilankangas kein Delta ist.

#### DER SALPAUSSELKÄ ZWISCHEN HEVOSOJA UND TUOHIKOTTI

Von der Wegkreuzung nach Hevosojä am östlichen Ende des Plateaus Anttilankangas wird der Salpausselkä wieder Osartig. Ungefähr 500 m weiter ostwärts erhebt sich ein Os ca. 5—10 m über die Umgebung. Es ist ungefähr 150—180 m lang und die Richtung westöstlich. Auch dieser Teil des Salpausselkä von Hevosojä bis Tuohikotti ist ein richtiger Os, auf dessen Scheitel die Landstrasse von SW nach NE verläuft (Abb. 2). Die Höhe schwankt in diesem Teil zwischen 110 und 125 m ü. d. M., und die höchste Stelle liegt sogar 155 m ü. d. M.

Nicht weit von der Wegkreuzung Hevosojä ostwärts tritt Urfels im Salpausselkä an die Oberfläche, in der sich eine recht weite Spalte auftut. Diese Spalte war damals, als das Inlandeis nördlich des Zweiten Salpausselkä lag, ein Urstromtal,

durch dessen das Wasser von Norden nach Süden geflossen hat. Am Süden des Urstromtales kann man noch deltaförmige Bildungen finden, die wahrscheinlich während dieser Zeit entstanden sind, als das Wasser an der Nordseite des Salpausselkä hoch stand und über diese Schwelle strömen konnte.

Östlich des Urstromtales setzt sich der Salpausselkä osartig fort und nördlich des Dorfes Kääpäälä findet sich ein Parallelos, dessen Richtung ost-westlich ist. In der Mitte dieses Oses ragt Grundfels ca. 1 m über die lose Bildungen und ostwärts des Felses kommen grosse Steinblöcke vor, die ostwärts kleiner werden und schliesslich vollständig verschwinden. Zwischen diesen Parallelosen finden sich Sandablagerungen, die sortiert sind und wagerecht liegen. Erst unweit des Dorfes Tuohikotti verbreitert sich der Os wieder und wird eine weite flache Ebene. An dieser Stelle, wo der Salpausselkä seine osartige Form verliert, erstrecken sich an der Nordseite zwei kleine Ose, die ca. 150—200 m lang sind. Wie die Untersuchungen bestätigt haben, liegt das Osmaterial auf der Grundmoräne, und umgekehrte Fälle kamen nicht vor. Wie aus dem Obigen ersichtlich, besteht der Salpausselkä zwischen Hevos-oja und Tuohikotti nur aus Osen, die zum Teil während späterer Zeit verflacht sind. Nirgends war Randmoräne zu finden, ausgenommen die einzelnen kleinen Bildungen, die an zwei Stellen am Nordrand vorkamen.

#### KALLINKANGAS

In dem bei dem Dorfe Tuohikotti einsetzenden Plateau Kallinkangas liegen wieder zwei Parallelose, die über die Oberfläche der Ebene reichen. Diese Ose haben west-östliche Richtung und sind an einigen Stellen von Toteisgruben unterbrochen. Leiviskä (1920) beschreibt diese Teile des Zweiten Salpausselkä sehr oberflächlich, und diese beiden niedrigen Ose sind in seiner Arbeit mit keinem Wort erwähnt. Er beschreibt wohl einige andere Ose, die auch von Westen nach Osten laufen und deutlich höher sind als die obengenannten. Zum Schluss schreibt Leiviskä (1920): »Ungefähr 13 km von Tuohikotti wird die fortwährend ebene dahinlaufende Heide von einem mitten auf ihr aufragenden Felsen unterbrochen, worauf die Landschaft eine Zeitlang sumpfig und felsig ist und Moorsetzen zwischen die niedrigen Hügel und die Heidebruchstücke eindringen.« Auch in diesem Plateau kommen Ose vor, deren Zwischenraum später ausgefüllt und gebnet worden ist

#### JÄRVITAIPALE

Seine Name hat Järvitaipale dadurch erhalten, dass in dieser Gegend des Salpausselkä die Seen Löytösenlampi, Pyöreäjärvi, Kauriolampi, Torkkelinlampi, Matalajärvi, Riihijärvi und viele kleinere Seen vorkommen (Abb. 2). Alle obengenannten Seen liegen zwischen höheren Felsen und Osen, die von Westen nach Osten und von Norden nach Süden laufen. An diesen Stellen, wo jetzt die Seen auftreten, lagen



Abb. 3. Querschnitt durch den Salpausselkä in Järvitaipale.

während des Abschmelzens des Inlandeises grössere oder kleinere Toteisblöcke. Erst nachdem dieses Toteis abgeschmolzt war, erfüllte es die hinterlassenen Vertiefungen mit Wasser. Die an dieser Stelle aufragenden hohen Felsen haben das Inlandeis so zerrissen, dass jetzt in der Umgebung von Järvitaipale schöne Längs- und Querose vorhanden sind (Abb. 3). Westlich der Seen Kauriolampi und Pyöreäjärvi geht ein Os in NS- Richtung quer über dem Salpausselkä und verbreitert sich am Südennde zu einem weiten Plateau. Zwischen den Seen Matalajärvi und Riihijärvi liegt ein Os, dessen Richtung west-östlich ist und der ca. 8—10 m über die Umgebung steigt. Östlich der Seen erhebt sich der Os ungefähr ca. 14 m Höhe, über der Salpausselkä reichenden Osrücken. Nicht weit von dem obengenannten Os südwärts tritt, von einer Mulde getrennt, südlich der Landstrasse ein Os auf, ein Begleiter des ersteren. Weiter östlich kommen noch einige kurze Ose im Salpausselkä vor, die alle dieselbe west-östliche Richtung haben wie der Salpausselkä selbst. Von dem Seegebiet nach Osten wird die Landschaft ebener, und die steinigen Hügel werden auch niedriger. Leviskä hat kein Querprofil durch den Järvitaipale wiedergegeben, und auch die Beschreibungen sind so mangelhaft, dass man keine richtige Vorstellung von dieser Stelle erhält. Obgleich die Landschaft in dieser Umgebung sehr zerrissen ist, sind auch die vorhandenen Ose an dieser Stelle zuerst entstanden, und erst danach haben die Sandablagerungen die Zwischenräume zwischen den Osen ausgefüllt. Die Quer- und Längsöse bestätigen uns, dass das Inlandeis in dieser Zeit, als die Ose entstanden, nicht viel bewegt hat, sonst hätte das Eis die Ose vernichtet.

### SIILINKANGAS

Vom Järvitaipale und von der durch Moore zerrissenen Strecke des Salpausselkä ostwärts fängt die Heide Siilinkangas an. Dieses Plateau breitet sich als steinfreie *Calluna*-Heide an beiden Seiten der Landstrasse aus, die nach Savitaipale führt.



Abb. 4. Ostseite des Grundfelsens nicht weit von Järvitaipale.

Die nordwestliche Hälfte ist unebener als die südlichere, und da kommen Osrücken, Felsen und Toteisgruben überall vor. In einigen Gruben gibt es kleine Weiher, an deren Ufern Ose vorkommen. Auf der Oberfläche dieser Heide liegen waagerechte, vom Wasser sortierte Sandablagerungen. Während der Entstehung dieser Heide muss das Ufer recht nahe gewesen sein, so dass die Uferwellen die Oberfläche ausebnen konnten. In der Mitte sowie am Südrande des Plateaus kommen nackte Felsen vor, deren Westseite von dem Inlandeis abgeschliffen worden und auf deren Ostseite die Felsen scharfkantig geblieben sind (Abb. 4). Diese Felsen zeigen uns, dass das Inlandeis am Anfang von Westen nach Osten bewegt hat und erst nachdem die nördliche Richtung genommen bekam.

#### DER SALPAUSSELKÄ ZWISCHEN SIILINKANGAS UND SAVITAIPALE

Von der Wegkreuzung Mäntyharju nach Osten wird die Heide Siilinkangas schmaler, und auch Toteisgruben kommen häufiger vor. Nördlich des Salpausselkä liegt der buchtenreiche See Virmajärvi. Am Südufer des Sees erstreckt sich niedrige Ose, alle in WE-Richtung. Ungefähr 6 km von der Heide Siilinkangas nach Osten läuft der Salpausselkä osartig weiter. An dieser Stelle, wo der grubenreiche Salpausselkä endet, geht ein Os quer über den Salpausselkä, dessen Richtung NW-SE ist. Östlich des Queroses breitet sich die Ackerhügellandschaft des Dorfes Vainikka am Südufer des Sees Virmajärvi. Der Salpausselkä setzt sich durch das Dorf Vainikka als niedrige steinige Hügellandschaft fort, bis am anderen Ende Dorfes wieder ein Os, mit dem Namen Heidunlachi, anfängt.

Am Anfang ist dieser Os ziemlich schmal, wird aber nach Osten breiter und auf der Oberfläche unebener. Am NE-Ende des Oses kommen Felsen vor und unter-

brechen beinahe völlig die Osbildung. Leiviskä (1920) hat sein Profil 372 an dieser Stelle, wo der Os breit ist und seine äussere Form nicht mehr gut hervortritt, aufgenommen. Der Os erstreckt sich bis zu dem See Säänjärvi, wo er dann zwei Verzweigungen bildet. Diese beiden Teile, die ca.  $\frac{1}{2}$  km voneinander entfernt liegen, reichen bis zu dem Huuhanjärvi, wo sie sich wieder vereinigen. Allmählich wird der Os zu einem, das sich bis zu dem Kirchdorf Savitaipale fortsetzt und dessen Nordseite mit Gruben und Aufschüttungen bedeckt ist. Östlich der Wegkreuzung nach Luumäki finden sich am Nordrande des Plateaus vier Parallelose, die sich 4—5 m über die Oberfläche der Umgebund erheben und die Richtung N 30 E haben. Am Ostende des Plateaus erhebt sich ein Os ungefähr 10—15 m über die Umgebung und ist 300 m lang.

Etwa 2.5 km westwärts der Kirche Savitaipale geht das Plateau in eine Grubenlandschaft über, die sich am südöstlichen Ende des Sees Kuolimojärvi zu einem breiten Osknoten erweitert. An diesen Osknoten schliessen sich beiderseits des Sees Kuolimojärvi nach NW gehende Ose. In der Umgebung des Kirchdorfes Savitaipale sowie bis 2 km ostwärts kommen in Salpausselkäplateau tiefe Toteisgruben vor, die zum Teil mit Wasser erfüllt sind. Wie aus Obigem hervorgeht, treten auch in diesem Teil des Salpausselkä häufig Ose auf, die alle dieselbe Richtung haben wie der Salpausselkä.

#### DER SALPAUSSELKÄ ZWISCHEN SAVITAIPALE UND SAIMAA

Etwa 2 km vom Kirchdorf Savitaipale nach NE endet die Grubenlandschaft, und der Salpausselkä wird wieder schmaler und osartiger. Dieser osartige Salpausselkä setzt sich bis zu dem Dorf Hyrkkälä fort und endet da, wo ein Fels aufragt. In dieser Gegend findet man überall Felsen, die von Sandablagerungen umgeben sind. Weiter ostwärts wandelt sich der Salpausselkä wieder in eine Osheide, die bald in einen ziemlich breiten Osrücken übergeht. Auf der Oberfläche des Osrückens sind einige Kammbildungen zu sehen, die Ost-westliche Richtung haben und die eigentlich obere Teile von Parallelosen sind.

An der Grenze der Kirchspiele Savitaipale und Taipalsaari setzt wieder ein Plateau ein, das eine beträchtliche Breite erreicht. Dieses Plateau, Taipalsaari genannt, setzt sich nach NE fort und wird bis 4 km breit. Am Nordrande erhebt sich bei dem Dorfe Solkinen ein einzelner Oshügel, auf dessen Scheitel eine Grube liegt, die dan Os in zwei Gipfel teilt. Ein anderer gesonderter Osrücken steigt NE vom Dorfe Pönnilä auf und ist durch ein Moor von dem Proximalabhang des Salpausselkä getrennt. Wie im Untersuchungsgebiet überall, finden sich auch hier auf der Oberfläche des Plateaus Unebenheiten und kesselige Gruben, wo einst Toteis vorhanden war. Auf Oberfläche des Plateaus sieht man einige niedrige Osrücken, die miteinander parallel und in der Richtung des Salpausselkä verlaufen. Das NE-Ende des Plateaus, Sarviniemi, ist eine ziemlich niedrige zweiteilige Landzunge oder



Abb. 5. Südseite des Oses im zweiten Salpausselkä am Ufer des Sees Saimaa.

Oszunge, die sich noch unter dem Spiegel des Sees Saimaa als unterseeischer Rücken fortsetzt (Abb. 5).

Wie aus der obigen Beschreibung zu ersehen, kommen in Zweiten Salpausselkä zwischen dem Kirchdorf Jaala und dem See Saimaa insgesamt über 40 längere oder kürzere Ose vor, die alle die Richtung des Salpausselkä haben. Mehrere sind gut erhalten und ragen über die Oberfläche des Salpausselkä auf. Andere wiederum liegen im Sand oder Grus und bilden dadurch breite Plateaus, wie z. B. Anttilankangas, Taipalsaari u. a. Einige gut erhaltene Ose steigen sogar bis 10 oder 15 m über die Umgebung auf, und beide Hänge sind unzerstört. Wäre das Inlandeis während seiner letzten Bewegung über diese Ose hinweg gegangen, so hätte es auch sie zerstören müssen.

#### ÜBER DIE ENTSTEHUNG DER OSE IM SALPAUSSELKÄ

Besondere Aufmerksamkeit haben die Geologen in Fennoskandien den Osen gewidmet, denn diese Bildungen sind in den peripheren Teilen des Vergletscherungsgebietes gut entwickelt. Über die Entstehung der Ose sind mehrere Theorien aufgestellt worden. Von diesen Theorien sind zu nennen: Inlandeistheorie, Oberflächenstromtheorie, Bodenstromtheorie, Deltatheorie und Innenmoränentheorie. Keine von diesen Theorien kann die Entstehung der Ose in allen Gegenden, wo sie vorkommen, befriedigend erklären.

In Finnland hat die Deltatheorie in den letzten Jahren Anklang gefunden. So kommt Sauramo (1958) zu dem Schluss, dass alle Ose in Finnland subaquatisch entstanden wären. Leiviskä (1928) dagegen erweist, dass die Ose in Finnland in den

inneren Teilen des bewegten Inlandeises während der Zeit des Abschmelzens aus Innenmoräne entstanden seien. Einige Ose hätten sich sogar unmittelbar am Inlandeiserande gebildet. In diesem Falle könnte der Eisrand auf beiden Seiten des Oses gelegen haben und nicht nur auf der einen Seite. Über die Vorstellung Leiviskäs schreibt Sauramo das Ergebnis über die Unabhängigkeit der Ose von dem Niveau des Wasserspiegels nicht stichhaltig sei. Sauramo beendet seine Arbeit mit den Worten: »Also scheint es mir, dass die in den Geologenkreisen der gesamten Welt allgemein vertretene Ansicht aufrecht bleibt, nach welcher die Ose Wassersedimente sind, die im Randgebiete des Landeises als hintereinander folgende Akkumulationen entstanden, und zwar in den meisten Fällen am nächsten in der Weise, wie es die Deltatheorie darstellt.«

Verfasser der vorliegenden Untersuchung konnte bei den Feldarbeiten feststellen, dass diese über 40 Ose, die im Zweiten Salpausselkä zwischen Kirchdorf Jaala und dem See Saimaa in der Richtung des Salpausselkä verlaufen, nicht als Deltabildungen entstanden sind. Einige Ose sind 10—15 m höher als die Umgebund, und beide Hänge sind steil und bilden häufig Böschungen von 30—35°. Hätte Wasser diese Ose als Deltabildungen ausgebildet, so müssten auch Wassersedimente nördlich des Inneren Salpausselkä in dieser Gegend zu finden sein. Da aber jegliche Wassersedimente völlig fehlen, haben diese Ose nicht als Deltabildungen im Wasser entstehen können. Auch fehlen in der Umgebung jegliche alte Uferbildungen, die bestätigen hätten, dass das Wasser jemals so hoch gewesen wäre, dass diese Ose als Deltaen hätten entstehen können. Gegen Deltatheorie spricht auch diese Tatsache, dass naheliegende Ose verschieden hoch emporsteigen und die Oberfläche des Wassers konnte nie so viel schwanken, dass diese Ose entstehen konnten.

Alle obengeschilderten Ose, die im Zweiten Salpausselkä vorkommen und die gleiche Richtung wie der Salpausselkä selbst haben, sind in Spalten des Inlandeises ausgebildet worden (Abb. 6). Auch könnten Tunnel im Inlandeis gewesen sein, in denen das Schmelzwasser Material für Osbildungen verfrachtet hätte. Leiviskä (*op. cit.*) schreibt über diese Osbildungen, dass sie könnten auch in dieser Weise entstanden, dass das Inlandeis an einer Seite lag und die andere Seite blossgelegt war. Die ausführlicheren Untersuchungen haben erwiesen, dass die obengenannten Ose nicht so entstanden sind, denn beide Hänge sind gleich steil. Alle diese osartige Bildungen, die so entstanden sind, wie Leiviskä gedacht hat, sind einseitig ausgebildet, und der innere Aufbau ist auch nicht so strukturiert wie bei diesen Osen (Abb. 6). Aus dieser Abbildung ist zu ersehen, dass das geschichtete Osmaterial gleichmässig nach bei den Seiten des Oses abfällt. Ein derartiger Aufbau bei den Osen kommt nur dann vor, wenn sie in Eispalten oder Tunnel aufgeschüttet worden sind und erst danach das Eis auf beiden Seiten abgeschmozen ist.

Jetzt erhebt sich die Frage, warum diese Spalten oder Tunnel im Inlandeis an dieser Stelle entstanden sind, wo jetzt der Innere Salpausselkä liegt? Es ist sehr schwer auf diese Frage zu antworten. Die Felsen, die im Untersuchungsgebiet im Salpausselkä häufig vorkommen, erreichen sich 1—3 m über die Oberfläche des



Abb. 6. Kiesgrube im zweiten Salpausselkä bei Selänpää.

glazifluvialen Osmaterials. Diese aufragenden Felsen haben wahrscheinlich das Inlandeis von unten zerrissen, und das Schmelzwasser konnte in diesen Rissen fließen und im Eis vorhandenen Sand und Grus verfrachten. Auch Leiviskä schreibt, dass Felsen vorhanden sind und häufig an diesen Stellen vorkommen, wo Ose liegen.

Damals, als die obengenannten Osen entstanden sind, war das Inlandeis schon recht dünn und lag südlich sowie nördlich des Zweiten Salpausselkä. Wie weit das Eis damals nach Süden reichte, ist schwer zu sagen, denn man findet Felsen noch bei der Stadt Kotka, dessen Westseiten niedergeschliffen sind und auf denen auch West-östliche Schrammen vorhanden sind.

### DIE BEWEGUNG DES INLANDEISES

Schon am Ende vorigen Jahrhunderts haben Geologen in Karelrien Kreuzschrammen den Felsen gefunden und feststellen können, dass das Inlandeis zwei Bewegungsrichtungen hatte. Im Jahre 1917 veröffentlichten Frosterus und Wilkman eine Kartenblatterklärung über die Umgebung der Stadt Joensuu, in der sie auch zwei Bewegungen des Eises feststellen, von denen die jüngere Bewegung west-östliche ist.

Im Jahre 1955 veröffentlichte Aurola seine Untersuchung über die Verbreitung der Asbestblöcke von Paakkila, des Serpentinegesteins von Kontisalmi, der Erzblöcke in Karhusaari nach Saksela, der Erzblöcke in den Kirchspielen Eno und Tuupovaara, der Erzblöcke von Hevoskumpu und molybdänglanzhaltiger Blöcke in der Umgebung von Suovaara. Mehrere dieser Erzverbreitungsfächern haben WNW-Richtung und bestätigen, dass das Inlandeis während der letzten Bewegung eine mehr west-östliche Richtung eingeschlagen hat. Dasselbe zeigt auch die von Frosterus und

Wilkman 1917 veröffentlichte Schrammenkarte von der Umgebung der Stadt Joensuu. Repo veröffentlichte 1957 seine Untersuchung über dieselben Gegend; er konnte viele west-östliche Schrammen finden, die deutlich bestätigen, dass das Inlandeis in west-östlicher Richtung gewandert ist.

Der Verfasser dieser Untersuchung hat auch die Frage nach der Bewegung des Inlandeises im Untersuchungsgebiet erforscht. Im Salpausselkä zwischen Jaala und Saimaa kommen viele Felsen vor, die sich ca. 1—3 m über die Oberfläche erheben. Viele dieser Felsen ragen am westlichen Ende der Ose auf und mehrere derart, dass loses glazifluviales Material auch an ihrer Westseite liegt. Bei diesen Felsen, die zwischen Jaala und Selänpää am westlichen Ende der Ose vorkommen, sind Ost- und auch Südseite scharfkantig, so dass das Inlandeis dort grössere Blöcke abgerissen hat. Diese Blöcke liegen jetzt recht nahe bei ihren Abrissstellen und weisen, dass das Inlandeis sich nicht sehr weite Strecken bewegt hat. Hätte es sich über längere Strecken verschoben, so hätte es auch die jetzt gut erhaltenen Osen vernichtet.

Im südlichen Teil der Heite Anttilankangas, ca. 4 km von der Wegkreuzung Kouvola—Tuohikotti—Selänpää, liegt südlich der Landstrasse ein Felsen, der ungefähr 1—3 m über die Umgebung oder Inneren Salpausselkä aufsteigt. Auf diesem Felsen waren Kreuzschrammen zu finden, die von Westen nach Osten und von Norden nach Süden verlaufen. Ebenso waren Süd- und Ostseite des Felsens scharfkantig und West- und Nordseite abgeschliffen. Hier haben wir mit den typischen Distal- und Proximalseiten zu tun, die in Finnland überall vorkommen. Nordwärts des Dorfes Kääpäälä kommt ein Parallelos vor, der west-östliche Richtung hat und an dessen westlichen Ende ein Felsen steht. Von diesem Felsen hat das Inlandeis grössere Blöcke abgerissen und weiter nach Osten transportiert. Diese Blöcke liegen noch auf dem Osrücken und sie werden allmählich kleiner, je weiter man nach Osten geht und verschwinden völlig am östlichen Ende des Oses.

Weiter östlich findet man noch viele Felsen in dem Salpausselkä, deren Ostseite scharfkantig und Westseite abgeschliffen ist und an denen neben den N-S-Schrammen auch W-E-gerichtete vorkommen. Aus den Kreuzschrammen konnte man feststellen, dass west-östliche Schrammen älter sind.

Alle vorgeführte Felsen und Schrammen bestätigen unwiederleglich, dass das Inlandeis sich in der Untersuchungsgebiet während der Entstehung des Zweiten Salpausselkä von Westen nach Osten bewegt hat. Während dieser Zeit entstanden supra-aquatisch die Ose, die jetzt im Zweiten Salpausselkä zwischen Jaala und Saimaa von Westen nach Osten verlaufen. Erst später entstanden die Uferablagerungen südlich des Salpausselkä und schmolz das Toteis an der Nordseite ab. Da auf der Nordseite grössere Wasseransammlungen fehlten, konnten Uferablagerungen diese Toteisgruben nicht ausfüllen, wie es auf der Südseite durch Wasser geschehen ist. Erst nachdem hat die letzte Inlandeisbewegung von Norden die kleine Moränenschichten auf die Nordseite des Zweiten Salpausselkä gebracht.

*Manuskript eingegangen am 21. Januar, 1966*

## LITERATURVERZEICHNIS

- AUROLA, E. (1955) Über die Geschiebeverfrachtung in Nordkarelien. Geol. tutkimuslaitos. Geotekn. julk. 56.
- BERGHELL, H. (1893) Beobachtungen über den Bau und die Configuration der Randmoränen im östlichen Finnland. Fennia 8, 5.
- BRENNER, Th. och TANNER, V. (1930) Södra Salpausselkä byggnad i Järnvägsskärningen för Lahti—Heinola banan. Referat: Der Bau des Südlichen Salpausselkä im Eisenbahneinschnitte der Lahti—Heinola—Bahn. Fennia 52, 9.
- FROSTERUS, B. (1890) Några iakttagelser skiktade moräner samt rullstens-åsar. Referat: Einige Beobachtungen über geschichtete Moräne und »Åsar». Fennia 3, 8.
- »— ja WILKMAN, W. W. (1917) Joensuun maalaajikartan selitys. Lehti D 3. Suomen Geologinen Toimikunta.
- LEIVISKÄ, I. (1920) Der Salpausselkä. Fennia 41, 3.
- »— (1927) Zwei Profile durch den Salpausselkä in Lohja. Fennia 47, 11.
- »— (1928) Über die Ose Mittelfinnlands. Die Entstehung des Materials und der Formen der Ose. Fennia 51, 4.
- »— (1951) Drei eiszeitliche Randmoräne. Fennia 74, 1.
- METZGER, A. A. Th. (1927) Über ein Profil durch die obersten Schichten des Salpausselkä zwischen Lohja und Keskilohja. Fennia 47, 7.
- MÖLDER, K. (1948) Die Verbreitung der Dacitblöcke in der Moräne in der Umgebund des Sees Lappajärvi. Bull. Comm. géol. Finlande. 142.
- »— (1960) Toisen Salpausselän syntytavasta Jaalan kirkonkylän ja Saimaan välisellä alueella. Geologi 1.
- OKKO, V. (1958) The second Salpausselkä at Jylisjärvi, East of Hämeenlinna. Fennia 81, 4.
- RAMSAY, W. (1891) Ueber den Salpausselkä in östlichen Finnland. Fennia 4, 2.
- »— (1921) Salpausselkä såsom geografiske benämning. En historik och förslag till nomenklatur. Referat: Salpausselkä als geographische Benennung. Historik und Vorschlag einer Nomenklatur. Fennia 42, 9.
- REPO, R. (1957) Untersuchungen über die Bewegung des Inlandeises in Nordkarelien. Bull. Comm. géol. Finlande 179.
- ROSBERG, J. E. (1892) Ytbildningar i ryska och finska Karelen med särskild hänsyn till de karelska randmoränerna. Fennia 7, 2.
- »— (1899) Ytbildningar i Karelen med särskild hänsyn till ändmoränerna. II. Referat: Oberflächenbildungen in Karelen mit besonderer Berücksichtigung der Endmoräne. Fennia 14, 7.
- SAURAMO, M. (1931) Zur Frage des inneren Baus des Salpausselkä in Finland. Zeitschr. f. Gletscherk. XIX. H. 4/5.
- »— (1958) Die Geschichte der Ostsee. Ann. Acad. Scient. Fennicae. Serie A. III. Geologica-Geographica 51.
- SEDERHOLM, J. J. (1889). On istidens bildningar i det inre af Finland. Auszug: Ueber die Bildungen der Eiszeit im inneren Finnland. Fennia 58, 3.
- TANNER, V. (1933) On the Nature of the Salpausselkä Ridges in Finland. Some old and new Data. Fennia 58, 3.

## ORBICULAR ROCK IN KURU, FINLAND

BY

AHTI SIMONEN

*Geological Survey of Finland, Otaniemi*

### ABSTRACT

The mode of occurrence and the petrographic characteristics of a new body of orbicular rock in Kuru have been briefly described. Two types of orbicules, esboitic and granitic in composition, occur in a partly granitized granodioritic matrix. The origin of the orbicular rock, due to sodium and potassium metasomatism, esboitization and granitization of the primary quartz dioritic rock, has been discussed.

### CONTENTS

	Page
Introduction .....	93
Mode of occurrence .....	94
Orbicules .....	95
Matrix .....	102
Concluding remarks .....	103
Acknowledgements .....	107
References .....	107

### INTRODUCTION

In the summer of 1960 a farmer, Mr. Albinus Suojärvi, found a peculiar orbicular rock exposed under a fallen tree in the village of Pengonpohja, Kuru parish. Later, in December 1960, Mr. Harma, an elementary school teacher, sent a short notice to the Geological Survey on the structure of the discovered rock, including a photograph. On the basis of this notice it was apparent that the rock in question was a new occurrence of orbicular rock in Finland. In the summer of 1961, detailed field work on the outcrop and collection of material for laboratory research were carried out. The results of these studies will be presented briefly in this paper and the origin of the orbicular rock in Kuru will be discussed.



FIG. 1. Geological map of the Parkusjärvi region. 1, gabbro; 2, granodiorite; 3, granite; 4, orbicular rock.

#### MODE OF OCCURRENCE

The orbicular rock in Kuru is situated south of Lake Parkusjärvi in the area belonging to the plutonic rock complex of Central Finland. The latest geological map sheet with explanations of the surrounding rock crust of the new orbicular rock has been made by Simonen (1952), who has also summarized the main characteristics of the plutonic rock province, the so-called granite province in Central Finland, which shows a continuous series from basic plutonic rock types to granites (Simonen 1960).

A geological sketch map of the environment of the orbicular rock is given in Fig. 1. It shows that the orbicular rock occurs as a fragment-like body in the plutonic rock complex along the contact zone between granodiorite and granite. Small

bodies of hornblende gabbros occur as fragments both in the granodiorite and granite. The granodiorite is grey-coloured and slightly foliated. Its main minerals are plagioclase ( $An_{30-35}$ ), quartz, potash feldspar, hornblende and biotite. The granite is red-coloured, even-grained or porphyritic and its main minerals are potash feldspar, quartz, plagioclase ( $An_{15-20}$ ) and biotite. The granite penetrates the granodiorite.

The map of the occurrence of the orbicular rock is given in Fig. 2. The maximum observed length of the body is 26 metres and its breadth about 16 metres. The direction of elongation of the orbicular rock body coincides roughly with the local N—S. strike of the surrounding rock crust.

The orbicular rock occurs as two mapable varieties. In the most southern and southeastern part of the occurrence the orbicules consist mainly of plagioclase. The coarse-grained nucleus of the orbicule is mainly plagioclase and is surrounded by a fine-grained, grey-coloured plagioclase shell (Fig. 3). These types of orbicule, rich in plagioclase, are called esboitic orbicules, after the orbicular rock in Espoo (Esbo), which is characterized by an oligoclastic composition typical of many orbicular rocks. In the northern and northwestern part of the occurrence the orbicules have, however, a pink-coloured outer shell of potash feldspar around the esboitic inner parts (Fig. 4). These orbicules, showing a granitic bulk composition, will be called granitic orbicules. The contact between the above-mentioned two principal types of the orbicular rock is gradational. Along the contact zone thin outer shells of potash feldspar (Fig. 5) appear around the esboitic orbicules, which are replaced by more granitic orbicules as the outer potash feldspar shells become gradually thicker.

The matrix between the orbicules is heterogeneous. The primary quartz dioritic matrix, occurring only as relics, has been almost totally altered by granitization into the secondary matrix of granodiorite and granite.

The map of the orbicular rock body (Fig. 2) shows that its western contact is covered by soil, but in the northeastern part the orbicular rock is bordered by granodiorite and in the southeastern part by granite. In the most southern part the contact between orbicular rock and granite is marked by a peculiar, two centimetre thick grey-coloured rim consisting of plagioclase (Fig. 6). Usually, however, this plagioclase rim is lacking. The granodiorite and granite along the contacts do not penetrate the orbicules. However, some narrow aplite granite veins, emplaced along the joints, cut sharply through the orbicular rock and orbicules (*cf.* Figs. 3 and 5). Some small faults cutting the orbicules (Fig. 7) also occur.

## ORBICULES

The orbicules of the Kuru rock, measuring 10—20 centimetres in diameter, consist of two or three different parts which are as follows: coarse-grained nucleus, grey-coloured zone of plagioclase and outer zone of potash feldspar. The outer zone of potash feldspar is entirely absent in the so-called esboitic types of orbicules.

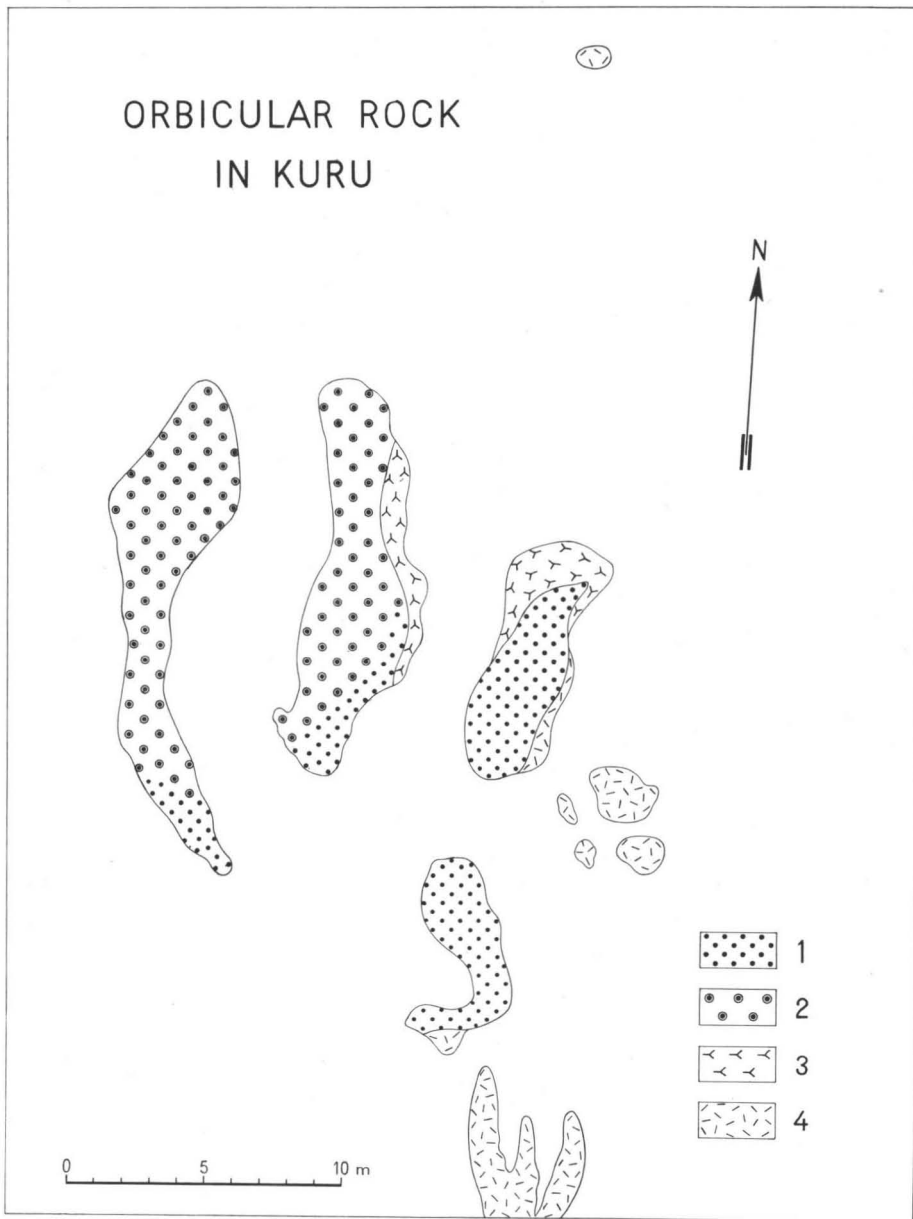


FIG. 2. Geological map of the orbicular rock in Kuru, 1, esboitic orbicules; 2, granitic orbicules; 3, granodiorite; 4, granite.

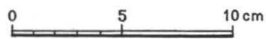
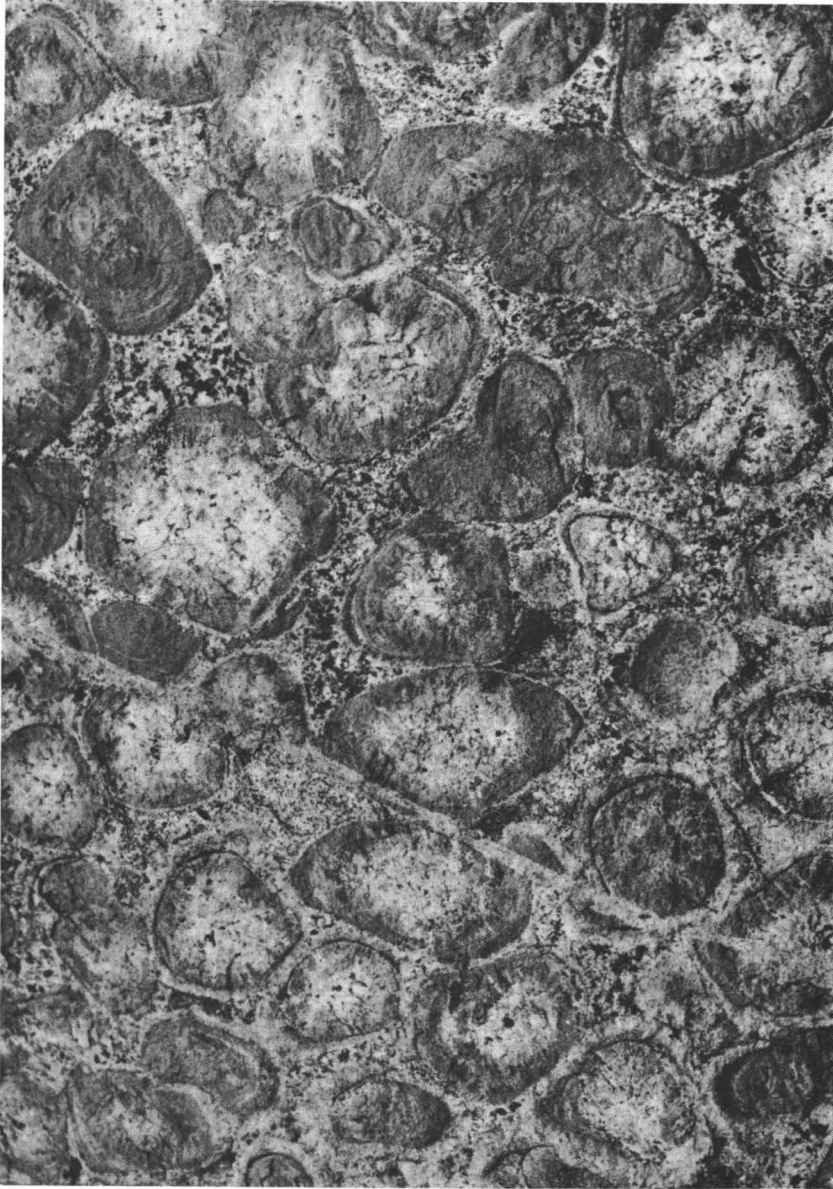


FIG. 3. Orbicular rock of Kuru with esboitic orbicules. Narrow granite dike cuts the orbicules. Photo: E. Halme.



0 5 10 cm

FIG. 4. Orbicular rock of Kuru with strongly developed potash feldspar shells around esboitic inner parts. Photo: E. Halme.

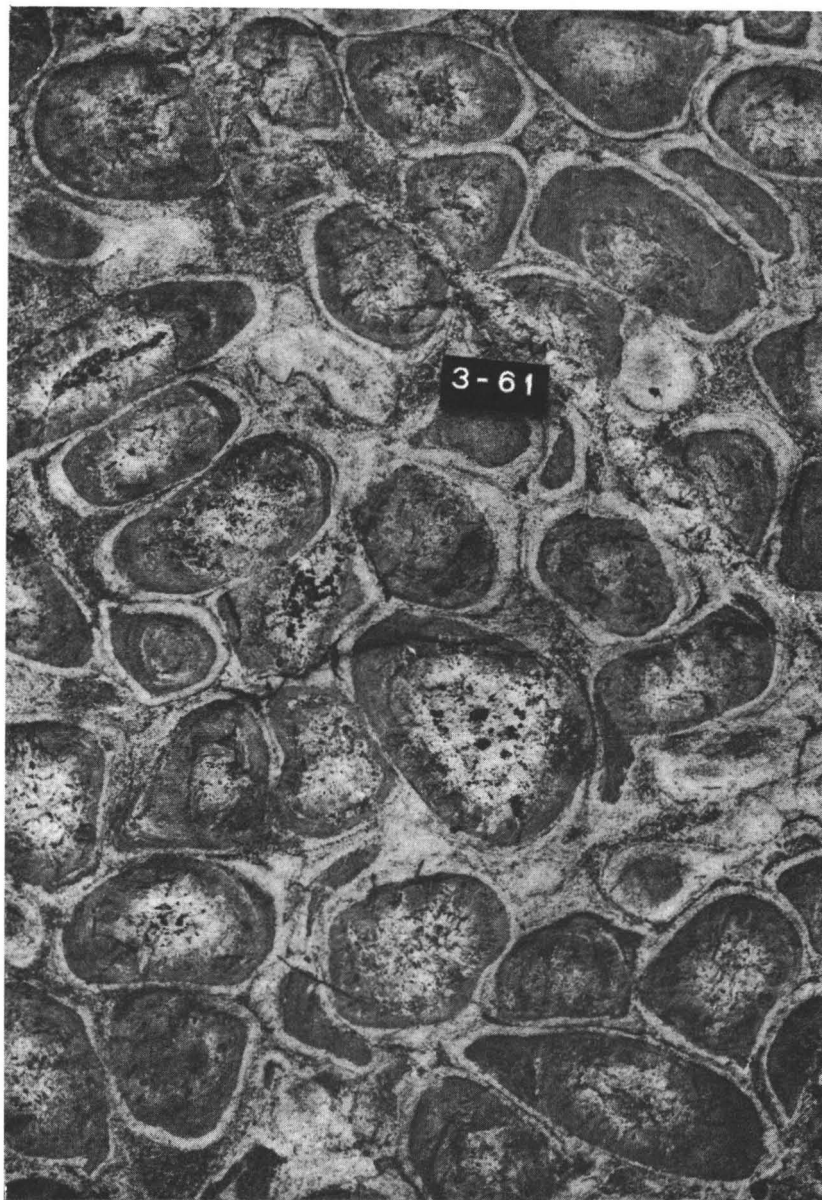


FIG. 5. Orbicular rock of Kuru with thin outer shells of potash feldspar around esboitic inner parts. Narrow granite vein cuts the orbicules. Photo: E. Halme.

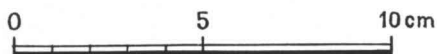
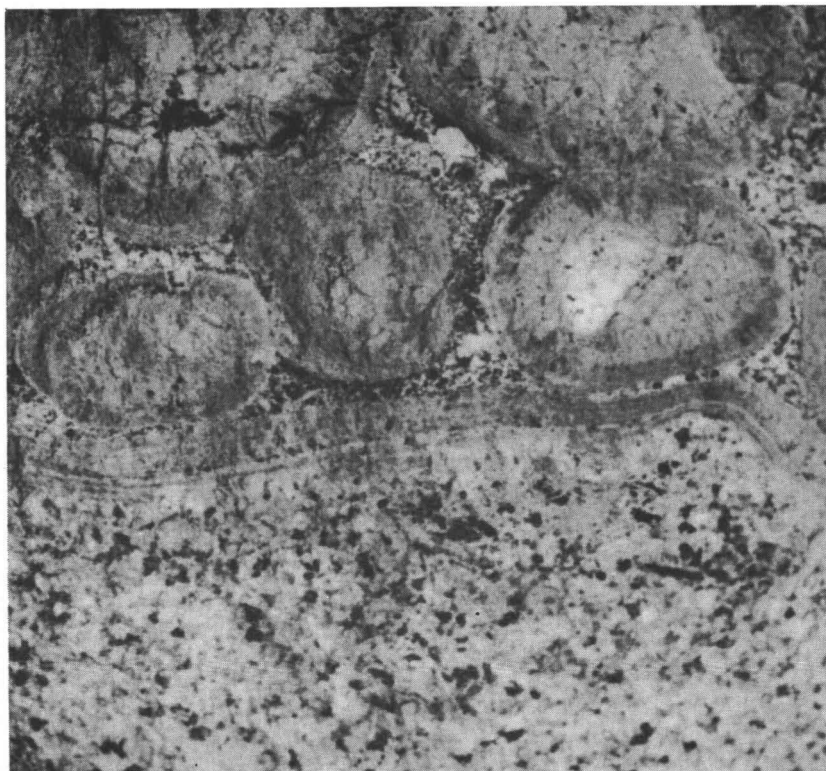


FIG. 6. Grey-coloured rim of plagioclase along the contact between the orbicular rock and granite. Photo: E. Halme.

*Nucleus of orbicule.* — The coarse-grained, light-coloured nuclei of the orbicules consist mainly of plagioclase and they are very similar to the esboitic nuclei in many other orbicular rocks. The plagioclase is andesine, whose An-content varies between the limits  $An_{35}$ — $An_{38}$ . Small quartz grains occupy the space between the plagioclase crystals and big hornblende grains with distinguishable crystal faces occur sporadically. Hornblende is partly altered into biotite. Biotite and chlorite occur as small flakes. Apatite and magnetite are accessory minerals.

The chemical composition of the nucleus is given in Table 1, anal. 1. It shows typical esboitic composition with high values of  $Al_2O_3$ , CaO and  $Na_2O$ .

*Grey-coloured plagioclase zone.* — The coarse-grained plagioclase nucleus passes gradually into a darker grey zone of plagioclase. The inner part of this zone contains sometimes grey-coloured plagioclase in a radiating arrangement while the outer part

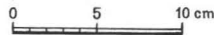


FIG. 7. Fault cutting the orbicular rock. Photo: E. Halme.

is composed of a fine-grained plagioclase mass with typical granoblastic texture. The inner, radiating plagioclase zone is usually lacking, in which case the light-coloured coarse-grained plagioclase nucleus passes gradually into the fine-grained, grey-coloured zone of plagioclase with granoblastic texture.

The grey-coloured plagioclase is andesine, whose An-content varies between the limits  $An_{33-37}$ . Small magnetite grains are common and some biotite flakes occur. Apatite is an accessory mineral.

The chemical composition of the fine-grained, grey-coloured plagioclase zone is given in Table 1, anal. 2. The composition is esboitic, but more basic than that of the nucleus.

*Outer zone of potash feldspar.* — The pink-coloured outer zone of the so-called granitic orbicules consists of potash feldspar and it borders sharply against the fine-grained plagioclase zone as well as against the matrix between the orbicules. The different development of the potash feldspar outer zone causes the most remarkable variations in the character of the orbicules. The thickness of the outer zone is usually 2—3 centimetres. In some cases the potash feldspar zone is only weakly developed and in the so-called esboitic orbicules it is entirely absent.

The potash feldspar is microcline with the degree of triclinity 0.9. It sometimes shows radial arrangement. A very few small quartz grains are observed as inclusions in microcline. Between the crystals of microcline there are small almost entirely sericitized remains of plagioclase grains. Magnetite and apatite are accessory minerals.

The chemical composition of the outer potash feldspar zone is given in Table 1, anal. 3. It is extremely rich in potassium and is entirely different from the esboitic composition of the nucleus and the grey-coloured plagioclase zone.

### MATRIX

The matrix of the orbicular rock in Kuru is heterogeneous consisting of quartz dioritic, granodioritic and granitic parts. The grey-coloured granodiorite which is fairly rich in potash feldspar is the main component of the matrix.

The medium-grained, grey-coloured quartz diorite occurs as small remains between the esboitic orbicules. Its main minerals are plagioclase ( $An_{35-38}$ ), quartz, hornblende and biotite. Secondary grains of microcline occur in the granulated mass between bigger mineral grains.

The quartz diorite must be considered as primary matrix material which has been changed by the metasomatic replacement processes into granodiorite and granite. Replacement processes upon the pre-existing minerals are due to granitization, characterized especially by the secondary increase of potassium. All gradational forms from the quartz diorite into granodiorite and further into granite can be observed and many structural relics of primary matrix have been found in partly altered gradational varieties.

The predominant matrix between both esboitic and granitic orbicules is granodiorite, whose main minerals are plagioclase ( $An_{32-35}$ ), microcline, quartz, hornblende and biotite. The potash feldspar has metasomatically corroded the primary quartz dioritic fabric so that remnants of the plagioclase grains occur as inclusions in the porphyroblasts of potash feldspar. The hornblende is partly altered into biotite and the amount of mafic minerals decreases with the secondary increase of potash feldspar.

The metasomatic granitization of the primary matrix has also produced granites in which the amount of potash feldspar is higher than that of the plagioclase. Some highly granitized parts are red-coloured granites, poor in mafic components. Hornblende has been totally altered into biotite, the content of which is low. The plagioclase ( $An_{25-32}$ ) of the granite is more albitic than that of the quartz dioritic or granodioritic matrix.

Two chemical analyses of granitized secondary matrix are given in Table 2. Anal. 1 represents a highly granitized granodiorite where the relics of the primary matrix are seen. Anal. 2 is from a red-coloured granitic type poor in mafic components, and in this variety the textural relics of the primary quartz dioritic matrix are only faintly seen.

TABLE 1.

Chemical analyses of different parts of an orbicule in the orbicular rock of Kuru.  
Anal. P. Ojanperä.

Constituents	1	2	3
SiO <sub>2</sub> .....	61.89	54.64	64.73
TiO <sub>2</sub> .....	0.34	1.03	0.06
Al <sub>2</sub> O <sub>3</sub> .....	20.19	22.31	18.70
Fe <sub>2</sub> O <sub>3</sub> .....	1.37	4.63	0.06
FeO .....	2.01	3.10	0.19
MnO .....	0.05	0.06	0.01
MgO .....	0.48	0.12	0.04
CaO .....	5.26	6.19	0.42
Na <sub>2</sub> O .....	5.15	6.76	2.45
K <sub>2</sub> O .....	2.33	0.62	12.84
P <sub>2</sub> O <sub>5</sub> .....	0.13	0.06	0.03
H <sub>2</sub> O+ .....	0.53	0.28	0.17
H <sub>2</sub> O- .....	0.06	0.10	0.05
Total	99.79	99.90	99.75

## N o r m s

q .....	10.48	—	0.37
or .....	13.77	3.66	75.87
ab .....	43.58	56.98	20.73
an .....	25.09	28.70	1.89
ne .....	—	0.13	—
cor .....	—	—	0.08
di .....	0.13	1.17	—
wo .....	—	0.09	—
fs .....	2.05	—	0.22
en .....	1.17	—	0.10
mt .....	1.99	6.71	0.09
il .....	0.65	1.96	0.11
ap .....	0.31	0.14	0.07

1. Nucleus of orbicule.
2. Fine-grained, grey-coloured zone of plagioclase.
3. Outer zone of potash feldspar

The granitization of the matrix has not caused a marked corrosion of the orbicules, as is the case in some other orbicular rocks. Only occasionally some few microcline porphyroblasts have been observed in the esboitic parts of the orbicules. This indicates that the granitization is later than the esboitic crystallization of the orbicules.

## CONCLUDING REMARKS

The orbicular rock in Kuru is the fourth occurrence of orbicular rock in place in the Precambrian rock crust of Finland. Earlier the occurrences of Virvik, Espoo (Esbo) and Kemijärvi were found and described by Finnish geologists (Frosterus 1893, Sederholm 1928, Eskola 1938, and Simonen 1938 and 1940). In addition to

TABLE 2.  
Chemical analyses of partly granitized matrix in the orbicular rock of Kuru.  
Anal. P. Ojanperä.

Constituents	1	2
SiO <sub>2</sub> .....	69.19	77.05
TiO <sub>2</sub> .....	0.46	0.12
Al <sub>2</sub> O <sub>3</sub> .....	15.08	12.48
Fe <sub>2</sub> O <sub>3</sub> .....	0.89	0.45
FeO .....	2.07	0.53
MnO .....	0.03	0.01
MgO .....	0.71	0.19
CaO .....	1.81	1.83
Na <sub>2</sub> O .....	2.81	2.63
K <sub>2</sub> O .....	5.97	4.05
P <sub>2</sub> O <sub>5</sub> .....	0.12	0.07
H <sub>2</sub> O + .....	0.45	0.24
H <sub>2</sub> O - .....	0.11	0.06
Total	99.70	99.71

## N o r m s

q .....	24.31	42.05
or .....	35.28	23.93
ab .....	23.78	22.25
an .....	8.21	8.63
c .....	0.99	0.61
fs .....	2.39	0.42
en .....	1.77	0.47
mt .....	1.29	0.65
il .....	0.87	0.23
ap .....	0.29	0.17

1. Secondary matrix, grey-coloured.
2. Secondary matrix, red-coloured.

the above-mentioned occurrences in situ, most of the orbicular rocks in Finland have been found as Pleistocene glacial boulders.

The orbicular rock in Kuru has many petrographical and compositional characteristics similar to the other Finnish orbicular rocks. Especially it contains varieties related to the well-known orbicular rocks in Espoo (Esbo) and Kemijärvi. The orbicules consisting only of plagioclase are similar to the so-called esboitic orbicules of the Espoo rock, while the orbicules with microcline outer zones around esboitic inner parts are related to the granitic orbicules of the Kemijärvi rock. The simultaneous occurrence of both esboitic and granitic orbicules in the Kuru rock is interesting, because it indicates that the concretionary crystallizations of both principal types of orbicule have taken place under similar conditions. Furthermore, it is possible to conclude that the esboitic orbicules, forming the inner parts of the granitic orbicules, must be considered as an embryonic stage in the evolution of the granitic orbicules.

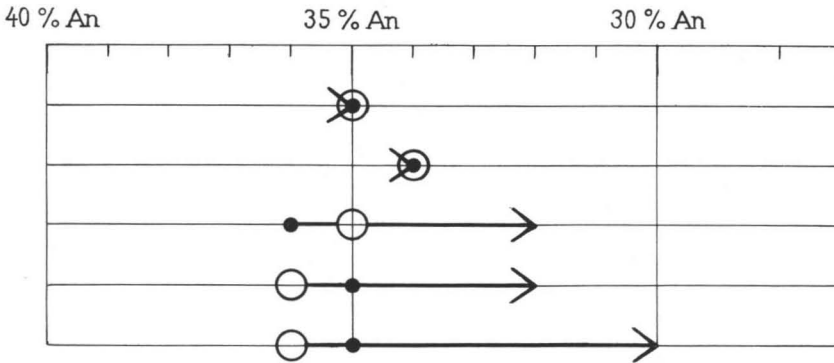


FIG. 8. The composition of plagioclase in the different parts of the Kuru rock. Dot = nucleus of orbicule; ring = grey-colored plagioclase zone of orbicule; arrowhead = matrix around orbicule.

The feldspars are the predominant minerals determining the structure of the orbicules. The compositions of the plagioclases in different parts of the orbicular rock in Kuru are presented in Fig. 8. The determinations show that the compositions of the plagioclases in different parts of the orbicules are very similar. Furthermore, the composition of the plagioclase in the orbicules is occasionally similar to that of the matrix plagioclase. However, the plagioclase of the granitized matrix is sometimes more albitic than that of the orbicules. These statements about the composition of the plagioclase in different parts of the orbicular rock in Kuru are similar to those about many other orbicular rocks (*cf.* Eskola 1938).

The normative proportions Or : Ab : An of the different parts of the orbicular rock in Kuru are given in Fig. 9. The variety of Kuru rock with the esboitic orbicules, without microclinc outer shells, is not a true esboite, because its matrix is not esboitic, but has the composition of a partly granitized rock. This variety of Kuru rock is related to the orbicular rock in Lintusaari, described by Eskola (1938), where the esboitic orbicules occur in the granitic matrix. The variety of Kuru rock with granitic orbicules, divided extremely sharply into an esboitic inner part and a microclinc outer zone, is related to the orbicular rock in Kemijärvi described by Simonen (1940). It is characteristic of this variety that the orbicules consist of both esboitic and microclinc parts and that they are in the granitic or partly granitized matrix.

The origin of the orbicules of most of the orbicular rocks is due to a concretionary crystallization characterized by the diffusion of material from the surroundings to the nuclei. In the Kuru rock, the crystallization of the plagioclase nucleus has started the concretionary formation of the orbicule. This crystallization, due to diffusion, metamorphic recrystallization and metasomatic processes, has taken place in the primary quartz dioritic rock, which is found only as relics in the heterogeneous

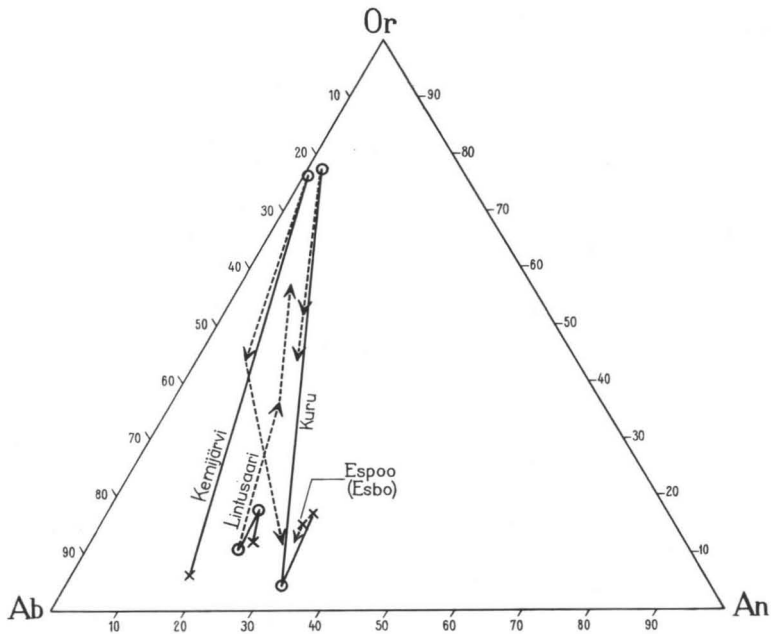


FIG. 9. Normative proportions Or : Ab : An in some orbicular rocks. Based on the data presented by Eskola (1938) and Simonen (1940). Cross = nucleus of orbicule; ring = zone of orbicule; arrowhead = matrix around orbicule.

matrix of the orbicular rock. The transition of the quartz diorite into an esboitic, plagioclase-rich nucleus is characterized by inward diffusion of sodium and outward diffusion of feric components. This peculiar type of metasomatic process has been called by the present author (Simonen 1940) as esboitization. The relics of the big recrystallized hornblende grains with crystal faces sometimes found in the nucleus show that the metamorphic recrystallization has also taken place at an early stage of the formation of the nucleus.

The concretionary crystallization of the esboitic material has also caused the development of the grey-coloured plagioclase shell around the nucleus. The inner part of this plagioclase shell is sometimes coarse-grained and radial while the outer parts are fine-grained and granoblastic in texture. Usually the radial part of the plagioclase shell is lacking in which case the light-coloured nucleus passes gradually into the more fine-grained, grey-coloured zone of plagioclase. The chemical composition of the grey-coloured plagioclase shell is more basic than that of the nucleus. This feature, contradictory to the laws of magmatic differentiation, is characteristic of esboitic crystallization. The grey-coloured plagioclase shell is a basic front of esboitic orbicules due to the outward diffusion of the mafic components during the process of the esboitic crystallization.

The esboitic orbicules of the Kuru rock represent embryonic orbicules in the crystallization of the granitic orbicules, because they have served as crystallization nuclei for the microclitic outer zone. The start of crystallization of the microclitic outer zone marks a radical change in the development of the orbicules. The potassium metasomatism replaced the sodium metasomatism which prevailed during the concretionary crystallization of the esboitic inner parts of the orbicules. The diffusion of potassium is connected to the metasomatic granitization of the primary quartz dioritic matrix into the heterogeneous secondary matrix which consists of granodiorite and granite. The esboitic orbicules have been very resistant to granitization, but some few microcline porphyroblasts in the esboitic parts of the orbicules show distinctly, however, that the diffusion of potassium has taken place later than that of sodium.

The evolution of the orbicular rock in Kuru briefly outlined above is related to the origin of many other orbicular rocks, which are interpreted as being products of concretionary crystallization caused by processes of metamorphic differentiation and metasomatism in a solid rock (Eskola 1938 and Simonen 1940). The Kuru rock with plagioclase-rich inner parts surrounded by microcline outer shells shows a peculiar and sharp fractionation of the alkalis during the process of diffusion. The diffusion of sodium, giving rise to the soda metasomatism or esboitization of the plagioclase-rich inner parts, is older than the diffusion of potassium which caused the crystallization of the microclitic outer shell and the granitization of the matrix.

*Acknowledgements* — Mrs. Toini Mikkola, M. A., and Mr. Pekka Kallio, M. A., have assisted in the optical and X-ray determinations. The chemical analyses were made by Mr. Pentti Ojanperä, M. A. The author wishes to express his sincere gratitude to all these persons.

*Manuscript received, February 10, 1966*

#### REFERENCES

- ESKOLA, PENTTI (1938). On the esboitic crystallization of orbicular rocks. *Journ. Geol.* 46, pp. 448—485.
- FROSTERUS, B. (1893). Ueber ein neues Vorkommnis von Kugelgranit unfern Wirvik bei Borgå in Finnland nebst Bemerkungen über ähnliche Bildungen. *Min. Petr. Mitt.* 13, pp. 1—34.
- SEDERHOLM, J. J. (1928). On orbicular granites, spotted and nodular granites etc. and the rapakivi texture. *Bull. Comm. géol. Finlande* 83, pp. 1—105.
- SIMONEN, AHTI (1938). Chemical study of the orbicular rock in Kemijärvi. *Bull. Comm. géol. Finlande* 123; *C. R. Soc. géol. Finlande* 12, pp. 47—49.
- »— (1940). Orbicular rocks in Kemijärvi and Esbo. *Bull. Comm. géol. Finlande* 128; *C. R. Soc. géol. Finlande* 14, pp. 107—140.
- »— (1952). Suomen geologinen kartta. Geological map of Finland. Lehti — Sheet — 2124. Viljakkala—Teisko. Kallioperäkartan selitys. Explanation to the map of rocks. Pp. 1—74.
- »— (1960). Plutonic rocks of the Svecofennides in Finland. *Bull. Comm. géol. Finlande* 189, pp. 1—101.



## SOME FEATURES OF THE SALMENKYLÄ GABBRO IN KANGASNIEMI COMMUNE, FINLAND

BY

ANTTI SAVOLAHTI and RAIMO KUJANSUU

*Institute of Geology and Mineralogy, University of Helsinki*

### ABSTRACT

A medium-grained pyroxene gabbro and a pegmatoid gabbro situated in an outcrop of the Salmenkylä pyroxene gabbro body in the commune of Kangasniemi are described. A chemical analysis and X-ray diffraction powder data are presented for the diopsidic augite and hypersthene contained in the pegmatoid gabbro.

### INTRODUCTION

The Salmenkylä gabbro area is situated in the eastern part of Central Finland, 3.5 km north of the church of Kangasniemi. It extends from the southern and eastern sides of Kotajärvi to the southern side of Jousjärvi (62°02' N lat. and 26°38' E long.). Described previously by Frosterus (1902) in connection with his explanatory notes for the petrographic map of Mikkeli and by Kranck (1923, 1923 a) in his *pro gradu* thesis, the gabbro area runs N—S, is nearly four kilometers long and has a maximum width of about two kilometers. According to both Frosterus and Kranck, it runs along the eastern edge of a broad granitic central massif. At its northern and southern ends, between, the granite and the gabbro, there are small stretches of mica gneiss.

The mineral composition of the Salmenkylä gabbro body varies somewhat in different portions of it. In its marginal zone there occur varieties containing considerable amounts of hornblende. For the most part, they seem to be products of dislocation metamorphosis (Savolahti 1964 a, p. 94). The marginal zone of the body at many places is fine-grained and contains a little olivine.

The present study is concerned with a medium-grained gabbro from the outcrop situated on the southern side of Kotajärvi as well as with a coarse-grained pegmatoid gabbro that occurs in the same outcrop.

#### MEDIUM-GRAINED GABBRO

The main part of the Salmenkylä gabbro body consists of medium-grained gabbro. The color of its weathered surface is brownish gray. The principal mineral constituents of the rock are plagioclase, hypersthene and diopsidic augite, in addition to which there is a certain amount of biotite. Accessory constituents are apatite and various ore minerals. The pyroxene is weakly uralitized and the plagioclase saussuritized.

The plagioclase ( $\alpha < 1.561, \gamma > 1.567, \text{An}_{60-64}$ ) occurs as bright, elongated crystals from one to three mm long and 0.3 to one mm wide. The principal mineral of the rock is plagioclase, which occurs as nearly euhedral and weakly zoned grains. Twinning occurs abundantly in conformity to the albite law, and there are combinations likewise in accordance with it and the pericline or Karlsbad's law. The plagioclase contains pyroxene and ore grains as inclusions. A slight potash feldspar content is to be observed in the marginal parts of plagioclase grains and their interstices.

The diopsidic augite ( $\alpha' = 1.689, \gamma' = 1.713$  — the refractive indices measured on a (110) cleavage flake (Parker 1961), approx. 30 mol-% CaFe-component) occurs as clusters of crystals, which vary in size between 0.5 and 2 mm. Inclusions are present in abundance, among them being biotite and ore grains — the ore occurring also as exsolutions. The augite is only slightly uralitized.

The hypersthene ( $\gamma = 1.710$ , approx. 37 mol-% Fe-component) is slightly pleochroic:  $\alpha$  = reddish,  $\gamma$  = bluish yellow (nearly colorless). Like the augite, it occurs as clusters of crystals, and the size of the individual crystals varies between 0.5 and 1.5 mm. At their edges the grains have only slightly altered to amphibole. Present are inclusions of ore grains (there is also a weak occurrence of the Schiller structure), augite and plagioclase.

The biotite is conspicuously pleochroic:  $\gamma = \beta$  = dark reddish brown,  $\alpha$  = brownish yellow, tending to be rather colorless. It occurs chiefly as tiny flakes in the pyroxene, elsewhere as an occasional grain measuring 0.2–0.4 mm, mostly in association with ore grains.

The apatite occurs as tiny xenomorphic crystals situated among grains of other constituents.

Opaque minerals in the gabbro include pyrrhotite and magnetite as well as chalcopyrite and sphalerite. No ilmenite has been detected, but in the hypersthene and the diopsidic augite slight amounts of sphene occur. There are appreciable amounts of the opaque minerals first mentioned but not much chalcopyrite or sphalerite. The grain sizes range from 0.2 to 1 mm.

## PEGMATOID GABBRO

The medium-grained gabbro contains coarse-grained, gabbro-pegmatoidic splotches of irregular shape. In mineral composition it corresponds closely to the foregoing.

The plagioclase ( $\alpha = 1.557$ ,  $\gamma = 1.565$ ,  $An_{53-58}$ ), which appears to be slightly poorer in anorthite here than in the medium-grained gabbro, occurs as fairly pure, only slightly saussuritized strips from two to four mm long. There are rather few inclusions, mainly biotite, pyroxene, apatite and — along the grain edges and in the interstices — some anhedral potash feldspar.

Diopside augite ( $\alpha = 1.684$ ,  $\beta = 1.690$ ,  $\gamma = 1.713$ ,  $c \wedge \gamma = 42^\circ$ ,  $2V\gamma = 58^\circ$ , approx. 30 mol-% CaFe component) is present as ragged grains averaging 1–2 mm in size, but there also occur large, poikilitic grains measuring between 5 and 10 mm, with inclusions of plagioclase, biotite and ore grains. Ore is present further as exsolutions, and hornblende occurs as an alteration product. The mode of intergrowth of the hornblende and the diopsidic augite is in many cases similar to the description given by, for example, Savolahti and Kurki (1964, p. 179) with regard to the peridotite of Rauhamäki. The chemical analysis of the mineral and its X-ray diffraction powder data are presented in Table No. 1, revealing that it contains more CaO and less  $Al_2O_3$  and FeO than does the augite of Ansio described by Savolahti (1964, p. 105).

The hypersthene ( $\gamma = 1.712$ ,  $2V\alpha = 63^\circ$ , approx. 40 mol-% Fe-component) is weakly pleochroic, consisting of irregularly shaped grains, which vary in size between 1.5 and 7 mm. The hypersthene contains augite lamellae, and the mode of intergrowth of the minerals is to be observed in stereographic projection (Fig. 1), which reveals that the b-axes of the minerals run parallel, as do the c-axes, and that the axis planes are perpendicular to each other. The intergrowth plane is (100). Occurring in the hypersthene as inclusions are ore grains, plagioclase and augite. The chemical analysis of the hypersthene is presented in Table No. 2, along with the X-ray diffraction powder data. The CaO content is apt to be excessive because it has not been possible to remove all the tiny augite lamellae from the hypersthene. A closely corresponding composition occurs in the hypersthene from Hakone-Toge, Hakone volcano, Kanagawa Prefecture, Japan (Kuno 1950, p. 964). The composition of the hypersthene is also revealed by the X-ray diffraction powder data, inasmuch as  $d(1031) - d(060) = 0.011\text{\AA}$  corresponds to the results obtained for hypersthene (Zwaan 1954).

The biotite ( $\gamma = 1.647$ ) is markedly pleochroic:  $\gamma =$  dark reddish brown and  $\alpha =$  brownish yellow. It occurs mainly as inclusions in the pyroxene, and elsewhere it is found only as an occasional grain averaging 0.6 mm in size.

The apatite occurs as xenomorphic crystals between grains of other constituents and as inclusions in the plagioclase. The grains are fairly large, measuring 0.5–2 mm, in some cases, though more generally the diameter gives a measurement varying between 0.1 and 0.2 mm.

TABLE 1.

Chemical composition (analyst, S. Turkka) and X-ray diffraction powder data (Copper  $K\alpha$  radiation, Nickel filter.) for diopsidic augite from Salmenkylä. Kangasniemi, Finland. Chemical composition (analyst, A. Heikkinen for augite (2) from Ansio. Padasjoki, Finland.)

	1		2		1		
	Weight per cent		No	d (Å)	I/I <sub>0</sub>		
SiO <sub>2</sub> .....	51.76	49.38	1 .....	3.33	10		
TiO <sub>2</sub> .....	0.55	1.25	2 .....	3.21	30		
Al <sub>2</sub> O <sub>3</sub> .....	1.47	2.28	3 .....	3.09	10		
Fe <sub>2</sub> O <sub>3</sub> .....	2.35	2.24	4 .....	2.983	100		
FeO .....	8.76	11.62	5 .....	2.942	60		
MnO .....	0.23	0.29	6 .....	2.883	45		
MgO .....	13.48	13.86	7 .....	2.560	35		
CaO .....	20.30	17.97	8 .....	2.512	50		
Na <sub>2</sub> O .....	—	0.50	9 .....	2.297	20		
K <sub>2</sub> O .....	—	0.05	10 .....	2.213	10		
P <sub>2</sub> O <sub>5</sub> .....	—	0.19	11 .....	2.207	10		
H <sub>2</sub> O+ .....	0.53	0.23	12 .....	2.196	10		
H <sub>2</sub> O- .....	0.16	0.02	13 .....	2.151	15		
Total	99.59	100.00	14 .....	2.128	35		
			15 .....	2.106	15		
			16 .....	2.038	20		
			17 .....	2.016	10		
			18 .....	1.851	10		
			19 .....	1.752	20		
			20 .....	1.623	20		
			21 .....	1.563	10		
			22 .....	1.550	10		
			23 .....	1.524	10		
			24 .....	1.505	10		
			25 .....	1.488	10		
			26 .....	1.423	35		
			27 .....	1.408	10		
			28 .....	1.332	10		
			29 .....	1.283	10		
Numbers of ions on the basis of 6 oxygens							
Si .....	1.93	1.88					
Ti .....	0.02	0.04					
Al .....	0.06	0.10					
Fe <sup>3+</sup> .....	0.07	0.07					
Fe <sup>2+</sup> .....	0.27	0.37					
Mn .....	0.01	0.01					
Mg .....	0.75	0.79					
Ca .....	0.81	0.73					
Na .....	—	0.04					

## CONCLUSIONS

The two varieties of rock from the pyroxene gabbro body of Salmenkylä described in this paper are very much alike in mineral composition and with regard to the nature of the constituent minerals. A comparison of the composition of the minerals making up the medium-grained portion with that of the pegmatoidic portion reveals that the plagioclase contained in the coarse-grained rock is slightly richer in albite and the hypersthene somewhat richer in Fe than in the case of the medium-grained rock. The composition of the diopsidic augite is approximately the same in both cases. These very slight differences would suggest that the pegmatoid part of the gabbro body crystallized at the same time and even somewhat later than the medium-grained part (*cf.* Savolabti 1966).

TABLE 2.

Chemical composition (analyst, S. Turkka) and X-ray diffraction powder data for hypersthene from Salmenkylä. (Copper  $K\alpha$  radiation, Nickel filter.) Kangasniemi, Finland.

	Weight per cent	No	hkl	d (Å)	I/I <sub>0</sub>
SiO <sub>2</sub> .....	53.36	1 .....	021	3.32	10
TiO <sub>2</sub> .....	0.25	2 .....	420	3.17	100
Al <sub>2</sub> O <sub>3</sub> .....	1.79	2 .....	221		
Fe <sub>2</sub> O <sub>3</sub> .....	1.79	3 .....	600	3.05	10
FeO .....	20.77	4 .....	321	2.950	30
MnO .....	0.39	5 .....	610	2.883	70
MgO .....	19.31	6 .....	230	2.832	30
CaO .....	2.54	7 .....	421	2.717	15
-H <sub>2</sub> O .....	0.10	8 .....	620	2.546	30
	100.63	9 .....	202	2.509	20
		10 .....	302	2.395	10
		11 .....	022	2.253	10
		12 .....	502	2.122	15
		13 .....	630	2.105	20
		14 .....	531	2.065	10
		15 .....	721	2.030	20
		16 .....	820	1.994	15
		17 .....	440	1.965	20
		18 .....	250	1.740	10
		19 .....	1 200	1.525	10
		20 .....	1 031	1.492	20
		21 .....	060	1.481	20
		22 .....	1 131	1.395	15
		23 .....	1 400	1.311	10
		24 .....	004	1.300	10
		25 .....	860	1.224	15

Numbers of ions on the basis of 6 oxygens	
Si .....	1.97
Ti .....	0.01
Al .....	0.08
Fe <sup>+3</sup> .....	0.06
Fe <sup>+2</sup> .....	0.64
Mn .....	0.00
Mg .....	1.06
Ca .....	0.10

According to Frosterus (1902) and Kranck (1923), the gabbro of Salmenkylä belongs to the Keuruu type of gabbros and is older than the late granites of the type found in the interior of the country. Sederholm (1893) describes the gabbros classified in this group to be found in Orivesi and places them alongside the olivine diabase of Satakunta petrographically. Savolahti (1964 b) produces evidence that the olivine diabase of Padasjoki, which Frosterus (1902) classified among gabbros of the Keuruu type, is younger than the younger granites of the so-called hinterland type (as designated by Frosterus) that constitute its country rock.

The pyroxene gabbro of Salmenkylä differs petrographically from the diabases of Orivesi and Padasjoki. It has a scanty olivine content, found in the main only in the marginal zones. According to Kranck (1923), it is finer of grain in its marginal parts, however, than in the middle. Consequently, the very slight granitic veins occurring in its marginal portions cannot necessarily be taken to prove that it is of earlier origin than the granites comprising its country rock; rather can they be interpreted — as Kahma (1951, p. 27) did — as products of melting by the gabbro from

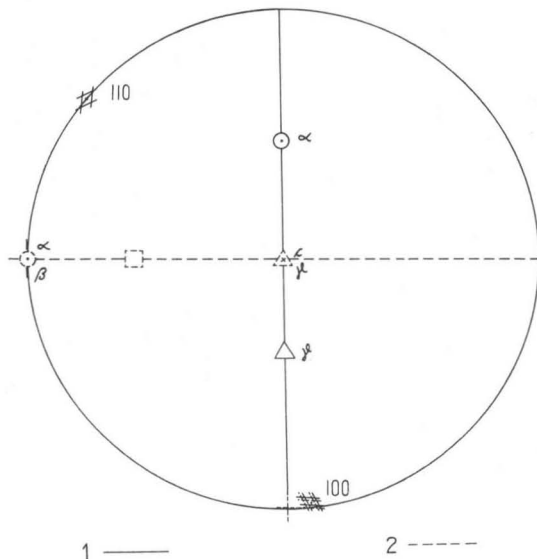


FIG. 1. Stereographic projection of intergrowth of diopside (1) and hypersthene (2). The projection shows the indicatrices, cleavages and c-axes of both minerals according to Reinhard (1931). Pyroxene gabbro. Salmenkylä, Kangasniemi.

its country rock. The gabbro of Salmenkylä petrographically resembles the enstatitic augite diabases of Central Finland described by Wilkman (1924) more than it does the olivine diabase of Satakunta.

*Manuscript received, February 16, 1966*

#### REFERENCES

- DEER, W. A., HOWIE, R. A., and ZUSSMAN, J. (1963) *Rock-forming minerals*. Vol. 2. London.
- FROSTERUS, B. (1902) Beskrifning till bergartskartan av kartbl. C 2, St. Michel. General geological map of Finland, 1 : 400 000.
- KAHMA, A. (1951) On the contact phenomena of the Satakunta diabase. *Bull. Comm. géol. Finlande* 152.
- KRANCK, E. H. (1923) Om tvänne gabbroområden i Kangasniemi socken. Manuscript. Institute of Geology, University of Helsinki.
- »— (1923 a) Om tvänne gabbro-områden i Kangasniemi socken. *Helsingin Geol. yhd. Tiedonantoja 1921—1923*, pp. 22—24.
- KUNO, H. (1950) Petrology of Hakone volcano and adjacent areas. *Japan. Bull. Geol. Soc. Am.* 61, pp. 957—1019.

- PARKER, R. B. (1961) Rapid determination of the approximate composition of amphiboles and pyroxenes. *Am. Mineralogist* 46, pp. 892—900.
- REINHARDT, M. (1931) *Universal Drehtischmethoden*. Basel.
- SAVOLAHTI, A. (1964 a) Observations on prehnite and its occurrence in Kangasniemi parish, Finland. *Bull. Comm. géol. Finlande* 215, pp. 89—98.
- »— (1964 b) Olivine diabase dike of Ansio in Padasjoki, Finland. *Bull. Comm. géol. Finlande* 215, pp. 99—111.
- »— (1966) The differentiation of gabbro-anorthosite intrusions and the formation in them of anorthosites. *Bull. Comm. géol. Finlande* 222, pp. 173—197.
- »— and KURKI, J. (1964) Observations of the nickeliferous ore block of Niemilahti in Kangaslampi and on small ultrabasic and basic bodies in the Rauhamäki—Kuronlahti district, Finland. *Bull. Comm. géol. Finlande* 215, pp. 171—192.
- SEDERHOLM, J. J. (1893) Om berggrunden i södra Finland. *Fennia* 8, 3.
- WILKMAN, W. W. (1924) Om diabasgångar i mellersta Finland. *Bull. Comm. géol. Finlande* 71.
- ZWAAN, P. C. (1954) On the determination of pyroxenes by X-ray powder diagrams. *Leidse Geol. Med.* 19, pp. 167—276.



# FRAMBOIDAL TEXTURE OF THE PYRITIC LAYER FOUND IN A PEAT BOG IN SE-FINLAND

BY

HEIKKI PAPUNEN

*Institute of Geology, University of Turku, Finland*

## ABSTRACT

A pyritic layer found in a Quaternary peat bog in SE-Finland shows framboidal and colloidal textures. The layer also contains pyritized remains of organic plants. Pyrite has a cell edge  $a_0 = 5.414 \pm 0.005 \text{ \AA}$ . The density is 4.10 and the chemical composition close to  $\text{FeS}_2$ . Framboidal pyrite texture is supposed to be caused by the reaction between absorbed iron hydroxide in the colloidal humus coacervate drops and hydrogen sulfide in the water.

## INTRODUCTION

A texture in sedimentary sulphide bearing formations which has been called »framboidal» or »vererzte Bakterien» has been described by many authors. The term framboidal was first used by Rust (1935). It is derived from the French word »Framboise» (Raspberry), and it means that there are small spherules composed of tiny idiomorphic crystals. The size of the spherules is under  $100 \mu$  and the mineral is generally pyrite but also chalcopyrite spherules are met with. Originally the texture was found in sulfide bearing shales, e.g. copper shales of Mansfeld, Meggen, Germany (Schneiderhöhn, 1923), but later on it was found also in recent shallow water deposits (Love, 1964).

The present study describes a pyrite formation found in a peat bog in SE-Finland, in which the microtexture shows certain similarities to the framboidal texture of shallow water muds.

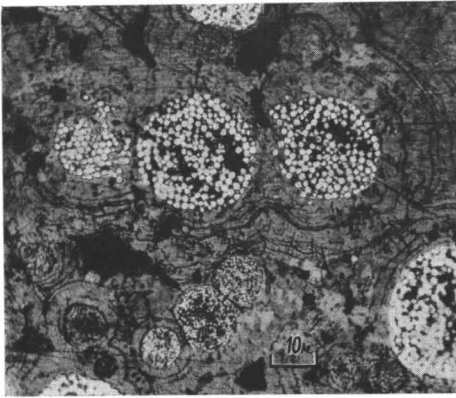


FIG. 1. Microtexture of the layer; pyrite spherules are white, pyrite with colloidal texture gray; holes are black. Polished section, slightly etched with  $\text{HNO}_3$ .

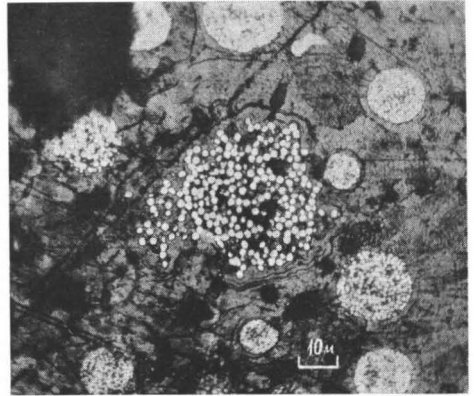


FIG. 2. Shattered pyrite spherule.

## OCCURRENCE

During the exploration work of Outokumpu Co in the summer of 1960 a peculiar rough layer was found in a Quaternary peat bog in the village of Toroppala, Kerimäki commune, SE-Finland. At first it was believed to be a bog iron ore (limonite) but later on it was verified by X-ray examination as pyrite. The layer was found when digging a bog drain. It lies at a depth of 0.7—1 m in moderately mouldered Sphagnum-peat. The layer has a thickness under 10 cm, generally not more than 0.5—1 cm. It is very hard and bronze-coloured at the fresh breaking. The lower side is often smooth or nearly so and the upper side rough, filled with outgrowths. In the thicker parts there are large holes and cavities. The layer extends over an area of a few ares, but as a whole it is very incoherent: here and there it is absent and the largest pieces taken from the bottom of the drain were about  $1/4 \text{ m}^2$  in size.

## MICROTEXTURE

Even in polished section the porous texture of the ore is seen clearly. Holes and small pores are numerous. Two components are seen in a newly polished section (Fig. 1). One of them is pyrite and reflects more than the other brownish, porous part, in which the pyrite occurs as centres of concentric zones. The texture becomes more clearly visible when etched with diluted  $\text{HNO}_3$  (1 : 1). The pyrite component occurs as small spherules composed of tiny idiomorphic crystals (Fig. 3). The spherules vary in diameter from 3 to  $45 \mu$ , and are on an average  $30 \mu$ . The sizes of the pyrite crystals are  $1/10$ — $1/12$  of the whole sphere, and vary thus from  $0.3$ — $4.5 \mu$ . The

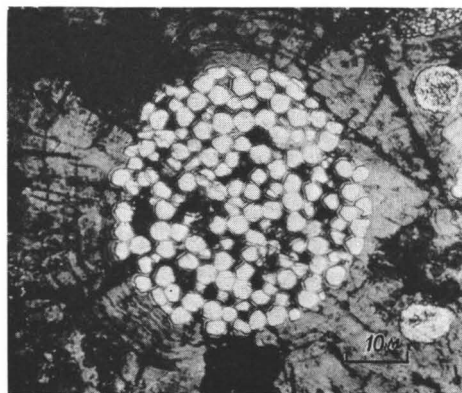


FIG. 3. Pyrite crystals in a spherule. Note the idiomorphic shape of crystals.

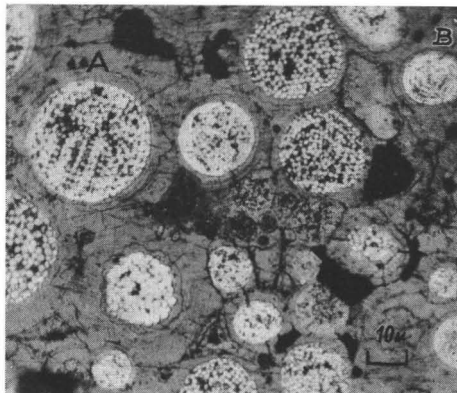


FIG. 4. Rectilinear (A) and circular (B) ordering of pyrite crystals in the framboidal spheres.

amounts of pyrite crystals in the spheres vary, but generally there are about one thousand of them in one spherule. Pyrite crystal aggregates are round in every section, but here and there a shattered sphere (Fig. 2) can be observed. Occasionally also tiny single pyrite grains are seen in the groundmass. Crystal forms of pyrite are cube and pyritohedron (Fig. 3). Sometimes the crystals in a sphere are in circular or rectilinear order (Fig. 4).

The crystal size depends on the size of the spherule (small sphere, tiny crystals), but within a spherule there is no difference in crystal size. Occasionally there are spheres with pyrite crystals only on the outer frame, or spheres with almost compact pyrite on the surface but only sparse crystals in the centres.

The texture of the pyrite described above is a typical framboidal texture (Bastin, 1960, p. 30).

The reflectivity of pyrite crystals does not change when etched with diluted  $\text{HNO}_3$ , whereas the porous low reflecting part around the pyrite spherules tarnishes quickly. At the same time a texture emerges, which has been interpreted as colloidal texture (Bastin 1960, p. 26). It is characterized by concentric curved fractures and porous concentric zones. In addition to them radial fractures occur (fig. 5). A framboidal pyrite crystal sphere is nearly always in the centre of this concentric colloidal texture.

In addition to the foregoing textures, casts of organic plants can be observed in places. Cross cuts of *Sphagnum* (Fig. 6) and leaf of *Mnium* (Fig. 7) have been identified. Remains of plants occur in greater abundance in the lower part of the pyritic layer and leaves of *Mnium* generally lie horizontally. There are some sharp-edged quartz grains in the lower part of the layer.

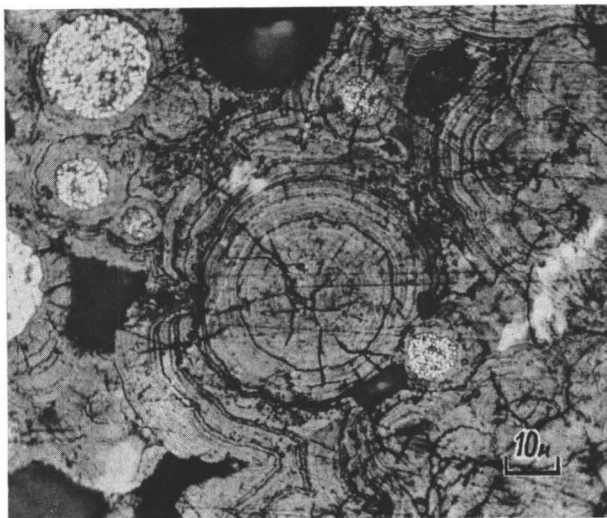


FIG. 5. Typical colloidal texture of the cryptocrystalline «groundmass».

#### X-RAY AND CHEMICAL INVESTIGATIONS

The layer has been investigated with X-ray diffraction. A Debye-Scherrer-powder camera with 114,6 mm diameter and filtered Fe-radiation was used. Crystals in spherules were found to be pyrite. No lines of marcasite can be observed in the powder patterns. The measured cell edge of pyrite is  $a_0 = 5.414 \pm 0.005 \text{ \AA}$ . The groundmass with colloidal texture also gives a pyrite-like pattern, reflexes are not, however, as sharp as in the pattern of well crystallized pyrite, but are broad and diffuse. This is possibly due to the small crystal size of the cryptocrystalline groundmass. With full justification this part with colloidal texture can be considered as so-called melnikovite-pyrite or gelpyrite (Ramdohr, 1960, p. 743). According to Berner (1964, a) «melnikovites» found in natural occurrences are probably cryptocrystalline pyrite or marcasite. The type melnikovite described by Doss was amorphous, black, magnetic, soluble in warm dilute HCl, sp.gr. 4.2—4.3 and had a composition of  $\text{FeS}_2$ . According to the studies of Berner (1964, a, p. 305) this was «a fine grained mixture of elemental sulfur and one or more of several known magnetic iron sulfides» (= cubic iron sulfide  $\text{Fe}_3\text{S}_4$  and tetragonal FeS). According to Polushkina and Sidorenko (1963) melnikovite has a composition close to  $\text{Fe}_3\text{S}_4$  and it is cubic with spinel structure and  $a_0 = 9.82\text{--}9.92 \text{ \AA}$ .

The chemical composition of the present pyrite layer proves to be almost stoichiometric  $\text{FeS}_2$ , Table 1. The density measured with pycnometer is 4.10.

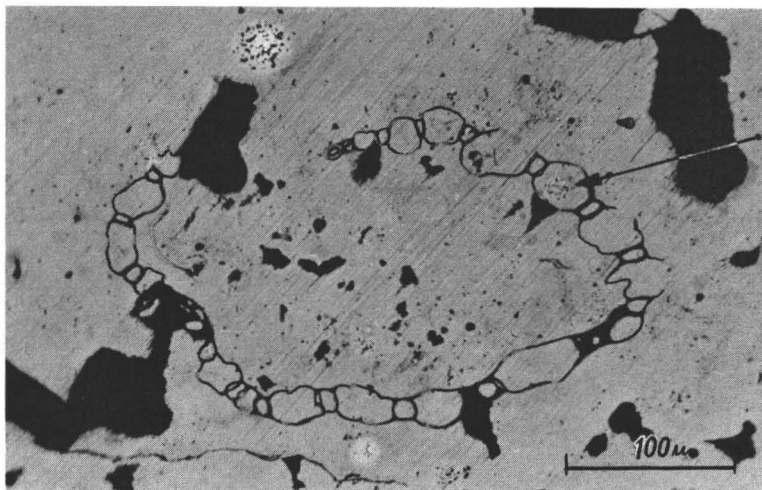


FIG. 6. Cross cut of pyritized *Sphagnum*. Note also a pyrite framboid inside cell of *Sphagnum* (arrow).

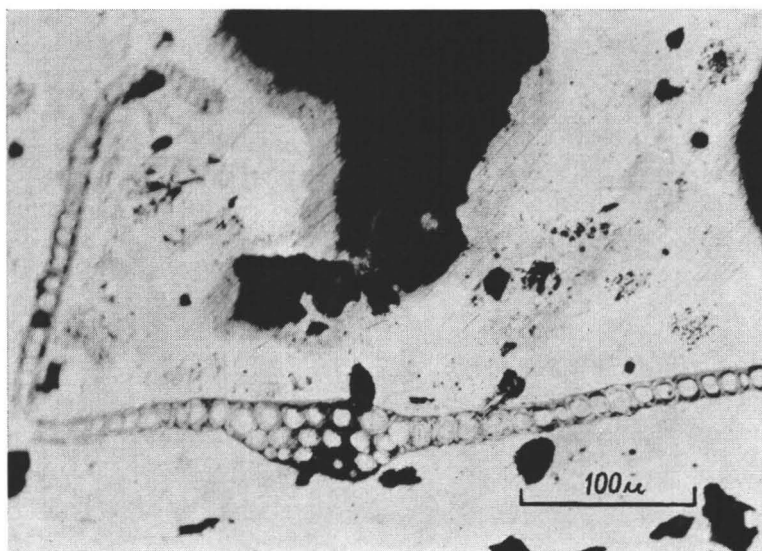


FIG. 7. Cross cut of pyritized *Mnium*.

TABLE 1.  
Chemical composition of the pyrite layer. Analyst Rolf Lappalainen.

	wt-%	Mol.-prop.	Number of ions
Fe .....	43.8	78.42	0.94
S .....	53.4	166.51	2
insoluble (mainly quartz) .....	1.2	—	—
Total	98.4		

## ORIGIN

### Origin of the framboidal pyrite and of the sedimentary pyrite in general

Schneiderhöhn (1923) was the first to describe this type of texture in the copper shale of Mansfeld. He considered that the formation of ore deposit took place on the sea floor and the sulfide spherules were colonies of sulfur depositing bacteria. It was he who used the term »vererzte Bakterien» (fossil bacteria) for this type of texture.

Rust (1935) explained that the framboidal texture in the deposit of Cornwall Mine, Missouri is probably metacolloidal in origin and was formed by the crystallization of a globule of pyrite gel, crystallization starting simultaneously at many points. In an alternative hypothesis of Rust, the texture might be considered to have been formed by a bunching of tiny pyrite crystals which floated in a chalcopyrite gel.

Schouten (1946) shows with many examples that in a sedimentogenous sulphide deposit »fossil bacteria» in the sense of Schneiderhöhn cannot be the origin of pyrite spheres. According to him the pyrite in sulphide bearing slates was formed prior to the entry of other ore forming solutions. Pyrite spheres are thus authigenic, but other sulfides have been formed later.

According to Love (1964) the framboidal pyrite spherules are also frequent in recent shallow water deposits investigated within the area of Christchurch Harbour in south England as well as in Long Island Sound, U.S.A. Fresh water lake mud from Queechy Pond, New York, was also investigated. In these deposits pyrite is the dominant sulphide, while marcasite was not found. It occurs as tiny cube crystals and framboidal small crystal spheres. Love (1964) calls this »early diagenetic pyrite» and writes (p. 13) that »a clear statement on the mode of origin of the authigenic sulphide in those sediments is lacking at present although as a generalisation it is safe to say that the sulphide radical is essentially the resultant of micro-biological processes in an anaerobic environment.» He also states that this diagenetic pyrite probably developed before the sediment reached anaerobic conditions, because spheres have been found inside cells and in other restricted places.

B. Ohlson of the University of Turku (personal communication) has recently found small opaque spheres in the mud from the bottom of lake Kaks Kerranjärvi,

near Turku, SW-Finland. Heavy liquid separation and optical study of a polished section proved the mineral to be pyrite and the texture similar to the framboidal spherules described by Love (1964).

Kaplan *et al.* (1963) have made investigations of sulfides and of the sulfur isotopic composition of the sea floor sediments. They have observed that the sulfur occurring in the sediments is mainly in the form of pyrite which, however, shows variations in the Fe to S ratio compared with stoichiometric  $\text{FeS}_2$ . The pyrite of the sea floor is S-deficient. Great variations also occur in the isotopic composition of pyrite. Two major possibilities exist for the origin of pyrite. Either it is contributed by runoff from land or it is of authigenic origin. The sulphur content in sediments and interstitial waters, and the regularity observed in the sulphur isotopic composition of sulfates and pyrite indicate that most pyrite is formed at the sediment-water interface. Biological reduction of the sulfates is the main process which liberates sulfur for the sulfide precipitation.

According to Berner (1964, b, p. 830) the first formed iron sulphide resulting from the reaction of bacterially produced hydrogen sulfide with detrital iron minerals in many marine sediments is not pyrite but a black pigmented, X-ray amorphous or weakly diffracting tetragonal form of  $\text{FeS}$ . The subsequent transformation of  $\text{FeS}$  into pyrite readily takes place, however. This transformation can be observed in sediments from a number of localities. This tetragonal  $\text{FeS}$  has also been called »kansite» and »mackinawite».

### Conditions under which the pyritic layer is formed

Ferrous sulfide occurring in the sediments is principally formed by the reaction of iron and sulfide ion. The slow decaying of the peat in a bog binds oxygen and thus bottom waters are oxygen-deficient and can contain hydrogen sulfide in high concentrations. According to C. E. ZoBell (1963, p. 558) hydrogen sulfide finds its way into natural gases and waters 1) from the reaction of mineral acids on metallic sulfides, 2) sulfate reduction or 3) from decomposing protein. In the present case the microbial decomposition of the remains of organic plants and animals causes the liberation of hydrogen sulfide in bottom waters. Numerous species of bacteria can participate in this process. Clarke (1953) has shown that most species of sulfur-bacteria liberate hydrogen sulfide from cysteine. Less common are bacteria which form hydrogen sulfide from cystine, thiosulphate or sulfate.

Iron comes into ground waters through the weathering of iron bearing minerals. When oxygen exists in an insufficient amount ferrous iron dissolves as ferrous bicarbonate,  $\text{Fe}(\text{HCO}_3)_2$ , and is precipitated as siderite when carbon dioxide is removed from the solution. If, on the contrary, there is oxygen and abundant humic matter dissolved in water, iron forms iron hydroxide. The colloidal humic acids are of great importance in the absorption and transportation of iron hydroxide. It is

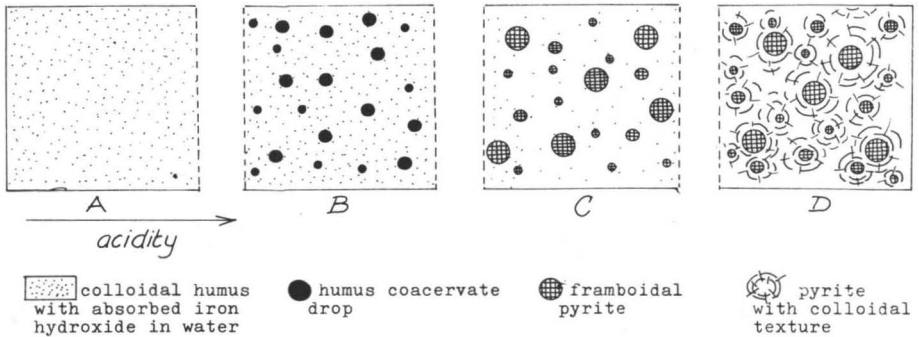


FIG. 8. Schematic illustration of the formation of pyritic layer. Explanation in the text.

thus possible that the iron of the present pyrite layer was absorbed in humus colloids (illustrated in Fig. 8, A).

Humus partly consists of spherical particles about  $0.02 \mu$  in diameter and all its physical properties are caused by its colloidal character. For example the acidity of the water in which humus occurs governs the particle size of humus materials and their adsorbed substances. Increase in acidity results in concentration of humus solutions (Swain 1963, p. 137). The humus with adsorbed iron hydroxide can with increasing acidity form spherical coacervations in water (Fig. 8, B). If now there were enough air, the liberated iron would precipitate as limonite, bog iron ore. But on the contrary in the bog the bottom waters can also be oxygen-deficient and can contain hydrogen sulfide abundantly. This reacts with liberated iron hydroxide forming iron sulfide, and reaction occurs between the iron hydroxide in a humus drop and the hydrogen sulfide in water. Crystallization products, framboidal pyrite spherules, with their varying sizes resemble small emulsion drops (type »oil in water«). Crystallization started from the surface of the sphere and occasionally one can see spheres with crystals only on the outer frame. As reaction continues crystallization extends inwards. Due to low concentrations of the ions, the crystallization is undisturbed and crystals become idiomorphic.

This is the mechanism, which forms framboidal pyrite spheres (Fig. 8, C).

After the precipitation all adsorbed iron hydroxide is liberated and reacts with the sulfide ion in water forming the cryptocrystalline pyrite with colloidal texture (Fig. 8, D). The occurrence of framboidal spheres as centres of colloidal texture proves that the frambooids formed first and then the melnikovite-pyrite.

Often the pyrite with colloidal texture is not formed because concentrations are too low. In those cases only separate pyrite spherules occur in the sediment, in the same manner as in shallow water muds. It is most probable that the pyrite occurs as framboidal spheres also in numerous Finnish shallow water deposits. The discovery of them is not, however, easy because of the small size of the opaque spherules (under  $100 \mu$ ).

*Acknowledgements* — I am indebted to Professor P. Haapala of the Outokumpu Co. for permission to publish the present study. I wish also to express my gratitude to Professor K. J. Neuvonen of the University of Turku, who kindly read the manuscript and made valuable suggestions. Professor P. Kallio and Dr Y. Mäkinen of the University of Turku have identified the remains of plants and R. Lappalainen, M. Sc. has made the chemical analysis. To them I express my special gratitude.

*Manuscript received, February 28, 1966*

## REFERENCES

- BASTIN, E. S. (1960) Interpretation of Ore Textures, Geol. Soc. America Memoir 45.
- BERNER, R. A. (1964 a) Iron sulfides formed from aqueous solution at low temperatures and atmospheric pressure. *Jour. Geology*, 72, pp. 293—306.
- BERNER, R. A. (1964 b) Stability fields of iron minerals in anaerobic marine sediments. *Jour. Geology* 72, pp. 826—834.
- CLARKE, PATRICIA H. (1953) Hydrogen sulphide production by bacteria. *Jour. Gen. Microbiol.* 8, pp. 397—407.
- KAPLAN, R., EMERY, K. O., RITTENBERG, S. C. (1963) The distribution and isotopic abundance of sulfur in recent marine sediments of Southern California. *Geoch. Cosmoch. Acta*, 27, pp. 297—331.
- LOVE, L. G. (1964) Early diagenetic pyrite in fine-grained sediments and the genesis of sulphide ores. In »Sedimentology and Ore Genesis», editor G. C. Amstutz, Elsevier, Amsterdam.
- POLUSHKINA, A. P. & SIDORENKO, G. A. (1963) Melnikovite as a mineral species. *Mem. All.—Union Min. Soc.* 92, pp. 547—554 (in Russian); *Min Abstr.* Vol 17 No 4, 1965, p. 388.
- RAMDOHR, P. (1960) Die Erzminerale und Ihre Verwachsungen, Akademie Verlag, Berlin.
- RUST, G. W. (1935) Colloidal primary copper ores at Cornwall Mines, southeastern Missouri. *Jour. Geology*, 43, pp. 398—426.
- SCHNEIDERHÖHN, H. (1923) Chalkographische Untersuchung des Mansfelder Kupferschiefers; *Neues Jahrb. Mineral.* Vol. 47, pp. 14—38.
- SCHOUTEN, C. (1946) The role of sulfur bacteria in the formation of so-called sedimentary copper ores and pyrite ore bodies. *Econ. Geology*, 41, pp. 517—538.
- SWAIN, F. M. (1963) Geochemistry of Humus. in »Organic Geochemistry», editor Irving A. Breger, Pergamon Press, London.
- ZOBELL, C. E. (1963) Organic Geochemistry of Sulphur, in »Organic Geochemistry», editor Irving A. Breger, Pergamon Press, London.



# ON THE PRECAMBRIAN MICROFOSSIL FLORA IN THE SILTSTONE OF MUHOS, FINLAND

BY

RISTO TYNNI and JAAKKO SIIVOLA

*Geological Survey of Finland, Otaniemi*

## ABSTRACT

A drilling through the Muhos formation (Jotnian) in Liminka, west-central Finland, was carried out in 1959 by the Oulujoki Company and the Imatran Voima Company. A study of the core samples by the authors has revealed probable Precambrian microfossils which can be divided into algal colonies and spore-like structures. A report of electron microprobe studies is also given.

## INTRODUCTION

The so-called Jotnian formations which are unfolded and comparatively unmetamorphosed belong to the younger Precambrian sedimentary rocks of Finland. Among others they comprise the Muhos formation south of Oulu (Brenner, 1941, 1944, Ödman, Härme, Mikkola and Simonen 1949, Okko 1954, Simonen and Kouvo 1955, Simonen 1960). Older than the Muhos formation are the sedimentary rocks of the Bothnian and Karelidic zone. The age of the Muhos formation is about 1 300 m.y. (Simonen 1960, Kouvo pers. comm.) and that of the Karelidic formation group about 1 900 m.y. (Kouvo 1958).

In 1890 Sederholm had found bag-like structures of carbon, *Corycium aenigmaticum* in the Bothnian phyllite of the Tampere area and had explained them as organogenic, possibly algal remnants. The organogenic origin of the carbon bags was supported by the studies of Rankama (1948). Along the Kemijoki River Sederholm also found stromatolitic structures (Sederholm 1932). Stromatolite investigations were continued in Tervola, on the Kemijoki River (Härme and Perttunen 1964).

By comparing and checking Marmo (1959) concluded that the same spore types occurred in the Muhos formation that Timofejev had found in the Jotnian formations

of Lake Onega. After the discovery of the Muhos formation (Brenner, 1941) K. Mölder investigated the possible microfossils. New possibilities of detecting microfossils appeared when the Oulujoki Company and the Imatran Voima Co. under the direction of Mr. J. Kalla carried out deep drillings in Liminka. The deep drilling reached a depth of more than 1 000 metres. In the following some preliminary results of research work on the microfossils met with in the drill cores are reported. Other investigations on drill samples were made by J. Kalla. He will publish his results later.

#### POSSIBLE MICROFOSSILS

The Muhos formation is in places reddish, greenish grey or dark grey in colour. Besides silt, the sediment comprises clay and fine sand fractions. Particularly in the greyish portions the varved structure is occasionally visible. Varving is partly caused by variations in the grain size and partly by colour variations of the sediment. The reddish portion would correspond to a sediment formed on the continent under oxydizing conditions (*c.f.* Lokka 1950, Simonen and Kouvo 1955), and the greyish one in many cases agrees with the later reduction product of the sediment. An exception is the carbon-bearing dark grey portion of sediment which corresponds to the initial reduction horizon (Kalla, pers. comm.).

Orientating research revealed that the Muhos sedimentary rock contained microfossils sparsely, for which reason only a few thin sections were studied. Instead hydrofluoric acid and heavy liquid ( $K_2CdJ_4$ ) methods were used to dissolve and separate the silicate material of the mechanically down-broken sediment. After the dispersion of specific sediment samples in water the material accumulated on the surface was studied for microfossils. Mr. Raimo Rätty of the Institute of Technology in Otniemi has investigated under an electron microscope such material from a sample taken from a depth of about 234 m. Mostly the HF-method was employed. The residue was studied by optical microscope with 250—1 300 x magnification. Possible microfossils occurred mainly in the reduced parts of the sediment. A corresponding observation has been earlier recorded by Lipman and Timofejev (1957). Research on the microflora of the Muhos formation was impeded by sporadic secondary occurrences, particularly in the coarser reddish portions. According to comparative analyses that impediment was due to contamination caused by bentonite, Cretaceous sediment, which was used during the drilling.

Generally speaking even the reduced part of the sediment, as far as is known from the few investigated samples, is poor in fossil structures. It contains dark material which is insoluble in HF and at least partly composed of indefinite pyritized or carbonized algae or spore remnants. This is supported by the fact that in the places richest in dark remnants are also found the structures identifiable as fossils. However, after treatment or possibly even before, they are so worn-out that they cannot be more precisely determined. Also the material accumulated on the surface

of the water contains possible microfossils. They are amorphous, round and colonial structures (Fig. 1 and 2), which would be destroyed in hydrofluoric acid.

Although more precise fossil determinations could not be performed, the possible microfossils can be divided into two groups at least: algal colonies and spore types. The former occurrences are more rare. Examples of algal colonies are in Fig. 3. A varying number of thin-walled cells over  $10\ \mu$  in diameter form a spherical or more irregular mass in an algal colony. The number of cells is generally more than 15, and the colony  $< 40\ \mu$  in diameter, but also chain-like accumulations of cells occur. The former resemble flagellates of present flora as regards their size, shape and assemblage. Similar, but thicker-walled green algae were found in the Precambrian strata of Central Australia (the age of the strata 700—900 m.y.) by Barghoorn and Schopf (1965). On the other hand, the algal colony type resembles the microfossil *Symplassospaeridium subcoalitum* found in the upper Cambrium of the Baltic region and presented by Timofejev (1959).

With the magnification used spore type is the most common among the observed microfossils in HF-residue. It corresponds plausibly to algal spores in the systematic classification by Timofejev (1959). They vary in size, some 20—70  $\mu$ , are rounded in form, even triangular in the most distinct cases, and in some cases reticular in surface structure. Also elliptical, reticular structures occur which resemble the *Huronispora* microfossils met with in the Gunflint formation (Barghoorn and Tyler 1965). The spores presented by Timofejev from Jotnian sediments are similar in appearance to some met with in the Muhos formation, but because the latter were too worn-out more accurate identification could not be made. It is quite possible that the genus *Mycreroligo-triletum* occurs in the Muhos formation and additionally some unidentified algal spore species.

Fig. 7 shows one of the best preserved spores which one of us (Tynni) has tentatively named, *Muhospora reticulata* n.gen. It is triangularly spherical with reticular microstructure and its size is 66  $\mu$ .

## MICROPROBE ANALYSIS

In order to get more information on these possible microfossiles an effort was made to analyse one sample with the electron microprobe. The main purpose of this analysis was to get knowledge on the structure of these microfossiles and the element concentrations in them.

One polished section was prepared for this study of a siltstone sample taken from 218 metres' depth. This mainly consists of greenish grey varved material. The polished section was first investigated under an optical microscope. During the microscopic studies a lot of colonies were found which closely resembled those shown in figs. 2, 3 and 4. Several of these colonies were examined by the electron microprobe. Some results are shown in the figure 9. The poor quality of the electron image is due

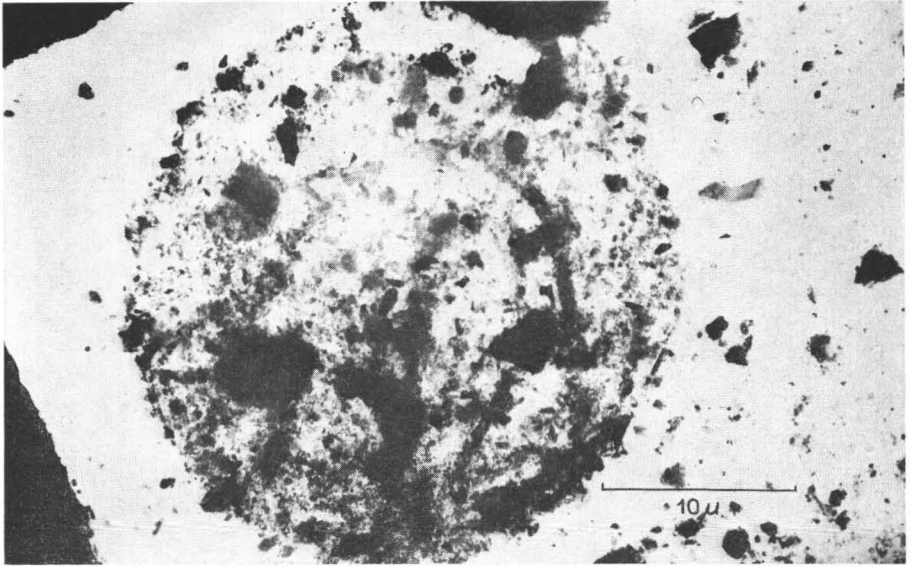


Fig. 1. Round organic structure from a depth of about 234 metres. Photo: Raimo Rätty.

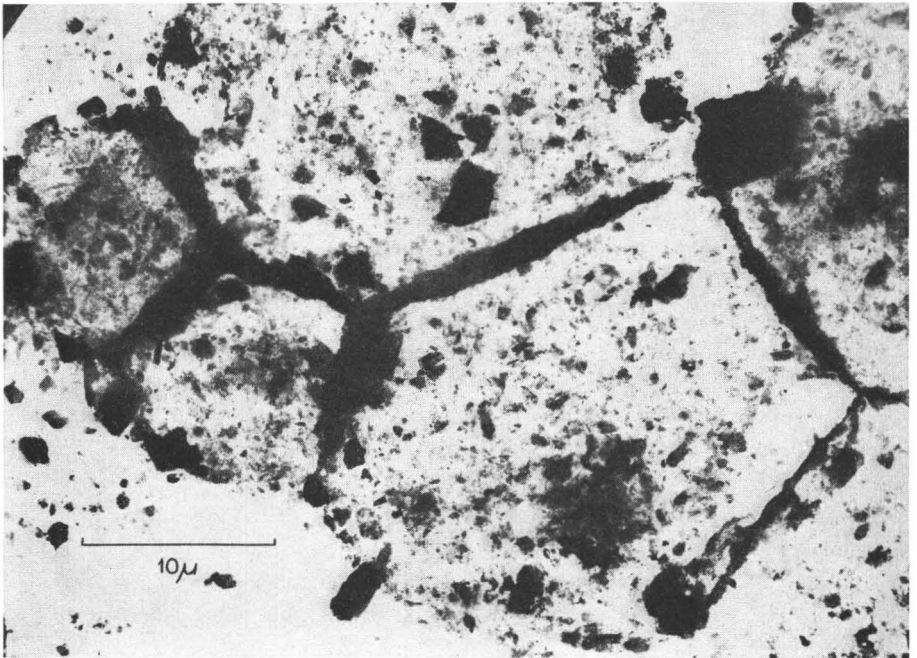


Fig. 2. Colony-like structure from the same level. Photo: Raimo Rätty.

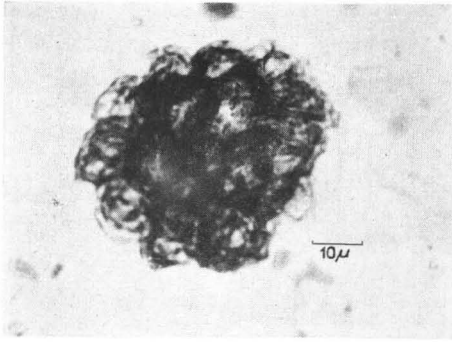


FIG. 3. Algal colony from a depth of 234.65 metres. Photo: Erkki Halme.

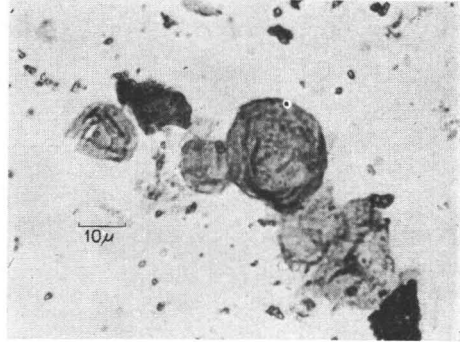
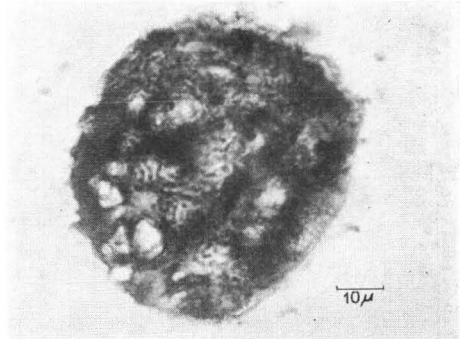
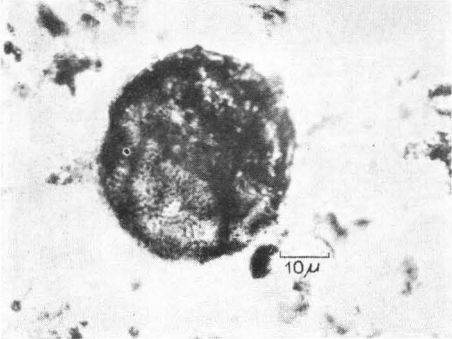


FIG. 4. Probable algal cells from a depth of about 234 metres. Photo: Erkki Halme.



FIGS. 5 and 6. Spore-like structure from a depth of 233.5 metres. Photo: Erkki Halme.

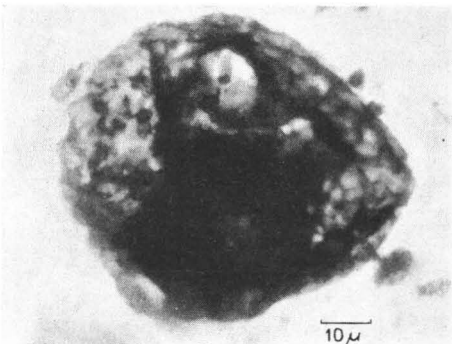


FIG. 7. *Mubospora reticulata*, n. gen. from a depth of 233.5 metres. Photo: Erkki Halme.

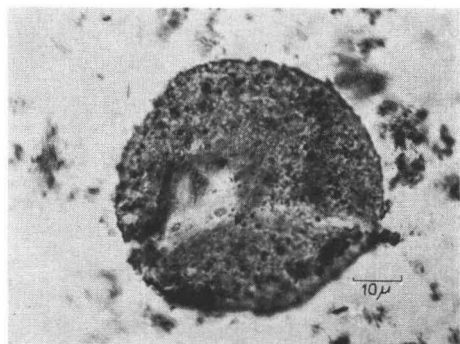


FIG. 8. Rare spore type from a depth of 218.75 metres. Photo: Erkki Halme.

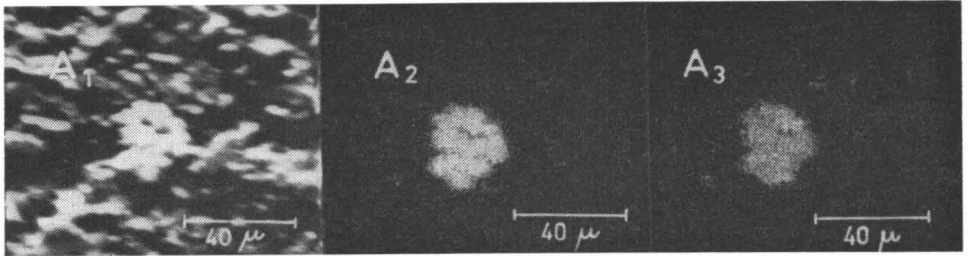


FIG. 9.  $A_1$  Electron image of one possible microfossil. Compare the structure *e.g.* with the one shown in fig. 3.  $A_2$  and  $A_3$ . X — ray images, Cu  $K\alpha_1$  and S  $K\alpha$  respectively. The same structure can be seen also in these images.

to the siltstone sample which was very difficult to get well polished. It was established that the colonies always contained either Cu and S (chalcosite), Fe and S (pyrite) or Cu, Fe and S (chalcopyrite). In many cases pyrite and chalcopyrite occur together in the same colony. It is worth mentioning that no other element, *e.g.* Mn and V, was detected in these objects. Carbon is unfortunately out of scope of the microanalyser used. The concentration of sulfides in the colonies possibly explains the well preserved structures of these microfossils.

#### COMPARISON WITH SOME OTHER STUDIES DEALING WITH PRECAMBRIAN MICROFOSSILS

Notions on the occurrence of spore type in the Precambrian sedimentary formations have been presented in the USSR during the past decades (among others, Naumova 1949, Lipman and Timofejev 1957, Timofejev 1959). Convincing Precambrian microfossils have been studied *e.g.* by Barghoorn and Tyler (1965) since 1953 and by Cloud, Jr. (1965). A formation rich in microfossils is the Gunflint iron formation. Although its age is about 2 000 m.y. structural remnants discernible under an ordinary microscope are much more abundant than in the Muhos formation. Their different age is exhibited by the differences of the most common types of microfossils. The micro-organisms of the Gunflint formation are filament structures of blue-green algae, iron bacteria or green algae, spore-like bodies are smaller in size than the corresponding ones found in the Muhos formation. It deserves mentioning that largish algal structures occur in the lower part of the Gunflint formation.

In sedimentary beds, still older than the Gunflint formation, in Witwatersrand, South Africa, Schidlowski (1965) has found two types of microfossils, 4–21  $\mu$  in size. They are possibly sulphur bacteria. Pyrite has caused these microfossils to preserve well.

Algal structures have been found in strata older than the previous ones, namely in South Rhodesia, in beds some 2 600 m.y. old. Even in a stratum about 2 800 m.y. in age Hoering has verified organic algal structure (Abelson 1963).

Microfossils presented by Barghoorn and Schopf (1965) from a late-Precambrian stratum in Central Australia, comprise algal structures, part of which resemble those found in the Muhos formation, but the greatest similarities, excluding details, exist between the subject of the present study and the microfossils of the Jotnian formation of Lake Onega.

*Manuscript received, February 28, 1966*

## REFERENCES

- ABELSON, P. H. (1963) Chemicals from ancient life. Carnegie Institution of Washington, Lecture and reception, May 9.
- BARGHOORN, E. S. & SCHOPF, J. W. (1965) Microorganismus from the Late Precambrian of Central Australia. *Science*, Vol. 150, pp. 337—339.
- BARGHOORN, E. S. & TYLER, S. A. (1965) Microorganism from the Gunflint chert. *Science*, Vol. 147, pp. 563—577.
- BRENNER, TH. (1941) Ein ungewöhnliches Kalkschlammsteinsediment von Muhos in Mittelfinnland. *Geol. Rundschau*, Bd. 32, pp. 535—549.
- »— (1944) Die Bodenbildungen des Muhos-Sediments bei Kieksi. *C. R. Soc. géol. Finlande* 16, pp. 189—196; *Bull. Comm. géol. Finlande* 132.
- CLOUD, P. E., JR. (1965) Significance of the Gunflint (Precambrian) microflora. *Science*, Vol. 148, p. 27—35.
- HÄRME, M. & PERTTUNEN, V. (1964) Stromatolite structures in Precambrian dolomite in Tervola, North Finland. *C. R. Soc. Géol. Finlande* 35, pp. 79—82; *Bull. Comm. géol. Finlande* 212.
- KOUVO, O. (1958) Radioactive age of some Finnish pre-Cambrian minerals. *Bull. Comm. géol. Finlande* 182.
- MARMO, V. (1959) Elämän merkkejä prekambrisissa kivissä. Summary: On the Precambrian fossils. *Terra*, pp. 150—156.
- OKKO, V. (1954) Muhossedimentets utbredning. *Geologi* 6, p. 43. Helsinki.
- RANKAMA, K. (1948) New evidence of the origin of pre-Cambrian carbon. *Geol. Soc. America Bull.* Vol. 59, pp. 389—416.
- SCHIDLOWSKI, M. (1965) Probable life-forms from the Precambrian of the Witwaterstrand Systems (South Africa). *Nature*, Vol. 205, p. 895—896.
- SEDERHOLM, J. J. (1932) On the geology of Fennoscandia. *Bull. Comm. géol. Finlande* 98.
- SIMONEN, A. (1960) Pre-Quaternary rocks in Finland. *Bull. Comm. géol. Finlande* 191.
- SIMONEN, A. and KOUVO, O. (1955) Sandstones in Finland. *C. R. Soc. géol. Finlande* 28, pp. 57—88, *Bull. Comm. géol. Finlande* 168.
- TIMOFEJEV, B. V. (1958) Über das Alter sächsischer Grauwacken. *Geologie (Berlin)*, Jg. 7, pp. 826—845.
- ÖDMAN, O. H., HÄRME, M., MIKKOLA, A. och SIMONEN, A. (1949) Den svensk-finska geologiska exkursionen i Tornedalen sommaren 1948. *Geol. Fören. i Stockholm Förh.*, Bd. 71, pp. 113—126.
- Липман, Р. А. и Тимофеев, Б. В. (1957) Об органических остатках в докембрии. Методика геологического картирования метаморфических комплексов. Москва.
- Наумова, С. Н. (1949) Споры Нижнего кембрия. *Изв. АН СССР, сер. геол.*, № 4.
- Тимофеев, Б. В. (1959) Древнейшая флора Прибалтики и ее стратиграфическое значение. *Труды ВНИГРИ*, вып. 129. Ленинград.



## RELATIONSHIP BETWEEN GÖTZENITE AND ROSENBUSCHITE

BY

TH. G. SAHAMA \*, ESKO SAARI \* and KAI HYTÖNEN \*\*

\* *University of Helsinki, Finland*

\*\* *The Geological Survey, Otaniemi, Finland*

### INTRODUCTION

In connection with the study of the lavas of the Nyiragongo volcano in the Congo, two of us published a description of the mineral named götzenite which was first discovered in a boulder on the rim of Mt. Shaheru, an extinct southern tributary of Nyiragongo (Sahama and Hytönen, 1957 a). Chemically götzenite was found to be closely related to calcium rinkite from Yukspor, Kola. Because the data available for calcium rinkite at that time, summarized by Fersman and Bohnstedt (1937), were very incomplete, a detailed comparison of the two minerals with each other could not be made.

After the powder pattern of calcium rinkite, published by Slepnev (1957), had become available and further chemical, optical and X-ray data had been obtained by Sahama (1960) on the Yukspor material, the identity of götzenite with calcium rinkite was definitely established. Later on, a new occurrence of the mineral in the Ukraine was published by Val'ter, Yeremenko and Stremovskiy (1963).

As was shown by Sahama and Hytönen (1957 b), the unit cell of götzenite, though related, is definitely different from that of the mosandrite-johnstrupite-rinkite group. Mosandrite, johstrupite and rinkite were studied using specimens from original type localities. They were found to be triclinic with unit cell dimensions virtually identical to each other. Slepnev (*op. cit.*) and Fleischer (1958 b) agree in considering this mineral group one single species. Fleischer (*op. cit.*) points out that the name mosandrite has priority and, accordingly, the names johnstrupite and rinkite should be dropped. For this reason and, further, because the composition of götzenite is closer to an end-member (absence of Ce, Y, Nb, Sr), the name calcium rinkite should be

abandoned (Fleischer, 1958 a; Sahama, 1960) in favor of götzenite. This suggestion has been approved by the New Minerals Commission of the International Mineralogical Association (*cf.* Bull. Soc. française Miner. Crist., T. LXXXV, p. 195, 1962). Therefore, throughout this paper, the name götzenite will be used for the mineral.

The discussion about götzenite received an important contribution from Neumann (1962). On preparing a collection of data for powder patterns of silicate minerals (Neumann, Sverdrup and Saebö, 1957), he noticed the fact that the powder pattern of götzenite is strikingly similar to that of rosenbuschite, suggesting a structural relationship between the two minerals. At the time when Neumann made his observation and published his remarks, the crystal structures of both rosenbuschite and götzenite were unknown. The crystal structure of götzenite still awaits determination. That of rosenbuschite, however, has been studied later by Shibajeva and Belov (1962) using the unit cell dimensions that were given by Peacock (1937).

The remarks made by Neumann (*op. cit.*), for which the authors would like to express their gratitude, and the crystal structure work by Shibajeva and Belov (*op. cit.*) make it evident that the mineral götzenite and its position in the general classification of silicate minerals needs reconsideration and seem to justify the comments to be presented in the following.

#### X-RAY CRYSTALLOGRAPHY

Like rosenbuschite, götzenite is triclinic and fibrous in appearance. The unit cell data for götzenite, compared with those for rosenbuschite, are compiled in Table 1. In the setting used by Peacock (1937) and later adopted by Shibajeva and Belov (1962) the fiber axis of rosenbuschite is taken as  $c$ -axis. This fiber axis shows a pronounced subcell with  $c_0/2$ . Because of the analogy of the götzenite cell with that of the wollastonite-pectolite family, the prism axis of götzenite was taken by Sahama and Hytönen (1957 a) as the crystallographic  $b$ -axis. The crystal structure of pectolite was presented by Buerger (1956) showing that the fiber axis of the mineral, taken as  $b$ -axis, exhibits also a substructure with period  $b_0/2$ . However, to make the data for götzenite more readily comparable with those for rosenbuschite, the  $b$ - and  $c$ -axes of götzenite as originally given by Sahama and Hytönen (*op. cit.*) have been interchanged in the compilation of Table 1. In this compilation the fiber axis with substructure is taken as  $c$ -axis for both minerals.

The unit cell originally obtained for götzenite (Table 1, column 5) was very oblique. Professor Horace Winchell (personal communication) kindly drew attention to the fact that the original cell could be transformed into a new less oblique cell with the same volume. The dimensions of this new reduced cell (Table 1, column 4) have been adopted in the compilation of crystal data published by the American Crystallographic Association and edited by Donnay (1963). Table 1, column 3, to be given below, presents the dimensions of this new cell refined by powder pattern.

TABLE 1.  
Unit cell data for rosenbuschite and götzenite

	Rosenbuschite		Götzenite *	
	Peacock (1937) **	This paper ***	Sahama (1960) ****	Sahama and Hytönen (1957 a) *****
$a_0$ .....	10.14 Å	9.667 Å	9.65 Å	10.93 Å
$b_0$ .....	11.41	5.731	5.74	5.74
$c_0$ .....	7.28	7.334	7.32	7.32
$\alpha$ .....	91° 21'	90°	90°	90°
$\beta$ .....	99° 38.5'	101.05°	101.1°	120°
$\gamma$ .....	111° 54.5'	101.31°	101.3°	100°

\*  $b$ - and  $c$ -axes interchanged from the original setting (Sahama and Hytönen, 1957 a) to make götzenite more easily comparable with rosenbuschite.

\*\* Å from kX.

\*\*\* Refined by powder pattern.

\*\*\*\* Reduced cell.

\*\*\*\*\* Original data obtained from rotation and Weissenberg photographs.

In his paper, Neumann (1962; Table 5, p. 185) compares the unit cell data for rosenbuschite as given by Peacock (1937) with those for götzenite as given by Sahama and Hytönen (1957 a). On the basis of the data compiled in his table Neumann makes the following remarks:

»Angles of the unit cell are the same within a few percent, and so are the lengths of the axes with these two modifications 1) one axis in the unit cell of rosenbuschite is twice as long as in götzenite, and 2)  $c_0$  of rosenbuschite equals  $b_0$  of götzenite while  $b_0$  of rosenbuschite equals  $c_0$  of götzenite. The reason for this discrepancy is hardly a different choice of axes, as the angles  $\beta$  and  $\gamma$  are nearly identical. It would seem hard to find a reasonable explanation, and it is tempting to suggest that the values for  $b_0$  and  $c_0$  may have been interchanged at some stage of the process leading from the Weissenberg camera to the ready printed paper.»

In conclusion Neumann suggests that rosenbuschite and götzenite are isomorphous species which may or may not form mixed crystals.

Now, the data used by Neumann for götzenite refer to the original oblique cell. The less oblique cell suggested by Horace Winchell is preferable and is used throughout this paper. Further, Neumann's suggestion that the numerical values for  $b_0$  and  $c_0$  (not for  $\beta$  and  $\gamma$ ) for götzenite have been erroneously interchanged in the paper by Sahama and Hytönen (1957 a) was tested on the original Weissenberg photographs preserved in the personal archive of X-ray films kept by one of use (Th. G. S.). The test was easily made because of the fact that the  $b$ -axis in the notation of Sahama and Hytönen (*op. cit.*), which coincides with the fiber axis of the mineral, is morphologically unique and is the only one of the axes that shows a pronounced subcell. It was found that there has been no mistake in the data given. A rotation photograph about this axis yielded a period of 7.32 Å and a subsequent Weissenberg photograph

TABLE 2.  
Indexed powder pattern of götzenite. Filtered copper radiation.

<i>hkl</i>	I	$2\theta_{\text{meas.}}$	$d_{\text{meas.}}$	$d_{\text{calc.}}$
*210 .....	15	22.24	3.997	3.995
102 .....	5	24.70	3.604	3.602
*300 .....	100	28.775	3.102	3.102
*012 .....	100	29.90	2.988	2.988
112 .....	10	31.26	2.863	2.874
020 .....	7	31.68	2.829	2.812
*220 .....	40	33.815	2.653	2.650
*310 .....	25	35.725	2.512	2.514
*320 .....	10	38.725	2.323	2.325
122 .....	15	39.83	2.261	2.265
220 .....	7	40.71	2.214	2.219
402 .....	5	41.945	2.152	2.154
322 .....	5	43.935	2.058	2.068
420 .....	7	45.575	1.988	1.998
*312 .....	50	47.535	1.911	1.915
510 .....	15	48.495	1.876	1.882
*104 .....	15	49.685	1.833	1.835
502 .....	10	50.72	1.798	1.802
232 .....	25	54.24	1.690	1.693
422 .....	7	55.815	1.646	1.649
322 .....	10	57.81	1.594	1.593
610 .....	10	58.635	1.574	1.578
132 .....	10	59.88	1.543	1.548
224 .....	15	62.635	1.482	1.487

\* Line used for calculating the unit cell dimensions.

with an unchanged adjustment of the crystal gave an interaxial angle of 100°. The discrepancy pointed out by Neumann is simply a different choice of axes. Accordingly, Neumann's compilation of the unit cell data for rosenbuschite and götzenite should be replaced by the data of Table 1 of this paper. However, using the data of this table the relationship between the two minerals, suggested by Neumann, becomes even more conspicuous.

To study the relationship between the powder patterns of götzenite and rosenbuschite, that of götzenite was indexed using the IBM-1620 computer of the computing center at the University of Helsinki. The results of the computation are given in Table 2. The  $d$ -values were read from the graphs published by Parrish and Mack (1963) and, accordingly, differ slightly from the original values given by Sahama and Hytönen (1957 a). The  $hkl$  indices listed in the table have been tested on the basis of the available single crystal photographs of the mineral. The reflections indicated by the indices are all strong on the single crystal photographs, by far the strongest among the possible reflections which correspond to the measured

TABLE 3.  
Powder pattern of rosenbuschite with possible indices. Filtered copper radiation.

Possible <i>hkl</i>	I	$d_{\text{meas.}}$	$\theta_{\text{meas.}}$	$\theta_{\text{calc.}}$
	Neumann (1962)			
001 .....	20	7.20	6.15	6.19
$\bar{1}20$ .....	20	5.58	7.94	7.96
$2\bar{2}0$ * .....	10	4.44	10.00	10.13
$1\bar{1}1$ .....	20	4.30	10.33	10.39
$0\bar{2}1$ .....	10	4.14	10.73	10.67
{ $1\bar{2}0$ .....	40	3.96	11.23	{ 11.16
{ $2\bar{2}1$ .....				{ 11.20
{ $2\bar{1}0$ .....				{ 11.87
{ $1\bar{2}1$ .....	10	3.71	11.99	{ 12.20
$10\bar{2}$ * .....	10	3.55	12.53	12.56
{ $1\bar{3}1$ .....	10	3.31	13.45	{ 13.44
{ $3\bar{1}0$ .....				{ 13.47
$1\bar{1}\bar{2}$ .....	20	3.27	13.62	13.67
$3\bar{2}0$ .....	10	3.24	13.75	13.76
$300$ * .....	80	3.06	14.58	14.48
{ $1\bar{2}\bar{2}$ * .....	100	2.94	15.19	{ 15.24
{ $0\bar{2}\bar{2}$ * .....				{ 15.40
{ $1\bar{2}0$ .....	10	2.83	15.80	{ 15.80
{ $3\bar{1}1$ .....				{ 15.83
$240$ * .....	10	2.78	16.09	16.09
$040$ * .....	40	2.63	17.03	17.00
$340$ * .....	40	2.48	18.10	17.79
$320$ * .....	10	2.30	19.57	19.49
$14\bar{2}$ * .....	20	2.23	20.21	20.25
$440$ * .....	30	2.20	20.50	20.60
$1\bar{3}\bar{3}$ .....	10	2.04	22.18	22.19
{ $5\bar{2}0$ * .....	10	1.98	22.89	{ 22.75
{ $240$ * .....				{ 22.77
{ $44\bar{2}$ * .....				{ 22.86
$23\bar{2}$ .....	60	1.89	24.05	24.05
$4\bar{3}\bar{2}$ .....	20	1.86	24.46	24.48
{ $3\bar{2}\bar{2}$ * .....	40	1.82	25.04	{ 25.02
{ $104$ * .....				{ 25.14
$2\bar{6}\bar{2}$ * .....	20	1.70	26.94	27.10

\* The indices marked with an asterisk correspond to those of a götzenite line (the  $k$  index twice that of the götzenite line).

$d$ -value of a powder line. The eight lines marked with an asterisk in Table 2 were used for calculating the unit cell dimensions (Table 1, column 3).

Using the IBM-1620 computer an attempt was also made to index the powder pattern of rosenbuschite as given by Neumann (1962; Table 4, p. 184). The results, summarized in Table 3, are based on the unit cell dimensions of rosenbuschite compiled in Table 1. Because no single crystal photographs were available of rosen-

buschite, the intensities of the reflections indicated by the  $hkl$  indices could not be tested in the same way as for götzenite. Therefore, the indices listed in Table 3 must be considered only tentative.

If rosenbuschite and götzenite were isostructural or even isomorphous with each other as was suggested by Neumann, then the indices of the powder lines of rosenbuschite should be largely analogous to those of götzenite. A complete analogy cannot be anticipated for two reasons. First, as is illustrated by the data of Table 1, the unit cell dimensions of the two minerals differ markedly from each other. This is true especially for  $a_0$  and  $\gamma$ . (In addition, the  $b$ -axis of rosenbuschite is roughly twice that of götzenite.) Second, in the rosenbuschite structure zirconium plays the role of the titanium of the götzenite structure. This replacement of Ti by Zr expectedly affects the intensities of some reflections. A comparison of Tables 2 and 3 with each other reveals the fact that most of the  $hkl$  indices listed in Table 2 for the götzenite lines can be assigned to the rosenbuschite lines of Table 3 (with  $k$  index doubled). Such lines are marked with an asterisk in Table 3. Accordingly, it seems that the apparent similarity between the powder patterns of rosenbuschite and götzenite is not merely accidental but points to a structural relationship between the two minerals.

The following reservation must be made on the discussion presented above. Of the unit cell dimensions given by Peacock only  $c_0$  and  $\gamma^*$  have been obtained through direct measurement with  $\pm 0.05 \text{ \AA}$  for  $c_0$  and  $\pm 10'$  for  $\gamma^*$ . The rest of his data has been calculated from measurements on Weissenberg photographs. For that reason, the values given by Peacock may be subject to some errors. On the other hand, the  $d$ -values for the powder lines of rosenbuschite listed by Neumann have been given with two decimals. Accordingly, both the measured and calculated  $\theta$ -angles of Table 3 may be somewhat inaccurate.

## CHEMICAL COMPOSITION

Neumann (1962) discusses also the relationship between the chemical compositions of rosenbuschite and götzenite. He gives a very complete new chemical analysis of rosenbuschite on the basis of which he arrives at a model formula  $X_{12}Y_4Si_8O_{32}(F, OH)_4$  where X is mainly Ca, Na and RE, and Y is mainly Zr and Ti. Since the atomic ratio of Ca to Na is closely 3:2, the simplified formula can be written  $Ca_2NaZrSi_2O_8F$ , neglecting the low content of RE replacing CaNa, and some Ti replacing Zr. This formula is virtually identical with that proposed by Shibajeva and Belov (1962) on the basis of their crystal structure analysis, *viz.*  $(Ca, Na)_3ZrSi_2O_7(O, F)_2$ , with four formula weights per unit cell. With respect to götzenite Neumann states:

»In comparison with the unit cell content of rosenbuschite, götzenite contains more Ca and F, which may be caused by a few per cent fluorite in the analyzed material which, if finely

TABLE 4.

Chemical analyses of götzenite. Omitting P<sub>2</sub>O<sub>5</sub>, Cl, SO<sub>3</sub>, H<sub>2</sub>O—. Calculated free from CaCO<sub>3</sub>.

	Azov Region, Ukraine	Yukspor, Kola	Shaheru, Congo
SiO <sub>2</sub> .....	32.47 %	32.34 %	32.50 %
TiO <sub>2</sub> .....	11.34	8.74	9.72
ZrO <sub>2</sub> .....	1.04	0.19	**
Nb <sub>2</sub> O <sub>5</sub> .....	0.65	3.36	0.00
Al <sub>2</sub> O <sub>3</sub> .....	4.50	0.45	4.26
Fe <sub>2</sub> O <sub>3</sub> * .....	0.89	0.18	0.85
MgO .....	**	0.04	0.29
MnO .....	0.85	0.62	0.07
RE <sub>2</sub> O <sub>3</sub> .....	2.39	1.84	0.00
CaO .....	31.87	38.95	41.80
BaO .....	**	0.00	0.09
SrO .....	1.35	0.87	0.00
Na <sub>2</sub> O .....	6.73	6.32	4.85
K <sub>2</sub> O .....	0.44	0.09	0.14
F .....	6.85	9.15	8.33
H <sub>2</sub> O+ .....	1.51	0.57	0.26
	102.88	103.71	103.16
—O .....	2.88	3.85	3.54
Total	100.00	99.86	99.62

\* Total iron.

\*\* Not determined.

grained, could easily escape recognition by optical as well as x-ray methods. If a content of 3.4 per cent fluorite is postulated the unit cell content of götzenite can be recalculated to X<sub>6.37</sub>Y<sub>1.66</sub>Si<sub>4</sub>O<sub>15.19</sub>(F, OH)<sub>2.81</sub>. On the assumptions, firstly, that some F replaces O, and secondly, that about 5 per cent of the large ions (mainly Ca) enter the Y sites in the lattice this formula becomes X<sub>6.03</sub>Y<sub>2.00</sub>Si<sub>4.00</sub>O<sub>16.00</sub>(F, OH)<sub>2.00</sub> remarkably close to a model cell formula X<sub>6</sub>Y<sub>2</sub>Si<sub>4</sub>O<sub>16</sub>(F, OH)<sub>2</sub> half of that given above for rosenbuschite.»

Because these remarks made by Neumann are very interesting, they will be discussed in the following, mainly on the basis of Table 4. This table reproduces the most reliable analyses of götzenite from all three localities where the mineral has been found. The analysis of the Ukraine mineral represents the analysis No. 1 given by Val'ter, Yeremenko and Stremovskiy (1963). The analysis of the Kola mineral is taken from Sahama (1960) and that of the Congo mineral from Sahama and Hytönen (1957 a). Neumann suggested that the material for the Congo mineral subjected to analysis was possibly contaminated by some amount of fluorite, say, 3.4 %. Such a contamination would be entirely possible because the specific gravity of fluorite, viz. 3.18, is only slightly higher than that reported for götzenite (Ukraine 3.17; Kola 3.106; Congo 3.138). In a heavy liquid separation traces of fluorite could remain in the final material to be analyzed. In addition, Table 4 reveals the fact that both the Congo mineral and the Kola mineral contain considerably more Ca and F

TABLE 5.  
Unit cell content of götzenite. Based on a total of 30 atoms per cell.

	Azov Region, Ukraine	Yukspor, Kola	Shaheru, Congo
Si .....	3.97	3.94	3.87
Ti .....	1.04	0.81	0.88
Zr .....	0.06	0.01	—
Nb .....	0.04	0.18	0.00
Al .....	0.65	0.06	0.60
Fe .....	0.08	0.01	0.08
Mg .....	—	0.01	0.05
Mn .....	0.09	0.06	0.01
RE .....	0.11	0.08	0.00
Ca .....	4.18	5.09	5.34
Ba .....	—	—	0.00
Sr .....	0.10	0.06	0.00
Na .....	1.59	1.50	1.12
K .....	0.07	0.01	0.02
O .....	14.14	14.18	14.69
F .....	2.65	3.53	3.14
OH .....	1.23	0.46	0.20

than the Ukraine mineral. Accordingly, it seems feasible to suggest that the Kola and Congo materials were contaminated by some amount of fluorite and the Ukraine material was not.

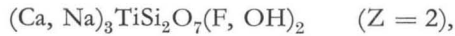
On the other hand, the specimen (numbered S. 80) in which the Congo götzenite occurs has been fully described by Sahama and Meyer (1958). The mineralogical composition of the rock is very complicated. The list of fourteen constituents found does not, however, contain fluorite. In thin section, fluorite has not been detected in the rock. Nor was any fluorite discovered in the powdered material used for analysis. A content of 3.4 % should easily be detectable through grain counting under the microscope. The Kola specimen was also studied in thin section. No fluorite was found in the rock, nor in the analyzed material, nor do Fersman and Bohnstedt (1937) mention any fluorite associated with götzenite at the Kola locality. The only one of the götzenite localities which is known to contain fluorite in association with götzenite is that of the Ukraine. Val'ter, Yeremenko and Stremovskiy (1963) specifically mention fluorite associated with götzenite, yet, the Ukraine mineral shows the lowest contents of Ca and F.

From the facts mentioned it is concluded that neither of the analyses of Table 4 suffers from any significant contamination of fluorite and that the peculiarities in chemical composition must be interpreted in some other way.

The unit cell content of götzenite was calculated on the basis of the three analyses

reproduced in Table 4. The calculation, made in the way described by Hey (1939; 1954), revealed the fact that the total number of atoms in the cell approaches 30 for all three specimens. For that reason it was assumed that the true number of atomic sites in the ideal götzenite structure is exactly 30 per cell. Accordingly, the cell content was calculated following the principle expressed by Donnay (1964). The results of this calculation are compiled in Table 5.

The data of Table 5 make it evident that the Ukraine mineral corresponds closely to the simplified formula  $(\text{Ca}, \text{Na})_6\text{Ti}_2\text{Si}_4\text{O}_{14}(\text{F}, \text{OH})_4$  in which CaNa includes also RE, Sr and K, and Ti includes also Zr, Nb, Al, Fe, (Mg) and Mn. This formula, in the form



is virtually identical to that arrived at by Val'ter, Yeremenko and Stremovskiy (1963). The figures for the Kola and Congo mineral compiled in Table 5 will also satisfy the formula given for the Ukraine mineral if the suggestion of Neumann is accepted, according to which part of the Ca occupies the sites of Ti in the structure. In Russian literature dealing with the crystal structures of the complex titanium and zirconium silicate minerals, this view is generally accepted. A small part of Al will replace Si and some O will replace (F, OH). The ratio of Ca to Na is not constant suggesting that these two cations occupy equivalent sites in the structure.

In the form given, the formula for götzenite is analogous to that of rosenbuschite, the difference being in the number of formula weights in the unit cell. The formula for götzenite presupposes that, like rosenbuschite, götzenite belongs to the sorosilicates with separate  $\text{Si}_2\text{O}_7$  groups. This assumption, though highly probable, still needs verification.

*Acknowledgements* — The authors are indebted to professor E. Wm. Heinrich of Ann Arbor, Michigan, for calling attention to the paper by Val'ter *et al.* and to Dr. A. Vormaa, of the Geological Survey of Finland, for fruitful discussions.

*Manuscript received, March 2, 1966*

## REFERENCES

- BUERGER, M. J. (1956) The determination of the crystal structure of pectolite  $\text{Ca}_2\text{NaHSi}_3\text{O}_8$ . *Zeitschr. Krist.*, Bd. 108, S. 248.
- DONNAY, J. D. H. (1963) *Crystal Data*, ACA Monograph No. 5.
- DONNAY, G. (1964) Using the cell content to derive the formula of a mineral from its chemical analysis. *Carnegie Inst. Washington Year Book* 63, p. 239.
- FERSMAN, A. E. and BOHNSTEDT, E. M. (1937) *Minerals of the Khibina and Lovozero tundras*. Lomosssov Inst. Acad. Sci. USSR.
- FLEISCHER, MICHAEL (1958 a) Abstract in *Amer. Miner.*, vol. 43, p. 790.
- »— (1958 b) Abstract in *Amer. Miner.*, vol. 43, p. 795.

- HEY, M. H. (1939) On the presentation of chemical analyses of minerals. *Min. Mag.*, vol. 25, p. 402.  
 —»— (1954) A further note on the presentation of chemical analyses of minerals. *Min. Mag.*, vol. 30, p. 481.
- NEUMANN, HENRICH, SVERDRUP, THOR and SÆBÖ, P. CHR. (1957) X-ray powder patterns for mineral identification. III Silicates. *Vid.-Akad. Avh.*, I, M.-N. Kl., No. 6.
- NEUMAN, HENRICH (1962) Contributions to the mineralogy of Norway, No. 13. Rosenbuschite and its relation to götzenite. *Norsk Geol. Tidskr.*, Bd. 42, p. 179.
- PARRISH, WILLIAM and MACK, MARIAN (1963) *Data for X-ray analysis*. Second Edition, Vol. I. Philips Technical Library.
- PEACOCK, M. A. (1937) On rosenbuschite. *Norsk Geol. Tidskr.*, Bd. 17, p. 17.
- SAHAMA, TH. G. and HYTÖNEN, KAI (1957 a) Götzenite and combeite, two new silicates from the Belgian Congo, *Min. Mag.*, vol. 31, p. 503.  
 —»— (1957 b) Unit cell of mosandrite, johnstrupite and rinkite. *Geol. För. Stockholm Förh.*, Bd. 79, p. 791.
- SAHAMA, TH. G. and MEYER, A. (1958) Study of the volcano Nyiragongo, A progress report. *Exploration du Parc National Albert, Mission d'Etudes Vulcanologiques*, Fasc. 2.
- SAHAMA, TH. G. (1960) Identity of calcium rinkite and götzenite. *Amer. Miner.*, vol. 45, p. 221.
- SHIBAJEVA, R. P. and BELOV, N. V. (1962) Crystal structure of rosenbuschite. *Dokl. Akad. Nauk USSR*, 143, No. 6. (in Russian).
- SLEPNEV, YU. S. (1957) The minerals of the rinkite group. *Izvestiya Akad. Nauk USSR, Ser. Geol.*, No. 3, p. 63 (in English translation).
- VAL'TER, A. A., YEREMENKO, G. K. and STREMOVSKIY, A. M. (1963) Calcium rinkite from alkalic rocks of the Ukraine. *Dokl. Akad. Sci. USSR, Earth Science Section*, vol. 150, 0. 112 (in English translation).

## ALKALI AMPHIBOLE OF OTANMÄKI, FINLAND

BY

KAI HYTÖNEN and AULIS HEIKKINEN

### ABSTRACT

An amphibole occurring as fissure filling in an alkali granite in Otanmäki, Finland, has an intermediate composition slightly closer to the alkali amphiboles than to the common hornblendes, approximating to:  $(\text{Na},\text{K})_{1.3} \text{Ca}_{0.8} \text{Fe}_{3.6}^{2+} \text{Mg}_{0.1} \text{Fe}_{1.1}^{3+} \text{Ti}_{0.1} \text{Al}_{1.1} \text{Si}_{7.4} \text{O}_{22.7} (\text{OH})_{1.4} \text{F}_{0.1}$ . The optical properties are characteristically identical with those of alkali amphiboles. Unit cell dimensions are very close to those of an arfvedsonite from Greenland and also to those of an amphibole from Nigeria, with composition intermediate between the hastingsites and alkali amphiboles.

### INTRODUCTION

The alkali amphibole that forms the subject of the present study was first described by Pääkkönen (1956, pp. 19—20) in a paper on the ilmenite-magnetite ore field of Otanmäki, Vuolijoki, eastern Finland. The amphibole was observed in fissures of a gneissose granite and the composition, based on optical properties, was assumed to be riebeckitic. Later, when the same granite of Otanmäki was studied by Marmo *et al.* (1966), an alkali amphibole was found with optical properties resembling those described by Pääkkönen. Further, a similar amphibole was observed in the alkali granite of Honkamäki, ca. 8 kilometres WNW of Otanmäki. As there are only few known observations of alkali amphibole in this country, a closer study of the amphibole was undertaken.

In this paper Hytönen is responsible for the physical and X-ray data and the writing, Heikkinen for the chemical analysis.

### OCCURRENCE

The amphibole that was selected for the present study occurs as fissure filling in an alkali granite at the western foot of the Otanmäki hill, near the Vanadium plant

TABLE 1.

Chemical analysis and weight norm of the alkali granite at the Vanadium plant, Otanmäki (Marmo *et. al.*, 1966).  
Anal. P. Ojanperä, V. Hoffrén and A. Heikkinen.

SiO <sub>2</sub> .....	71.19	Q .....	20.2
TiO <sub>2</sub> .....	0.32	ab .....	34.2
Al <sub>2</sub> O <sub>3</sub> .....	13.51	or .....	37.2
Fe <sub>2</sub> O <sub>3</sub> .....	1.50	Salic .....	91.6
FeO .....	1.41		
MnO .....	0.07		
MgO .....	0.03	ac .....	4.3
CaO .....	0.30	Na <sub>2</sub> SiO <sub>3</sub> .....	0.1
Na <sub>2</sub> O .....	4.66	wo .....	0.4
K <sub>2</sub> O .....	6.29	en .....	0.1
P <sub>2</sub> O <sub>5</sub> .....	0.09	hy .....	2.2
CO <sub>2</sub> .....	0.00	ap .....	0.2
H <sub>2</sub> O+ .....	0.32	il .....	0.6
H <sub>2</sub> O— .....	0.06	Femic .....	7.9
F .....	0.01	Rest .....	0.3
Nb <sub>2</sub> O <sub>5</sub> .....	0.01		
ZrO <sub>2</sub> .....	0.02		
SrO .....	0.0		
Rb <sub>2</sub> O .....	0.02		
	99.81		

of the Otanmäki Company. The fissures are up to 0.5 cm—1 cm wide and continue at least for 10 cm—20 cm. As main constituents they contain strongly undulatory quartz, microcline, brown mica, an unidentified brown mineral and quite large grains of alkali amphibole, measuring up to 5 mm—10 mm in length.

Chemical analysis of the alkali granite, made from a specimen free from fissures, was presented by Marmo *et al.* (*op. cit.*). The analysis is reproduced in Table 1. Instead of reproducing the calculated mode from Marmo *et al.*, the weight norm was computed and is presented in Table 1. The rock is peralkaline, i.e. the molecular proportion of alumina is less than that of soda plus potash. Attention should be paid to the presence of 4.3 per cent acmite (Na<sub>2</sub>O.Fe<sub>2</sub>O<sub>3</sub>.4SiO<sub>2</sub>) and 0.1 per cent sodium metasilicate (Na<sub>2</sub>O.SiO<sub>2</sub>) in the norm.

As main constituents the alkali granite contains cross-hatched and perthitic microcline (triclinicity 0.95), albite (An<sub>3</sub>Ab<sub>97</sub>), quartz with undulatory extinction and alkali amphibole that is strongly pleochroic with colours varying from light brown to dark greenish blue.

## EXPERIMENTAL

The amphibole was collected from one of the fissure specimens by hand picking, crushed, ground to —0.15 millimetres and purified with Clerici's solution in a centrifuge and with a Frantz-type isodynamic separator. The purity of the sample

TABLE 2.  
Physical properties of the Otanmäki amphibole

Optical properties	
This paper	Pääkkönen, 1956
$\alpha$ $1.696 \pm 0.002$	$\alpha$ 1.692
$\beta$ $1.704 \pm 0.003$	
$\gamma$ $1.707 \pm 0.003$	$\gamma$ 1.707
$\gamma - \alpha$ 0.011	$\gamma - \alpha$ 0.015
axial plane $\perp$ (010)	
$b = Z$	
$c \wedge Y$ $7^\circ - 13^\circ$	$c \wedge X$ $0^\circ - 4^\circ$
$2V\alpha$ $62^\circ - 66^\circ$	$2V\gamma$ $78^\circ, 80^\circ, 84^\circ$
Pleochroism:	Pleochroism:
X light brown	X dark blue
Y dark bluish green	Y yellow green
Z dark brownish green	Z deep blue
absorption:	
$Z \approx Y > X$	
Specific gravity measured (pycnometer)	3.429
Specific gravity calculated	3.407
Unit cell dimensions	
$a_0$ 9.940 Å	
$b_0$ 18.173 Å	
$c_0$ 5.329 Å	
$\beta$ $104^\circ 22'$	
$V$ 932.5 Å <sup>3</sup>	
space group C2/m	

to be analyzed was checked by microscopic examination. Foreign grains and inclusions (diameter  $\sim 5\mu$ ) total up to ca. one per cent of the sample.

The optical properties, the measured and calculated specific gravity and the unit cell dimensions of the amphibole are listed in Table 2, first column. In the second column we have reproduced the optical data published by Pääkkönen (*op. cit.*) for a separate alkali amphibole sample of Otanmäki.

The refractive indices were determined by the immersions method in sodium light, the orientation of the indicatrix and  $2V$  were measured with the universal stage. In sections parallel or almost parallel to (010) the extinction is incomplete both in white and monochromatic light. In the position closest to maximum absorption characteristic anomalous reddish interference colours appear in white light. Incomplete extinction and strong absorption decrease the accuracy of the measurement of the optical properties.

A thin section examination of the fissure specimen reveals that the amphibole is not quite homogeneous which is shown by the variation of the colour of the mine-

TABLE 2.  
Physical properties of the Otanmäki amphibole

Optical properties	
This paper	Pääkkönen, 1956
$\alpha$ 1.696 $\pm$ 0.002	$\alpha$ 1.692
$\beta$ 1.704 $\pm$ 0.003	
$\gamma$ 1.707 $\pm$ 0.003	$\gamma$ 1.707
$\gamma - \alpha$ 0.011	$\gamma - \alpha$ 0.015
axial plane $\perp$ (010)	
b = Z	
c $\wedge$ Y 7°—13°	c $\wedge$ X 0°—4°
2V $\alpha$ 62°—66°	2V $\gamma$ 78°, 80°, 84°
Pleochroism:	Pleochroism:
X light brown	X dark blue
Y dark bluish green	Y yellow green
Z dark brownish green	Z deep blue
absorption:	
Z $\approx$ Y > X	
Specific gravity measured (pycnometer)	3.429
Specific gravity calculated	3.407
Unit cell dimensions	
a <sub>0</sub> 9.940 Å	
b <sub>0</sub> 18.173 Å	
c <sub>0</sub> 5.329 Å	
$\beta$ 104°22'	
V 932.5 Å <sup>3</sup>	
space group C2/m	

to be analyzed was checked by microscopic examination. Foreign grains and inclusions (diameter  $\sim 5\mu$ ) total up to ca. one per cent of the sample.

The optical properties, the measured and calculated specific gravity and the unit cell dimensions of the amphibole are listed in Table 2, first column. In the second column we have reproduced the optical data published by Pääkkönen (*op. cit.*) for a separate alkali amphibole sample of Otanmäki.

The refractive indices were determined by the immersions method in sodium light, the orientation of the indicatrix and 2V were measured with the universal stage. In sections parallel or almost parallel to (010) the extinction is incomplete both in white and monochromatic light. In the position closest to maximum absorption characteristic anomalous reddish interference colours appear in white light. Incomplete extinction and strong absorption decrease the accuracy of the measurement of the optical properties.

A thin section examination of the fissure specimen reveals that the amphibole is not quite homogeneous which is shown by the variation of the colour of the mine-

TABLE 3.

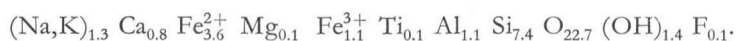
Indexed powder diffraction pattern of the Otanmäki amphibole. Geiger counter X-ray diffractometer. Filtered iron radiation with quartz standard.

hkl	I	$2\theta_{\text{meas}}$	$d_{\text{meas}}$	$d_{\text{calc}}$
110	100	13.10	8.49	8.51
200	3	23.23	4.81	4.82
040	5	24.64	4.54	4.54
131	5	32.88	3.420	3.419
240	11	34.06	3.305	3.304
310	60	35.69	3.159	3.161
330	15	39.91	2.836	2.836
151	15	41.47	2.734	2.732
061	4	43.50	2.612	2.612
$\bar{2}02$	3	44.55	2.554	2.554
400 } 350 }	4	47.43	2.407	{ 2.407 2.406
$\bar{3}51$	5	48.58	2.353	2.355
261	5	52.57	2.186	2.184
351	3	56.64	2.0405	2.0403
461	5	70.88	1.6694	1.6690
$\bar{6}61$	5	83.69	1.4510	1.4510

acter and the orientation of the indicatrix (*e.g.* Miyashiro, 1957). Therefore, it is not surprising to find a difference of this type in the optical properties of the amphibole of two separate specimens of the Otanmäki granite.

The unit-cell dimensions and space group were determined from single crystal a-axis zero-level and b-axis zero-, first- and second-level precession photographs. The indexing of the powder pattern, given in Table 3, was based on the crystallographic data obtained from the single-crystal study. The intensity I was measured from the peak area in the diffractometer pattern.

The result of the chemical analysis and the content of half of the unit-cell, calculated on the basis of the specific gravity and the X-ray data, is presented in table 4, first column. Neglecting the minor constituents, the formula of the Otanmäki amphibole may be written:

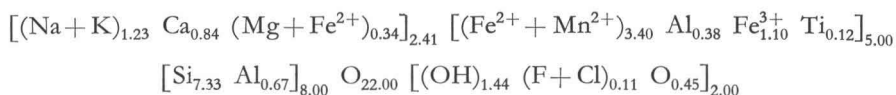


The composition of the amphibole is characterized by the predominance of the alkalis over Ca, by the high content of ferrous iron and by the low Mg.

The classification of the amphibole group is usually based on the character of the predominant ion in the X position of the structure, *i.e.* Na+K and Ca (*e.g.* Deer, Howie and Zussman, 1963, vol. 2, p. 208; Sundius, 1946). A comparison reveals that the Otanmäki amphibole, with regard to the ratio of alkalis to calcium, has an intermediate position slightly closer to the alkali amphiboles than to the common calciferous hornblendes.

To illustrate the relationship between the composition of the Otanmäki amphibole and those of the calcic and alkali amphiboles, a three-dimensional diagram from a paper of Smith (1959) is reproduced in a slightly modified form in Figure 2. Because of the predominance of ferrous iron over magnesium in the Otanmäki amphibole, the magnesian end members in the original diagram of Smith have been replaced by the ferrous end members in Figure 2. The calcic amphiboles (actinolite, ferroedenite, hastingsite and ferro-tschermakite) form the quadrilateral basis, the alkali amphiboles (ferro-richterite, arfvedsonite and riebeckite) have been erected on the vertical ordinate. The formulas of these end-members are shown in the figure. Al includes aluminum plus  $\text{Fe}^{3+}$ . In the diagram for all four valence states of amphiboles planes can be erected which express the amounts of the ions.

To locate the point of the Otanmäki amphibole within this diagram, the formula in Table 4 was re-calculated, following the general way of presenting amphibole formulas (*e.g.* Smith, *op. cit.*, and Ghose, 1965) as  $\text{X}_{2-3}\text{Y}_5\text{Z}_8\text{O}_{22}(\text{OH}, \text{F}, \text{O})_2$ , where X is Na, K, Ca, Mg,  $\text{Fe}^{2+}$ ,  $\text{Mn}^{2+}$ , Y is Mg,  $\text{Fe}^{2+}$ ,  $\text{Mn}^{2+}$ , Al,  $\text{Fe}^{3+}$ ,  $\text{Ti}^{4+}$  and Z is Si, Al. The calculation gave:



The point of the Otanmäki amphibole is shown as a large black sphere at the distant corner of an inset rectangle that has been constructed to facilitate orientation within the three-dimensional diagram. Examination of the diagram shows that the point lies in a position that is slightly closer to the alkali amphiboles than to the calcic amphiboles. Further, it is slightly closer to the riebeckite corner than to the corners of the two other alkali amphiboles, arfvedsonite and ferro-richterite.

To obtain information on the composition of the blue portions, the amphibole was examined with the electron probe micro-analyzer (Geoscan/Cambridge). Intensity measurements show that the contents of Si, total Fe, Mg, Mn, Na and K are practically the same in the blue portions as in the main portion, whereas the calcium content of the blue portions is half that of the main portion.

Accordingly, assuming that the analysis of Table 4, first column, represents the composition of the main portion of the amphibole, with 0.85 atoms of calcium in half of the unit-cell, the content of Ca in the blue portions would be ca. 0.4. In other words, the composition of the blue portions is clearly closer to the alkali amphiboles than the main portion (see Figure 2). This conclusion would eventually, although not necessarily, need an increase in the sodium content. However, the ability to detect small variations in relatively low sodium contents with the electron probe microanalyzer is limited due to the low atomic number of sodium. The rather low content of calcium in the blue portions corresponds with their intense blue colour and almost parallel extinction, both of which are properties typical of the alkali amphibole riebeckite.

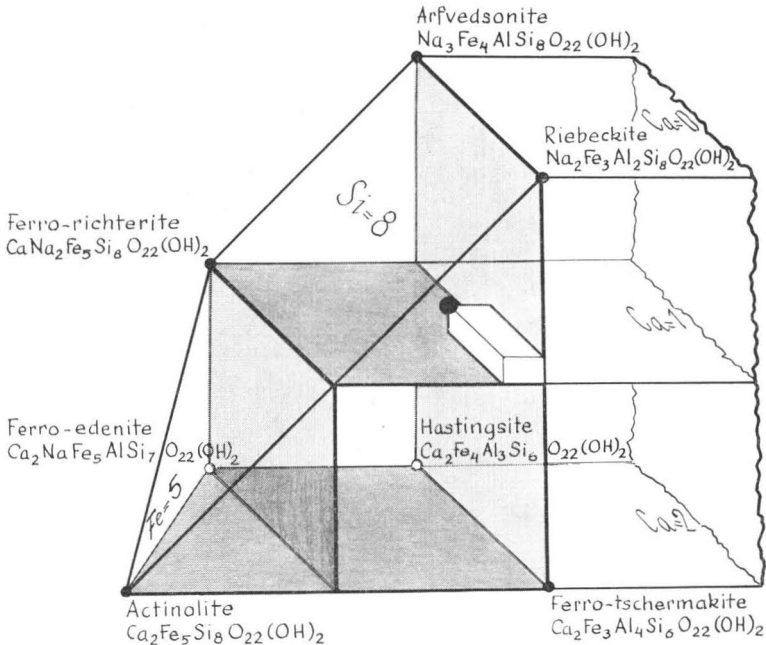


FIGURE 2. Three-dimensional diagram showing the compositional variation in amphiboles, modified from J. V. Smith (1959). The position of the Otanmäki amphibole is shown as a large black sphere at the distant corner of the inset rectangle.

## COMPARISON

In the following, some of the data presented in the previous chapter will be compared with those given for amphiboles in the literature.

Due to the high iron content of the Otanmäki amphibole, the values of the specific gravity and the refractive indices are fairly high, as in the iron-rich amphibole end members. Pleochroism, absorption and the relatively low value of the birefringence are of a type commonly observed in the amphiboles of the riebeckite-glaucophane series and arfvedsonites.

The optical orientation is normal-symmetric, i.e. the optic axial plane is perpendicular to (010) and  $b = Z$ , with the extinction angle  $c \wedge Y = \text{small}$  ( $7^\circ$ – $13^\circ$ ). Amphiboles with such an optical orientation have been observed in the glaucophane-riebeckite series, where they have usually been called crossite (*e.g.* Miyashiro, 1957). The name crossite was originally given by Palache (1894). On the other hand, some crossites show parallel-symmetric optical orientation. Further, some writers regard crossite as having been defined by a composition which is intermediate between glaucophane and magnesioriebeckite (*e.g.* Deer, Howie and Zussman, 1963, vol. 2,

TABLE 4.

Chemical composition and some physical properties of the Otanmäki amphibole (column 1) and of four other alkali amphiboles.

	1	2	3	4	5
SiO <sub>2</sub> .....	45.99	50.88	38.56	47.46	46.57
TiO <sub>2</sub> .....	1.00	1.86	0.96	0.74	1.43
Al <sub>2</sub> O <sub>3</sub> .....	5.57	8.53	10.31	2.43	1.89
Fe <sub>2</sub> O <sub>3</sub> .....	9.19	4.25	13.12	11.85	3.73
FeO .....	26.00	13.41	18.72	24.44	31.38
MnO .....	1.08	0.23	1.91	0.56	0.68
MgO .....	0.49	8.50	1.24	0.46	0.30
CaO .....	4.93	5.19	5.78	1.19	5.90
Na <sub>2</sub> O .....	3.26	4.63	4.71	6.89	4.54
K <sub>2</sub> O .....	1.10	0.03	2.73	1.59	1.18
P <sub>2</sub> O <sub>5</sub> .....	0.02	—	—	0.16	—
H <sub>2</sub> O+ .....	1.35	2.44	1.66	2.03	—
H <sub>2</sub> O— .....	0.00	0.00	0.00	0.22	0.13
F .....	0.20	—	0.30	—	3.84
Cl .....	0.02	—	0.15	—	—
—O = F <sub>2</sub> , Cl <sub>2</sub> ..	100.20	99.95	100.15	100.02	101.57
	0.08	—	0.16	—	1.62
	100.12	99.95	99.99	100.02	99.95
Si .....	7.36 } 8.00	7.32 } 8.00	6.20 } 8.00	7.52 } 8.00	7.57 } 8.00
Al <sup>iv</sup> .....	0.64 }	0.68 }	1.80 }	0.45 }	0.36 }
Ti <sup>iv</sup> .....	— }	— }	— }	0.03 }	0.07 }
Al <sup>vi</sup> .....	0.41 }	0.75 }	0.15 }	— }	— }
Ti <sup>vi</sup> .....	0.12 } 1.64	0.21 } 1.43	0.11 } 1.85	0.06 } 1.47	0.10 } 0.56
Fe <sup>3+</sup> .....	1.11 }	0.47 }	1.59 }	1.41 }	0.46 }
Fe <sup>2+</sup> .....	3.48 }	1.60 }	2.52 }	3.24 }	4.26 }
Mn .....	0.15 } 3.75	0.03 } 3.47	0.26 } 3.08	0.08 } 3.43	0.09 } 4.42
Mg .....	0.12 }	1.84 }	0.30 }	0.11 }	0.07 }
Ca .....	0.85 }	0.80 }	1.00 }	0.20 }	1.03 }
Na .....	1.01 } 2.09	1.30 } 2.10	1.47 } 3.03	2.11 } 2.63	1.43 } 2.70
K .....	0.23 }	— }	0.56 }	0.32 }	0.24 }
OH .....	1.44 }	2.33 }	1.78 }	2.14 }	— }
F .....	0.10 }	— }	0.15 }	— }	1.95 }
Cl .....	0.01 }	— }	0.04 }	— }	— }
O .....	22.64 }	21.67 }	22.03 }	21.69 }	— }
a <sub>0</sub> .....	9.940 Å			9.94 Å	9.923 Å
b <sub>0</sub> .....	18.173 Å			18.17 Å	18.180 Å
c <sub>0</sub> .....	5.329 Å			5.34 Å	5.319 Å
β .....	104°22'			104°24'	104°9'
	α 1.696 β 1.704 γ 1.707 b = Z c ∧ Y 7°—13°	α 1.645  γ 1.654  c ∧ Y 11°	α 1.705 β 1.713 γ 1.715 b = Z		α' 1.693  γ' 1.701

- Otanmäki amphibole. The content of half of the unit-cell calculated on the basis of the specific gravity and the unit-cell volume.
- Crossite from crossite-amphibolite, Knockormal, South Ayrshire, Scotland (Bloxam and Allen, 1960). Formula calculated on the basis of 24 (O, OH).
- Mbozi amphibole from syenite-gabbro complex, south-west Tanganyika (Brock, Gellatly and von Knorring, 1964). Anal. M. H. Kerr. Formula calculated on the basis of 24 (O, OH, F, Cl).

p. 334). A comparison of the crossite analyses (*e.g.* Palache, *op. cit.*, Machatschki, 1943; Holgate, 1951; Switzer, 1951; Bloxam and Allen, 1960) with that of the Otanmäki amphibole reveals a difference mainly in the contents of ferrous iron, magnesium and, of course, in the total alkalis. Mainly due to the lower iron content, the values of the refractive indices of the crossites are lower than those of the Otanmäki amphibole. On the other hand, there are certain similarities in the chemistry between some crossites and that of the Otanmäki amphibole.

For comparison the chemical analysis together with some optical data of a crossite from Knockormal, Ayrshire, Scotland (Bloxam and Allen, *op. cit.*) have been reproduced in Table 4, column 2.

Recently Brock, Gellatly and von Knorring (1964) have described two iron rich alkali amphiboles, one from Mbozi, S. W. Tanganyika, the other from Darkainle, Borama district, Somali Republic, with refractive indices, birefringence, pleochroism, anomalous interference colours and optical orientation particularly similar to those of the Otanmäki amphibole. Also the *d*-values of the strongest lines in the powder diffraction patterns of the Mbozi and Darkainle amphiboles are quite close to those listed in Table 3 in this paper. For comparison, the chemical analysis and optical data of the Mbozi amphibole have been reproduced in Table 4, column 3. The composition, especially of the Mbozi amphibole, approaches very close to the theoretical end-member  $\text{Na}_2\text{CaFe}_3^{2+}\text{Fe}_2^{3+}\text{Al}_2\text{Si}_6\text{O}_{22}(\text{OH})_2$ , for which the new name mboziite has been proposed.

In Figure 3 a diagram has been reproduced in simplified form from Jans (1964) showing the variation of the position of the optic axial plane of the amphiboles as a function of the contents of Ca in X-position and (Mg+Al) in Y-position in the structure. The point of the Otanmäki amphibole within this diagram is shown as a black circle. It lies in the field of amphiboles with normal-symmetric optical orientation.

Incomplete extinction has been observed on a number of alkali amphiboles and has been studied by various methods. Eskola and Sahlstein (1930) and Sahama (1956) have observed in some alkali amphiboles a striation on (010), parallel with the *c*-axis, and have attributed the incomplete extinction as indicating an intergrowth of two amphibole components with slightly different composition. An alternative view, based on measurement of transmittance of light of two arfvedsonites and one riebeckite, was proposed by Shoda (1957 and 1958), who showed that the orientations of the absorption axes and the axes of the indicatrix are not coincident. This author concludes that the anomalous optical properties of the three alkali amphiboles may be due to the elliptic vibration of light wave, resulting from the strong absorption of the mineral. There is no report of striations in Shoda's papers.

4. Arfvedsonite from Tunugliarfik, Greenland (Kawahara, 1963). Anal. H. Haramura. The content of half of the unit-cell calculated on the basis of the specific gravity (3.37) and the unit-cell volume ( $934.2 \text{ \AA}^3$ ).
5. Alkali amphibole from quartz-fayalite porphyry, Liruei Complex, Jos Plateau, Nigeria (Borley and Frost, 1963). The formula has been calculated on the basis of 23 oxygen atoms as it was not possible to determine  $\text{H}_2\text{O}+$ .

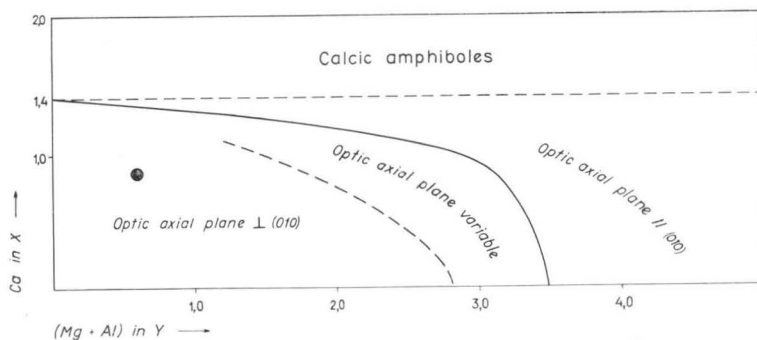


FIGURE 3. Variation of the position of the optic axial plane of the amphiboles as a function of the contents of Ca in X-position and (Mg+Al) in Y-position. Simplified from Jans (1964). Black circle = Otanmäki amphibole.

As the Otanmäki amphibole shows no striation on (100) and the reflections in the precession photographs taken show no doubling, it is concluded, that the mineral represents a single homogeneous phase rather than an intergrowth of two amphibole components. Accordingly, the incomplete extinction of the Otanmäki amphibole appears to be of the type described by Shoda.

The unit-cell dimensions and the powder diffraction pattern of the Otanmäki amphibole correspond with those of the monoclinic amphiboles in general. Of the roughly 10 amphiboles listed in the X-ray powder data file up to 1964, an arfvedsonite from Nunarsuatsiak, Tunugdliarfik, Greenland (ASTM 14—633; Kawahara, 1963), shows unit cell dimensions and a powder diffraction pattern almost identical with those of the Otanmäki amphibole. Chemically these two amphiboles correspond closely in their high contents of  $\text{Fe}^{2+}$  and  $\text{Fe}^{3+}$  and low Mg and differ from each other mainly in the contents of Ca and Na. This arfvedsonite from Greenland also shows incomplete extinction (Shoda, 1958). Chemical analysis and unit-cell dimensions of the arfvedsonite are reproduced in Table 4, column 4.

For the other amphiboles listed in the X-ray powder data file the unit-cell dimensions clearly differ from those of the Otanmäki amphibole, the lengths of the unit-cell edges being usually shorter, and hence the unit-cell volume smaller.

An unnamed amphibole from a quartz-fayalite porphyry, Liruei complex, Jos Plateau, Nigeria (Borley and Frost, 1963; sample number A 25), has an intermediate composition that is slightly closer to the arfvedsonites and the riebeckitic arfvedsonites than to the hastingsites from the Nigerian granites. Optically this amphibole resembles the alkali amphiboles. Its unit-cell parameters are intermediate between the two types of amphibole suggesting, according to Frost, evidence of limited solid solution between the hastingsites and the alkali amphiboles from the Nigerian granites.

Chemically this Nigerian amphibole (Table 4, column 5) corresponds with the Otanmäki amphibole in the content of high total iron, low magnesium and also in the contents of calcium and total alkalis. Also the refractive indices, colour and the unit-cell dimensions of these two amphiboles are close to each other.

*Acknowledgements* — Thanks are due to the following persons of the Geological Survey of Finland: to Dr. Atso Vormaa for advice in the single crystal X-ray work and critical reading of the manuscript, to Mr. J. Siivola, Mag. Phil., for the electron probe micro-analysis, and to Mrs. Toini Mikkola, Mag. Phil., and Mrs. Kerttu Järvinen, for the drawings.

The authors also wish to thank Mr. Ole Lindholm, Mag. Phil., and the Otanmäki Company for assistance in collection of the specimen, and prof. Th. G. Sahama, of the University of Helsinki, for directing the authors attention to the unpublished thesis of H. Jans.

*Manuscript received, March 2, 1966*

#### REFERENCES

- BLOXAM, T. W. and ALLEN, J. B. (1960). Glaucofan-shist, eclogite, and associated rocks from Knocknoral in the Girvan-Ballantrae complex, South Ayrshire. *Transactions of the Royal Society of Edinburgh*, vol. LXIV, No 1, 1—27.
- BORLEY, G. and FROST, M. T. (1963). Some observations on igneous ferrohastingsites. *Mineralog. Mag.*, vol. 33, No 263, 646—662.
- BROCK, P. W. G., GELLATLY, D. C. and VON KNORRING, O. (1964) Mboziite, a new sodic amphibole end member. *Mineralog. Mag.*, vol. 33, No 267, 1057—1065.
- DEER, W. A., HOWIE, R. A. and ZUSSMAN, J. (1963) *Rock-forming minerals*, vol. 2, chain silicates. Longmans, Green and Co. Ltd., London.
- ESKOLA, PENTTI and SAHLSTEIN (SAHAMA), TH. G. (1930) Über die unvollkommene Auslöschung einiger Amphibole. *C. R. Soc. Géol. Finlande*, 3; *Bull. Comm. Géol. Finlande* 92, 89—95.
- GHOSE, S. (1965) A scheme of cation distribution in the amphiboles. *Mineralog. Mag.*, vol. 35, No 269, 46—54.
- HOLGATE, N. (1951) On crossite from Anglesey. *Mineralog. Mag.*, vol. 29, No 215, 792—798.
- JANS, HENK S. J. (1964) De Plaats van borgniezite in de groep van de alkali-amfibolen volgens zijn chemische samenstelling en fysische eigenschappen. Thesis. Catholic University of Louvain, Belgium.
- KAWAHARA, A. (1963) X-ray studies of some alkaline amphiboles. *Mineralog. Jour. (Japan)*, vol. 4, No 1, 30—40.
- MACHATSCHKI, F. (1943) Die Formel des Crossits von Vodno. *Neues Jahrb. Min., Monatshefte*, Abt. A, 17.
- MARMO, V., HOFFRÉN, V., HYTÖNEN, K., KALLIO, P., LINDHOLM, O. and SIIVOLA, J. (1966) On the granites of Honkamäki and Otanmäki, Finland, with special reference to the mineralogy of accessories. *Bull. Comm. Géol. Finlande* No 221.
- MIYASHIRO, A. (1957) Chemistry, optics and genesis of the alkali-amphiboles. *Journ. Fac. Sci. Univ. Tokyo*, sec. II, vol. 11, pt. 1, 57—83.
- PALACHE, C. (1894) On a rock from the vicinity of Berkeley containing a new soda amphibole. *Bull. Dept. Geol. Sci., Univ. California*, vol. 1, 181—192.
- PÄÄKKÖNEN, VEIKKO (1956) Otanmäki, the ilmenite-magnetite ore field in Finland. *Bull. Comm. Géol. Finlande* No 171.

- SAHAMA, TH. G. (1956) Optical anomalies in arfvedsonite from Greenland. *Amer. Mineral.*, vol. 41, Nos. 5 and 6, 509—512.
- SHODA, T. (1957) On probable elliptic vibration of light in heikolite. *Mineralog. Jour. (Japan)*, vol. 2, No 2, 114—133.
- »— (1958) Elliptic vibration of light of some alkali amphiboles. *Mineralog. Jour. (Japan)*, vol. 2, No 4, 269—278.
- SMITH, J. V. (1959) Graphical representation of amphibole compositions. *Amer. Mineral.*, vol. 44, 437—440.
- SUNDIUS, N. (1946) The classification of the hornblendes and the solid solution relations in the amphibole group. *Sveriges Geologiska Undersökning*, Ser. C, No 480, 1—36.
- SWITZER, G. (1951) Mineralogy of the California glaucophane shists. *Bull. California Division of Mines*, No 161, 51—70.

# ON A PECULIAR BRECCIA AT HIRVIJÄRVI, VIRRAT, CENTRAL FINLAND

BY

PENTTI RASTAS and VLADI MARMO

*Geological Survey of Finland, Otaniemi*

## ABSTRACT

The large granodiorite area to the west of Hirvijärvi contains scattered large fragments of various volcanic rocks from doleritic to granitic in composition. In several places, these fragments, measuring from some decimetres to several metres across, are sufficiently abundant to form a breccia. The particular locality described in the present paper is only some 150 by 200 m in size, and forms practically a single body with basic volcanogenic fragments brecciated by coarse granite porphyry-like rock, the whole mass being enclosed and at places cut by the surrounding granodiorite.

## CONTENTS

	Page
Introduction .....	157
Volcanic breccia .....	160
Petrology of the breccia .....	161
Dicussion .....	166
References .....	168

## INTRODUCTION

Within the area of the map quadrangle sheet Virrat (2214), Central Finland (Marmo, 1965), there is an area, to the west of Lake Hirvijärvi (Fig. 1) characterized by the presence of large fragments of various composition enclosed by the granodiorite forming the main rock of the area. These fragments are predominantly of volcanic origin except to the north-east of Hirvijärvi, where the fragments are of diorite, genetically and closely related to the diorite area on the northern and eastern side of the lake mentioned above. On the western shore of this lake, acid rocks of volcanic origin occur that are probably related to the basic and intermediate volcanic

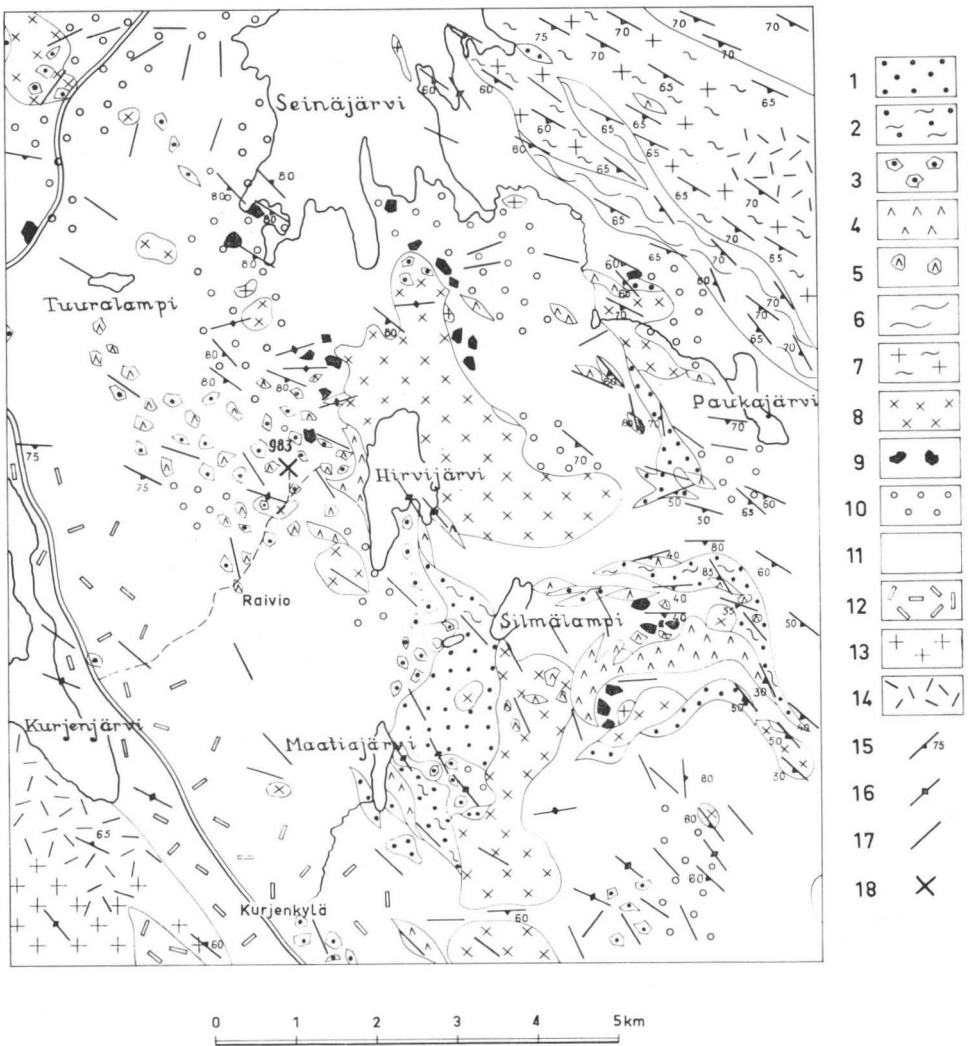


FIG. 1. Geology around the examined area (983 on the map). 1 = basic and intermediate volcanics, tuffs, amphibolite; 2 = volcanic gneiss; 3 = small fragments of metavolcanic rocks; 4 = acid volcanics, tuffite, »leptites»; 5 = fragments of acid volcanics; 6 = mica gneiss; 7 = granite gneiss; 8 = gabbro and diorite; 9 = fragments of diorite; 10 = quartz diorite; 11 = granodiorite; 12 = porphyroblastic granodiorite; 13 = granite, mostly coarse-grained; 14 = porphyroblastic granite; 15 = strike and dip; 16 = vertical dip; 17 = gneissosity; 18 = locality showed in Figs. 2 and 3.

rocks to the south of Lake Hirvijärvi. There they are also brecciated by a quartz diorite along the western margin, as well as to the east of Maatiajärvi. All the mentioned rock types also occur as fragments in the quartz- and granodiorites of the breccia mentioned above.

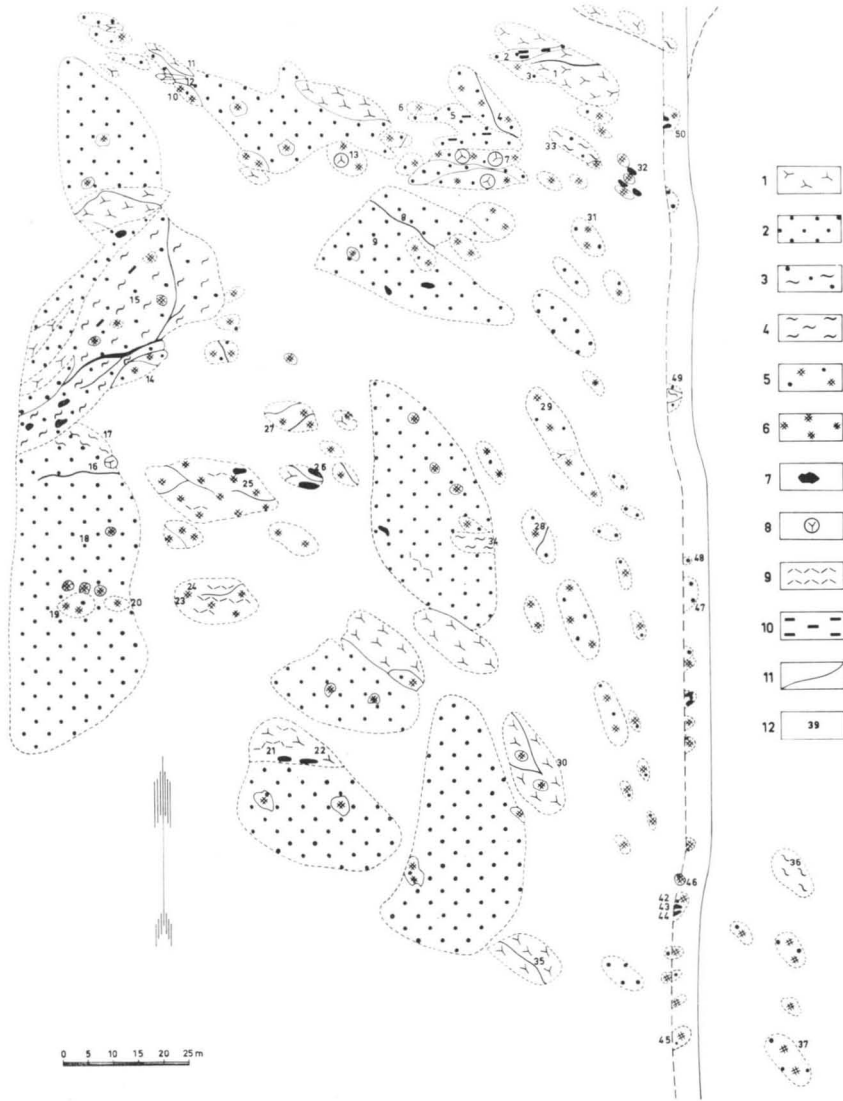


FIG. 2. Geology of the outcrops of the area 983 of Fig. 1. 1 = quartz- and granodiorite; 2 = granite porphyry; 3 = gneissose granite porphyry; 4 = acid gneiss; 5 = metadolerite and plagioclase porphyrite; 6 = amphibolite; 7 = diorite and gabbro; 8 = inclusions of quartz- and granodiorite; 9 = fragmentary streaks and clusters of acid gneiss; 10 = plagioclase insets; 11 = granite and aplite veinlets; 12 = sampling point.

Within this area, an especially interesting spot is at point 983 of the map (Fig. 1). A coherent body of complex breccia, some 150 by 200 m in size, seems to be enclosed by granodiorite. This particular body will be described below (Figs. 2 and 3).

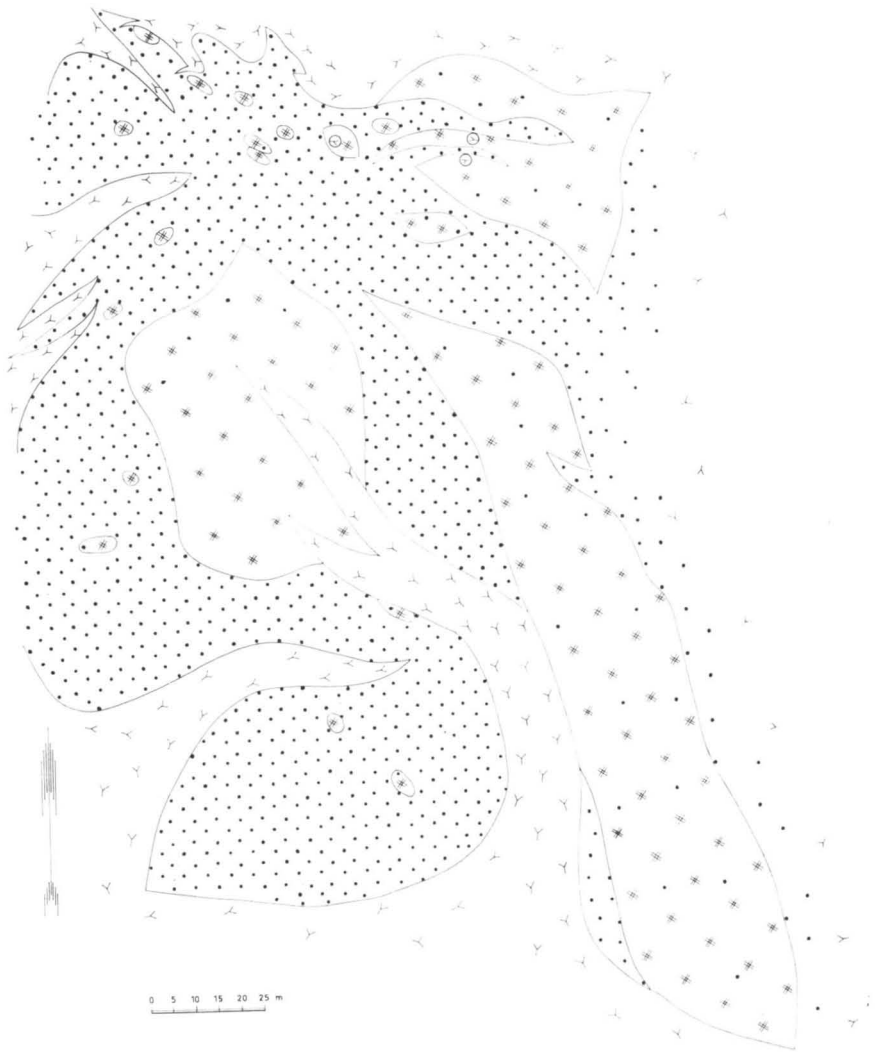


FIG. 3. Supposed rock boundaries of the area shown in Fig. 2. The legend is the same as in Fig. 2.

### VOLCANIC BRECCIA

The breccia, illustrated in Fig. 2 in which only the originally or artificially out-cropped places are shown, is made up mainly of the acid granite porphyry rock, which brecciates and encloses the basic rock types of various composition and texture. Furthermore, there is also younger grano- and quartzdiorite penetrating the whole



FIG. 4. A granodiorite inclusion in the metadoleritic fragment. The scale on the label is 5 cm.

breccia, but also occurring as inclusions in the basic fragments. The very youngest components are the narrow veinlets of granite and aplite.

In Fig. 3 the supposed contacts within the same area as shown in Fig. 2 are indicated. This figure readily gives the following impression: The oldest rock types present are the small inclusions of granodiorite composition enclosed by the basic rocks — metadolerite and plagioclase porphyrite (Fig. 4). This granodiorite is probably much older than the surrounding quartz- and granodiorite enclosing the whole brecciated mass shown in Fig. 3. The basic rocks form large, mainly lenticular fragments, probably belonging to the same ancient basic flows met with to the south of Hirvijärvi. These rocks have been brecciated by granite porphyry, originally acid extrusions. The enclosing granodiorite penetrates the whole breccia as dykes and veins.

#### PETROLOGY OF THE BRECCIA

*Granite porphyry.* This name is used for the porphyric granite-looking rock similar to that occurring as coherent beds on the western shore of Lake Hirvijärvi, and also forming the breccia considered in this paper. The size of the potash feldspar insets is 1 to 10 mm across, and the average grain size of the ground mass is 0.2 to 0.5 mm. The average composition of granite porphyry is revealed by the chemical analysis of Table 1 and its mineralogy by the following determinations by point counting (Table 2).

TABLE 1.  
Chemical composition of the brecciating granite porphyry. Analyst: A. Heikkinen

SiO <sub>2</sub> .....	70.42	<i>Calculated mode:</i>	
TiO <sub>2</sub> .....	0.37	Quartz .....	29.40
ZrO <sub>2</sub> .....	0.04	Albite .....	24.63
Al <sub>2</sub> O <sub>3</sub> .....	14.48	Anorthite .....	8.62
Fe <sub>2</sub> O <sub>3</sub> .....	0.97	K-feldspar .....	26.69
FeO .....	2.10	Biotite .....	8.00
MnO .....	0.07	Magnetite .....	1.39
MgO .....	0.85	Fluorite .....	0.14
CaO .....	2.05	Sphene .....	0.35
SrO .....	0.03	Apatite .....	0.34
BaO .....	0.10	Rest .....	0.79
Na <sub>2</sub> O .....	2.90		
K <sub>2</sub> O .....	5.30		
Rb <sub>2</sub> O .....	0.02		
P <sub>2</sub> O <sub>5</sub> .....	0.08		
CO <sub>2</sub> .....	0.00		
H <sub>2</sub> O+ .....	0.49		
H <sub>2</sub> O- .....	0.03		
F .....	0.09		
	100.39		
		Total	100.35
less for-O = F <sub>2</sub> .....	0.04		
	100.35		

TABLE 2.  
Modal composition of granite porphyry

Sampling point	9	12	47	47 a	gneissose varieties	
					15	17
Quartz .....	31.0 %	31.0 %	36.0 %	25.0 %	38.0 %	31.0 %
Plagioclase .....	30.0	30.0	27.0	30.0	26.0	33.0
(An % in Plag.) .....	(20—25)	(30—33)	(30)	(25)	(25—30)	(27—30)
K-feldspar .....	30.0	31.0	25.0	33.0	29.0	27.0
Biotite .....	7.5	7.0	11.0	11.0	6.0	7.5
Accessories .....	1.5	1.0	1.0	1.0	1.0	1.5

The microtexture of the rock is seen in Fig. 5. In a fine- to medium-grained matrix there are insets mainly of potash feldspar, sometimes also of oligoclase. The triclinicity of the potash feldspar insets varies from 0 to 1. In two cases examined (samples 9 and 18) a faint maxima at 0.4 and 0.2 could be observed. The insets are often enveloped by a fine-grained mixture of quartz, plagioclase and potash feldspar (Fig. 5). The common accessories are magnetite, epidote, apatite, sphene, orthite, zircon and sometimes also fluorite. According to the chemical analysis (Table 1) the composition is truly granitic. Furthermore, the contents of F, Rb<sub>2</sub>O, SrO, ZrO<sub>2</sub> and especially of BaO are unusual in syn- or latekinematic granites, but are more com-



FIG. 5. Granite porphyry. Point 9 on Fig. 2. The insets are mainly microcline, to the left also consisting of plagioclase. N+, Magn. 8×. Photo: E. Halme.

mon in younger intrusive granites formed at somewhat elevated temperatures; they are not uncommon in granite porphyries. This, together with the microtexture of the rock, entitles also this rock to be classified with granite porphyries — considering them here as somewhat recrystallized acidic extrusives.

The gneissose varieties of this rock occur (see Fig. 2), with the preserved porphyritic texture (Fig. 6). Sometimes, and especially outside the area shown in Figs. 2 and 3, a grading into a more coarse-grained granodiorite-like rock takes place. Such a gradational zone is common especially around the granite porphyry inclusions within the quartz- and granodiorite embracing the breccia mass.

*Basic fragments* of the breccia (Table 3) are mostly ophitic in texture, but of rather varying grain-size. Among them those of plagioclase porphyrite and amphibolite with plagioclase insets ( $An_{40-50}$ ) are most common. They often form fairly large fragments (see Fig. 3) which are brecciated by granite porphyry (Fig. 7). But the texture of these basic rock types often grades into one which resembles more closely a porphyritic dolerite with pronounced ophitic plagioclase (Fig. 8). On the other hand, there are also gradations into fine-grained gabbroic rocks which may also occur as single but comparatively small acicular fragments (Figs. 9 and 10). All such fragments seem to be closely related to the plagioclase and uralite porphyrities occurring to the south of Lake Hirvijärvi and in the breccia here concerned they form inclusions of considerable size (Fig. 3) — up to several tens of meters across.

The breccia also contains fragments of *diorite* which are sometimes large, their size varying from some decimeters to several meters across. The diorite is similar

TABLE 3.  
Modal composition of some fragments of basic rocks

Rock type	Metadolerite				Plagioclase porphyrite		Fine-grained gabbro	Diorite	
	14	29	37	42	19	43	3	26	50
Quartz . . . .	20 %	0.5 %	2.0 %	0.5 %	5.0 %	1.0 %	1.3 %	5.0 %	4.0 %
Plagioclase ..	47.0	49.0	41.0	50.0	38.5	30.0	42.0	38.0	53.0
(An % in Plag.) . . . .	(45—50)	(40—45)	(30—35)	(40—50)	(25—30)	(30—40)	(35)	(30—35)	(~40)
K-felspar . . .	—	—	—	—	—	—	—	4.0	—
Biotite . . . .	7.0	4.0	11.0	7.0	13.0	13.5	14.0	13.0	11.0
Hornblende . .	42.0	39.0	44.5	36.5	41.5	52.5	41.5	39.0	31.0
Pyroxene . . .	1.0	5.0	—	—	—	—	—	—	—
Accessories . .	1.0	2.5	1.5	6.0	2.0	3.0	1.2	1.0	1.0

to that occupying a large coherent area NE of Lake Hirvijärvi and is supposedly in close relation to that. It should also be mentioned that it sometimes contains up to 3.5 % magnetite. A few grains of calcite have been encountered in thin sections.

*Acid fragment* are not very abundant, but a gneiss-like rock probably also of volcanic origin occurs as xenoliths of various size both in the granite porphyry and in the basic fragments as inclusions. The xenoliths of an older granodiorite enclosed by metadoleritic fragments have already been mentioned (p. 161).

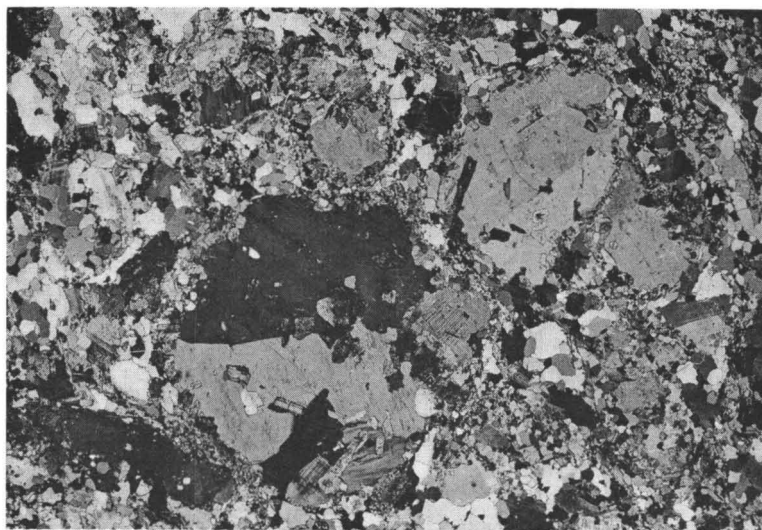


FIG. 6. Gneissose portion of granite porphyry, 15 in Fig. 2. Insets consist of plagioclase and K-feldspar. N+. Magn. 10×. Photo: E. Halme.



FIG. 7. Metadoleritic large fragment brecciated by granite porphyry. 8 in Fig. 2. Scale on the label is 5 cm.

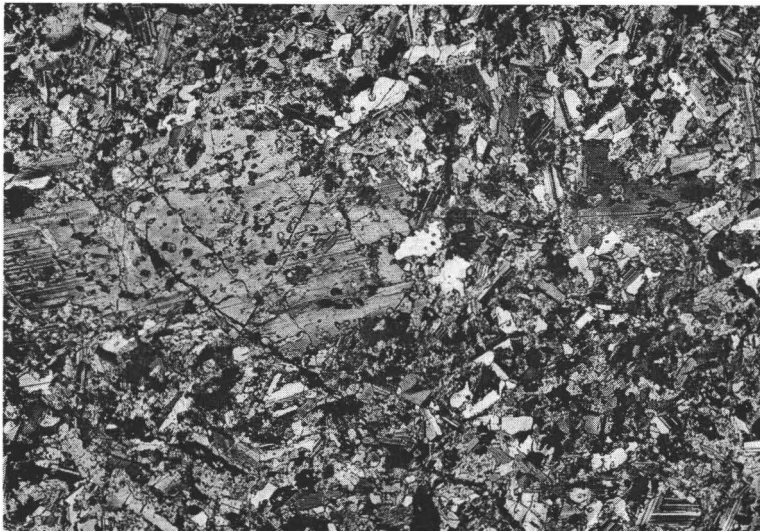


FIG. 8. Ophitic dolerite. 29 in Fig. 2. Contains scattered plagioclase insets. N+. Magn. 12 $\times$ . Photo: E. Halme.

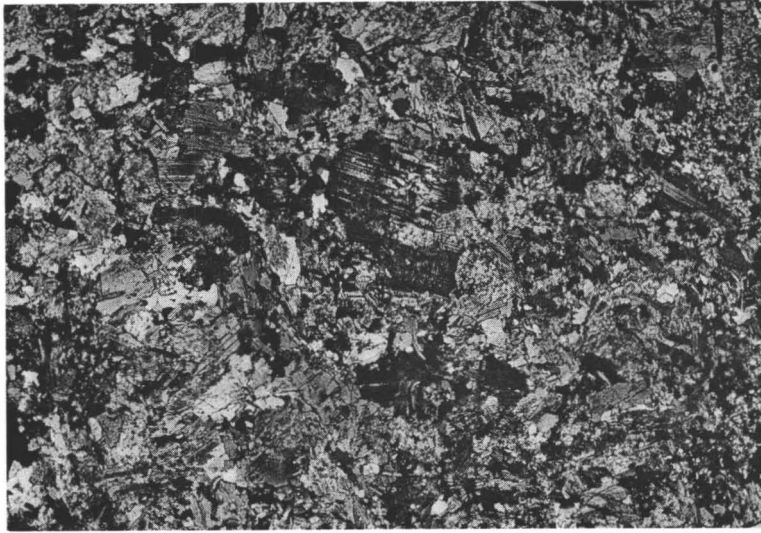


FIG. 9. Even-grained variety of dolerite resembling a fine-grained gabbro. 3 in Fig. 2. N+, Magn. 12 $\times$ . Photo: E. Halme.

*Aplitic and granitic* veins are the very youngest constituents of the breccia. They occur cross-cutting everything including the embracing grano- and quartzdiorites. Also aplitic has a tendency to contain microcline insets (Fig. 11), and in this sense it much resembles the aplitic-like granite porphyry of map sheet 2214 (Marmo, 1965), but which is outside the area mainly considered in the present paper.

## DISCUSSION

The description of the geology and petrography of the complex breccia embraced and cut by grano- and quartzdiorites occupying large areas, indicates that prior to the formation of the embracing acid rocks a complex geological evolution had taken place. The granodioritic inclusions in the basic fragments (p. 161) indicate the presence of such rocks before the volcanic extrusions. The volcanic activity began with basic flows, and the present doleritic and possibly also the dioritic fragments of the breccia may be derived from hypabyssal rocks to be considered as comagmatic with the basic flows themselves. The next stage in this evolution was that characterized by granite porphyries. Whether they were true flows, hypabyssal intrusions or both can only be guessed at. The intensive brecciation seen at the examined spot is rather in favour of the hypabyssal intrusions, thus also explaining the strikingly large size of the basic fragments. To the east of this place, however, there is also clear evidence for the acid flows (Marmo, 1965).

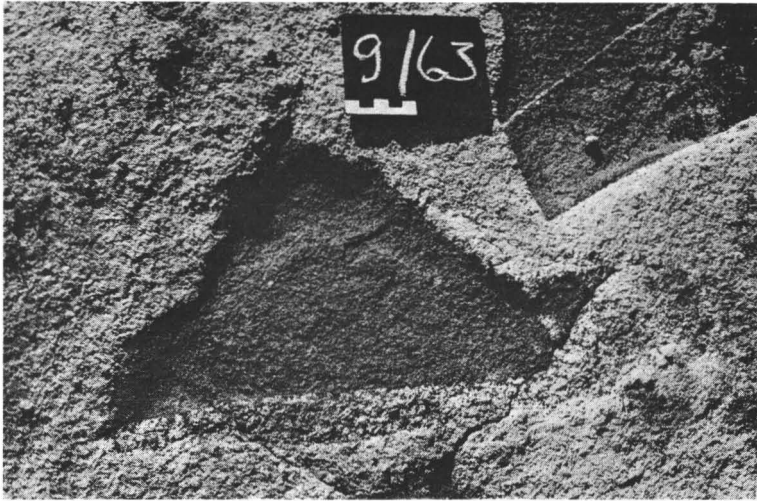


FIG. 10. Basic, partly gabbroic, partly ophitic doleritic clusters in granodiorite resembling coarse granite porphyry.

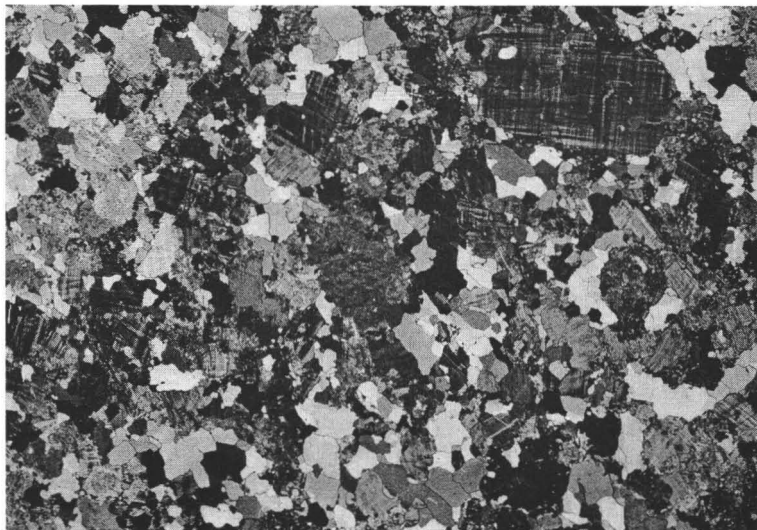


FIG. 11. Aplitic granite. 16 in Fig. 2. N+, Magn. 10×. Photo: E. Halme.

The surrounding grano- and quartzdiorites have been obviously formed from acid volcanic and sedimentogeneous materials, as could be shown at a more extensive examination of these rocks (Marmo, 1965). However, in places their homogeneity indicates an intrusive character, which may be interpreted as being paligenetic products with omnipresent remnants of the pre-existing rocks, to which also belongs the breccia described above.

*Manuscript received, March 5, 1966*

#### REFERENCES

- MARMO, VLADI (1965) Kallioperäkartan selitys 2214, Virrat. English summary. Explanation to the map of rocks. Suomen geologinen kartta 1 : 100 000.

## ON THE BARIUM-CONTENT OF SOME GRANITES OF FINLAND

BY

VLADI MARMO and JAAKKO SIIVOLA

*Geological Survey of Finland, Otaniemi*

### ABSTRACT

For the present paper, 13 granites containing BaO have been subjected to microprobe analyses and thereby it was established that practically all the BaO is in potash feldspar, containing 0.19 to 0.65 % BaO. The results have been tentatively discussed.

### INTRODUCTION

According to Rankama and Sahama (1950), rocks rich in barium or strontium are usually rich in both. In the granitic rocks, however, the enrichment is not striking. Furthermore, the mentioned elements only exceptionally form independent minerals in igneous rocks but rather are concealed in the main rock-forming minerals and barium preferably in the potash feldspar. The cited authors also pointed out that the potash feldspar formed during the early steps of the crystallization interval contain, as a rule, more strontium and barium than do the potash feldspars which are the last to crystallize. Barium may also replace potassium in the mica structure, up to 9 per cent of it may be present in barian muscovite, or as much as 6.16 per cent in barian biotite; this content is, however, low in the micas from late crystallates, the early-crystallized biotites being sometimes rich in barium (Engelhardt, 1936).

In general, the barium-contents of granites are seldom determined or indicated in chemical analyses. On the other hand, if this element is present in larger quantities, it comes out during the analytical procedure and can hardly be overlooked. Most granites seem to be very short or devoid of barium, but there are definite types of granites which regularly contain barium. According to Sahama (1945), for instance, the rapakivi granites of eastern Fennoscandia contain up to 0.09 % Ba (0.01 % Sr). Some younger granites may contain up to 0.06—0.07 % Ba (0.009—0.925 % Sr) etc.

TABLE 1.

Number of sample	K <sub>2</sub> O % in rock	K-feldspar % in rock	BaO % in rock (calc.)	BaO % in rock (anal.)	SO <sub>3</sub> % (if determ.)	Intensities			BaO % in K-feldspar	Remarks
						I Ba BaLa <sub>1</sub>	B Back-ground	I-B Ba		
1	6.80	40	—	0.47	0.06	1 382	129	1 253	0.90	Tebo, Sierra Leone. Used as standard
2	5.74	34	0.22	0.09	—	1 014	114	900	0.65	
3	5.79	34	0.15	0.09	—	714	118	596	0.43	*) K-feldspar amount estimated
4	—	(35) *	0.14	—	—	673	113	560	0.40	
5	4.82	29	0.05	0.08	—	341	107	234	0.17	
6	6.49	38	0.11	0.13	—	525	111	414	0.30	*) K-feldspar amount estimated
7	—	(30) *	0.05	—	—	373	121	252	0.18	
8	4.73	28	0.09	—	—	544	112	432	0.31	
9	6.09	36	0.03	0.05	—	242	124	118	0.09	*) K-feldspar amount estimated
10	6.09	36	0.08	0.05	—	420	114	306	0.22	
11	5.21	31	0.09	0.13	—	498	101	397	0.28	
12	5.80	34	0.10	0.03	—	531	112	419	0.30	*) K-feldspar amount estimated
13	—	(35) *	0.05	—	—	268	105	163	0.12	
14	5.30	27	0.13	0.10	—	789	102	687	0.49	

2. Granite, Obnäs (Lokka, 1934)
3. » Värnäs, Obnäs (Lokka, 1934)
4. » Bodom
5. » Äva, Ahvenanmaa (Lokka, 1934)
6. » Onas, Porvoo (Lokka, 1934)
7. Tirillite, Petäjävesi
8. » Tullisenlampi, Lemi (Simonen, 1961)
9. Rapakivi, even-grained, Taivassalo (Lokka, 1934)
10. » Taivassalo (Lokka, 1934)
11. » Laitila (Lokka, 1934)
12. » Vinkkilä, Vehmaa (Lokka, 1934)
13. » Lappi, TL
14. Granite porphyry, Virrat (Rastas-Marmo, 1966)

Because the barium-content of granites was confined to some of them only, all of which seemed to be similar to a certain, the question arose as to whether the behavior of barium of granites could have some bearing on general granite problems, too.

Furthermore it was found out that the barium may not always be concealed in feldspar or mica, but may also occur there as independent mineral—baryte, as was the case for the granite of Tebo, Sierra Leone, which contained 0.47 % BaO, part of which was in potash feldspar (0.9 %), none or less than 0.09 % in mica, but 0.11 % as baryte (Marmo, 1966).

Therefore, it was decided to examine this problem tentatively in some granites, known from previous work to be barium-bearing.

It should also be mentioned that the modern development of granite petrology pays increasing attention to the accessory element distribution among granites in general. As a matter of fact, as early as 1939, Sahama and Rankama (1939) emphasized the possibility of using the accessory elements as Index Elements for the further classification of granites. This possibility remained uninvestigated in detail by the

cited authors, but certainly their work indicated some very important points of view. As mentioned above, future petrology will pay more attention to the accessory constituents of granites, and there is already a trend visible along these lines.

### MATERIAL INVESTIGATED

Based on the literature, 13 granites containing 0.03 to 0.13 % BaO were chosen. Specimens of the granites were used for microprobe analytical examinations. The polished sections were first checked for baryte because this mineral was present in the granite of Tebo, Sierra Leone (Marmo, 1966), but it was not detected. Then, for each polished section, ten arbitrarily chosen points within potash feldspar were taken to determine the intensity of the  $BaLa_1$ -line. The granite of Tebo (see above) was thereby used as the standard. To ensure that the chosen point was within a potash feldspar grain the K  $K\alpha$ -intensity was simultaneously determined. The time of measurement was 100 seconds. The background was determined using quartz.

For all the samples the BaO-content of micas was likewise examined and thereby it was found out, that, on an average, it is less than one tenth of the BaO-content of the respective potash feldspar.

Table 1 includes all these determinations. From the known total analyses of the rocks, the modal potash feldspar content was calculated (see Table 1).

In a similar way the BaO-content of the total rock could be also calculated and then compared with the value given by the total chemical analysis of the resp. rock.

In Table 1 all the intensity values are the means of ten measurements.

### CONCLUSIONS

If considering the values presented in Table 1, the following observation can be made: there is no correlation between potassium and barium, the latter obviously being entirely independently distributed but mainly incorporated into K-feldspar. Furthermore, the highest BaO-contents in K-feldspar are in those granites (2, 3, 4 of Table 1), which are probably postkinematic, and which are of more or less obscure character. No 14 is a granite porphyry forming the brecciating rock, probably of volcanic origin, of a peculiar breccia within a granodiorite area (Rastas and Marmo, 1966). All these rocks bear a potash feldspar of varying triclinicity and containing more than 0.40 % BaO. The next group — rapakivi granites and tirilite, also usually associating rapakivi or other orthoclase-bearing granites — contains, on an average, more than 0.20 % BaO in K-feldspar. Also these granites are postkinematic. Late-kinematic and other granites with microcline of highly developed triclinicity have not been included in the present study, because the BaO-content of them is generally conspicuously low. Thus there seems to be a tendency for BaO to occur in particular group of granites only.

The present paper is to be taken merely as a preliminary account, and the conclusion reached as a tentative one. It is hoped, however, that this paper will initiate further study into this and other related questions.

*Manuscript received, March 11, 1966*

#### REFERENCES

- ENGELHARDT, WOLF VON (1936) Die Geochemie des Barium. *Chemie Erde*, vol. 10, p. 187.
- LOKKA, LAURI (1934) Neuere chemische Analysen von finnischen Gesteinen. *Bull. Comm. géol. Finlande* 105.
- MARMO, VLADI (1966) Monzonitic hornblende granite of Tebo, Central Sierra Leone. *Bull. Comm. géol. Finlande* 222, p. 53.
- RANKAMA, KALERVO and SAHAMA, TH. G. (1950) *Geochemistry*. Chicago.
- RASTAS, PENTTI and MARMO, VLADI (1966) On a peculiar breccia at Hirvijärvi, Virrat, Central Finland. *Bull. Comm. géol. Finlande* 222, p.
- SAHAMA, TH. G. (1945) On the chemistry of the east Fennoscandian rapakivi granites. *Bull. Comm. géol. Finlande* 136, p. 15.
- »— and RANKAMA, KALERVO (1939) Preliminary notes on the geochemical properties of the Maarianvaara granite. *Bull. Comm. géol. Finlande* 125, p. 5.
- SIMONEN, AHTI (1961) Olivine from rapakivi. *Bull. Comm. géol. Finlande* 196, p. 371.

# THE DIFFERENTIATION OF GABBRO- ANORTHOSITE INTRUSIONS AND THE FORMATION OF ANORTHOSITES

BY

ANTTI SAVOLAHTI

*Institute of Geology and Mineralogy, University of Helsinki*

## ABSTRACT

The main rocks composing the gabbro-anorthosite intrusions of the region of Ahvenisto, Finland, are as follows, listed in order from the oldest to the youngest: pegmatoid gabbros and pegmatoid anorthosites, anorthosites, gabbro-anorthosites, and anorthosite-gabbros. The marginal varieties of the intrusions are described as a separate category. In addition, descriptions are given of late-stage differentiates, autometamorphic and autometamorphic processes as well as, finally, metamorphic and metasomatic phenomena.

Anorthosite lenses formed at a stage of crystallization when the rate of genesis of plagioclase nuclei in the magma was greatest — and this stage did not coincide with the inception of crystallization.

## CONTENTS

	Page
Introduction .....	174
Structure of the gabbro-anorthosite intrusions, principal rocks and their inter- relations .....	177
Description of the principal rocks contained in the gabbro-anorthosite intrusions	178
Introduction .....	178
Pegmatoid gabbros and pegmatoid anorthosites .....	180
Anorthosites .....	186
Gabbro-anorthosites and anorthosite-gabbros .....	187
Marginal varieties of the gabbro-anorthosite intrusions .....	190
Late crystallizations of the gabbro-anorthosite intrusions and the autometa- morphic and autometamorphic processes .....	191
Metamorphism in gabbro-anorthosite intrusions .....	192
Conclusions .....	193
Acknowledgement .....	195
References .....	195

## INTRODUCTION

The Ahvenisto massif is situated in southern Finland between 26° and 27° E longitude and 61° and 61°30' N latitude. It has been previously described by, among others, Frosterus (1902), Wahl (1925) and Savolahti (1956).

The Ahvenisto massif consists of many magma bodies differing in composition and age (Savolahti 1956, p. 79). The oldest intrusive group in it forms a gabbro-anorthosite complex, which half surrounds an occurrence of biotite rapakivi in the shape of an incomplete arch (Fig. 1).

The rapakivi is younger than the gabbro-anorthosite, and there exists no evidence to suggest that these rocks had evolved through crystallization differentiation from the same magma. The close association of these rocks does not suffice as proof (*cf.*, Eskola 1961, p. 122). With reference to this matter, Turner and Verhoogen (1951, p. 256; 1960, p. 324) have written: »But it is perhaps well to remember at this stage that common mutual association of rocks is no infallible criterion of origin from a common source. No one, for example, would consider graywacke and peridotite to be derivatives of common magma merely because these two kinds of rock so frequently are found side by side in folded geosynclines.» Savolahti (1959, p. 94), for his part, observes that, taken statistically, there is an equal probability of all the different varieties of rock occurring in association. And he adds that if certain rocks occur more commonly in association with each other than with others, evidence must be found to explain why the frequent close association of such rocks occurs. No hypothesis can be accepted as proof one way or another. For example, in the case at hand, since many of the rapakivis are known to be situated in places where block movements have occurred, and which at the same time represent zones of weakness in the earth's crust, the unusual frequency of the simultaneous occurrence of rapakivis and basic rocks may be due simply to these factors. Magmas may have naturally intruded into such places at different times and from different levels more readily than into other places. Of course, intrusions can take place successively also from the same magma chamber — as apparently was the case in the formation of the gabbro-anorthosite complex. But before one can make legitimate assumptions concerning common parent magmas, there must exist other clear evidences of their occurrence than the mere common association of the rocks (*cf.*, Hjelmquist 1961).

On the other hand, evidence can be produced to support the contention that the rapakivis of the Ahvenisto region and the basic rocks occurring in association with them have no other connection than their having intruded into the same place (Savolahti 1956, pp. 34—45, 79—82; 1962, pp. 80—81). In his early day, Frosterus (1900) marked on his General Geological Map of Mikkeli (Sheet C2) the occurrence in the northern part of the Ahvenisto region granites older than the rapakivis but intersecting the basic rocks, although he was not bold enough to describe them in the explanatory text accompanying the map (Frosterus 1902) or to mark them on the detailed map of the Ahvenisto region under discussion in the present paper. Seder-

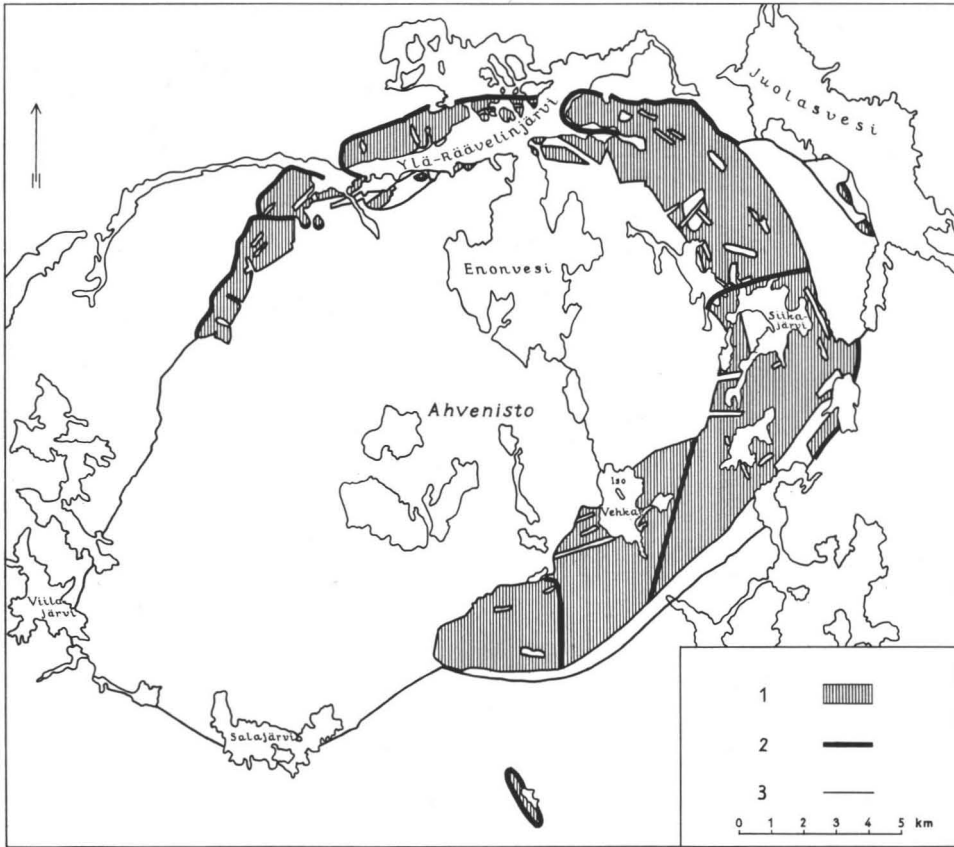


FIG. 1. Map of the gabbro-anorthosite intrusions of Ahvenisto and the younger intrusions intersecting them. 1) Gabbro-anorthosite intrusions. 2) Boundary of the gabbro-anorthosite intrusions against older rocks. 3) Boundary between the gabbro-anorthosite intrusions and the younger intrusions intersecting them.

holm (1928, p. 84) doubted the view that the rapakivis and the basic rocks found in association with them had originated from the same magma. Eskola (1957, p. 296) wrote in his textbook of geology and mineralogy that in the border zones of all the rapakivi areas there occur diabases, some of which are older than the rapakivis and even older than certain granites of the bedrock type, as along the margins of the Ahvenisto rapakivi in the commune of Mäntyharju, apart from the Viipuri region; and he added that other diabases, again, are younger than the rapakivi, as the olivine diabases of Ala-Satakunta, which penetrate both the rapakivi and sandstone as dikes and sills (see also Eskola 1961 and 1963). In any case, it may be said that the separation of the rapakivis and gabbro-anorthosites in the Ahvenisto region — if they

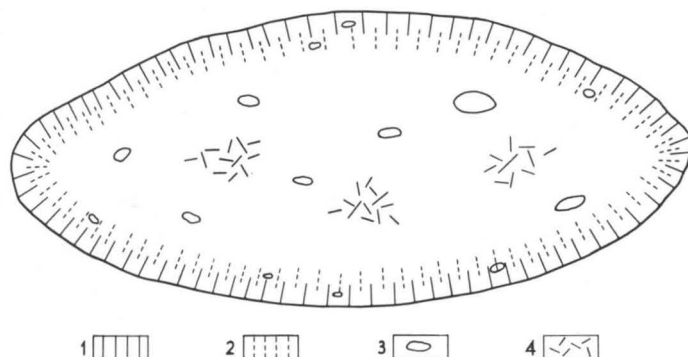


FIG. 2. Schematic picture of the structure of the gabbro-anorthosite intrusions. 1) Marginal varieties. 2) Latest crystallizations. 3) Anorthosite lenses. 4) Pegmatoid gabbros and anorthosites.

had derived from a common parent magma — did not take place after the intrusion *in situ*.

Evidence of the genetic lack of kinship between rocks apparently belonging together in close association has previously been presented by, among others, Buddington (1939) in his extensive study on the Adirondack region. This region had earlier provided Balk (1931) with material to support his hypothesis regarding the origin of anorthosites, which gained acceptance even in the pages of academic textbooks. This hypothesis probably represented the most far-reaching application of the in itself tenable theory of crystallization differentiation.

The investigation of the crystallization temperatures and crystallization courses of the principal minerals of basalt magmas (tholeiites, alkali basalts and high-alumina basalts) has also given results (Yoder and Tilley 1957, p. 159) that suggest that these magmas cannot occur as parent magmas through the crystallization differentiation of which large quantities of rocks of granitic composition evolve. Winkler (1962, p. 225) likewise reports a result indicating the same thing — the solidus of basalt is far higher than the liquidus of granite and even higher than the crystallization temperature of rapakivis.

The gabbro-anorthosite complex of Ahvenisto (Fig. 1) is divided into separate, independent intrusions, in each of which differentiation took place during the crystallization of the magma and even afterward (Fig. 2). They exhibit all the various stages of this differentiation — also nearly all the possible stages that have been project (see, *e.g.*, Buddington 1939, pp. 19—68, Kranck 1961, pp. 302—303, and Hess 1960). To be sure, the layered structures frequently described nowadays (Wager 1953, Ferguson and Pulvertaft 1963, Loomis 1963, Pulvertaft 1965, Speed 1963, Cameron 1963, and Wager, Brown, and Waldsworth 1960) are only slightly in evidence. Every gabbro-anorthosite intrusion constitutes an entirety in itself, which is

presupposed by the process of intruding, cooling and, in particular, the differentiation embodied in the theory of differentiation by crystallization.

Previously (Savolahti 1956, 1962), descriptions have been published on the way the rapakivis of the Ahvenisto region form intrusives in line with the theory referred to. What has happened there is a peculiar, inverse differentiation, clear evidence of which can likewise be cited (Savolahti 1956, pp. 83—93; 1962, pp. 79—92). A magma of rapakivi composition that differentiates in this way cannot (at least, not on a large scale) evolve out of K- and Si-poor and Ca-rich magma. This truth was suspected even by Bowen, the distinguished developer of the theory of differentiation by crystallization, having written as he did (Schairer and Bowen 1947, p. 87): »If all plagioclases were like anorthite in this respect (meaning crystallizing relations with potash feldspar), such a relation between the feldspars as that shown in rapakivi could presumably never have developed» — insofar as investigations into the crystallization of potash feldspars under vapour pressure (Bowen and Tuttle 1950) yield the same result and later experimental studies, summarized by, among others, Tuttle and Bowen (1958), lend further support to the matter.

The differentiation of the gabbro-anorthosite intrusions of the Ahvenisto region has not yet been depicted anywhere, although their varying rock types have been described fairly extensively (Frosterus 1902 and Savolahti 1956). The purpose of the present study is to delve into this matter. The grounds given in this introduction suffice, in the author's view, as justification.

## STRUCTURE OF THE GABBRO-ANORTHOSITE INTRUSIONS, PRINCIPAL ROCKS AND THEIR INTER-RELATIONS

The gabbro-anorthosite intrusions (Fig. 2) vary in size and shape, most commonly being elongated bodies. All of them have a fine-grained chilled contact with country rock of earlier origin. This phenomenon has also on occasion been observed in their contacts with other gabbro-anorthosite intrusions (Savolahti 1956, p. 31). The rock composing the marginal zones of the intrusions grades by degrees toward the center into coarse-grained gabbro-anorthosite (Fig. 3). In places, narrow, winding veins bordering indistinctly on their country rock penetrate the marginal zone from the body of gabbro-anorthosite. In many cases, they are darker of color than their country rock, and they have often been observed to contain amphiboles. Calcite and apatite are enriched into these veins and into the portion of the marginal zones on the side of the gabbro-anorthosite where the increase in the grain size of the intrusive rocks is most marked.

Gabbro-anorthosites constitute the principal rock of the intrusions. Here and there, they contain coarse-grained, pegmatoid patches of rock varying from gabbro to anorthosite in composition. This occurs more frequently in the middle portions of the intrusions, the patches being indistinctly situated against the gabbro-anorthosite.

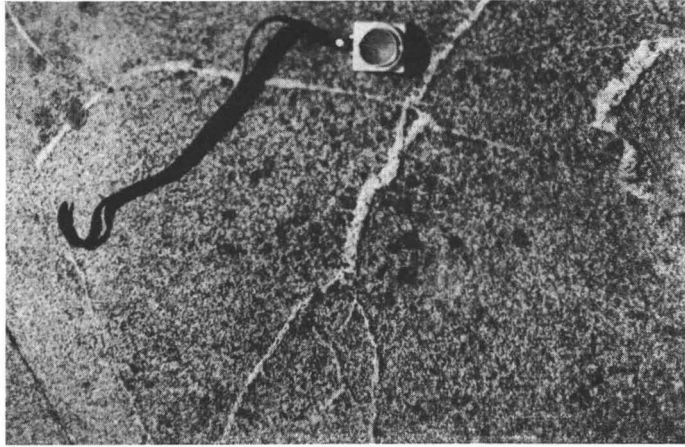


FIG. 3. Transition of a marginal variety of gabbro-anorthosite intrusion into a gabbro-anorthosite. South side of Lake Rääveli, Paistjärvi, commune of Heinola, region of Ahvenisto.

Figure 4 illustrates such a pegmatoid gabbro, in which plagioclase and hypersthene occur in nearly equal abundance.

Anorthosite lenses of varying size also occur in the gabbro-anorthosite intrusions (Fig. 5). The size of these lenses ranges from a few centimeters to dozens of meters; some of them may, perhaps, measure over a hundred meters in length. They border sharply on their country rock. Whether the anorthosites had become enriched into any particular part of the intrusions is difficult so say, for they have been found, at least to some extent, in all portions of the intrusions.

Present in the gabbro-anorthosite intrusions are a few small albite-diabase dikes, which are the most recent crystallizations.

The intrusions further bear witness to autometamorphic and autometasomatic as well as metamorphic and metasomatic processes. The latter include rocks metamorphosed through cataclasis and mylonitization as well as later intrusive action.

## DESCRIPTION OF THE PRINCIPAL ROCKS CONTAINED IN THE GABBRO-ANORTHOSITE INTRUSIONS

### Introduction

Although it might at first strike the reader as odd, it is pertinent, considered in the light of the genesis of the intrusions, to describe the rocks in the following order: pegmatoid gabbros and pegmatoid anorthosites, anorthosites, gabbro-anorthosites, varieties of rock contained in the border zones, and late crystallizations.

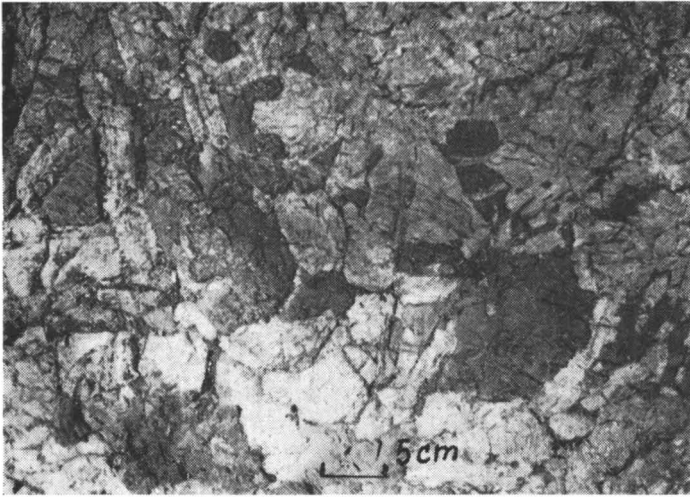


FIG. 4. Pegmatoid gabbro, with large grains of poikilitic hypersthene and plagioclase. North side of Siikajärvi, Mäntyharju, region of Ahvenisto (SAVOLAHTI 1956, p. 29).



FIG. 5. Anorthosite lens (pale) in a gabbro-anorthosite intrusion. Hietaniemi, Mäntyharju, region of Ahvenisto.

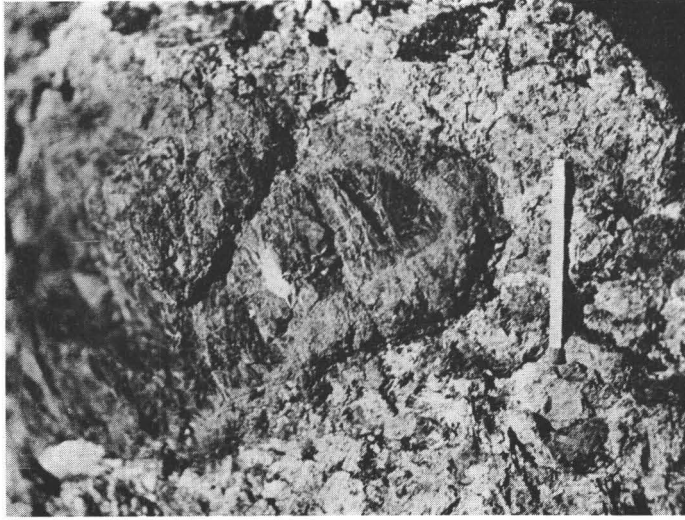


FIG. 6. Zoned hypersthene grain. Sharp boundary between zones. North side of Siikajärvi, Hietaniemi, Mäntyharju, region of Ahvenisto (Photo by Erkki Viluksela).

### **Pegmatoid Gabbros and Pegmatoid Anorthosites**

The pegmatoid gabbros and pegmatoid anorthosites are very coarse-grained (average grain size: 1—20 cm). In outward appearance, they look like pegmatites. The varieties of these rocks cannot in general be differentiated regionally, and their interrelations vary greatly. Genetically, they represent one and the same rock. In some cases, the passage of different types is gradual, sometimes abrupt. In the latter case, now it is the pegmatoid gabbro, now the pegmatoid anorthosite, that cuts across the other. With respect to grain size, the variation is similar: one is suddenly likely to run across a place where the grain size is strikingly larger or smaller than immediately adjacent to it, and the intersecting relationship of the rocks of differing grain size is similar to what has been described in the foregoing as prevailing between pegmatoid gabbros of different types.

Plagioclase and hypersthene are the principal minerals of these rocks, and they vary considerably in proportional content. In one spot the rock is apt to be nearly pure plagioclase, while immediately next to it the mineral content might be more than half hypersthene. The composition of the plagioclase is  $An_{50-68}$ , and according to the variation in the hypersthene content, for example, the composition of the plagioclase has not been observed to vary. In addition to hypersthene, these rocks contain small amounts of olivine, biotite, quartz, potash feldspar, ore and oxides as well as pyrites, including, *e.g.*, chalcopyrite and apatite and, at least as secondary constituents, amphibole and chlorite.

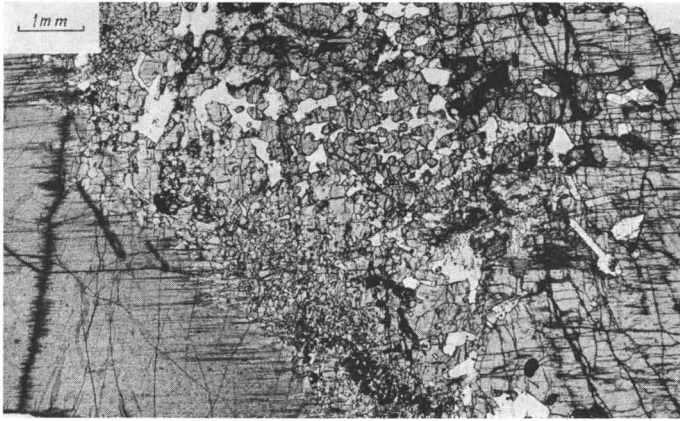


FIG. 7. Portion of the same hypersthene grain shown in Fig. 6. The hypersthene of the middle portion of the grain is lamellic, whereas that of the marginal portion is not. The joint between the two portions contains a zone of varying thickness rich in inclusions. 1 Nicol. North side of Siikajärvi, Hietaniemi, Mäntyharju, region of Ahvenisto.

On the northwestern side of Siikajärvi, at Hietaniemi, there is a pegmatoid gabbro (Savolahti 1956, p. 28), a portion of the hypersthene grains of which are beautifully zoned. In this pegmatoid gabbro the composition of the plagioclase is  $An_{53}$  ( $\alpha = 1.556$ ,  $\gamma = 1.563$ ). Figure 6 shows a large hypersthene grain, the center of which is dark brown, being surrounded by a brown zone about 0.5 cm wide. The difference in color, which is visible on the surface of the weathered rock, between the different parts is apparently due to the fact that, being richer in Fe than the center, the marginal portion of the hypersthene grain is rusty, for on the fresh surface of the rock no appreciable color difference between the parts can be noticed. The line of demarcation between the central and marginal parts of the hypersthene grain is fairly sharp (Fig. 6). These hypersthene grains of different compositions have become intergrown in such a way that their corresponding optic axes ( $\alpha$ ,  $\beta$ ,  $\gamma$ ) and thus their corresponding crystallographic axes ( $b$ ,  $a$ ,  $c$ ) join together. Fig. 7 gives a microscopic picture of the hypersthene grain under consideration, the view being nearly at right angles to the  $b$ -axis of the hypersthene. At the boundary between the central and marginal portions of the hypersthene grain there runs a zone of varying thickness rich in inclusions.

The hypersthene of the central portion (Fig. 7) contains very thin exsolution lamellae. They are so thin that they cannot be properly examined under the microscope. They have an oblique extinction between crossed nicols and their refractive indices deviate from those of the parent crystal. The hypersthene of the central portion has been exsolved following crystallization. The exsolution probably took place upon the crystallization of the marginal zone and, to a certain extent, also prior to that.

TABLE 1.

Chemical composition (analyst, A. Heikkinen) and physical properties of the hypersthene of the middle portion. Zoned hypersthene. Hietaniemi, Mäntyharju, region of Ahvenisto.

Weight per cent				
SiO <sub>2</sub> .....	49.52	Si .....	7.21	} Z = 8.00
Al <sub>2</sub> O <sub>3</sub> .....	7.45	Al .....	1.28	
TiO <sub>2</sub> .....	0.44	Ti .....	0.05	} Y = 0.64
Fe <sub>2</sub> O <sub>3</sub> .....	0.96	Fe <sup>3+</sup> .....	0.10	
FeO .....	15.70	Fe <sup>2+</sup> .....	1.92	} X = 7.12
MnO .....	0.24	Mn .....	0.03	
MgO .....	23.81	Mg .....	5.17	} W = 0.30
CaO .....	1.86	Ca .....	0.29	
Na <sub>2</sub> O .....	0.05	Na .....	0.01	
K <sub>2</sub> O .....	0.00			
P <sub>2</sub> O <sub>5</sub> .....	0.02			
CO <sub>2</sub> .....	0.00			
H <sub>2</sub> O+ .....	0.00			
H <sub>2</sub> O- .....	0.04			
Total			100.09	

## Physical properties

$\alpha$	= 1.692
$\gamma$	= 1.705
$2V\alpha$	= 77°
D	= 3.46

Figure 7 further reveals how the hypersthene grades over in part before the joint to take on the character of the marginal zone.

When Mg—Fe silicate crystallizes from magmas, it almost invariably assumes the orthorhombic, stable at temperatures below 1 140° at the magnesian end and below 955° at the other extreme (Bowen and Schairer 1935). Hess (1960, p. 39) writes about pyroxenes' serving as a geologic thermometer: »On cooling, the pigeonite thus formed inverts to orthopyroxene of the Stillwater type, whereas the orthopyroxene which crystallized as such from the magma becomes orthopyroxene of the Bushveld type. In both the Stillwater and Bushveld complexes, the inversion curve was crossed when the crystals had an Mg : Fe ratio of 70 : 30. This would indicate a temperature near 1 100° C. Inasmuch as all the crystallization up to this point was below the inversion curve, the initial crystallization from the Stillwater and Bushveld magmas must have taken place below approximately 1 140° C., the inversion temperature for enstatite to clinoenstatite. In the Stillwater the pigeonite began to crystallize at a horizon represented by the highest outcrop stratigraphically or, as will be seen from later discussion, after about 60 per cent of the magma had crystallized. The temperature change during the first 60 per cent of crystallization is very small.»

According to the studies of Yoder and Tilley (1962, p. 390), orthorhombic pyroxene can crystallize from quartz-dolerite at temperatures above the Bowen and Schairer (1935) inversion curve, where the pyroxene would be expected to crystal-

TABLE 2.

Chemical composition (analyst, A. Heikkinen) and physical properties of the hypersthene of the marginal portion. Zoned hypersthene. Hietaniemi, Mäntyharju, region of Ahvenisto.

Weight per cent				
SiO <sub>2</sub> .....	51.09	Si .....	7.66	} Z = 8.00
Al <sub>2</sub> O <sub>3</sub> .....	1.45	Al .....	0.25	
TiO <sub>2</sub> .....	0.50	Ti .....	0.05	} Y = 0.16
Fe <sub>2</sub> O <sub>3</sub> .....	1.70	Fe <sup>3+</sup> .....	0.20	
FeO .....	20.97	Fe <sup>2+</sup> .....	2.63	} X = 7.62
MnO .....	0.38	Mn .....	0.05	
MgO .....	22.08	Mg .....	4.94	
CaO .....	1.64	Ca .....	0.26	W = 0.26
Na <sub>2</sub> O .....	0.00			
K <sub>2</sub> O .....	0.00			
P <sub>2</sub> O <sub>5</sub> .....	0.04			
CO <sub>2</sub> .....	0.00			
H <sub>2</sub> O+ .....	0.03			
H <sub>2</sub> O- .....	0.04			
Total				
				99.92

Physical properties

- $\alpha = 1.696$
- $\gamma = 1.709$
- $2V\alpha = 57^\circ$
- D = 3.49

lize in monoclinic form. Moreover, »because of the uncertainty of the nature of the inversion, of the inversion temperature, and the observed pressure effects, the writers (Yoder and Tilley 1962, p. 391) do not believe that magma temperatures can be estimated from observation of the orthopyroxene-clinopyroxene inversion at this time».

The hypersthene of the marginal zone, at least when seen under the microscope, is wholly homogeneous (Fig. 7).

The chemical composition and physical properties of the middle portion of the zoned hypersthene grain are given in Table 1 and those of the marginal portion correspondingly in Table 2. The hypersthene of the middle portion contains more Mg, Ca and, especially, Al, and less of Fe<sup>2+</sup> and Fe<sup>3+</sup> than does the hypersthene of the marginal portion. The greater amount of Mg in the hypersthene of the middle portion, as compared to its content in the marginal portion, is natural. The abundance of Ca and Al in the middle portion evidently is due to the fact that the diadochy is large when the crystallization temperature is high. Stranger, at first, is the marked increase in the ratio Fe:Al as the crystallization temperature decreases, or as a shift is made to the hypersthene of the marginal portion. This is due evidently only because the Al replaces Si, but not iron, and because the degree of oxidation of iron is higher at late stages of crystallization than at the beginning.

The properties of the hypersthene in the marginal zone correspond well to the diagrams of Hess (1960, p. 27), which date back to the year 1952. The properties

of the hypersthene situated in the middle portion likewise fit, except that the axis angle ( $2V\alpha$ ) is greater than in Hess's (1960) diagram.

Green (1963) has demonstrated a high  $Al_2O_3$ -content in enstatite augen in high-temperature peridotite and a low  $Al_2O_3$ -content in recrystallized enstatite. He has further reported that the  $Al_2O_3$ -values are low along the edges of the augens. Banno (1964) contends, in the light of his observations, that increasing pressure reduces the  $Al_2O_3$ -content of orthopyroxene associated with garnet and clinopyroxene, and he adds that his arguments do »not stand against» the view in a P—T field where garnet is unstable, increasing pressure favors the formation of  $Al_2O_3$ -rich orthopyroxene.

According to Hess (1960, p. 31), the calcium content of orthopyroxene is of interest petrologically, for it may throw some light on the conditions of crystallization. The middle portion of the hypersthene of Hietaniemi contains 1.86 per cent of CaO and the marginal portion of the grains 1.64 per cent. These hypersthene have scarcely any other impurities than slight amounts of some other hypersthene. Probably 1.65 per cent CaO is near the maximum  $Ca^{2+}$  that the orthopyroxene structure can hold at the temperature of ordinary magmatic crystallization (Hess 1960, p. 31). Hess (1960, p. 33) further writes that the amount of CaO in orthopyroxene is also probably a function of the temperature of crystallization.

In the boundary zone between the marginal and middle portions of the zoned hypersthene, and for some distance toward the margin, there is an abundance of olivine and also plagioclase (though less than the former) as inclusions. Hypersthene of the marginal portion is also to be found in the part of the boundary zone rich in inclusions. No inclusions appear to occur in the hypersthene of the middle portion — but when the hypersthene were separated, inclusions were discovered there, too.

The composition of the plagioclase contained in the hypersthene of the middle portion as inclusions was  $An_{64-68}$  ( $\alpha = 1.562$ ,  $\gamma = 1.569$ ). The composition of the plagioclase contained as inclusions in the hypersthene of the marginal portion was  $An_{58}$  ( $\alpha = 1.558$ ,  $\gamma = 1.566$ ), or approximately the same — perhaps slightly greater — An-content as in the pegmatoid gabbros and anorthosites in general. It will be noted that the An-content of plagioclase present in the hypersthene of the middle portion as inclusions considerably exceeds that of the plagioclase contained in the hypersthene of the marginal portion, in the pegmatoid gabbros and in the pegmatoid anorthosites and of the plagioclase in general met with in the different varieties of rock represented in the gabbro-anorthosite intrusions. Conclusion: The hypersthene of the middle portion crystallized at a very early stage, but even prior to that the gabbro-anorthosite intrusions harbored the crystallization of uncommonly anorthite-rich plagioclase, which has remained as inclusions within the hypersthene of the middle portion and been preserved there alone as what might be described as armored relicts.

The composition of the olivine in the inclusion-rich boundary zone and the marginal portion is 60 per cent of Fo-component ( $2V\alpha = 80^\circ$ ,  $\alpha = 1.716$ ,  $\gamma = 1.756$ ,

TABLE 3.

Chemical composition of hypersthènes. Eerolampi, Paistjärvi, commune of Heinola, region of Ahvenisto. (LOKKA 1941, pp.21 and 29).

	1	2	1	2
Weight per cent				
SiO <sub>2</sub> .....	49.30	49.32	7.21 } Z = 8.00	7.18 } Z = 8.00
TiO <sub>2</sub> .....	0.38	0.81	0.04 }	0.09 }
Al <sub>2</sub> O <sub>3</sub> .....	5.23	6.39	0.90 } Y = 0.50	1.10 } Y = 0.48
Fe <sub>2</sub> O <sub>3</sub> .....	3.26	1.02	0.35 }	0.11 }
FeO .....	15.26	16.40	1.86 }	2.00 }
MnO .....	0.36	0.26	0.04 } X = 7.23	0.04 } X = 7.18
MgO .....	24.42	23.52	5.33 }	5.14 }
CaO .....	2.04	2.02	0.32 } W = 0.32	0.28 } W = 0.28
Alkalien .....	—	0.00		
H <sub>2</sub> O+ .....	0.17	0.37		
H <sub>2</sub> O— .....	—	0.08		
F .....	—	0.03		
Total	100.41	100.22		
—O .....		0.01		
Total		100.21		

$d_{130} = 2.792$ ). The  $d_{130}$ -value fits into the curves drawn by Yoder and Sahama (1957). Very few inclusions of olivine are present in the hypersthene of the middle portion; the composition of olivine in them would seem, according to the refractive indices, which are only a couple of thousandth parts smaller than in the marginal portion, to be only slightly richer in Mg than in the other portion. The scantiness or, perhaps, even absence, to some extent, of olivine inclusions from the main part of the hypersthene content of the middle portion indicates that the olivine started to crystallize only during the crystallization of the hypersthene of the middle portion — and, perhaps, not until the very final stages of its crystallization. On the other hand, olivine no longer occurs in the outermost parts of the hypersthene of the marginal portion or, in general, in the rocks of the gabbro-anorthosite intrusions. In exceptional instances, olivine may be found in the marginal zones of the intrusions in forms other as »armored» relicts. Conclusion: the interval during which the olivine crystallized was evidently rather short, occurring in the main during the initial stage of crystallization of the hypersthene of the marginal portion.

Table 3 presents two chemical analyses (performed by Lokka in 1943) of rocks from the vicinity of Eerolampi, in the region of Ahvenisto, that resemble the ones described in this chapter. Both analyses, which were probably made from samples taken from the same place, correspond closely to the analysis made of the middle portion of the hypersthene of Siikajärvi. In these analyses, Mg and Al, for example, vary somewhat, and there are fewer of the cations mentioned than in the hypersthene of the zoned grains of the middle portion at Siikajärvi and more of them than in the

TABLE 4.

Chemical composition of anorthosite. Island in Lake Ylä-Rääveli, east of Kuhaniemi, Pertunmaa, region of Ahvenisto. Average mineral composition of the anorthosites contained in the Ahvenisto massif.

Weight per cent		Niggli values		Volume per cent	
SiO <sub>2</sub> .....	53.33	si .....	153	Plagioclase (An <sub>53-58</sub> ) .	90.8
Al <sub>2</sub> O <sub>3</sub> .....	27.79	al .....	47	Potash feldspar and	
Fe <sub>2</sub> O <sub>3</sub> .....	0.09	fm .....	2.2	quartz .....	4.6
FeO .....	0.49	c .....	37.2	Mafic minerals .....	4.1
MgO .....	0.17	alk .....	13.5	Opaque minerals ....	0.3
MnO .....	0.01	k .....	0.08	Carbonate .....	0.1
CaO .....	12.11	mg .....	0.31	Apatite .....	0.1
Na <sub>2</sub> O .....	4.46	c/fm .....	16.62		
K <sub>2</sub> O .....	0.25	qz .....	-1		
P <sub>2</sub> O <sub>5</sub> .....	0.07				
H <sub>2</sub> O+ .....	0.66				
H <sub>2</sub> O- .....	0.02				
Total	100.03				100.0

hypersthene of the marginal portion of the same grains. The Eerolampi hypersthene has not been described as zoned, but such a feature would naturally explain the variations in composition revealed by the analyses (Table 3). The hypersthene grains of the Eerolampi rock are to some extent quite large, measuring, as they do, as much as 50 centimeters in length.

### Anorthosites

The anorthosites vary considerably in color: brownish, light gray and blue-gray. The grain size varies between 2 and 5 millimeters, being consistently smaller than the grains of the gabbro-anorthosites, which range from 5 to 20 mm, and very much smaller than those of the pegmatoid gabbros and pegmatoid anorthosites. The anorthosites are frequently observed to contain a sparse scattering of 1—10-cm long plagioclase phenocrysts. Mafic minerals (orthopyroxene, amphibole and biotite) are present in them under 10 per cent by volume. The composition of the plagioclase in them is An<sub>52-58</sub>. The phenocryst plagioclase has not been seen to be any richer in anorthite.

The chemical analysis of the anorthosites and the Niggli values computed from it are presented in Table 4, which also includes the modal mineral composition of the anorthosites as computed from Savolabti's Table 3 (1956, p. 24). The mineral composition corresponds in general to the values given for anorthosites of this type. A noteworthy feature of the chemical and mineral compositions of the anorthosites here discussed — as well as in general — is the scantiness of phosphorus and the scantiness or even complete absence of apatite (Rosenbusch 1923, pp. 30, 201, 240; Johannsen 1937, pp. 199—201; Buddington 1939, p. 30; and Turner and Verhoogen

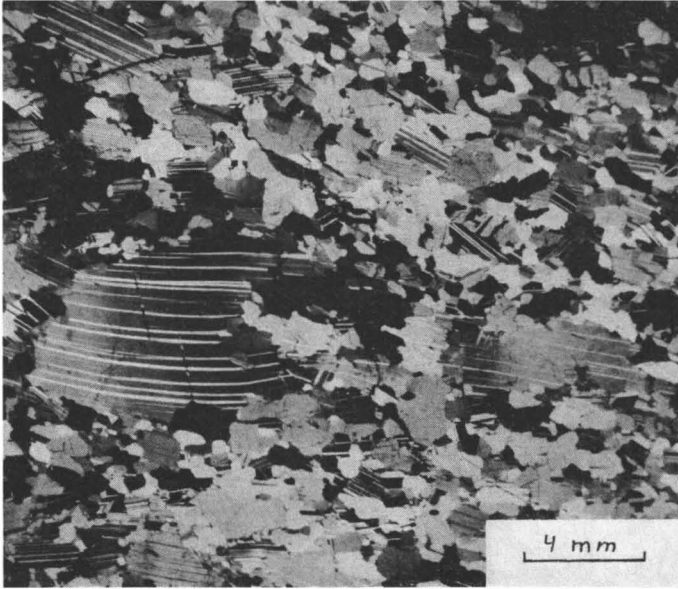


FIG. 8. Microscopic view of anorthosite. The lamellae of the plagioclase are twisted and the grains somewhat parallel in structure. Crossed nicols. Kuortti, Pertunmaa, region of Ahvenisto.

1951, p. 255). According to Wager (1963, p. 6), the cumulus minerals (plagioclase, olivine, pyroxene and iron ores) are essentially free from phosphorus.

Figures 8 and 9 show the microscopic texture of two anorthosites of differing structural type. In the one, the habit is oriented, in the other, it is unoriented. Moreover, in the one, the lamellae of the plagioclase grains are twisted, in the other, they are not.

#### **Gabbro-anorthosites and anorthosite-gabbros**

Gabbro-anorthosites are the most common rock contained in the gabbro-anorthosite intrusions. In color, they are most generally a bluish dark gray. The color of these rocks, too, varies. The grain size of the plagioclase contained in the gabbro-anorthosites ranges from 5 to 20 mm, and they have a sparse scattering of different-sized plagioclase phenocrysts, which usually measure between 1 and 10 cm (Fig. 10). Table 5 presents the chemical analysis and Niggli values for a certain typical gabbro-anorthosite, together with the average, modal mineral composition of the gabbro-anorthosites. The mean of the modal mineral composition has been computed from Table 4 (Savolahti 1956, p. 25). Since the plagioclase phenocrysts have not been included in the individual computations of the mineral compositions, the count for

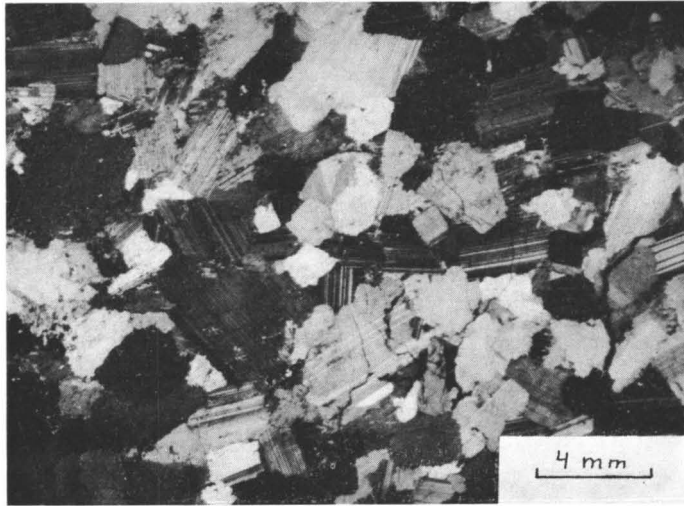


FIG. 9. Microscopic view of anorthosite. The plagioclase contains a slight amount of alternation products. The lamellae in the grains are untwisted. Crossed nicols. Nurmaa, Mäntyharju, region of Ahvenisto.

the pale minerals turns out to be somewhat too small in the averaging. Accordingly, the true figure for the pale minerals is greater than that shown in Table 5. The contrarywise results is influenced by the fact that among the gabbro-anorthosites are rocks which it would be better — and even necessary — to term anorthosite-gabbros, in view of their abundance of mafic minerals. However, they undoubtedly represent a small minority, although no calculations have been made as to the distribution of these different types. This conception must have been shared by Frosterus (1902), since he gave all the basic rocks of the Ahvenisto region the common designation of »labrador rocks». Sederholm (1916; 1932, p. 25; 1934, p. 55) also took the same view. The composition of the plagioclase in these rocks varies within the range  $An_{48-58}$ . According to the refractive indices and axis angles (Savolahti 1956, pp. 25—27), the rhombic pyroxene is slightly richer in iron than is the hypersthene of the marginal portion of the zoned grains of the pegmatoid gabbro of Siikajärvi.

The gabbro-anorthosites have an ophitic or megaophitic habit, but in places in the steep rock walls plagioclase laths may be seen situated in a nearly horizontal position. The effect is one of a parallel structure. Kahma (1951, p. 14) has previously observed this kind of orientation in the olivine diabase of Satakunta. Such phenomena seem to suggest an incipient igneous layering structure. The types of gabbro anorthosites rich in mafic minerals are likely to have formed partly in that manner, although such beautiful banding structures as have been described by, for example, Pulvertaft (1965) from Greenland have not come to light in the Ahvenisto region. Anorthosite-gabbros are probably produced in other ways, too. The scarcity of

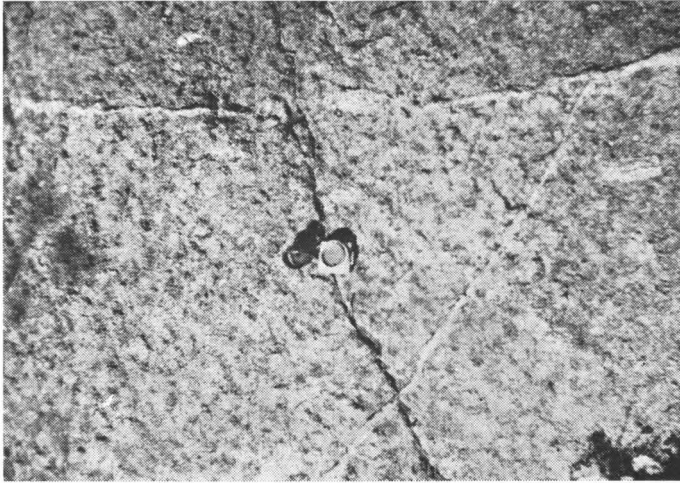


FIG. 10. Gabbro-anorthosite. Kuhaniemi, Kuortti, Pertunmaa, region of Ahvenisto (SAVOLAHTI 1956, p. 40).

TABLE 5.

Chemical composition of gabbro-anorthosite. Hietaniemi, Mäntyharju, region of Ahvenisto. Average mineral composition of the gabbro-anorthosites and anorthosite-gabbros contained in the Ahvenisto massif.

Weight per cent		Niggli values		Volume per cent	
SiO <sub>2</sub> .....	52.84	si .....	146	Plagioclase (An <sub>48-58</sub> ) .	70.6
Al <sub>2</sub> O <sub>3</sub> .....	22.14	al .....	36	Potash feldspar .....	3.8
Fe <sub>2</sub> O <sub>3</sub> .....	1.76	fm .....	23	Quartz .....	2.4
FeO .....	4.93	c .....	29	Pyroxene .....	3.7
MgO .....	1.91	alk .....	12	Amphibole .....	12.6
MnO .....	0.05	k .....	0.18	Biotite (Chlorite) ....	3.6
CaO .....	9.74	mg .....	0.34	Epidote .....	1.2
Na <sub>2</sub> O .....	3.70	c/fm .....	1.25	Opaque minerals .....	1.3
K <sub>2</sub> O .....	1.24	qz .....	-2	Apatite .....	0.8
TiO <sub>2</sub> .....	0.90				
P <sub>2</sub> O <sub>5</sub> .....	0.27				
H <sub>2</sub> O+ .....	0.44				
H <sub>2</sub> O- .....	0.08				
Total	100.02				100.0

igneous layering structures in the gabbro-anorthosite intrusions of Ahvenisto may, to some extent, be due to their chemical composition, which presuppose a greater viscosity than in the case of basalts in general, as well as, in part, to the way in which the intrusive processes occurred.

### Marginal varieties of gabbro-anorthosite intrusions

The marginal varieties of the gabbro-anorthosite intrusions are fine- or medium-grained rocks containing plagioclase phenocrysts in greater or smaller amounts and, in some cases, also hypersthene phenocrysts. In structure they are ophitic with a subparallel arrangement of plagioclase laths. In the northwest corner of the gabbro-anorthosite complex as well as along its southwest margin and on the southern side of Näätijärvi, some slight evidences of rhythmic banding may be seen.

The marginal varieties contain the same minerals as do the gabbro-anorthosites, and the composition of the plagioclase is likewise approximately the same as in the gabbro-anorthosites. In addition, they contain monoclinic pyroxene. Mafic minerals, however, are present in substantially greater amounts than in gabbro-anorthosites on the average. According to Haker (1909, p. 133), this is very common, as has been observed in, *e.g.*, the Adirondacks (Buddington 1939, pp. 1, 47) — and the same thing prevails in, among other rocks, the diabases of Petolahti (Ervamaa 1962, p. 12). Among other differences, in comparison with gabbro-anorthosites, are the fact that they reveal the presence in spots of olivine and that a lamellar intergrowth of rhombic and monoclinic pyroxene can be observed in them.

It should further be emphasized that the magnitude and amount of phenocrysts vary in different varieties, the measurements ranging from one centimeter to over half a meter, and that variation also occurs in their mineral composition (Savolahti 1956, pp. 30—33). Thus do the rocks composing the marginal zones of the different intrusions differ from each other also megascopically. This, too, is in many instances evidence of the occurrence of numerous different intrusions.

The refractive indices of one large hypersthene grain 20 cm long found in a marginal variety of rock are:  $\alpha = 1.693$ ,  $\beta = 1.703$ ,  $\gamma = 1.706$ ; while the composition of a nearby plagioclase grain 50 cm is  $An_{58}$  ( $\alpha = 1.557$ ,  $\gamma = 1.566$ ).

At one place, where the marginal zone grades over by degrees into normal gabbro-anorthosite, there are several occurrences of amphibole-rich gabbro, which penetrates the marginal zone as indistinct veins. This gabbro contains aggregates of carbonate and apatite in greater than ordinary abundance. Present in it are, among other things, large apatite crystals, which, despite their good idiomorphism, appear to have crystallized at a relatively late stage (Savolahti 1956, p. 21). Everything points to the fact that the volatile materials of the magma had become concentrated at this point in the intrusions, for from this point outward the grains diminish greatly in size.

Wegman (1938, pp. 83—92) reports having found carbonate — even veins of carbonate — contained in diabase dikes a short distance toward the center from their contacts in southwestern Greenland, and that the occurrences bear witness to movements having taken place after the intrusions. Keto (1959) has carried out quantitative determinations of the mineral contents and grain sizes in an olivine diabase dike 40 meters broad at Ika-Pynt, Greenland. The determinations revealed that a short distance from the contact, inside the dike, where grain size begins to diminish markedly, apatite, carbonate and hydrous silicates have become enriched.

### Late crystallizations of the gabbro-anorthosite intrusions and the autometamorphic and autometasomatic processes

Reference has been made, in connection with the foregoing description of the marginal zones of the gabbro-anorthosite intrusions, to the enrichment of volatile materials into them and to the penetration of indistinct gabbro veins from gabbro anorthosites into their marginal varieties. These veins border vaguely on their country rock, and they still reveal the presence of minerals from the country rock as relicts (Savolahti 1956, p. 22). In their formation, a significant part was evidently played by solutions and volatiles penetrating from the magma into rock that had already largely crystallized, meaning that these veins represent, at last in part, replacement veins, as it were, and are the end products of autometasomatic processes.

Autometamorphic and autometasomatic processes generated by residual solutions and volatiles have also occurred in other portions of the intrusions. NNE of Enonvesi (Savolahti 1956, p. 29) there is a certain example, in which the hypersthene grains of a pegmatoid gabbro have undergone partial alteration. At the edges and in the fissures of the hypersthene grains there are bands of cummingtonite and in certain cases the entire hypersthene grain has changed to cummingtonite. Adjacent to plagioclase, these cummingtonite bands have a very thin biotite edge ( $\gamma = \beta = 1.601$ ). A certain amount of biotite is also contained in the middle of the cummingtonite bands and aggregates, being wedged in between the cummingtonite grains. The rock thereby altered is cut across by narrow (1—5 mm), pale gray veins, which consist mostly of feldspar and quartz. The veins do not appear to come from any granite occurrence or other external intrusion, and in some instances they are cut off at both ends. In all probability, they represent late crystallizations of gabbro-anorthosite intrusions. The cummingtonite bands and aggregates are either contemporaneous with the afore-described veins or are younger, for the veins running through this pegmatoid gabbro cut across plagioclase and hypersthene grains but do not cut through the cummingtonite aggregates and bands even when they intersect a hypersthene grain around and inside which are cummingtonite bands.

Table 6 presents a chemical analysis and the physical properties for cummingtonite.

How common and intense these autometamorphic and autometasomatic processes have been in these intrusions, it is difficult to determine, for even after they ceased there occurred in the area contact metamorphoses and contact metasomatoses, caused by younger magma intrusions, as well as dislocation metamorphoses, induced by later movements. The magma intrusions and movements might, conceivably, have been to some extent synchronous. Undoubtedly, a part of even those gabbro-anorthosites in which the mafic minerals have wholly altered into amphiboles, chlorite and biotite were produced by the late solutions of the gabbro-anorthosite intrusions themselves.

Representing the latest crystallizations in the gabbro-anorthosite intrusions are

TABLE 6.

Chemical composition (analyst, A. Heikkinen) and physical properties of cummingtonite. Enonvesi NNE, Hietaniemi, Mäntyharju, region of Ahvenisto.

Weight per cent				
SiO <sub>2</sub> .....	53.02	Si .....	7.86	} Z = 8.00
TiO <sub>2</sub> .....	0.26	Ti .....	0.03	
Al <sub>2</sub> O <sub>3</sub> .....	1.00	Al .....	0.18	} Y = 0.12
Fe <sub>2</sub> O <sub>3</sub> .....	0.55	Fe <sup>3+</sup> .....	0.05	
FeO .....	22.19	Fe <sup>2+</sup> .....	2.75	} X = 6.43
MnO .....	0.77	Mn .....	0.10	
MgO .....	16.21	Mg .....	3.58	
CaO .....	3.94	Ca .....	0.62	} W = 0.71
Na <sub>2</sub> O .....	0.16	Na .....	0.05	
K <sub>2</sub> O .....	0.20	K .....	0.04	
P <sub>2</sub> O <sub>5</sub> .....	0.03	P .....		} (OH, P <sub>2</sub> O <sub>5</sub> ) = 1.55
H <sub>2</sub> O+ .....	1.56	OH .....	1.55	
H <sub>2</sub> O- .....	0.06			
Total				

## Physical properties

$a$	= 1.643
$\beta$	= 1.652
$\gamma$	= 1.666
$2V\gamma$	= 73°
$c \wedge \gamma$	= 13°
$b$	= $\beta$
$D$	= 3.26

a few albite-dabase dikes. They are coarse-grained and ophitic in structure. Their principal minerals are albite and chlorite, in addition to which one finds pistacite quartz, ore, apatite and potash feldspar (Savolahti 1956, p. 29). The composition of the final crystallization appears to be rich in Na, just as has frequently been observed to be the case with rocks of this description elsewhere as well.

## METAMORPHISM IN GABBRO-ANORTHOSITE INTRUSIONS

In the village of Enolahti, situated on a headland of Siikajärvi, a beautiful example may be seen of a contact metamorphism into gabbro-anorthosite caused by later intrusions. Situated on top of a gabbro-anorthosite intrusion, there is a rapakivi sill gently sloping westward. Directly under the rapakivi, the mafic minerals of the gabbro-anorthosite are totally chloritized and the plagioclase conspicuously epidotized, giving the entire rock a greenish yellow color. As much as ten meters deeper down, the contact metamorphism induced by the rapakivi is clearly and conspicuously evident. The mode of occurrence of the chlorite here is bizarre. When a sample is knocked off a rock, its fresh surface is seen to contain dark, poikilitic grains a couple of centimeters in diameter with plagioclase inclusions and with a

metallic glitter. It requires closer examination to identify them as chlorite. In all likelihood, they had originally been orthopyroxene grains, which eventually underwent chloritization. It is at a distance of more than 20 meters that the gabbro-anorthosites take on their typical outward appearance and mineral composition.

Later intrusions have also induced the formation of metasomatic porphyroblasts in the rocks of the gabbro-anorthosite intrusions (Savolahti 1956, pp. 59—60).

The gabbro-anorthosite intrusions display many shearing and crushing zones which bear witness to dislocation metamorphism (Savolahti 1956, pp. 57—59). The anorthite content of the plagioclase contained in the original rock of these zones has decreased, being approximately  $An_{25}$ , and at the same time calcite and epidote have been introduced into the rock. Its mafic minerals have altered into chlorite and amphibole. The same kind of mineral composition has been reported to occur in a certain mylonitized anorthosite in western Greenland (Sørensen 1955, p. 37). The rock itself in gabbro-anorthosite intrusions has in many cases turned a lighter hue than that of the original rock. This seems to be due to the fact that the altered plagioclase is lighter of color than the original plagioclase. In addition, those properties of the light and dark minerals that resist physical and chemical weathering may have changed. As a result, the weathering relations between the various minerals may also have changed. The mafic minerals may, for example, have corroded into hollows. Rocks thus altered resemble anorthosites more than they do the original rocks. During such a process, the chemical composition of the rocks need not always have changed so as to approximate that of anorthosite to any higher degree than originally. By this the author does not wish to deny that anorthosites could and might, indeed, have evolved through such a process or that chemical changes might also have taken place in these rocks. The author's intention is only to demonstrate that the outward appearance of a rock can give rise to an erroneous conception with regard to the chemical composition of the rock.

### CONCLUSIONS

The magma from which the gabbro-anorthosite intrusions of Ahvenisto have crystallized was very probably nearly identical in chemical composition to the gabbro-anorthosite presented in Table 5. Accordingly, this magma would have contained appreciably more  $SiO_2$ ,  $Fe_2O_3$ ,  $Al_2O_3$  and  $Na_2O$  and less  $FeO$ ,  $CaO$  and, especially,  $MgO$  than did the high-alumina basalts corresponding most nearly to it in composition that were experimentally investigated by Yoder and Tilley (1962, p. 362).

Yoder and Tilley (1962, p. 382) have submitted the following significant conclusions deriving from their studies of basalts: »1. Each of the major silicate phases may appear as the primary silicate phase. 2. The temperature at which the primary silicate appears lies within a narrow range irrespective of the kind of primary silicate phase ( $1.160^\circ$  to  $1.240^\circ$  C). 3. All major silicate phases appear within a small tem-

perature interval ( $< 80^{\circ}$  C). 4. All major silicate phases begin crystallizing together at about the same temperature ( $1.155^{\circ}$  to  $1.170^{\circ}$  C). 5. Total range of crystallization is small ( $135^{\circ}$  to  $195^{\circ}$  C).

The chemical composition of the gabbro-anorthosites of the Ahvenisto region probably presupposes a slightly lower crystallization temperature than that of the aforementioned basalts. Moreover, the former have perhaps crystallized under slightly higher pressure than the latter.

It was the plagioclase, with a composition of  $An_{65}$ , that first began to crystallize from the gabbro-anorthosite magma, immediately followed by the Al-rich pyroxene, now occurring as lamellic hypersthene (Table 1). At the final stage of the crystallization of this pyroxene, the olivine ( $Fo_{60}$ ) crystallized. According to MacDonald (1949), most common phenocrysts in basalt are olivine and many of them contain plagioclase, but the conditions of crystallization and the composition of the magma there were somewhat different. After that, there crystallized the hypersthene (Table 2) in which no lamellae occur, partly around the first-mentioned, lamellic hypersthene, partly as independent grains. The plagioclase ( $An_{58-53}$ ) crystallized concurrently with it.

The composition of the plagioclase phenocrysts present in various places in the gabbro-anorthosite intrusions is  $An_{58-53}$ . The plagioclase ( $An_{65}$ ) occurring in the lamellic hypersthene as inclusions has not been met with as phenocrysts. On the other hand, hypersthene phenocrysts have been met with here and there in the marginal zones of the gabbro-anorthosite intrusions, the refractive indices of which correspond more closely to those of lamellic hypersthene than of hypersthene in which no lamellae occur. Olivine has been met with — except as inclusions in the hypersthene of pegmatoid gabbros — only in the marginal zones of intrusions, but not as phenocrysts even there. The pegmatoid gabbros thus include the minerals that crystallized first in these intrusions, though their crystallization lasted a long time.

Anorthosite lenses occur in all parts of the intrusions. The grain size of their minerals is distinctly smaller than that of the gabbro-anorthosites. The composition of the plagioclase in them is  $An_{53-58}$ . Locally, there evidently occurred a sudden appearance of nuclei in great abundance and a partial removal of intercumulus liquid. The sudden formation of nuclei seems to have taken place at a time when the rate of generation of plagioclase nuclei in the magma was very high — and it was not highest during the crystallization of plagioclase ( $An_{65}$ ). Since anorthosite lenses occur also in the fine-grained marginal zones of the intrusions, they had appeared, perhaps, even prior to the intrusive action as well as possibly afterward, too. This would also explain the twisted shape of the lamellae of the plagioclase grains to be observed in spots in these anorthosites. The present author does not presume to contend that all the anorthosites of the intrusions had originated in this fashion, but in the case of some he is unable to offer any other explanation. The pegmatoid anorthosites occurring in association with the pegmatoid gabbros have not been counted among the aforementioned anorthosites.

The gabbro-anorthosites, including the several varieties of the rock, constitute the principal rock component of the gabbro-anorthosite intrusions. The composition of the plagioclase contained in them is  $An_{58-48}$  and the refractive indices of their hypersthene content are partly greater than those of the marginal portion of the zoned hypersthene present in the pegmatoid gabbros.

Since the pegmatoid gabbros and anorthosites are among the oldest minerals present in the gabbro-anorthosite intrusions of the Ahvenisto region, we may regard them as the portions of the magma that differentiated first. True, crystallization continued in them long after the first minerals crystallized; but this, according to Wager, Brown and Wadsworth (1960), is something to be expected in cumulates. There followed the crystallization of the fine- and medium-grained anorthosites at a time when the rate of formation of the plagioclase nuclei was highest in the magma. The rocks of the marginal zones underwent rapid crystallization after the intrusion of the magma, which, perhaps, occurred during the crystallization of the fine-grained anorthosites. In the light of the compositions of the minerals, we may conclude that the crystallization of the gabbro-anorthosites and their varieties lasted longer than did that of the other principal rocks.

The main crystallization of the intrusions took place as a whole within very narrow limits of temperature, as in the case, according to Yoder and Tilley (1962), of basalts.

The emergence of the principal varieties of rock was followed by late-stage crystallizations, the autometamorphic and autometasomatic rocks, and the rocks metamorphosed by later intrusions and dislocations.

*Acknowledgements* — Professor Martti Saksela, my superior, has kindly read the manuscript of this study and recommended that it be included in the series published by the Geological Society of Finland. For this, I wish to thank him.

*Manuscript received, March 15, 1966*

## REFERENCES

- BALK, R. (1931) Structural geology of the Adirondack anorthosite. A structural study of the problem of the magmatic differentiation. *Miner. Petr. Mitt.* 41, pp. 308—434.
- BANNO, S. (1964) Alumina content of orthopyroxene as a geologic barometer. *Japanese Journal of Geology and Geography* 25, Nos. 2—4, pp. 115—121.
- BOWEN, N. L. (1917) The problem of the anorthosites. *Jour. Geol.* 38, pp. 289—302.
- »— (1928) *The evolution of the igneous rocks.* Princeton.
- »— and SCHAIRER, J. F. (1935) The system,  $MgO-FeO-SiO_2$ . *Amer. Jour. Science* 29, pp. 151—217.
- »— and TUTTLE, O. F. (1950) The system  $NaAlSi_3O_8-KAlSi_3O_8-H_2O$ . *Jour. Geol.* 58, pp. 489—511.
- BUDDINGTON, A. F. (1939) Adirondack igneous rocks and their metamorphism. *Geol. Soc. Am., Mem.* 7.

- CAMERON, E. N. (1963) Structure and rock sequences of the Critical Zone of the eastern Bushveld Complex. Mineral. Soc. Amer. Spec. Paper 1, pp. 93—107.
- ERVAMAA, P. (1962) The Petolahti diabase and associated nickel-copper-pyrrhotite ore, Finland. Bull. Comm. géol. Finlande 199.
- ESKOLA, P. E. (1957) Kidetietaan, mineralogian ja geologian alkeet. Werner Söderström Osakeyhtiö. Helsinki.
- »— (1961) Granitentstehung bei Orogenese und Epirogenese. Geol. Rundschau 50, pp. 105—123.
- »— (1963) The Precambrian of Finland. The Precambrian 1, pp. 145—263.
- FERGUSON, J., and PULVERTAFT, T. C. R. (1963) Contrasted styles of igneous layering in the Cardar Province of south Greenland. Mineral. Soc. Amer. Spec. Paper 1, pp. 10—21.
- FROSTERUS, B. (1902) Beskrifning till bergartskartan av kartbl. C 2, St. Michel. General geological map of Finland (1900), 1 : 400 000.
- GORBATSCHEW, R. (1961) Dolerites of the Eskilstuna region. Sveriges Geol. Undersökn., Ser C, Avhandl. och Uppsat. 580.
- GREEN, D. H. (1963) Alumina content of enstatite in a venezuelan high-temperature peridotite. Geol. Soc. Amer. Bull. 74, pp. 1397—1402.
- HAKER, A. (1909) The natural history of igneous rocks. Methuen & Co, London.
- HESS, H. H. (1960) Stillwater igneous complex, Montana. Geol. Soc. Amer. Mem. 80.
- HIETANEN, A. (1956) Anorthosite in Bodol Butte Quadrangle, Idaho. Bull. Geol. Soc. Am. 67, p. 1710.
- HJELMQUIST, S. (1961) The relation between diabase, granite, and porphyry at Bullberget in Dalarna, Central Sweden. A proof of magmatic granite formation. Bull. Inst. Univ. Upsala 40, pp. 69—80.
- JOHANNSEN, A. (1937) A descriptive petrography of igneous rocks, volume III. The University of Chicago Press. Chicago.
- KAHMA, A. (1951) On contact phenomena of the Satakunta diabase. Bull. Comm. géol. Finlande 152.
- KETO, L. (1959) Ika-Pyntin juonikivilajeista. Manuscript. Institute of Geology. University of Helsinki.
- KRANCK, E. H. (1961) Tectonic position of the anorthosites of eastern Canada. Bull. Comm. géol. Finlande 196, pp. 299—320.
- LOKKA, L. (1943) Beiträge zur Kenntnis des Chemismus der finnischen Minerale. Bull. Comm. géol. Finlande 129.
- LOOMIS, A. A. (1963) Noritic anorthosite bodies in the Sierra Nevada batholith. Mineral. Soc. Amer. Spec. Paper 1, pp. 62—68.
- MAC DONALD, G. A. (1949) Hawaiian petrographic province. Bull. geol. Soc. Amer. 60, pp. 1541—1596.
- PULVERTAFT, T. C. R. (1965) The Eqaloqarfia layered dyke, Nunarsuit, south Greenland. Medd. Grønland 169, 10.
- ROSENBUSCH, H. (1923) Elemente der Gesteinslehre. Vierte Auflage. E. Schweizerbart'sche Verlagsbuchhandlung (Erwin Nägele) G. m. b. H. Stuttgart.
- SAVOLAHTI, A. (1956) The Ahvenisto massif in Finland. Bull. Comm. géol. Finlande 174.
- »— (1959) Petrologiaan kohdistuvaa kritiikkiä (with english summary). Geologi 11, pp. 88—95.
- »— (1962) The rapakivi problem and the rules of idiomorphism in minerals. Bull. Comm. géol. Finlande 204, pp. 33—111.
- SCHAIRER, J. F. und BOWEN, N. L. (1947) The system anorthite-leucite-silica. Bull. Comm. géol. Finlande 140, pp. 67—87.
- SEDERHOLM, J. J. (1916) On synantetic minerals and related phenomena. (Reaction rims, corona minerals, kelyphite, myrmekite, etc.) Bull. Comm. géol. Finlande 48.
- »— (1928) On orbicular granites, spotted and nodular granites etc. and on the rapakivi texture. Bull. Comm. géol. Finlande 83.

- SEDERHOLM, J. J. (1932) On the geology of Fennoskandia with special reference to the Pre-Cambrian. Bull. Comm. géol. Finlande 98.
- »— (1934) On migmatites and associated Pre-Cambrian rocks of southwestern Finland. Part III. Bull. Comm. géol. Finlande 107.
- SPEED, R. C. (1963) Layered picrite-anorthositic gabbro sheet, West Humboldt Range, Nevada. Mineral. Soc. Amer. Spec. Paper 1, pp. 69—77.
- SØRENSEN, H. (1955) Anorthosite from Buksefjorden; West Greenland. Medd. Dansk Geol. For. i København 13, pp. 31—41.
- TURNER, F. J., and VERHOOGEN, J. (1951) Igneous and metamorphic petrology. First edition. New York.
- »— and —»— (1960) Igneous and metamorphic petrology. Second edition. New York.
- TUTTLE, O. F., and BOWEN, N. L. (1958) Origin of granite in the light of experimental studies in the system  $\text{NaAlSi}_3\text{O}_8$ — $\text{KAlSi}_3\text{O}_8$ — $\text{SiO}_2$ — $\text{H}_2\text{O}$ . Geol. Soc. Am. Mem. 74.
- WAGER, L. R. (1953) Layered intrusions. Bull. Geol. Soc. Danmark 12, Part 3, pp. 335—349.
- »— (1963) The mechanism of adcumulus growth in the layered series of the Skaergaard intrusion. Mineral. Soc. Amer. Spec. Paper 1, pp. 1—9.
- WAGER, L. R., BROWN, G. M., and WADSWORTH, W. J. (1960) Types of igneous cumulates. Journal petrology 1, pp. 73—85.
- WAHL, W. (1925) Die Gesteine des Wiborger Rapakivigebietes. Fennia 45, 20.
- WEGMANN, C. E. (1938) Geological investigations in Southern Greenland. I. On the structural divisions of Southern Greenland. Medd. Grønland 113, 2.
- WINKLER, H. G. F. (1962) Viel Basalt und wenig Gabbro — wenig Rhyolith und viel Granit. Beiträge z. Mineral. u. Petrogr. 8, pp. 222—231.
- YODER, H. S., and SAHAMA, TH. G. (1957) Olivine X-ray determinative curve. Am. mineralogist 42, pp. 475—491.
- »— and TILLEY, C. E. (1957) Basalt magmas. Carnegie Inst. Wash., Year Book 56, pp. 156—161.
- »— and —»— (1962) Origin of basalt magmas: An experimental study of natural and syntetic rock systems. Journal Petrology 3, pp. 342—532.



# ON THE PETROGRAPHY OF THE METAMORPHIC SCHIST BELT OF HAUTAJÄRVI, KIURUVESI COMMUNE, FINLAND

BY

A. SAVOLAHTI and REINO MARJONEN

*Institute of Geology and Mineralogy, University of Helsinki*

## ABSTRACT

The metamorphic schists of Hautajärvi include the following varieties of rock: black schists, diopside amphibolites, garnet-bearing mica gneisses, cummingtonite-biotite gneisses, hornblende gneisses, amphibolites, mica gneisses, plagioclase gneisses, anthophyllite-biotite gneisses and diopside gneisses. Associated with them are diabases, porphyritic granites and pegmatites. This paper presents a petrographic description of the rocks mentioned, their mode of occurrence, in many cases the modal mineral composition and the optic properties of the minerals. In the case of one amphibolite's amphibole, a chemical analysis, the optic properties and the X-ray data are given. The paper further includes a brief description of the eruptive rocks found in the region: diabases, porphyritic granites and pegmatites.

## CONTENTS

	Page
Introduction .....	200
Eruptive Rocks of Hautajärvi .....	200
Diabases .....	200
Porphyritic Granites .....	203
Pegmatites .....	203
Metamorphic Schists of Hautajärvi .....	203
Black Schists .....	203
Diopside Amphibolites .....	204
Garnet-bearing Mica Gneisses .....	206
Cummingtonite-Biotite Gneisses and Hornblende Gneisses, with Their Lenses and Intercalations .....	207
Mica Gneisses, with Their Lenses and Intercalations .....	211
Plagioclase Gneisses, with Their Intercalations .....	213
Anthophyllite-Biotite Gneiss and Diopside Gneisses .....	215

Discussion .....	216
Acknowledgments .....	216
References .....	217

## INTRODUCTION

Hautajärvi is situated in the commune of Kiuruvesi, some 40 kilometres west of the town of Iisalmi, in the northern part of the ancient province of Savo, in eastern Finland. Previously, the area under consideration has been geologically described by Mäkinen (1916) and Wilkman (1931).

According to Wilkman, the Hautajärvi area is crossed by a belt of fine-grained, dark gray hornblende gneiss, which is foliated and distinctly banded, with alternating layers of mica gneiss. Next to the mica gneiss, according to the same source, are rusty layers rich in pyrrhotite.

The maps of the Hautajärvi area drawn on the basis of airborne magnetic and electric surveys show very strong anomalies. This circumstance led to a remapping by the Exploration Department of the Outokumpu Company in the summer of 1959. The job was later completed, resulting in the revision of some parts of the maps.

The purpose of the present study is to describe the rocks of the Hautajärvi schist belt and their modes of occurrence.

The strike of the schistosity of the rocks at Hautajärvi is generally N 30°—60° W and the dip 40°—85° SW. In the eastern part of the area the dip is less steep than in the western part. The strike of the schistosity of the strongly metamorphosed rocks seems to be more toward the west than that of the slightly metamorphosed rocks. The lineation is very steep and trends toward the southwest. The fold axis is nearly horizontal. The basal direction of the schists has been discovered anywhere.

The schists are described in geographical sequence from the western margin of the schist belt toward the east. Finally, there is a description of the anthophyllite-biotite gneisses and diopside gneisses situated in the southern and southwestern part of Hautajärvi, near the porphyritic granite.

Associated with the schists of Hautajärvi are eruptive rocks, which are briefly described before the schists; the latter are situated adjacent to porphyritic granites along their southern and southwestern margins (Fig. 1). In two places the schists are intersected by a diabase dike, which at one point evidently also penetrates the porphyritic granite. In addition, the schists contain pegmatites to a certain extent.

## ERUPTIVE ROCKS OF HAUTAJÄRVI

### Diabases

Some 800 metres to the north from the middle of Hautajärvi there runs a diabase dike. The diabase in the dike is gray of color, coarse-grained and ophitic, and its

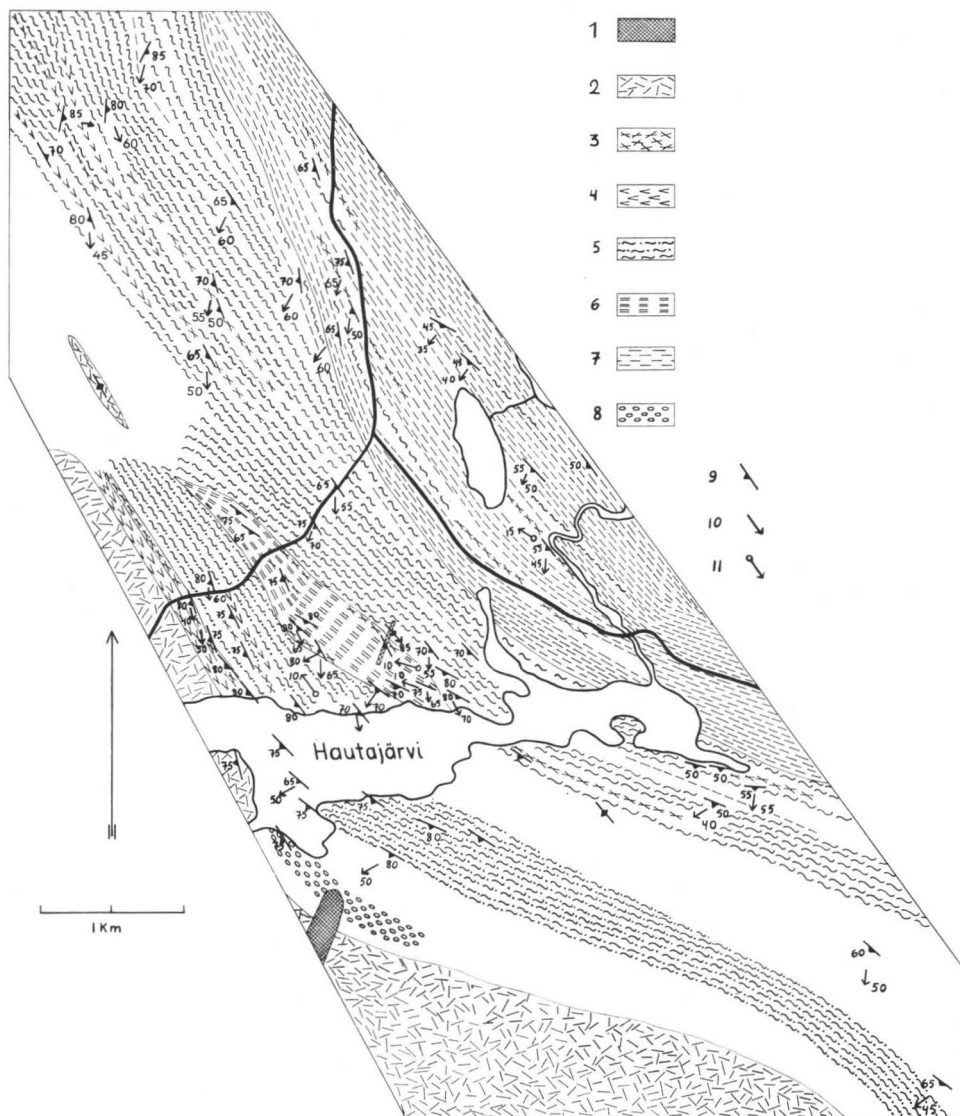


FIG. 1. Map of the schist area of Hautajärvi. 1) Diabase. 2) Porphyritic granite and pegmatite. 3) Diopside amphibolite and amphibolite. 4) Black schists. 5) Garnet-bearing mica gneiss and mica gneiss. 6) Cummingtonite-biotite gneiss and hornblende gneiss. 7) Plagioclase gneiss. 8) Anthophyllite-biotite gneiss and diopside gneiss. 9) Schistosity. 10) Lincation. 11) Fold axis.

mineral composition, in terms of percentages by volume, is as follows: plagioclase 47.4, diopsidic augite 15.6, hypersthene 1.3, hornblende 28.5, biotite 4.8, apatite 0.4 and opaque minerals 0.2.

Plagioclase ( $An_{55-63}$ ) occurs as long, narrow, idiomorphic, twinned grains. The pyroxenes occur mainly as large poikilitic grains, which in most instances are surrounded by a ring of hornblende — to some extent appearing to be a reaction rim; in many cases, they have partly altered to hornblende from inside the grain.

Hypersthene ( $\alpha = 1.719, \gamma = 1.735, Fs_{52}$ ) is present in far smaller amounts than is diopsidic augite. Diopsidic augite ( $\alpha = 1.680, \gamma = 1.711, c \wedge \gamma = 37^\circ$ ) contains very thin lamellae, which have an extinction different from of the main portion of the crystal. The latter in some cases reveals the presence of a little tremolite as an alteration product.

The hornblende ( $\alpha = 1.660 =$  pale green,  $\beta =$  yellowish green,  $\gamma = 1.680 =$  brownish green,  $c \wedge \gamma = 15^\circ, 2V\alpha = 68^\circ$ ) in places contains biotite flakes. Ordinarily, the biotite ( $\gamma = 1.639$ ) occurs as rings around allotriomorphic opaque mineral grains, these rings being in turn surrounded by hornblende, in which they in some spots have the character of inclusions.

The diabase in the dike situated on the southern side of Hautajärvi is appreciably coarser of grain than the aforescribed diabase. It is ophitic in texture and further differs from the former in that no diopsidic augite has been met with in it but only hypersthene. The mineral composition of the diabase is as follows: plagioclase, hypersthene, gedrite, biotite, apatite and opaque minerals.

Plagioclase ( $\alpha = 1.562, \gamma = 1.570, An_{65}$ ) occurs as grains 0.5 cm broad, 1.5 cm long, the largest measuring as much as 1.5 cm in breadth and 25 cm in length. The hypersthene ( $2V\alpha = 64^\circ, \alpha = 1.691, \gamma = 1.704, Fs_{32}$ ) is unevenly distributed. In places it occurs as anhedral, poikilitic grains measuring as much as  $2 \times 5$  cm in size and protruding several millimeters above the surface of the rock. Similarly elevated are roundish titanomagnetite crystals measuring 0.5—1.5 cm.

In spots the plagioclase contains inclusions of tiny, wormshaped hypersthene grains (Fig. 2), which have a simultaneous extinction between crossed nicols under the microscope not only among themselves but also, in many instances, with adjacent larger hypersthene grains. Frequently, the impression is given that the inclusions are relicts of hypersthene that has been replaced by the plagioclase. In some spots there are inclusions of gedrite ( $2V\gamma = 78^\circ$ ). On occasion the hypersthene has been observed to have altered into an aggregate composed of tiny gedrite grains. The plagioclase containing hypersthene inclusions is slightly richer in albite than is the rock elsewhere.

Adjacent to the hypersthene in the plagioclase are biotite flakes ( $\gamma = 1.653$ ), which have become attached to the hypersthene. In many instances, they run parallel to the prismatic direction of the pyroxene. Occurrences of such biotite have also been described in their papers by Christophe-Michel-Lévy and Goñi (1964).

Frequently associated with the gedrite are large allotriomorphic apatite grains.

Wilkman (1924) has described enstatite-augite diabase dikes and hornblende diabase dikes occurring in, among other places, Sonkajärvi. Petrographically, the pyroxene diabase dikes of Hautajärvi resemble those first mentioned.

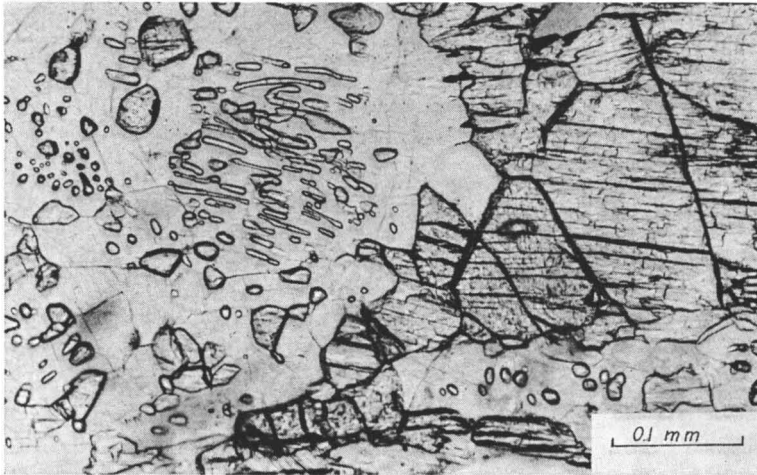


FIG. 2. Worm-like hypersthene and gedrite inclusions in plagioclase. Microphoto, 1 nic. Diabase. South side of Hautajärvi, Kiuruvesi.

### Porphyritic granites

The schist area borders along its southern and southwestern margins on porphyritic granites. Wilkman (1938) has distinguished four different types of rock in the porphyritic granite area situated south of Hautajärvi: pyroxene-quartz diorite, pyroxene granite, ordinary porphyritic granite and pyroxene granodiorite.

### Pegmatites

The schists contain to some extent pegmatite veins. In the northern part of the area there is a pegmatite vein roughly 40 meters broad and running N 30° W. To a large extent, it is pure quartz, but in spots it has pure microcline and, in addition, small amounts of albite. The pegmatite is sheared.

## THE METAMORPHIC SCHISTS OF HAUTAJÄRVI

### Black schists

The black schists are poorly visible in outcrops. In most cases, it is necessary to dig to expose them. This was done, for example, at several places near the western margin of the diopside amphibolite bed.

The black schists occur in the area as two different types, with respect to their chief mineral constituents: a biotite-quartz type and a diopside-amphibole type. The principal constituents of both types include not only graphite but also pyrrhotite

and hydro-pyrrhotite (germ. »Wasserkies«; Saksela, 1947, p. 208), pyrite and, evidently, ilmenite.

The mineral composition of the biotite-quartz type, which is more prevalent in the western part of the bed, is as follows, in terms of percentages by volume: plagioclase 17.5, microcline 10.1, quartz 5.0, biotite 6.0, leucoxene and apatite 2.7, and opaque minerals 58.7. The plagioclase is classified as albite. The quartz occurs as tiny grains and also as lenticular grain clusters. The biotite's  $\gamma$  is very pale brown. The leucoxene is pleochroic and is present mainly in association with opaque minerals.

In the diopside-amphibole type, the amphibole is weakly pleochroic ( $\gamma$  = grayish green) and  $c \wedge \gamma = 30^\circ$ . The diopside is euhedral and its  $c \wedge \gamma = 42^\circ$ . The plagioclase is andesine. In addition, the rock contains clinozoisite, quartz, anhedral and euhedral sphene in abundance, large allotriomorphic apatite grains and sericite.

The diopside-amphibole type reveals the presence of microscopically thin laminae containing various minerals: sphene, quartz and layers with an abundance of epidote, other layers with abundant epidote, diopside and hornblende as well as laminae containing large amounts of hornblende and plagioclase.

Both black schist types occur as intercalations within each other. Black schists occur to some extent as narrow intercalations also in the diopside amphibolite situated on their eastern side, and they are to be found elsewhere as well in the schist area of Hautajärvi (Fig. 1).

Saksela (1933) reports the following mineral assemblages as occurring in black schists: chlorite, microcline, quartz and albite; biotite, microcline, intermediary plagioclase and quartz; actinolite, microcline, sphene and albite; actinolite, intermediary plagioclase, microcline and quartz. Saksela (1933 a) has described a black schists formation a black schists from Karhunsaaari. The carbon and sulfide material is regarded by Saksela (1933 a, p. 37) as original, as indicated by the structure of black schists, and in composition they represent dolomite-bearing clay sediments.

Marmo (1960) distinguishes the presence in sulphite and graphite schists of, *e.g.*, sulphide schists of pelite composition and sulphide-graphide schists of calcareous composition.

Marmo and Metzger (1953) have described from the Hiirola area black schists consisting principally of biotite, quartz and graphite.

Peltola (1960) divides the black schists into three categories: argillaceous, calcareous and arenaceous varieties. Of these, the argillaceous schists correspond to the biotite-quartz type of the Hautajärvi area, and the calcareous ones to the diopside-bearing schists.

### Diopside amphibolites

The thickest diopside amphibolite bed occurs immediately to the east of the black schists.

TABLE 1.

Mineral compositions of diopside amphibolite in percentages by volume: hornblende-rich band (1 and 2), diopside-rich band (3), and plagioclase-rich band (4). North side of Hautajärvi, Kiuruvesi.

	1	2	3	4
Quartz .....	1.4	—	—	—
Plagioclase .....	28.5	21.1	10.2	56.0
Hornblende .....	62.5	72.1	5.0	5.2
Diopside .....	0.7	—	59.0	32.0
Epidote .....	—	—	11.4	—
Opaque minerals .....	5.8	4.5	3.7	2.7
Sphene .....	—	0.9	6.2	1.2
Apatite .....	—	0.9	0.7	0.6
Carbonate .....	—	—	3.0	—
Other minerals .....	1.1	0.5	0.8	2.3
Total	100.0	100.0	100.0	100.0

The diopside amphibolites are banded, and the bands are foliated and broken up. The thickest bed consists of three different types of rock: 1) greenish gray stretches of rock containing diopside in abundance, 2) blackish gray stretches containing abundant hornblende, and 3) rock of a coarser than normal grain containing garnet, diopside and considerable amounts of plagioclase (Table 1). In addition, it contains in the cleavages pyrrhotite situated at right angles to the schistosity. The portions of the rock containing abundant diopside occur as narrow bands of varying thickness, as lenses and as folds shaped like an »S». The lenses contain larger hornblende, diopside, quartz and calcite crystals. Garnet occurs more in the eastern part of the bed, while it is commonly lacking in the western marginal portions.

The bands containing abundant hornblende represent fine-grained amphibolites more nearly than anything else. They show a clearer schistosity than do the other types. The composition of the plagioclase in them is  $An_{50}$  ( $\alpha'$  on 001 cleavage plates is 1.554 and  $\gamma'$  on 001 cleavage plates is 1.561). The following optic properties have been measured from the hornblende:  $\alpha = 1.665$ ,  $\beta = 1.681$ ,  $\gamma = 1.689$ ,  $\gamma - \alpha = 0.025$ ,  $c \wedge \gamma = 21^\circ$  and  $2V\alpha = 68^\circ$ .

The diopside occurs as euhedral, greenish grains, of which a number are conspicuously uraltized. The diopside ( $\alpha = 1.701$ ,  $\gamma = 1.732$ ,  $2V\gamma = 59^\circ$ ,  $c \wedge \gamma = 41^\circ$ ) appears also as large, allotropic grains, notably in coarse-grained, diopside-rich bands. The epidote ( $\alpha = 1.704$ ,  $\gamma = 1.714$ ) generally occurs as allotropic grains of anomalous blue in interference color. In places it occurs as rings around many mineral grains, such as plagioclase, diopside, hornblende and sphene (Fig. 3). In some cases, the epidote grains contain abundant inclusions shaped like worms, which may be quartz. The hornblende ( $\gamma =$  dark green,  $\alpha =$  golden brown) occurs in allotropic and frequently poikilitic form in diopside- and epidote-rich bands. There is also a little tremolite. The composition of the plagioclase in the pale veins is  $An_{(55-70)}$ . ( $\alpha'$  on 001 cleavage plates is 1.551 and  $\gamma'$  on



FIG. 3. Epidote surrounds hornblende, diopside, plagioclase and sphene. Diopside amphibolite. Microphoto, crossed nicols. North side of Hautajärvi, Kiuruvesi.

001 cleavage plates is 1.571). The rock further contains *c a r b o n a t e*, of which a part of it represents an intergrowth with plagioclase, occurring as winding bands, as well as sphene, opaque minerals, quartz and biotite. Surrounding the opaque minerals in many cases is a ring of sphene. The biotite content is slight, whereas there is an abundance of sphene, occurring as large grains, the degree of idiomorphism of which varies.

Eskola (1914) has described diopside amphibolites from the Orijärvi region, which are distinctly layered, frequently appearing as alternating layers with leptite. According to Eskola, these diopside amphibolites are of sedimentary origin: they formed from metamorphic calcareous slates with a probable mixture of volcanic matter.

#### Garnet-bearing mica gneisses

Garnet-bearing mica gneiss is situated on the immediate eastern side of the thick diopside amphibolite bed. It is stratified, with feldspar-quartz-rich layers alternating with mica-rich ones. In many instances, the mica gneiss is veined. To some extent, augen gneiss is also to be found — for example, on the southern side of Hautajärvi. Table 2 gives the mineral composition of two types of mica gneiss in percentages by volume, exclusive of garnet. In addition, they have yielded a few narrow layers of granite gneiss.

Here and there, the garnet-bearing mica gneiss contains layers of amphibolite and diopside amphibolite as well as black schist. The aforementioned rocks occur

TABLE 2.

Mineral composition of two garnet-bearing mica gneisses, in percentages by volume, without garnet. North side of Hautajärvi, Kiuruvesi.

	1	2
Quartz .....	22.1	31.9
Plagioclase .....	52.1	45.7
Potash feldspar .....	<0.1	<0.1
Biotite .....	23.0	21.6
Muscovite .....	1.0	—
Apatite .....	0.8	<0.1
Zircon .....	0.1	<0.1
Opaque minerals .....	0.3	0.1
Chlorite .....	0.2	0.1
Carbonate .....	0.4	—
Other minerals .....	—	0.3
Total	100.0	100.0

in the mica gneiss in places also as small lenses. Moreover, carbonate-bearing lenses have come to light, probably being present more along the western margin of the bed.

The amount of garnet ( $n = 1.788$ ) present in the garnet-bearing mica gneiss varies — in spots it is abundant, but in other places there is very little of it. It is found in both mica-poor and mica-rich varieties. The garnet grains are reddish brown, in some cases as large as a thumb's end, in other cases smaller than the head of a pin. Large garnet porphyroblasts have been met with in abundance, particularly in the mica gneiss resembling augen gneiss situated on the southern side of Hautajärvi. The principal mafic mineral is biotite ( $\gamma = \beta = 1.666$ ). Muscovite occurs in varying amounts, especially in places marked by the presence of rock taking the form of augen gneiss. To a certain extent, it would appear to have originated through the alteration of biotite. Also chlorite is present in spots to a minor extent as an alteration product of biotite. The composition of the plagioclase is  $An_{33}$  ( $\alpha = 1.545$ ). There is very little potash feldspar. On occasion, apatite is to be found in considerable abundance.

#### Cummingtonite-biotite gneisses and hornblende-biotite gneisses with their lenses and intercalations

East of the garnet-bearing mica gneiss is situated a rather broad, non-homogeneous bed. The main rock constituents are garnet-bearing cummingtonite-biotite gneiss and hornblende-biotite gneiss, in addition to biotite gneiss, granite gneiss and biotite amphibolite. Situated in the western margin of the bed is a layer of fine-grained amphibolite containing cummingtonite porphyroblasts, and in the eastern margin fine-grained diopside amphibolite. Here and there, it contains different kinds of lenses.

TABLE 3.

Mineral compositions of different varieties of rock contained in cummingtonite-biotite gneisses and hornblende-biotite gneiss layers: 1) Cummingtonite-biotite gneiss. 2) Hornblende-biotite gneiss. 3) Biotite gneiss. 4) Biotite gneiss. North side of Hautajärvi, Kiuruvesi.

	1	2	3	4
Quartz .....	4.6	16.1	19.8	6.3
Plagioclase .....	34.0	29.0	42.8	62.2
Biotite .....	15.7	27.9	33.0	26.0
Hornblende .....	16.0	20.6	0.4	—
Cummingtonite .....	24.2	—	—	—
Diopside .....	—	2.7	—	—
Sphene .....	—	2.0	1.3	—
Apatite .....	—	1.4	1.3	1.1
Opaque minerals .....	1.8	0.2	—	0.8
Garnet .....	2.1	—	—	—
Chlorite .....	—	—	—	1.1
Muscovite .....	—	—	—	1.4
Carbonate .....	—	—	—	0.9
Other minerals .....	0.6	0.1	1.4	9.2
Total	100.0	100.0	100.0	100.0

The garnet-bearing cummingtonite-biotite gneiss is rather small-grained, pale brownish gray and veined. Embedded in it are narrow, garnet-bearing bands, in which the garnet generally occurs as grains measuring 2 mm, and narrow amphibole layers, in which the amphibole occurs as grains 1—2 cm in length, and 3-mm thick, or as radiating clusters of grains 5 cm long 2 cm broad. The biotite ( $\gamma = 1.651 =$  dark brown) is poikiloblastic and it contains inclusions of plagioclase, in particular. The cummingtonite ( $c \wedge \gamma = 18^\circ$ ,  $\alpha = 1.650$ ,  $\gamma = 1.679$ ) occurs as colorless, polysynthetically twinned prisms and grain clusters. The garnets are rather large, allotriomorphic porphyroblasts with inclusions of quartz, cummingtonite and opaque minerals. The hornblende is pleochroic from green to pale brownish green and its  $\gamma = 1.680$  and  $c \wedge \gamma = 20^\circ$ . In addition, the rock contains plagioclase ( $An_{40}$ ) as well as quartz, opaque minerals and sphene (Table 3, No. 1). The gneiss further reveals the presence of pegmatites, which contain sulphide disseminations to the extent of causing the rock to weather.

Table 3 also shows the mineral composition of the hornblende-biotite gneiss (No 2) and the biotite gneiss (Nos. 3 and 4) in percentages by volume. The last-mentioned is diopside-bearing. The gray, white and brown, variegated biotite amphibolite, which has an abundance of biotite, contains hornblende and plagioclase, occurring in some cases as porphyroblasts with ragged edges and many large inclusions. This rock further contains a little cummingtonite.

The garnet-bearing cummingtonite-biotite gneiss contains carbonate-bearing, greenish gray lenses with a dark gray amphibolite edge a couple of centimeters wide. The composition of the plagioclase along the margin of the amphibolite is

TABLE 4.

Chemical composition of hornblende in amphibolite (analyst: A. Heikkinen). North side of Hautajärvi, Kiuruvesi.

Weight per cent			
SiO <sub>2</sub> .....	44.52	Si .....	6.567
Al <sub>2</sub> O <sub>3</sub> .....	11.25	Al .....	1.974
TiO <sub>2</sub> .....	0.76	Ti .....	0.080
Fe <sub>2</sub> O <sub>3</sub> .....	2.95	Fe <sup>3+</sup> .....	0.322
FeO .....	15.48	Fe <sup>2+</sup> .....	1.928
MnO .....	0.18	Mn .....	0.027
MgO .....	9.58	Mg .....	2.134
CaO .....	11.78	Ca .....	1.892
Na <sub>2</sub> O .....	1.49	Na .....	0.450
K <sub>2</sub> O .....	0.49	K .....	0.088
P <sub>2</sub> O <sub>5</sub> .....	0.03	P .....	0.018
H <sub>2</sub> O+ .....	1.75	OH- .....	1.738
	100.25		

} 8.00  
 } 5.03  
 } 2.43  
 } 1.76

Physical properties

$\alpha = 1.662$   
 $\beta = 1.677$   
 $\gamma = 1.686$

Specific gravity = 3.30

$c \wedge \gamma = 15^\circ$   
 $2V\alpha = 70^\circ$

An<sub>52</sub> ( $\alpha = 1.554, \gamma = 1.564$ ). And the hornblende contained in it has yielded the following measurements with respect to the optic properties:  $\alpha = 1.662, \beta = 1.677, \gamma = 1.684, c \wedge \gamma = 23^\circ$  and  $2V\alpha = 73^\circ$ . The composition of the plagioclase in the carbonate-bearing lens is An<sub>90</sub> ( $\alpha = 1.573, \beta = 1.579, \gamma = 1.585$  and  $2V\gamma = 78^\circ$ ). In addition, it contains the following minerals: diopside ( $\alpha = 1.702, \gamma = 1.732, 2V\gamma = 59^\circ$  and  $c \wedge \gamma = 44^\circ$ ), actinolite ( $\alpha = 1.646, \beta = 1.657, \gamma = 1.667$ ), calcite ( $\omega = 1.663$ ), garnet, sphene and sericite.

Interbedded in the western part of the rock is fine-grained, bluish gray amphibolite, which contains a fair abundance of light gray, 1—3-mm, round or square — in some instances, oval — cummingtonite porphyroblasts ( $\alpha = 1.658, \beta = 1.676, \gamma = 1.691$  and  $c \wedge \gamma = 17^\circ$ ). The composition of the plagioclase in the amphibolite is An<sub>35</sub> ( $\alpha = 1.548, \gamma = 1.554$ ) while the refractive indices of the hornblende are:  $\alpha = 1.664, \beta = 1.680$  and  $\gamma = 1.688$ ).

The bluish, dark gray amphibolite situated north of the foregoing contains large, radiating clusters of amphibole grains, which megascopically resemble gedrite but in thin section can be readily distinguished as hornblende. Consequently, this amphibole has been separated and analyzed and its X-ray data been determined (Tables 4 and 5).

Hornblendes of nearly identical composition chemically have been described by Buddington (1952) and Miyashiro (1958).

The composition of the plagioclase in this amphibolite is An<sub>44</sub> ( $\alpha = 1.551, \gamma = 1.559$ ). In addition, it contains slight amounts of biotite ( $\gamma = \beta = 1.621$ ) and chlorite ( $\gamma = 1.631$ ).

TABLE 5.

X-ray diffraction powder data of hornblende in amphibolite. (Iron  $K\alpha$  radiation, Mangan filter).  
Hautajärvi, Kiuruvesi.

No	$2\theta$	d	$I/I_0$	No	$2\theta$	d	$I/I_0$
1	12.44	8.93	10	14	48.92	2.338	25
2	13.33	8.34	100	15	49.25	2.323	10
3	22.08	5.05	10	16	53.28	2.159	20
4	24.87	4.49	10	17	56.50	2.045	10
5	33.34	3.37	25	18	57.45	2.014	15
6	34.51	3.26	20	19	57.96	1.998	10
7	36.22	3.114	100	20	61.62	1.890	10
8	38.54	2.933	20	21	71.88	1.649	15
9	40.47	2.799	15	22	75.24	1.586	10
10	41.48	2.733	15	23	77.44	1.548	10
11	41.97	2.703	35	24	80.30	1.501	10
12	43.88	2.591	20	25	83.26	1.457	10
13	44.71	2.545	20	26	84.49	1.440	15

TABLE 6.

Mineral compositions of diopside amphibolite in percentages by volume, and the optic properties of the minerals. (1) Diopside-rich band, and 2) hornblende-rich band). North side of Hautajärvi, Kiuruvesi.

	1	2
Plagioclase	39.3	25.6
Diopside	51.5	—
Hornblende	6.4	61.5
Cummingtonite	—	7.5
Opaque minerals	2.8	5.4
Total	100.0	100.0
Plagioclase $\alpha$	1.551	1.552
$\beta$	1.554	1.555
$\gamma$	1.556	1.560
An	43	46
Diopside $\alpha$	1.700	1.700
$\beta$	1.708	1.709
$\gamma$	1.730	1.731
Hornblende $\alpha$	1.670	1.666
$\beta$	1.685	1.683
$\gamma$	1.692	1.689

Situated along the eastern margin of the bed is fine-grained, streaked diopside amphibolite. Its mineral composition in percentages by volume and its optic properties are given in Table 6. NNW of this diopside amphibolite can be found similar diopside amphibolite, with the difference that it contains garnet. The rock is in places conspicuously brecciated (Fig. 4), the brecciating material being mainly

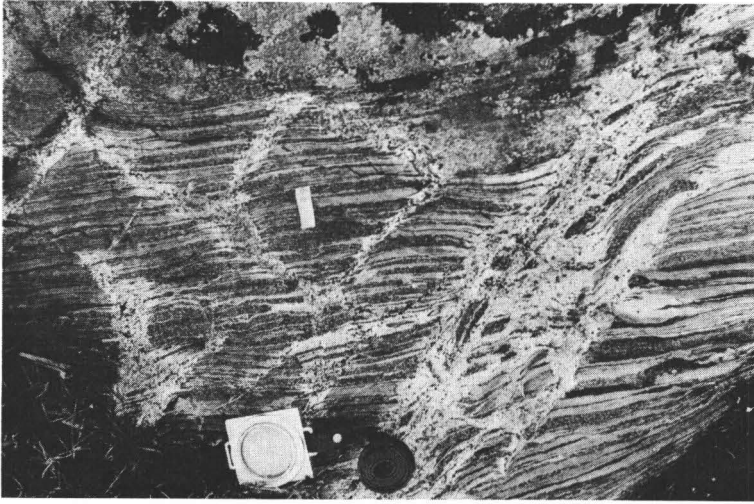


Fig. 4. Brecciated diopside amphibolite. North side of Hautajärvi, Kiuruvesi.

TABLE 7.

Mineral compositions of mica gneisses in percentages by volume. North side of Hautajärvi, Kiuruvesi.

	1	2
Plagioclase .....	49.0	49.5
Quartz .....	13.3	12.5
Biotite .....	35.5	37.4
Other minerals .....	2.2	0.6
Total	100.0	100.0

plagioclase and quartz as well as epidote and chlorite. Farther to the north there are interbedded occurrences of gray amphibolite with a considerable content of carbonate as well as black schists.

**Mica gneisses, with their lenses and intercalations**

The mica gneiss bed situated next in an easterly direction resembles the garnet-bearing mica gneiss, though it contains substantially less garnet and more numerous intercalations of plagioclase gneiss. The mica gneisses are likewise partly laminated, partly having the appearance of veined gneiss and partly that of augen gneiss. Present in them are intercalations of various amphibolites and diopside amphibolites; these layers are narrow and not very numerous. Black schists also occur as narrow intercalations. Table 7 presents the mineral composition of two mica gneisses dif-



FIG. 5. Foliated amphibolite lenses in mica gneiss. North side of Hautajärvi, Kiuruvesi.



FIG. 6. Banded amphibolite. North side of Hautajärvi, Kiuruvesi.

TABLE 8.

Mineral composition, in percentages by volume, of plagioclase gneiss from 1) mica-poor band, and 2) mica-bearing band, as well as 3) mica gneiss occurring in it as an intercalation. North side Hautajärvi, Kiuruvesi.

	1	2	3
Quartz .....	4.2	11.5	18.2
Plagioclase .....	89.5	70.4	50.4
Potash feldspar .....	5.7	5.9	—
Biotite .....	—	7.9	31.0
Epidote .....	—	0.4	—
Sphene .....	—	0.2	—
Apatite .....	—	0.3	—
Muscovite .....	—	2.9	—
Opaque minerals .....	—	0.4	—
Other minerals .....	0.6	0.1	0.4
Total	100.0	100.0	100.0

fering macroscopically in appearance. The principal minerals constituting the rock are plagioclase, quartz and biotite, in addition to which there are present slight amounts of muscovite, chlorite, carbonate and opaque minerals as well as, in spots, garnet.

The mica gneiss resembling augen gneiss in places contains narrow, partially foliated amphibolite lenses (Fig. 5) and also rectangular amphibolite fragments, both cases possibly representing breakages off narrow layers. Also found in it as an intercalation has been streaky diopside amphibolite (Fig. 6). The mineral composition of its dark gray portion, expressed in terms of percentages by volume, is: plagioclase 23.2, quartz 3.0, hornblende 66.0, sphene 2.6, epidote 3.3, opaque minerals 1.4 and other minerals 0.5. The composition of the plagioclase in it is  $An_{37}$  ( $\alpha = 1.547$ ,  $\gamma = 1.556$ ), the refractive indices of the hornblende being:  $\alpha = 1.661$   $\gamma = 1.683$ . Some of the pale gray bands are elevated, others depressed. The elevated bands are rich in quartz, while the depressed ones contain abundant epidote ( $\alpha = 1.712$ ,  $\gamma = 1.724$ ). The composition of the plagioclase in the depressed bands is  $An_{(62-74)}$  ( $\alpha = 1.561$ ,  $\gamma = 1.576$ ).

### Plagioclase gneisses, with their intercalations

Plagioclase gneiss occurs east of the mica gneiss. It is not easy to draw the line between them because they are present in each other as intercalations. The plagioclase gneisses are partly banded, even to the extent of taking on the appearance of veined gneiss, and partly in the guise of augen gneiss. Also brecciated types have been run across. The types resembling augen gneiss and veined gneiss contain more pegmatites than the other types do. The plagioclase gneisses are fine-grained, pale gray or gray rocks. Their principal minerals are plagioclase  $An_{25}$ , quartz, biotite

( $\gamma = 1.646$ ) and potash feldspar, the accessory constituents being epidote, sphene, apatite, muscovite, chlorite and opaque minerals. The potash feldspar ordinarily occurs only as antiperthite. In Table 8, Nos. 1 and 2 represent the mineral composition of two banded plagioclase gneisses in percentages by volume.

The plagioclase gneiss contains various intercalations and lenses, such as different amphibolites and mica gneisses. In Table 8, No. 3 is a mineral composition analysis of a mica gneiss intercalation.

One intercalation consists of streaky diopside amphibolite, in which dark gray amphibolite layers alternate with layers of diopside ( $\alpha = 1.689$ ,  $\beta = 1.698$  and  $\gamma = 1.720$ ) and epidote ( $\alpha = 1.716$ ,  $\beta = 1.722$  and  $\gamma = 1.727$ ). The latter are invariably coarser of grain than the former, and they always have a black hornblende border ( $\alpha = 1.653$ ,  $\beta = 1.667$  and  $\gamma = 1.674$ ). The composition of the plagioclase in the diopside amphibolite is  $An_{45}$  ( $\alpha = 1.551$  and  $\gamma = 1.560$ ) and in the amphibolite  $An_{35-38}$  ( $\alpha = 1.546$  and  $\gamma = 1.556$ ). The refractive indices of the hornblende in the latter are:  $\alpha = 1.657$ ,  $\beta = 1.672$  and  $\gamma = 1.678$ . The banded diopside amphibolite further contains quartz, sphene, apatite and opaque minerals.

Present in this diopside amphibolite are also bands and lenses containing pure quartz, running parallel to the schistosity and measuring 0.1—0.5 cm in width. They are extraordinary in that the quartz contained in them is conspicuously oriented and the grains are intergrown. In places each band appears to consist of a single quartz crystal. Metamorphism seems to have played a prominent part in the production of their present habit. Since the bands containing diopside and epidote are coarser of grain than the amphibolite, and since the former has a black hornblende border, there is a likelihood that metamorphism contributed also to the origin of the bands composed of diopside and epidote.

The mica gneiss situated next to the power station at Ryönäjoki (Table 8, No. 3) contains a layer 10 cm thick with occurrences of amphibole, diopside and carbonate. This layer is subdivided into separate boudins. The surface of the outcrop running parallel to the plane of schistosity and the bedding contains numerous lenses situated close together. It may be observed from a vantage point perpendicular to the layer that, on the other hand, the lenses belong to the same layer.

The lenses are zoned. Outermost next to the mica gneiss lies a very narrow rim, which is composed principally of cumingtonite ( $\alpha = 1.652$  and  $\gamma = 1.686$ ), plagioclase ( $An_{75}$ ) and quartz. There follows a fine-grained, black-gray rim approximately 1 cm wide, which consists of plagioclase ( $\alpha = 1.569$ ,  $\gamma = 1.580$ ,  $An_{85}$ ) and hornblende. The center of the lenses is coarse-grained and greenish gray and contains an abundance of poikiloblastic diopside grains ( $\alpha = 1.680$ ,  $\gamma = 1.720$ ), plagioclase ( $An_{85}$ ), quartz and calcite ( $\omega = 1.663$ ). The remaining minerals of the lenses and the mineral composition in percentages by volume are presented in Table 9. The rims containing hornblende and cumingtonite have been combined in the computations.

TABLE 9.

Mineral composition of zoned lens contained in mica gneiss, in percentages by volume. (1) Amphibole-rich marginal zone containing cummingtonite, and 2) diopside-rich middle portion of the lens). North side of Hautajärvi, Kiuruvesi.

	1	2
Quartz .....	12.2	19.1
Plagioclase .....	28.8	24.2
Hornblende .....	48.4	5.2
Diopside .....	—	39.1
Cummingtonite .....	3.8	—
Carbonate .....	—	2.0
Apatite .....	—	0.4
Sphene .....	—	4.4
Opaque .....	6.8	5.2
Other minerals .....	—	0.4
Total	100.0	100.0

Here and there in the plagioclase gneiss there also occur portions of rock of nearly amphibolite composition that have undergone a high degree of metamorphism.

### Anthophyllite-biotite gneiss and diopside gneisses

On the southern and southwestern sides of Hautajärvi near the porphyritic granites, there occur alternating layers of various diopside gneisses and anthophyllite-biotite gneisses. The schistosity of the rocks is rather weak: in some cases, their orientation can be observed under the microscope only by using a test plate. We shall concern ourselves here briefly with a few of the principal types.

The mineral constituents of one type, the anthophyllite-biotite gneiss, are: plagioclase  $An_{35}$ , biotite, gedrite, cordierite, garnet and hypersthene. Brown biotite ( $\gamma = \beta = 1.640$ ) and cordierite ( $\alpha = 1.543$ ,  $\gamma = 1.552$ ) occur together, and in their stead there appear garnet ( $n = 1.798$ ) and gedrite ( $\alpha = 1.654$ ,  $\gamma = 1.675$ ). Hypersthene occurs in some spots as a relict in gedrite. The margins of the gedrite reveal the presence of slight amounts of hornblende and green biotite. In addition, the rock contains a little quartz, opaque minerals and apatite. Pinite is present in the cordierite as an alteration product. The rock contains as lenses 5-cm long spheres composed of quartz, plagioclase and epidote.

The second type, diopside-plagioclase gneiss, consists chiefly of allotriomorphic plagioclase and pyroxene, which occurs as broken, irregularly shaped grains, frequently taking the form of porphyroblasts (Table 10). The plagioclase ( $An_{40}$ ) contains potash feldspar as antiperthite. The edges and cracks between segments of the diopside contain hornblende and, furthermore, biotite. Cummingtonite occurs slightly, chiefly in association with hypersthene, being colorless and polysynthetically twinned. The biotite flakes are in many cases chloritized at their edges, with horn-

TABLE 10.

Mineral composition, in percentages by volume, of diopside-plagioclase gneiss (1) and diopside gneiss (2). South side of Hautajärvi, Kiuruvesi.

	1	2
Plagioclase .....	66.6	13.4
Diopside .....	15.6	} 43.9
Hypersthene .....	7.3	
Hornblende .....	3.8	19.4
Biotite .....	3.3	18.3
Quartz .....	0.9	—
Carbonate .....	—	0.3
Opaque minerals .....	1.5	3.1
Other minerals .....	1.0	1.6
Total	100.0	100.0

blende enveloping them. Further, the rock has tiny apatite grains, opaque minerals, around which occur hornblende, quartz, epidote and carbonate.

The third type, consisting of dark gray, coarse-grained diopside gneiss, is characterized by the presence of, in addition to the diopside grains, finer-grained plagioclase ( $An_{40}$ ), hornblende ( $2V\alpha = 73^\circ$ ,  $c \wedge \gamma = 20^\circ$ ,  $\gamma = \alpha = 0.028$ ), biotite, hypersthene ( $2V\alpha = 50^\circ$ ) and diopside ( $2V\gamma = 61^\circ$ ,  $c \wedge \gamma = 44^\circ$ ), as the main constituent minerals. The pyroxene shows evidence of alteration into amphibole.

## DISCUSSION

The magnetic and electric anomalies of the Hautajärvi schist area are probably due in the main to the sulfide-bearing black schists, judging by the circumstance that these schists have frequently been observed to occur at points where the anomalies register maxima. The schist belt is relatively narrow, but it contains a highly varied series of schists, which differ in composition. To a large extent, at least, the schists are sedimentogeneous. The presence of, for example, black schists, diopside amphibolites, mica gneisses and plagioclase gneisses indicates that considerable changes have taken place in the sedimentation milieu. The schists of Hautajärvi metamorphosed under conditions of amphibolite facies, and the schist area as a whole provides an admirable example of the amphibolite facies commonly met with in Finland.

*Acknowledgements* — The authors wish to express their gratitude to the National Research Council for Sciences for financial aid received to support their research. They also wish to acknowledge the assistance given by the Institute of Geology and Mineralogy of the University of Helsinki and the Exploration Department of the Outokumpu Company. Further, they are greatly indebted to professor Martti Saksela his invaluable aid in reading the manuscript and pointing out errors.

*Manuscript received, March 15, 1966*

## REFERENCES

- BUDDINGTON, A. F. (1952) Chemical petrology and mineralogy of some metamorphosed Adirondack gabbroic, syenitic and quartz syenitic rocks. *Amer. Journ. Sci.*, Bowen vol., p. 37.
- CHRISTOPHE-MICHEL-LÉVY, M. et GOŃI, J. (1964) Étude minéralogique et géochimique d'une latite vitreuse a biotite et plagioclase. *Bull. Soc. franc. Minér. Crist.* LXXXVII, p. 385—92.
- DEER, W. A., HOWIE, R. A., and ZUSSMAN, J. (1963) *Rock Forming Minerals*. Vol. 1—4. London.
- ESKOLA, P. (1914) On the Petrology of the Orijärvi Region in south-western Finland. *Bull. Comm. géol. Finlande* 40.
- MARMO, V. (1960) On the sulphide and sulphide-graphite schists of Finland. *Bull. Comm. géol. Finlande* 190.
- MARMO, V. and METZGER, A. TH. (1953) Geology of the Hirola district, North of Mikkeli, south-eastern Finland. *Bull. Comm. géol. Finlande* 159.
- MÄKINEN, E. (1916) Översikt av de prekambryska bildningarna i mellersta Österbotten i Finland. *Bull. Comm. géol. Finlande* 47.
- MIYASHIRO, A. (1958) Regional metamorphism of the Gosaisyo-Takanuki district in the central Abukuma plateau. *Journ. Fac. Sci. Univ. Tokyo, sect. II*, vol. 11, p. 219.
- PELTOLA, E. (1960) On the black schists in the Outokumpu region in eastern Finland. *Bull. Comm. géol. Finlande* 192.
- SAKSELA, MARTTI (1933) *Kivilajikartan selitys*. Lehti B 4 Kokkola.
- »— (1933 a) Die Kieserzlagertätte von Karhunsaaari in Nordkarelien, Finnland. *Geol. Fören. Förhandl. i Stockholm* 55, pp. 29—58.
- »— (1947) Über eine antimonreiche Paragenese in Ylöjärvi, SW-Finnland. *Bull. Comm. géol. Finlande* 140, pp. 199—222.
- »— (1957) Die Entstehung der Outokumpu-Erze im Lichte der tektonisch-metamorphen Stoffmobilisierung. *Neues Jb. Mineral. Abh.* 91, 278—303. Festband, Schneiderhöhn. Stuttgart.
- WILKMAN, W. W. (1924) Om diabasgångar i mellersta Finland. *Bull. Comm. géol. Finlande* 71.
- »— (1931) *Kivilajikartan selitys*, C 4—Kajaani. With map, 1929. General geological map of Finland, 1 : 400 000.
- »— (1938) *Kivilajikartan selitys*, C 3—Kuopio, With map, 1935. General geological map of Finland, 1 : 400 000.



## A COMPUTER PROGRAM FOR BOULDER TRAIN ANALYSIS

BY

T. A. HÄKLI and P. KEROLA

*Outokumpu Co.*

### ABSTRACT

A tentative model for the boulder frequency distribution function

$$F(x, y) = N_0 \cdot e^{-kx} \frac{1}{(S_0 + Ax) \sqrt{2\pi}} \cdot e^{-\frac{y^2}{(S_0 + Ax)^2}}$$

is derived. Based on this model a computer program has been written for an IBM 1440 computer. The program has been used to analyse some boulder trains. The results are reported and discussed and some applications suggested. The program, written in Fortran, is given in full in the Appendix.

### INTRODUCTION

In areas recently glaciated, as in Fennoscandia, the tracing of ore-boulders has for long been a widely and successfully used prospecting method. This method, as well as boulder trains have been described by various authors (Sauramo, 1924; Hyypä, 1945; Okko and Peltola, 1958).

At present the use of computers for resolving problems in mining and exploration is gaining in popularity. In particular, much work has been done in developing programs which make possible the calculation of ore reserves (Hewlett, 1963), the evaluation of the location of shafts, the controlling of mining operations and the testing of geological models in problems which involve areally distributed data (Miller, 1956; Whitten, 1962 a, 1962 b, 1963).

The reasonable usage of computers requires that a reliable mathematical model is available, otherwise it may well happen that the computer will soon be running the operator, instead of the operator the computer. In this paper a tentative model for the distribution function of the boulders in a boulder train is given. Based on the

model a computer program has been made which calculates the required parameters characterising the frequency distribution. As an application of the program a few typical cases are reported and discussed.

### FREQUENCY DISTRIBUTION FUNCTION

Consider glacial ice moving over an outcrop. The effect of this movement is twofold. Boulders are loosened from the outcrop and later deposited into moraine together with other glacial drift. For a better approach to the problem let the orthogonal coordinate axes be placed in such a way that the origo is situated at the outcrop, with the x-axis parallel to the movement of the glacier. For convenience's sake, let the x-values increase in the direction of the movement. If it is further supposed that the number of boulders does not increase due to breaking during transportation, it is obvious that the number of the boulders ( $dn$ ) caught by moraine at a small distance ( $dx$ ) is proportional to the number of the boulders ( $n$ ) present

$$(1) \quad \frac{dn}{dx} = -kn$$

where  $k$  is a constant, whose value depends on the ability of moraine to stop or »absorb» boulders. If the above differential equation is integrated, it becomes

$$(2) \quad n = n_0 \cdot e^{-kx}$$

where  $n$  is the number of boulders passing a particular plane perpendicular to the x-axes at a distance of  $x$  from the origo,  $n_0$  is the total number of boulders loosened by the glacier ice from the outcrop, and  $k = \text{an »absorption» coefficient}$ .

It may be assumed that the movement of the glacier is rectilinear. However, the boulders do not strictly follow the direction of the ice but, due to thrusting and colliding with each other and with other moraine material, they deviate at random from the course of the glacier. The deviations are neither systematic nor constant but are equally likely to be positive or negative. Small deviations are more frequent than large ones and under these conditions it is obvious that the distribution of the boulders in y-direction obeys — at least approximately — the normal distribution law, *viz.*,

$$(3) \quad F(y) = \frac{1}{S \sqrt{2\pi}} \cdot e^{-\frac{y^2}{2S^2}}$$

where  $s$  is standard deviation.

The number of boulders deviating to left and to right at a small transportation distance is proportional to the amount of boulders present. As a consequence the frequency remains practically unaltered near the centre line of the train, provided the

absorption effect of morain is omitted, due to the fact that the gradient of the frequency in  $y$ -direction is gentle. On the flanks where the frequency gradient is steep more boulders are transported towards the edge than towards the centre with the consequence that the boulder train tends to widen with increasing distance from the outcrop. Hence  $S$  is not constant, but a function of the distance  $x$ . It can be supposed that this dependence of the width of the boulder train on the distance from the outcrop is a simple, linear one. Making now the transformation  $S = S_0 + Ax$ , where  $S_0 =$  the standard deviation on the outcrop ( $x = 0$ ),  $x =$  the distance from the outcrop and  $A =$  a constant, the value of which depends on the angle at which the boulder train opens, the equation (3) converts into

$$F(x, y) = \frac{1}{(S_0 + Ax) \sqrt{2\pi}} \cdot e^{-\frac{y^2}{2(S_0 + Ax)^2}} \quad (4)$$

From the equations (2) and (4) one now obtains

$$F(x, y) = n_0 \cdot e^{-kx} \frac{1}{(S_0 + Ax) \sqrt{2\pi}} \cdot e^{-\frac{y^2}{2(S_0 + Ax)^2}} \quad (5)$$

as the expression for the distribution function of the boulders passing a particular point in the boulder train.

The number of boulders stopped by moraine at a point in the boulder train is directly proportional to the total sum of the boulders passing that point and, consequently, the expression for the distribution function of the boulders in the boulder train is similar to the function (5), except that  $n_0$  is now replaced by  $N_0$ , *viz.*,

$$F(x, y) = N_0 \cdot e^{-kx} \frac{1}{(S_0 + Ax) \sqrt{2\pi}} \cdot e^{-\frac{y^2}{2(S_0 + Ax)^2}} \quad (6)$$

where  $N_0$  is the number of boulders on the plane perpendicular to the movement of the glacier at the lee edge of the outcrop (*i.e.*  $x = 0$ ).

## APPLICATIONS

The above derived equation (6) has some straight-forward applications which, in addition to being of academic interest could also be of aid to prospectors.

Thus in practice it may happen that a boulder train cannot be followed up to the outcrop due to various difficulties. The location of the boulder source can, however, be estimated by using the frequency information obtained from the accessible part of the boulder train. Under these conditions it is advisable to place the  $Y$ -axis at the place up to which the boulder train has been traced. The values for the parametres

are now calculated based on the available data. At the outcrop the value for  $S$  cannot be negative and, consequently

$$0 < S < S_0$$

Inserting these limit values into the equation

$$S_0 + AX = S$$

and solving it for  $X$ , the location of the outcrop can reasonably well be confined within a relatively small area.

The equation (6) can also be used for the evaluation of the total number ( $n_0$ ) of the boulders. It is easy to see that if the equation (6) is integrated with respect to  $x$  over  $(0, \infty)$  and with respect to  $y$  over  $(-\infty, \infty)$

$$n_0 = \frac{N_0}{k}$$

Again, if the average volume ( $\bar{V}$ ) of the boulders and the thickness ( $L$ ) of the layer eroded by the glacier from the outcrop are known, the area ( $A$ ) of the outcrop is

$$A = \frac{n_0 \cdot \bar{V}}{L}$$

Should the area of the outcrop have been established by direct measurements then the above equation permits the evaluation of the thickness of the layer eroded by ice.

Equation (5) gives still another useful parameter *viz.*, the average transportation distance ( $\bar{d}$ ). It is obtained by totalling all the distances and dividing the sum by the number of the boulders. Consequently

$$\bar{d} = \frac{1}{k}$$

where  $k$  is »absorption» coefficient.

#### PROGRAM DESCRIPTION

Based on the equation (6) a computer program has been developed for IBM 1 440 computer. The intelligent use of the program requires that the coordinate axes be placed in such a way that the  $X$ -axis is at least approximately parallel to the boulder train axis. A square grid system is laid over the boulder train parallel to the coordinate axes and the frequencies determined by counting the numbers of boulders within each square. The centres of the squares are situated at the grid points, the sides of the squares being of the same length as the grid interval. The grid interval should be

selected so that the random local variations in frequencies are not shown too clearly. In most cases an interval of 100 or 200 metres is entirely satisfactory.

Because of storage limitations, the program operates in three phases. In the first phase the program requires as input the coordinates of the grid points, the observed frequencies and the grid interval. The values for  $N$ ,  $S$  and that for the centre of the boulder train,  $Y$ , are evaluated for every profile. The second phase computes the parameters of the equation (6) *i.e.*  $N_0$ ,  $k$ ,  $S_0$  and  $A$  by the least squares method and also evaluates the standard deviations and the correlation coefficients. By the same method the parameters of the equation  $Y = Y_0 + Bx$  for the boulder train axis are solved and printed out together with those of the equation (6). In the third phase the theoretical frequencies are calculated at the observed grid points using the output of the phase II. The differences between the observed and calculated frequencies are also computed. Finally, if desired, the program performs the Chi-square test to provide a measure for the goodness of fit between the observed and calculated frequencies. For various reasons this test is not always worth doing unless the terrain is relatively even and the number of boulders high enough to keep the random local variation in the observed frequencies within reasonable limits. For further details the interested reader is advised to see the appendix.

### SOME EXAMPLES

To test the validity of the above derived distribution function and to find out applications for the program some trains of uranium-bearing quartzite boulders were analysed. These boulder trains were chosen as testing material because uranium-bearing boulders are easily detectable with scintillometers, with the consequence that practically all the boulders on or near by the surface can be discovered.

#### The Pk-1 boulder train

This boulder train is composed of about 850 known quartzite boulders which are spread over a rather hilly terrain. The source of the boulders is under a lake which has not permitted the following of the boulders up to the outcrop. The quartzite hills have caused some distortion and irregularities to the frequency distribution by pushing the boulders towards the valleys between the hills.

For the frequency distribution analyses the Y-axis was placed near by the shore of the lake and frequencies counted only from that line on. Two grid intervals were used. At first the interval was chosen to be 200 metres. This is so small that the local fluctuations of the frequencies caused by an uneven terrain and perhaps also by the breaking of some boulders are distinctive, as is seen in Fig. 1 in which the observed frequencies are expressed as contours drawn with an interval of 100 boulders per  $\text{km}^2$ .

The computation of the train parameters was performed using all the measured frequencies. The results are compiled in Table 1.

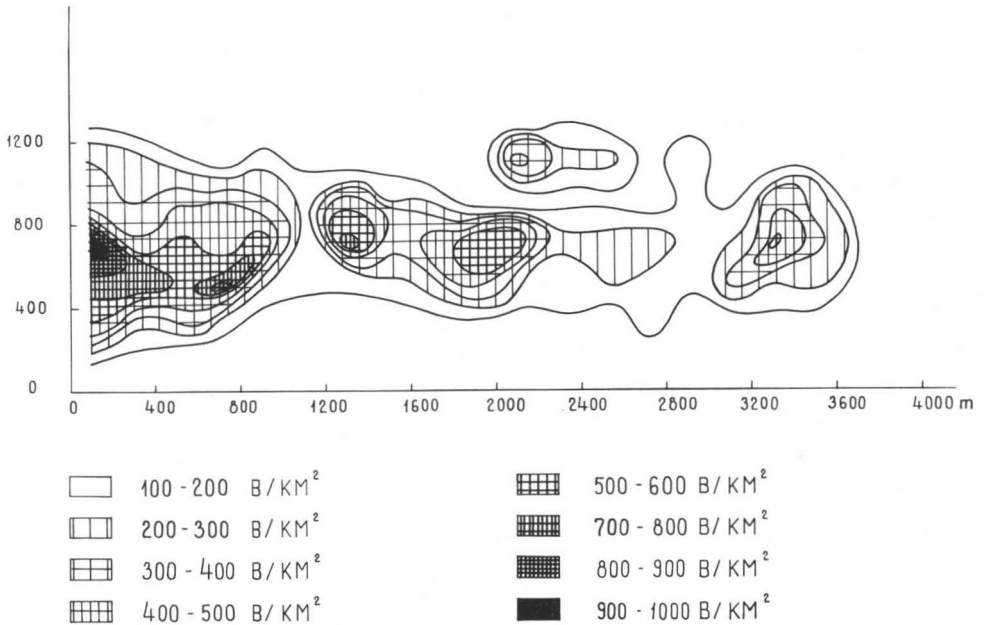


FIG. 1. The Pk-1 boulder train. Observed frequencies. Grid interval 200 m. The frequencies are given as boulders per km<sup>2</sup>.

An examination of Table 1 reveals the relatively high value of the correlation coefficient R connected with the absorption coefficient k. This indicates that the decreasing of the boulder frequency as a function of the distance from the source obeys well the exponential law.

The boulder train widens only a little with distance. If 4S is taken as the width of the boulder train the widening is no more than 25 metres per kilometre as is shown by the low value of  $A = 0.0072112$ . Moreover,  $R = 0.17265$  indicates a poor correlation between the distance from the source and the width of the boulder train. This is, no doubt, due to the terrain effect and to the very small widening angle of the train. The calculated distribution of the boulder frequencies based on the above parameters is presented in Fig. 2.

TABLE 1.

The Pk-1 boulder train. The calculated parameters. The grid interval 200 metres.

$N_0 = 0.3620716$	$S_0 = 198.39055$	$Y_0 = 695.206$
$K = 0.000335122$	$A = 0.0072112$	$B = 0.0086683$
$SD = 0.40655$	$SD = 47.64598$	$SD = 75.22206$
$R = -0.69050$	$R = 0.17265$	$R = 0.13228$

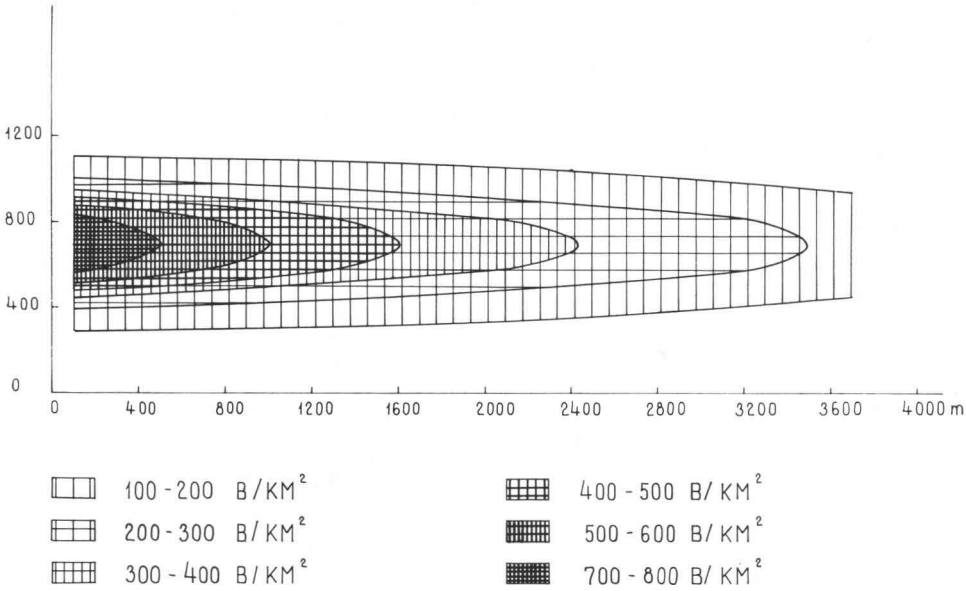


FIG. 2. The Pk-1 boulder train. Computed frequencies. Grid interval 200 m.

The influence of the change of the grid interval upon the frequencies was studied by reanalysing the boulder train using 400 metres as a distance between the grid points. The effect was that of a distinct smoothing, which was to be anticipated, and the observed and the calculated frequency patterns now resemble each other more than in the previous case. (See Figs. 3 and 4). The computed parameters are presented in Table 2.

If these values are compared with those of Table 1 it is realised that the difference between the two sets of parameters is surprisingly small. In the case of the 400 m grid interval the boulder train is slightly wider and the value for  $k$  somewhat greater than in the former case. As a consequence the calculated mean transportation distances also vary only little, being 2.98 km and 2.87 km, respectively.

TABLE 2.

The Pk-1 boulder train. The calculated parameters. The grid interval 400 metres.

$N_0 = 0.3798773$ $K = 0.0003491435$ $SD = 0.31800$ $R = -0.81575$	$S_0 = 213.23794$ $A = 0.0072676$ $SD = 36.52046$ $R = 0.24766$	$Y_0 = 707.514$ $B = 0.0071505$ $SD = 67.00297$ $R = -0.13581$
---	--	---

TABLE 3.

The Pk-1 boulder train. The observed and calculated frequencies. The grid interval 400 metres.

X	Y	Frequency observed	Frequency calculated
200.	200.	0.000169	0.000041
200.	600.	0.000662	0.000583
200.	1 000.	0.000300	0.000258
600.	200.	0.000113	0.000039
600.	600.	0.000557	0.000505
600.	1 000.	0.000232	0.000223
1 000.	200.	0.000000	0.000037
1 000.	600.	0.000250	0.000437
1 000.	1 000.	0.000169	0.000193
1 400.	200.	0.000000	0.000035
1 400.	600.	0.000325	0.000378
1 400.	1 000.	0.000169	0.000166
1 400.	1 400.	0.000012	0.000003
1 800.	200.	0.000000	0.000033
1 800.	600.	0.000425	0.000327
1 800.	1 000.	0.000056	0.000144
1 800.	1 400.	0.000006	0.000003
2 200.	200.	0.000019	0.000031
2 200.	600.	0.000294	0.000283
2 200.	1 000.	0.000175	0.000124
2 200.	1 400.	0.000019	0.000003
2 600.	200.	0.000031	0.000029
2 600.	600.	0.000225	0.000245
2 600.	1 000.	0.000100	0.000107
3 000.	200	0.000000	0.000027
3 000.	600.	0.000212	0.000212
3 000.	1 000.	0.000094	0.000093
3 000.	1 400.	0.000019	0.000002
3 400.	200.	0.000031	0.000025
3 400.	600.	0.000325	0.000183
3 400.	1 000.	0.000156	0.000080
3 800.	200.	0.000050	0.000023
3 800.	600.	0.000087	0.000158
3 800.	1 000.	0.000038	0.000069

In Table 3 the measured and calculated frequencies of the Pk-1 boulder train are compiled. The grid interval was 400 metres.

#### The Pk-2 boulder train

This train of about 500 uranium-bearing quartzite boulders is situated in the same area as the Pk-1 train. On the whole it is not as regular as that of the previous example. The boulder train crosses a small lake and, in addition, the morain is covered by overburden in some places with the consequence that reliable frequencies can only be measured along some selected profiles.

Two hundred metres proved to be the most suitable grid interval and the boulder frequencies were observed along the profiles of  $X = 400$ ,  $X = 1\ 000$ ,  $X = 1\ 600$ ,  $X = 2\ 800$  and  $X = 3\ 200$ . Based on this information the parameters listed in Table 4

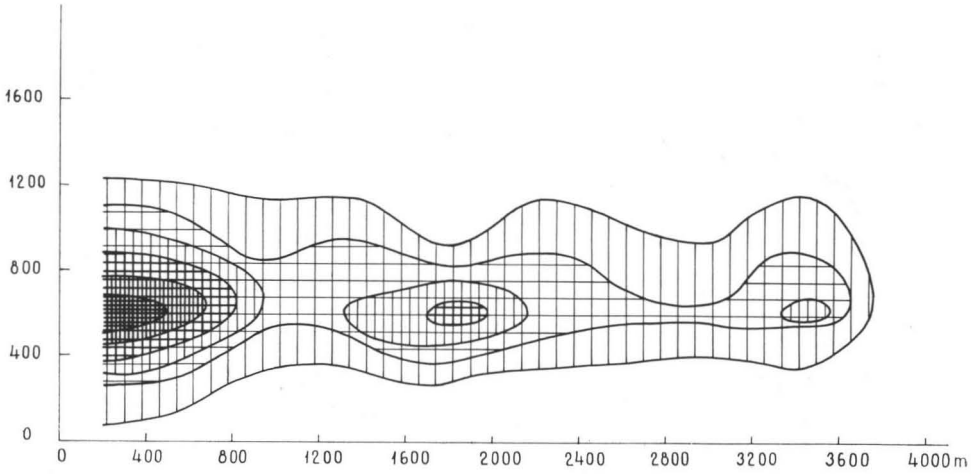


FIG. 3. The Pk-1 boulder train. Observed frequencies. Grid interval 400 m.

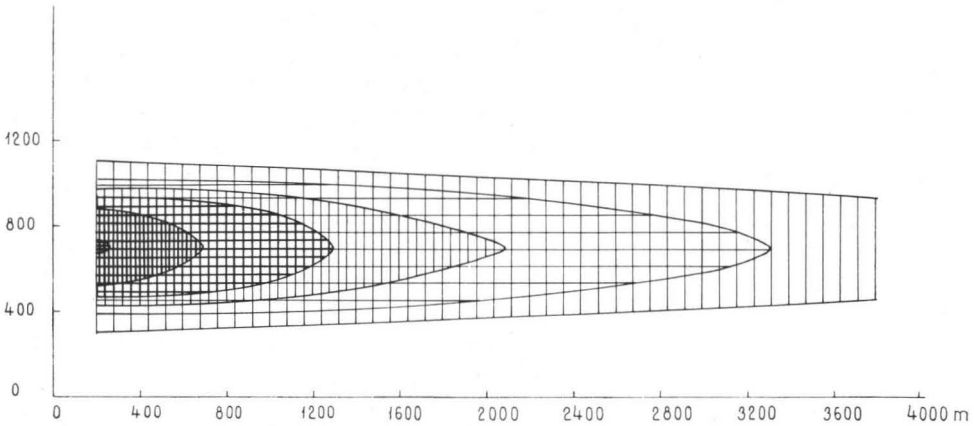


FIG. 4. The Pk-1 boulder train. Computed frequencies. Grid interval 400 m.

TABLE 4.

The Pk-2 boulder train. The computed parameters. The grid interval 200 metres.

$N_0 = 0.2216692$	$S_0 = 72.10224$	$Y_0 = 589.356$
$K = 0.0002276653$	$A = 0.0387678$	$B = 0.0063341$
$SD = 0.07049$	$SD = 15.91933$	$SD = 69.85809$
$R = -0.97527$	$R = 0.95768$	$R = -0.12294$

were solved. The contours of the observed and calculated frequencies are presented in Fig. 5 and Fig. 6.

If these values are compared with those of Table 1 and Table 2 it is noticed that the  $k$  for the Pk-2 is clearly smaller than the  $k$ s for the Pk-1. This means a greater average transportation distance (about 4.4 km), which could be attributed to the more even terrain in this case. Also it is noteworthy that the  $R$ s for  $k$  and  $A$  are very close to  $-1$  and  $1$ , respectively, indicating that the decreasing of the boulder frequency obeys excellently the exponential law and that the boulder train widens very regularly in spite of the slight bending observed at the proximal end of the train. As a matter of fact there is good reason to believe that this bending is only ostensible and caused by the fact that the terrain there is not favourable to boulder finding.

#### A multi-source boulder train

A complicated case arises when several boulder trains overlap forming a multi-source frequency distribution. If the outcrops are situated in a row parallel to the transportation direction the observed boulder frequencies may show only a slight variation with distance, and the localization of the sources becomes difficult.

The different components can, however, be sorted out by applying the above described computer program successively to the selected parts of the boulder train. Should the outcrops not be too close to each other the procedure could be as follows for instance. Beginning from the proximal end of the boulder train the observed frequencies, which are estimated to be caused by the first outcrop only, are fed into the computer. Based on this information the first and second phase of the program evaluates the parameters of the frequency distribution function for the boulders originating from the first outcrop. Phase III reads all the data cards from the beginning of the boulder train to, say, about  $X = 3\ 000$  and computes the theoretical frequencies caused by the first outcrop at every grid point. The differences between the observed and calculated frequencies are now computed and printed out. By plotting the differences on a map and drawing the frequency contours it is easy to see the location of the second outcrop without the disturbing effect of the first boulder source.

If the boulder train involves more than two successive outcrops the above procedure must be repeated several times. The idea is to eliminate the boulder frequencies of the previous sources by calculating the theoretical frequencies and subtracting them from the observed ones. The outcrops appear now as positive differences.

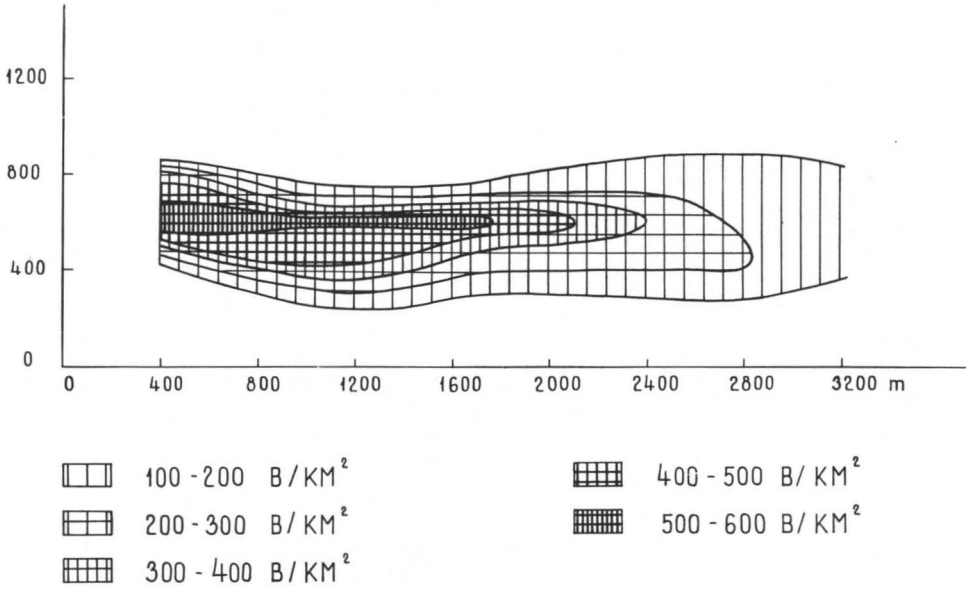


FIG. 5. The Pk-2 boulder train. Observed frequencies. Grid interval 200 m.

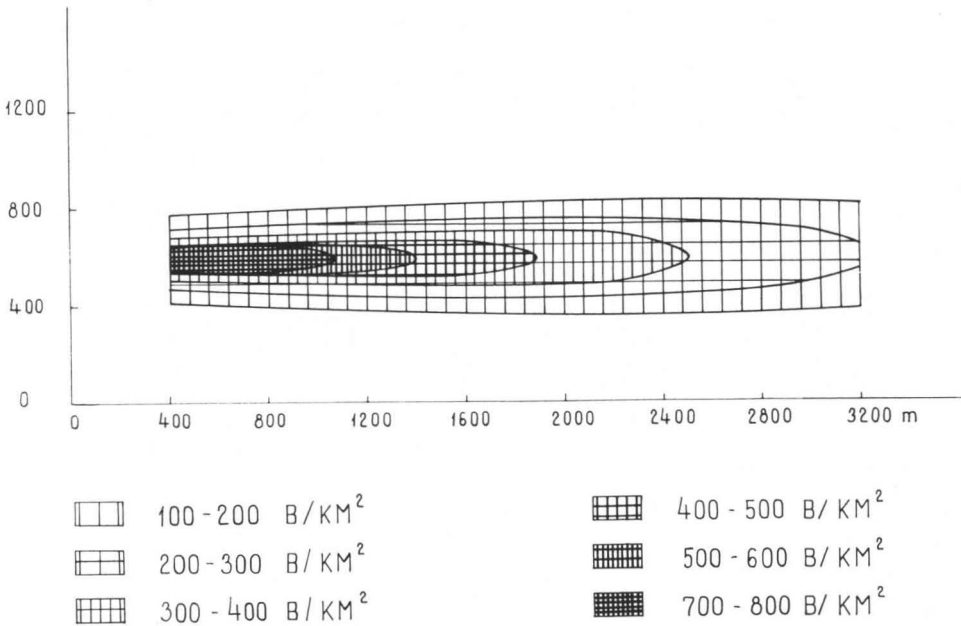


FIG. 6. The Pk-2 boulder train. Computed frequencies. Grid interval 200 m.

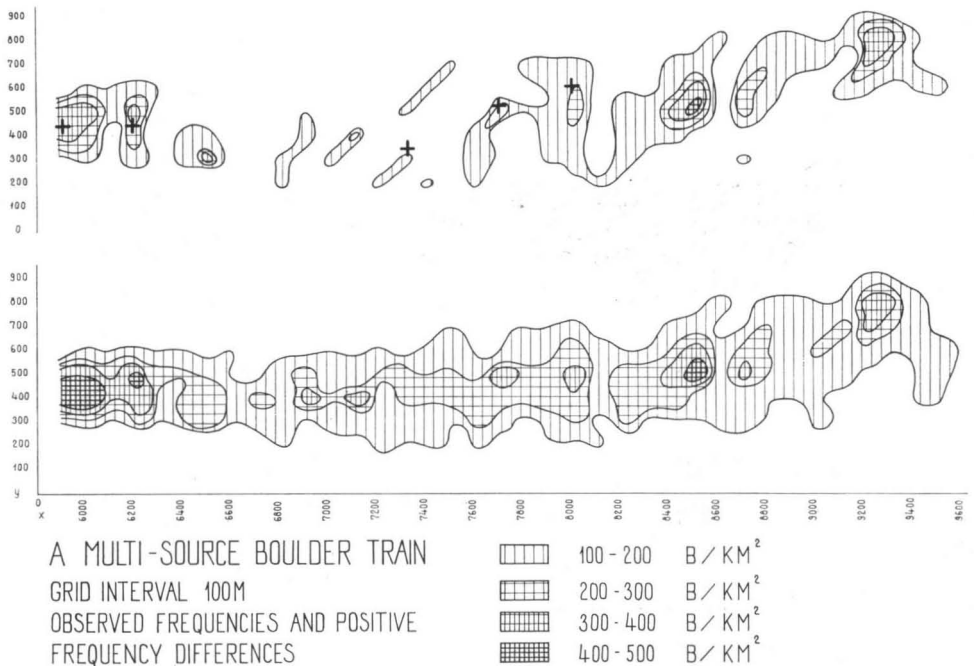


FIG. 7. A part of a multi-source boulder train. At the bottom the observed frequencies and at the top the positive differences between the observed and computed frequencies are presented as contours. The verified mineralisations in the bed rock are marked by crosses.

Fig. 7 serves to illustrate the application of this method. In this figure the frequency contours for a selected part of a long multi-source boulder train are shown. One of the outcrops is situated at the very left end at about  $X = 5\,900$ . To compute the parameters for this outcrop the data cards from  $X = 5\,900$  to  $X = 8\,000$  were fed into the computer. The calculated frequencies were subtracted from the observed ones and printed out. The positive differences presented as contours in the upper part of Fig. 7 can be attributed to two different reasons. The smaller narrow anomalies running diagonally to the boulder train axes are obviously due to the shallow valleys which have caught more boulders than the terrain between them, giving rise to an abnormally high boulder frequency at these places. The higher anomalies e.g. further down the boulder train show features which can best be interpreted as having been caused by new boulder sources.

The outcrop at the left is also shown in Fig. 7 as a positive frequency difference. This is due to the fact that the boulders chosen for the parameter evaluations do not all originate from that source. In fact some of them come from several small outcrops situated between  $X = 6\,300$  and  $X = 8\,000$ . Because of these outcrops the values

for  $k$  and  $N_0$  become too small and the corresponding standard deviations abnormally high, with the consequence that the differences of the boulder frequencies will not be completely eliminated at that outcrop.

## CONCLUSIONS

The comparison of the observed and calculated frequencies in some investigated boulder trains indicates that the model tentatively introduced in this paper can describe satisfactorily the distribution of boulder frequency within boulder trains. It appears that, in most cases, the observed discrepancies are attributable either to the terrain effect or to the too small total number of boulders present, which gives rise to relatively high random local variations in boulder frequencies. Also the breaking of boulders during transportation may be another source of error since no allowance has been made for this effect while deriving the distribution function.

The program is especially suitable for the estimation of the values for  $k$ , which can further be used for the calculation of the average transportation distance. Again, it gives the direction of the transportation very accurately. Finally, the program can be successfully applied to multi-source boulder train analysis. Under favourable conditions it is possible to estimate the locations of the outcrops and also to get some idea about their sizes and forms.

**Appendix:** The Fortran program for evaluating the parameters of the boulder frequency distribution function as applied to an IBM 1440 computer.

The present program, which is based on an overlay system, is designed to operate in three phases due to storage limitations and all data should be recorded on the 80-column IBM cards.

The first phase reads the title card on which the desired information is recorded in columns 21 through 40. This data is immediately printed out.

The program now reads the following card which contains the maximum X-coordinate ( $A$ ) of the deck and the grid interval ( $CY$ ) punched in format (F8.2, F5.0).

Following some initialization, the third card is read on which the X-coordinate of the first profile ( $K$ ) and the number of observations along the same profile ( $NN$ ) are given in format (2 I5).

The program now accepts data cards of the first profile. Each card contains the X- and Y-coordinate and the observed frequency expressed as boulders per  $m^2$  of one location only. The format requires:

```

columns  1 through  8 X-coordinate
          9 through 16 Y-coordinate
         17 through 24 Frequency

```

SEQ	STMNT	MACODER STATEMENT
	C	OUTOKUMPU CO
	C	BOULDER FREQUENCY DISTRIBUTION FUNCTION FOR BOULDER TRAINS
	C	P A R T O N E IBM 1440 12K
1		DIMENSION X%50□, FLN%50, 3□, Y%20□, F%20□
2		READ 90
3	90	FORMAT %20X20H HEAD-LINE, TEMPOR. □
4		PRINT 90
5		LÄ 0
6		READ 98, A, CY
7	98	FORMAT %F8.2, F5.0□
8	99	FORMAT %2I5□
9	3	SUM Ä0.
10		SSUMÄ0.
11		SIGÄ0.
12		LÄL+1
13		READ 99, N, K
14		X%L□ÄK
15		JÄ1
16		DO 1IA1, N
17		READ 100, Y%I□, F%I□
18		SUMÄSUM+CY*F%I□
19	1	SSUMÄSSUM+F%I□*CY*Y%I□
20		FLN%L, J□ÄSSUM/SUM
21		DO 2 IÄ1, N
22	2	SIGÄSIG+CY*F%I□* %FLN%L, J□-Y%I□□**2.
23		JÄ2
24		FLN%L, J□ÄSQRTF%SIG/SUM□
25		JÄ 3
26		FLN%L, J□ÄLOGF%SUM□
27	100	FORMAT %8X F8.2, F8.6 □
28		IF %X%L□-Ä□ 3, 4, 4
29	4	X%50□ Ä L
		END

FIG. 8. Phase I.

The program evaluates for the profile: the centre of the boulder train,  $S$  and  $\ln N$ , which are stored for the next phase.

Each profile is treated in a similar way. The data cards are preceded by a card containing  $K$  and  $NN$  for the profile. That is repeated until  $X = \text{maximum}$  is reached which indicates the end of phase I.

The maximum number of profiles the program accepts is 49 and it is also required that the  $X$ -values should be multiples of 100. The number of observations per profile should not exceed 20.

The second phase calculates the values for  $N_0$ ,  $k$ ,  $S_0$ ,  $A$ ,  $Y_0$  and  $B$  with the least squares method based on the information obtained from phase I. Also the standard deviations and the correlation coefficients connected with the above parameters are evaluated and all results printed out.

Phase III is a very useful adjunct to the previous program. Based on the parameters solved in Phase II it calculates the theoretical frequencies at every data point and prints them out together with the  $X$ - and  $Y$ -coordinates and the observed frequencies. In addition, it performs the Chi-square test, if desired.

```

SEQ  STMT  MACRODER STATEMENT
      C      OUTOKUMPU OY
      C      PART TWO
1     120   FORMAT %//10X44HBOULDER FREQ.DISTR.FUNCT. FOR BOULDER TRAINS///□
2     DIMENSION X%50□,FLN%50,3□, A0%3□,A1%3□
3     JÄ1
4     PRINT 120
5     NNA X%50□
6     KPLÄO
7     15    SXÄO.
8     SYÄO.
9     SXXÄO.
10    SXYÄO.
11    SYYÄO.
12    DO 5IA1,NN
13    SXÄSX+X%I□
14    SYÄSY+FLN%I, J□
15    SXXÄSXX+X%I□*X%I□
16    SYYÄSYY+FLN%I, J□*FLN%I, J□
17    5     SXYÄSXY+X%I□*FLN%I, J□
18    NÄ1-1
19    FNÄN
20    S11ÄSXX-SX**2/FN
21    S01ÄSXY-SX*SY/FN
22    S00ÄSYY-SY**2/FN
23    KPLÄKPL+1
24    A1%J□ÄS01/S11
25    A0%J□ÄSY/FN-A1%J□*SX/FM
26    RÄS01/SQRTF%S00*S11□
27    SDA SQRTF%S00-A1%J□*S01□/□FN-2.□□
28    IF%KPL-2□12,13,14
29    12    PRINT 106
30    106   FORMAT%15X29HCOEFF. FOR BOULDER TRAIN AXIS/□
31    PRINT 107, A0%J□,A1%J□
32    107   FORMAT%15X3HYO ,F9.3/15X7HB ,F9.7□
33    JÄ2
34    PRINT 104,SD,R
35    GO TO 15
36    13    PRINT 105, A0%J□,A1%J□
37    PRINT 104,SD,R
38    105   FORMAT %15X6HCOEFF.,/15X5HSD ,F9.5/15X7HA ,F9.7/□
39    JÄ3
40    GO TO 15
41    14    ANÄEXPFA0%J□□
42    PRINT 103, AN,A1%J□
43    A0%J□ÄAN
44    103   FORMAT%15X6HCOEFF.,/15X7HNO ,F9.7/15X7HK ,F12.10/□
45    PRINT 104,SD,R
46    104   FORMAT %15X5HSD ,F9.5/15X5HR ,F9.5///□
47    PAUSE
      END

```

FIG. 9. Phase II.

To ease the data handling, the program has been written in such a way that phase III reads the same data deck as phase I and searches for the value 99999. to indicate that all data cards have been read.

It is important to note that to make use of the Fortran program presented in Figures 8, 9 and 10 the following instructions should be followed.

All three phases must be translated. From phases II and III the C1-and the C2-cards should be removed. The final halts of phases I and II must be replaced by a branch to calling routine (N000 is replaced by BA26), for which the disc routine area can be used.

```

SEQ  STMT  MACODER STATEMENT
C      BOULDER FREQUENCY DISTRIBUTION FUNCTION FOR BOULDER TRAINS
C      CHI-SQUARE ANALYSIS
C      PART THREE
C      SAME CARDS AS IN 1:ST PART
C      LAST CARD WITH X-VALUE 100000. Y- 1.
1      DIMENSION P%50, FLN%50, 3, A0%3, A1%3
2      A1%3 X -1.*A1%3
3      PRINT 112
4      112  FORMAT %1H1, 23X1HX, 16X1HY, 14X1HF, 16X5HFREQ. 4X6H/DIFF. //
5      SUMA0.
6      READ 120 ,CY
7      120  FORMAT %/8X, F5.0
8      BCYXCY*CY
9      18   READ 113 ,X,Y,F
10     113  FORMAT %F8.0, F8.2, F8.6
11     IF %Y 18, 18, 19
12     19   IF %X-99999. 16, 17, 17
13     16   YN X Y-A0%1-A1%1*X
14     ACO X A0%2+A1%2*X
15     FREQ X A0%3*EXPF %A1%3*X / %ACO*2.5067 * EXPF%YN*Y/%-2.*
16     1   ACO*ACO
17     PRINT 114 ,X,Y ,F, FREQ
18     114  FORMAT %15X, F12.0, 5X, F12.0, 5X, F12.6, 5X, F12.9//
19     ADIF X F-FREQ
20     PRINT 116, ADIF
21     116  FORMAT %76XF9.6//
22     13   DIFF X FREQ - F
23     SUM X SUM+DIFF **2./FREQ
24     GO TO 18
25     SUM X SUM*BCY
26     PRINT 115, SUM, CY
27     115  FORMAT ///15X11HCHI-SQUARE , F12.8, 18X4HCY , F5.0
        PAUSE
        END

```

FIG. 10. Phase III.

The punched calling routine clears storage for reading and branches to loading. On the A26 the following information is punched: /080', 001'LA53081' M % G1001R' B001'G, where ' and G stand for a wordmark and a group mark, respectively.

The Fortran routine load cards can be removed from phases II and III if the object deck is wanted to be smaller.

Statement 2 should be removed from the source deck of phase III if the A1 (3) has a negative internal notation after phase II.

*Acknowledgements* — The present authors wish to express their gratitude to the Outokumpu Co. for permission to publish this paper.

Cordial thanks are also due to professor O. Lokki who has critically read the manuscript giving valuable suggestions.

*Manuscript received, March 16, 1966*

## REFERENCES

- HEWLETT, RICHARD F. (1963) A basic computer program for computing grade and tonnage of ore using statistical and polygonal methods. Bureau of Mines, Report of investigations 6292.
- HYYPÄ, ESA (1945) Tracing the source of the pyrite stones from Vihanti on the basis of glacial geology. Bull. Comm. Geol. Finlande No 142, pp. 97—122.
- MILLER, R. L. (1956) Trend surfaces: their application to analysis and description of environments of sedimentation. The relation of sediment-size parameters to current-wave system and physiography. Jour. Geology, V 64. pp. 425—446.
- OKKO, VEIKKO and PELTOLA, ESKO (1958) On Outokumpu boulder train. Bull. Comm. Geol. Finlande No 180. pp. 113—134.
- SAURAMO, MATTI (1924) Tracing of glacial boulders and its application in prospecting. Bull. Comm. Geol. Finlande No 67. pp. 1—37.
- WHITTEN, E. H. T. (1962 a) Areal variability of alkalis in the Malsburg granite, Germany. N. Jb. Miner. Mh. pp. 193—200.
- »— (1962 b) A new method for determination of the average composition of a granite massif. Geochim. et Cosmochim. Acta, Vol. 26, pp. 545—560.
- »— (1963) A surface-fitting program suitable for testing geological models which involve areally-distributed data. Technical report No 2 of ONR Task No 389—135. Northwestern University, Evanston, Illinois.



## RADIOCARBON AGES OF THE RÅBACKA BOG, SOUTHERN FINLAND

BY

K. VIRKKALA

*Geological Survey of Finland, Otaniemi*

Geologically interpreted radiocarbon datings of samples from the southern half of the Finnish mainland are rather few in number. Donner has two datings (Barendsen, Deevey, Gralenski 1957; Donner 1951; *cf.* also Okko 1960), Okko (1960, 1965) has published three datings, Hyyppä (1963) one dating, Salmi (1963 a and b) six, Tolonen (1963) two, Alhonen (1964) one and Aario (1965 a, b and c) eleven dating. Two of Aario's samples represent, however, disturbed, layers. In addition, there are two radiocarbon determinations of which no forest-historically zoned pollen diagrams are available as yet (Hyyppä, Isola, Hoffrén 1963; Hyyppä, Toivonen, Isola 1964).

Eight of the 28 radiocarbon determinations deal with the rational *Picea* limit and eleven with pollen zones V and IV. They are Donner's (*op. cit.*) datings from the Lahti area, Salmi's (1963) two datings from Kihniö and one dating from Saarijärvi, Hyyppä's (1963) dating from Porvoo, Aario's (1965 a and b) four datings from the Päijänne lake basin and Tolonen's (1963) dating from East Finland.<sup>1)</sup>

Because the majority of the radiocarbon dated Finnish samples derive from North Finland, it is important that also the southern part of the country should be covered by dependable radiocarbon datings. In this way it will be possible to control the synchronicity of the forest-historical zoning applied to Finnish pollen diagrams with the zoning of Central-European sequences. The present study aims at filling part of the radiocarbon-chronological gap in South Finland.

The Råbacka bog, situated about 40 km north of Helsinki, was selected for the control site because the characteristic features of southern Finnish pollen diagram are very well developed here (Mölder, Valovirta, Virkkala 1957; Virkkala 1959).

<sup>1)</sup> During type-setting of this paper 15 radiocarbon datings of Boreal or older deposits have been published. Hyvärinen (1966) has 12 datings some of which are rather unreliable and Tynni (1966) has three datings.

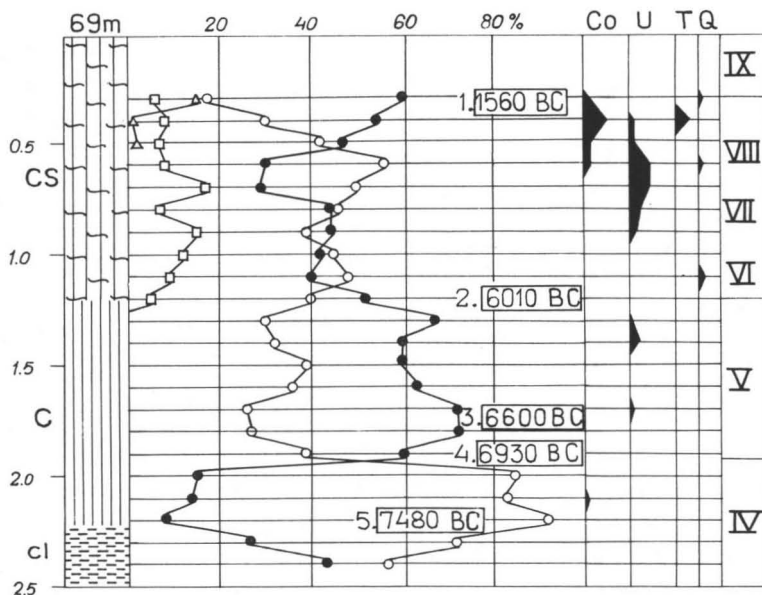


FIG. 1. Stratigraphy, pollen diagram and results of radiocarbon determinations of the Råbacka bog. CS = *Carex-Sphagnum* peat, C = *Carex* peat, cl = clay.

The peat profile and the pollen diagram of the Råbacka bog, shown in Fig. 1, were drawn according to a re-investigation carried out solely for the selection of samples to be studied by the radiocarbon method. The position of the samples and the results of the radiocarbon measurements are shown in the figure.

Sample 1 represents the beginning of the strong expansion of the spruce in this region. Its age, 1 560 B.C., is younger than the previously published datings from the Finnish mainland (Aario 1965 b). The sample is from a layer quite close to the surface of the bog; therefore, roots of recent and subrecent plants may have caused the apparent young age. It seems to be a general feature in the radiocarbon ages determined from peat samples that, owing to plant roots penetrating the peat substratum, the ages tend to be somewhat too young (Butzer 1964). It is also possible that water flowing downwards when the sample is being taken up has an effect in the same direction.

Sample 2 represents zone transition V/VI or the beginning of the *Alnus* curve. The age, 6 010 B.C., is of the same order as the age 6 100 B.C. published by Salmi (1963 a) from Kihniö, situated about 200 km NNW of Råbacka. The corresponding horizon in Aario's (1965 a) material from Central Finland is younger, about 5 250 B.C.

Sample 3 was taken from the layer that exhibits the Boreal maximum in the *Pinus* curve. The radiocarbon age obtained, 6 600 B.C., is practically identical with the age of the corresponding horizon, 6 540 B.C., in Salmi's (1963 b) material from Central

Finland. The age of the *Pinus* maximum in the Lapaneva bog at Kihniö (Salmi 1963 a) seems to correspond to the upper *Pinus* maximum in the Råbacka profile. The growth of peat in the Boreal period at Lapaneva may have been slow enough to cause a fusion of the two *Pinus* maxima, thus rendering an apparent age too young for the true Boreal *Pinus* maximum.

Sample 4 represents zone transition IV/V, age 6 930 B.C. Previously only Aario (1965 c) has published a dating of this zone boundary, namely 7 100 B.C. in the Päijänne basin.

The lowermost sample, sample 5, 7 480 B.C., represents the maximum of the *Betula* curve in zone IV. The radiocarbon age of the corresponding horizon is 7 640 B.C. in the Porvoo area (Hyyppä 1963), 7 190 B.C. in East Finland (Tolonen 1963). In the Päijänne basin the age of the end phase of the *Betula* maximum is 7 200 B.C. (Aario 1965 c). At Kihniö in West Finland the age of the *Betula* maximum is 7 900 B.C. (Salmi 1963 a) but it seems to represent the early Pre-Boreal rise of the curve. The radiocarbon age obtained from Kihniö — if it really can be depended on — indicates that this area was deglaciated by zone transition III/IV at the latest, a development suggested for the region north of Tampere by the present writer (Virkkala 1962). Further radiocarbon data for the later half of the Pre-Boreal period are the age 7 900 B.C. at Pölläkkälä on the Karelian Isthmus and 6 450 B.C. at Mantsinsaari island on Lake Ladoga (Hyyppä, Hoffrén, Isola 1962; Hyyppä 1943, 1963). Viewed against the other radiocarbon ages of the Pre-Boreal time, the Mantsinsaari age seems too young.

In conclusion it may be stated that the radiocarbon ages obtained from the peat sequence at Råbacka comply with the previous datings and with the forest-historical and paleoclimatological chronology attained by other methods (*e.g.*, Sauramo 1958, p. 44). For the time being, the radiocarbon determinations of samples from southern Finland are too few to yield a definite dating of the zone boundaries and other distinct horizons in the pollen diagrams.

*Acknowledgments.* — Mr. Pentti Alhonen, Mag. Phil., did the pollenanalytical work. The National Research Council for Sciences granted financial support. The author wishes to express his gratitude for the assistance received. Isotopes Inc, U.S.A., is responsible for the radiocarbon measurements.

*Manuscript received, 17 March, 1966*

#### REFERENCES

- AARIO, RISTO (1965 a) Development of ancient Lake Päijänne and the history of the surrounding forests. *Ann. Acad. Sci. Fenn. A.* 81.  
 —»— (1965 b) Die Fichtenverhäufung im Lichte von C<sup>14</sup>-Bestimmungen und die Altersverhältnisse der finnischen Pollenzone. *Bull. Comm. géol. Finlande* 218.  
 —»— (1965 c) Die quartäre Schichtenfolge am Flösskanal von Kimola, Südfinnland. *Ann. Acad. Sci. Fenn. A.* 86.

- ALHONEN, P. (1964) Radiocarbon age of waternut (*Trapa natans* L.) in the sediments of Lake Karhejärvi, SW-Finland. Mem. Soc. Fauna Flora Fenn. 40.
- BARENDSSEN, G. W., DEEVEY, E. S. and GRALENSKI, L. J. (1957) Yale natural radiocarbon measurements III. Science 126.
- BUTZER, K. (1964) Environment and archeology. London.
- HYVÄRINEN, H. (1966) Studies on the late-Quaternary history of Pielis-Karelia, eastern Finland. Soc. Sci. Fenn. Comm. Biol. Vol. 19. Nr. 4.
- HYYPÄ, E. (1943) Beiträge zur Kenntnis der Ladoga- und Ancylustransgressionen. Bull. Comm. géol. Finlande 128.
- »— (1963) On the Late-Quaternary history of the Baltic Sea. Fennia 89, No:1.
- HYYPÄ, E., HOFFRÉN, V. and ISOLA, A. (1962) Geological Survey of Finland. Radiocarbon measurements I. Radiocarbon 4.
- HYYPÄ, E., ISOLA, A. and HOFFRÉN, V. (1963) Geological Survey of Finland. Radiocarbon measurements II. Radiocarbon 5.
- HYYPÄ, E., TOIVONEN, A. V. P. and ISOLA, A. (1964) Geological Survey of Finland. Radiocarbon measurements III. Radiocarbon 6.
- MÖLDER, K., VALOVIRTA, V. and VIRKKALA, K. (1957) Über Spätglazialzeit und frühe Postglazialzeit in Südfinnland. Bull. Comm. géol. Finlande 178.
- OKKO, V. (1960) The age of the subfossil roots of *Alnus glutinosa*, Tuusula, Southern Finland. Bull. Comm. géol. Finlande 188.
- »— (1965) Kallaveden suurtulvasta. Savotar V.
- SALMI, M. (1963 a) Radiocarbon determinations from the bog profile of Lapaneva, Kihniö, Western Finland. Bull. Comm. géol. Finlande 204.
- »— (1963 b) On the subfossil Pediastrum algae and molluscs in the Late-Quaternary sediments of Finnish Lapland. Arch. Soc. Zool. Bot. Fennicae »Vanamo» 18:2.
- SAURAMO, M. (1958) Die Geschichte der Ostsee. Ann. Acad. Sci. Fenn. A, 51.
- TOLONEN, K. (1963) Über die Entwicklung eines nordkarelischen Moores im Lichte der C<sup>14</sup>-Datierung. Das Moor Puohtiinsuo in Ilomantsi (Ost-Finnland). Arch. Soc. Zool. Bot. Fenn. »Vanamo», 18:1.
- TYNNI, R. (1966) Über spät- und postglaziale Uferverschiebung in der Gegend von Askola, Südfinnland. Bull. Comm. géol. Finlande 223.
- VIRKKALA, K. (1959) Maaperäkartan selitys. Lehti 2 043. Kerava. 1 : 100 000. Suomen geologinen kartta. Geologinen tutkimuslaitos.
- »— (1962) Maaperäkartan selitys. Lehti 2 123. Tampere. 1 : 100 000. Suomen geologinen kartta. Geologinen tutkimuslaitos. Explanation to the map of superficial deposits. Sheet 2 123. Tampere. 1 : 100 000. Geological map of Finland. The Geological Survey of Finland.

# ON THE RARE EARTH MINERALS FROM THE PYÖRÖNMAA PEGMATITE IN KANGASALA, SW-FINLAND

BY

ATSO VORMA, PENTTI OJANPERÄ, VÄINÖ HOFFRÉN,  
JAAKKO SIIVOLA and ARVO LÖFGREN

*Geological Survey of Finland, Otaniemi*

## ABSTRACT

This paper gives a mineralogical description of the RE-pegmatite of Pyörönmaa, Kangasala in SW Finland. The yttrium minerals: yttrian spessartine, xenotime, gadolinite, calcio-gadolinite, britholite-(Y), thalenite, fergusonite and tenerite are described. All of these minerals are new to Finland. The occurrence of synchysite-(Nd) is established.

RE-element distribution in the various minerals is discussed. Comparison of the Pyörönmaa pegmatite is made in respect to other well known pegmatite provinces in Finland and to some abroad.

## CONTENTS

	Page
Introduction .....	242
The mode of occurrence .....	242
Allanite .....	246
Yttrian spessartine .....	249
Zircon and xenotime .....	252
Gadolinite and calcio-gadolinite .....	253
Britholite-(Y) .....	257
Thalenite .....	260
Fergusonite .....	264
Tenerite .....	268
Discussion .....	270
Acknowledgments .....	273
References .....	273

## INTRODUCTION

In connection with the pegmatite studies performed by the Ore Department of the Geological Survey of Finland a small pegmatite body was encountered near the village of Pyörönmaa in Kangasala and preliminary investigations were made by the late Mr. Arvo Vesasalo, Lic. Phil. The pegmatite body is located 6 km to the north of the town of Valkeakoski and 400 m to the west of the southern shore of the lake Vähä Leppäjärvi. The geological environment of the pegmatite is described in the geological maps of Finland nos. 2 123 (Tampere) and 2 124 (Kangasala) by Mr. Arvo Matisto, Lic. Phil. The pegmatite itself is situated in the southern part of a granite body measuring up to 8 km in diameter and being partly even-grained partly porphyritic.

Arvo Vesasalo collected with Prof. K. J. Neuvonen a great number of specimens from the radioactive minerals present in the pegmatite for further laboratory study. After the early death of Arvo Vesasalo the material was kindly given to the present authors by K. J. Neuvonen who had initiated the laboratory studies of the specimens concerned. One of the present authors (A. Vormaa) has also later investigated the pegmatite quarry itself and collected part of the material investigated. Some of the specimens are derived from the walls of the quarry, some have been collected from the dump. In addition, some specimens for this study were given by Arvo Matisto. The mineralogical and X-ray diffraction work of this paper was performed by Atso Vormaa, who also compiled the manuscript. Wet chemical analyses and flame photometric analyses were done by Pentti Ojanperä, microprobe <sup>1)</sup> analyses by Jaakko Siivola, X-ray fluorescence analyses by Väinö Hoffrén and the spectrochemical ones by Arvo Löfgren.

## THE MODE OF OCCURRENCE

According to the field studies of Arvo Vesasalo in 1956 the mineralogical composition of the pegmatite is mainly potash feldspar, plagioclase and quartz; biotite, garnet and allanite occur as minor constituents. The pegmatite has been quarried, the quarry being somewhat 20 m long and 10 m broad. At present the quarry is water-filled (Fig. 1).

Fig. 2 shows the zoned structure of Pyörönmaa pegmatite. The pegmatite can be divided into three zones, the wall zone composed of graphic granite, the intermediate zone of feldspar (microcline and albite,  $An_5$ ) and the cores of quartz. The greater part of the radioactive mineral specimens investigated during this study were collected from the dump in connection with albite. Fig. 2 indicates the radioactive minerals to be located in the intermediate feldspar rich zone. In this zone the individual albite crystals measure up to tens of centimeters in places.

<sup>1)</sup> All the microprobe work concerning this paper has been performed using the two channel electron probe microanalyser model »Geoscan» manufactured by Cambridge Inst. Co. Ltd. England.

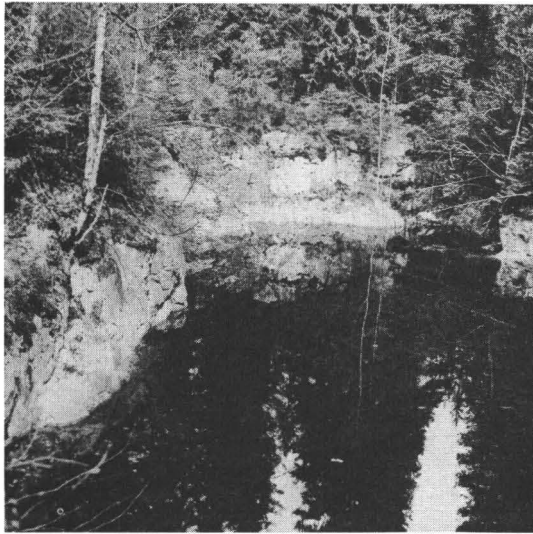


Fig. 1. The pegmatite quarry of Pyörönmaa, Kangasala.  
Photo: A. Vorma

The size of the radioactive anomalies varies from one to two square decimeters, occasionally more. These anomalies consist almost exclusively of black allanite (Fig. 3) which in places is brown in colour due to alteration. Occasionally fergusonite, however, forms the major part of the radioactive minerals present. In addition to allanite and fergusonite, some other RE-minerals occur as minor constituents.

The following minerals have been encountered in the intermediate zone of Pyörönmaa pegmatite.

#### Silicates

- Albite ( $An_8$ )
- Microcline microperthite
- Biotite
- Chlorite
- Allanite
- Yttrian spessartine
- Zircon (+anderbergite)
- Muscovite (sericite)
- Gadolinite
- Calcio-gadolinite
- Britholite-(Y)
- Thalenite

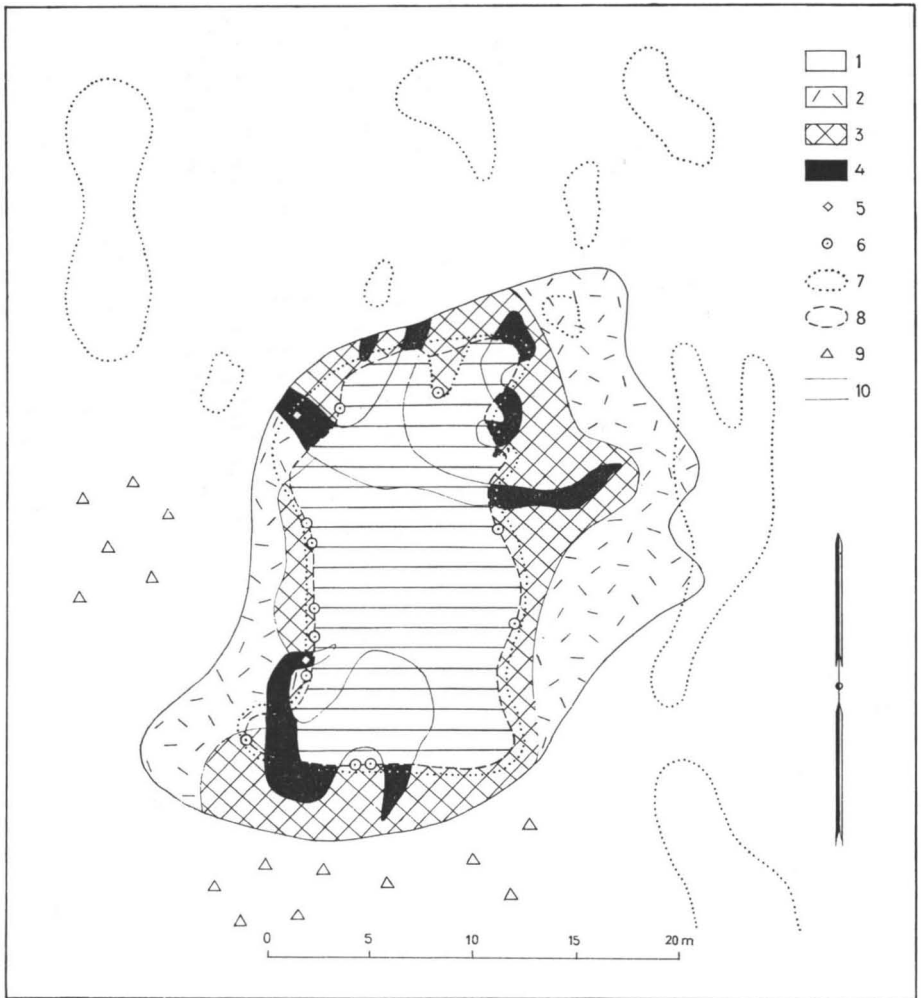


FIG. 2. The map showing the zonal structure of the Pyörönmaa pegmatite. According to Arvo Vesasalo. 1, granite. 2, graphic potash feldspar. 3, feldspar. 4, quartz. 5, gneiss inclusion. 6, radioactive anomaly. 7, outcrop. 8, quarried. 9, dump. 10, water.

Thorite (as inclusion in thalenite)

Y-Al-silicate, unidentified (intergrown with albite)

Y-Fe-silicate, unidentified (as inclusion in britholite-(Y))

Y-Fe-silicate, unidentified (replacement product of britholite-(Y))

Y-Ca-silicate, unidentified (replacement product of britholite-(Y))

Y-silicate, unidentified (replacement product of thalenite)

Al-Y-silicate, unidentified (as inclusion in thalenite)

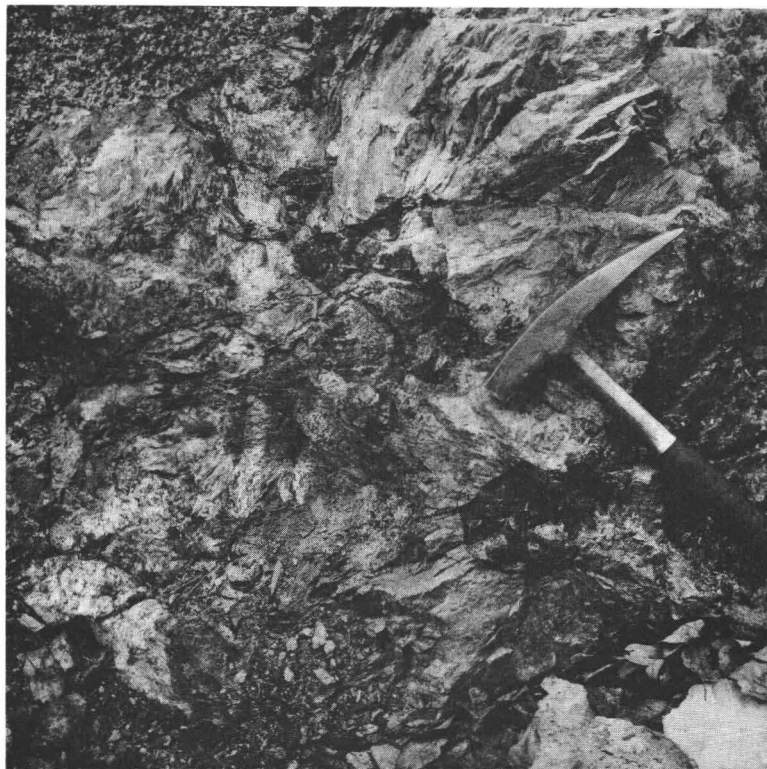


FIG. 3. Coarse allanite (black) embedded in albite. Photo: A. Vormaa

### Carbonates

Synchysite-(Nd) (replacement product of calcio-gadolinite)

Bastnaesite-(Ce) (replacement product of allanite)

Tengerite (a supergene carbonate)

Calcite

### Oxides

Quartz

Fergusonite (3 varieties)

— strongly hydrated, metamict

— slightly hydrated, metamict

— crystalline, monoclinic

Uraninite

### Phosphates

Xenotime

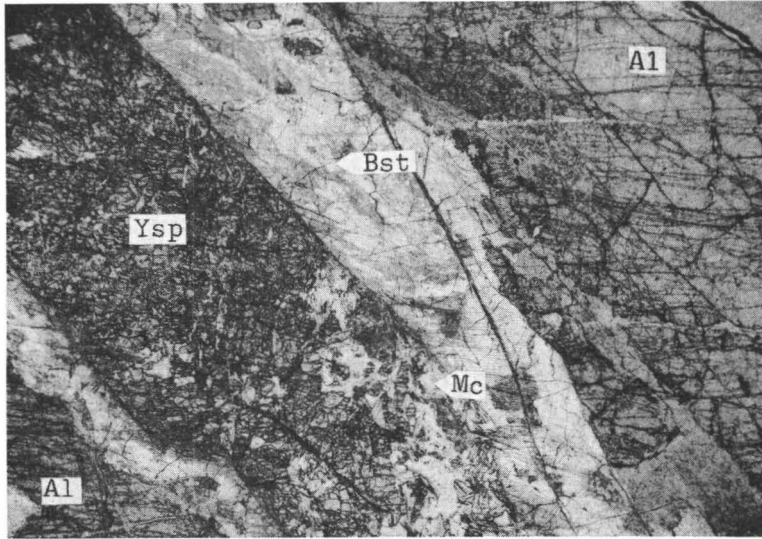


FIG. 4. Yttrian spessartine (Ysp) and muscovite (Mc) as fissure filling in allanite (Al). The light marginal zones between garnet and allanite are rich in bastnaesite (Bst). Magn. 8 x. Photo: Erkki Halme.

The study of the Pyörönmaa pegmatite is still in progress and the list above can be regarded only as provisional, since quite a few specimens are still waiting for further study. However, it was felt of current interest to give a short description of the minerals so far dealt with.

#### ALLANITE

Allanite occurs in the intermediate zone in connection with albite. The crystals are mostly prismatic, in places, however, of indefinite habit; massive or rounded grains of very different size. The crystal size measures upwards from a few centimeters to tens of centimeters. The colour is black. Often, however, the margins are brown, the core still being black. In places the colour of the mineral is completely altered into brown of different shades.

Fergusonite, thalenite, xenotime, zircon, britholite-(Y) and uraninite have been found in association with allanite. Yttrian spessartine, found as fracture fillings in allanite, (Fig. 4) shows an age difference between these minerals. Albite, also, has frequently been found as fracture fillings in allanite.

Lokka investigated the alteration of allanites from the adjacent Varala pegmatite (Lokka 1950, pp. 18—20) and from Impilahti on the northern shore of Lake Ladoga (*op.cit.*, pp. 24—25). The most conspicuous features during the alteration of allanites he recorded were:

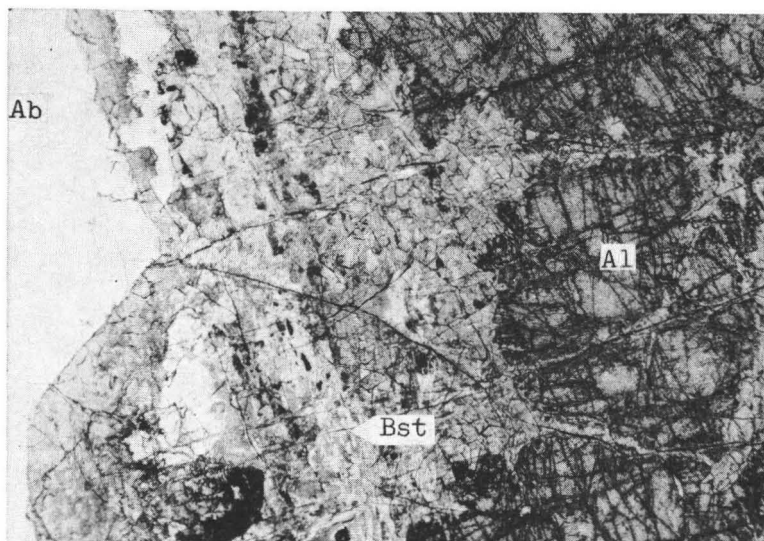


FIG. 5. Fresh, although metamict allanite (Al) replaced by bastnaesite (Bst) rich material. The large light grain is albite (Ab). Magn. 28 x. Photo: Erkki Halme.

1. The colour changes from black to reddish brown, bluish grey or light brown.
2. The water content increases considerably.
3.  $\text{CO}_2$ , that does not belong to the fresh allanite is found up to 6–7 wt.-% in the strongly altered crystals.
4. The alkali content of fresh allanite is insignificant but in the altered grains alkalis are found in considerable amount.
5. Oxidization of ferrous iron into ferric iron. As both  $\text{FeO}$  and  $\text{Fe}_2\text{O}_3$  dissolve somewhat in water containing  $\text{CO}_2$ , part of the iron has probably been leached away as easily soluble bicarbonate. In connection with a more abundant alkali-immigration it is likely that most of the iron has been leached away.
6. Rare earths,  $\text{ThO}_2$  and  $\text{Al}_2\text{O}_3$  are found in the alteration products in the same amounts as in the unaltered grains.

Now returning back to the alteration of Pyörönmaa allanites, all the crystals investigated so far either by optical or X-ray diffraction methods show the allanite to be in metamict state. The black allanite with the specific gravity varying from 3.27 to 3.56 gave an X-ray powder pattern of  $(\text{Ce}, \text{Th})\text{O}_2$  with some additional unidentified lines after having been heated in air to  $1\,000^\circ\text{C}$  for one hour. Some specimens develop the  $\text{CeO}_2$  phase already after having been heated at  $700^\circ\text{C}$  for three hours. The diffraction lines, however, are then weak and broad. The reddish brown alteration product of allanite develops the same cubic  $\text{CeO}_2$  phase. Often, however, a cubic phase with spinel structure was observed in addition to the  $\text{CeO}_2$  phase. The cell size,  $a_0 = 8.10 \text{ \AA}$ , refers to hercynite.

TABLE 1

X-ray powder data for the bastnaesite from Pyörönmaa and for bastnaesite ASTM 11—340

1			2	
<i>d</i> ( <i>A</i> )	<i>I</i>	<i>hkl</i>	<i>d</i> ( <i>A</i> )	<i>I</i>
4.9	w b	002	4.88	40
3.55	s b	110	3.564	70
2.86	s b	112	2.879	100
		202	2.610	1
		004	2.445	9
		104	2.273	3
		203	2.238	3
2.04	s b	300	2.057	40
2.00	s b	114	2.016	40
1.88	s b	302	1.898	40
1.78	m b	220	1.783	9
1.67	m b	222	1.674	21
		006	1.629	1
1.57	w b	304	1.573	15
		116	1.481	9
		224	1.439	11
		410	1.347	7
1.29	w b	412	1.298	15

+ additional lines

w = weak, m = medium, s = strong, b = broad

1. Pyörönmaa pegmatite, Kangasala, Finland.  $\text{CuK}\alpha$ -radiation, Debye-Scherrer camera. The preparation consists of a metamict alteration product of allanite where bastnaesite is disseminated.
2. ASTM 11—340.

Under the microscope the reddish brown alteration product is seen to fill the fractures of fresh but metamict allanite (Figs. 4 and 5). In places the fresh allanite is almost completely replaced by this reddish brown unhomogeneous alteration product. Often a very fine-grained anisotropic mineral can be seen between crossed nicols disseminated in the otherwise isotropic alteration product of allanite. Whenever this anisotropic mineral is seen the colour in the host mineral — alteration product of allanite — has turned to light brown or yellowish.

X-ray powder data of this anisotropic mineral show it to be bastnaesite,  $\text{Ce}(\text{F}/\text{CO}_3)$  (Table 1). Microprobe analysis shows Ce to prevail over Nd which in turn prevails over La.

The occurrence of bastnaesite among the alteration products of allanite is in accordance with the high  $\text{CO}_2$  contents recorded by Lokka (1950) in the altered allanites from the adjacent Varala pegmatite.

No chemical analyses have been performed on the Pyörönmaa allanite other than qualitative spectrographic analyses by A. Löfgren. These indicate high Ce and Al contents, low Y content and an absence of Be. These determinations were run at the initial stage of investigation of the minerals from Pyörönmaa pegmatite to distinguish allanite from gadolinite.

## YTTRIAN SPESSARTINE

Yttrian spessartine is a fairly common mineral in the Pyörönmaa pegmatite. The mineral occurs mostly as crystals measuring up to 1—3 cm embedded in coarse albite. The crystal form {211} is poorly developed. Striation is a common feature on the crystal faces. The colour of the mineral is brownish red with a slight violet shade.

In places yttrian spessartine has been found in connection with allanite as fissure fillings. Fig. 4 shows yttrian spessartine and a dioctahedral mica veinlet cutting allanite, indicating at least a local age difference between garnet and allanite. This refers to the earlier crystallization of the lighter lanthanons (Ce-earths) than that of Y and heavy lanthanons.

The density of yttrian spessartine was determined with a pycnometer. The result gave 4.225 g/cc. Refractive indices were determined with the single variation method using a Hartman dispersion net. For the most important lines the indices are as follows: *F* 1.825, *E* 1.820, *D* 1.813 (Na), and *C* 1.809. The refractive index,  $n_{\text{Na}} = 1.813$ , is in excellent accordance with the composition of garnet. A. Sriramadas, 1957, gives the refractive index for a garnet with 43 % almandine and 57 % spessartine as 1.813. Four mol. per cent yttrigarnet will increase the refractive index of spessartine about 0.0009 (Yoder and Keith, 1951, p. 526). The unit cell size was determined with a Debye-Scherrer camera with Straumanis technique using  $\text{FeK}\alpha_1$  and  $\text{FeK}\alpha_2$  radiation. This gave for  $a_0$  11.610 Å.

The chemical analysis (Table 2) of the yttrian spessartine was made from the material occurring as large crystals embedded in albite and separated with clerici solution. The wet chemical part of the analysis is by Pentti Ojanperä, spectrographic work by Arvo Löfgren and the X-ray fluorescence analysis by Väinö Hoffrén.

The wet chemical analysis was performed using the conventional methods of silicate analysis. Due to the high manganese content, Mn, however, was precipitated with  $(\text{NH}_4)_2\text{S}$  before the investigation of the alkaline earth group. The rare earths were determined separately. Due to the method used,  $\text{Sc}_2\text{O}_3$  did not belong to this group. The precipitate of rare earths was first investigated semiquantitatively by X-ray fluorescence methods. Yttrium, however, due to its high concentration, was also quantitatively determined by X-ray fluorescence methods from the original material. Also  $\text{Sc}_2\text{O}_3$  was quantitatively determined from the original material by optical spectrographic methods. The group precipitate of rare earths was quantitatively separated into components by optical spectrograph.

The unit cell content was calculated using the equation

$$G = \frac{M \times 1.660}{V}$$

where  $G$  is the observed density (= 4.225 g/cc),  $M$  the molecular weight of the unit cell content, and  $V$  the volume of the unit cell (= 1 565 Å<sup>3</sup>). From this equation

TABLE 2

The chemical composition and the unit cell content of yttrian spessartine from Pyörönmaa pegmatite, Kangasala, Finland

	Wt.-% oxides	Mass of each oxide in the cell	Mol. no. of oxides in the cell	Number of elements in the cell	
SiO <sub>2</sub> .....	35.62	1 418.7	23.61	Si .....	23.61
Al <sub>2</sub> O <sub>3</sub> .....	18.81	749.2	7.35	Al .....	14.70
TiO <sub>2</sub> .....	.03	1.2	.015	Ti .....	.015
Fe <sub>2</sub> O <sub>3</sub> .....	2.63	104.8	.66	Fe <sup>3+</sup> .....	1.32
FeO .....	16.01	637.7	8.88	Fe <sup>2+</sup> .....	8.88
MnO .....	21.28	847.6	11.95	Mn .....	11.95
MgO .....	.04	1.6	.040	Mg .....	.040
CaO .....	1.52	60.5	1.08	Ca .....	1.08
Li <sub>2</sub> O .....	.18	7.2	.24	Li .....	.48
Na <sub>2</sub> O .....	.13	5.2	.084	Na .....	.17
K <sub>2</sub> O .....	.05	2.0	.021	K .....	.042
Y <sub>2</sub> O <sub>3</sub> .....	2.10	83.6	.37	Y .....	.74
Yb <sub>2</sub> O <sub>3</sub> .....	.63	25.1	.064	Yb .....	.13
Er <sub>2</sub> O <sub>3</sub> .....	.27	10.8	.028	Er .....	.056
Dy <sub>2</sub> O <sub>3</sub> .....	.12	4.8	.013	Dy .....	.026
Lu <sub>2</sub> O <sub>3</sub> .....	.11	4.4	.011	Lu .....	.022
Ho <sub>2</sub> O <sub>3</sub> .....	.05	2.0	.005	Ho .....	.010
Tm <sub>2</sub> O <sub>3</sub> .....	.05	2.0	.005	Tm .....	.010
Gd <sub>2</sub> O <sub>3</sub> .....	.02	.8	.002	Gd .....	.004
Sc <sub>2</sub> O <sub>3</sub> .....	.03	1.2	.009	Sc .....	.018
H <sub>2</sub> O+ .....	.11	4.4	.24	OH .....	.48
	99.79			O .....	95.10
					95.58
				-O = 1/2 (OH) .....	.24
				O, OH .....	95.34

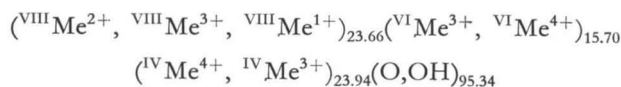
$$\text{VIII Me}^1 + \text{VIII Me}^{3+} \text{ replaces } 2\text{VIII Me}^{2+}$$

$$\text{VIII Me}^3 + \text{IV Al}^{3+} \text{ replaces } \text{VIII Me}^{2+} + \text{IV Si}^{4+}$$

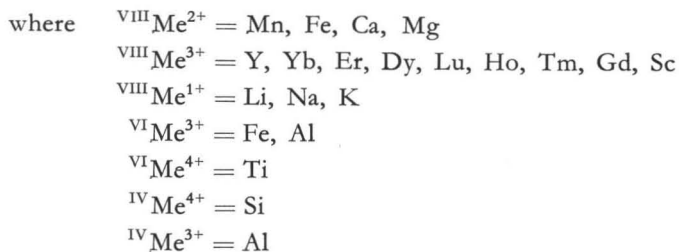
$$\therefore 0.69 (\text{VIII Me}^1 + \text{VIII Me}^{3+}) \text{ replaces } 1.38\text{VIII Me}^{2+} \text{ and}$$

$$(1.02 - 0.69) (\text{VIII Me}^3 + \text{IV Al}^{3+}) \text{ replaces } 0.33 \text{VIII Me}^{2+} + \text{IV Si}^{4+}$$

$M$  was derived as 3 983. Using this value for  $M$ , the mass of each oxide in the unit cell was calculated (Table 2); these divided by the corresponding molecular weights yielded the number of oxides in the cell. Next the number of each element in the cell was calculated. Following the suggestion of Jaffe (1951, p. 147) that  $\text{Y}^{3+}\text{Al}^{3+}$  replaces  $\text{Mn}^{2+}\text{Si}^{4+}$ , and  $\text{Na}^{1+}\text{Y}^{3+}$  replaces  $2\text{Mn}^{2+}$  (*op.cit.*, p.150) the substitution of elements in the Pyörönmaa yttrian spessartine has been thought to be as indicated in the footnote of Table 2. On this basis the following unit cell content was derived



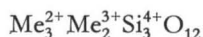
where VIII, VI, IV indicate the coordination number in respect to oxygen and



On the basis of  $Z = 8$ , the formula can be written as



which is very near to the theoretical structure formula of garnets



The chemical analysis of Pyörönmaa garnet corresponds to a garnet with 50.6 mol. per cent  $\text{Mn}_3\text{Al}_2\text{Si}_3\text{O}_{12}$  (spessartine), 37.6 mol. per cent  $\text{Fe}_3\text{Al}_2\text{Si}_3\text{O}_{12}$  (almandine), 4.6 mol. per cent of  $\text{Ca}_3\text{Fe}_2\text{Si}_3\text{O}_{12}$  (andradite) and 4.3 mol. per cent  $\text{Y}_3\text{Al}_2\text{Al}_3\text{O}_{12}$  (yttrogarnet). The remaining 2.9 mol. per cent consists of alkalis in the position of  $24c$  (Wyckoff notation) and ferric iron in  $16a$  (see also the substitution scheme in the footnote of Table 2).

The rare earth content, 3.35 wt.-%  $\text{RE}_2\text{O}_3$ , is so far the highest recorded for natural spessartines.

The garnet occurring as fissure fillings in allanite was investigated by microprobe analyser. The composition is identical with the yttrian spessartine occurring as large crystals embedded in albite and analyzed above.

So far no other yttrian spessartines have been reported from Finland. Therefore, some garnet specimens originating from the Tammela pegmatite province in SW Finland and from the Varala pegmatite quite near Pyörönmaa were investigated for yttrium. The garnet from Varala pegmatite was the only one to contain an appreciable amount of yttrium. An X-ray fluorescence analysis by V. Hoffrén using the accurately analyzed Pyörönmaa yttrian spessartine as standard gave for the Varala garnet 25.4 wt.-% FeO (total iron), 15.7 wt.-% MnO and 1.1 wt.-%  $\text{Y}_2\text{O}_3$ , corresponding to almandine with 38 mol. per cent spessartine and 1.7 mol. per cent yttrogarnet. In addition to yttrium no other RE-elements were determined. The refractive index of the Varala yttrian garnet is 1.816 and the unit cell edge 11.596 Å. The mineral occurs as crystals with the  $\{211\}$  form well developed. The specimen studied consisted of crystals measuring up to one centimeter.

Jaffe, 1951, emphasized the significance of the pegmatite garnets to contain essentially spessartine and almandine. He also discussed the role of accessory elements associated with the garnets of pegmatites and granites (*op.cit.*, pp. 142—153). Yttrium is shown to be the most important accessory element. Almost all of the manganese

rich garnets he investigated contained yttrium as an accessory element, some even more than 2 wt.-%  $Y_2O_3$ . As trace elements Jaffe detected yttrium in 39 out of 40 spessartine specimens.

The old yttrian spessartine analyses quoted in Jaffe's paper include more than 2 per cent yttrium (2.64 % »YO» in a spessartine reported 1868 by Websky; 2.45 % rare earths in a spessartine from Japan originally reported by Iimori 1938). The new yttrium determinations in Jaffe's work gave  $Y_2O_3$  contents as high as *e.g.*, 2.48 wt.-% (+ spectrographic traces of Sc, Gd, Dy, La, Ce, Nd, Pr), 2.01 wt.-% (+ traces of Yb, Dy, Er, Ho) and 1.36 wt.-%  $Y_2O_3$  (+ traces of Dy and Gd) for spessartines from pegmatites.

Concerning other trace constituents found in spessartines mention should be made that Jaffe detected Li and Na in the majority of specimens investigated in concentrations between 0.1—0.5 wt.-% substituting for divalent cations.

## ZIRCON AND XENOTIME

Zircon and xenotime are here treated together because they are isostructural minerals and often occur intimately intergrown in the Pyörönmaa pegmatite. The minerals are commonly encountered in connection with other RE minerals of the intermediate zone.

The colour of zircon is usually reddish in various shades. The colouring is due to very strong pigmentation. In places the colour is greenish grey especially when the mineral occurs as fissure fillings in allanite. The largest crystals of zircon are up to 10 mm:s in length. Both well developed prism faces and pyramidal faces are found: mostly, however, the crystal form is poorly developed.

Between crossed nicols zircon is isotropic due to the metamict state. Between parallel nicols the mineral is almost opaque due to very strong pigmentation. Often »schlieren» of a strongly anisotropic mineral is seen in zircon which has been identified as xenotime both by microprobe analyser and by X-ray powder diffraction methods. The »schlieren» are very narrow and partly submicroscopic in nature. Microprobe analyser indicates the intensity figures of P and Zr as varying reciprocally from point to point indicating that zircon and xenotime do not form a solid solution, but that an exsolution has taken place.

In places, zircon grades colourless in thin section. In such a grain microprobe analysis indicated, besides the high Zr and Si contents, 12 wt. per cent  $Y_2O_3$  but no phosphorus. In addition, 1 per cent MnO and 2—3 per cent CaO is present. Additional study on this anderbergite-like mineral is needed (Dana 1895, p. 487).

Xenotime, when occurring as single crystals, is always well crystallized and strongly anisotropic. The largest xenotime crystals found measure up to 1—2 mm. Microprobe analysis reveals that in addition to Y and P xenotime contains up to 5 wt.-%  $SiO_2$ .

The X-ray powder pattern of xenotime is characteristic of the species concerned. The powder pattern of the material, consisting of Y and P rich zircon, gives diffuse lines indicating a zircon structure with expanded cell size, larger than that of zircon but smaller than that of xenotime. Heat treatment produces the splitting of lines into powder patterns characteristic of zircon and xenotime.

## GADOLINITE AND CALCIO-GADOLINITE

Among the rare earth mineral specimens from the Pyörönmaa pegmatite, gadolinite forms a very small part. The manner of occurrence of the fresh but metamict gadolinite could not be deduced with the help of specimens concerned, the specimens being practically monomineralic, *viz.*, crystal fragments with conchoidal surfaces, the fragments measuring up to two centimeters.

The colour of the Pyörönmaa gadolinite is black, in thin splinters dark green. The fracture is conchoidal. The mineral is X-ray amorphous. Heated to 1 000°C in air for one hour the X-ray powder pattern is identical to that of the Lövböle gadolinite from Kemiö, SW Finland. The X-ray powder data for the heated Pyörönmaa gadolinite is given in Table 3, column 1.

The index of refraction is 1.775. Density, determined by the Berman density balance, is 4.11. The optical spectrograph revealed Fe, Be, Y (+ RE), and Si as the major components.

The mineral here called calcio-gadolinite belongs to the gadolinite-datolite group. The mineral occurs embedded in albite as strongly altered wedge-shaped crystals (Fig. 6). The composition determined with the optical spectrograph is near to that of gadolinite above containing essentially Si, Y, Be, Ca and Fe. The iron content of the gadolinite concerned is low, and the calcium content high compared with the iron and calcium contents of the black gadolinite above.

Megascopically the mineral is reddish-brown; especially the margins are brown with conchoidal fracture. The centres of the crystals are very inhomogeneous, lighter in colour and replaced partly by synchysite. Microscopic investigation reveals that the marginal parts (Fig. 7) are anisotropic, crystalline (A). The middle parts of the crystals also often show anisotropic irregular regions (B) having the same optical orientation as the marginal parts. All these strongly support the idea that these anisotropic areas represent the original mineral. However, the occurrence of narrow anisotropic rims (C) along the fractures of the metamict material with the same optical orientation as the margins of the crystals point to a reverse direction of reaction — to recrystallization. Microprobe analysis shows the composition in all three above mentioned cases (A—C) to be identical and



TABLE 3

X-ray powder data of gadolinite and calcio-gadolinite from Pyörönmaa pegmatite from Kangasala, SW Finland and of gadolinites from Norway

Phases in 1-5	1.		2.		3.		4.		5.		6.	
	<i>d</i> ( <i>A</i> )	<i>I</i>	<i>d</i> ( <i>A</i> )	<i>I</i>	<i>d</i> ( <i>A</i> )	<i>I</i>	<i>d</i> ( <i>A</i> )	<i>I</i>	<i>d</i> ( <i>A</i> )	<i>I</i>	<i>d</i> ( <i>A</i> )	<i>I</i>
			6.10	mw							5.99	20
<i>G</i> .....	5.4	vw										
Adhesive? ...	4.70	s	4.85	w	4.74	s	4.70	4	4.75	7	4.77	20
			4.15	m	4.10	m						
			3.76	m							3.79	30
											3.65	10
$\gamma, G$ .....	3.47	vwv	3.45	m b	3.47	ms	3.50	2	3.50	6	3.43	50
<i>G</i> (?) .....							3.40	1			3.33	5
$\gamma$ .....					3.25	m			3.26	5		
?	3.20	vs										
<i>G</i> .....	3.10	vw	3.13	s	3.11	m	3.10	8	3.12	5	3.14	100
<i>G</i> .....	3.00	m	3.00	w		w	3.01	2	3.03	2	3.00	60
<i>G</i> .....	2.92	w			2.93	w	2.94	3	2.95	2		
$\gamma$ .....					2.885	mw			2.89	5		
<i>G</i> .....	2.80	ms	2.85	vs	2.810	mw	2.82	10	2.82	5	2.86	80
$\gamma$ .....	2.68	ms			2.678	vs			2.69	10	2.75	5
<i>G</i> .....	2.54	ms	2.57	ms	2.560	m	2.55	9	2.55	6	2.55	60
?			2.475	vwv	2.515	vw					2.46	20
<i>G</i> .....	2.35	w	2.366	vwv	2.357	w	2.37	4	2.38	4	2.40	10
$\gamma$ .....					2.306	w			2.30	2	2.34	30
$\gamma$ .....									2.28	1		
<i>G</i> .....	2.25	w	2.224	vw	2.245	w	2.25	2	2.24	1	2.26	50
<i>G</i> .....	2.20	w	2.207	mw	2.195	w	2.21	3	2.20	2	2.20	70
<i>G</i> .....	2.10	vw	2.120	vwv	2.157	w	2.12	1	2.16	2	2.11	10
$\gamma$ .....					2.065	mw			2.07	3		
<i>G</i> .....	2.03	vw b	2.045	vwv	2.020	vw	2.03	1	2.02	1	2.05	10
<i>G</i> .....	1.95	w	1.978	m	1.951	vw	1.96	5	1.96	2	2.00	40
											1.957	5
$\gamma$ .....	1.90	vw	1.904	w	1.911	s			1.92	7	1.922	5
<i>G</i> .....	1.85	mw	1.874	mw	1.857	w	1.87	5 b	1.87	4 b	1.881	40
$\gamma$ .....					1.813	vw			1.82	1		
<i>G</i> .....	1.75	m	1.770	m b	1.757	ms	1.77	5 b	1.76	4 b	1.781	40
											1.749	10
<i>G</i> .....					1.705	w			1.72	2	1.722	30
<i>G</i> .....	1.68	} w b			1.690	w			1.70	2	1.684	10
<i>G, \gamma</i> .....				1.659	m vb	1.652	s	1.66	5	1.66	8	1.650
<i>G</i> .....	1.63				1.613	m	1.64	3	1.62	4		
<i>G</i> .....	1.57	mw b	1.573	vw	1.571	w b	1.58	3 b	1.57	1	1.573	5
<i>G</i> (?) .....					1.518	vwv						
<i>G</i> (?) .....					1.493	vwv						
<i>G</i> (?) .....					1.442	vwv						
$\gamma, G$ .....	1.40	m vb			1.418	ms	1.42	1 b	1.43	4 b		
$\gamma$ .....					1.388	w			1.40	1		
$\gamma$ .....	+ additional	+ additional	+ additional	+ additional	1.297	w			1.303	3	+ additional	+ additional
<i>G</i> .....	lines	lines	lines	lines			1.290	1			lines	lines
?					1.279	vwv						
<i>G</i> .....							1.250	1				
$\gamma$ .....					1.243	vwv			1.250	1 b		
?					1.211	vwv						
$\gamma$ .....					1.173	m			1.180	5		
$\gamma$ .....									1.168	1 b	+ additional	+ additional
											lines	lines



FIG. 6. Calcio-gadolinite (wedge-shaped crystals) embedded in albite. The white centres of calcio-gadolinite crystals are rich in synchysite-(Nd). Photo: Erkki Halmé.

The metamict material gave the same relative composition between the elements above. The intensity figures, however, were relatively smaller due to the hydration of the mineral. Boron and phosphorus were investigated by optical spectrograph but could not be detected.

The X-ray powder pattern of the anisotropical material (A above) is given in Table 3, column 2. In column 4 the powder data of Hitterö gadolinite from Norway are reproduced (Lima de Faria, 1964) and in column 6 those of the isostructural phosphate, herderite. Comparison of these data leaves no doubt that the mineral

---

s = strong, m = medium, w = weak, v = very, b = broad,  $G$  = gadolinite phase,  $\gamma = ?$  ( $G$  and  $\gamma$ , Lima de Faria, 1964, Table 14)

1. Black gadolinite. Heated in air at 1 000°C for one hour. Pyörönmaa, Kangasala, Finland.
2. Reddish-brown gadolinite (calcio-gadolinite). Unheated material. Pyörönmaa, Kangasala, Finland. All the lines are diffuse and difficult to measure accurately.
3. Reddish-brown gadolinite (calcio-gadolinite). Heated in air at 1 000°C for one hour. Pyörönmaa, Kangasala, Finland.
4. Gadolinite. Hitterö, Norway (Lima de Faria, 1964, table 14).
5. Gadolinite. Heated in air at 1 300°C for one hour. Norway (Lima de Faria, loc.cit.).
6. Herderite. ASTM 6 -0338.



FIG. 7. Calcio-gadolinite. Right margin albite. Between the inhomogeneous metamict calcio-gadolinite and albite there is a rim of crystalline calcio-gadolinite. The narrow light rims around the fissures in calcio-gadolinite have the same optical orientation as the crystalline gadolinite mentioned above and as the large yellowish-brown homogeneous region in the middle of the crystal. Magn. 11 x. Photo: Erkki Halme.

in column 2 does belong to the gadolinite group. Column 3 of the same table gives the powder data for the heated material from Pyörönmaa. Column 5 in turn gives the X-ray powder pattern of a Norwegian gadolinite heated in air at 1 300°C for one hour. The phases in column 5 are according to Lima de Faria (*op.cit.*) the gadolinite phase *G* and the  $\gamma$  phase (still unidentified, but characteristic to heated gadolinites). The same phases are present in the column 3.

Silicates belonging to the gadolinite-datolite group and being devoid of boron are gadolinite ( $Y_2FeBe_2Si_2O_8O_2$ ) and the nonferrous analogue of gadolinite, the so called »Tuva mineral» of Semenov, Dusmatov and Samsonova (1964) ( $Y_2Be_2Si_2O_8(OH)_2$ ). All the other members of this group — datolite, homilite, erdmannite, and the »Tadzhik mineral» of Semenov and al. — are boron bearing and can thus be omitted. Calcio-gadolinite has been described by Nakai (1938) and is regarded as a variety of gadolinite (Hinze and Chudoba, 1960, p. 63). As the gadolinite-datolite structure type is represented by a large number of mineral species (Semenov *et al.*, 1964) and there seem to exist extensive miscibility between various species, the variety name calcio-gadolinite is here adopted provisionally for the Pyörönmaa Ca-rich gadolinite, albeit the calcio-gadolinite of Nakai is rich in iron and that of Pyörönmaa rather poor.

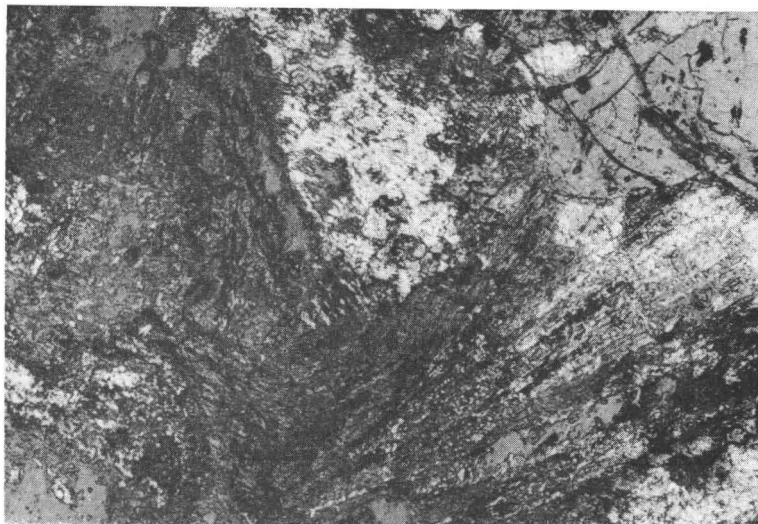


FIG. 8. Synchysite-(Nd), white, and calcio-gadolinite, grey. Magn. 150 x, Nic. +  $-16^\circ$ . Photo: Erkki Halme.

The metamict calcio-gadolinite of the Pyörönmaa pegmatite is in many places replaced by a white carbonate (Fig. 8). X-ray powder data of this mineral show it to belong to the synchysite-doverite group (Table 4). Microprobe analysis shows Nd to be the prevailing rare earth element. In addition Ca, Ce, Y and La are the other major components. The presence of fluorine and carbonate was tested by the conventional methods. Thus the mineral in question is essentially  $\text{NdCaF}(\text{CO}_3)_2$ , or synchysite-(Nd) if using the terminology of Levinson (1966).

The d-spacings of the synchysite-(Nd) are represented in the Table 4 with the corresponding data for synchysite-(Y) ( $\text{YCaF}(\text{CO}_3)_2$ ) and synchysite-(Ce) ( $\text{CeCaF}(\text{CO}_3)_2$ ) for comparison. Most of the extraneous lines of the powder data of synchysite-(Nd) can be attributed to calcio-gadolinite.

#### BRITHOLITE-(Y)

The mineral identified as britholite-(Y) occurs in Pyörönmaa pegmatite as crystals measuring up to 2 cm intimately associated with other RE minerals, especially with fergusonite. The colour is dark reddish brown, in thin splinters yellowish brown. In thin section the colour is greenish-grey. The marginal parts of the crystals are mostly replaced by other RE silicates.

Britholite-(Y) from Pyörönmaa is X-ray amorphous. In some specimens broad diffuse haloes occur on the photographs recorded with a Debye-Scherrer camera. These haloes can be interpreted as representing the strongest lines of the apatite

TABLE 4  
Comparison of X-ray powder data of synchysites

	1.		2.		3.		Remarks
<i>hkl</i> <sup>1)</sup>	<i>d</i> (Å)	<i>I</i>	<i>d</i> (Å)	<i>I</i>	<i>d</i> (Å)	<i>I</i>	
0 0 1 .....	9.09	5	9.1	m	9.1	s	Extraneous
	5.6	0.5					
0 0 2 .....	4.50	5	4.53	m	4.55	m	Extraneous
0 2 0, 1 1 0 .....	3.47	7	3.52	s	3.56	s	
			3.32	vwv	3.49	vw	Extraneous
0 2 1, 1 1 1 .....	3.22	1			3.31	m	
			3.13	vw			Extraneous
0 0 3 .....	3.00	4	3.03	vw	3.07	w	
			2.99	vwv	3.04	w	Extraneous
			2.85	vwv			
0 2 2, 1 1 2 .....	2.75	8	2.78	s	2.81	s	Extraneous
	2.62	1	2.55	vw	2.42	vwv	
1 1 3 .....					2.31	w	Extraneous
0 0 4 .....	2.25	3	2.27	w	2.28	w	
			2.20	vw	2.23	vw	Extraneous
	2.04	0.5			2.15	vw	
1 3 0, 2 0 0 .....	2.00	9	2.035	ms	2.05	ms	Extraneous
1 3 1 .....			1.980	vw	2.002	w	
0 2 4, 1 1 4 .....	1.89	10	1.908	m	1.918	m	Extraneous
	1.86	1					
1 3 2, 2 0 2 .....	1.83	9	1.861	m	1.870	ms	Extraneous
0 0 5 .....					1.821	vw	
0 4 0, 2 2 0 .....	1.73	2	1.768	w	1.781	w	Extraneous
0 4 1, 2 2 1 .....	1.70	1	1.740	vw	1.749	w	
1 3 3, 2 0 3 .....	1.66	1			1.704	w	Extraneous
	1.64	0.5					
0 4 2, 2 2 2 .....	1.62	6	1.645	m	1.658	m	Extraneous
1 3 4, 2 0 4 .....	1.49	6	1.519	mw			
	1.46	0.5					Extraneous
	1.39	0.5					
0 4 4, 2 2 4 .....	1.37	9	1.389	mw			Extraneous
1 3 5, 2 0 5 .....	1.34	1					
1 5 0, 2 4 0, 3 1 0 ..	1.31	1					Extraneous
0 0 7 .....	1.28	0.5					
1 5 2, 2 4 2, 3 1 2 ..	1.26	7	1.276	m (b)			Extraneous
1 5 3, 2 4 3, 1 3 6 ..	1.20	4	1.214	w			
3 1 3, 2 0 6 .....			1.145	w			

s = strong, ms = medium strong, m = medium, mw = medium weak, w = weak, vw = very weak, vvw = very very weak, b = broad.

<sup>1)</sup> Indexing by Levinson and Borup 1962, Smith et al. 1960.

1. Doverite (= synchysite-(Y)). Cotopaxi, Colorado (Levinson and Borup, 1962).

2. Synchysite-(Nd). Pyörönmaa, Kangasala, Finland.

3. Synchysite (= synchysite-(Ce)). Quincy, Mass. (Smith, Stone, Ross and Levine, 1960).

structure. Heated to 1 000°C in air for one hour the apatite-type structure is completely restored. The powder pattern of the heated material is identical with that of fluorapatite; the cell size, however, slightly deviates from that of the latter. The Pyörönmaa britholite-(Y) has  $a_0 = 9.39 \text{ \AA}$  and  $c_0 = 6.78 \text{ \AA}$  (calculated from the fully

TABLE 5

Partial chemical analysis of the britholite-(Y) from Pyörönmaa, Kangasala, Finland and the chemical analysis of the abukumalite (= britholite-(Y)) from Iisaka, Abukuma-Mountains, Fukushima Pref., Japan

	Pyörönmaa britholite-(Y)		Iisaka abukumalite
	1.	2.	3.
SiO <sub>2</sub> .....	23		20.84
P <sub>2</sub> O <sub>5</sub> .....	0		5.84
CaO .....	11		13.53
MgO .....			0.22
MnO .....	6	2	1.13
FeO .....	4	3	
Fe <sub>2</sub> O <sub>3</sub> .....			2.10
Al <sub>2</sub> O <sub>3</sub> .....			1.05
Ce-earths .....			6.45
Y-earths .....			45.98
Y <sub>2</sub> O <sub>3</sub> .....	44	41	
Yb <sub>2</sub> O <sub>3</sub> .....	3	3	
Er <sub>2</sub> O <sub>3</sub> .....		3	
Dy <sub>2</sub> O <sub>3</sub> .....		2	
Gd <sub>2</sub> O <sub>3</sub> .....		2	
ThO <sub>2</sub> .....			0.90
H <sub>2</sub> O(—) .....			0.16
H <sub>2</sub> O(+) .....			0.57
CO <sub>2</sub> .....			0.08
F .....			0.45
Loss of ignition (900°C) .....		2.1	
			99.30 %

1. Partial microprobe analysis of homogeneous part of Pyörönmaa britholite-(Y).

2. Partial X-ray fluorescence analysis of one large britholite-(Y) crystal, Pyörönmaa, Kangasala.

3. Hata, 1938 (ref. from Hintze: Handbuch der Mineralogie, Ergänzungsband II, p. 2).

indexed X-ray powder pattern recorded with a Debye-Scherrer camera). The corresponding figures of fluorapatite are 9.36 Å and 6.88 Å (Jaffe and Molinski, 1962, p.15). The differences in the cell size are due to the substitution of Y<sup>3+</sup> for Ca<sup>2+</sup> and of Si<sup>4+</sup> for P<sup>5+</sup>. Trömel and Eitel, 1957, give the cell size as:  $a_0 = 9.31$  Å and  $c_0 = 6.58$  Å for the synthetic abukumalite (=britholite-(Y)), Ca<sub>2</sub>Y<sub>3</sub>(SiO<sub>4</sub>)<sub>3</sub>(OH, F). The rare earth silicate apatites with La and Ce predominating (e.g., lessingite, beckelinite, and britholite-(Ce) have cell sizes considerably larger than that of fluorapatite (Gay, 1957,; Jaffe and Molinski, 1962, Table II).

The chemical composition of the Pyörönmaa britholite-(Y) was tested by optical spectrometer and microprobe analyser (Table 5). The result indicates the mineral to be a Y-Ca-silicate being devoid of phosphorus (compare apatites) and boron (compare the borosilicates with apatite structure: heated spencite (=tritomite-(Y)) and tritomite-A (Jaffe and Molinski, *loc.cit.*). Rare earth distribution was determined by X-ray fluorescence methods (Table 5, column 2).<sup>1)</sup>

<sup>1)</sup> Optical spectrograph revealed, in addition to the elements in Table 5, the following RE elements: La, Ce, Pr, Nd, Tb, Ho, Tm, Lu, and Sc.

TABLE 6

Partial microprobe analyses of the inclusions and alterations products of britholite-(Y)

	1.	2.	3.
SiO <sub>2</sub> .....	29	31	25
CaO .....	1	1	7
FeO .....	9	9	3
MnO .....	1	1	1
Y <sub>2</sub> O <sub>3</sub> .....	39	22	39
Yb <sub>2</sub> O <sub>3</sub> .....	4	5	4

1. Gadolinite? Inclusion in britholite-(Y). Microprobe analysis also indicates high intensity figures for Gd and Dy.
2. Reddish alteration product of britholite-(Y).
3. Colourless alteration product of britholite-(Y), occurring as a rim between albite and the reddish alteration product.

The specific gravity determined with the Berman density balance (suspension in toluene) is 3.54. The mean index of refraction is ca. 1.750—1.755. The index, however, is very variable due to alteration of the mineral. The mineral is optically isotropic because of the metamict state.

As inclusions there are some rounded reddish brown grains (0.1 mm in diameter) of metamict (?) unidentified mineral. The partial chemical analysis refers to gadolinite (?) (Table 6, column 1).

The alteration of britholite-(Y) is in places far advanced (Fig. 9). The marginal parts of the crystals are often replaced by an anisotropic reddish-brown Y-Fe-silicate (partial microprobe analysis in Table 6, column 2). The X-ray powder data could not be interpreted to correspond to any known mineral species. In places the alteration rim has, besides albite, another unidentified silicate (Y-Ca-silicate; partial microprobe analysis in Table 6, column 3).

### THALENITE

Thalenite has so far been identified in one specimen from the Pyörönmaa pegmatite. The mineral occurs as an allotriomorphic grain measuring up to 1 cm associated with fergusonite, allanite, zircon, xenotime, albite and some unidentified Y-silicates (Fig. 10). Thorite and an unknown Al-Y-silicate occur as inclusions (Fig. 11). At one end of the crystal thalenite is partly replaced by an anisotropic as yet unidentified Y-silicate (microprobe analysis gives 31 wt.-% SiO<sub>2</sub>, 30 % Y<sub>2</sub>O<sub>3</sub> and 1 % CaO).

Thalenite from Pyörönmaa is optically isotropic due to the metamict state. The mean refractive index for Na light is 1.663. The colour is dark reddish brown, in thin splinters yellowish brown, transparent. In thin section the colour is pink.

The thalenite investigated is X-ray amorphous. Heated in air at 1 000°C for one hour the X-ray powder pattern indicates the  $\gamma$  phase of yttrialite (Lima de Faria,

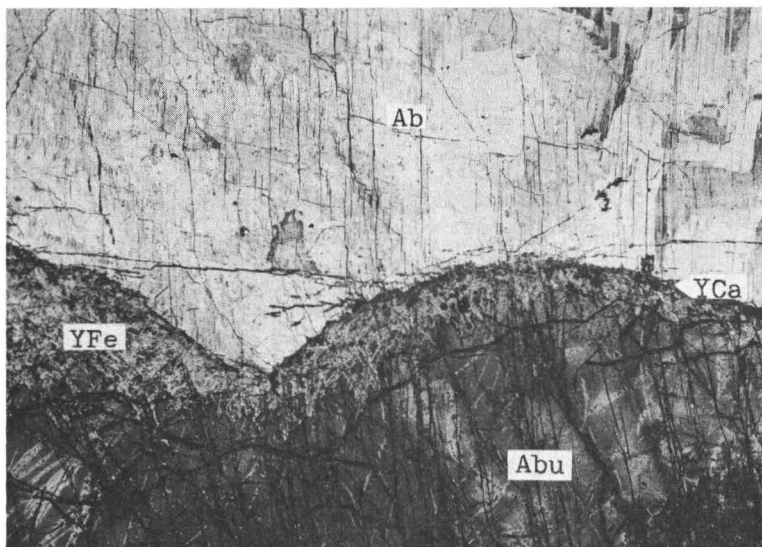


FIG. 9. Britholite-(Y) (Abu) replaced by an unidentified Y-Fe-silicate (YFe) and an unidentified Y-Ca-silicate (YCa). Upper part of the figure is albite (Ab). Magn. 7 x, Photo: Erkki Halme.

1964, pp. 33—34) as predominating. Yttrialite has been regarded as thorian thalenite ( $Y_2Si_2O_7$ ). Lima de Faria, however, points out that none of the phases which yttrialites develop by heating corresponds to the thalenite phase and accordingly he does not consider yttrialite as a variety of thalenite but as a species apart. The development of the  $y$  phase from the Pyörönmaa thalenite which is almost thorium free, however, is in discordance with Lima de Faria's opinion that thalenite and yttrialite are two separate species. The development of the  $y$  phase, which is different from the thalenite phase corresponding to unheated crystalline material, strongly contradicts the opinion that the  $y$  phase is the original yttrialite phase.

Table 7 shows that the X-ray powder data of Pyörönmaa thalenite fits those of yttrialites from Iimori, Japan and Bluffton, USA quite well. In addition to the lines of the  $y$  phase, the powder pattern of Pyörönmaa thalenite consists of a few lines which do not belong to the  $y$  phase. These, however, can be interpreted as the  $\alpha$  and  $\epsilon$  phases which Lima de Faria found as recrystallization products of yttrialites heated at 1 300°C for one hour. Column 4 of Table 7 gives the powder data for the  $\alpha$  phase, columns 5 those of the cubic  $\epsilon$  phase.

Microprobe analysis of Pyörönmaa thalenite indicated ca. 30 %  $Y_2O_3$ . In addition Yb, Fe, Dy, Ho and Lu are present. Si is as a major component. Mention should be made that the contents of Ce-earths and Th are very small.

Thorite (Th, U)  $SiO_4$ , in which microprobe analysis indicates Th to prevail over U, occurs as inclusions in thalenite forming crystals measuring up to 0.3 mm.

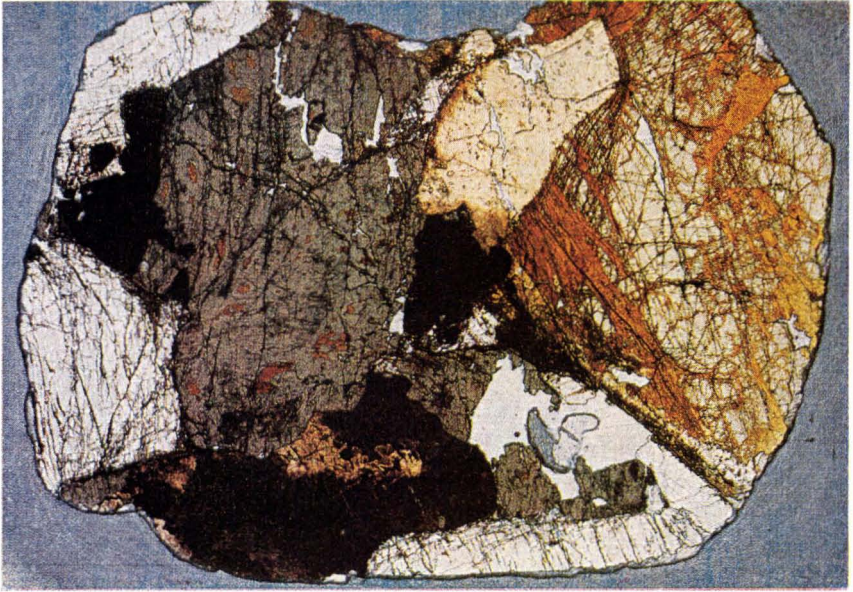


FIG. 10. Strongly hydrated fergusonite (green), less hydrated fergusonite (brown inclusions in green), thalenite (pink), zircon (black), albite (white), allanite (light green to the right). The yellowish brown mineral in the largest zircon grain is the Y-rich zircon mentioned in the text. Magn. 2.3 x. Photo: Erkki Halme.

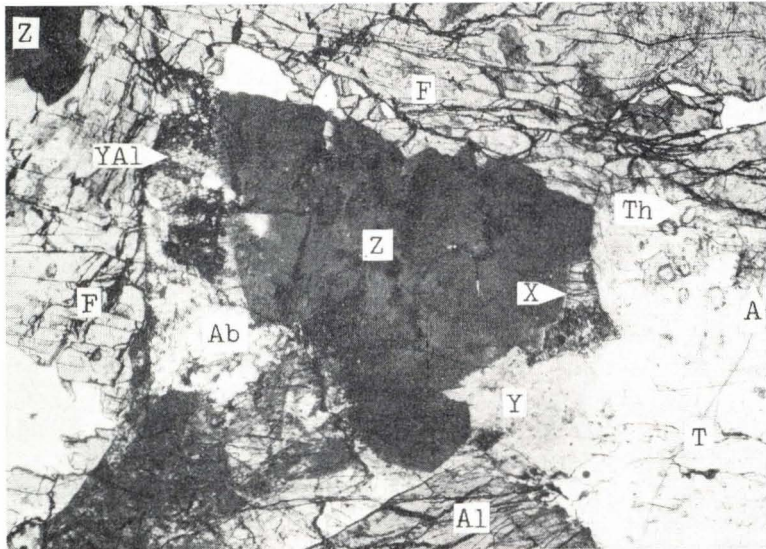


FIG. 11. Partial magnification of Fig. 10. Zircon (Z), fergusonite (F), thalenite (T), xenotime (X), albite (Ab), thorite (Th), allanite (Al), unknown Al-Y-silicate (A), unknown Y-Al-silicate (YAl), unknown Y-silicate (Y). Magn. 5 x. Photo: Erkki Halme.

TABLE 7  
X-ray powder data of heated thalenite and yttrialites

1.		2.		3.		4.		5.	
<i>d</i> (Å)	<i>I</i>								
						6.6	2	6.6	1
						5.8	2	5.8	2
4.70	m	4.7	4	4.6	4				
4.31	vw					4.4	6 b	4.35	5
4.04	m	4.05	3	4.00	4				
3.49	s	3.50	7	3.49	7				
3.30	vw					3.30	4	3.30	4
3.20	w	3.21	1	3.20	2				
						3.15	2	3.11	7
3.06	vs b	3.08	10	3.05	10				
						3.00	10	3.00	10
2.89	w					2.89	7 b	2.90	6
								2.86	3
2.80	vw					2.80	5	2.80	5
2.700	vw					2.70	5	2.70	7
2.635	m	2.65	6	2.64	6				
2.398	m	2.41	6	2.40	6				
2.327	vw	2.34	1	2.34	1				
						2.20	2 b	2.19	2 b
						2.14	2 b	2.15	2 b
						2.10	2 b	2.10	2 b
2.061	m	2.06	7	2.06	7				
2.022	m	2.03	5	2.02	6				
1.914	w b	1.89	2	1.88	4			1.91	8
1.864	w b	1.86	1	1.86	2			1.86	1
								1.84	1
1.801	vw					1.81	8	1.81	8
						1.78	3	1.78	3
1.746	ms	1.75	9	1.75	9				
1.700	vw	1.71	1	1.71	1			1.72	1
								1.70	1
1.681	vw	1.68	1	1.68	1			1.68	1
1.631	w					1.63	2	1.63	9
1.596	mw	1.61	6	1.60	6			1.61	1
1.549	m	1.55	8	1.55	10				
1.530	vw	1.53	2	1.53	2				
1.457	w b	1.46	1 b	1.47	1 b	1.50	1 b	1.50	1 b
1.377	mw	1.380	4	1.380	6	1.45	2 b	1.46	1 b
								1.350	1 vb
1.344	vw								
1.319	vw	1.322	1	1.325	1				
1.294	w	1.298	2	1.298	2				
1.259	mw	1.260	3	1.260	5				
1.236	w	1.240	1	1.240	1			1.241	3
								1.210	3
1.201	vw	1.205	1	1.208	1				
1.187	w	1.190	2	1.190	4				
1.172	vw			1.172	1 b				
		1.155	1	1.155	1 b				
						1.145	1 vb	1.145	1 vb
1.119	vw b	1.125	1 vb	1.125	1 vb				
1.097	vw							1.105	2
1.069	mw	1.071	2 b	1.071	4				
				1.063	1				

Table 7. (continued)

1.		2.		3.		4.		5.	
<i>d(A)</i>	<i>I</i>								
1.053	w	1.054	1	1.055	2				
1.033	vw	1.036	1	1.037	1			1.040	4
1.0075	mw	1.012	2	1.014	4				
.9913	w	.996	1	.997	2				
.9730	mw	.975	2 b	.976	4				
				.969	1				
.9310	vw								
.9127	mw							.915	3
.8973	mw								
.8512	m								
.8386	w								
.8326	mw								
.8241	w								
.8055	mw								
.7992	w								
.7894	ms								

s = strong, m = medium, w = weak, v = very, b = broad.

1. Thalenite. Heated in air at 1 000°C for one hour. Pyörönmaa, Kangasala, Finland.
2. Yttrialite. Heated in air at 1 000°C for one hour. Swishōyama, Iisaka, Fukushima Prefecture, Japan. (Lima de Faria 1964, Table 14).
3. Yttrialite. Heated in air at 1 000°C for one hour. Near Bluffton, Llano Co., Texas, USA. (Lima de Faria 1964, Table 14).
4. Yttrialite. Heated in N<sub>2</sub> at 1 300°C for one hour. Swishōyama, Iisaka, Fukushima Prefecture, Japan. (Lima de Faria 1964, Table 14).
5. Yttrialite. Heated in air at 1 300°C for one hour. Swishōyama, Iisaka, Fukushima Prefecture, Japan. (Lima de Faria 1964, Table 14).

In addition, an unidentified isotropic Al-Y-silicate occurs as an inclusion (a rectangular crystal measuring up to 0.4 mm). A partial microprobe analysis of this gave 38 % SiO<sub>2</sub>, 37 % Al<sub>2</sub>O<sub>3</sub>, 6 % Y<sub>2</sub>O<sub>3</sub>, 4.5 % CaO and 4 % FeO.

#### FERGUSONITE

Fergusonite, YNbO<sub>4</sub>, occurs in connection with allanite and other RE minerals in the intermediate zone as crystals measuring up to 5 cm. Some of the fergusonite specimens have been collected from the dump and some from the western wall of the quarry. The habit of the mineral is prismatic, the crystal faces, however, are so poorly developed that no goniometric measurements could be made. The colour varies from greenish-yellow to brownish-yellow. The mineral is transparent in very thin splinters. The luster is vitreous. It is isotropic due to the metamict state. The refractive index varies slightly from grain to grain: mostly it is slightly more than 2.06. The fracture is conchoidal. Some of the crystals are very brittle (strongly hydrated). Density, determined with a Berman density balance (suspension in toluene), varies

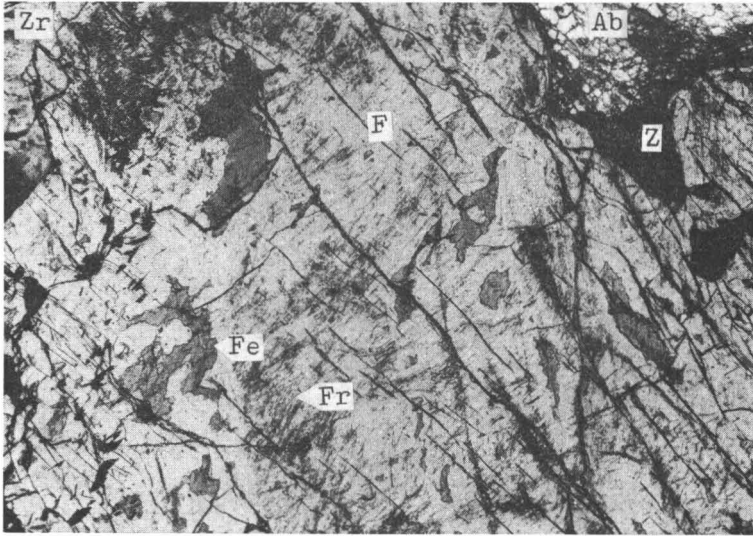


FIG. 12. Partial magnification of Fig. 10. Fergusonite, hydrated (F), fergusonite, less hydrated (Fe), network of monoclinic fergusonite (Fr), zircon (Z), albite (Ab), Y-bearing zircon (Zr). Magn. 5 x. Photo: Erkki Halme.

from grain to grain from 4.75 to 5.48, indicating inhomogeneity of the material (partly due to hydration).

A thin section of fergusonite (Figs. 10 and 12) shows the mineral to be inhomogeneous. The host fergusonite is greenish and completely isotropic. As inclusions there are irregular regions of greenish-brown fergusonite; also isotropic. Between crossed nicols it is seen, that in places there is a network of anisotropic mineral, which could not be distinguished from the greenish fergusonite without an analyser. The anisotropic material inside one single fergusonite crystal has a parallel optical orientation.

In addition to the inhomogeneities in fergusonite mentioned above, uraninite has also been encountered occasionally as inclusions.

Fergusonite was identified by the standard heat treatment of metamict minerals developed by Lima de Faria (1964). The recrystallized phases were investigated by X-ray powder diffraction methods and the chemical composition was determined with X-ray fluorescence methods. The unheated material (host) is X-ray amorphous. Heated in air at 700°C for three hours the mineral gives the powder pattern of tetragonal fergusonite (Table 8). Heated in air at 1 000°C for one hour the monoclinic  $YNbO_4$  is developed. The X-ray fluorescence analysis is given in Table 9. This comprises also the inclusions, which in this case are greenish-brown fergusonite and the anisotropic material. The chemical analysis fits with other published fergusonite analyses very well.

TABLE 8  
X-ray powder data of heated fergusonite from Pyörönmaa, Kangasala,  
SW Finland

1.			2.		
<i>hkl</i>	<i>d</i> (Å)	<i>I</i>	<i>hkl</i>	<i>d</i> (Å)	<i>I</i>
			0 2 0	5.44	< 1
			1 1 0	4.73	< 1
1 1 2	3.04	10	1 2 1	3.10	10
0 0 4	2.74	2	0 3 1, 1 2 1	2.96	10
2 0 0	2.593	3	0 4 0	2.74	2
			2 0 0	2.64	1
				2.573	< 1
1 1 4	2.191	< 1	0 0 2	2.515	1
			1 1 2, 1 4 1	2.161	1
2 0 4	1.879	4	$\bar{2}$ 3 1, 1 5 0, 0 5 1	2.006	< 1
2 2 0	1.830	1	2 4 0, 2 3 1, $\bar{2}$ 0 2	1.901	4
			0 4 2	1.855	3
1 1 6	1.631	2	2 0 2, 3 1 0	1.758	1
3 1 2	1.568	3 b	$\bar{1}$ 6 1, $\bar{3}$ 2 1	1.642	2
2 2 4	1.523	≈ 1	$\bar{2}$ 5 1	1.624	2
0 0 8	1.369	< 1	3 2 1, 2 5 1, $\bar{2}$ 4 2	1.565	3 b
			0 7 1, 1 2 3	1.504	1
4 0 0	1.287	1	$\bar{2}$ 1 3	1.481	< 1
			0 8 0	1.371	< 1
				1.319	< 1
				1.288	≈ 1
	1.216	2 b		1.265	≈ 1
				1.238	≈ 1
	1.164	≈ 1 b		1.215	2
	1.099	≈ 1 b		1.190	1 b
				1.146	1 b
				1.112	1 b
				1.082	1 b
				1.048	1 b
				.999	< 1 b
				.985	≈ 1 b
				.954	< 1 b
				.913	< 1 b
				.858	< 1 b
				.835	< 1 b
				.813	< 1 b

$a_0 = 5.18 \text{ \AA}$   
 $c_0 = 10.96 \text{ \AA}$   
Tetragonal

$a_0 = 5.30 \text{ \AA}$ ,  $b_0 = 10.96 \text{ \AA}$ ,  $c_0 = 5.05 \text{ \AA}$   
 $\beta \approx 95.3^\circ$   
Monoclinic

1. Heated in air at 700°C for three hours.

2. Heated in air at 1 000°C for one hour.

Intensities are by visual estimations (b = broad).

Debye-Scherrer method; CuK $\alpha$ -radiation.

TABLE 9

Semi-quantitative XRF-analysis of the fergusonite from  
Pyörönmaa pegmatite, Kangasala, Finland

Nb <sub>2</sub> O <sub>5</sub> .....	35 wt.-%
Ta <sub>2</sub> O <sub>5</sub> .....	10
Y <sub>2</sub> O <sub>3</sub> .....	29
Yb <sub>2</sub> O <sub>3</sub> .....	4
Er <sub>2</sub> O <sub>3</sub> .....	3
Dy <sub>2</sub> O <sub>3</sub> .....	2
Lu <sub>2</sub> O <sub>3</sub> .....	1
(Ho, Gd) <sub>2</sub> O <sub>3</sub> .....	1
UO <sub>2</sub> .....	3
ThO <sub>2</sub> .....	2
PbO .....	1
<hr/>	
	91 wt.-%
<i>Loss of ignition at 800°C</i>	3.70 %

Concerning the inclusions in the host fergusonite, the greenish brown material was also subjected to the same heat treatment as the host fergusonite and to subsequent X-ray study. The phases developed were identical with those of the host fergusonite. The unheated anisotropic material, investigated by X-ray powder diffraction methods, gave the powder pattern of monoclinic fergusonite with a slightly expanded lattice. Thus we can conclude that inside one morphologically single fergusonite crystal there are three varieties, two being in metamict state and the third in crystalline state. Semi-quantitative partial microprobe analyses are given for these three varieties in Table 10.

These analyses indicate the same Nb:Ta:Y ratio in both metamict varieties. Intensity figures indicate the greenish-brown material to be less hydrated than the greenish host. The occurrence of the anisotropic monoclinic fergusonite in the strongly hydrated part of fergusonite points to the possibility of interpreting it as a recrystallized

TABLE 10

Semi-quantitative partial microprobe analysis of the different fergusonite varieties of Pyörönmaa  
pegmatite, SW Finland

	1.	2.	3.
Nb <sub>2</sub> O <sub>5</sub> .....	35 %	39 %	47 %
Ta <sub>2</sub> O <sub>5</sub> .....	10	12	11
Y <sub>2</sub> O <sub>3</sub> .....	28	35	42
CaO .....			1

1. Strongly hydrated fergusonite (the host).
2. Greenish-brown fergusonite; as inclusions in the host.
3. Anisotropic fergusonite; recrystallization product of the host mineral.

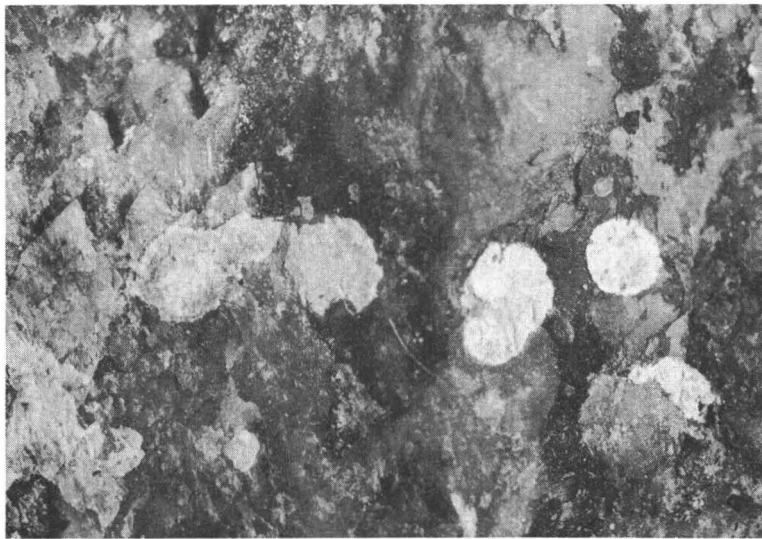


FIG. 13. Tengerite incrustations as radial aggregates on albite. Pyörönmaa, Kangasala, SW Finland. Magn. 8.5 x. Photo: Erkki Halme.

zation product, and not as an original structure of fergusonite. Also the composition of this monoclinic fergusonite (column 3, Table 10) indicates more advanced fractionating of Nb and Ta if compared to those in metamict material. It is emphasized that the analyses in the table are only semiquantitative; the relative values, however, are accurate.

The occurrence of fergusonite in the Pyörönmaa pegmatite is also noteworthy in that this is the first known fergusonite occurrence inside the Finnish borders.

#### TENGERITE

Tengerite occurs in the Pyörönmaa pegmatite as a supergene mineral as white powdery fillings in the fractures of other minerals and on their surfaces, especially on albite. Chemical analysis indicates that the mineral is a hydrous carbonate of yttrium and calcium. Often the incrustations are of circular shape (radial aggregates) measuring about 1—2 mm across (Fig. 13). The mineral has a pearly luster. It is soluble in diluted hydrochloric acid with a vigorous effervescence.

For the chemical analysis 7.2 mg of tengerite were separated under a binocular. The  $H_2O(-)$  was determined by drying 4.09 mg of the mineral at  $110^\circ C$  for 17 hours (weight loss was 5.4 wt.-%). The total ignition loss amounted to 39.4 wt.-%. 3.14 mg of pure tengerite was now heated in a micro Penfield tube. The total  $H_2O$  derived was 7.0 wt.-%. These figures give the  $H_2O(+)$ ,  $H_2O(-)$  and  $CO_2$  contents 1.6 %, 5.4 %

TABLE 11

Chemical analysis of the tengerite from Pyörönmaa pegmatite, Kangasala, SW Finland and of the tengerite from Iisaka, Japan

	1.	2.
Y <sub>2</sub> O <sub>3</sub> .....	29.0	
Lu <sub>2</sub> O <sub>3</sub> .....	<i>trace</i>	
Yb <sub>2</sub> O <sub>3</sub> .....	2.2	
Tm <sub>2</sub> O <sub>3</sub> .....	0.9	
Er <sub>2</sub> O <sub>3</sub> .....	4.0	
Ho <sub>2</sub> O <sub>3</sub> .....	<i>trace</i>	
Dy <sub>2</sub> O <sub>3</sub> .....	6.8	
Tb <sub>2</sub> O <sub>3</sub> .....	1.2	
Gd <sub>2</sub> O <sub>3</sub> .....	4.6	
Y-earths .....	(48.7)	49.0
Eu <sub>2</sub> O <sub>3</sub> .....	<i>n.d.</i>	
Sm <sub>2</sub> O <sub>3</sub> .....	1.8	
Nd <sub>2</sub> O <sub>3</sub> .....	1.3	
Pr <sub>2</sub> O <sub>3</sub> .....	0.3	
Ce <sub>2</sub> O <sub>3</sub> .....	0.7	
La <sub>2</sub> O <sub>3</sub> .....	0.2	
Ce-earths .....	(4.3)	1.3
CaO .....	3.2	8.3
Fe <sub>2</sub> O <sub>3</sub> .....	0.4	<i>trace</i>
Al <sub>2</sub> O <sub>3</sub> .....	<i>n.d.</i>	<i>trace</i>
BeO .....	<i>n.d.</i>	0.7
ThO <sub>2</sub> .....		0.3
PbO .....	<i>n.d.</i>	0.2
TiO <sub>2</sub> .....	<i>n.d.</i>	0.0
UO <sub>3</sub> .....		0.0
MnO .....	<i>n.d.</i>	0.0
MgO .....	<i>n.d.</i>	0.0
SiO <sub>2</sub> .....	<i>n.d.</i>	0.8
CO <sub>2</sub> .....	32.4	28.7
H <sub>2</sub> O(-) .....	5.4	0.3
H <sub>2</sub> O(+) .....	1.6	10.1
<i>Total</i> .....	96.0	99.7

*n.d.* = not detected

1. Tengerite from Pyörönmaa, Kangasala, SW Finland. Rare earths, Ca, Fe, Al, Pb, Ti, Mn, Mg, and Si determined by microprobe, Be by optical spectrograph.
2. Tengerite from Iisaka, Fukushima Prefecture, Japan (Iimori, 1938).

and 32.4 % respectively (determination by P. Ojanperä). The metal oxides were determined by the microprobe analyser. The results are given in Table 11.

The X-ray powder data of the mineral is given in the Table 12.

The manner of occurrence of the Pyörönmaa tengerite is similar to that of Iisaka tengerite (Iimori, 1938). The Pyörönmaa tengerite is devoid of Be (by optical spectrograph) as is that of Iisaka. The other tengerites described are rich in beryllium and must be regarded as a species apart (Hey, 1955, p. 80).

The chemical analysis of the Iisaka tengerite (Table 11) is in some respects different from that of Pyörönmaa tengerite. The most marked difference is in

TABLE 12  
X-ray powder data of the tengerite from the Pyörönmaa  
pegmatite, Kangasala, SW Finland

<i>d</i> (Å)	<i>I</i>	<i>d</i> (Å)	<i>I</i>
9.9	m	2.432	w
6.51	m	2.405	w
5.82	s	2.289	vw
5.18	vw	2.210	vw
4.61	s	2.148	w (b)
3.82	s	2.096	vw
3.603	w	2.051	mw
3.445	vw	2.008	vw
3.307	vw	1.975	mw
3.173	vw	1.904	vw
2.933	s	1.870	w
2.685	w	1.843	w
2.576	vw	1.782	vw
2.542	m	1.729	vw

Debye-Scherrer camera. Camera dia. 57.3 mm,  $\text{CuK}\alpha$ -radiation.

s = strong, m = medium, w = weak, v = very, b = broad.

the  $\text{H}_2\text{O}$  contents. Iisaka tengerite has low (—) and high (+) water contents. In the Pyörönmaa tengerite the situation is vice versa. However, the Pyörönmaa material is here named tengerite. After the X-ray powder data of the Iisaka tengerite is available one can conclude whether these are identical minerals or not.

The refractive indices of Pyörönmaa tengerite are:  $\gamma = 1.627$  and  $\alpha = 1.569$ ;  $Z \parallel$  elongation. Iisaka tengerite has  $\alpha = 1.622$  and  $\gamma = 1.642$  (Iimori, 1938).

Material with the same X-ray powder pattern as Pyörönmaa tengerite has also been found as fracture fillings in the Lövböle gadolinite from Kemiö, SW Finland (Fig. 14).

## DISCUSSION

In the preceding pages a short description of some rare minerals occurring in the Pyörönmaa pegmatite is given. Some of the minerals are new to Finland (thalenite, britholite-(Y), calcio-gadolinite, yttrian spessartine, synchysite-(Nd), tengerite, fergusonite and the many Y-silicates still unidentified).

All the rare earth minerals occur in the intermediate zone of the pegmatite. The zone is very rich in albite, some of which evidently crystallized before the first RE mineral, allanite. The occurrence of albite as fracture fillings in allanite proves the crystallization of albite to have been continued after the allanite had crystallized. The Ce-earth silicate, allanite, is older than the Y rich silicates and fergusonite. The present study has not managed to establish any reliable time-table for the order

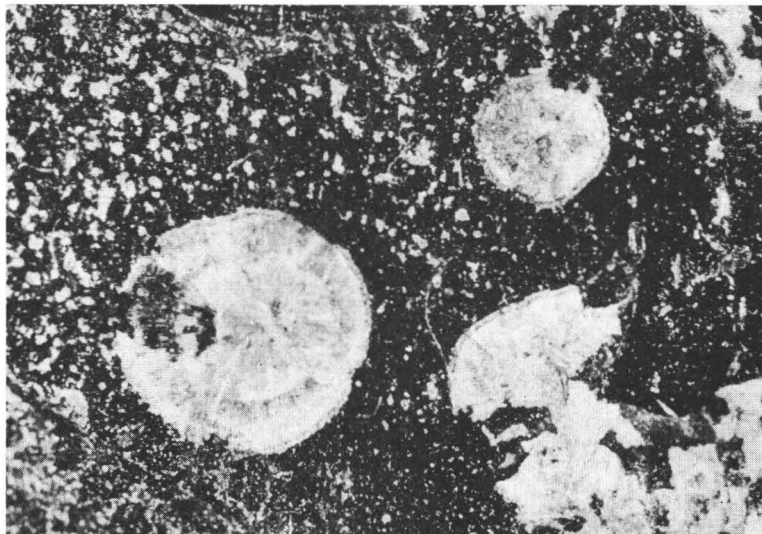


FIG. 14. Radial aggregates of tenerite on gadolinite. Lövböle, Kemiö, SW Finland. Magn. 17 x. Photo: Erkki Halme.

of crystallization of yttrian spessartine, calcio-gadolinite, zircon, britholite-(Y) and thalenite. It is probable that all of them have crystallized simultaneously. The next stage in the formation of pegmatite seems to have been the replacement of Y silicates by other Y silicates, which, unfortunately, are still awaiting further study. The last stage in the evolution of the intermediate zone was the replacement of RE silicates by RE carbonates (synchysite and bastnaesite, accompanied by calcite). The supergene alteration of the RE minerals continuously creates new minerals, such as tenerite.

The distribution of RE elements in the various minerals of Pyörönmaa pegmatite is by no means clear and needs more investigation. However, it can be stated, that the crystallization was initiated with the separation of Ce-earths to form allanite. Also it has been established that all the younger RE silicates of Pyörönmaa pegmatite are rich in Y-earths. In yttrian spessartine, fergusonite and britholite-(Y) the distributions of RE elements are almost identical (Fig. 15). The situation is, however, not the same for all the Y rich minerals in the pegmatite concerned. In calcio-gadolinite and tenerite (Fig. 15), *e.g.*, Dy is the next prevailing RE element after Y. In the gadolinite-like inclusion in britholite-(Y) Gd and Dy are high compared *e.g.*, with Er. In the carbonate (bastnaesite) which replaces allanite, Ce prevails as is to be expected. The carbonate (synchysite-(Nd)) replacing calcio-gadolinite, however, has a different RE distribution from the host mineral. In calcio-gadolinite the prevailing RE elements are Y and Dy, but in synchysite Nd, Ce and Y, in this order.

Eskola (1963, p. 230) called attention to the fact that the pegmatite province west of Pitkäranta on the northern shore of Lake Lagoda is characterized by the occurrence

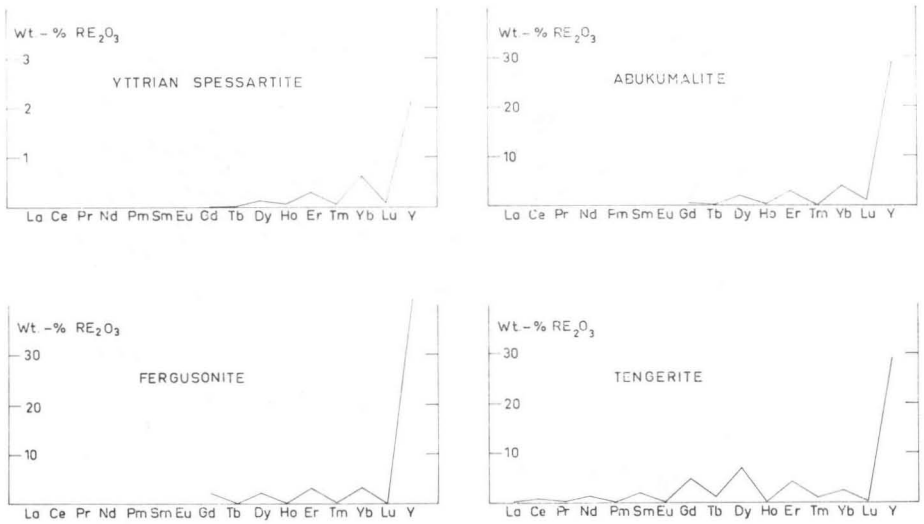


FIG. 15. Distribution of rare earth elements in yttrian spessartine, fergusonite, britholite-(Y) (= abukumalite) and tengerite from Pyörönmaa pegmatite, Kangasala, SW Finland.

of wiikite, monazite and other lanthanite minerals, and that the elements of this assemblage are entirely different from those of the Svecofennian in western Finland (Tammela, Kemiö, Eräjärvi and Kuortane pegmatite provinces according to v. Volborth 1956), but strangely enough, have much in common with the pegmatites of the Stockholm area in Sweden. The mineral and element assemblage of Pyörönmaa pegmatite corresponds closely to those of the Ytterby pegmatite near Stockholm. In the Ytterby pegmatite *e.g.*, allanite, gadolinite, fergusonite, yttriotantalite, xenotime and anderbergite (yttrian zircon) have been reported (Brotzen, 1959, pp. 19–20). Apatite, magnetite, pyrite, native bismuth and molybdenite are found occasionally. Beryl, chrysoberyl, cordierite and tourmaline are very rare in Ytterby pegmatite. Mention should be made that muscovite is far less common than biotite and that garnet is quite common (yttrian spessartine?). The zonal structure of Ytterby pegmatite is similar to that of Pyörönmaa. The wall zone is made up of graphic granite. The border zone, which is absent in places, is granitic. The rare minerals are mainly confined to the intermediate zone (microcline zone), the outermost part of which is rather rich in oligoclase and biotite. Quartz lenses form the cores.

Brotzen (*op.cit.*, p. 19) regards Ytterby pegmatite as being genetically related to the Stockholm granite (late kinematic granite).

The Pyörönmaa pegmatite is inside a late kinematic Svecofennian granite body. About 14 km to the north-east of the Pyörönmaa pegmatite the well known Varala pegmatite is situated (Lokka, 1935, 1950; Matisto, 1964). The Varala pegmatite quarry is mineralogically known due to the amount of allanite found there. The

pegmatite itself is confined to even-grained granite that may be an apophyse of the same granite body in which also the Pyörönmaa pegmatite is situated. The study on the minerals of the Varala pegmatite is in progress. The occurrence of allanite and of *e.g.*, yttrian spessartine refers to a similar element assemblage as those in Pyörönmaa and Ytterby pegmatites. Mention should also be made that biotite is the prevailing mica in the Varala pegmatite.

These comparisons indicate that in Kangasala there exist pegmatites similar to those in the Stockholm area (*e.g.*, Ytterby) and on the northern shore of Lake Ladoga. The mineral and element assemblage of this pegmatite province is different from those of the other well known Finnish pegmatite provinces, *i.e.*, Tammela (Mäkinen, 1912; Aurola, 1963), Kemiö (Pehrman, 1945), Eräjärvi (v. Volborth, 1954) and Kuortane (Haapala, 1964) all of which can be described as lithium-beryllium pegmatites. The genesis of some of these have been related to the synorogenic Svecofennian rocks (See Aurola, *op. cit.*, pp. 24—29; Haapala, *op. cit.*, pp. 130—134).

*Acknowledgments* — The authors wish to thank Prof. K. J. Neuvonen of the University of Turku and the late Mr. Arvo Vesalio Lic.Phil., of the Geological Survey for many samples. We also wish to thank Prof. Vladi Marmo, the Director of the Geological Survey of Finland for the many fruitful discussions and suggestions and for giving permission to publish the map in fig. 2. Also our thanks are due to Mr. Arvo Matisto, Lic.Phil., for many specimens of Pyörönmaa pegmatite, to Mrs. Toini Mikkola, Mag.Phil., for determining most of the refractive indices in this study as well as to Mr. Erkki Halme, for taking the photographs.

*Manuscript received, March 22, 1966*

## REFERENCES

- ASTM — Powder diffraction data file, sets 1—14. American Society for Testing and Materials.
- AUROLA, ERKKI (1963) On the pegmatites in the Torro area, southwestern Finland. Bull. Comm. géol. Finlande 206, pp.1—32.
- BROTZEN, O. (1959) Outline of mineralization in zoned granitic pegmatites. Geol. För. Stockholm Förh., vol. 81, no. 496, pp. 1—98.
- DANA, E. S. (1895) The system of mineralogy, 6th ed., New York.
- ESKOLA, PENTTI (1963) The precambrian of Finland. Interscience Publishers.
- GAY, P. (1957) An X-ray investigation of some rare-earth silicates: cerite, lessingite, beckelite, britholite, and stillwellite. Miner. Mag., vol. 31, no. 237, pp. 455—468.
- HAAPALA, ILMARI (1964) Peräseinäjoen, Alavuden ja Etelä-Kuortaneen graniittipegmatiiteista. (Thesis). Manuscript in the archives of the Dept. of Geology and Mineralogy of the University of Helsinki.
- HEY, MAX H. (1955) An index of mineral species and varieties. British Museum.
- HINZE, KARL und CHUDOBA, KARL F. (1960) Handbuch der Mineralogie. Ergänzungsband II, Berlin.
- IIMORI, TAKEO (1938) Tengerite found in Iisaka, and its chemical composition, Sci. Papers, Inst. Chem. Res., Tokyo, 34, pp. 832—841.
- JAFFE, HOWARD W. (1951) The role of yttrium and other minor elements in the garnet group. Am. Mineral, vol. 36, nos. 1—2, pp. 133—155.

- JAFFE, HOWARD W. and MOLINSKI, VICTOR J. (1962) Spencite, the yttrium analogue of tritomite from Sussex County, New Jersey. *Am. Mineral.*, vol. 47, nos. 1—2, pp. 9—25.
- LEVINSON, A. A. and R. A. BORUP (1962) Doverite from Cotopaxi, Colorado. *Am. Mineral.* vol. 47, pp. 337—343.
- LEVINSON, A. A. (1966) A system of nomenclature for rare-earth minerals. *Am. Mineral.* vol. 51, pp. 152—158.
- LIMA de FARIA, J. (1964) Identification of metamict minerals by X-ray powder photographs. *Estudos, Ensaios e Documentos No. 112, Junta de Investigações do Ultramar, Lisboa.*
- LOKKA, LAURI (1935) Über den Chemismus der Minerale (Orthit, Biotit u.a.) eines Feldspatbruches in Kangasala, SW-Finland. *Bull. Comm. géol. Finlande* 111, pp. 1—40.
- »— (1950) Contributions to the knowledge of the chemistry of radioactive minerals of Finland. *Bull. Comm. géol. Finlande*, 149, pp. 1—76.
- MÄKINEN, EERO (1912) Die Granitpegmatite von Tammela in Finland und ihre Minerale. *Bull. Comm. géol. Finlande* 35, pp. 1—101.
- MATISTO, ARVO (1961) Suomen geologinen kartta, 1 : 100 000 — Geological Map of Finland, 1 : 100 000, No. 2123, Tampere.
- »— (1964) Suomen geologinen kartta, 1 : 100 000 — Geological Map of Finland, 1 : 100 000, No. 2124, Kangasala.
- NAKAI, TOSHIO (1938) On calcio-gadolinite from Tadati, Nagano Prefecture. *Bull. Chem. Soc. Japan*, 13, pp. 591—594.
- PEHRMAN, GUNNAR (1945) Die Granitpegmatite von Kimito (SW-Finland) und ihre Minerale. *Medd. från Åbo Akad. Geol.-Miner. Inst. no. 26.* pp. 1—84.
- SEMENOV, E. I., DUSMATOV, V. D. and SAMSONOVA, N. S. (1964) Yttrium-beryllium minerals of the datolite group. *Soviet Physics; Crystallography*, 8, pp. 539—541.
- SMITH, WILLIAM LEE, STONE, JEROME, ROSS, DAPHE R. and LEVINE, HARRY (1960) Doverite, a possible new yttrium fluocarbonate from Dover, Morris County, New Jersey. *Am. Mineral.* vol. 45, pp. 92—98.
- SRIRAMADAS, A. (1957) Diagrams for the correlation of unit cell edges and refractive indices with the chemical composition of garnets. *Am. Mineral.*, vol. 42, No. 3—4, pp. 294—298.
- TRÖMEL, G. and EITEL, W. (1957) Die Synthese von Silikatapatiten der Britholith-Abukumalit Gruppe. *Zeit. Krist.* 109, pp. 231—239.
- v. VOLBORTH, A. (1954) Phosphatminerale aus dem Lithiumpegmatit von Viitaniemi, Eräjärvi, Zentral-Finnland. *Ann. Acad. Sci. Fennicae, Ser. A, III, No. 39,* pp. 1—90.
- »— (1956) Die Mineralparagenese im Lithiumpegmatit von Viitaniemi (Zentralfinland) vom geochemischen Standpunkt. *Tscherm. Miner. u. Petrog. Mitt.*, F. 3, Bd. 5, H. 4, pp. 273—283.
- YODER, H. S. and KEITH, M. L. (1951) Complete substitution of aluminium for silicon; the system  $3\text{MnO} \cdot \text{Al}_2\text{O}_3 \cdot 3\text{SiO}_2 - 3\text{Y}_2\text{O}_3 \cdot 5\text{Al}_2\text{O}_3$ . *Am. Mineral.*, vol. 36, nos. 7—8, pp. 519—533.

# PALEOMAGNETISM OF THE DIKE SYSTEMS IN FINLAND

## II REMANENT MAGNETIZATION OF DOLERITES IN THE VAASA ARCHIPELAGO

BY

K. J. NEUVONEN

*Institute of Geology, University of Turku, Finland*

### ABSTRACT

The strength and direction of the remanent magnetization of a dolerite dike system in western Finland is observed to be similar to that previously measured for Jotnian dolerite dikes in southwestern Finland. Consequently, both systems can be considered to be almost of the same age. The position of the paleomagnetic pole measured is Longitude 164°E and Latitude 7°N.

### CONTENTS

	Page
Introduction .....	275
Samples and measurements .....	276
Demagnetization .....	277
Discussion of results .....	278
References .....	281

### INTRODUCTION

The direction of the remanent magnetization measured on the Jotnian olivine dolerites in southwestern Finland (Neuvonen, 1965) was stable and showed so little variation that the results obtained encouraged the extension of magnetical measurements to other dolerite systems in Finland as well.

TABLE 1.

Mineral composition (mode) of some dolerite samples from Vaasa archipelago used for magnetic measurements.

Sample No	235.1	237.1	240.1	244.1	246.1
Plagioclase (An 55—65) .....	62.2	63.0	76.1	68.9	55.3
Olivine .....	11.5	28.9	14.2	14.5	10.3
Augite .....		1.5	1.5	12.0	24.2
Hypersthene .....	23.7				
Magnetite .....	1.6	3.7	3.8	2.7	8.9
Biotite, hornblende, and chlorite .....	1.0	2.3	2.5	1.7	1.1
Accessories .....		0.6	1.9	0.2	0.2
	100.0	100.0	100.0	100.0	100.0

A dolerite dike system is known to occur in western Finland in the archipelago outside the town of Vaasa (Saksela, 1933, Laitakari, 1942 and Nykänen, 1960). Medium coarse dolerite occurs in the area on several small islands and forms sub-parallel dikes in NW-SE direction. The rock is well preserved and is petrographically very similar to the Jotnian dolerite in Satakunta, southwestern Finland. Table 1 shows the mineral composition of some of the dikes. On an average, the plagioclase content is somewhat higher than in the Satakunta area. Additional mode analyses and a chemical analysis of the Vaasa dolerites are given by Nykänen (1960). The age of dikes in the Vaasa area is not known. Since they cut through the Precambrian basement complex in a manner similar to the Jotnian dikes in southwestern Finland and are fully undeformed, they are generally assumed to be of Jotnian age (Laitakari, 1942). It should be remembered, however, that in Sweden, on the other side of the Gulf of Bothnia, there are dolerite dike systems which are considered to be still younger.

#### SAMPLES AND MEASUREMENTS

The sampling, demagnetization and measuring techniques used were mainly the same as those employed during the previous work (Neuvonen, 1965). Fifteen vertically drilled and oriented samples, 32 mm in diameter, were collected from thirteen on the islands in the area. The samples were cut into 32 mm high cylindrical specimens, altogether 108 in number. The strength and direction of the remanent magnetization was determined by measuring the specimens in 12 different positions with an astatic magnetometer. The direction of the natural remanent magnetization in the samples was calculated and combined from the specimen measurements using the statistical method of Fisher (1953).

First measurements were made on untreated specimens as soon after collection as possible. Table 2 lists the collection sites, the direction and intensity values of the remanent magnetization and the paleomagnetic pole positions calculated.

TABLE 2.

Direction of remanent magnetization of Vaasa dolerites mesured before demagnetization.

Sample No	Locality			Magnetic direction					Intensity c.g.s./cm <sup>3</sup>	Pole position		
	Name	Lat. N	Long. E	Decl.	Incl.	$\alpha_{95}$	k	N		Lat.	Long.	
233.1	Rågskäret .....	63.0	20.9	35°	-22°	6°	67.4	7	11	10 <sup>-4</sup>	11°N	166°E
234.1	Strömmings- bådan .....	63.0	20.7	35°	-7°	7°	51.1	8	14	»	18°N	163°E
235.1	Fälskär .....	63.1	20.8	35°	-18°	2°	930.2	5	16	»	13°N	165°E
235.2	Fälskär .....	63.1	20.8	36°	-21°	1°	627.9	8	15	»	11°N	165°E
236.1	Lågbådan .....	63.1	20.8	34°	-7°	5°	74.9	9	12	»	18°N	165°E
237.1	Storskär E .....	63.1	20.9	41°	-17°	5°	110.0	6	17	»	12°N	160°E
238.1	Storskär N .....	63.1	20.9	42°	-1°	3°	189.1	9	11	»	19°N	156°E
239.1	Fåfångkobben ..	63.1	20.9	46°	-11°	5°	90.1	9	14	»	13°N	154°E
240.1	Rönnskär .....	63.1	20.9	45°	+14°	4°	250.0	6	12	»	25°N	150°E
241.1	Hamnskär .....	63.1	20.9	45°	-17°	3°	245.6	8	13	»	11°N	156°E
242.1	Krokskär .....	63.1	20.9	38°	-11°	5°	142.1	6	18	»	16°N	161°E
243.1	Kobberget .....	62.9	21.0	72°	-9°	5°	96.0	8	6	»	4°N	129°E
244.1	Brusen .....	62.9	21.0	35°	-26°	13°	21.1	6	13	»	9°N	167°E
245.1	Bergbådan .....	63.0	21.1	32°	-24°	3°	336.5	8	13	»	11°N	170°E
246.1	W om Bergbådan	63.0	21.1	33°	-20°	2°	379.3	5	18	»	13°N	167°E
Mean of all samples		63.0	20.9	40°	-13°	6.8°	46.7	15	$\delta_m = 7.0^\circ$ $\delta_p = 3.5^\circ$		13°N	160°E

The magnetic directions so measured do not vary greatly. All samples show declination between north and east and all but one sample have negative (upwards) inclinations. Positive inclination was observed, however, in quite a few specimens originating at the top ends of the sample cores drilled. The same thing was observed in many Jotnian dolerite samples in the Satakunta region, where it was found out (Neuvonen, 1965) that the positive inclination on the top most specimens was caused by secondary magnetization connected with the surface weathering of the rock.

### DEMAGNETIZATION

The secondary magnetization is, fortunately, weak and can be »cleaned» out by partial demagnetization in an alternating magnetic field (As and Zijdeveld, 1958) or by heating (Chamalaun and Creer, 1964). Both methods were successfully employed on the Satakunta dolerites and the use of the methods was verified by trials with »pilot» specimens before demagnetization of all of the samples from the Vaasa region. The apparatus and the methods were the same as described previously (Neuvonen, 1965). Every second specimen of each sample core was demagnetized with an alternating magnetic field and the rest of the specimens were heat treated. Table 3 lists the magnetic directions measured after demagnetization of the specimens in 300 oersteds (peak) field and Table 4 shows the magnetic orientation found after heating. The heat treatment was performed by immersing the specimens (as many as

TABLE 3.  
Remanent magnetisation of the dolerites from Vaasa archipelago measured after  
A.C. demagnetisation.

No Sample	Locality			Magnetic direction					Intensity c.g.s./cm <sup>3</sup>	Position of the virtual Pole	
	Name	Lat. N	Long. E	Decl.	Incl.	$\alpha_{95}$	k	N		Lat.	Long.
233.1	Rädskäret . . . . .	63.0	20.9	30°	—36°	10°	46.5	4	1.4.10 <sup>-4</sup>	4°N	173°E
234.1	Strömning- bådan . . . . .	63.0	20.7	42°	—29°	6°	120.0	4	2.4 »	5°N	160°E
235.1	Fälskär . . . . .	63.1	20.8	35°	—32°	2°	2 857.1	3	4.4 »	5°N	168°E
235.2	Fälskär . . . . .	63.1	20.8	32°	—36°	3°	535.7	4	4.2 »	3°N	171°E
236.1	Lägbådan . . . . .	63.1	20.8	34°	—28°	4°	303.0	5	2.6 »	7°N	168°E
237.1	Storskär, E . . . . .	63.1	20.9	36°	—37°	3°	281.7	3	3.8 »	2°N	167°E
238.1	Storskär, N . . . . .	63.1	20.8	34°	—28°	6°	96.9	5	2.3 »	8°N	167°E
239.1	Fäfangkobben . . . . .	63.1	20.9	36°	—38°	8°	65.6	5	3.5 »	1°N	168°E
240.1	Rönnskär . . . . .	63.1	20.9	35°	—5°	22°	13.4	3	1.3 »	19°N	164°E
241.1	Hamnskär . . . . .	63.1	20.9	36°	—35°	2°	937.5	4	3.7 »	3°N	167°E
242.1	Krokskär . . . . .	63.1	20.9	39°	—29°	4°	392.2	4	4.3 »	6°N	162°E
243.1	Kobberget . . . . .	62.9	21.0	65°	—37°	23°	9.6	4	0.9 »	8°	142°E
244.1	Brusen . . . . .	62.9	21.0	28°	—35°	7°	144.9	3	1.6 »	5°N	175°E
245.1	Bergbådan . . . . .	63.0	21.1	39°	—12°	11°	39.6	4	0.7 »	20°N	160°E
246.1	W om Bergbådan	63.0	21.1	33°	—38°	4°	363.6	3	2.7 »	2°N	171°E
Mean of all samples		63.0	20.9	37°	—30°	5.8°	46.7	15		6°N	166°E

ten a time) for several hours in heavy oil (Cyless) at 300°C or in a fine sand bath at 400°C. Heating, cooling and the a.c. demagnetization were carried out in zero magnetic field inside an Helmholtz coil. The demagnetization improved the measurements. The negative inclination also increased for all the samples measured. The magnetic directions revealed are very similar for both cleaning methods and the results can be combined. This is done in Table 5.

## DISCUSSION OF RESULTS

After cleaning the secondary magnetization, all the samples measured show very similar magnetic orientation. This indicates that all the dolerite dikes measured belong to a suite of a same age. In addition, the magnetic direction revealed by the Vaasa dolerites is highly similar to that measured on the Jotnian dikes in the Satakunta region. The mean direction of all samples in the Satakunta area is  $D = +46^\circ$ ,  $I = -34^\circ$  compared with  $D = +38^\circ$ ,  $I = -29^\circ$  as determined for the Vaasa dolerites in this study. Consequently, the geomagnetic fields during the crystallization of these two dolerite dike systems did not notably differ from each other.

On the other hand, the paleomagnetic pole positions (Fig. 1) calculated on the basis of the present measurements (Long. 164°E, Lat. 7°N) lies very close to the pole determined for the Satakunta dolerites (Long. 158°E, Lat. 2°N). The circles of confidence ( $p = 0.05$ ) are almost equal in size and they clearly overlap. This might

TABLE 4.  
Direction of remanent magnetization of Vaasa dolerites measured after thermal treatment at 300°—400°C.

Sample No	Magnetic directions			k	N	Intensity c.g.s./cm <sup>3</sup>
	Decl.	Incl.	$\alpha_{95}$			
233.1	30°	—29°	9°	74.9	3	10.10 <sup>-4</sup>
234.1	36°	—25°	6°	154.6	4	11 »
235.1	35°	—26°	—°	—	2	13 »
235.2	36°	—26°	3°	517.2	4	12 »
236.1	31°	—24°	7°	88.2	4	9 »
237.1	38°	—29°	4°	392.2	3	11 »
238.1	40°	—19°	7°	89.8	4	8 »
239.1	39°	—26°	5°	180.7	4	11 »
240.1	46°	+ 2°	8°	93.9	3	9 »
241.1	46°	—25°	2°	1 153.9	4	12 »
242.1	37°	—20°	2°	1 111.1	3	14 »
243.1	71°	—19°	7°	115.4	4	5 »
244.1	33°	—25°	3°	714.3	3	11 »
245.1	36°	—32°	3°	600.0	4	11 »
246.1	35°	—28°	—°	—	2	15 »
Mean	39°	—25°	58°	47.3	15	

TABLE 5.  
Direction of remanent magnetization of Vaasa dolerites measured after removal of the secondary magnetization by a.c. or thermal treatment

Sample No	Locality			Magnetic direction					Pole position	
	Name	Lat. N	Long. E	Decl.	Incl.	$\alpha_{95}$	k	N	Lat.	Long.
233.1	Rågskäret . . . . .	63.0	20.9	30°	—33°	7°	59.1	7	6°N	172°E
234.1	Strömning- bådan . . . . .	63.0	20.7	39°	—27°	5°	118.6	8	7°N	163°E
235.1	Fälskär . . . . .	63.1	20.8	35°	—23°	4°	317.5	5	7°N	167°E
235.2	Fälskär . . . . .	63.1	20.8	34°	—31°	4°	177.2	8	6°N	168°E
236.1	Lågbådan . . . . .	63.1	20.8	33°	—27°	4°	142.4	9	9°N	169°E
237.1	Storskär E . . . . .	63.1	20.9	37°	—33°	4°	185.9	6	4°N	166°E
238.1	Storskär N . . . . .	63.1	20.8	37°	—24°	5°	72.4	9	9°N	164°E
239.1	Fäfangkobben . . . . .	63.1	20.8	38°	—33°	6°	61.6	9	4°N	165°E
240.1	Rönnskär . . . . .	63.1	20.9	41°	— 4°	11°	25.2	6	18°N	158°E
241.1	Hamnskär . . . . .	63.1	20.9	41°	—30°	5°	120.1	8	5°N	162°E
242.1	Krokskär . . . . .	63.1	20.9	38°	—24°	4°	192.3	6	9°N	164°E
243.1	Kobberget . . . . .	62.9	21.0	69°	—28°	12°	15.9	8	4°	137°E
244.1	Brusen . . . . .	62.9	21.0	31°	—31°	4°	235.9	6	4°N	172°E
245.1	Bergbådan . . . . .	63.0	21.1	37°	—22°	8°	35.1	8	10°N	164°E
246.1	W om Bergbodan	63.0	21.1	34°	—34°	5°	140.4	5	4°N	169°E
Mean of all samples		63.0	20.9	38°	—29°	5.0°	53.9	15		

Pole position: latitude 7°N, longitude 164°E,  $\delta m = 5.5^\circ$ ,  $\delta p = 3.2^\circ$

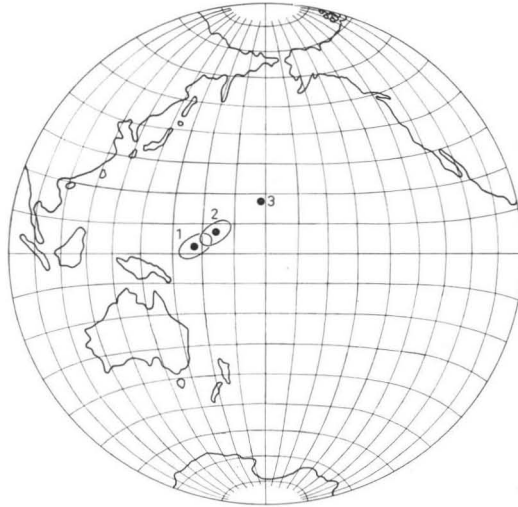


FIG. 1. Paleomagnetic poles. 1) Pole and the oval of confidence ( $p = 0.05$ ) determined by the magnetic directions of the Satakunta dolerites. 2) Paleomagnetic pole determined on the Vaasa dolerites. 3) position measured on the Norwegian sparagmites by Harland and Bidgood (1959).

mean that the two poles can be considered to be just one and the two dolerite suites to belong together. To test whether the two pole directions are identical, the statistical method given by Watson and Irving (1957) can be used. The identity of dispersions of the two populations must, however, be tested first. In the Vaasa area 15 sites ( $N_1 = 15$ ) give an estimate  $k_1 = 61.04$  and 18 Satakunta dolerite sites ( $N_2 = 18$ ) give an estimate  $k_2 = 53.87$ . The ratio of the variances

$$F_{28,34} = 61.04/53.87 = 1.13$$

is not significant, and there is no reason for supposing the two populations to have different dispersions.

The identity of the two polar vectors can now be tested by the statistic

$$(N-2) (R_1 + R_2 - R)/(N-R_1-R_2)$$

in which  $N = 33$ ,  $R_1 = 17.722$  (Satakunta),  $R_2 = 14.740$  (Vaasa), and  $R = 32.359$  (resultant of all directions). It gives for 2 and 2 ( $N-2$ ) degrees of freedom,

$$F_{2,62} = 5.89$$

which is significant at level  $p = 0.05$  but not significant at level 0.01. Thus the data give no or very little reason for supposing the two polar vectors to be identical.

The paleomagnetic poles determined by the Jotnian dolerites and by the Vaasa dolerites are close to a pole determined by Harland and Bidgood (1959) for the sparagmites in southeastern Norway. This is the only paleomagnetic pole of Precambrian age measured in Europe which, as quoted by Irving (1964), lies near the poles now determined. The sparagmite formation in Norway is, according to present knowledge, about 300 m.y. younger than the Jotnian dolerites. Since the Vaasa dolerite pole lies between the other poles (Fig. 1), the age of the Vaasa dolerites might also be assumed to be between those of the Jotnian and sparagmite formations. Since the Vaasa dolerite pole is very close to that of the Jotnian dolerites the difference in age can only be very small, *viz.* less than 100 m.y. Many more paleomagnetic measurements and age determinations must be done, however, before reliable conclusions can be drawn concerning the age relations of the dike systems and other rocks in Finland.

*Acknowledgements.* — Sincere thanks are due to all the persons who helped and assisted me during this study. Thanks are also given to The National Scientific Research Council for the grant which made this work possible.

*Manuscript received, 25 March, 1966*

#### REFERENCES

- As. J. A. and ZIJDERVELD, J. D. A. (1958) Magnetic clearing of rocks in paleomagnetic research. Royal Astron. Soc. Geoph. Journ., Vol. 1, pp. 308—319.
- CHAMALAUN, F. H. and CREER, K. M. (1964) Thermal demagnetization studies on the old sandstone of the Anglo-Welsh cuvette. Journ. Geoph. Research, Vol. 69, pp. 1 607—1 616.
- FISHER, R. A. (1953) Dispersion on a sphere. Royal Soc. London Proc., ser. A, Vol. 217, pp. 295—305.
- HARLAND, W. B. and BIDGOOD, D. E. T. (1959) Paleomagnetism in some Norwegian sparagmites and the late Pre-Cambrian ice age. Nature, Vol. 184, pp. 1 860—1 862.
- IRVING, E. (1964) Paleomagnetism and its application to geological and geophysical problems. John Wiley & Sons, inc., New York/Sydney.
- LAITAKARI, AARNE (1942) Kivilajikartan selitys B 3, Vaasa. Zusammenfassung. General geological map of Finland, 1 : 400 000.
- NEUVONEN, K. J. (1965) Paleomagnetism of the dike systems in Finland. I. Remanent magnetization of Jotnian olivine dolerites in southwestern Finland. Compt. Rend. Soc. géol. Finlande, Vol. 37, pp. 153—168.
- NYKÄNEN, OSMO (1960) Kallioperäkartan selitys 1242-Korsnäs, English summary: Explanation to the map of rocks. Geological map of Finland, 1 : 100 000.
- SAKSELA, MARTTI (1933) Pre-Quaternary rocks B 3, Vaasa; General geological map of Finland, 1 : 400 000.
- WATSON, G. S., and IRVIN, E. (1957) Statistical methods in rock magnetism. Monthly Notices Roy. Astron. Soc. Geoph. Suppl., Vol. 7, pp. 289—300.



# PLAGIOCLASE ZONING IN A GABBROIC DIKE FROM ALATORNIO, NORTHERN FINLAND

BY

MAUNU HÄRME and JAAKKO SHIVOLA

*Geological Survey of Finland, Otaniemi*

## ABSTRACT

This is a preliminary report on the study of the zoned structure of a plagioclase. The oscillatory variation of Ca-content in a zoned plagioclase is determined with an electron probe microanalyser. The cause of the zoning is discussed; the oscillation of the hydrostatic pressure in the melt during the crystallization is probably one of the primary causes in the formation of a zoned structure.

## INTRODUCTION

The zoning in plagioclases is conspicuous especially in extrusive and hypabyssal rocks. It is common also in the plagioclases of plutonic and metamorphic rocks but in these cases the boundary lines between the different zones are usually not as sharp as in the extrusive rocks. The compositional and structural determinations by means of optical and X-ray methods are, on account of the density of the zoning, often very difficult and inaccurate but a new possibility for compositional study is given by the electron probe microanalyser (Geoscan).

According to classic opinion (*e.g.* Bowen, 1928) the An-content of an igneous plagioclase depends on the composition of the melt from which it is crystallizing. Often, however, the very sharp boundaries between the zones in the plagioclases of the igneous rocks give reason to suspect that also other factors than the composition of the magma have been involved in the crystallization and caused the compositional variations of the An-content of the different zones.

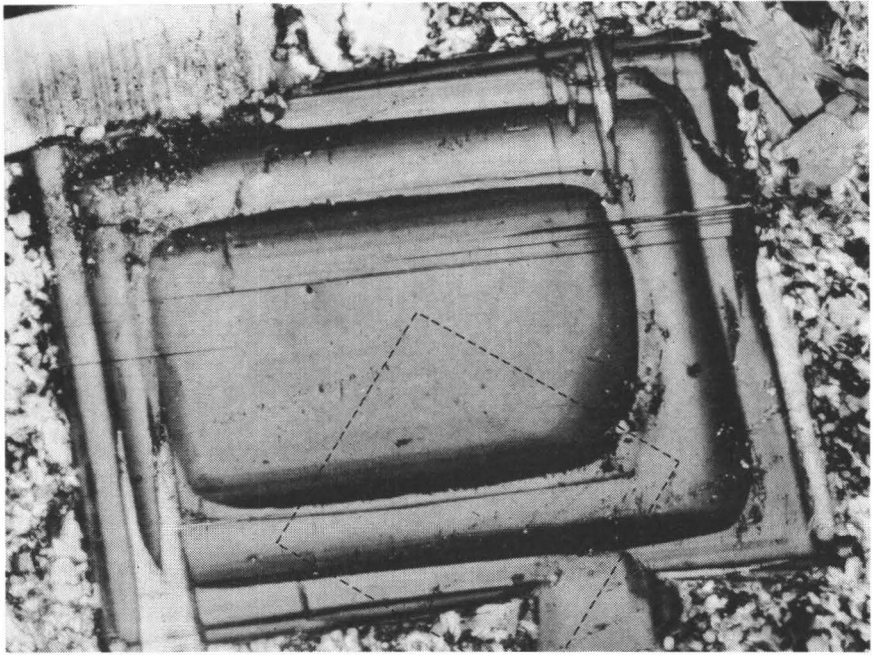


FIG. 1a. Euhedral zoned plagioclase from a porphyritic marginal variety of a gabbroic dike. The margin of the center zone shows corrosion to have taken place before the crystallization of the next broad zone. Palonkalliot. Alatornio. Nic. +. Magn about 125 x.

## PETROGRAPHY

A plagioclase from the chilled contact of a gabbroic dike has been the object of this study. The dike is about 10 meters broad and is situated in a mica schist in the parish of Alatornio, northern Finland. The dike belongs to the igneous Haparanda suite (*cf.* Ödman, Härme, Mikkola and Simonen, 1949; Härme, 1949; A. Mikkola, 1949). It is typical of the rocks of this suite that their plagioclases have a well developed zoned structure. The pyroxenes and amphiboles often show also a noticeable zoning. Kouvo (1950) has made detailed optical determinations on the plagioclases of the rocks of this suite. He has also discussed the causes of the zoning and pointed out the possible effect of hydrostatic pressure during magmatic crystallization as one cause.

The central part of the afore-mentioned dike is an even-grained gabbroic rock rich in plagioclase. Towards the margins the rock gradually passes over into a porphyritic variety in which the plagioclase phenocrysts lie in a fine-grained groundmass. These phenocrysts have a well developed zoned structure.

Figs. 1 a and b are photomicrographs of a zoned plagioclase grain. The plagioclase shows zoning on a large scale but inside the main zones minor rectilinear oscillatory

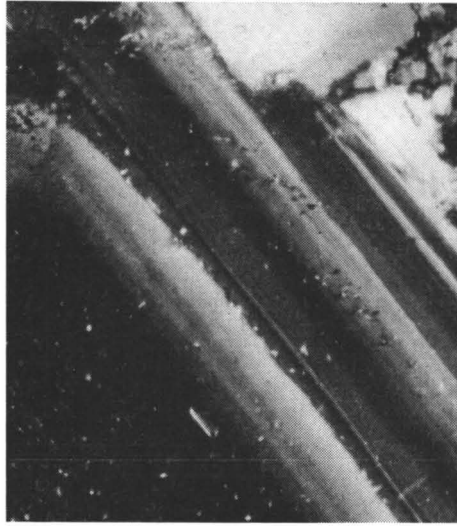


FIG. 1b. A part of the zoned plagioclase seen in Fig. 1a (bounded by the broken line). Nic. +. Magn. about 250 x.

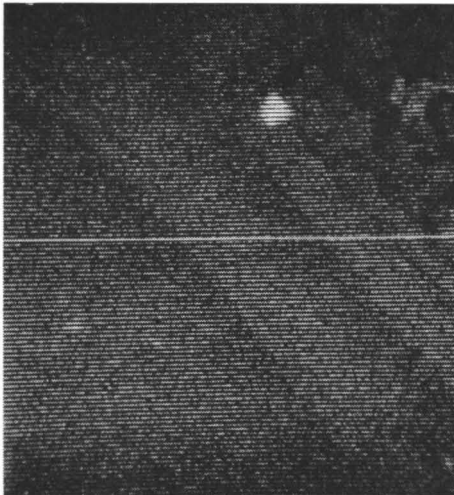


FIG. 2. X-ray image (Ca K $\alpha$  radiation) of that part of plagioclase seen in the same scale in Fig. 1b.

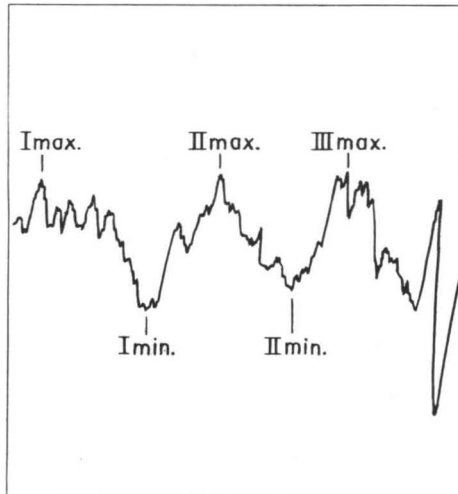


FIG. 3. Ca K $\alpha$  intensity along the line indicated in Fig. 2 (determined by J. Siivola).

TABLE 1.

CaO-contents (determined by J. Siivola) and the corresponding An-contents of the maxima and minima in the CaK $\alpha$  intensity diagram in Fig. 3.

	CaO-content %	Calculated An-content %
Core of the plagioclase .....	19.3	95.7
I maximum .....	19.8	98.2
I minimum .....	13.3	66.0
II maximum .....	20.2	100.2
II minimum .....	13.9	68.9
III maximum .....	19.6	97.2
(standard) .....	(12.8)	(63.5)

zones occur. The borderline between the center area and the next main zone cuts obliquely the minor zoning of the center area. Obviously corrosion has taken place before the crystallization of the next main zone. Fig. 2 is an X-ray image (Ca K $\alpha$  radiation) showing the variations of the Ca-content in the zoned marginal part of the same plagioclase. Fig. 3 is the Ca K $\alpha$  intensity along a line across the zones. The diagram shows sharp oscillation, and both increase and decrease of the Ca-content. The CaO-contents of the maxima and minima as well as the corresponding percentages of the anorthite are presented numerically in Table 1. The An-contents of the maxima are very high, and obviously a Ca-rich composition is also a peculiar case to form great compositional differences between the various zones of a plagioclase. An optic study reveals few inclusions in this plagioclase but the II maximum is probably caused by a Ca-rich inclusion because it shows a somewhat higher CaO-content (*cf.* Table 1) than a pure anorthite. On the other hand, that deviation is perhaps due to an analytical error.

The zoning of this plagioclase reveals periodicity on a large scale (Fig. 3, between the maxima and minima) but within the large periods sharp irregular oscillation of the Ca-content occurs, discernible also optically (Fig. 1b) as zoning on a small scale. No clear tendency of the An-content to decrease from the core towards the margin is observable in this plagioclase.

## DISCUSSION

When considering the causes of the formation of this kind of zoned structure it can be stated that three factors have an effect on the crystallization: the composition of the melt, the crystallization temperature and the prevailing hydrostatic pressure. The borderlines between the different zones in plagioclases of igneous rocks are sometimes very sharp, and this feature indicates that sudden changes of the crystallization conditions have taken place. Rapid great changes of the composition of

the melt are less likely. The quick changes of temperature in both directions are also unlikely in a large magma chamber. The factor which may change suddenly in a melt is the hydrostatic pressure. The changes of temperature and pressure are interdependent but primarily sudden changes in the hydrostatic pressure are more likely to occur than those in the temperature.

The structures of plagioclases are complex and vary according to their chemical compositions (Deer, Howie and Zussman, 1964, p. 95). Tuttle and Bowen (1958, p. 15) have stated that the stability of some structures of albite depends on pressure and temperature. According to experimental work it is known that the annealing can change the structural order and even change the structure of the plagioclase (*e.g.* Tuttle and Bowen, 1950; Gay, 1953, 1954, 1961; Gay and Bown, 1956; Smith and Gay, 1958; Megaw, 1961; Laves and Goldsmith, 1961; Marfunin, 1962). Thus — when the structure depends on the composition, and the structure may change with the temperature — it is possible that also the pressure may have an effect on the composition of a crystallizing plagioclase. The effect of the hydrostatic pressure on the composition of the plagioclase is not known on the basis of experimental work but many facts in the field point out that the pressure is also a significant factor in the crystallization. If this is true then also the tectonic history must have an influence on the magmatic crystallization differentiation.

Studies dealing with the role of pressure in crystallization are few in number. Carr has made optical determinations on the zoned plagioclase of the Skaergaard gabbro (Greenland) and (Carr, 1954, p. 372) has presented the opinion that »zoning was mainly caused by variation in hydrostatic pressure due to vertical movement of the convecting magma and crystals.« Ewart (1963) has studied some volcanic rocks of New Zealand and found that their plagioclase has extremely well-developed oscillatory zoning. He has regarded it (p. 429) »as due to the movement of crystals within the magma into zones of varying vapour pressure. Many crystals show sharp discontinuities of some zones which are attributed to sharp decreases in vapour pressure, possibly due to previous eruptions.«

In this preliminary study the variation diagram of Ca-content is given only because it best revealed the compositional variations in the studied zoned plagioclase. Many facts, however, give reason to suppose that the contents of some accessory elements may also vary significantly in the zoned plagioclase and cause optical differences between the zones. It is still to be noted that some pyroxenes and amphiboles of the rocks of the same Haparanda suite have a zoned structure and in these minerals the Mg/Fe ratio varies significantly in different zones.

*Manuscript received, March 26, 1966*

## REFERENCES

- BOWEN, N. L. (1928) The evolution of the igneous rocks. Princeton University Press. Princeton, New Jersey.
- CARR, J. (1954) Zoned plagioclases in layered gabbros of the Skaergaard intrusion, east Greenland. *Mineral. Mag.* 30, No. 225, p. 367.
- DEER, W. A., HOWIE, R. A. and ZUSSMAN, J. (1964) Rock-forming minerals. Vol. 4. Longmans, Green and Co Ltd. London.
- EWART, A. (1963) Petrology and petrogenesis of the Quaternary pumice ash in the Taupo area, New Zealand. *J. of Petrol.* 4, No. 3, p. 392.
- GAY, P. (1953) The structures of the plagioclase feldspars: III. An X-ray study of anorthites and bytownites. *Mineral. Mag.* 30, No. 222, p. 169.
- (1954) The structures of the plagioclase feldspars. V. The heat-treatment of lime-rich plagioclases. *Mineral. Mag.* 30, No. 226, p. 428.
- (1961) Some recent work on the plagioclase feldspars. *Cursillos y Conferencias del »Lucas Mallada«*. Fasc. VIII, p. 159.
- GAY, P. and BOWN, M. G. (1956) The structure of the plagioclase feldspars: VII. The heat treatment of intermediate plagioclases. *Mineral. Mag.* 31, No. 235, p. 306.
- HÄRME, MAUNU (1949) On the stratigraphical and structural geology of the Kemi area, northern Finland. *Bull. Comm. géol. Finlande* 147.
- KOUVO, OLAVI (1950) Haaparantasarjan kivilajeista ja niissä esiintyvistä mineraalien vyöhykerakenteista. Pro gradu. Manuscript at Geology Department of the University of Helsinki.
- LAVES, F. and GOLDSMITH, J. R. (1961) Comments on the anorthite papers by Megaw and coworkers presented at this symposium. *Cursillos y Conferencias del »Lucas Mallada«*. Fasc. VIII, p. 155.
- MARFUNIN, A. S. (1962) Some petrological aspects of order-disorder in feldspars. *Mineral. Mag.* 33, No. 259, p. 298.
- MEGAW, H. D. (1961) Effects of temperature and composition in the plagioclases and other feldspars. *Cursillos y Conferencias del Instituto »Lucas Mallada«*. Fasc. VIII, p. 149.
- MIKKOLA, AIMO (1949) On the geology of the area North of the Gulf of Bothnia. *Bull. Comm. géol. Finlande* 146.
- SMITH, J. V. and GAY, P. (1958) The powder patterns and lattice parameters of plagioclase feldspars. II. *Mineral. Mag.* 31, No. 240, p. 744.
- TUTTLE, O. F. and BOWEN, N. L. (1950) High-temperature albite and contiguous feldspars. *J. of Geol.* 58, p. 572.
- (1958) Origin of the granite in the light of experimental studies in the system  $\text{NaAlSi}_3\text{O}_8$ — $\text{KAlSi}_3\text{O}_8$ — $\text{SiO}_2$ — $\text{H}_2\text{O}$ . *Geol. Soc. America, Mem.* 74.
- ÖDMAN, OLOF H., HÄRME, M., MIKKOLA, A. och SIMONEN, AHTI (1949) Den svensk-finska geologiska exkursionen i Tornedalen sommaren 1948. *Geol. Fören. i Stockholm Förh.* 71, H. 1, p. 113.

## ON THE TITANIFEROUS ORE OXIDES IN SOME SUBSILICIC DIKES AND SILLS

BY

O. VAASJOKI and KAUKO PUUSTINEN

*Institute of Geology and Mineralogy, University of Helsinki*

### ABSTRACT

Distinct difference exists with regard to iron titanium oxides and their fabrics in samples of diabases either from Precambrian or Tertiary age. The old diabases, representing occurrences of deep erosional level, are characterized by magnetites forming abundant intergrowths with exsolved ulvite. The ore oxides in samples of the young diabase, associating Tertiary plateau basalt formation, are characterized by skeletal grains of titanomagnetite and ilmenite. The geological features of sample localities and the petrography of sampled rocks have been explained.

### CONTENTS

	Page
Introduction .....	288
Description of Localities and Samples .....	290
Valamo Area .....	290
Syväri Area .....	292
Kvandalen Disko .....	292
The Ore Microscopic Observations .....	294
Remarks on the Relations of the Fe-Ti-Phases in the Samples Studied .....	298
Conclusion .....	300
Acknowledgement .....	300
References .....	301

### INTRODUCTION

The dependence obviously existing between the properties in mineralogy and fabrics of titaniferous iron ore components and the properties of the host involved has been a subject of a number of significant investigations (*e.g.* Ramdohr, 1939 and

1956; Buddington *et al.*, 1955 and 1964; Vincent *et al.*, 1954 and Vincent, 1960). This subject was dealt also by Vaasjoki and Heikkinen in the course of a previous study on titaniferous magnetites (1962). In that connection it was pointed out that dense intergrowths of magnetite and ulvite especially characterize the fabrics of titaniferous magnetites associated with doleritic or diabasic rocks. On this topic additional observations and comments will be offered in the paper at hand.

The samples studied principally form two separate groups; one part is from formations intruded during Precambrian Jotnian time while another part is from a diabase of Tertiary age. The first mentioned is represented by samples from Valamo and Syväri (Svir) areas which are situated in Karelia, U.S.S.R. (Fig. 1). The specimens from these areas belong to the collection sampled by Dr. Professor Emeritus W. Wahl at the beginning of this century. For the present study the collection was made available by the Museum of Geology and Mineralogy of the University of Helsinki. The term Karelian diabase as used here will cover the formations of both localities mentioned. The specimens of Tertiary diabase belong to material collected by the first author in summer of 1963 from Disko island, West Greenland. In purpose to furnish the reader by sufficient information on the geologic character of the formations represented by specimens studied, short descriptions on the sample localities have been included. In case of Karelian samples this has been based on the relevant descriptions given in the earlier literature on the matter. The information on the sample locality in Disko is based on field notes carried out by the first author.

A background for the present investigation has been a study for master thesis carried out by the second author on petrographic features of the aforementioned diabase formations. The work was insisted and guided by the first author. The observations on the opaque materials, however, inspired a continued separate study concentrating especially on the fabrics of iron titanium minerals as demonstrated in the paper at hand. In the text to follow these minerals, for the sake of convenience have been usually expressed by term ore oxides.

## DESCRIPTION OF LOCALITIES AND SAMPLES

### Valamo area

The main island and surrounding archipelago of Valamo situated in the lake of Ladoga close to SE-border of Finland (Fig. 1) are composed of diabasic rocks which also are present in the islands of Mantsi, Lunkula and Konevitsa. Similar rocks as dikes of differing size also occur in the mainland of the western and northern shores of Ladoga. The lithology, stratigraphy and petrography of these subsilicic rocks have been dealt with in several earlier connections. Here especially the investigations by von Chrustschoff (1891), Sederholm (1893 and 1927) and Hackman (1933) are referred to. These earlier investigations, however, have not given closer considerations on the opaque components incorporating the diabasic rocks in question.

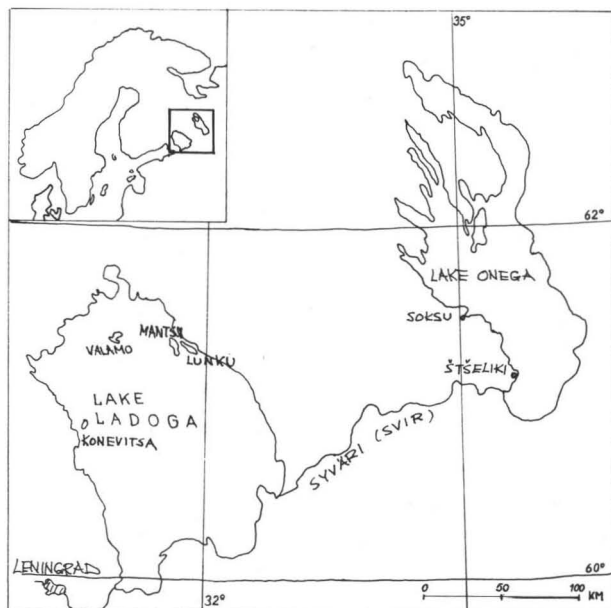


FIG. 1. Map showing the sample localities in Karelia, U.S.S.R.

The dominating rock in Valamo region is a medium grained, dark colored quartz diabase which locally may be accompanied by lighter colored, more silicic varieties. Frequent occurrence of aphanitic, glassy subsilicic veins in association with Valamo formations is most typical like the abundance of veinous, granophyric portions.

In this connection the dominating, texturally subophitic quartz diabase is considered only. The major components in the rock are plagioclase ( $An_{60}$ ) and monoclinic pyroxene which commonly is augite with  $2V_z = 44^\circ$  and  $c \wedge Z = 45^\circ$ . Sometimes the pyroxene approaches pigeonite in composition as indicated by smaller value of optic axis angle ( $2V_z = 20^\circ$ ). Amphibole, biotite and serpentine exist in minor amounts and they generally are alteration products after the pyroxenes. Accessory apatite is abundantly present. In agreement with the common field occurrence of granophyric portions small dimensioned intergrowths of potash feldspar and quartz appear as characteristic microscopic feature in these rocks. On places the alteration of silicatic components is present in a remarkable degree.

The opaque minerals are variably present as accessory components and are dominated by ore oxides. Sulphide minerals like pyrite, pyrrhotite and chalcopyrite usually in minute grains are sporadic in occurrence.

### Syväri area

The diabase rocks of Syväri region occur in large outcrops and have been demonstrated already close to or in change of 19th century especially by Helmersen (1860 and 1882), Jakowleff (1905), Ramsay (1906) and Wahl (1908).

The areas intruded by diabase sills in the Syväri region in the first hand are known as areas of horizontal or slightly tilted beds of unmetamorphic sandstones of late Precambrian Jotnian age. An illustrating example on the relationship between a diabase sill and the intruded sandstone from the vicinity of Štšeliki village, Syväri region, has been demonstrated by Ramsay (1906). The sill cropping out in this locality is ca. 30 meters thick and forms ridges stretching ca. 3.5 kilometers to North from the village mentioned. At its footwall the diabase borders to sandstone. Along the contact the sandstone has been recrystallized while the diabase is forming a dense, aphanitic border variety. In its central part the ridge has been cut by a fault running in direction N25°W (Fig. 2).

Because the diabase rocks in the Syväri region regularly occupy the uppermost part in the outcrops it is apparent as proposed by Wahl (1908) that the hanging wall parts of the sandstone formation have been eroded. According to Wahl the diabases in the Syväri area originated as one large sill the intrusion of which probably took advantage of fault zone running in direction SSE—NNW in the immediate vicinity of the western shore of the lake Onega. As evidenced by presence of a number of fault lines the originally uniform sill, however, has been dislocated by later block movements (*cf.* Fig. 2).

The dominating rocks amongst the Syväri diabases is a darkish gray, fine grained quartz diabase. It is associated with a medium to coarse grained variety which usually shows strong alteration phenomena. In immediate contact with sandstone the diabases are dense and aphanitic in appearance.

The dominating, fine grained diabase is microscopically rather homogeneous, slightly altered and texturally subophitic. The major components are plagioclase ( $An_{60}$ ) and monoclinic pyroxenes which are represented by augite ( $2V_z = 42^\circ$ ) and pigeonite ( $2V_z = 12^\circ$ ). Minor amphibole occurs as small independent laths or as an alteration product after pyroxenes. The assemblage of typical accessory minerals include biotite, apatite and opaque grains. Micrographic textures of potash feldspar and quartz corresponding to those observed in the samples from Valamo area, have been noticed here and there.

### Kvandalen, Disko

Disko island, West Greenland, forms a well known locality of formations belonging to the Brito Arctic basalt province. It is also known as an area of basalt flows containing native iron. The series of these rocks, the eruption of which commenced during the Eocene, are excellently exposed in the valley of Kvandalen in NE-part of Disko. The total length of this canyon like valley system is almost 40 kilometers

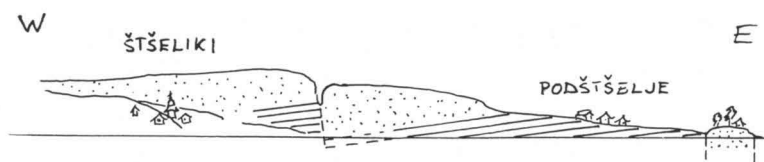


FIG. 2. Section of the occurrence of quartz diabase at Stselik, Karelia, U.S.S.R.  
Ruled = sandstone, dotted = diabase. According to Ramsay (1906).

while the width varies between 5—10 kilometers. The height of the basalt plateau on either side of the valley varies between ca. 300—1 400 meters whereby the height of the plateau escarpment as shown in Fig. 3 is around 600 meters. A river system runs at the bottom of the valley.

It is obvious that in relation to each other the plateau formations and underlying sediments of southern and northern side of the valley have been vertically displaced and that the valley actually follows one of the major faults in the region. In the northern side the lowermost visible horizon comprises dominantly pale colored sandstones intercalated by narrow beds of slaty and/or bituminous materials. In the river banks in the bottom of the valley the sediments generally crop out in sections 30—50 meters high. The series of plateau formations consists of layered basaltic materials composed of alternating beds of basalt flows, tuffaceous materials or so-called interbasaltic breccias of ignimbrite character. Frequent diabases occur as sills or dikes.

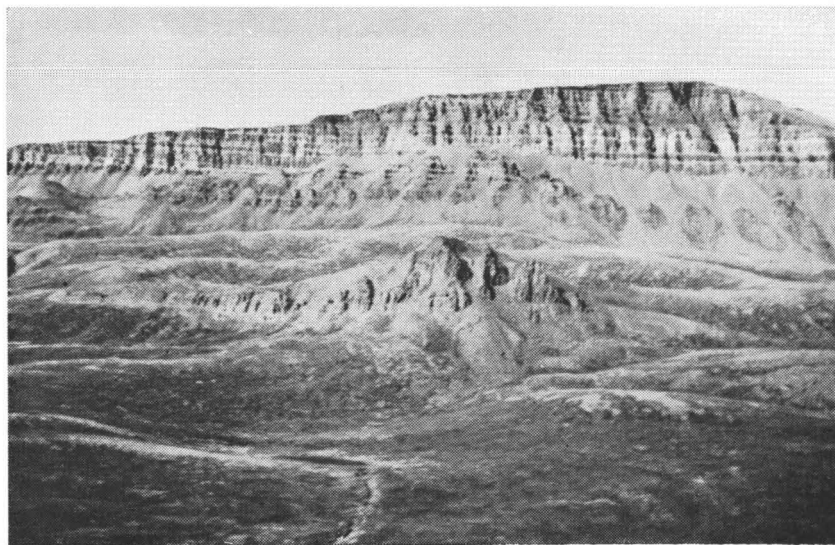


FIG. 3. A view to the formations in Kvandalen, Disko, West Greenland. The northern side of the valley with plateau escarpment. Photo by O. Vaasjoki.

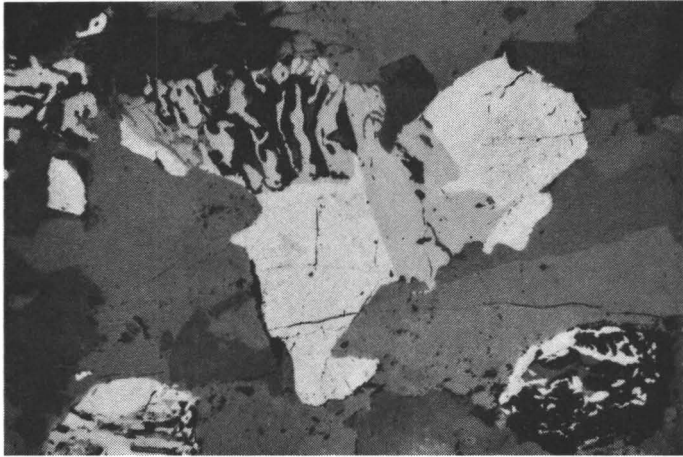


FIG. 4. Aggregate of myrmecitic ilmenite and magnetite in diabase. The magnetite is inhomogeneous due to a tendency of granule exsolution of titaniferous phases (greyish areas in the magnetite). In the middle platy portion of ilmenite. Stselik, Karelia, U.S.S.R. + nic., 50 x.

With regard to the petrographic composition the basalt flows in Kvandalen are tholeiites dominated by the presence of pyroxenes and plagioclase while the olivine occurs in minor amounts only or is entirely missing. The rocks appropriately might be called as olivine bearing basalt or as plagioclase basalt.

The samples used for the present study have been taken from a 5 meters thick dike of diabase piercing the river bank sediments in a locality which is situated in the central part of the Kvandalen valley. The occurrence obviously is a member of a swarm of diabase dikes running in direction  $N15^{\circ}W$  which approximately conjoins the direction of the valley system in Kvandalen. The elevation of the river plain in the sample locality is ca. 150 meters.

Microscopically the sampled rock is rather fine grained and texturally ophitic. The main constituents are plagioclase ( $An_{60}$ ) and monoclinic pyroxene. Strongly serpentinized olivine and opaque grains occur abundantly. The plagioclase grains are averagely 0.5 mm in length and some of them show a zonar structure. The pyroxene is diopsidic augite with  $2V_z = 51^{\circ}$  and  $\epsilon \wedge Z = 42^{\circ}$ . The olivine ( $2V_z = 86^{\circ}$ ) occur as grains averaging 0.2 mm in diameter. The grains are commonly serpentinized along grain borders and cracks in varyable amounts. The opaque material comprises both magnetite and ilmenite.

#### THE ORE MICROSCOPIC OBSERVATIONS

In all sampes investigated in the course of the present study the ore oxides form the predominant part of the opaque materials.

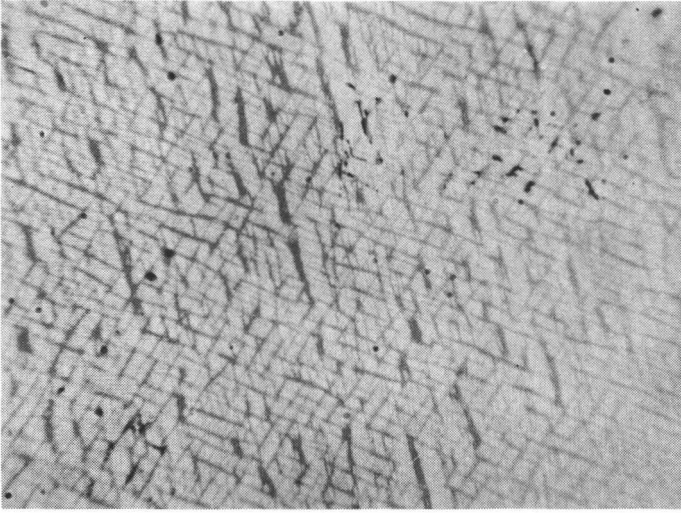


FIG. 5. Magnetite with network probably containing lamellae of ilmenite and ulvite. The lamellae in directions (111) and (100) planes. Diabase. Valamo island. Karelia, U.S.S.R. Oil im. One nicol, 1050 x.

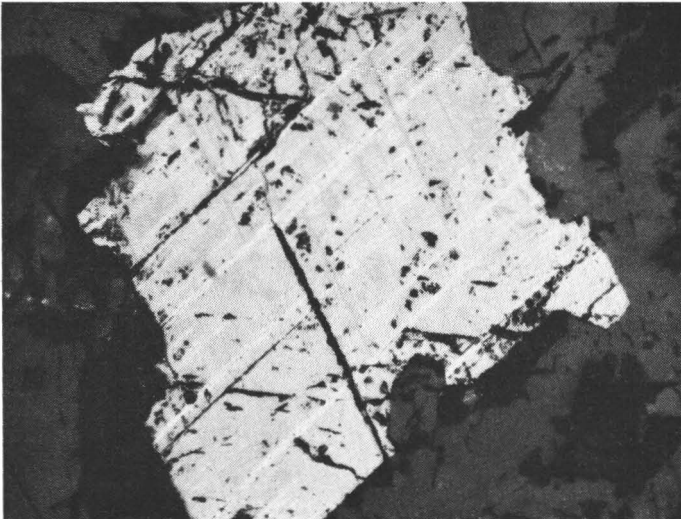


FIG. 6. Magnetite with lamellae of ilmenite along (111) planes. Irregular greyish flecks in the magnetite reveal a tendency of granule exsolution of titaniferous phases. Diabase. Stselik, Karelia, U.S.S.R. + nic., 130 x.

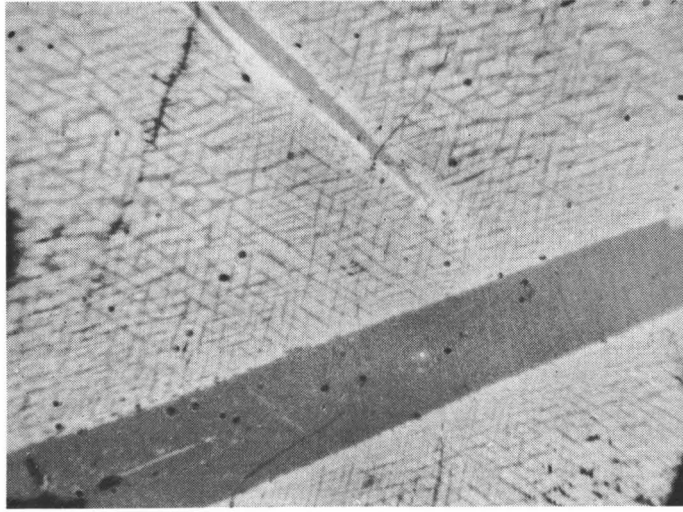


FIG. 7. Magnetite with ilmenite and ulvite. The thick lamellae of ilmenite in directions (111). Network of small lamellae along (111) probably ilmenite. In direction (100) faint lamellae traceable. Diabase. Valamo island, Karelia, U.S.S.R. Oil im. One nicol, 1050 x.

On basis of the preceding descriptions on the specimens studied it is obvious that the Karelian diabases are most similar in petrographic properties. This is even true when comparing the observations carried out under the reflected light on samples representing a common quartz diabase belonging to either one of the Karelian localities.

The ore oxides in the samples studied include ilmenite and titaniferous magnetite as individual grains or as aggregates formed of both of these minerals. The ilmenite forms myrmecite like textures with micaceous non-opaque material so far not identified (Fig. 4). In appearance ilmenite is homogeneous revealing no intergrowths with hematite.

Because the magnetite regularly seems to envelop the grains of the myrmecitic ilmenite the latter possibly might have crystallized as first phase in the aggregates in question. The magnetite commonly shows according to (100) a network texture which is resembling those *e.g.* demonstrated by Ramdohr (1960, Fig. 537) and is interpreted as ulvite intergrowths (Fig. 5). Likewise the magnetite is characterized by abundant lamellae or granules of ilmenite. The lamellae occur in all sets or in one set of (111) planes of the host (Figs. 6,7 and 8). In the specimens of Syväri region in especially a more or less intense replacement of magnetite by maghemite is a common phenomenon.

In the samples of olivine diabase collected from Kvandalen, Disko island, the magnetite and ilmenite are always present as separate grains. The magnetite has a

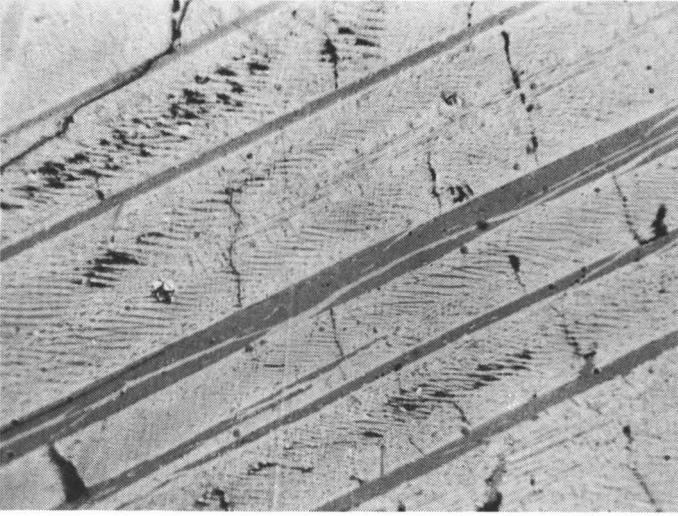


FIG. 8. Magnetite with parallel thick lamellae of ilmenite. Between these systems parallel thin lamellae probably ulvite. Diabase. Valamo island, Karelia, U.S.S.R. Oil im. One nicol, 600 x.

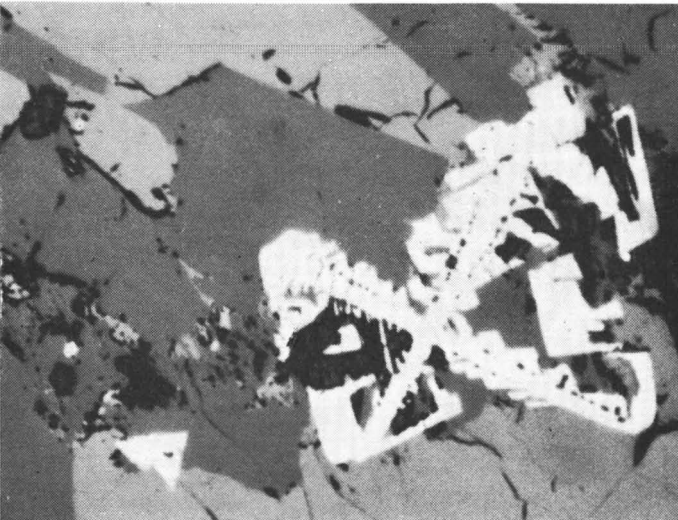


FIG. 9. Grain of skeletal magnetite in diabase. Kvandalen, Disko, West Greenland. One nicol, 160 x.

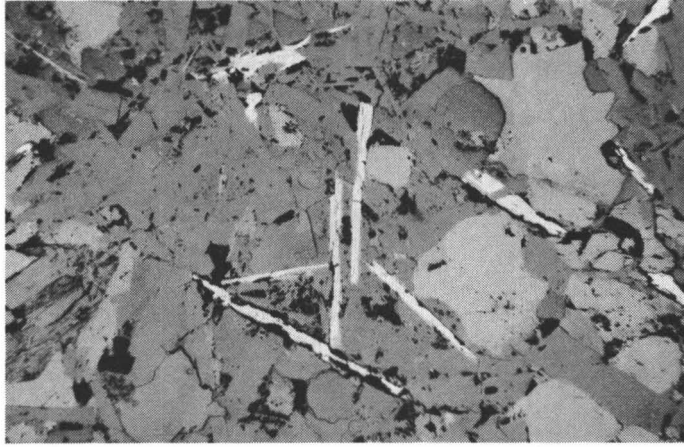


FIG. 10. Needles of ilmenite (white) in diabase. Kvandalen, Disko, West Greenland. One nicol, 50 x.

most specific skeletal appearance in all samples studied (Fig. 9). When using strong magnification these skeletal grains reveal, though most sparsely, faint lamellae of ilmenite. The ilmenite is in form of longitudinal, needle like grains (Fig. 10). Similarly as in the Karelian quartz diabases the ilmenite is homogeneous which means that no intergrowths with hematite have been observed.

Some preliminary determinations for testing the content of titanium in the homogeneous parts of this magnetite were carried out by means of the electron micro probe analyzer at the Geological Survey of Finland. The runs performed by Mr. Jaakko Siivola, M. A., revealed a titanium content, which in the order of magnitude corresponds to that observed in the ulvite and ilmenite bearing magnetites in the specimens of Karelian diabases. Accordingly the magnetite present in the samples from Kvandalen obviously is to be considered practically homogeneous titanomagnetite though slight lamellae of exsolved ilmenite are occasionally observed here and there.

#### REMARKS ON THE RELATIONS OF THE Fe-Ti-PHASES IN THE SAMPLES STUDIED

The intergrowths formed between magnetite, ilmenite and/or ulvite and hematite as observed in the titaniferous iron ores have gained considerable interest during the latest years. Besides the opinion that at high temperatures the ilmenite forms solid solutions with magnetite it has been assumed that the  $\text{TiO}_2$ -content primarily incorporated the titaniferous magnetite as  $\text{Fe}_2\text{TiO}_4$  (Foslie, 1928) and that the formation

of ilmenite thus followed by an oxidation. In favor of the latter hypothesis especially the works by Mogensen (1946), Ramdohr (1953), Vincent *et al.* (1957), Vincent (1960) and Basta (1960) have to be mentioned, whereby the first author of this paper as well has taken advantage of Foslie's principle in some earlier investigations on the titaniferous iron ores (Vaasjoki, 1948; Vaasjoki and Heikkinen, 1962). Recently Buddington and Lindsley (1964) have especially emphasized the significance of oxidation on the magnetite ulvite solid solution and conclude that increasing degrees of oxidation and diffusion result in titaniferous iron ores in a systematic series of fabrics. A principally analogical thesis would be drawn on basis of conclusions arrived at by Vaasjoki and Heikkinen (1962).

In the samples of Karelian diabases the ilmenite occurs as separate grains or as discrete portions within the magnetite. In the former case it is characterized by the myrmecitic replacement textures. Exactly similar textures in association with Bushveld gabbros have been described by Ramdohr (1960, Fig. 534). According to his interpretation such texture would be considered as a relict after dissolution of magnetite from a composite grain of the two minerals. Independently of this possibility, as pointed out in preceding text, it seems that the myrmecitic ilmenite might have been the first phase to be crystallized among the ore oxides studied. The discrete portions of ilmenite within the magnetite (Figs. 4 and 6) either in form of wider laths and flecks or as typical lamellae undoubtedly are products of unmixing from an initial titaniferous magnetite and would be explained as products of an internal granule exsolution (*cf.* Buddington and Lindsley, 1964). The discrete portions of ilmenite like the system of thin ilmenite network in direction of (111) planes of the magnetite (Fig. 5), probably represent products of exsolution through oxidation.

The impressively skeletal shapes of the magnetites and the needle like ilmenite spontaneously arrest one's attention while looking at the specimens of Kvandalen under the reflected light. As illustrated in Fig. 9, the skeletal forms of magnetite have been controlled by a stronger growth in directions of the three-fold symmetry axes. In case of the ilmenite needles (Fig. 10), which as well are skeletal in character, the crystal growth obviously has been strongest in direction perpendicular to the three-fold inversion axis. As is known from metallurgy the skeletal dendritic forms belong to phenomena of rapidly supercooled melts. Even in the case at hand the main factor for the uncomplete crystallization as revealed by the skeletal grains presumably was a rapid decrease in temperature below the melting point of the titaniferous magnetite in the still fluid parts of erupting material. On the other hand the occasional lamellae of ilmenite prove that the cooling during the eruption of material including the skeletally formed high temperature mixcrystals was sluggish enough for enabling the process of exsolution in some degree. As is well known (*e.g.* Ramdohr, 1960; Vaasjoki and Heikkinen, 1962) the titaniferous magnetites associating materials of surface flows are homogeneous in appearance.

## CONCLUSION

In the foregoing the ore oxides and associated fabrics present in some diabasic rocks of late Precambrian age have been compared to those as observed in samples collected from a diabase of Tertiary age. The observations performed have given results according to which the properties studied are most analogical in the samples from the two Karelian localities. A profound difference is obvious, however, when comparing the ore oxide phases and fabrics present in Karelian diabases to those present in the diabase from Kvandalen, Disko. This of course accords well to the fact that the rocks in question belong to entirely different categories with regard to their general relations in space and time.

The field geologic and petrographic properties of the Karelian diabases suggest that the exposed portions at the present erosional level represent material which probably was crystallized in relatively deep-seated though still in hypabyssal zone. The frequent occurrence of granophyric portions eventually indicate conditions of retarded cooling facilitating the differentiation within the original tholeiitic material. The fabrics as observed in the ore oxides in the Karelian diabase samples on the other hand might refer to conditions prevailing in a zone »of intermediate partial pressures of oxygen where it is possible to develop both ilmenite lamellae in (111) planes by partial oxidation and ulvite lamellae in (100) planes by true exsolution» (Buddington and Lindsley, 1964).

The presence of maghemite in the samples of the Karelian diabases is a phenomenon which probably accounts for the effects of deuteric character. It is acceptable that both the alteration of silicatic minerals into hydrous species and the alteration of ore oxides into maghemite are related to diaphthoric changes in association of the block movements.

In relation to the Karelian diabases that from Kvandalen, though still belonging to the suite of hypabyssal rocks, represents formations of a higher stratigraphic level where the conditions of crystallization assumingly approached to those which prevail while the basaltic surface flows crystallize. Therefore, due to relatively rapid cooling *e.g.* chances for unmixing or oxidation of iron titanium bearing phases have been close to minimum. The skeletal forms of ore oxides probably evidence a crystallization of a supercooled melt.

The absence of hematite and ilmenite hematite intergrowths in all the samples studied is a feature in common which obviously relates to intermediate or relatively low partial pressures of oxygen during the crystallization of ore oxides.

The results of this investigation, even if based on restricted material, forward the opinion that well developed ulvite textures especially characterize the ore oxides associating rocks formed in deep-seated hypabyssal conditions.

*Acknowledgement.* — The authors wish to express their gratitude to the Museum of Geology and Mineralogy, University of Helsinki, for making samples of Karelian diabases available for this study.

*Manuscript received, March 31, 1966*

## REFERENCES

- BASTA, E. Z. (1960) Natural and synthetic titanomagnetites. *N. Jb. Min. Abh.* 94, pp. 1017—48.
- BUDDINGTON, A. F., FAHEY, JOSEPH and VLISIDIS, ANGELINA (1955) Thermometric and Petrographic Significance of Titaniferous Magnetite. *Amer. Journ. Sci.* 253, pp. 497—532.
- »— and LINDSLEY, D. H. (1964) Iron-Titanium Oxide Minerals and Synthetic Equivalents. *J. of Petr.* Vol. 5, No 2, pp. 310—357.
- VON CHRUSTSCHOFF, K. (1891) Über das Gestein der Insel Valamo in Ladogasee. *Geol. Fören. Stockholm Förh.* 13, pp. 149—174.
- FOSLIE, ST. (1928) Gleichgewichtsverhältnisse bei einigen Titaneisenerzen. *Fennia* 50, N:o 26 pp. 1—15.
- HACKMAN, V. (1933) Geological Map of Finland, Explanation, Sheet D 2, Savonlinna.
- HELMERSEN, G. (1860) Das Olonez Bergrevier. *Memoires de l'acad. imp. des Sc. de St. Petersburg*, VII Serie, Tome III, N:o 6.
- »— (1882) Geologische und physico-geographische Beobachtungen in Olonezer Bergrevier. Beiträge zur Kenntnis des russischen Reiches, zweite Folge V, St. Petersburg.
- JAKOWLEFF, S. A. (1905) Über granitähnliche Gänge in Diabase an der Süd-Westküste des Onegasee (Diabas-apliten), *Travanx Soc. Imp. Nat. St. Petersburg*, Vol. XXXIII, Sec. Geol. et de Min., pp. 53—102.
- MOGENSEN, E. (1946) A ferrotitanite ore from Södra Ulvöen. *Geol. Fören. Stockholm Förh.* 68, pp. 378—588.
- RAMDOHR, PAUL (1939) Wichtige neue Beobachtungen an Magnetit, Hämatit, Ilmenit und Rutil. *Abhandl. Berliner Ak. Wiss. Math.-nat. Kl.* 14, pp. 1—14.
- »— (1953) Ulvöspinel and its Significance in Titaniferous Iron Ores. *Econ. Geol.* 48, pp. 677—688.
- »— (1956) Die Beziehungen von Fe-Ti-Erzen aus magmatischen Gesteinen. *Bull. Comm. géol. Finlande* 173.
- »— (1960) Die Erzminerale und ihre Verwachsungen. Berlin.
- RAMSAY, WILHELM (1906) Beiträge zur Geologie der präkambrischen Bildungen im Gouvernement Olonez. I. *Fennia* 22, N:o 7, pp. 1—27.
- SEDERHOLM, J. J. (1893) Om berggrunden i södra Finland. *Fennia* 8, N:o 3.
- »— (1927) Om de jotniska och s.k. subjotniska bergarterna. *Geol. Fören. Stockholm Förh.* 49, pp. 397—426.
- VAAJOKI, O. (1947) On the microstructure of titaniferous iron ore at Otanmäki. *C. R. Soc. géol. Finlande* 140. *Bull. Comm. géol. Finlande* 140, pp. 107—114.
- »— and HEIKKINEN, AULIS (1962) On the significance of some textural and compositional properties of the magnetites of titaniferous iron ore. *Bull. Comm. géol. Finlande* 204. *C. R. Soc. géol. Finlande* 34, pp. 141—158.
- WAHL, WALTER (1908) Beiträge zur Geologie der präkambrischen Bildungen in Gouvernement Olonez, II. Die Gesteine der Westküste des Onega-Sees. *Fennia* 24, N:o 3, pp. 1—94.
- VINCENT, E. A. (1960) Ulvöspinel in the Skaergaard intrusion, Greenland. *N. Jb. Miner., Abh.* 94, Festband Ramdohr, pp. 993—1016.
- »— and PHILLIPS, R. (1954) Iron titanium oxide ore minerals in layered gabbros of the Skaergaard intrusion, East Greenland. *Geochim. et Cosmochim. Acta*, 6, pp. 1—26.
- VINCENT, E. A., WRIGHT, J. B., CHEVALIER, R. and MATHIEU, S. (1957) Heating experiments on some natural titaniferous magnetites. *Miner. Mag.* 31, pp. 624—55.



# ON THE FAULTS AND DIABASIC FORMATIONS IN HERAJOKI REGION, KARELIA, EAST FINLAND

BY

O. VAASJOKI

*Institute of Geology and Mineralogy, University of Helsinki*

## ABSTRACT

The paper deals with observations carried out on the fault lines and diabasic formations in an area of Precambrian orogenic belt. Dependence between the fault tectonics and the emplacement and location of diabase formations has been discussed. Attention has been paid to vertical dislocations evidenced by occurrences of diabasic rocks exposed at the same erosional level but obviously being products of crystallization in differing depth zones.

## CONTENTS

	Page
Introduction .....	303
On the Faults .....	305
The Diabasic Dikes and Sills .....	306
The Diabasic Occurrences in Hirvivaara and Pärnälä, Herajoki Region .....	308
Conclusion .....	309
References .....	310

## INTRODUCTION

In the paper at hand the author represents his observations and conclusions on faults and diabase dikes as present in Herajoki area situated on the SSW side of the lake Pielinen in Karelia, East Finland (Fig. 1). The observations were carried out during the summer of 1965 in frames of field program undertaken by the firm Suomen Mineraali Osakeyhtiö (The Finnish Mineral Company). The investigations

created in the first hand tended for estimation on resources of kyanite-pyrophyllite deposits which since long have been known from the zones of quartzitic rocks in terrain to SW from the lake Pielinen (*cf.* Aurola, 1959).

The locality considered in this paper is a part of a wider area which would be called Koli-Kontiolahti-Kaltimo region, the geology of which has been described especially by Frosterus and Wilkman (1916), Väyrynen (1928 and 1930), Ojakangas (1965) and Gaal (1965). Lithologically the area comprises pre-Karelian gneissose granites, metamorphic Karelian sediments and post-tectonic dikes and sills of subsilicic, mainly diabasic intrusions. In fact, Koli-Kaltimo zone represents the outposts of the border of orogenic activity against the foreland formations and subsequently is most inspiring from geological point of view.

As an introduction to the general stratigraphic relations prevailing in the areas under consideration the standard section for Karelian formations as proposed by Väyrynen (1930) will be presented in the following.

#### Kalevian phyllites and mica schists

Jatulian	{	Marine phyllites and dolomites	Penetrated by uralite diabase sills
		Kainuan Quartzites	
		Sariolan Arkosis and Conglomerates	
		— Great Unconformity — Granite gneiss basement	

The observations of the present investigation are dealing with the lower portions of the sedimentary column *i.e.* the Jatulian quartzites, the basement gneisses and associated subsilicic dike and sill formations. It has to be noticed that the change from basal gneiss to Jatulian series is commonly gradational. Väyrynen (1939) interpreted this being a result of thrust shear, whereby even basal conglomerates, if having been present, were destroyed.

In a number of recent geological investigations carried out in Finland an increased attention has been paid on the fault tectonics. Besides the results presented in connection of the regional geological maps and their explanations, the fault tectonics has been the main topic in a few investigations of more local character. A map tending to a generalized outlook on the dominating fault lines in the Precambrian domain of Finland was recently represented by Härme (1960 and 1963). The compilation has been based mainly on the topographic maps, partly on aerial photographs and partly on published field observations. The map, in spite of including rather considerable amount of lines, however, does not contain any effort on systematic analysis *e.g.* between the directions illustrated and orogenic events. A remark that »in general the eskers follow the trend of the fault lines where these are predominantly oriented» (Härme, 1963) is most likely, while the compilation of fault lines, in the first hand, is based on the relevant features of the topographic maps and the eskers essentially effect on the relief contours represented in the ordinary topographic maps of Finland.

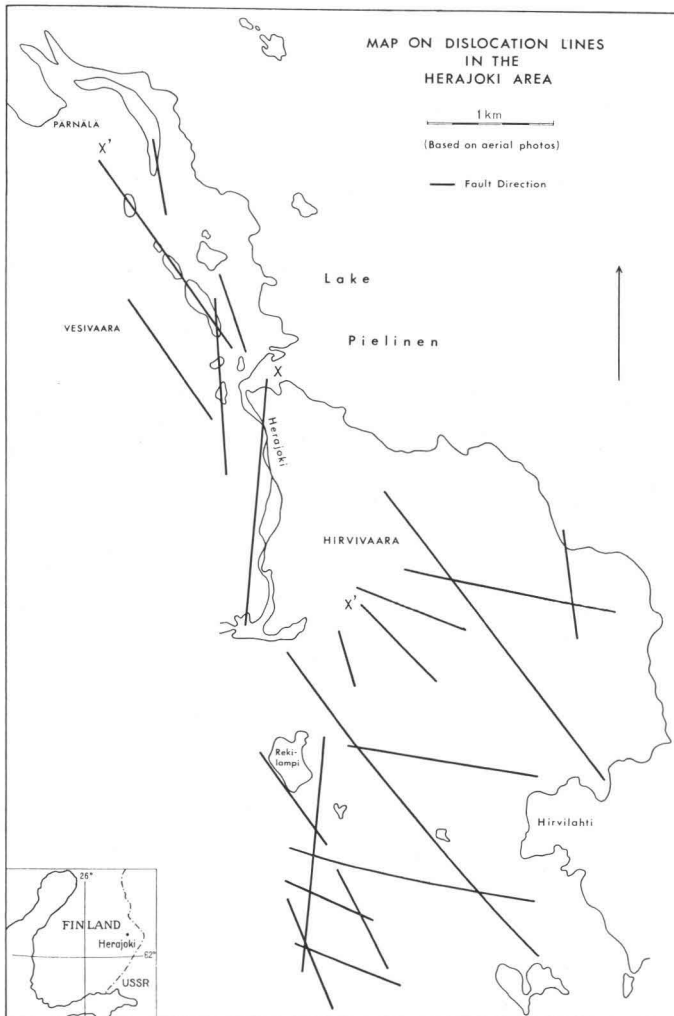


Fig. 1. The location of Herajoki area and the dominating lines of faults and joints.

### ON THE FAULTS.

The works by Frosterus and Wilkman (*op.cit.*) and Väyrynen (1928 and 1939) have to be mentioned as especially distinguished contributions with consideration to the investigations of fault tectonics in the Karelian zones. The results obtained by large are pertinent still today and the value of great number of observations at least has remained unchanged. It is therefore most astonishing that this valuable material in its whole seems to be ignored by Härme (1960 and 1963). For example Väyrynen

was the first to draw attention (1939) to the pronounced and important system of obvious fault lines running parallelly in direction NW—SE in the areas to W from lake Pielinen *i.e.* in the areas of thrust geosynclinal formations. These lines commonly are several tens of kilometers in length while one of the most striking runs in an approximate distance of 10 kilometers from the Herajoki region. In terrain this line is represented by chains of rocky valleys and watercourses. The most fascinating of these valleys is the canyon Kolvananuuro close to the boundary between the parishes of Kontiolahti and Eno.

In connection of this investigation concentrating into formations in the Herajoki area the fault lines have been traced by means of the aerial stereo pairs as well as by observations in terrain. The synthesis has been presented in Fig. 1 showing the dominating fault line directions. Among these the most profound are directions N10°E, N70°—80°W and N30°W.

A part of these lines (Fig. 2) undoubtedly indicate traces of shears produced by thrust movements, which in the area investigated have influenced from west to east (Väyrynen, 1939; Eskola, 1963). The lines caused by thrust have been termed as lines of first phase movements by Gaal (*op.cit.*).

A part of the lines in Fig. 2 indicate traces of planes of dislocations probably caused by the release of tensions created in proximity to the end of thrust movements. These effects Gaal ascribes (*op.cit.*) as dislocations of second phase movements which especially gave rise for origination of cataclastic shears facilitating the emplacement of post-tectonic hypabyssal formations.

The dislocations of second phase movements as defined by Gaal (*op.cit.*) are strikingly concentrated in the areas of quartzite formations. This may account for the mechanical properties of elasticity of differing materials in formations undertaken by movements, the hard quartzite being the most breakable (Eskola, 1963). This is well manifested by the present observations in the Herajoki area revealing a number of differing fault and joint directions crossing the areas occupied by Jatulian quartzites and/or rocks belonging to the formations of the old Karelian kraton (*cf.* Fig. 1). Great many of these lines eventually indicate traces of post-orogenic block movements which as well may have caused recurrent movements along the zones of pre-existing faults and shears.

## THE DIABASIC DIKES AND SILLS

Scattered all over the area under consideration there occur subsilicic dikes and sills. In massive occurrences the rock is rather fine grained and shows an ophitic texture. Within contacts these rocks are often more or less schistose resembling amphibolites in appearance. This is especially observed in occurrences situated in areas westwards from the Herajoki region (*cf.* Väyrynen, 1939). Under the microscope even the massive type reveals strong mineralogical alteration, and subsequently these

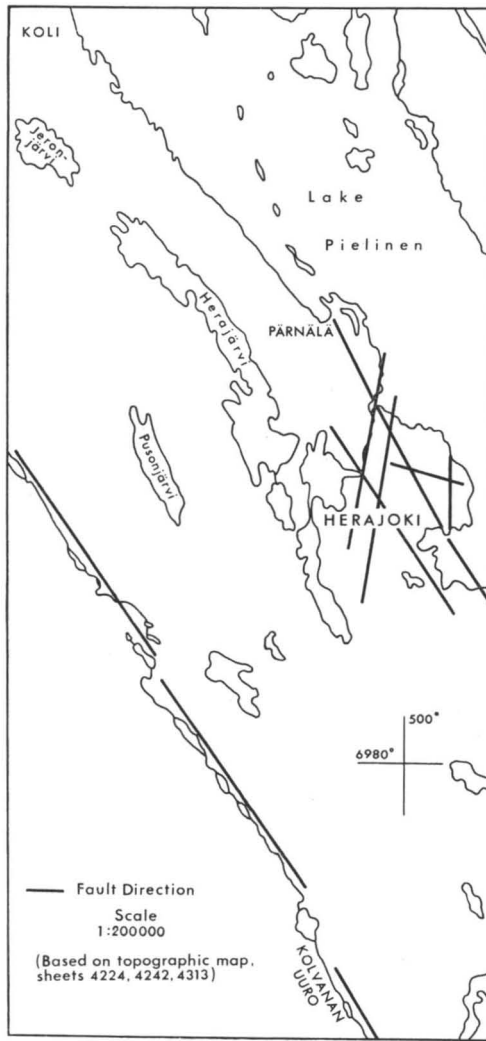


Fig. 2. A map showing the traces of major fault lines of the Herajoki area in relation to the direction of fault line including the Kolvananuuro formation.

rocks generally have been termed as metadiabase (Eskola, 1963). Here these rocks have been called simply as diabase in agreement to the usage adopted in Great Britain.

A typical representative of the diabases in the vicinity of lake Herajärvi closely neighbouring the area of the present study has been analyzed by Sahlbom (Frosterus and Wilkman *op.cit.*). The result shows a tholeiitic composition. According to the microscopic description the analyzed rock contains equal amounts of femic and salic

components and comprises completely uralitized pyroxene, labradoritic plagioclase and abundant epidote as main constituents. The description corresponds well to the mineralogical compositions as determined from the samples of the present study.

Frosterus and Wilkman (*op.cit.*) classify the analyzed rock as belonging to a group which they called Jatulian uralite diabases. Besides this group Frosterus and Wilkman separated another group called Kalevian metadiabases. These terms depend on whether the quartzite penetrated by a diabase was called Kalevian or Jatulian. On basis of the stratigraphic scheme proposed by him Väyrynen (*cf.* p. 3) pointed out that the separation of two groups of diabasic rocks is superfluous and he especially emphasized (1939) that the uralite diabases, though typical in the areas of Jatulian quartzites, have never been met with in the areas occupied by the Kalevian schists. This opinion obviously gains supportance by Gaal (*op.cit.*) who states that the veins of hypabyssal rocks in Koli-Kontiolahti region penetrate the precambrian basement formations as well as the clastic metamorphic rocks. Sharing in opinion that the diabases under consideration do not penetrate the Kalevian sediments Simonen has suggested (1960) that the diabase emplacement indicates a marked change in tectonic activity between stable platform (Jatulian sedimentation) and a subsiding geosyncline (Kalevian sedimentation). This obviously means that the eruptive activity producing diabases ceased before the sedimentation of the Kalevian formations. This possibility as well has been considered earlier by Väyrynen (1954).

#### THE DIABASIC OCCURRENCES IN HIRVIVAARA AND PÄRNÄLÄ, HERAJOKI REGION

Two localities in Herajoki area arise special interest because showing occurrences of diabasic rocks which obviously are products of two considerably differing depth zones. One of these localities is situated at the southern end of Hirvivaara quartzite ridge. The second locality with excellently exposed occurrences is situated on the shore of lake Pielinen in Pärnäälä in a distance of ca. 3 kilometers to N from the Hirvivaara ridge.

The diabase at the southern end of Hirvivaara has intruded as sills running in a general direction N30°W. Because of the scarcity of outcrops no reliable conclusion on the dip was obtainable though a rather flat lying position would be anticipated. The rock in the outcrops is massive, fine grained and distinctly ophitic in texture.

The diabase dike situated at Pärnäälä borders on both sides with the basal gneisses of the kraton formation, is vertical and runs in direction N30°W. Parallel to the dike runs a marked fault line which continues in a distance of at least 30 kilometers between Enojärvi in the south and Koli region in the north (X' in Fig. 1). Frosterus and Wilkman (*op.cit.*) already noticed this line and consider that it defines the trend of sheared zone. The diabase associating this direction at Pärnäälä is strikingly coarse grained and particularly characterized by abnormally long amphibole laths which

may reach a length of several centimeters. In relation to the occurrence of the fine grained diabase present in the quartzite horizon at Hirvivaara the occurrence at Pärnälä is distinguished by associated narrow, reddish granophyric veins.

The coarser grain of the diabase similarly as associated granophyric portions in the occurrence at Pärnälä evidence that this formation probably crystallized in greater depth than the diabase at Hirvivaara. The same tendency is revealed by the mode of the occurrence of the diabasic rocks under consideration. The formation at Pärnälä typically indicates dike intrusion controlled by kratogenic tectonics of the old basement whereas the diabase sill at Hirvivaara indicates intrusion controlled by thrust and joint tectonics of the suprazone. The fact that both of these diabasic formations, however, crop out at the same erosional level, suggests considerable vertical dislocation since the emplacement of the subsilicic rocks in question.

As illustrated in the geological map on Koli-Kaltimo area constructed by Gaal (*op.cit.*) the diabasic occurrences commonly display narrow, longitudinal forms oriented in direction  $N30^{\circ}W$  *i.e.* parallel to the directions determined for the diabasic intrusions at Pärnälä and Hirvivaara (X' in Fig. 1). It seems accordingly that the faults in direction  $N30^{\circ}W$  have been of a special significance with regard to the emplacement of diabasic materials. It is thus likely that the whole system of lines in approximate directions  $N30^{\circ}W$  has to be considered as indicating the traces of dislocations of the second phase movements as defined by Gaal (p. 4), though the activity which produced the diabasic materials seems to concentrate solely into shears existing within the zones of Jatulian quartzites.

The line in approximate direction  $N10^{\circ}E$  (X in Fig. 1) conjoining the direction of the Herajoki valley calls attention while obviously cutting the continuation of the diabasic dike described from Pärnälä. Accordingly this line probably demonstrates a trace of post-diabasic block movements. Additional lines of similar inheritance though in differing directions are present in Fig. 1. Väyrynen even considers that the faults responsible for lines parallel to that passing through Kolvananuuro are relatively young and presumably resulted in movements combined with isostatic readjustment in the course of the weathering down of the Karelian mountain chain (Väyrynen, 1939). It might be inferred, however, that the lines in question indicate the second phase movements by Gaal (*op.cit.*). It is acceptable that movements of later dates may have recurrently taken advantage of these old zones of weakness as already pointed out earlier.

## CONCLUSION

The observations carried out in the Herajoki region contribute the following conclusions:

— The intrusions of diabasic materials in thrust formations has been facilitated by cataclastic shears which probably originated in proximity to the end of thrust movements.

— The occurrence of diabases is restricted within the areas occupied by basement formations or by zones of the Jatulian quartzites.

— Diabasic rocks representing products of crystallization in different depth zones, while present at the same erosional level in Hirvivaara and Pärnälä, indicate vertical dislocations caused by post-diabasic block movements.

*Manuscript received, March 31, 1966*

#### REFERENCES

- AUROLA, ERKKI (1959). Kyaniitti- ja pyrofylliittiesiintymät Pohjois-Karjalassa. With an English summary. *Geoteknillisiä julkaisuja* 63. Helsinki.
- ESKOLA, PENTTI (1963). The Precambrian of Finland. The geologic systems. The Precambrian, Vol. 1, pp. 144—263.
- FROSTERUS, BENJ. and WILKMAN, W. W. (1916). Geologinen yleiskartta. The general geological map of Finland, D 3, Joensuu. Beskrifning till bergartskartan D 3, Joensuu. Résumé en français.
- GAAL, GABOR (1964). Jatul und karelische Molasse im S-Koligebiet in Nordkarelien und ihre Beziehungen zum Gebirgsbau des präkambrischen Orogens. *Bull. Comm. géol. Finlande* 213.
- HÄRME, MAUNU (1961). On the fault lines in Finland. *Bull. Comm. géol. Finlande* 196. C. R. Soc. géol. Finlande XXXIII, pp. 437—444.
- »— (1963). On the shear zones and fault lines in Finnish Precambrian strata. Symposium on recent crustal movements in Finland with bibliography. *Fennia* 89, N:o 1.
- OJAKANGAS, RIKHARD W. (1965). Petrography and sedimentation of the precambrian Jatulian quartzites of Finland. *Bull. Comm. géol. Finlande* 191.
- SIMONEN, AHTI (1960). Pre-Quaternary rocks in Finland. *Bull. Comm. géol. Finlande* 191.
- VÄYRYNEN, HEIKKI (1933). Über die Stratigraphie der karelischen Formationen. *Bull. Comm. géol. Finlande* 101. C. R. Soc. géol. Finlande VI, pp. 54—79.
- »— (1939) On the geology and tectonics of the Outokumpu ore field and region. *Bull. Comm. géol. Finlande* 124.
- »— (1954) Suomen kallioperä. Helsinki.

# STRUCTURAL CONTROL OF COMPOSITION IN THE ORIJÄRVI GRANODIORITE

BY

HEIKKI V. TUOMINEN

*Department of Mining, Institute of Technology, Otaniemi, Finland*

## ABSTRACT

The Orijärvi granodiorite is described as a pseudo-phacolith resulting from migration of elements toward the axial planes during folding. Different elements have migrated with different velocities, thus producing a chemical differentiation of the original layered complex. A mathematical model of the phenomenon is presented.

## CONTENTS

	Page
Introduction .....	311
Geological outline .....	312
Sampling .....	314
Variation of mineral composition .....	316
Variation of chemical composition .....	322
Model for chemical squeezing .....	322
Application to Orijärvi .....	325
References .....	326
Appendix .....	327

## INTRODUCTION

Formation of granitic rocks, whether by magmatic, anatectic or metamorphic differentiation, is presumably connected with the complementary phenomenon, formation of more basic rocks elsewhere. In terms of the most abundant cations of the crust, the process means a more or less effective separation of silicon and alkalies from magnesium, iron and calcium. It seems obvious, therefore, that the major compositional variation in series of differentiation containing granitic members is roughly similar irrespective of the type of the underlying process (*cf.* Chayes

1964). The investigations discussed in the present paper on the Orijärvi granodiorite seem to indicate that compositional variations resulting from chemical squeezing (Ramberg 1952, p. 221) may even be inseparable from compositional variations supposedly resulting from magmatic fractionation.

The present paper should be read in connection with an earlier paper by Tuominen (1961), where the structure of Orijärvi granodiorite has been discussed in greater detail (see also Tuominen 1966).

As in the earlier paper, the term granite is in conformance with the definition of Chayes (1957) and the subdivision (trondhjemite, granodiorite, adamellite) follows his classification. Terms such as pluton, phacolith, *etc.* are used in a descriptive sense only. With regard to Orijärvi granodiorite, the name granodiorite means the average composition of the pluton. All modal analyses are given in volume percentages.

## GEOLOGICAL OUTLINE

Orijärvi granodiorite is generally considered as a typical representative of synkinematic Svecofennian granites. These are slightly gneissose granitoid rocks in which sodic plagioclase usually is the dominant feldspar. Commonly they are agmatitic to streaky in structure but banded types also occur.

Fig. 1 shows the parts of the Orijärvi granodiorite mass essential for the present study. Rocks rich in cordierite and anthophyllite and related rocks are frequent between the curved dash-line and the contact of the granodiorite. The Kurksaari strike-slip fault forms the western border for the »magnesium metasomatic» area as well as for the granodiorite. Apparently this fault was formed simultaneously with the folding and granitization. The northeast striking thrust fault at the east end of Lake Orijärvi also has been active during the granitization. Both faults die out southward.

The intercalating shaded and white zones in Fig. 1 are, respectively, zones of higher and lower average magnetic intensity of the vertical component. The zonal variation of the magnetic intensity corresponds to a stratiform variation in the concentration of highly magnetic minerals, such as magnetite and pyrrhotite. The zones coincide with groups of layers of the following qualifications:

- Zone I. Amphibolite, leptite, marble, skarn, skarn-banded magnetite ore.
- Zone II. Leptite.
- Zone III. Amphibolite, leptite, marble, skarn, banded magnetite ore in skarn-type rock rich in apatite. Sulfide mineralization.
- Zone IV. Leptite interlayered with subordinate amphibolite.
- Zone V. Sequence upward: 1. Leptite with layers of marble and skarn, sulfide mineralization. 2. Leptite with polymict conglomerate. 3. Diopside amphibolite.
- Zone VI. Diopside amphibolite with subordinate leptitic layers.
- Zone VII. A zone of gradual change from VI to VIII, with grauwacke conglomerates.
- Zone VIII. Leptite with subordinate layers of diopside amphibolite or amphibolite.

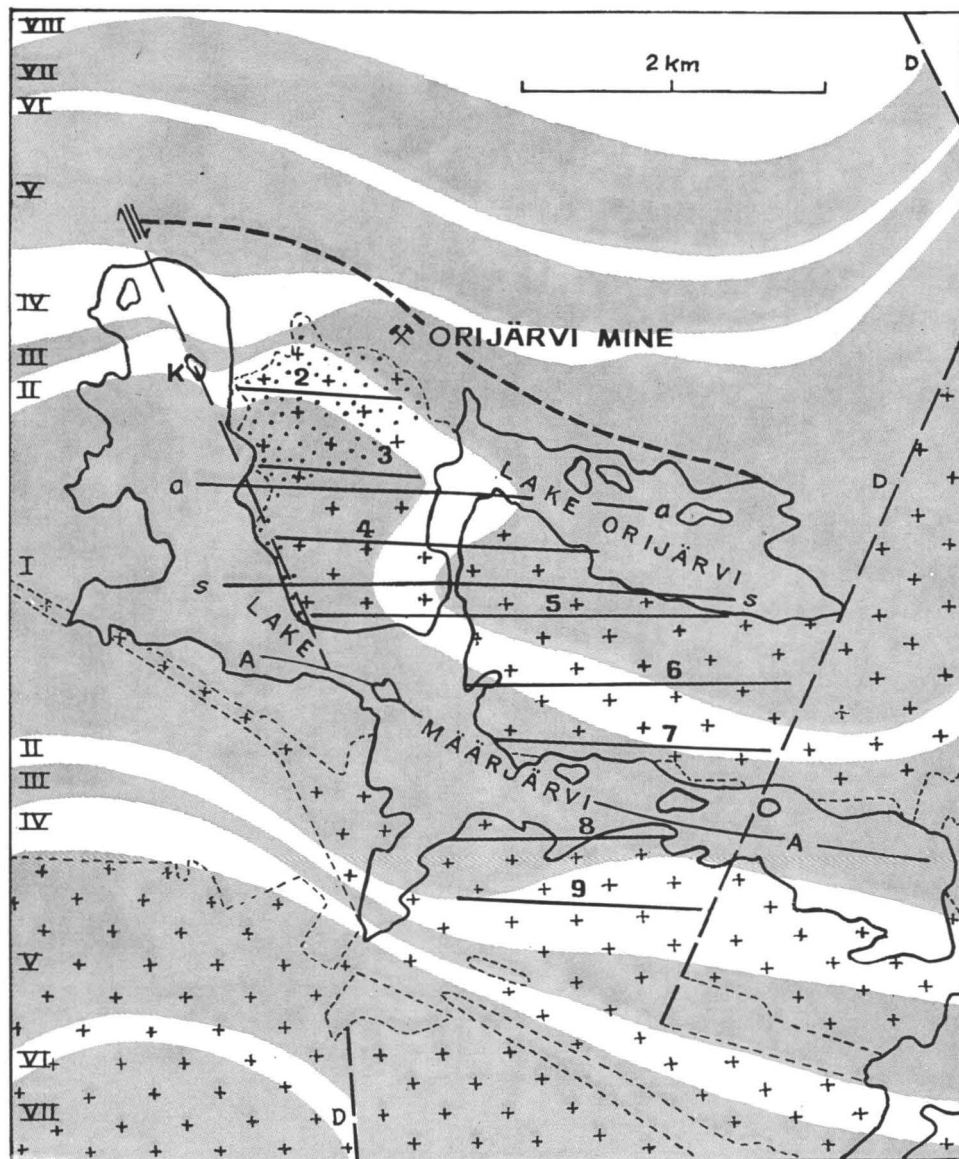


FIG. 1. Schematic map of Orijärvi granodiorite and surroundings. Crosses: granodiorite. Dots: porphyroblastic modification of granodiorite. »Magnesium metasomatic» rocks are common between curved dash line and border of granodiorite. A—A = Määrjärvi anticline. a—a = secondary anticline. s—s = secondary syncline. D = downthrown side of thrust fault. Arrows = strike-slip fault. K = Isle of Kurksaari. Shaded = zones of higher magnetic intensity. White = zones of lower magnetic intensity. Roman numbers I—VIII show apparent sequence of strata. The magnetic zoning seen on this map is compiled from measurements at over 50 000 stations. Sample lines are indicated by numbers 2—9.

Zones I—VIII represent the sequence of the observable strata from bottom to top. As can be seen from Fig. 1, the magnetic zones continue uninterrupted through the granodiorite, which suggests (Tuominen 1961) that the corresponding beds do the same.

The areas of the granodiorite considered in the present paper belong to the strongly folded zones I—III, of which zones I and III are characterized by iron formations and hence show a higher magnetic intensity. The low intensity zone II follows a layer of cordierite-bearing and other leptites poor in magnetic minerals. Because of intense small-scale folding and faulting, the border areas of the neighboring zones are mixtures of the layers from both zones. This means that the borders of the magnetic zones coincide only roughly with the borders of the corresponding strata.

As is the whole leptite belt, the granodiorite is folded upon axes plunging gently east. A schematic cross section perpendicular to this axial direction is shown in the upper part of Fig. 2. Both folds seen in the picture are asymmetric with their steeper limbs dipping south. The northernmost limb grades down the limb to rocks rich in cordierite and anthophyllite («magnesium metasomatic» rocks).

### SAMPLING

In order to study whether any regular correlation exists between the folded forms and the composition of the phacolith, 94 specimens were collected at intervals of 100 to 250 meters in a zigzag pattern along the lines 2 to 9 of Fig. 1. The zig-zagging and the uneven intervals were caused by uneven outcropping. The sample lines are approximately 500 meters apart. East of the crossing thrust fault the composition of the pluton has been strongly influenced by structures interfering with the main folding. For this reason the sampling was not extended beyond the fault.

To avoid «contamination», the specimens were taken as far as possible from the «dark inclusions» found all over the granodiorite mass. A thin section of each specimen, stained for identification of potash feldspar (microcline), was analyzed by the point counter method. Results are given in the Appendix in which the specimens are tabulated for lines as well as for zones.

The anorthite content of plagioclase was determined using standard optical methods without universal stage. For each slide this represents an average from three grains. As the variation in a single slide may be from 10 to 35 per cent An, the results are not very reliable. For this reason they are not given in the Appendix.

Color index, as used in this paper, includes everything else except quartz, potash feldspar and plagioclase. The carbonates found in a few specimens have for this reason been included in the color index. This seems justified as the carbonates add to the bulk basicity of the rock. In any case they have no influence on the results of the present study.

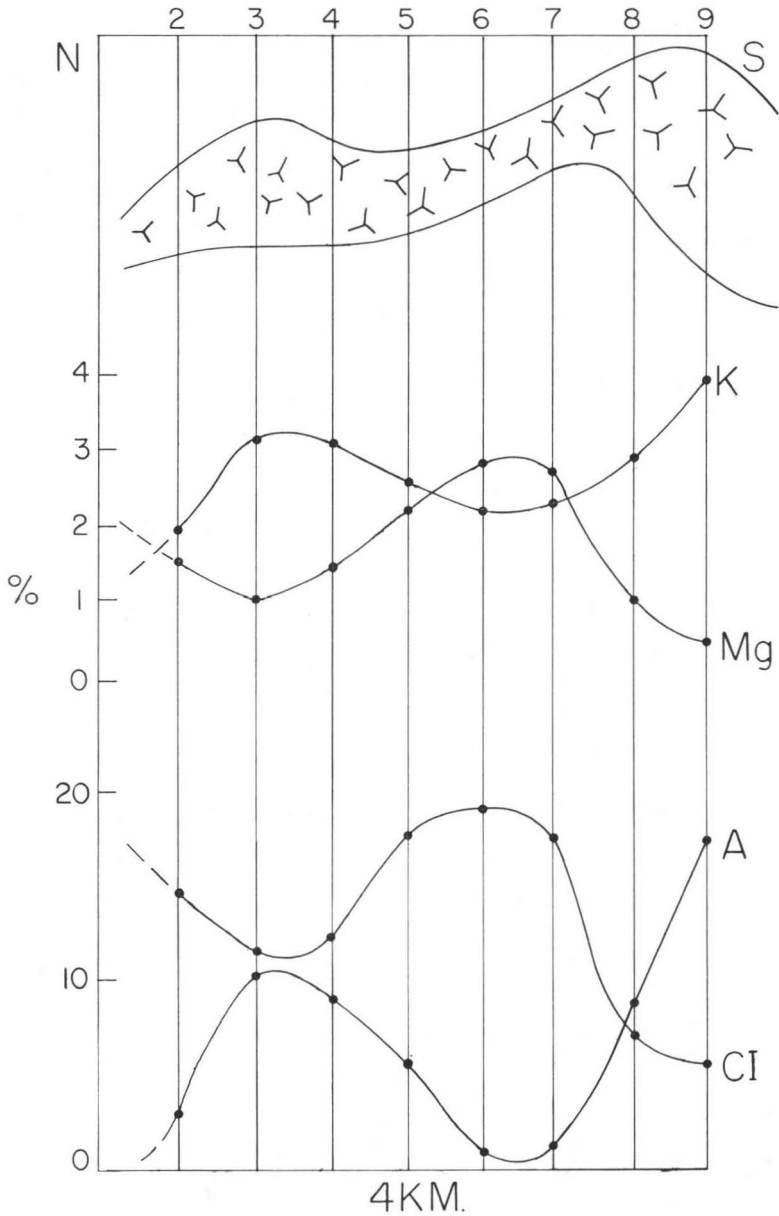


FIG. 2. Above: schematic cross section of Orijärvi granodiorite perpendicular to fold axis. — Center: average cation percentage variation of potassium and magnesium. — Below: average variation of color index (CI) and concentration of potash feldspar (A). Vertical lines numbered 2—9 represent the sample lines. Correspondence between composition and structure is evident.

All the specimens show traces of more or less strong secondary alteration. Intensive alteration of plagioclase, in particular, reduced the accuracy of the point counter analysis. Small amounts of chlorite are normally associated with biotite. In specimen 408 there is 17.4 per cent chlorite and no biotite at all, while the microcline content (29.0 per cent) is particularly high. No correlation, however, seems to exist between the amounts chlorite and potash feldspar.

In general the specimens come well within the range of the types described in detail by Eskola (1914 and 1952, p. 128), to whom in this respect the reader is referred. All the specimens of line 2 belong to the porphyroblastic type which consists of larger crystals and nodules of quartz and plagioclase (up to 4 mm in diameter) embedded in a microgranitoid matrix. This feature, still pronounced in the western half (specimens 301—306) of line 3, becomes weaker towards the south-east as the ground mass becomes coarser, but is recognizable all over the pluton.

At the time of sampling nothing was known of the relic zoning in the granodiorite, nor of the secondary fold situated at the north limb. The sampling was done in order to test whether the change in composition from trondhjemitic rocks of the lower parts of the north limb to the adamellitic rocks of the main crest zone was gradual. As there was a clear peak toward adamellitic composition at the center of the north limb, the result was considered negative and inexplicable. Only after the compilation of large scale magnetic maps (Tuominen 1957) had indicated the presence of the secondary fold, was the existence of the corresponding adamellitic peak explained. Since then the author has been looking forward to an opportunity for doing a statistically less biased sampling which would embrace the inclusions as well. However, as the old sampling still seems informative, and as no opportunity for a new sampling is in sight, the results are given below. Since methods of quick chemical rock analyses were not available at the time, the amount of chemical analyses had to be reduced to a minimum.

#### VARIATION OF MINERAL COMPOSITION

From the point counter analyses average compositions were calculated for each zone I—III, for each sample line, and for some combinations of them.

The average modal compositions for the magnetic zones have been given by Tuominen (1961, p. 509). As small adjustments have been made later in the allotment of the samples to the zones, new values for the zonal compositions are given in Table 1. There is, however, no significant difference between old and new values. The compositions of the three zones are very similar. However, the concentration of Ca-bearing minerals in zone II is lower than in zones I and III. The same applies to the anorthite content of plagioclase. These differences correspond very well to the differences appearing between the same zones west of the granodiorite.

TABLE 1  
Average modal composition of Orijärvi granodiorite by magnetic zones

Zone No. of slides	I 40	II 33	III 21
Quartz .....	35.4	36.9	33.7
Potash feldspar .....	7.6	6.3	4.5
Plagioclase .....	43.8	42.5	46.0
White mica .....	.2	1.0	.0
Biotite and chlorite .....	10.3	11.6	13.0
Hornblende .....	1.6	.8	1.2
Epidotes .....	.7	.9	1.3
Others .....	.4	.2	.3
	100.0	100.0	100.0
Color index .....	13.2	14.3	15.8
Opagues ( $\approx$ magnetite) .....	.2	.04	.2
% An in plagioclase .....	28	26	27

It is obvious that in a granitization process layers of nearby granitic composition do not change markedly. On the other hand, the compositions of, say, amphibolitic layers will approach a granitic composition. Consequently the differences between originally different layers are reduced. Nevertheless, there is a marked difference in the concentration of magnetite, which in zones I and III is five times higher than in zone II. According to the Kolmogorov—Smirnov test (Miller and Kahn 1962, p. 466) the confidence of these differences is much above the 95 per cent level. It seems probable, therefore, that the strata of the surrounding rocks continue through the pluton.

The average compositions of the sample lines are given in Table 2. The strongest variations are seen in the values of potash feldspar and color index. In Fig. 2 (lower graphs) these variations are compared with the folded forms of the phacolith. The concentration of potash feldspar (A) seems to increase from the limbs toward the crests of both folds, while the color index (CI) behaves in the opposite way. The verity of the maxima and minima of both curves, at 95 per cent confidence, was checked by using the Kolmogorov—Smirnov test with the results as given in Table 3 which can be read as the distance table of a road map.

For the following discussion sample lines 2, 5, 6 and 7 are considered to represent the limbs, and lines 3, 4, 8 and 9 the crests of the folds seen in Fig. 2. The modal compositions of the felsic fractions of the limb and crest specimens are seen in Figures 3 and 4, respectively. It is evident from these pictures that the crest areas contain much more potash feldspar than the limb areas. The average modal compositions of the limb and crest samples are given in Table 5. It appears from this table that at the crests the concentrations of quartz and potash feldspar are higher, whereas color index, plagioclase and the anorthite content of the latter are lower than at the limbs. This is also seen from Fig. 5 in which the statistical reliability of the diffe-

TABLE 2  
Average modal composition of Orijärvi granodiorite by sample lines.

Line	2	3	4	5	6	7	8	9
No. of slides	11	11	14	15	11	15	8	9
Quartz .....	38.0	35.4	34.1	33.0	34.6	32.2	41.7	40.5
Potash feldspar .....	2.9	10.2	9.1	5.9	0.8	1.2	8.7	17.0
Plagioclase .....	44.2	42.5	43.7	43.4	45.5	48.6	42.5	37.0
White mica .....	2.3	0.4	0.0	0.0	0.0	0.0	0.4	0.8
Biotite and chlorite .....	10.6	9.0	10.8	13.5	15.9	15.4	6.2	4.6
Hornblende .....	0.1	0.7	1.0	2.6	2.1	1.8	0.0	0.0
Epidotes .....	1.5	1.1	1.1	1.4	0.8	0.5	0.3	0.0
Others .....	0.4	0.7	0.2	0.2	0.3	0.3	0.2	0.1
	100.0	100.0	100.0	100.0	100.0	100.0	100.0	100.0
Color index .....	14.9	11.9	13.1	17.7	19.1	18.0	7.1	5.5

TABLE 3

Results of application of Kolmogorov-Smirnov test to comparison of differences in composition at various sample lines. Sig.05 gives the minimum deviation required for a given pair of values to indicate difference at 95 per cent level of confidence. Deviations not meeting this requirement are omitted. Q = quartz, A = potash feldspar, Pl = plagioclase, CI = color index.

3	A .....	.725						
	Pl .....	.545						
	CI .....	.545						
	Sig.05 .....	.545						
4	A .....	.725						
	Sig.05 .....	.520	.520					
5	A .....		.550					
	CI .....		.600	.600				
	Sig.05 .....	.515	.515	.490				
6	A .....		.910	.930	.640			
	Pl .....		.635					
	CI .....	.635	.820	.655				
	Sig.05 .....	.545	.545	.520	.515			
7	A .....		.840	.860	.600			
	Pl .....		.640					
	CI .....		.725					
	Sig.05 .....	.515	.515	.490	.480	.515		
8	Q .....		.750	.720	.665	.725	.810	
	A .....					.625	.560	
	CI .....	.910	.750	.660	.875	1.000	1.000	
	Sig.05 .....	.590	.590	.560	.560	.590	.560	
9	Q .....		.665	.635	.600	.675	.710	
	A .....	.725			.690	1.000	.935	
	Pl .....					.615	.665	
	CI .....	.910	1.000	.855	1.000	1.000	1.000	
	Sig.05 .....	.570	.570	.550	.540	.570	.540	.615
Line	2	3	4	5	6	7	8	

TABLE 4

Average modal composition of magnetic zones, by limbs and crests, in Orijärvi granodiorite.

Position	Zone I		Zone II		Zone III	
	Limbs	Crests	Limbs	Crests	Limbs	Crests
No. of slides	16	24	21	12	15	6
Quartz .....	32.0	37.6	36.1	38.2	33.6	33.9
Potash feldspar .....	3.5	10.3	2.1	13.8	3.1	8.1
Plagioclase .....	46.3	42.2	44.5	39.0	46.2	45.3
White mica .....	.0	.4	1.2	.6	.0	.0
Biotite and chlorite .....	14.1	7.8	13.8	7.4	14.0	10.8
Hornblende .....	3.1	.5	.8	.6	1.4	.4
Epidotes .....	.7	.7	1.2	.4	1.3	1.4
Others .....	.3	.5	.3	.0	.3	.1
	100.0	100.0	100.0	100.0	100.0	100.0
Color index .....	18.2	9.9	17.3	9.0	17.1	12.7
Opaques ( $\approx$ magnetite) ...	.25	.20	.05	.01	.3	.05
% An in plagioclase .....	29	27	28	23	29	24

TABLE 5

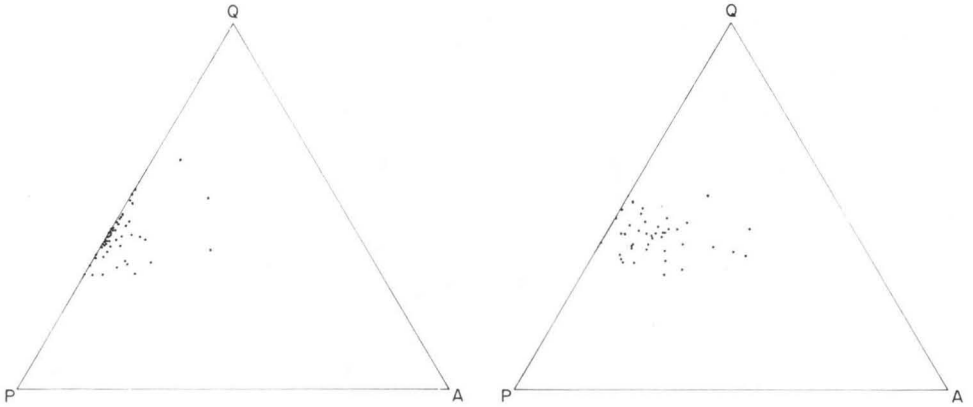
Average modal and chemical composition of limb and crest specimens of Orijärvi granodiorite.

Sample size								
	Limbs 52	Crests 42	Limbs 52	Crests 42	Limbs 52	Crests 42	Limbs 52	Crests 42
Quartz .....	34.2	37.3	SiO <sub>2</sub>	69.05	73.04	Si	65.60	69.16
Potash feldspar .....	2.8	11.0	TiO <sub>2</sub>	.37	.25	Ti	.26	.18
Plagioclase .....	45.5	41.7	Al <sub>2</sub> O <sub>3</sub>	14.14	13.25	Al	15.83	14.78
White mica .....	.5	.4	Fe <sub>2</sub> O <sub>3</sub>	1.53	1.05	Fe <sup>3+</sup>	1.09	.75
Biotite and chlorite .....	13.9	8.1	FeO	3.39	2.19	Fe <sup>2+</sup>	2.69	1.73
Hornblende .....	1.7	.5	MnO	.09	.05	Mn	.07	.04
Epidotes .....	1.1	.7	MgO	1.67	.78	Mg	2.36	1.10
Others .....	.3	.3	CaO	3.05	1.95	Ca	3.10	1.98
	100.0	100.0	Na <sub>2</sub> O	3.59	3.84	Na	6.61	7.04
Color index .....	17.5	10.0	K <sub>2</sub> O	1.93	2.67	K	2.34	3.22
Opaques ( $\approx$ magnetite) ...	.2	.1	P <sub>2</sub> O <sub>5</sub>	.03	.02	P	.03	.02
% An in plagioclase .....	28	24		98.84	99.07		100.00	100.00
						O	169.79	171.96

rences between the limb and crest samples has been tested. As is apparent from Table 4, the differences between the limb and crest compositions are observable in each zone as well.

It seems worthwhile to note that the concentration of magnetite drops from the limbs toward the crests (see Tables 4 and 5). This corresponds closely to the general dilution of iron resulting from the expansion of the original beds and related granitization, which both increase towards the axial planes of the folds.

Apart from the zoning, no systematic compositional variation parallel to the (strike of the) fold axis has been observed.



FIGURES 3—4. Modal composition of felsic fraction of Orijärvi samples. Q = quartz, A = potash feldspar, P = plagioclase. Fig. 3 = limbs, Fig. 4 = crests.

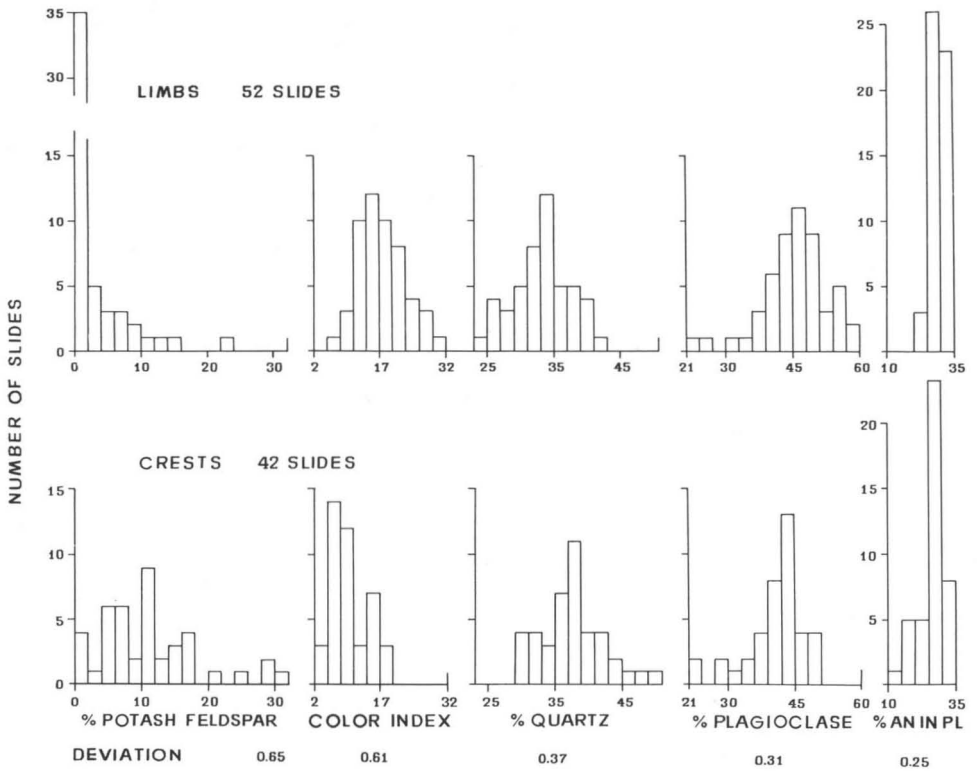


FIG. 5. Frequency distribution of percentage values for major components and anorthite content of plagioclase in the Orijärvi specimens. Upper row: limbs; lower row: crests. The deviations between crest and limb data are from Kolmogorov-Smirnov test. Minimum requirement for 95 per cent confidence is 0.28.

TABLE 6

Chemical bulk compositions of line samples from Orijärvi granodiorite<sup>1)</sup>. Above: oxide weight percentages<sup>2)</sup>; center: cation percentages<sup>3)</sup>; below: cation/magnesium ratios.

Line Sample size	2 11	3 11	4 14	5 15	6 11	7 15	8 8	9 9
SiO <sub>2</sub> .....	71.97	71.84	70.96	68.72	68.43	67.72	75.10	75.93
TiO <sub>2</sub> .....	0.31	0.29	0.31	0.36	0.38	0.42	0.20	0.16
Al <sub>2</sub> O <sub>3</sub> .....	13.90	13.37	13.68	14.03	14.04	14.50	12.74	12.88
Fe <sub>2</sub> O <sub>3</sub> .....	0.94	1.30	1.27	1.60	1.81	1.70	0.80	0.62
FeO .....	2.18	2.50	2.98	3.60	3.67	3.85	1.61	1.11
MnO .....	0.05	0.05	0.07	0.10	0.08	0.10	0.03	0.04
MgO .....	1.17	0.77	1.06	1.54	2.00	1.91	0.76	0.36
CaO .....	2.53	2.34	2.54	3.21	3.21	3.17	1.42	1.04
Na <sub>2</sub> O .....	4.09	3.85	3.54	3.48	3.33	3.53	4.16	4.00
K <sub>2</sub> O .....	1.67	2.53	2.59	2.17	1.86	1.93	2.32	3.27
P <sub>2</sub> O <sub>5</sub> .....	0.02	0.02	0.02	0.03	0.04	0.02	0.01	0.03
	98.83	98.86	99.02	98.84	98.85	98.85	99.15	99.44
Si .....	68.14	68.28	67.44	65.46	65.21	64.40	70.93	71.50
Ti .....	.22	.21	.22	.26	.27	.30	.14	.11
Al .....	15.51	14.97	15.32	15.75	15.77	16.25	14.18	14.29
Fe <sup>3</sup> .....	.67	.93	.91	1.15	1.30	1.22	.57	.44
Fe <sup>2</sup> .....	1.73	1.99	2.37	2.87	2.92	3.06	1.27	.87
Mg .....	1.65	1.09	1.50	2.18	2.84	2.70	1.07	.51
Ca .....	2.56	2.38	2.58	3.27	3.28	3.23	1.44	1.05
Na .....	7.50	7.09	6.52	6.42	6.15	6.50	7.61	7.30
K .....	2.02	3.07	3.14	2.64	2.26	2.34	2.79	3.93
	100.00	100.01	100.00	100.00	100.00	100.00	100.00	100.00
O .....	171.69	171.36	170.95	169.64	169.81	169.01	173.24	173.40
Fe .....	2.40	2.92	3.28	4.02	4.22	4.28	1.84	1.31
Si/Mg .....	41.29	62.62	44.94	30.00	22.97	23.80	66.34	141.6
Ti/Mg .....	.134	.190	.148	.118	.096	.111	.133	.224
Al/Mg .....	9.397	13.73	10.21	7.208	5.554	6.006	13.26	28.30
Fe <sup>3</sup> /Mg .....	.406	.852	.605	.525	.457	.449	.532	.870
Fe <sup>2</sup> /Mg .....	1.046	1.822	1.578	1.312	1.030	1.131	1.189	1.730
Ca/Mg .....	1.554	2.185	1.723	1.499	1.154	1.193	1.343	2.076
Na/Mg .....	4.546	6.502	4.344	2.940	2.166	2.404	7.119	14.45
K/Mg .....	1.223	2.813	2.092	1.206	.796	.865	2.613	7.775
Fe/Mg .....	1.451	2.674	2.183	1.837	1.487	1.581	1.720	2.599

<sup>1)</sup> Analyst: P. Ojanperä.

<sup>2)</sup> H<sub>2</sub>O not determined.

<sup>3)</sup> Mn and P omitted.

## VARIATION OF CHEMICAL COMPOSITION

In order to study the variation of the chemical composition with the folding, the specimens of each line were bulked and analyzed chemically. Results are given in Table 6. In the central part of the table the oxide percentages of the original analyses have been recalculated into cation percentages. The strongest variations are seen in the values for potassium and magnesium. As is shown in Fig. 2 their variation complies closely with the variation of potash feldspar and the color index, respectively, as well as with the folded forms of the phacolith. Potassium increases from the limbs toward the crests of both folds while magnesium behaves in the opposite way.

It seems obvious that this structural variation of the rock composition would also appear as a regular variation of components other than K and Mg. The concentrations of the other common cations do not follow the pattern of the single folds as clearly as do these two. However, variations in the concentration of the other elements can be studied as related to the variation of Mg, the tectonic pattern of which is known. In order to do this the ratios of the concentrations of other cations to the corresponding values for magnesium have been given in Table 6. It appears that the ratio Si/Mg increases from the limbs towards the crests of the folds. In the following this ratio has been considered as the coordinate giving the position in the folded forms.

## MODEL FOR CHEMICAL SQUEEZING

For simplicity let us assume that originally there was a homogenous layer of constant thickness consisting of the various elements 1, 2, . . . , n. The width of the layer is denoted by  $2x_0$ . The number of atoms of element  $\nu$ , per unit area of the layer, is denoted by  $M_\nu^{(0)}$ . Suppose now that the layer is folded along the axis  $x = 0$ . Due to chemical squeezing elements move towards the axial plane, different elements having different average speeds. For simplicity, a pure one-dimensional flow is presumed. It may be assumed that after a sufficiently long time the number of atoms of the element  $\nu$ , per unit area of the layer, corresponds approximately to the Gaussian law (see Fig. 6)

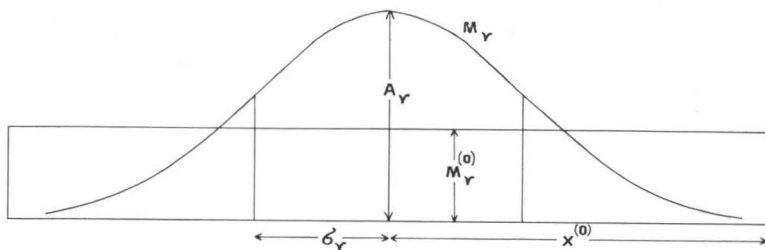


FIG. 6. Schematic representation of chemical squeezing of an element ( $\nu$ ) toward axial plain of fold. Originally even distribution of the element in a layer  $2x^{(0)}$  wide has been transformed into approximately Gaussian distribution.

$$M_v = A_v e^{-\frac{1}{2} \frac{x^2}{\sigma_v^2}} \quad (1)$$

where  $\sigma_v$  and  $A_v$  are constants,  $A_v$  representing the number of atoms per unit area at the axial plane. By integrating  $M_v$  from  $-\infty$  to  $+\infty$ , we obtain the total number of atoms per unit length of the fold. Hence

$$A_v = \frac{2x_0 M_v^{(0)}}{\sigma_v \sqrt{2\pi}}. \quad (2)$$

In fact, the quantities  $M_v$  are not known. Instead the corresponding percentage concentrations

$$C_v = 100 M_v / \sum_{i=1}^n M_i \quad (3)$$

are obtained from observations. Consider now three elements  $i$ ,  $j$  and  $k$ . First we have

$$\frac{M_i}{M_k} = \frac{C_i}{C_k} = \frac{\sigma_k}{\sigma_i} \frac{C_i^{(0)}}{C_k^{(0)}} e^{-\frac{1}{2} x^2 \left( \frac{1}{\sigma_i^2} - \frac{1}{\sigma_k^2} \right)}, \quad (4)$$

whence accordingly

$$\ln \frac{C_i}{C_k} - \ln \frac{\sigma_k}{\sigma_i} \frac{C_i^{(0)}}{C_k^{(0)}} = -\frac{1}{2} x^2 \left( \frac{1}{\sigma_i^2} - \frac{1}{\sigma_k^2} \right). \quad (5)$$

Dividing (5) by the analogous equation obtained by replacing the element  $i$  by element  $j$ ,

$$\ln \frac{C_i}{C_k} - \ln \frac{\sigma_k}{\sigma_i} \frac{C_i^{(0)}}{C_k^{(0)}} = \lambda_{ijk} \left( \ln \frac{C_j}{C_k} - \ln \frac{\sigma_k}{\sigma_j} \frac{C_j^{(0)}}{C_k^{(0)}} \right), \quad (6)$$

where

$$\lambda_{ijk} = \frac{\frac{1}{\sigma_i^2} - \frac{1}{\sigma_k^2}}{\frac{1}{\sigma_j^2} - \frac{1}{\sigma_k^2}}. \quad (7)$$

Hence

$$\log \frac{C_i}{C_k} = \lambda_{ijk} \log \frac{C_j}{C_k} + K_{ijk}, \quad (8)$$

where

$$K_{ijk} = \log \frac{\sigma_k}{\sigma_i} \frac{C_i^{(0)}}{C_k^{(0)}} - \lambda_{ijk} \log \frac{\sigma_k}{\sigma_j} \frac{C_j^{(0)}}{C_k^{(0)}}. \quad (9)$$

In equations (8) and (9) the logarithms are taken to base ten.

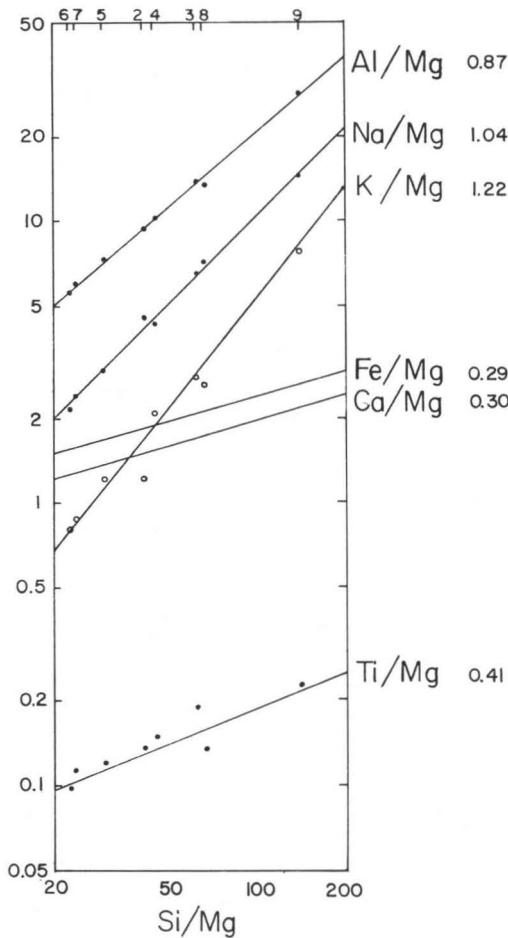


FIG. 7.

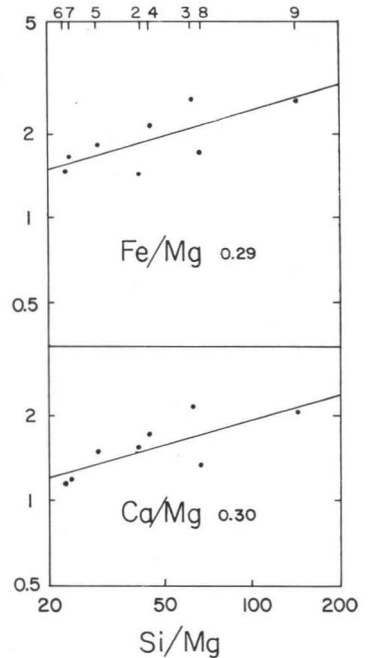


FIG. 8.

Fig. 7. Orijärvi line samples. Cation ratios Al/Mg, Na/Mg, Ti/Mg (dots) and K/Mg (circles) plotted against Si/Mg on logarithmic coordinates. Corresponding ratios Fe/Mg and Ca/Mg are shown separately in Fig. 8. Straight lines represent least-squares solutions. Numbers on the right are calculated values of the constants  $\lambda_{iSiMg}$ . Their standard deviations, counted from above, are .015, .02, .06, .10, .09, .06. The values of  $\lambda$  for  $i = Si$  and  $i = Mg$  are automatically fixed to unity and zero, respectively. Numbers along top refer to the sample lines.

Equation (8) shows that  $\log (C_i/C_k)$  is a linear function of  $\log (C_j/C_k)$ ,  $\lambda_{ijk}$  representing the slope. If  $\lambda_{ajk} > \lambda_{bjk}$ , this means that  $\sigma_a < \sigma_b$ , provided  $\sigma_j < \sigma_k$ .

In the case of Orijärvi, in fact, there are two folds of different size, which, for some reason, might have different values of the constants  $\sigma_v$ , say  $\sigma_v^{(1)}$  and  $\sigma_v^{(2)}$ . In this case it is natural to assume that  $\sigma_v^{(1)} = c \cdot \sigma_v^{(2)}$ , where  $c$  is the same constant

for all elements. As can be seen from equation (7), this means that  $\lambda_{ijk}$ -values are the same in both folds. Hence, when  $C_i/C_k$  is plotted as a function of  $C_j/C_k$ , it is permissible to mix samples belonging to the two folds.

#### APPLICATION TO ORIJÄRVI

In Figures 7 and 8 the model has been applied to the Orijärvi granodiorite. In this case silicon and magnesium have been selected for  $j$  and  $k$ , respectively, while  $i$  is the index of any element. We may conclude from the differences in the  $\lambda$ -values that the different elements have migrated toward the axial planes at different average velocities, decreasing in the order K-(Na, Si)-Al-(Ti, Ca, Fe)-Mg. No significant difference in this respect can be observed between Na and Si, nor between Ti, Ca, and Fe. It must be noted also that the ratio  $Fe^3/Fe^2$  increases with Si/Mg and hence has an influence upon the  $\lambda$ -value for the total iron.

Due to the different mobilities of the elements, the migration has resulted in a chemical fractionation of the original layered complex into a rock series ranging from cordierite-anthophyllite rocks and other basified rocks, situated lowest downlimb, via trondhjemites (tonalites) and granodiorites to adamellites of the axial zones. The major basification appears to have taken place in areas of strong shear and contraction while the granitoid rocks were formed in areas of expansion increasing toward the adamellitic end (Tuominen 1961, see also Bennington 1956, 1959). This differentiation, being related to the folding, took place mainly before the final recrystallization (drying up) of the complex.

If the differentiation proceeds to the right past the observed values of Fig. 7, it will lead to compositions where the amount of alkalis (and calcium) exceeds the equivalent amount of aluminum needed for feldspars. In this event the liberated alkalis may cause feldspathization and other related phenomena in the surrounding rocks where excess aluminum is available. Also the high K/Na ratios exceeding that of the eutectoid granites, characteristic of metasomatic microcline granites, may result from a differentiation of this type (Marmo 1962, p. 63; Eskola 1963 p. 220).

The above model is very similar to an earlier model (Tuominen 1964) presented by the author for the »liquid descent» of subalkalic series. Also the sequence of »mobility» obtained for the Orijärvi case is equivalent to that for the supposedly magmatic series. The experiments of Johannes and Winkler (1965) seem to indicate that fractionation of rocks at temperatures below melting may lead to sequences of the above type, i.e., melting temperatures are not necessary for such a fractionation. Nevertheless, whether partial melting has contributed to the later stages of the Orijärvi fractionation, remains, of course, open to discussion.

It seems obvious that the Gaussian distribution provides an approximation for the areas of expansion only. Outside these areas the logarithmic trends may

not be linear. Linearity, however, is not essential for the use of the logarithmic ratio plot. It can be shown that if, for a given abscissa,  $\lambda_{ajk} > \lambda_{bjk}$ , the ratio  $C_a/C_b$  increases at this point. In consequence the logarithmic ratio plot indicates the changes of ratios between all the components plotted on the diagram. I would like to point out also that the application of least-squares is not essential for the method. The slopes and their differences may normally be seen and estimated directly from the plots without any further calculation.

*Manuscript received, March 31, 1966*

#### REFERENCES

- BENNINGTON, K. O. (1956) Role of shearing stress and pressure in differentiation as illustrated by some mineral reactions in the system  $MgO-SiO_2-H_2O$ . *J. Geol.* 64, pp. 558—577.
- (1959) Energy transfer from differentiation in a differential pressure system under non-equilibrium conditions. *Ibid.* 67, pp. 171—198.
- CHAYES, F. (1957) A provisional reclassification of granite. *Geol. Mag.* 94, pp. 58—68.
- (1964) Variance-covariance relations in some published Harker diagrams of volcanic suites. *Jour. Petrology* 5, pp. 219—237.
- ESKOLA, P. E. (1914) On the petrology of the Orijärvi region in southwestern Finland. *Bull. Comm. géol. Finlande* 40; *Fennia* 37,3.
- (1952) A discussion of domes and granites and ores. *Bull. Comm. géol. Finlande* 157, pp. 125—144.
- (1963) The Precambrian of Finland. In Rankama (editor): *The Precambrian*, Vol.1; Interscience Publishers.
- JOHANNES, W. and WINKLER, H. (1965) Transport von Feldspäten und Quartz im Temperaturgefälle. *Beiträge zur Mineralogie und Petrographie* 11, pp. 250—271.
- MARMO, V. (1962) On granites. *Bull. Comm. géol. Finlande* 201.
- MILLER, R. L. and KAHN, J. S. (1962) *Statistical analysis in the geological sciences*. John Wiley & Sons.
- RAMBERG, H. (1952) *The origin of metamorphic and metasomatic rocks*. University of Chicago Press.
- TUOMINEN, H. V. (1957) The structure of an Archaen area, Orijärvi, Finland. *Bull. Comm. géol. Finlande* 177.
- (1961) The structural position of the Orijärvi granodiorite and the problem of synkinematic granites. *Bull. Comm. géol. Finlande* 196, pp. 499—515.
- (1964) The trends of differentiation in percentage diagrams. *Jour. Geol.* 72, pp. 855—860.
- (1966) On synkinematic Svecofennian plutonism. *Bull. Comm. géol. Finlande* 222, pp. 387—392.

## Appendix. Modal analyses of 94 specimens from Orijärvi granodiorite.

Q = quartz A = potash feldspar Pl = plagioclase

Mu = white mica Bi+Chl = biotite + chlorite

Hbl = hornblende Ep = epidotes

Others = apatite, sphene, opaques (+ garnet or carbonates where indicated)

CI = color index

Count for Mt = count for opaques ( $\approx$  magnetite)The specimens of each *Line* are listed from west to east.

Location and code no. of specimen	% Q	% A	% Pl	% Mu	% Bi + Chl	% Hbl	% Ep	% Others	CI	Count for Mt	Count length
<i>Line 2.</i>											
Zone II											
208 .....	38.4	0.1	54.3	1.0	5.6	—	0.3	0.3	7.2	—	1 474
207 .....	43.6	4.8	21.3	14.6	13.3	—	2.2	0.2	30.3	—	1 298
206 .....	31.4	0.4	55.8	4.8	6.7	—	0.5	0.5 <sup>1)</sup>	12.4	—	1 431
205 .....	34.7	0.4	52.6	0.2	12.1	—	—	—	12.3	—	1 450
204 c .....	42.8	1.3	40.5	0.4	15.0	—	—	—	15.4	—	1 431
204 b .....	45.6	0.2	37.8	1.4	13.5	—	1.4	0.1	16.4	1	1 557
204 a .....	45.7	0.1	40.2	0.1	13.7	—	0.1	0.1	14.0	—	1 509
203 .....	32.8	1.8	49.7	—	7.4	1.4	5.4	1.5 <sup>2)</sup>	15.7	—	1 478
202 .....	29.7	0.3	58.2	—	5.3 <sup>3)</sup>	—	5.0	1.5 <sup>4)</sup>	11.8	—	1 446
201 a .....	43.2	15.2	24.8	—	15.4	—	1.3	0.1	16.8	—	1 426
201 b .....	30.0	7.7	50.6	2.9	8.2	—	0.5	0.1	11.7	1	1 418
<i>Line 3</i>											
Zone I											
301 .....	33.5	14.3	41.4	0.5	10.3	—	—	—	10.8	—	1 465
302 .....	35.2	10.1	44.8	0.8	8.9	—	0.1	0.1	9.9	—	1 479
303 .....	37.6	6.1	38.6	—	16.3	—	1.4	—	17.7	—	1 539
304 .....	36.0	17.4	37.8	—	8.8	—	—	—	8.8	—	1 425
305 .....	38.7	12.2	37.3	1.1	7.6	1.1	1.7	0.3	11.8	2	1 380
306 .....	38.0	8.4	43.8	—	7.4	0.5	1.0	0.9	9.8	7	1 438
307 .....	27.8	17.0	44.5	2.1	6.4	—	0.8	1.4	10.7	12	1 465
308 .....	37.5	0.1	43.2	—	10.7	3.2	2.6	2.7 <sup>5)</sup>	19.2	—	1 485
309 .....	37.6	10.2	43.4	—	4.8	2.3	1.0	0.7	8.8	4	1 321
310 .....	32.9	9.9	43.8	—	10.5	—	2.3	0.6	13.4	—	1 492
311 .....	34.6	7.0	48.5	0.5	6.5	0.4	1.6	0.9	9.9	9	1 446
<i>Line 4</i>											
Zone I											
401 .....	34.0	5.7	53.5	0.7	6.1	—	—	—	6.8	—	1 467
402 .....	29.9	5.7	48.3	—	12.6	1.8	1.4	0.3	16.1	—	1 445
403 .....	38.5	11.8	39.6	—	8.8	0.7	0.3	0.3	10.1	4	1 511
404 .....	37.2	11.9	41.0	—	7.3	1.4	1.0	0.2	9.9	3	1 347
Zone II											
405 .....	29.0	6.7	48.0	—	10.7	4.4	1.2	—	16.3	—	1 402
406 .....	35.4	2.9	45.2	—	12.1	2.7	1.6	0.1	16.5	2	1 437
407 .....	40.9	4.6	40.5	—	11.6	0.7	1.7	—	14.0	—	1 395
408 .....	30.0	29.0	23.6	—	17.4 <sup>6)</sup>	—	—	—	17.4	—	1 459

Location and code no. of specimen	% Q	% A	% Pl	% Mu	% Bi + Chl	% Hbl	% Ep	% Others	CI	Count for Mt	Count length
<i>Zone III</i>											
409 .....	35.4	4.0	44.8	—	10.6	2.3	2.5	0.4	15.8	2	1 423
410 .....	32.9	6.1	45.2	—	14.3	0.3	1.1	0.1	15.8	2	1 468
411 .....	37.5	6.2	42.5	—	12.0	—	1.8	—	13.8	—	1 473
412 .....	29.7	14.6	40.6	—	14.5	—	0.6	—	15.1	—	1 466
413 .....	35.2	6.8	47.2	—	8.8	—	1.8	0.2	10.8	—	1 371
414 .....	32.6	10.8	51.5	—	4.8	—	0.3	—	5.1	—	1 499
<i>Line 5</i>											
<i>Zone I</i>											
501 .....	29.8	2.2	41.8	—	12.9	12.7	—	0.6	26.2	6	1 442
502 .....	27.0	10.8	40.0	—	14.0	7.5	0.6	0.1	22.2	1	1 404
503 .....	33.4	22.7	31.8	—	9.1	1.5	1.5	—	12.2	—	1 439
<i>Zone II</i>											
504 .....	35.1	2.5	41.0	—	9.7	11.1	0.6	—	21.4	—	1 428
505 .....	39.6	0.6	44.7	—	11.8	1.5	1.8	—	15.2	—	1 302
506 .....	26.6	6.1	43.5	—	19.8	1.6	2.4	—	23.8	—	1 473
<i>Zone III</i>											
507 .....	26.1	5.1	47.0	—	20.5	—	1.3	—	21.8	—	1 483
508 .....	32.0	6.1	38.8	—	20.0	0.9	1.7	0.5	23.1	7	1 458
509 .....	40.1	2.8	44.8	—	9.1	1.5	1.7	—	12.3	—	1 454
510 .....	33.8	13.7	33.9	—	13.4	0.4	4.8	—	18.5	—	1 406
511 .....	25.4	9.4	46.2	—	18.2	—	0.8	—	19.0	—	1 474
512 .....	32.3	0.1	48.3	—	18.3	—	1.0	—	19.3	—	1 470
513 .....	39.0	1.0	49.6	—	8.2	—	1.4	0.8	10.4	8	1 468
514 .....	37.8	5.0	47.2	—	8.1	—	1.5	0.4	10.0	5	1 424
515 .....	36.3	0.1	53.3	—	9.5	—	0.6	0.2	10.3	2	1 425
<i>Line 6</i>											
<i>Zone I</i>											
611 .....	32.2	3.8	46.3	—	13.4	2.8	1.5	—	17.7	—	1 429
<i>Zone II</i>											
610 .....	35.0	0.1	46.4	—	17.1	0.6	0.6	0.2	18.5	—	1 400
609 .....	38.8	0.3	36.2	—	23.8	—	0.8	0.1	24.7	—	1 523
608 .....	38.7	0.4	42.5	—	16.6	1.1	0.4	0.3	18.4	5	1 432
607 .....	34.4	0.3	45.6	—	19.0	—	0.7	—	19.7	—	1 426
<i>Zone III</i>											
606 .....	35.3	0.6	45.1	—	16.2	0.6	1.9	0.3	19.0	5	1 429
605 .....	39.2	0.5	43.8	—	14.4	0.3	1.1	0.7	16.5	12	1 481
604 .....	34.2	0.3	49.8	—	12.8	2.7	0.1	0.1	15.7	—	1 451
603 .....	34.8	0.3	47.6	—	16.4	—	0.7	0.2	17.3	3	1 418
602 .....	23.1	1.6	49.3	—	11.6	13.9	0.3	0.2	26.0	3	1 422
601 .....	35.0	0.1	48.4	—	13.0	1.0	0.8	1.7	16.5	23	1 435
<i>Line 7</i>											
<i>Zone I</i>											
701 .....	32.3	—	43.8	—	22.0	—	—	0.1 <sup>7)</sup>	22.1	—	1 410
702 a .....	37.1	3.6	56.4	—	6.0	5.7	1.0	—	12.7	—	1 457
702 b .....	41.1	0.1	54.1	—	7.3	7.0	0.4	—	14.7	—	1 495

Location and code no. of specimen	% Q	% A	% Pl	% Mu	% Bi + Chl	% Hbl	% Ep	% Others	Cl	Count for Mt	Count length
703 .....	36.3	0.3	45.9	—	13.6	2.9	1.0	—	17.5	—	1 496
704 .....	33.7	0.3	44.9	—	16.9	3.0	0.9	0.3	21.1	4	1 486
705 a .....	38.2	0.3	45.2	—	14.1	0.9	0.5	0.8	16.3	11	1 444
705 b .....	36.0	0.7	43.0	—	19.4	—	0.7	0.2	20.3	3	1 446
706 .....	29.4	0.2	49.1	—	18.5	1.4	0.8	0.6	21.3	9	1 467
707 .....	29.7	0.7	43.2	—	26.1	—	—	0.3 <sup>7)</sup>	26.4	—	1 483
708 .....	27.1	—	59.7	—	11.8	—	—	1.4	13.2	20	1 448
709 a .....	35.6	8.0	41.7	—	9.2	5.5	—	—	14.7	—	1 461
709 b .....	31.8	1.8	54.3	—	11.6	—	—	0.5	12.1	3	1 433
<i>Zone II</i>											
710 .....	33.5	0.5	53.4	—	11.7	—	0.3	0.6	12.6	8	1 414
711 .....	32.8	0.3	45.6	—	21.0 <sup>8)</sup>	—	0.3	—	21.3	—	1 497
712 .....	26.7	0.6	49.7	—	21.8	—	1.2	—	23.0	—	1 452
<i>Line 8</i>											
<i>Zone I</i>											
801 .....	37.7	25.9	33.8	0.5	1.6	—	—	0.5	2.6	8	1 443
802 .....	39.6	10.8	43.3	0.3	5.7	—	0.3	—	6.3	—	1 506
803 .....	42.4	16.1	35.4	0.4	4.6	—	1.0	0.1	6.1	1	1 423
804 .....	39.5	10.0	40.0	0.7	9.1	—	0.7	—	10.5	—	1 452
805 .....	47.2	1.9	43.7	0.7	6.1	—	0.1	0.3	7.2	4	1 452
806 .....	44.1	0.3	45.9	—	9.1	—	—	0.6 <sup>7)</sup>	9.7	—	1 417
807 .....	36.8	—	55.3	—	7.6	—	—	0.3	7.9	4	1 466
808 .....	46.2	4.6	42.6	0.3	6.2	—	0.1	—	6.6	—	1 490
<i>Line 9</i>											
<i>Zone I</i>											
908 .....	41.2	30.5	22.2	0.6	4.7	—	—	0.8	6.1	11	1 453
<i>Zone II</i>											
907 b .....	40.0	10.4	44.8	0.6	4.2	—	—	—	4.8	—	1 437
907 a .....	35.0	29.8	28.4	0.5	6.2	—	0.1	—	6.8	—	1 468
906 .....	42.4	4.2	48.4	1.3	3.6	—	—	0.1	5.0	—	1 410
905 .....	49.8	17.5	27.5	0.1	5.0	—	—	—	5.2	—	1 450
904 .....	44.2	11.3	39.0	1.9	3.6	—	—	—	5.5	—	1 492
903 .....	31.3	21.8	43.8	0.4	2.5	—	0.2	—	3.1	—	1 437
902 .....	38.5	12.1	40.9	1.3	6.2	—	—	—	7.5	—	1 409
901 .....	41.0	15.0	38.1	0.4	5.5	—	—	—	5.9	—	1 418

1) Carbonate 0.3 %

2) Carbonate 1.2 %

3) Chlorite 3.3 %

4) Carbonate 1.2 %

5) Carbonate 2.3 %

6) All chlorite

7) All garnet

8) Chlorite 4.1 %



# THE MINERALOGY AND GEOCHEMISTRY OF THE YLÖJÄRVI Cu-W DEPOSIT, SOUTHWEST FINLAND: MACKINAWITE-PYRRHOTITE- TROILITE ASSEMBLAGES

BY

A. HORRELL CLARK

*Department of Geology, University College London*

## ABSTRACT

The properties and paragenetic relationships of mackinawite in the Ylöjärvi deposit are briefly described. In several zones this mineral has preferentially replaced troilite which forms lamellar and granular intergrowths with intermediate hexagonal pyrrhotite ( $\text{Fe}_{0.9;2}\text{S}$ ), and is thus presumed to have crystallized at a later stage than the mutual exsolution of the hexagonal phases, at temperatures below  $\sim 139^\circ\text{C}$ , and, probably, in the range  $25^\circ\text{--}100^\circ\text{C}$ . Ylöjärvi mackinawite breaks down to pyrrhotite or troilite when heated in vacuo between  $130^\circ$  and  $140^\circ\text{C}$ , and a temperature of  $135\pm 5^\circ\text{C}$  is proposed as the upper stability limit for Ni- and Co-free tetragonal  $\text{Fe}_{1+x}\text{S}$ .

## INTRODUCTION

Mackinawite,  $(\text{Fe,Ni,Co})_{1+x}\text{S}$  with  $x \leq \sim 0.07$  (Kouvo *et al.*, 1963; Evans *et al.*, 1964), has recently been shown to be a comparatively widespread accessory mineral in several types of ore deposits and in sedimentary and igneous rocks (*e.g.*, Milton & Milton, 1958; Soeda, 1960; Berner, 1962, 1964; Kouvo *et al.*, 1963; Fujiki 1963; Evans *et al.*, 1962, 1964; Takeno & Soeda, 1964; Takeno 1965; Chamberlain & Delabio, 1965). Its paragenetic relationships with associated sulphides and silicates are broadly indicative of relatively low temperatures of formation, and Berner (1962, 1964) has synthesized an identical tetragonal  $\text{Fe}_{1+x}\text{S}$  phase in aqueous solutions at normal temperatures and pressures. Mackinawite occurs as a consistent accessory phase in the Pre-Cambrian Ylöjärvi copper-tungsten deposit, near Tampere, Finland (Himmi, 1960), where its textural relationships perhaps permit a more precise

estimation of its conditions of deposition than has been possible in the occurrences previously described. Kouvo *et al.* (1963) determined the composition of mackinawite from the Ylöjärvi deposit by electron microprobe analysis.

### ASPECTS OF THE MINERALOGY OF THE YLÖJÄRVI DEPOSIT

The mineralogy and geochemistry of the Ylöjärvi deposit have been studied in detail by the author (Clark, 1964, 1965a, 1965b), a major aim of this work being the investigation of the compositional variations of the ore minerals, and their interpretation on the basis of the available synthetic phase equilibrium data. In the Ylöjärvi deposit, the fragments in a vertical breccia pipe cutting regionally metamorphosed Bothnian (Svecofennidian) volcanic schists have been cemented by iron-rich tourmaline and associated arsenopyrite, chalcopyrite, pyrrhotite, pyrite, scheelite, and lesser concentrations of many other ore and gangue minerals. The solid solution ranges of the early-formed arsenopyrite (Clark, 1965b) and pyrrhotite (Clark, 1964), and the nature of the later ore mineral parageneses have been tentatively interpreted as indicating that sulphide deposition in the matrix of the breccias commenced at  $\sim 700^\circ\text{C}$ , under confining pressures probably exceeding 2000 bars, and that hypogene mineralization continued during progressive cooling to temperatures of the order of  $200^\circ\text{C}$ . Subsequently, extensive re-equilibration of several sulphides, and particularly pyrrhotite, accompanied the gradual exposure of the mineralized zone and the attainment of the prevailing temperatures of  $-10$  to  $+25^\circ\text{C}$ .

In the course of the present study particular attention was paid to the paragenetic and compositional relationships of the iron sulphides: pyrrhotite, mackinawite, pyrite and marcasite, in the deposit. Deposition of a minor early generation of pyrite preceded that of pyrrhotite, while the latter suffered late-stage, but hypogene, replacement by further pyrite and marcasite, approximately simultaneously with the introduction of a third pyrite phase. On the basis of the X-ray powder diffraction examination of 216 specimens it has been concluded that over sixty per cent of the pyrrhotite in the deposit exhibits a monoclinic or monoclinic + hexagonal crystal structure ( $46.3_6$ – $46.7_0$  and  $46.7_0$ – $47.1_0$  atomic per cent iron, respectively). The subordinate hexagonal pyrrhotite comprises: (a) a minor, very iron-deficient phase with continuous solid solution from  $46.2_3$  to  $\sim 47.5$  atomic per cent iron; (b) »intermediate hexagonal pyrrhotite» with a composition showing no appreciable variation from  $47.6_0$  atomic per cent iron; and (c) troilite, stoichiometric FeS. Intermediate hexagonal pyrrhotite and troilite form characteristic lamellar intergrowths, which in restricted zones have apparently undergone progressive segregation to granular and veiniform intergrowths and monomineralic patches and veinlets of the two phases.

A possible mechanism for the development of these complex pyrrhotite assemblages has been briefly outlined elsewhere (Clark, 1964) and a revised and more com-

prehensive discussion of the geochemistry of the pyrrhotite in the Ylöjärvi deposit is in the course of preparation. On the evidence at present available, it is considered that, whereas the monoclinic, monoclinic+hexagonal, intermediate hexagonal, and troilite modifications are low temperature (< 315°C max.) phases and show compositional limits conforming to the equilibrium phase relationships at approximately normal temperatures, the very iron-deficient hexagonal pyrrhotites may be true high temperature forms which persisted during cooling from initial crystallization temperatures in the range ~ 500—550°C. Their preservation in a pyrrhotite assemblage which has otherwise wholly equilibrated to very low temperatures cannot in this case be ascribed to abnormal minor element concentrations (Clark, 1964), and must be considered problematical.

Whereas the rigorous interpretation of the more iron-deficient pyrrhotite phases in the Ylöjärvi assemblages in terms of crystallization temperatures must await clarification of the phase relationships in the FeS-S partial system below ~ 315°C,<sup>1</sup> the published phase equilibrium data (*e.g.* Grønvold & Haraldsen, 1952; von Gehlen & Piller, 1965), suffice to indicate that the lamellar intergrowths of troilite and intermediate hexagonal pyrrhotite have resulted from exsolution at a low temperature solvus. The solvus curve, coinciding with the  $\alpha$ -transformation (Roberts, 1935), falls from a maximum temperature of  $139 \pm 2^\circ\text{C}$  at the stoichiometric composition (Moh & Kullerud, 1964) to progressively lower temperatures with increasing iron-deficiency. Intermediate hexagonal pyrrhotite coexisting with troilite in many deposits (Clark, 1964; von Gehlen & Piller, 1965) has been found to have a composition of  $47.6_9 \pm 0.02$  atomic per cent iron, and this composition probably indicates the position of the solvus at normal temperatures.

#### THE PROPERTIES AND PARAGENETIC RELATIONSHIPS OF MACKINAWITE

Mackinawite in the Ylöjärvi deposit is either closely associated with moderate-to-low temperature assemblages or exhibits apparently replacive relationships to early, higher temperature ore minerals. It forms irregular, subhedral to anhedral flakes and microveinlets, averaging 0.01—0.2 mm in maximum diameter but occasionally attaining 1.2 mm across, in the following environments: (a) in magnetite, frequently along zones of microfracturing and in marginal areas of magnetite grains enclosed by later chalcopyrite and cubanite (Fig. 1), and pyrrhotite; (b) in chalcopyrite, often in the immediate vicinity of exsolved plates of cubanite, the mackinawite being characteristically concentrated within and at the margins of the cubanite bodies (Fig. 1); (c) in pyrrhotite (monoclinic; monoclinic+hexagonal, intermediate hexagonal, and troilite modifications); (d) within or adjacent to grains of several of

<sup>1</sup> The results of an experimental investigation of the Fe-S system between 45° and 400°C are discussed in a paper being prepared for publication.

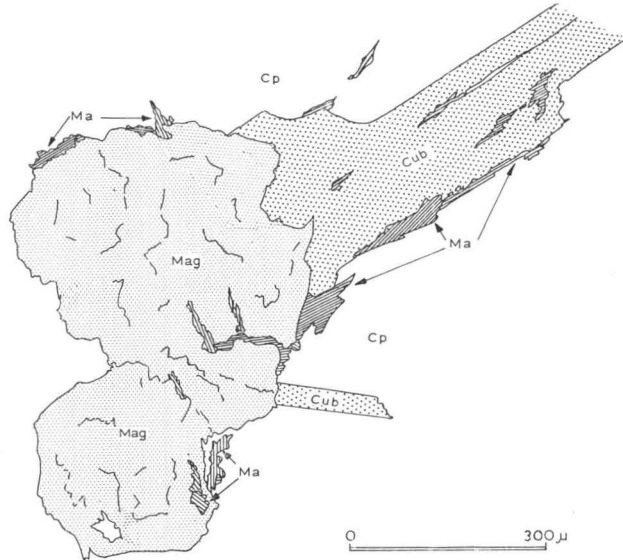


Fig. 1. Relationships between mackinawite (Ma), magnetite (Mag), chalcopyrite (Cp) and cubanite (Cub), Ylöjärvi mine, 285 m level orebody I.

the rare minerals of the intermediate-stage Pb-Ag-Bi-Sb paragenesis (galena, matildite, and native silver); (e) in late-stage chlorite-calcite-quartz veinlets cutting the above minerals.

The optical properties of the Ylöjärvi mackinawite are very similar to those described by earlier workers (Kouvo *et al.*, 1963; Evans *et al.*, 1964; Chamberlain & Delabio, 1965), and clearly differ from those of valleriite, *sensu stricto*. Thus, bronze or brown colours are not exhibited in plane-polarized light, and under incompletely crossed nicols (in air and oil) the mackinawite shows strong bluish-white to brown anisotropism. Reflectivity was not measured, but is of same order as that of the associated pyrrhotite and cubanite, and certainly higher than that of valleriite. The Vickers microhardness values of 16 grains were determined for various loads, using a Leitz Durimet instrument. As demonstrated by Chamberlain & Delabio (1965) the microhardness increases approximately linearly with increasing load, and was found to be  $52 \pm 3$  for a 50g load, in reasonable agreement with the value of 58 given by Chamberlain & Delabio (*op. cit.*), considering the difficulties inherent in indenting very thin flakes of such a well-cleaved, markedly anisotropic mineral. The microhardness of mackinawite may be affected by nickel and cobalt solid solution, perhaps accounting for the comparatively high (but unmeasured) hardness of the Outokumpu tetragonal  $(\text{Fe, Ni, Co})_{1+x}\text{S}$  (Kouvo *et al.*, 1963).

When compared with most other analysed mackinawites, that from the Ylöjärvi deposit is notable for its very low nickel and cobalt contents (each  $\sim 0.2$  weight

per cent; Kouvo *et al.*, 1963)<sup>1</sup>. Takeno (1965) has, however, described a mackinawite from the Kawayama mine, Japan, which contains negligible Ni and Co, and it is evident that these minor elements are not essential constituents of naturally occurring tetragonal  $\text{Fe}_{1+x}\text{S}$ . The nickel- and cobalt-poor composition of the Ylöjärvi mackinawite reflects the generally very minor concentration of these elements in the later sulphides in the deposit owing to their preferential incorporation in early-formed, stable arsenopyrite (Clark, 1965b), whereas in several other occurrences which have been described this mineral is closely associated with nickel- and cobalt-bearing sulphides and silicates.

Several relatively pure mackinawite fractions were examined using a 114.6 mm diameter Debye-Scherrer X-ray camera and a Nonius Guinier-de Wolff quadruple-focussing camera (filtered Co- $K\alpha$  radiation), and yielded X-ray powder patterns showing no significant differences from those of the type mackinawites (Evans *et al.*, 1964; Kouvo *et al.*, 1963), with the most intense reflections at  $5.03_3$  (relative intensity 100),  $2.96_5$  (65),  $3.31_0$  (90),  $1.836$  (50),  $1.808$  (80), and  $1.725$  (40) Å. Comparison of the powder data of synthetic tetragonal  $\text{Fe}_{1+x}\text{S}$  (Berner, 1962) with those of the nickel- and cobalt-bearing natural mackinawites reveals no appreciable variations in cell dimensions with minor element content.

Although the paragenetic relationships of mackinawite in the Ylöjärvi ores are suggestive of late-stage, low temperature formation, most of the observed textural associations are not indicative of a restricted temperature range. Mackinawite apparently replaced both chalcopyrite and cubanite, and formed after the exsolution of the latter phase. The position of the chalcopyrite-cubanite solvus is still undefined at low temperatures (Yund & Kullerud, 1961), however, and because the compositions of the original chalcopyrite-cubanite solid solutions in the Ylöjärvi assemblages varied between unknown limits and both phases have largely equilibrated since deposition to normal temperatures, these intergrowths cannot yield reliable maximum temperatures of formation. Similarly, the association of mackinawite with the monoclinic and monoclinic+hexagonal pyrrhotite assemblages is of little geothermometrical value, owing to the difficulty of distinguishing originally exsolved from introduced pyrite, and, therefore, of ascertaining whether mackinawite formation occurred earlier or later than the pyrrhotite-pyrite equilibration reactions at temperatures below  $\sim 315^\circ\text{C}$ .

The observed relationships between mackinawite and the troilite-intermediate pyrrhotite intergrowths, however, are considered to indicate more precisely the conditions of formation of the tetragonal iron sulphide in this environment. In several polished sections mackinawite exhibits a consistent association with troilite lamellae enclosed in intermediate pyrrhotite, (Figs. 2 A, 3). Mackinawite flakes and microveinlets are concentrated both within and at the margins of the troilite lamellae,

<sup>1</sup> Further electron microanalytical studies of mackinawites from the Ylöjärvi deposit and other localities are in progress.

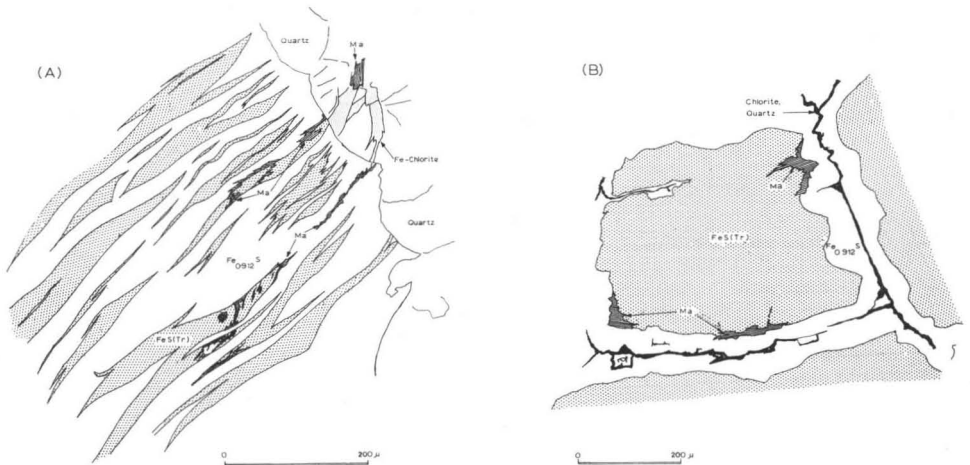


Fig. 2. Relationships between mackinawite (Ma), troilite, (FeS(TR)) and intermediate hexagonal pyrrhotite (Fe<sub>0.912</sub>S), Ylöjärvi mine, 285 m level, orebody IV.

particularly in the vicinity of pyrrhotite grain boundaries. In some zones preferential replacement of troilite has led to the partial pseudomorphism of the extremities of lamellae, and rare sinuous lamellae of mackinawite in intermediate pyrrhotite probably formed through complete replacement of small troilite bodies (Fig. 3). The intermediate pyrrhotite has also been replaced by mackinawite, but to a lesser extent. Mackinawite further occurs along grain boundaries in the granular and veiniform troilite-intermediate hexagonal pyrrhotite intergrowths (Fig. 2 B).

It is considered that these textural features clearly show that the mackinawite formed after the mutual exsolution of the troilite and intermediate pyrrhotite and the local diffusion of the hexagonal phases to form the coarser intergrowths. It should be stressed that many areas of troilite and intermediate pyrrhotite are apparently wholly free from mackinawite, and there is no evidence that the formation of the tetragonal phase was an integral stage in the development of the pyrrhotite assemblages. The possibility that mackinawite may itself have exsolved from the original pyrrhotite solid solutions cannot be entirely discounted, although the textural relationships between troilite and mackinawite and the morphology of the composite lamellae make this improbable.

#### TEMPERATURE OF FORMATION OF THE MACKINAWITE

Exsolution of the troilite and iron-deficient hexagonal pyrrhotite from initially homogeneous pyrrhotite solid solutions is assumed to have taken place at temperatures below  $\sim 139^{\circ}\text{C}$ . In zones where post-exsolution diffusion has not caused changes

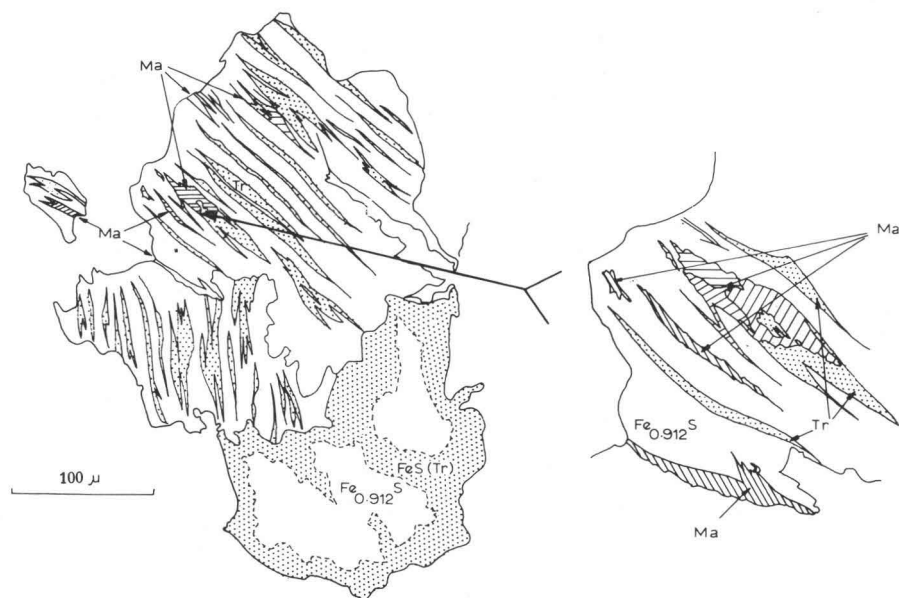


Fig. 3. Replacement of troilite lamellae by mackinawite, Ylöjärvi mine, 375 m level, orebody IV.

in the bulk compositions of the lamellar grains, relatively lower maximum temperatures of initial exsolution may be inferred from the trend of the solvus curve (and  $\alpha$ -transformation) with increasing iron-deficiency. Where the lamellar grains contain very minor concentrations of troilite (< 10 per cent) it is probably reasonable to assume that exsolution of this phase commenced at temperatures as low as  $\sim 50$ — $100^\circ\text{C}$ , although consideration of the precise conditions of exsolution must await the determination of the detailed phase relationships in this part of the Fe-S system. It is suggested that mackinawite may have crystallized under conditions closely approaching those at present prevailing in the mineralized zone. Although this mineral shows no spatial relationship to the rare supergene goethite — the deposit as a whole has been little affected by supergene alteration at the present level of exposure — mackinawite formation was »epigenetic» with respect to the equilibrating pyrrhotite solid solution assemblages on a microscopic scale, and tetragonal  $\text{Fe}_{1+x}\text{S}$  should perhaps be considered as a supergene phase in this environment.

Several heating experiments were carried out on intergrowths of mackinawite with other minerals in order to obtain a semi-quantitative confirmation of the proposed low temperature formation of this phase.

Pure fractions of mackinawite were not readily obtainable. The mackinawite-bearing intergrowths were removed from polished sections and hand-specimens, finely ground, and heated for various periods in evacuated silica glass tubes in »Kullerud-type» electrically-heated furnaces, temperatures being controlled to within

TABLE 1 (a—c)

Heating experiments on mackinawite-bearing assemblages, Ylöjärvi mine.

(a): Mackinawite — intermediate hexagonal pyrrhotite ( $\text{Fe}_{0.912}\text{S}$ ; 2.0701 Å<sup>1</sup>) — troilite (2.0932 Å) intergrowth.

Heating temperature (°C)	Heating period (hrs.)	Observations on phases present on quenching
50	2	no detectable changes in mackinawite and pyrrhotite X-ray patterns
	6	
	70	
103	48.5	mackinawite persists unchanged; troilite: 2.0929 Å; pyrrhotite: 2.0720 Å
130	6	mackinawite persists unchanged; troilite (trace): 2.0936 Å; pyrrhotite: 2.0739 Å
	32	
140	72	mackinawite persists unchanged; troilite (trace): 2.0939 Å; pyrrhotite: 2.0742 Å
	13	
155	96	mackinawite very faint, but no X-ray reflection shifts; troilite absent; pyrrhotite: 2.0755 Å
	96	

<sup>1</sup> All d-values represent pyrrhotite 102 substructure spacings

1—2°C and measured using chromel-alumel thermocouples. After annealing the runs were quenched in iced water and immediately X-rayed on a Nonius focussing camera (Co-K $\alpha$  radiation; NaCl and Ni as external standards). The results of these experiments are presented in Table 1 (a—c).

A precise indication of the stability relationships of natural mackinawite probably cannot be derived from these few data. The dangers inherent in deducing phase relationships and original crystallization conditions of sulphides from the results of annealing experiments on, necessarily, arbitrarily delimited assemblages are fully realized. Whether associated with troilite and intermediate hexagonal pyrrhotite, monoclinic pyrrhotite, or chlorite and quartz, however, the mackinawite apparently broke down consistently between 130° and 140°C. At lower temperature, no changes in either angular positions or relative intensities of reflections were detected in the composite powder patterns yielded by the mackinawite-monoclinic pyrrhotite and mackinawite-chlorite-quartz assemblages, and there was no evidence that mackinawite reacted with the associated phases below its apparent breakdown temperature. Between 100°C and 130°C the associated troilite and intermediate pyrrhotite clearly re-equilibrated, possibly only partially, to the annealing temperatures, the latter phase showing an increasing iron content.

TABLE 1: continued:

(b): Mackinawite — monoclinic pyrrhotite ( $2.0635$ ;  $2.0523 \text{ \AA}$ <sup>1</sup>) intergrowth.

Heating temperature (°C)	Heating period (hrs.)	Observations on phases present on quenching
103	6.5 74	mackinawite persists unchanged; monoclinic pyrrhotite: $2.0632$ ; $2.0523 \text{ \AA}$
130	32.5 96	mackinawite persists unchanged; monoclinic pyrrhotite: $2.0637$ ; $2.0520 \text{ \AA}$
140	96	mackinawite absent; monoclinic pyrrhotite: $2.0637$ ; $2.0522 \text{ \AA}$ ; traces of slightly iron-deficient hexagonal pyrrhotite

<sup>1</sup> d-values of monoclinic ( $408 + 228$ ) and ( $228 + 408$ ) composite reflections

(c): Mackinawite — chlorite — quartz intergrowth.

Heating temperature (°C)	Heating period (hrs.)	Observations on phases present on quenching
103	72	mackinawite, chlorite, and quartz patterns unchanged
130	5.5 42 96.5	mackinawite, chlorite, and quartz patterns essentially unchanged, but chlorite reflections slightly diffuse after 96.5 hours
140	13 94	mackinawite absent; traces of troilite ( $d_{102} = 2.0930 \text{ \AA}$ ); chlorite and quartz unchanged

Again, in this assemblage, mackinawite apparently resisted reaction with pyrrhotite below  $\sim 130^\circ\text{C}$ . Where associated with chlorite and quartz, mackinawite was converted on heating to troilite (with characteristic superstructure reflections) at  $\sim 140^\circ\text{C}$ , whereas a slightly iron-deficient hexagonal pyrrhotite was formed from mackinawite intergrown with monoclinic pyrrhotite. The X-ray powder patterns of mackinawite showed no measureable changes on heating below  $\sim 130^\circ\text{C}$ , and no intermediate phases between mackinawite and the pyrrhotites which formed on heating were detected.

## DISCUSSION

The approximate upper stability limit of  $\sim 130$ – $140^\circ\text{C}$ , tentatively proposed for the Ni-free Ylöjärvi mackinawite coincides with the temperature of the  $\alpha$ -transformation for stoichiometric hexagonal FeS, and is in very good agreement with the breakdown temperatures recorded in heating experiments carried out by Soeda

(1960; in Takeno, 1965), who observed that Ni-free mackinawite from the Kawayama mine, Japan, loses its characteristic pleochroism and anisotropism at 130–140°C. In contrast, cleanly separated tetragonal  $(\text{Fe, Ni, Co})_{1.046}\text{S}$  from the Outokumpu mine, Finland (Kouvo *et al.*, 1963) apparently broke down when heated in air at  $\sim 200$ –210°C. A strong endothermic reaction was detected in DTA runs at 245°C. and was ascribed to phase transformation of the tetragonal sulphide, although very weak exothermic peaks at 130°C. and 160°C might perhaps have been related to the incipient breakdown of this phase. The Outokumpu mackinawite, however, contained 8.28 weight per cent nickel (and 0.42 per cent Co), and it is probable that extensive minor element solid solution may be found to have a significant influence on the stability limit of this mineral. It should be stressed that attempts to reverse the mackinawite — pyrrhotite (or troilite) transition proved unsuccessful; mackinawite did not reappear in detectable quantities when the pyrrhotite assemblages which formed at 140°C, and in which mackinawite had originally been present, were re-annealed at 130° and 103°C for 50–60 days.

The equilibrium relationships of mackinawite in the Fe-S binary system are at present unknown. The author was unable to synthesize a tetragonal phase in comparatively extended evacuated tube experiments at 45, 74.5, and 115°C (in preparation). Troilite, showing no deviation from stoichiometry, and  $\alpha$ -iron alone formed in all runs having initial bulk compositions in the range 63.6–65.0 weight per cent iron, after heating periods of up to 6.5 months. Furthermore, no mackinawite was formed when small proportions of nickel (equivalent to 3–8 weight per cent) were added in the initial synthesis of the pyrrhotites. Berner (1962, 1964) succeeded in synthesizing both tetragonal  $\text{Fe}_{1+x}\text{S}$  and hexagonal FeS in aqueous solutions by reaction of  $\text{H}_2\text{S}$  with metallic iron and steel at 40–42°C and 80–85°C, while at 20–25°C tetragonal  $\text{Fe}_{1+x}\text{S}$  alone formed under similar conditions. Troilite and mackinawite are not, however, strictly polymorphous, and there is little evidence that naturally-occurring troilite is unstable (or metastable), in the absence of pyrite, at temperatures below  $\sim 40^\circ\text{C}$ . Troilite suffers very rapid tarnishing in polished sections (*e.g.*, Kouvo *et al.*, 1963), but appears to be essentially unaltered in natural environments. As suggested by Berner (1964), a comparative consideration of the phase relationships in the generally similar Fe-Se system may be instructive in this context. The published experimental data for this system (summarized by Grønvold & Westrum, 1959, and Tröften & Kullerud, 1961) indicate that at temperatures below  $\sim 335$ –350°C the stable phases are tetragonal  $\text{Fe}_{1+x}\text{Se}$  ( $\text{Fe}_{1.04-1.05}\text{Se}$ ), comparable to mackinawite, and hexagonal (to monoclinic)  $\text{Fe}_{1-x}\text{Se}$  with a modified NiAs structure, corresponding to pyrrhotite but showing an iron rich solid solution limit of approximately  $\text{Fe}_{0.88}\text{Se}$  below 350°C. By analogy, the possibility that stoichiometric hexagonal FeS may in fact be metastable at very low temperatures cannot be wholly discounted. In the light of the prevalence of low-temperature modifications in natural pyrrhotite associations it might be expected that intergrowths of tetragonal  $\text{Fe}_{1+x}\text{Se}$  and hexagonal  $\text{Fe}_{1-x}\text{Se}$  would occur in favourable environments, but ferroselite

(FeSe<sub>2</sub>) has not yet been observed to occur in association with other iron selenides, and strict comparisons of natural iron sulphide and selenide assemblages cannot be made.

Until the stability relationships of mackinawite are established experimentally it is tentatively suggested that this phase, having a composition in the range Fe<sub>1.04—1.07</sub> occupies a narrow, probably vertical field between those of troilite and  $\alpha$ -iron below  $\sim 135 \pm 5^\circ\text{C}$ . Continuous solid solution between troilite and mackinawite is considered to be very improbable. The clearly shown replacement of troilite by mackinawite in the Ylöjärvi deposit possibly reflects abrupt local variations in sulphur or oxygen fugacities during the penetration of the ores by late-stage hypogene or supergene fluids, rather than the inherent instability of troilite at very low temperatures.

The generally markedly differing environments of formation of (terrestrial) troilite and mackinawite should be stressed. Troilite is almost invariably closely associated with iron-deficient pyrrhotite phases (except, perhaps, in recent sediments), and is considered to have formed through low-temperature equilibration of pyrrhotite assemblages in the course of post-deposition cooling. In contrast, mackinawite is characteristically associated and intergrown with Cu-Fe or Fe-Ni sulphides, and appears to have exsolved from or to have replaced those minerals, whereas troilite never shows ordered intergrowths with sulphides other than pyrrhotite in terrestrial rocks. Although nickel and cobalt are not invariably present in natural mackinawites, the crystallization of this mineral may have been often stimulated by the expulsion of these minor elements during the low temperature exsolution and equilibration of, say, chalcopyrite-cubanite solid solutions. Mackinawite is sometimes the sole nickel- or cobalt-bearing constituent in sulphide assemblages, and then appears to have »scavenged» these elements during its formation. Preliminary electron microprobe examination of troilite-pyrrhotite intergrowths has, on the other hand, shown that minor nickel and cobalt (and copper) are preferentially concentrated in the iron-deficient phase, troilite showing little capacity for their incorporation.

*Acknowledgements* — The microscopic and X-ray studies of the Ylöjärvi assemblages were carried out in the Department of Geology, the University of Manchester, during tenure of a Research Studentship, and under the direction of Professor E. A. Vincent, while the heating experiments and experimental studies referred to in this paper were undertaken in the Department of Geological Sciences, McGill University, Montreal, during tenure of a National Research Council of Canada Postdoctoral Fellowship, and with the kind assistance of Professor L. A. Clark. The writer is grateful to Outokumpu Oy, and to Professor P. Haapala and Mr. R. Himmi in particular, who provided facilities for the field work at the Ylöjärvi mine. Dr. R. A. Howie kindly reviewed the manuscript.

*Manuscript received, March 31, 1966*

## REFERENCES

- BERNER, R. A., (1962) Tetragonal iron sulfide. *Science*, 137, 669.
- »— (1964) Iron sulfides formed from aqueous solution at low temperatures and atmospheric pressure. *J. Geol.*, 72, 293—306.
- CHAMBERLAIN, J. A., & DELABIO, R. N., (1965) Mackinawite and valleriite in the Muskox intrusion. *Amer. Min.*, 50, 682—695.
- CLARK, A. H., (1964) Pyrrhotite-sphalerite relations in the Ylöjärvi deposit, southwest Finland: a summary. *Geologi*, 16, 145—150.
- »— (1965a) The mineralogy and geochemistry of the Ylöjärvi Cu-W deposit, southwest Finland: a bismuth-bearing apatite. *Comptes Rend. Soc. géol. Finlande*, 37, 195—199.
- »— (1965b) The composition and conditions of formation of arsenopyrite and löllingite in the Ylöjärvi copper-tungsten deposit, southwest Finland. *Bull. Comm. géol. Finlande* 217.
- EVANS, H. T., MILTON, C., CHAO, E. C. T., ADLER, I., MEAD, C., INGRAM, B., & BERNER, R. A., (1964) Valleriite and the new iron sulfide, mackinawite, U. S. Geol. Surv. Prof. Paper 475-D, D64—D69.
- FUJIKI, Y., (1963) Paragenetic relations of the ore minerals from the Komori mine: on the exsolution textures of Cu-Fe-S system minerals, (in Japanese). *Mining Geol.*, 13, 339—350.
- GEHLEN, K. von., & PILLER, H., (1965) Optics of hexagonal pyrrhotine ( $\sim\text{Fe}_9\text{S}_{10}$ ). *Min. Mag.*, 35, 335—346.
- GRØNVOLD, F., & HARALDSEN, H., (1952) On the phase relations of synthetic and natural pyrrhotites ( $\text{Fe}_{1-x}\text{S}$ ). *Acta Chem. Scand.*, 6, 1 452—1 469.
- GRØNVOLD, F., & WESTRUM, E. F., JR., (1959) Low temperature heat capacities and thermodynamic properties of the iron selenides  $\text{Fe}_{1.04}\text{Se}$ ,  $\text{Fe}_7\text{Se}_8$ , and  $\text{Fe}_3\text{Se}_4$ , from 5 to 350°K. *Acta Chem. Scand.*, 13, 241—248.
- HIMMI, R., (1960) The Ylöjärvi mine: in *Mining Geology, Finland — Guide to excursions A36 and C31*, Int. Geol. Congress.
- KOUVO, O., VUORELAINE, Y., & LONG, J.V.P., (1963) A tetragonal iron sulfide. *Amer. Min.*, 48, 511—524.
- MILTON, C., & MILTON, D.J., (1958) Nickel-gold ore of the Mackinaw mine, Snohomish county, Washington. *Econ. Geol.*, 53, 426—447.
- MOH, G. H., & KULLERUD, G., (1964) The Fe-S system. *Carnegie Instn. Wash. Year Book* 63, 207—208.
- ROBERTS, H. S., (9135) Polymorphism in the FeS-S solid solutions: 1. Thermal study. *J. Amer. Chem. Soc.*, 57, 1 034—1 038.
- SOEDA, A., (1960) Valleriite in the cubanite-bearing ores from the Chugoku district, Japan (in Japanese). *Mining Geol.*, 10, 346—358.
- TAKENO, S., (1965) A note on mackinawite (so-called valleriite) from the Kawayama mine, Japan. *Geol. Rept. Hiroshima Univ.*, 14, 59—76.
- »— & SOEDA, A., (1964) Thermal studies of so-called valleriite from the Kawayama mine: Preliminary report (in Japanese). *J. Geol. Soc. Japan*, 70, 395.
- TRÖFTEN, P., & KULLERUD, G., (1961) The Fe-Se system. *Carnegie Instn. Wash. Year Book* 60, 176.
- YUND, R. A., & KULLERUD, G., (1961) The system Cu-Fe-S. *Carnegie Instn. Wash. Book* 60, 180—181.

# ON ROCKS CONTAINING GARNET, HYPER- STHENE, CORDIERITE AND GEDRITE IN THE KIURUVESI REGION, FINLAND

## PART I: JUURIKKAJÄRVI

BY

ANTTI SAVOLAHTI

*Institute of Geology and Mineralogy, University of Helsinki*

### ABSTRACT

Description are given of the different varieties of rock, their mode of occurrence and their relationships. Supplementing the text are twelve new chemical analyses of both the rocks and the minerals. The genesis of the rocks is discussed.

### CONTENTS

	Page
Introduction .....	344
The outcrop on the southeastern side of Lake Juurikka .....	346
Relationships of the rocks contained in the outcrop .....	346
Quartz-bearing amphibolite .....	349
Gedrite- and plagioclase-bearing quartzite .....	349
Rock lenses containing garnet, hypersthene, cordierite and gedrite .....	351
Hypersthene-gedrite gneiss .....	356
Conclusions .....	356
The outcrop situated southeast of Lake Juurikka .....	358
Relationship of the rocks in the outcrop .....	358
Hypersthene rock and diopside-hypersthene rock .....	360
Garnet-hypersthene-cordierite-gedrite gneiss .....	361
Garnet-hypersthene-gedrite-bearing gneiss and quartz-feldspar schist .....	361
Conclusions .....	362
The breccia on the northernmost point of land on the eastern shore of Lake Juurikka .....	362
Introduction .....	362
Fragments in the breccia .....	363

	Page
Brecciated rock .....	363
The surroundings of the breccia .....	367
The outcrop on the southern end of Lake Juurikka .....	368
Relationships of the rocks in the outcrop .....	368
Non-homogeneous cordierite gneiss .....	368
Quartz-feldspar schist .....	372
Peridotite .....	373
Conclusions .....	374
Hornblende-pyroxene gneiss from the outcrop on the west shore of Lake Juurikka	375
The highway cuts southeast by south of Lake Juurikka .....	376
Introduction .....	376
Hypersthene- and hornblende-bearing diopside gneiss .....	376
Quartz-bearing amphibolite .....	378
Diopside-bearing biotite amphibolite .....	379
Hypersthene-bearing gneiss .....	379
Conclusions .....	380
Pyroxene-bearing dioritic and granitic gneisses .....	381
Porphyritic granites .....	381
Discussion .....	382
Acknowledgments .....	384
References .....	384

## INTRODUCTION

In many places in the commune of Kiuruvesi, which is situated in the region of northern Savo, Finland, there are garnet-, hypersthene-, cordierite- and/or gedrite-bearing rocks. Occurrences of these rocks have been found, for example, in the vicinities of Niemiskylä, Kalliokylä and Toiviaiskylä. The rocks in the last-mentioned area show, perhaps, more variety than elsewhere, and the outcrops there probably afford the investigator the most ample opportunities for making observations of genetic significance. In the vicinity of Kalliokylä, hypersthene is rarely met with; and in the Niemiskylä area there are fewer outcrops than at Toiviaiskylä. It is for this reason that the research material collected in the surroundings of Lake Juurikka (Juurikkajärvi), Toiviaiskylä, has been taken up first for consideration. The lake is situated about five miles from the church of Kiuruvesi to the SSW.

I did the field work for the present series of studies during the summers of 1959—1961 in association with the exploration department of the Outokumpu Company. During the summer of 1962, I further checked certain of my observations, in addition to which I took some extra photographs. In the summer of 1959, I was armed with rapid aerial photographic maps covering the entire Kiuruvesi region of my investigation on the scale of 1 : 20 000, while, in the summer of 1960, I was also provided with aerial photographs of the vicinity of Lake Juurikka on a scale of 1 : 8 000. It was not possible as yet to mark down even on the latter photographs the variations in rock occurrences in detail. For this reason and in order to give the reader a more

# THE JUURIKKA REGION

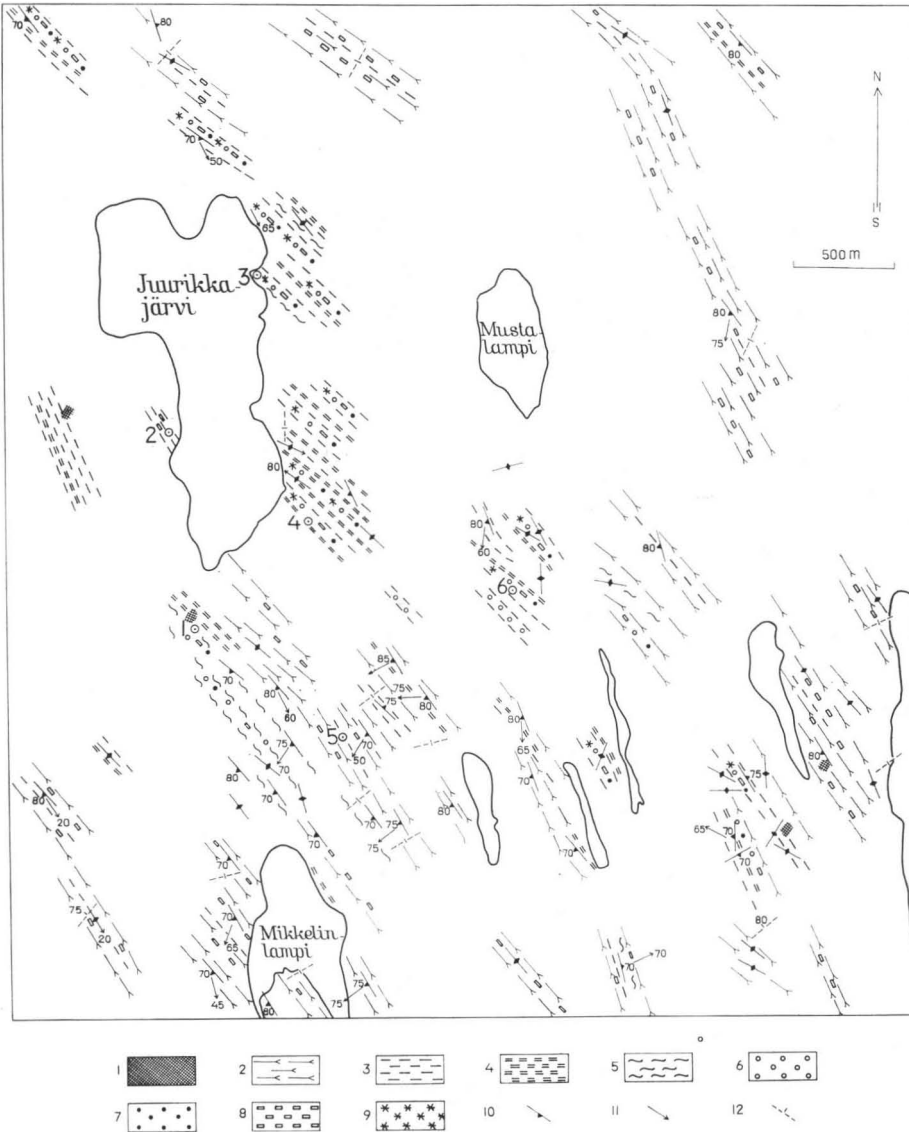


FIG. 1. Map of the vicinity of Lake Juurikka (Juurikkajärvi). 1) Peridotite, 2) Dioritic and granitic gneisses, 3) Amphibolitic rocks, 4) Quartz-feldspar schists, 5) Mica gneiss, 6) Garnet, 7) Cordierite, 8) Hypersthene, 9) Gedrite, 10) Foliation, 11) Lineation, 12) Cleavage.

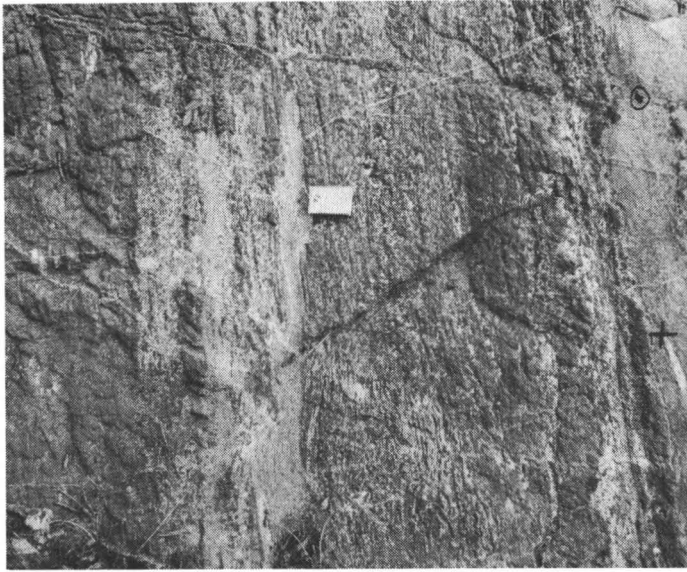


FIG. 2. The main part of the figures represents hypersthene-gedrite gneiss, which contains a few cordierite xenoblasts and garnet porphyroblasts. Here and there occur relicts of quartz-bearing amphibolite. (The cross and the point are on the same spot as in Fig. 3.)  
Point 4, Lake Juurikka, Toivaiaskylä, Kiuruvesi.

objective picture of these rocks and their mode of occurrence, I have deviated from the usual manner of presentation and undertaken to describe the structure of a few selected outcrops and their component rocks in detail. The outcrops described are marked in Figure 1. As a result, we arrive at a simultaneous description of the rocks situated in the region and their various relations without any generalizations.

No detailed geological study of the surroundings of Juurikkajärvi has previously appeared. Mäkinen (1916) marked the occurrence of mignatites and quartz diorites around the lake as well as of porphyritic granites at the eastern edge of the vicinity. The general geological map of Finland (Wilkman 1929) shows veined gneiss and granite gneiss in the surroundings of Lake Juurikka as well as porphyritic granites along the eastern border of the area. The explanatory text published to elucidate the general map (Wilkman 1931) makes only very scant mention of this area.

## THE OUTCROP ON THE SOUTHEASTERN SIDE OF LAKE JUURIKKA

### **Relationships of the rocks contained in the outcrop**

About 150 meters from the southeastern shore of Juurikkajärvi in the direction SEE, there is an outcrop (Point 4) containing quartz-bearing amphibolite, plagio-



FIG. 3. The center and the right edge of the figure contain quartz-bearing amphibolite, with narrow monomineral veins and lenses (hypersthene, gedrite and quartz). At the right edge of the figure there is hypersthene-gedrite gneiss. Point 4, Lake Juurikka, Toivaiaskylä, Kiuruvesi.

clase- and gedrite-bearing quartzite, and coarse-grained rock lenses consisting of garnet, hypersthene, cordierite and gedrite as well as hypersthene-gedrite gneiss. The relationship of these rocks can be observed fairly easily in this outcrop (Figs. 2, 3 and 4). The cross and the point in Figs. 2 and 3 are in the same place. The left edge of Fig. 4 starts near the right edge of Fig. 3. Southwest is in all three figures to the right.

The middle portion and the right edge of Fig. 3 represent the least metamorphosed rock contained in the outcrop. The same kind of quartz-bearing amphibolite extends over to the left margin of the next figure (No. 4). In places this amphibolite is slightly banded. The amphibole content varies in the different bands somewhat. The different bands are not sharply bounded against each other, however, and they do not differ very much. Furthermore, this amphibolite contains, among other things, narrow (approximately 1 cm in width and less), lenticular, monomineral veins of varying thickness, which, though slight winding, nevertheless conform in the main to the schistosity (Fig. 3). Quartz, hypersthene and gedrite occur as lenticular veins of this kind. In many cases, the entire vein seems to consist of a single crystal: no lines of separation can be detected between the mineral grains and throughout the vein the mineral displays cleavages running in the same direction. The structure and mode of occurrence of these lenticular veins indicates their having originated during

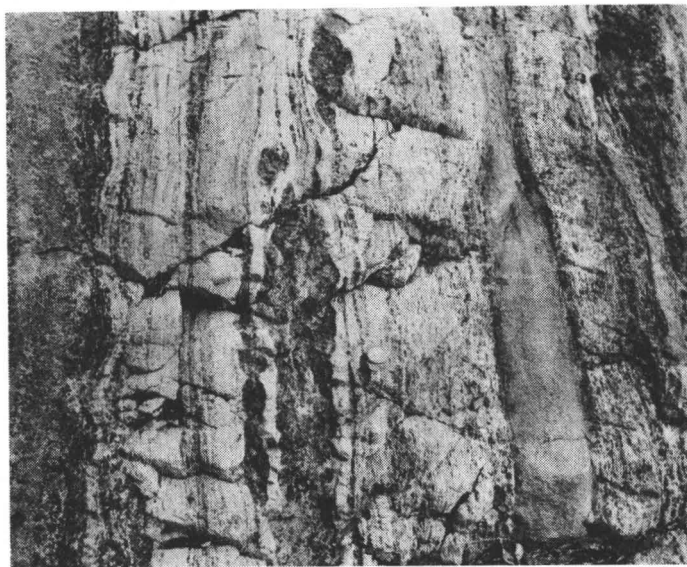


FIG. 4. The left margin of the figure shows quartz-bearing amphibolite, which also occurs as an inclusion at the right edge. The light gray represents plagioclase- and gedrite-bearing quartzite. The quartzite has coarse-grained rock lenses containing garnet, hypersthene, cordierite and gedrite. Point 4, Lake Juurikka, Toivaiskylä, Kiuruvesi.

the period of metamorphism, which evidently also played a part in the genesis of certain other quartz-bearing veins of coarser grain than the average for amphibolite.

Toward the right, the quartz-bearing amphibolite is followed (Fig. 4) by a very light gray, somewhat banded, conspicuously tectonized gedrite- and plagioclase-bearing quartzite. The banded nature of the rock is due to the variableness in, to some extent, the amounts of mafic and of light minerals and, partly, in the grain size of the minerals as well as, to a further extent, in the degree of tectonization of the rock.

In this quartzite, the quartz-bearing amphibolite occurs as narrow, elongated inclusions, one of which may be seen in Fig. 4. The upper end of the inclusion (Fig. 4) appears to fade away gradually into the quartzite. The same amphibolite is also present in the quartzite in vague, ghostlike form. Moreover, the quartzite has coarse-grained rock lenses as inclusions containing garnet, hypersthene, cordierite and gedrite (Fig. 4).

Mafic minerals have in many cases crystallized along the contact of the quartz-bearing amphibolite and the gedrite- and plagioclase-bearing quartzite (Fig. 4). In Fig. 2, an abundance of mafic minerals has crystallized in the quartz-bearing amphibolite, giving the rock a blackish gray hue. Relicts of quartz-bearing amphibolite are further visible in this hypersthene-gedrite gneiss. Immediately beyond the left margin of Fig. 2, this hypersthene-gedrite gneiss runs against markedly tectonized

gedrite- and plagioclase-bearing quartzite of the kind described in the foregoing. The zone involved in the latter case is considerably broader than in the former.

### Quartz-bearing amphibolite

The quartz-bearing amphibolite is a medium-grained, greenish rock, which takes on a light yellowish gray hue on the weathered surface of the outcrop. In places this amphibolite is slightly banded. The principal minerals in the quartz-bearing amphibolite are plagioclase, hornblende and quartz. There are also small amounts of orthorhombic amphibole, apatite and opaque minerals.

The plagioclase ( $\alpha = 1.550$ ,  $\gamma = 1.557$ ; An<sub>43</sub>) grains average 1 mm in length and are nearly rectangular in shape. The hornblende ( $\alpha = 1.655 =$  yellowish,  $\beta = 1.669 =$  yellowish green,  $\gamma = 1.675 =$  bluish green,  $c : \gamma = 19^\circ$ ; 35—40 mol. per cent (Fe<sup>2+</sup>, Mn, Ti)-component) grains average 0.5 mm in length, some of them being euhedral and some anhedral. Near a certain mylonitic zone, the hornblende has partially turned to anthophyllite ( $\alpha = 1.644$ ,  $\beta = 1.649$ ,  $\gamma = 1.661$ ; 35—45 mol. per cent Fe<sup>2+</sup>-component). The anthophyllite grains in many instances display the habit of hornblende, but a hornblende grain of this description usually consists of very many, sometimes even fibrous anthophyllite grains. The anthophyllite grain clusters generally contain small opaque inclusions, which are frequently observed to form a ring along the edge of the cluster. Adjacent to plagioclase, the grain clusters have a very narrow anthophyllite ring, sharply bounded against them but penetrating the plagioclase in toothlike fashion. The ring has an extinction simultaneous to that of the main crystals. Gedrite occurs much more commonly in this exposure than does anthophyllite, but the author lacks sufficient observation material to give a detailed description of the relationship of the hornblende and the gedrite, on the one hand, and of the anthophyllite and the gedrite, on the other, in this outcrop. Rather large opaque grains occur in greater amounts wherever the hornblende has not changed to anthophyllite. There is more quartz, which occurs as larger grains and to a greater extent with an undulating extinction, in places where the hornblende has altered to anthophyllite than elsewhere. In such places also the apatite occurs as larger grains than elsewhere.

Table 1 presents a chemical analysis of the quartz-bearing amphibolite. The norm includes quite a considerable amount of quartz. Very little K<sub>2</sub>O occurs in the rock. Orthoclase does not appear at all in the norm.

### Gedrite- and plagioclase-bearing quartzite

Gedrite- and plagioclase-bearing quartzite is a very light gray, banded and markedly tectonized rock. Its principal minerals are quartz, plagioclase and gedrite. To a slight extent it contains hypersthene, microcline, opaque minerals and alternation products.

TABLE 1.  
Chemical composition of quartz-bearing amphibolite (analyst: A. Heikkinen).  
Point 4, Lake Juurikka, Toiviaisskylä, Kiuruvesi.

	Weight per cent	Weight norm	Molecular norm	Niggli values
SiO <sub>2</sub> .....	54.93	or ... —	Or .. —	si ..... 149
TiO <sub>2</sub> .....	1.53	ab ... 25.7	Ab .. 28.0	al ..... 23
Al <sub>2</sub> O <sub>3</sub> .....	14.43	an ... 25.9	An .. 26.5	fm ..... 53
Fe <sub>2</sub> O <sub>3</sub> .....	7.11	Q ... 15.8	Q ... 15.4	c ..... 18
FeO .....	7.83	Σ' 67.4	Σ' 69.9	alk ..... 8
MnO .....	0.20			ti ..... 3
MgO .....	4.91	wo .. 0.1	C .... 0.1	h ..... 3
CaO .....	5.50	en ... 12.3	en ... 14.0	k ..... 0.04
Na <sub>2</sub> O .....	3.03	fs ... 6.3	Fs ... 5.6	mg ... 0.38
K <sub>2</sub> O .....	0.02	il .... 2.9	Il .... 2.2	o ..... 0.28
P <sub>2</sub> O <sub>5</sub> .....	0.13	mt ... 10.4	Mt ... 7.8	c/fm .. 0.30
CO <sub>2</sub> .....	0.0	ap ... 0.3	Ap .. 0.4	qz .... +17
H <sub>2</sub> O+ .....	0.34	fr ... 0.1	Fr ... —	
H <sub>2</sub> O— .....	0.01			
F .....	0.06			
Cl .....	0.01			
Σ	100.04	Σ 99.8	Σ 100.0	
—O .....	0.03			
Σ	100.01			

The quartz occurs generally, as in granulites (Eskola 1952, Scheumann 1961), as so-called platy quartz. In places it forms, to some extent, long bands of grains, in which in many cases the grains have become intergrown so as to form a single large grain; while, again, the quartz occurs in part as tiny crushed particles, which form narrow ribbons.

The composition of the plagioclase is An<sub>20</sub> ( $\alpha = 1.538$ ,  $\gamma = 1.546$ ). It is noticeably richer in albite than in the quartz-bearing amphibolite, or in other rocks contained in this outcrop. The twin lamellae of the plagioclase grains are in many instances bent.

The gedrite ( $\alpha = 1.662 =$  greenish,  $\beta = 1.671$ ,  $\gamma = 1.683 =$  violet-gray green,  $2V\gamma = 85^\circ$ ; 50 per cent Fe<sup>2+</sup>-component) occurs everywhere in the quartzite, though to a greater extent in the dark gray bands of the quartzite. The gedrite laths are frequently seen to be bent, and even rolled. They occur on the foliation plane, forming, among themselves long, irregular ribbons. In the more tectonized places, the grains have broken into very small, roundish particles.

The hypersthene ( $\alpha = 1.715 =$  hyacinth red,  $\beta =$  straw yellow,  $\gamma = 1.730 =$  sky blue,  $2V\alpha = 68^\circ$ ; 55 per cent Fe<sup>2+</sup>-component) occurs only in the dark gray bands of the quartzite. It is usually found as inclusions in gedrite and in fissures and along the edges of the grains has in many cases turned into a yellowish brown, fine-grained mass. The hypersthene appears to be an unstable mineral when contained

in quartzite — at least in its more highly tectonized portions — and it generally is present in gedrite only as armored relicts.

The microcline content is scanty and it has a beautiful quadrille texture.

Cordierite ( $\alpha = 1.543$ ,  $\gamma = 1.553$ ; 30 per cent  $\text{Fe}_2\text{Al}_4\text{Si}_5\text{O}_{18}$ -component<sup>1)</sup>) has been met with, but only in small amounts. In thin section, it has been observed with certainty only close to rock lenses containing garnet, hypersthene, cordierite and gedrite, and even in such cases it has been markedly pinitized. In this quartzite, the cordierite is an unstable mineral.

### Rock lenses containing garnet, hypersthene, cordierite and gedrite

The gedrite- and plagioclase-bearing quartzite contains various coarse-grained lenses of rock composed of garnet, hypersthene, cordierite and gedrite (Fig. 4). These lenses may be divided into two categories: 1) those containing abundant garnet, and 2) those containing abundant hypersthene. Between these two categories, however, there is no sharp line of demarcation, both of them revealing varying amounts of garnet, hypersthene, cordierite, gedrite, plagioclase and/or quartz. The lenses further contain small amounts of the following minerals: opaques, hercynite, biotite, zircon, pinitite, apatite, fibrous amphibole, chlorite, potash feldspar and rutile. In the distribution of the minerals in the lenses, no other regularity has been observed than that in lenses rich in garnet, this mineral tends to occur in the middle portion.

The garnet ( $n = 1.790$ — $1.787$ ,  $\text{FeO} = 27.49$  per cent by weight, or almandine = 60 molecular per cent; *cf. p.* 363 and Eskola 1952, p. 153) occurs in many instances as large poikiloblasts and grain clusters. It is reddish brown and it contains large hypersthene, cordierite and gedrite inclusions as well as small inclusions of plagioclase and opaque minerals. In its cleavages, the garnet reveals the presence in many spots of some chlorite and fibrous amphibole.

The hypersthene occurs to some extent as smallish prismatic grains and to a further extent as large anhedral poikiloblasts, the latter having inclusions of cordierite, opaques, plagioclase and gedrite. The large hypersthene grains are frequently seen to be surrounded by a gedrite ring, which is usually narrow but in some instances rather broad (Fig. 5). The ring generally consists of a single crystal, the c-axis of which joins the c-axis of the hypersthene. In these rocks the hypersthene is quite pleochroic:  $\alpha =$  hyacinth red,  $\beta =$  straw yellow,  $\gamma =$  sky blue; and it also contains Schiller inclusions. Table 2 presents the chemical composition of the hypersthene separated from the rock of one lens, together with its physical properties. According to this evidence, the hypersthene contains a fair abundance of aluminum. The maximum percentage of  $\text{Al}_2\text{O}_3$  found in hypersthene taken from granulites in

<sup>1)</sup> The pulverized quartzite rock was run several times through a Franz isodynamic separator to insure the elimination of the quartz and the feldspars. Thereafter, it proved easy to determine the indices of refraction of the cordierite.



FIG. 5. Microphoto. A portion of a hypersthene grain with gedrite inclusions and a surrounding gedrite ring. 1 nic. Lake Juurikka, Toivaiskylä, Kiuruvesi.

TABLE 2.

Chemical composition (analyst: S. Turkka) and physical properties of hypersthene from rock lenses containing garnet, hypersthene, cordierite and gedrite. Point 4, Lake Juurikka, Toivaiskylä, Kiuruvesi.

Weight per cent					
SiO <sub>2</sub> .....	49.72	Si .....	1.86	Z = 2.00	$\left\{ \begin{array}{l} \text{Si} = 1.86 \\ \text{Al} = 0.14 \end{array} \right.$
Al <sub>2</sub> O <sub>3</sub> .....	6.47	Al .....	0.29	$\left. \begin{array}{l} \text{Ti} \dots\dots\dots 0.01 \\ \text{Fe}^{3+} \dots\dots\dots 0.08 \\ \text{Fe}^{2+} \dots\dots\dots 0.71 \end{array} \right\} \text{Y} = 0.24$	
TiO <sub>2</sub> .....	0.25	Ti .....	0.01		
Fe <sub>2</sub> O <sub>3</sub> .....	2.80	Fe <sup>3+</sup> .....	0.08		
FeO .....	22.57	Fe <sup>2+</sup> .....	0.71	$\left. \begin{array}{l} \text{Mn} \dots\dots\dots 0.01 \\ \text{Mg} \dots\dots\dots 0.97 \end{array} \right\} \text{X} = 1.69$	
MnO .....	0.25	Mn .....	0.01		
MgO .....	17.43	Mg .....	0.97	$\left. \begin{array}{l} \text{Mg} \dots\dots\dots 0.97 \\ \text{Ca} \dots\dots\dots 0.02 \end{array} \right\} \text{W} = 0.02$	
CaO .....	0.46	Ca .....	0.02		
	$\Sigma$ 99.95				
Physical properties:					
<i>a</i> = 1.707					
<i>β</i> = 1.718					
<i>γ</i> = 1.723					
D = 3.54					

Lapland was 8.26 (Eskola 1952). It is Banno's (1964) observation that increasing pressure reduces the Al<sub>2</sub>O<sub>3</sub> content of orthopyroxene associated with garnet and clinopyroxene.

Hypersthene grains present in different lenses and even in different parts of the same lens have yielded different optic values, which have the following range: *γ* =

TABLE 3.

Chemical composition (analyst: S. Turkka) and physical properties of cordierite from rock lenses containing garnet, hypersthene, cordierite and gedrite. Point 4, Lake Juurikka, Toivaiaskylä, Kiuruvesi.

Weight per cent					
SiO <sub>2</sub> .....	49.17	Si .....	4.93	Z = 6.00	$\left\{ \begin{array}{l} \text{Si} = 4.93 \\ \text{Al} = 1.07 \end{array} \right.$
Al <sub>2</sub> O <sub>3</sub> .....	34.09	Al .....	4.03	$\left. \begin{array}{l} \text{Fe}^{3+} \\ \text{Mn} \end{array} \right\} Y = 3.07$	
Fe <sub>2</sub> O <sub>3</sub> .....	1.49	Fe <sup>3+</sup> .....	0.11		$\left. \begin{array}{l} \text{Fe}^{2+} \\ \text{Mg} \\ \text{Ca} \end{array} \right\} X = 0.94$
MnO .....	0.02	Mn .....	0.00		
FeO .....	3.95	Fe <sup>2+</sup> .....	0.33		
MgO .....	10.67	Mg .....	1.60		
CaO .....	0.13	Ca .....	0.01		
H <sub>2</sub> O+ .....	0.92				
H <sub>2</sub> O- .....	—				
	Σ 100.44				
Physical properties:					
α = 1.537					
γ = 1.546					
2Vα = 82°					
D = 2.59					

1.730—1.718, β = 1.727—1.714<sup>1)</sup>, α = 1.714—1.705, 2Vα = 69°—80°. This corresponds in composition to a variation of from 43 to 53 per cent with respect to the Fs-component. The optic angle of the hypersthene is appreciably greater than generally is true. Parras (1958) made the same observation in his study of the charnockites of the West Uusimaa complex in Finland.

The cordierite occurs to a certain extent as large xenoblasts and partly as clusters of small grains. The large grains are in many cases twinned. The cordierite xenoblasts contain an abundance of small hypersthene grains as well as large, ragged hypersthene grains. They also contain opaque minerals and hercynites as inclusions. In addition, the cordierite reveals the presence of zircon, which has pleochroic haloes and, in spots, a little pinite. Also the chemical composition of the cordierite varies somewhat, for the optic determinations made from different grains vary: γ = 1.550—1.546, α = 1.540—1.537, 2Vα = 78°—86°, although the variation in composition is than in the case of hypersthene. According to the optic properties, the cordierite contains approximately 25 per cent of the Fe<sub>2</sub>Al<sub>4</sub>Si<sub>5</sub>O<sub>18</sub>-component. Table 3 presents a chemical analysis and certain physical properties of cordierite. It will be seen to be relatively rich in magnesium, as are, for example, the cordierites of granulites (Eskola 1952). See also Schreyer and Yoder (1964).

The gedrite likewise occurs in part as small prismatic grains and in part as large poikiloblastic grains or clusters of tiny grains. The gedrite contains within itself hypersthene, cordierite, plagioclase, biotite and opaque minerals. It does not

<sup>1)</sup> Determinations of β have not been made from all the grains.

TABLE 4.

Chemical composition (analyst: S. Turkka) and physical properties of gedrite from rock lenses containing garnet, hypersthene, cordierite and gedrite. Point 4, Lake Juurikka, Toivaiaskylä, Kiuruvesi.

Weight per cent					
SiO <sub>2</sub> .....	42.48	Si .....	6.21	Z = 8	} Si = 6.21 Al = 1.79
Al <sub>2</sub> O <sub>3</sub> .....	17.00	Al .....	2.93	} Y = 1.50	
TiO <sub>2</sub> .....	0.36	Ti .....	0.04		} X = 5.58
Fe <sub>2</sub> O <sub>3</sub> .....	2.91	Fe <sup>3+</sup> .....	0.32	} W = 0.57	
FeO .....	17.40	Fe <sup>2+</sup> .....	2.13		
MnO .....	0.17	Mn .....	0.02		
MgO .....	15.74	Mg .....	3.43		
CaO .....	0.72	Ca .....	0.11		
Na <sub>2</sub> O .....	1.54	Na .....	0.44		
K <sub>2</sub> O .....	0.08	K .....	0.02		
H <sub>2</sub> O+ .....	1.44	(OH)— .....	1.41		
H <sub>2</sub> O— .....	0.00				
	Σ 99.84				
Physical properties:					
α = 1.663					
β = 1.671					
γ = 1.682					
2Vγ = 69°					
D = 3.35					

occur in the form of fibrous grains. To be sure, fibrous amphibole does appear slightly as an alternation product of garnet and hypersthene, though it represents a very late generation. The gedrite also reveals the presence of inclusions like the Schiller inclusions found in the hypersthene. The chemical analysis and the physical properties of the gedrite are presented in Table 4. Also the chemical composition of the gedrite varies according to the optic determinations in different grains and in different places:  $\gamma = 1.682$ — $1.675$ ,  $\beta = 1.673$ — $1.663$ ,  $\alpha = 1.656$ ,  $2V\gamma = 65^\circ$ — $72^\circ$ . According to the optic properties, its composition varies between 40 and 50 per cent with respect to the Fe''-component. Having read the study published by Schreyer and Yoder (1964), I see no theoretical obstructions to the occurrence, under favorable circumstance, of gedrite in association with cordierite and hypersthene.

The composition of the plagioclase is An<sub>45</sub> ( $\gamma = 1.558$ ,  $\alpha = 1.550$ ). The biotite is reddish brown and its  $\gamma = 1.662$ . It appears as a number of rather large flakes and as some small ones contained in the gedrite as inclusions. Quartz is present to a slight extent as small anhedral grains in the interstices between cordierite grains. It is also on occasion met with as large grains. Hercynite is found as grain clusters in association with opaques and cordierite. Apatite occurs as a few large grains, some of which are highly euhedral and some quite anhedral.

The petrography of the rock lenses containing garnet, hypersthene, cordierite and gedrite indicates that the minerals named all crystallized in them at the same

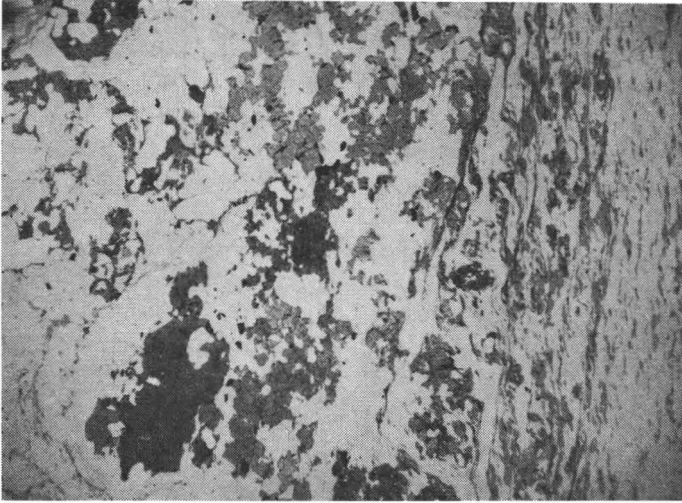


FIG. 6. Appearing toward the right margin of the figure is gedrite- and plagioclase-bearing quartzite, and on the left side rock lenses containing garnet, hypersthene, cordierite and gedrite. Microphoto, 1 nic.,  $\times 10$ .  
Point 4, Lake Juurikka, Toivaiskylä, Kiuruvesi.

time, for they all exist as inclusions within each other. These four minerals appear in relation to each other as a completely balanced mineral paragenesis. Garnet, it is true, has not been met with in places marked by the occurrence of gedrite-rich lenses, but this does not yet prove that this mineral cannot occur also in such places. The composition of the minerals in the lenses seems to vary according to whether any given mineral occurs as an inclusion within another one or outside it. The optic axial angle of hypersthene ( $2V\alpha$ ) appears to be distinctly greater in those grains that occur as inclusions in gedrite than in the ones on the outside. Similarly, the optic axial angle of gedrite ( $2V\gamma$ ) is larger in grains found in hypersthene as inclusions than in the ones situated outside this mineral. These variations in composition are understandable if we consider that during the genesis of the lenses different minerals crystallized at diverse places and at various times in different amounts and that the PT- and concentration-conditions did not remain constant throughout the entire time of formation of the lenses.

The contact between the gedrite- and plagioclase-bearing quartzite and the rock lenses containing garnet, hypersthene, cordierite and gedrite is to be seen in the microscopic photograph No. 6. At the right edge of the picture there appears gedrite- and plagioclase-bearing quartzite and at the left edge rock lenses containing garnet, hypersthene, cordierite and gedrite. Near the contact, the lens has been crushed into a fine-grained mylonitic rock. Around such rock lenses one does not always see a mylonitic joint like this.

### Hypersthene-gedrite gneiss

Figure 2 shows an abundance of hypersthene-gedrite gneiss, which immediately beyond the right margin of the figure is bounded by an occurrence of gedrite- and plagioclase-bearing quartzite. This hypersthene-gedrite gneiss appears to be coarse of grain. In part, this is due to the fact that the hypersthene and gedrite grains have separately taken the same positions, and, in part, to the fact that the hypersthene and the gedrite form in it large poikiloblasts. Hypersthene and gedrite are the principal minerals of the rock. The Fe''-component ( $\alpha$  = hyacinth red = 1.708,  $\beta$  = straw yellow,  $\gamma$  = sky blue = 1.722) accounts for 47 per cent of the hypersthene. In the gedrite the Fe''-component ( $\alpha$  = 1.662 = greenish,  $\gamma$  = 1.682 = violet-gray green) makes up 48 per cent of the total composition. Here and there in this rock there are blue cordierite xenoblasts of various sizes-ranging from, in many cases, only 2 mm to, in some cases, nearly 50 mm in diameter- and/or clusters of cordierite grains. Reddish brown garnet is also found in it to some extent, the grains of this mineral occurring in clusters and/or as porphyroblasts measuring as much as ten centimeters in length. The rock further contains a little plagioclase of andesine composition, quartz and opaques.

### Conclusions

The original chemical composition of the rocks contained in the outcrop situated at Point 4 probably corresponded to the chemical composition of the quartz-bearing amphibolite (Table 1). The quartz-bearing amphibolite is somewhat stratified, and it contains layers somewhat richer in, on the one hand, mafic minerals and, on the other, feldspars and quartz than the average. The original composition of the outcrop has not here, perhaps, varied, as indicated by the ghostlike quartz-bearing amphibolite relicts in the different rocks found in the outcrop. A further indication is the conspicuous scantiness in them of, *inter alia*, K-bearing minerals.

The quartz-bearing amphibolite contains monomineral lenses and lenticular veins, which, to judge by their very structure and mode of occurrence, clearly did not evolve until the period of metamorphism. The hypersthene-gedrite gneiss reveals the presence of ghostlike but nevertheless plainly distinguishable relicts of quartz-bearing amphibolite. Also the hypersthene-gedrite gneiss did not develop in the quartz-bearing amphibolite until the period of metasomatic metamorphism. There may, perhaps, be places in the hypersthene-gedrite gneiss that at the very beginning were a little richer in mafic minerals than the quartz-bearing amphibolite, but the occurrence of powerful metasomatic processes in connection with its genesis can scarcely be denied.

The gedrite- and plagioclase-bearing quartzite is a highly tectonized rock, which contains inclusions of quartz-bearing amphibolite. The upper end of the inclusion

shown in Fig. 4 gradually disappears into the quartzite, which also reveals the presence of ghostlike relicts of quartz-bearing amphibolite. It may be concluded on these grounds that a certain variety of quartz-bearing amphibolite, which may in spots have been slightly richer in felsic minerals than the type analyzed, was involved in powerful tectonic processes and that from it evolved gedrite- and plagioclase-bearing quartzite. The plagioclase of andesine composition and amphibole have dispersed and been replaced by plagioclase of oligoclase composition and, in the main, gedrite as well as an abundance of quartz. It is in this way that the gedrite- and plagioclase-bearing quartzite originated.

Some of the ions released by the tectonic processes wandered into the quartz-bearing amphibolite, forming in the rock monomineral lenses and veins and changing part of the amphibolite into hypersthene-gedrite gneiss. Certain of the released ions caused the formation in the quartzite of coarse-grained (pegmatoid) lenses. This explains the origin of the rock lenses containing garnet, hypersthene, cordierite and gedrite. The event to some extent resembled the formation of porphyroblasts in mylonite. In part, there also took place metamorphic differentiation (Eskola 1932; *cf.* Eskola 1933 a). Sahlsten (1935) has described eclogite lenses situated in paragneisses in eastern Greenland that in structure and mode of occurrence bear a resemblance to rock lenses containing garnet, hypersthene, cordierite and gedrite, and he regards them as the product of metamorphic differentiation.

Here in the same outcrop one finds three varieties of rock, which differ from each other with respect to the circumstances of origin: 1- quartz-bearing amphibolite, which in a different environment would be classified as a rock of an amphibolitic facies and which has to some extent disappeared; 2- gedrite- and plagioclase-bearing quartzite, which was involved in powerful tectonic processes; and 3- hypersthene-gedrite rock and rocks containing garnet, hypersthene, cordierite and gedrite, which, in the light of their habit and mineral composition, should be classified as belonging to the granulite facies.

Kranck (1931) considers the simultaneous occurrence of polymetamorphics in the kinzigite area of the Helsinki archipelago as a foregone conclusion, and he distinguishes two main mineral facies; amphibolite and prasinite facies, of which he regards the former as the older and the latter as associated with orogenial movements. Seki (1957) describes polymetamorphic phenomena in Kitakami and distinguishes two metamorphisms, of which the earlier is one of a lower degree and the later one of a higher degree. (See also Andreatta 1961). It is also possible, to be sure, that what is involved here are only different phases of the same regional metamorphism. But in the formation of a mineral assemblage, tectonic phenomena played a significant role, for the three last-mentioned rocks, though possessing a different mineral assemblage, evolved during the time they were active.

In rocks containing garnet, hypersthene, cordierite and gedrite and in hypersthene-gedrite rock the mineral assemblage is: garnet, hypersthene, cordierite and gedrite as well as, in many instances, plagioclase, hercynite and quartz. The present author

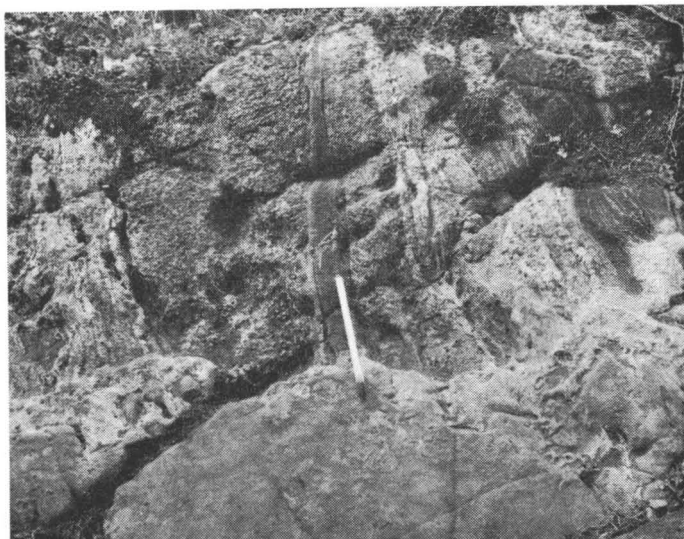


FIG. 7. Toward the bottom of the figure one will see a fine-grained diabase dike, and toward the upper edge various metamorphic rocks. At the contact occurs aplitic rock. Point 6, Lake Juurikka, Toivaiskylä, Kiuruvesi.

has seen no mention in the literature of such a mineral assemblage in equilibrium — as in the situation at hand is evidently true. No circumstance has come to light through microscopic examinations, at least, that gives any support to the argument that this mineral paragenesis might not be in equilibrium in these rocks. Perhaps the facies conditions here lie somewhere between the granulite and the amphibolite facies. Perhaps, too, during the tectonic processes, when the crystallization of these rocks took place, the chemical composition of the crystallizing material varied more than, for example, in thermometamorphism.

## THE OUTCROP SITUATED SOUTHEAST OF LAKE JUURIKKA

### **Relationships of the rocks in the outcrop**

Some 500 meters to the southeast from the outcrop situated on the southeastern side of Juurikkajärvi (Point 4), there is Point 6. Outcrops are situated there that have even more varied rocks than the ones observed in the first-mentioned area. The following rocks can be distinguished there: hypersthene rock and hypersthene-diopside rock, amphibolite and hornblende schist, garnet-hypersthene-cordierite-gedrite gneiss, garnet-, hypersthene- and gedrite-bearing gneiss, and quartz-feldspar schist.

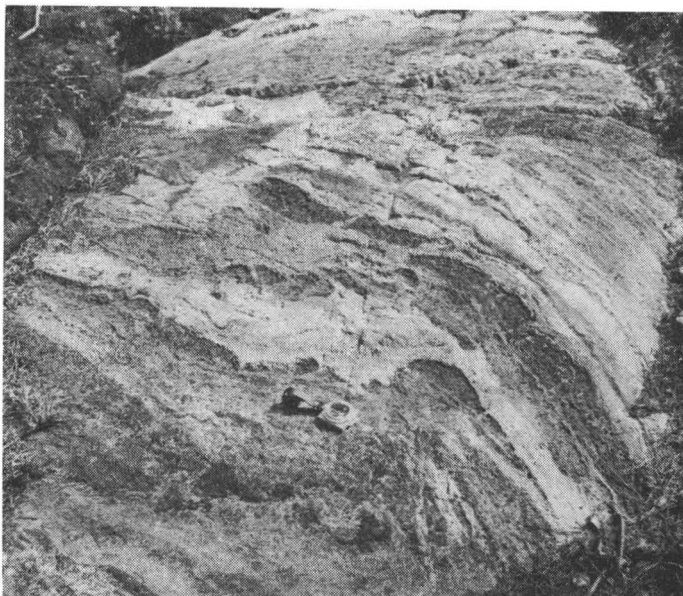


FIG. 8. Lower portion rocks containing mafic minerals in abundance. Upper portion rocks containing felsic minerals in abundance. Point 6, Lake Juurikka, Toiviaiskylä, Kiuruvesi.

Fig. 7 shows alternating layers of amphibolite, hornblende schist, hypersthene-diopside rock, garnet-hypersthene-cordierite-gedrite gneiss and a few narrow layers of quartz-feldspar schist. This entire series of metamorphic rocks is intersected by a fine-grained black-gray diabase (Fig. 7, lower margin). The diabase contains a few small fragments of wall rock. Between the series of metamorphic rock and the diabase there occurs fine-grained, pale gray, aplitic rock. This so-called aplite occurs as irregularly winding veins, mainly found in the diabase. The mineral composition of the aplite veins in terms of per cent by volume is as follows: quartz 40.5, oligoclase 45.1, biotite (and muscovite) 13.7, apatite and zircon 0.4, and opaques 0.3 per cent. No potash feldspar has been detected in it.

Fig. 8 depicts a site a few meters north of Fig. 7. On its left side there are metamorphic rocks containing a fair abundance of mafic minerals as well as garnet, hypersthene, gedrite and cordierite; while the right side of the figure is claimed by a light gray garnet- and gedrite-bearing gneiss with narrow layers of quartz-feldspar schist. At the border between the rocks, the varieties of the right and left sides are situated together as intercalations. In Fig. 9, which represents a separate exposure a few meters north of Fig. 8, there occurs a garnet-, hypersthene- and gedrite-bearing gneiss. The gneiss here is coarser of grain than in Fig. 8, and it is no longer so distinctly oriented. It contains quartz-feldspar layers and layers rich in mafic minerals.

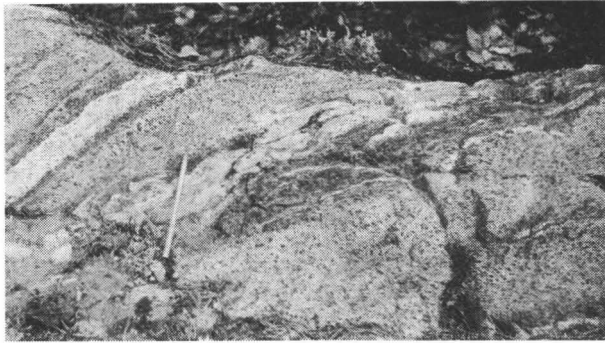


FIG. 9. Garnet-hypersthene- and gedrite-bearing gneiss. Point 6, Lake Juurikka, Toivaiskylä, Kiuruvesi.

### Hypersthene rock and diopside-hypersthene rock

The hypersthene rock is black-gray and its grain size is roughly 1 mm. It has a high content of hypersthene ( $2V\alpha = 70^\circ$ ), or some 70 per cent by volume. Its other minerals are diopside, hornblende, plagioclase ( $An_{90}$ ), opaques (*e.g.*, pyrrhotite) and zoisite.

The diopside-hypersthene rock, which resembles the preceding, contains approximately the same amount of diopside ( $2V\gamma = 56^\circ$ ,  $c:\gamma = 38^\circ$ ) as it does hypersthene ( $2V\alpha = 69^\circ$ ). In addition, it contains hornblende ( $2V\gamma = 78^\circ$ ,  $c:\gamma = 18^\circ$ ), plagioclase ( $An_{90}$ ), carbonate, opaques and zoisite.

These rocks include varieties with a cummingtonite content, but they are hard to distinguish megascopically. The following optic properties have been measured for the minerals contained in a cummingtonite-bearing specimen: plagioclase ( $\alpha = 1.573$ ,  $\gamma = 1.584$ ;  $An_{90}$ ), hypersthene ( $\alpha = 1.698$ ,  $\gamma = 1.712$ ; 38 mol. per cent Fs-component), diopside ( $\alpha = 1.692$ ,  $\gamma = 1.720$ ; 40 mol. per cent  $CaFe''$ -component), hornblende ( $\alpha = 1.658$ ,  $\beta = 1.672$ ,  $\gamma = 1.679$ , 43 mol. per cent (Fe'', Mn, Ti)-component) and cummingtonite ( $\alpha = 1.633$ ,  $\gamma = 1.661$ ,  $c:\gamma = 20^\circ$ ; 40 mol. per cent  $Fe''$ -component).

The hypersthene and, in particular, the diopside in all these rocks contain an abundance of indefinite hornblende inclusions. In some cases, the uralitization of the diopside grains has reached to a high degree. The rest of the hornblende has wandered around and in between the pyroxene grains. The diopside also contains quite small zoisite grains, which give the effect of being of a secondary nature. In the hypersthene, one finds thin lamellae running parallel to the *c*-axis. Carbonate occurs in the plagioclase as inclusions.

### Garnet-hypersthene-cordierite-gedrite gneiss

The garnet-hypersthene-cordierite-gedrite gneiss is indistinctly banded and dark gray. The distribution of the minerals in it is irregular, making it difficult to determine accurately the relative abundance of the mineral contents. The rock contains bands rich in garnet that also contain, *i n t e r a l i a*, hypersthene. The gneiss grains vary between 1 mm and 1 cm in length. In places the rock also has layers rich in garnet and hypersthene. The mineral composition of the gneiss is as follows: garnet, hypersthene, gedrite, plagioclase, cordierite, quartz, opaques, biotite, pinite and apatite.

The composition of the *h y p e r s t h e n e* involves 42 mol. per cent of the Fs-component ( $\alpha = 1.702$ ,  $\beta = 1.713$ ,  $\gamma = 1.716$ ). The mineral is distinctly pleochroic, though not very conspicuously so, and it is comparatively anhedral. The composition of the *g e d r i t e*: 50 mol. per cent Fe''-component ( $\alpha = 1.664$ ,  $\beta = 1.671$ ,  $\gamma = 1.683$ ). Wherever gedrite occurs in abundance, the edges and fissures of the hypersthene grains situated in it as inclusions are covered by a fine-grained, yellow stuff. The composition of the *p l a g i o c l a s e* is  $An_{35}$  ( $\alpha = 1.546$ ,  $\gamma = 1.554$ ). The mineral is comparatively euhedral and it does not contain any appreciable amount of alteration products. The composition of the *c o r d i e r i t e* is 17 mol. per cent of the  $Fe_2Al_4Si_5O_{18}$ -component. It occurs as rather large twinned porphyroblasts with a little pinite in places.

### Garnet-hypersthene-gedrite-bearing gneiss and quartz-feldspar schist

The garnet-hypersthene-gedrite-bearing gneiss is light gray, and its grain size is 1 mm or less. The rock contains larger grains of reddish brown garnet, greenish black-gray gedrite, and brownish black-gray hypersthene. The finer-grained varieties of the rock are distinctly schistose; but in the coarser-grained varieties, the schistosity is indistinct, with only the gedrite and, to some extent, the hypersthene having in some degree settled in definite levels. The light gray portion is quartz and plagioclase. The three specimens available for examination have revealed the presence of neither cordierite nor potash feldspar.

The composition of the *h y p e r s t h e n e* includes 50 mol. per cent of the Fs-component ( $\alpha = 1.713 = \text{hyacinth red}$ ,  $\gamma = 1.729 = \text{sky blue}$ ). The composition of the *g e d r i t e*: 48 mol. per cent Fe''-component ( $\alpha = 1.662 = \text{light greenish yellow}$ ,  $\gamma = 1.681 = \text{yellowish green}$ ). The garnet ( $n = 1793$ ) evidently corresponds in composition to the garnet of the granulite. The composition of the *p l a g i o c l a s e* is  $An_{30}$  ( $\alpha = 1.544$ ,  $\gamma = 1.551$ ). The *q u a r t z* content exceeds that of plagioclase.

The quartz-feldspar schists likewise contain small amounts of garnet.

### Conclusions

In spite of their marked metamorphism, these outcrops show that they have contained a number of schist layers greatly differing from each other in composition. But apparent in them are the results of metamorphic differentiation and metasomatic changes, too. The dark gray »boudins» situated in the garnet-, hypersthene- and gedrite-bearing gneisses are obviously fragments of thin strata, and Fig. 8 shows in its left margin the banding of the rock prevailing in them. Nothing like this is to be seen (or argued) in the rock lenses containing garnet, cordierite, hypersthene and gedrite on the southeastern shore of Juurikkajärvi (Fig. 3). Neither the metamorphic nor metasomatic processes have been capable of destroying the bedding, although recrystallization and the metamorphic differentiation of certain layers have been rather far-reaching.

The distinct schistosity of the garnet-hypersthene-gedrite-bearing gneiss has disappeared (Fig. 9). Gradual change cannot be perceived — for we are confronted with two separate, if adjacent, outcrops.

The genesis of the narrow diabase vein shown in Fig. 7 is interesting. In the Kiuruvesi—Vieremä region, diabase veins occur in many places, consistently being situated in the marginal portions of metamorphic schist and gneiss beds or quite adjacent to them. Their mineral composition corresponds to the same facies as that of their country rocks. There are, for example, pyroxene diabases and amphibole diabases. Are they of different ages, as has been assumed, or have they taken their positions at a late stage of regional metamorphism, the facies conditions of which had differed in different parts of the region?

## THE BRECCIA ON THE NORTHERNMOST POINT OF LAND ON THE EASTERN SHORE OF LAKE JUURIKKA

### Introduction

There is a breccia in the shore rocks on the northernmost point of land (Point 3) on the eastern end of Lake Juurikka. The fragments in the breccia consist of blackish gray diopside amphibolite. They have twisted and rolled, forming angles of as much as 90° among themselves. In addition, the outcrop contains indeterminate relicts of mica schist. The brecciated rock itself is to a great extent altogether unoriented and massive, but non-homogeneous. The minerals are unevenly distributed in it. In addition, there can be distinguished in it at least two components of differing mineral composition, which appear to intersect each other. The brecciated rock had behaved quite intrusively. In the following, a description will be given of the fragments in the breccia as well as of the brecciated rock and the rocks surrounding the breccia.

### The fragments in the breccia

The fragments in the breccia consist in the main of a blackish gray, on places stratified diopside amphibolite. The amphibole lahts in the rock are between one and two millimeters long. The minerals contained in the rock are plagioclase, hornblende, diopside, hypersthene and a little biotite, as well as accessories.

The composition of the plagioclase is  $An_{72}$  ( $\alpha = 1.566$ ,  $\gamma = 1.575$ ). The composition of the hornblende includes 53 mol. per cent of the (Fe'', Mn, Ti)-component ( $\alpha = 1.664$ ,  $\gamma = 1.686$ ,  $c:\gamma = 15^\circ$ ). The composition of the diopside involves 45 mol. per cent of the (Ca, Fe'')-component ( $\alpha = 1.696$ ,  $\gamma = 1.723$ ,  $c:\gamma = 43^\circ$ ). The composition of the hypersthene: 32 mol. per cent Fe''-component ( $\alpha = 1.692 =$  hyacinth red,  $\beta = 1.704 =$  sky blue).

The mica schist does not occur as substantial fragments but as indeterminate relicts. The mineral components are biotite, quartz, garnet and a little plagioclase ( $An_{30}$ ), opaques, green spinel and chlorite. The index of refraction of the garnet ( $n$ ) is 1.786. The quartz is conspicuously undulatory in its extinction, its grains have preferred lattice orientation and their edges are toothed. The refractive index of the biotite ( $\gamma$ ) is 1.629, and the pleochroism:  $\alpha =$  yellowish and  $\gamma =$  brown.

### Brecciated rock

The brecciated rock is variegated in color, rough on the weathered surface of the outcrop, massive and non-homogeneous. The roughness of the weathered surface is due to the fact that the garnet in it has remained elevated while the hypersthene and the gedrite have eroded in to hollows. The non-homogeneous character of the rock, again, is due mainly to the fact that the component minerals are unevenly distributed. Furthermore, one can distinguish in it two types of rock sharply bordering on each other, which appear to intersect, too.

The dominant rock type contains reddish brown garnet, blue cordierite, very dark brown hypersthene, blackish gray gedrite, blackish brown biotite, watery gray quartz, light gray plagioclase and small amounts of opaques, sillimanite and chlorite. The minerals are hard to classify in order of abundance, for locally each of the seven first listed is apt to predominate.

The size of the garnet grains varies from under a millimeter to the end of a thumb. The large garnet porphyroblasts or xenocrysts show the presence of inclusions of quartz, opaques, biotite, cordierite and hypersthene. The little garnet grains are in many cases quite euhedral, but the large ones are highly anhedral, even tattered. A chemical analysis of the garnet contained in this rock is given in Table 5. According to the analysis the garnet consists 57 mol. per cent of the almandine component and 31 mol. per cent of the pyrope component. This composition corresponds to that of the garnet found in the cordierite-bearing granulites of Lapland (Eskola 1952, p. 164, and 1961, p. 175). In Tröger's (1959) classification, it corresponds most

TABLE 5.

Chemical composition (analyst: S. Turkka) and physical properties of garnet from the gedrite-cordierite granulite. Point 3, Lake Juurikka, Toivaiaskylä, Kiuruvesi.

Weight per cent			
SiO <sub>2</sub> .....	38.68	Si .....	6.01    Z = 6.00
TiO <sub>2</sub> .....	tr	—	
Al <sub>2</sub> O <sub>3</sub> .....	21.06	Al .....	3.86 } Y = 4.35
Fe <sub>2</sub> O <sub>3</sub> .....	4.12	Fe <sup>3+</sup> .....	0.49 } X = 5.28
FeO .....	26.22	Fe <sup>2+</sup> .....	3.40 } W = 0.19
MnO .....	0.36	Mn .....	0.05 }
MgO .....	7.91	Mg .....	1.83 }
CaO .....	1.10	Ca .....	0.19 }
H <sub>2</sub> O— .....	0.06		
	Σ 99.51		n = 1.790

nearly to the composition of the garnets contained in charnockite. In the triangular diagram of Coleman *et al.* (1965, p. 49), the composition of this garnet falls in to the field of Group B of the eclogites and the composition line of the charnockites and granulites.

The cordierite xenoblasts approximate in size the garnet porphyroblasts. The cordierite is usually twinned. Like quartz, it frequently has an undulatory extinction. When such an extinction occurs also in twinned grains, quartz cannot be involved. In some cases the cordierite grains have broken into small, angular fragments, which, still attached as they are to each other, compose a mosaic-like pattern. The cordierite contains inclusions of opaques, garnet, biotite and zircon. There is a scantiness of alteration products. Thin sillimanite needles are sometimes to be observed in fissures in the cordierite and along the margins of the grains. Table 6 presents a chemical analysis and the physical properties of the cordierite contained in this rock. The mineral is rich in Mg and contains 76 mol. per cent of the Mg<sub>2</sub>Al<sub>4</sub>Si<sub>5</sub>O<sub>18</sub>-component.

The hypersthene is in many instances poikiloblastic or poikilitic, or, then, it consists of grain clusters. It contains inclusions of gedrite, biotite, garnet, cordierite, quartz and opaques. It displays the strong pleochroism characteristic of the hypersthene of granulites:  $\alpha$  = hyacinth red,  $\beta$  = straw yellow and  $\gamma$  = sky blue). The Schiller structure is further characteristic of this hypersthene, but the pleochroism is not evidently due to filtering of the opaques. Howie (1963, p. 222) has shown that the strength of the pleochroism of orthopyroxenes is not related to the iron content and that it can be correlated with the alumina content and the contraction of the cell parameters. The cleavages in the hypersthene in some cases contain green chlorite. Table 7 presents a chemical analysis and the optical properties of the hypersthene. According to this table, the hypersthene is composed of: 50 mol. per cent of En-component, 5.80 per cent by weight of Al<sub>2</sub>O<sub>3</sub>, and 6.02 per cent of Fe<sub>2</sub>O<sub>3</sub>.

TABLE 6.

Chemical composition (analyst: S. Turkka) and physical properties of cordierite from the gedrite-cordierite granulite. Point 3, Lake Juurikka, Toivaiaskylä, Kiuruvesi.

Weight per cent					
SiO <sub>2</sub>	49.32	Si	4.96	Z = 6.00	} Si = 4.96 Al = 1.04
Al <sub>2</sub> O <sub>3</sub>	33.14	Al	3.93	} Y = 2.95	
TiO <sub>2</sub>	tr	Ti	—		} X = 1.99
Fe <sub>2</sub> O <sub>3</sub>	0.83	Fe <sup>3+</sup>	0.06	} W = 0.17	
FeO	5.05	Fe <sup>2+</sup>	0.42		
MnO	0.04	Mn	0.04		
MgO	10.24	Mg	1.53		
CaO	0.24	Ca	0.02		
Na <sub>2</sub> O	0.72	Na	0.14		
K <sub>2</sub> O	0.12	K	0.01		
H <sub>2</sub> O	0.92				
	$\Sigma$ 100.62				
Physical properties:					
$\alpha$	= 1.536				
$\beta$	= 1.540				
$\gamma$	= 1.544				
2V $\alpha$	= 88°				
D	= 2.59				

TABLE 7.

Chemical composition (analyst: S. Turkka) and physical properties of hypersthene from the gedrite-cordierite granulite. Point 3, Lake Juurikka, Toivaiaskylä, Kiuruvesi.

Weight per cent					
SiO <sub>2</sub>	47.52	Si	1.80	Z = 2.00	} Si = 1.80 Al = 0.20
Al <sub>2</sub> O <sub>3</sub>	5.80	Al	0.26	} Y = 0.24	
TiO <sub>2</sub>	0.50	Ti	0.01		} X = 1.71
Fe <sub>2</sub> O <sub>3</sub>	6.02	Fe <sup>3+</sup>	0.17		
FeO	22.20	Fe <sup>2+</sup>	0.70		
MnO	0.14	Mn	—		
MgO	17.33	Mg	0.98		
CaO	0.64	Ca	0.03		
	$\Sigma$ 100.15				
Optical properties:					
$\alpha$	= 1.712				
$\beta$	= 1.721				
$\gamma$	= 1.725				
2V $\alpha$	= 70°				

Also the gedrite occurs as large, separate grains, though in many instances it surrounds the hypersthene as small grains whose c-axes lie parallel to each other and to the c-axis of the hypersthene. The gedrite contains 40 mol. per cent of the Fe''-component ( $\alpha = 1.656$ ,  $\beta = 1.666$ ,  $\gamma = 1.675$ ).

TABLE 8.

Chemical composition (analyst: S. Turkka) and optical properties of biotite from the gedrite-cordierite granulite. Point 3, Lake Juurikka, Toivaiaskylä, Kiuruvesi.

Weight per cent					
SiO <sub>2</sub> .....	37.38	Si .....	5.41	Z = 8.00	} Si = 5.41 Al = 2.59
Al <sub>2</sub> O <sub>3</sub> .....	18.95	Al .....	3.24	} Y = 0.89	
TiO <sub>2</sub> .....	tr	Ti .....	—		} X = 4.85
Fe <sub>2</sub> O <sub>3</sub> .....	2.16	Fe <sup>3+</sup> .....	0.24	} W = 1.87	
FeO .....	12.35	Fe <sup>2+</sup> .....	1.50		} OH = 4.27
MnO .....	0.03	Mn .....	0.00		
MgO .....	15.53	Mg .....	3.35		
CaO .....	0.06	Ca .....	0.01		
Na <sub>2</sub> O .....	1.00	Na .....	0.28		
K <sub>2</sub> O .....	8.56	K .....	1.58		
H <sub>2</sub> O+ .....	4.43	OH .....	4.27		
H <sub>2</sub> O— .....	0.08				
	Σ 100.53				

Optical properties:  
 $\alpha$  = kellertävä  
 $\beta = \gamma = 1.637 = \text{ruskea}$

The biotite content is smaller than that of the other minerals described in the foregoing, but it occurs in largish heaps of flakes. Table 8 presents a chemical analysis of it and of its optical properties. It is also possible that the biotite analyzed represents the type described in the following.

The quartz and the plagioclase occur as small grains, though some of the latter mineral are of finger-tip size. The composition of the plagioclase is An<sub>16</sub> ( $\alpha = 1.535$ ,  $\gamma = 1.546$ ). The quartz has an undulatory extinction.

The mineral composition and properties of this rock almost fit granulites. The rock resembles the cordierite granulite of Lapland (Eskola 1952). It might, perhaps, be also termed gedrite-cordierite granulite.

The paler type among the brecciated rocks contains quartz and garnet as the principal minerals. The accessory minerals in it are plagioclase, biotite, cordierite undergoing conversion into pinitite, chlorite, zircon, spinel and opaques. In the cases examined, the plagioclase, biotite, and cordierite contained in the rock appear to be unstable minerals, and they occur only as armored relicts in the garnet. Green spinel occurs in the pinitized cordierite. Chlorite and quartz occur as intergrowths after the fashion of myrmekite. The quartz has a marked undulatory extinction and the lattices in the grains are clearly oriented, elongated and, to some extent, intergrown.

At least in part, this type represents the more tectonized variety of brecciated rock. Mica schist relicts have frequently been met with in this type of rock.

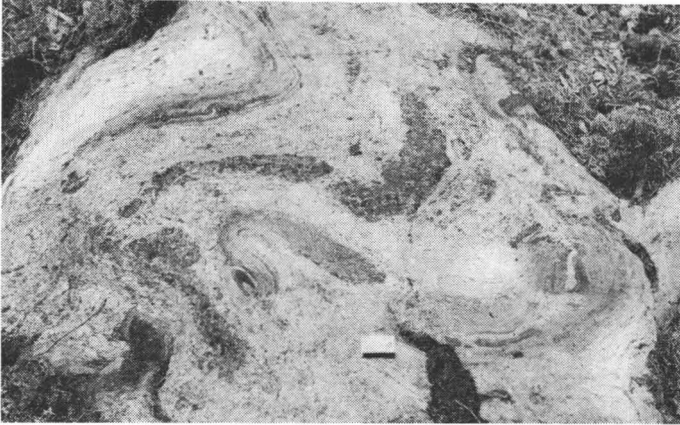


FIG. 10. Cordierite-gedrite granulite brecciates amphibolite. Five hundred meters from Point 3 toward the east, Lake Juurikka, Toivaiaskylä, Kiuruvesi.

### The surroundings of the breccia

On both sides of this breccia, there are layers of the same type of rock as that described from the southeastern side of Lake Juurikka: *e.g.*, gedrite- and plagioclase-bearing quartzites, quartz-bearing amphibolites and various rocks containing garnet, hypersthene, cordierite and gedrite. In addition, there are occurrences of diopside amphibolites, mica schists or gneisses, schists rich in feldspar and quartz, and gedrite-cordierite granulites. The diopside amphibolites have layers of coarser grain, which contain, *inter alia*, garnet and hypersthene. The mica schists and gneisses are commonly also banded. The coarser-grained bands are of different widths. In places the bands are only a few millimeters thick and lenticular. In the bands one finds porphyroblasts of garnet and cordierite, large grains of biotite and hypersthene, plagioclase — with antiperthite-, hercynite and sillimanite in the cordierite, quartz — which in some cases forms myrmekite in conjunction with biotite —, zircon and opaques. The principal minerals contained in the mica schist itself and the gneiss are biotite, plagioclase and quartz.

Similar breccias to those situated on the point of land at the northernmost end of Lake Juurikka and gedrite-cordierite granulites of the same kind occur in this locality in greater abundance than elsewhere. Fig. 10 presents another breccia of similar rock, which is situated some 500 meters east of the aforescribed breccia. The photograph was taken against the lineation with the lens directed perpendicular to the surface of the outcrop. Tectonic processes evidently played a considerable part in its genesis. It may be asked whether they are entirely tectonic breccias or eruptive breccias. At any rate, they are intrusive. Not far from these breccias toward

the NNE, there are rocks of, for example, hypersthene-granite composition. To be sure, no positive evidence exists of their magmatic origin, either, unless one accept as such purely petrographic and microscopic petrographic observations (*cf.* Nickel 1953, Savolahi 1963).

In these rocks, too, which are designated as gedrite-cordierite granulites, there occurs the mineral paragenesis hypersthene, garnet, cordierite and gedrite; and here, too, it seems to be quite in equilibrium. (See also Scheumann, Bossdorf and Bock 1961).

## THE OUTCROP ON THE SOUTHERN END OF LAKE JUURIKKA

### Relationships of the rocks in the outcrop

Some 100 meters toward the SSW from the most southern end of Lake Juurikka (Juurikkajärvi), there is a rather large outcrop (Point 1), in which one will observe three different kinds of rock, as judged by their mineral composition and their structure. The southwestern side of the outcrop consists of non-homogeneous cordierite gneiss, the NE side of quartz-feldspar schist and the northern side of peridotite.

The non-homogeneous cordierite gneiss has narrow layers of, *inter alia*, garnet-perthite gneisses and quartz-feldspar schists. There are more of the latter close to the quartz-feldspar schist, which has narrow intercalations of mica gneiss, with, perhaps, a cordierite content, and, in addition, a few rather small basic inclusions. At the boundary between the cordierite gneiss and the quartz feldspar schist, a few short veinlike formations penetrate the cordierite gneiss from the quartz-feldspar schist. They may, perhaps, be interpreted as evidence of incipient boudinage, for between these veins and the quartz-feldspar schist there exists no sharp line of demarcation.

The peridotite at the northern tip of the outcrop is lensshaped and measures approximately 10×20 meters. It may, perhaps, contain a bit more plagioclase than peridotite is supposed to have by definition (Streckeisen 1964). In a nearly south-eastern direction from the peridotite lens, an extension of the lens contains, parallel to the schistosity, small basic lenses, which probably originated through boudinage from narrow layers of basic rock.

### Non-homogeneous cordierite gneiss

The cordierite gneiss is a bluish dark-gray, fine-grained rock with medium-grained, yellowish gray veins 1 cm in width. The veins contain, among other minerals, hypersthene and garnet, and they do not always run closely parallel to the foliation of the rock.

The structure of the cordierite gneiss is granoblastic and its mineral components are quartz, cordierite, biotite, plagioclase and (sillimanite, opaques, hypersthene,

TABLE 9.

Chemical composition of the non-homogeneous cordierite gneiss (analyst: A. Heikkinen). Point 1, Lake Juurikka, Toivaitsylä, Kiuruvesi.

	Weight per cent	Weight norm	Molecular norm	Niggli values
SiO <sub>2</sub> .....	72.50	or .... 5.6	Or ... 6.0	si ..... 341
TiO <sub>2</sub> .....	0.62	ab .... 7.3	Ab ... 8.0	al ..... 37
Al <sub>2</sub> O <sub>3</sub> .....	13.50	an .... 3.9	An ... 4.5	fm ..... 51
Fe <sub>2</sub> O <sub>3</sub> .....	1.07	Q .... 53.1	Q .... 50.9	c ..... 5
FeO .....	4.06		69.9	alk ..... 7
MnO .....	0.10			ti ..... 4
MgO .....	4.41	en .... 10.9	En ... 12.6	h ..... 10
CaO .....	0.97	fs .... 5.7	Fs .... 5.0	k ..... 0.42
Na <sub>2</sub> O .....	0.84	C ..... 9.6	C ..... 10.7	mk ..... 0.60
K <sub>2</sub> O .....	0.97	il .... 1.2	Il ..... 1.0	c/fm .... 0.09
P <sub>2</sub> O <sub>5</sub> .....	0.04	mt .... 1.6	Mt ... 1.2	o ..... 0.08
CO <sub>2</sub> .....	0.05	fr .... 0.2	Cc .... 0.1	qz ..... 213
H <sub>2</sub> O+ .....	0.66	cc .... 0.1		
H <sub>2</sub> O- .....	0.02			
F .....	0.05			
Cl .....	0.01			
	99.87	99.2	100.0	
—O .....	0.02			
	99.85			

apatite and zircon). Table 9 presents a chemical analysis of this cordierite gneiss. The vein portions were totally removed from the analyzed specimen before the rock was pulverized.

The quartz has a conspicuously undulatory extinction. The cordierite occurs ordinarily as porphyroblasts twice as large as the other mineral grains. Its fissures and marginal portions contain sillimanite needles. The composition of the cordierite includes 22 mol. per cent of the Fe<sub>2</sub>Al<sub>4</sub>Si<sub>5</sub>O<sub>18</sub>-component. The biotite ( $\gamma = \beta = 1.646 =$  brown,  $\alpha =$  light brownish) has changed to green next to the cordierite. In certain cases, there are small anhedral hypersthene grains in association with the biotite, which in such cases, too, appears to be undergoing alteration. The composition of the plagioclase is An<sub>14</sub> ( $\alpha = 1.535$ ,  $\gamma = 1.544$ ).

The following minerals occur in the medium-grained, hypersthene- and garnet-bearing veins of the cordierite gneiss: quartz, hair-perthite, plagioclase, hypersthene, garnet, biotite, opaques, cordierite, hercynite, chlorite, zircon and apatite.

The grain size of the quartz in these veins is from one to two millimeters. The mineral is undulatory in its extinction and it is anhedral, in some cases even ragged. There is an abundant occurrence of hair-perthite. It appears in the rock as rather large, independent, anhedral grains, as splotches in the plagioclase (Fig. 11) and intergrown with plagioclase grains (Fig. 12). In the latter cases, the

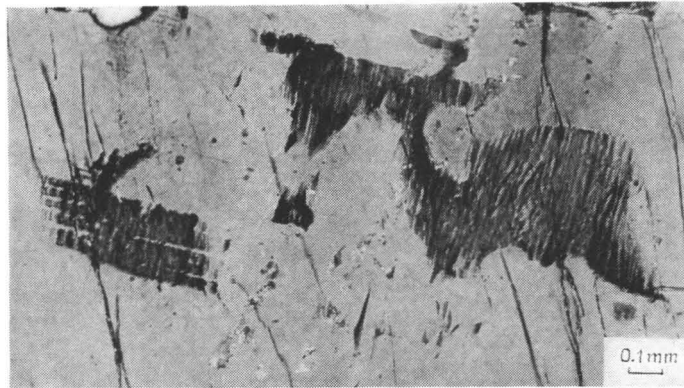


FIG. 11. Hair-perthite splashes in plagioclase. Non-homogeneous cordierite gneiss. Microphoto. Crossed nicols. Point 1, Lake Juurikka, Toiviaiskylä, Kiuruvesi.

border between the plagioclase grains and the hair-perthite grains is quite indeterminate. In some cases, hair-perthite grains display the quadrille structure of microcline. In places, the plagioclase ( $An_{14}$ ) contains antiperthite, and on occasion one will meet with myrmekite along the edges of the plagioclase grains. This rock has not noticeably revealed the presence of independent potash feldspar grains. The hypersthene is brownish black and poikiloblastic. The grains range as high as three millimeters in size. The  $Fe''$ -component ( $\alpha = 1.712 = \text{hyacinth red}$ ,  $\gamma = 1.727 = \text{sky blue}$ ) accounts for 50 mol. per cent of the total composition. The hypersthene contains inclusions of, especially, quartz and biotite. The garnet ( $n = 1.786$ ) is red-brown and anhedral, and its grains are approximately one millimeter in size. It holds inclusions of hypersthene, quartz and hair-perthite. Also present are intergrowths of garnet, opaques and hercynite. The biotite in these veins is appreciably coarser of grain than in the cordierite gneiss. The biotite and the hypersthene have in some instances grown together like myrmekite. In many cases, quartz-biotite myrmekite occurs in the same connection. The biotite has in places intergrown with hair-perthite in a way reminiscent of myrmekite. The cordierite is beautifully twinned, and it has inclusions of, *inter alia*, biotite. There is perhaps less of this mineral in these veins than in cordierite gneiss.

The fine-grained garnet-perthite gneiss that occurs intercalated in the cordierite gneiss is laminated. Some of the lamellae are bluish gray and others yellowish gray. Both kinds are quite narrow, particularly the former. The mineral composition of the gneiss is hair-perthite, quartz, biotite, plagioclase, garnet, cordierite, muscovite, sillimanite, chlorite and opaques. The cordierite and the biotite are disappearing from the pale lamellae. A chemical analysis of this gneiss is presented in Table 10. Both components of the gneiss have been included in the analyzed powder.

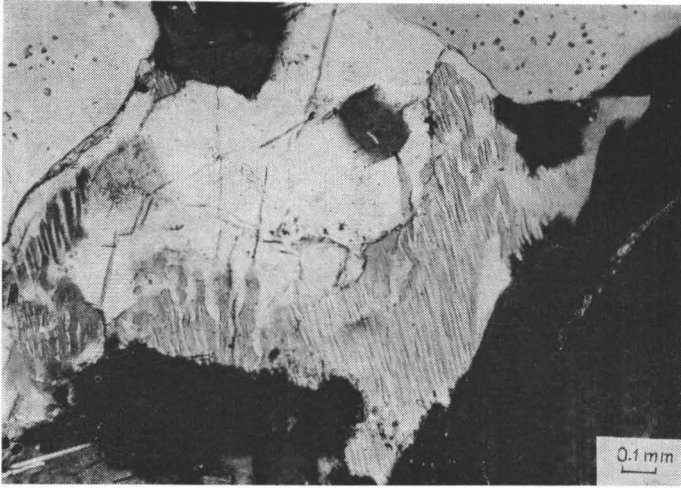


FIG. 12. Microperthite intergrown with plagioclase. Non-homogeneous cordierite gneiss. Microphoto, crossed nicols. Point 1, Lake Juurikka, Toivaiskylä, Kiuruvesi.

TABLE 10.

Chemical composition of garnet-perthite gneiss (analyst: A. Heikkinen). Point 1, Lake Juurikka, Toivaiskylä, Kiuruvesi.

	Weight per cent	Weight norm	Molecular norm	Niggli values
SiO <sub>2</sub> .....	79.35	or .... 13.4	Or .... 14.0	si ..... 544
TiO <sub>2</sub> .....	0.20	ab .... 24.1	Ab ... 26.4	al ..... 41
Al <sub>2</sub> O <sub>3</sub> .....	10.18	an ... 1.9	An ... 2.0	fm ..... 26
Fe <sub>2</sub> O <sub>3</sub> .....	0.50	Q .... 50.2	Q .... 48.1	c ..... 4
FeO .....	2.00	Σ 89.6	Σ 90.6	alk ..... 29
MnO .....	0.08			ti ..... 1
MgO .....	1.11	en .... 2.8	En ... 3.2	h ..... 9
CaO .....	0.58	fs .... 3.0	Fs .... 2.6	k ..... 0.34
Na <sub>2</sub> O .....	2.87	C ..... 2.3	C ..... 2.5	mg ..... 0.44
K <sub>2</sub> O .....	2.26	il .... 0.5	Il ..... 0.4	o ..... 0.10
P <sub>2</sub> O <sub>5</sub> .....	0.01	mt .... 0.7	Mt ... 0.5	c/fm .... 0.16
CO <sub>2</sub> .....	0.03	fr .... 0.2	Fr .... 0.2	qz ..... 328
H <sub>2</sub> O <sup>+</sup> .....	0.37	cc .... 0.1	Cc .... 0.1	
H <sub>2</sub> O <sup>-</sup> .....	0.06			
Cl .....	0.01			
F .....	0.08			
Σ	99.69	Σ 99.2	Σ 100.0	
—O .....	0.04			
Σ	99.65			

Hair-perthite ( $\gamma = 1.527$ ) occurs in the gneiss in the greatest amounts, perhaps, and it takes the form of rather large anhedral grains. In places the grains are broken and they also have an undulatory extinction. Some of them display the quadrille texture of microcline. The quartz has a very conspicuous undulatory extinction in the light bands, and to some extent it has been shattered into tiny particles. Garnet ( $n = 1.797$ ) is more abundantly present in the bluish gray bands, into which biotite ( $\gamma = \beta = 1.648 = \text{brown}$ ) has also been enriched. In addition, they contain quartz and hair-perthite. In the light bands, the biotite is partially green and partially chloritized. In these places the garnet is likewise in some cases chloritized. The cordierite ( $\alpha = 1.543$ ,  $\gamma = 1.555$ ) in many cases contains abundant chlorite and muscovite as clearly distinguishable flakes. It also contains sillimanite ( $\alpha = 1.658$ ,  $\gamma = 1.681$ ). The composition of the plagioclase is  $An_{17}$ .

The rock shows evidence of the fact that its banding is due, at least in some measure, to metamorphic differentiation.

#### Quartz-feldspar schist

The quartz-feldspar schist is a reddish pale brown and small, in some instances fine, of grain. It contains biotite-rich splotches and bands. The fabric is granoblastic. The mineral components are quartz- hair-perthite, plagioclase, microcline, biotite, opaques, garnet, zircon and apatite. The mineral composition of the rock in percentages by volume, as measured from one specimen, is as follows:

Quartz .....	46.1
Hair-perthite .....	36.7
Microcline .....	1.2
Plagioclase .....	12.1
Biotite .....	3.1
Other minerals .....	0.8
	Total 100.0

The quartz scarcely has an undulatory extinction. It occurs both as very tiny grains and as grains with a diameter of about 1 mm. The hair-perthite ranks among the largest-grained minerals composing the rock. The grains are anhedral and contain quartz, in especial, as inclusions. The quantity of the feldspar components of the grains varies. In numerous instances, there is more of the potash feldspar component in the marginal portion of a perthite grain than at the center. The marginal portion is likely to be made up even of pure microcline with a pronounced quadrille texture. Shreds of plagioclase are to be seen in some of the perthite grains. Fig. 13 shows a feldspar grain the upper part of which consists of plagioclase, the lower part of microcline and the middle part of perthite.

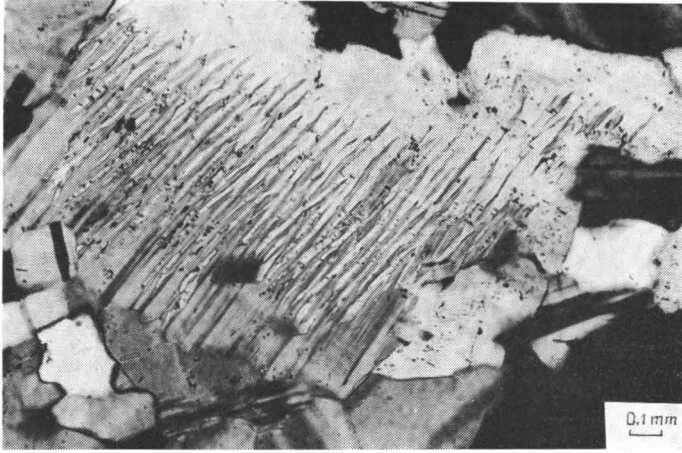


FIG. 13. Feldspar grain: upper portion plagioclase, lower portion microcline and middle portion micropertthite. Quartz-feldspar schist. Microphoto, crossed nicols. Lake Juurikka, Toivaiskylä, Kiuruvesi.

Plagioclase ( $An_{14}$ :  $\alpha = 1.535$ ,  $\gamma = 1.544$ ) occurs in greater abundance wherever there is a higher content of biotite than elsewhere. The main part of microcline ( $\alpha = 1.519$ ,  $\gamma = 1.526$ ) occurs as small, separate, anhedral grains. The biotite in this rock is both brown ( $\gamma = \beta = 1.647$ ) and green ( $\gamma = \beta = 1.619$ ). One sometimes finds in association with the biotite small amounts of tiny anhedral garnet grains.

### Peridotite

Peridotite from the weathered surface of the outcrop is greenish gray and rough, while taken from the fresh surface it is greenish blackgray. The grain size of the rock varies between one and three millimeters, in addition to which one will always find in it amphibole porphyroblasts three cm long. The mineral components are olivine, hypersthene, diopsidic augite, cummingtonite, tremolitic amphibole, hornblende, serpentine, chlorite, plagioclase, apatite, carbonate, epidote, opaques and quartz.

The composition of the olivine includes 25 mol. per cent of the Fa-component ( $2V\alpha = 84^\circ$ ). The grains measure approximately one millimeter or less. Some of them are quite fresh, some have in spots changed partly to green chlorite and some partly to yellow serpentine ( $2V\alpha = 62^\circ$ ). In some cases, the entire grain has undergone alteration to either serpentine or chlorite. In the alteration process, opaques have become eliminated.

The composition of the hypersthene includes 25 mol. per cent of the Fs-component ( $\alpha = 1.685$ ,  $\gamma = 1.695$ ,  $2V\alpha = 74^\circ$ ). Some of the hypersthene grains

have very thin lamellae situated parallel to the c-axis and possessing a diagonal extinction. Olivine and hypersthene occur in the hypersthene as inclusions. In spots the hypersthene has altered to cummingtonite, which ( $\alpha = 1.643$ ,  $\gamma = 1.675$  = greenish,  $2V\gamma = 84^\circ$ ) is present also around the hypersthene grains. Around it one sometimes finds colorless amphibole ( $c:\gamma = 15^\circ$ ).

Diopsidic augite ( $c:\gamma = 42^\circ$ ) occurs as considerably smaller grains than the hypersthene and it alters to amphibole. In many cases, the diopsidic augite occurring as a residue contains very small, wormlike inclusions, which are evidently the same amphibole into which the mineral is changing. This amphibole, which is pale of color ( $c:\gamma = 15^\circ$ ) and whose refractive indices are smaller than those of cummingtonite, probably represents tremolite.

The large amphibole porphyroblasts ( $\alpha = 1.658$  = greenish,  $\gamma = 1.685$  = brownish,  $c:\gamma = 23^\circ$ ) consist of hornblende. They contain nearly all the minerals composing the rock as inclusions. Noteworthy in these porphyroblasts is their undulatory extinction, which is due not to zoning but to movements.

Plagioclase ( $\alpha = 1.542$ ,  $\gamma = 1.578$ ;  $An_{(30-80)}$ ) occurs here and there as relatively large grains, which are full of small, wormlike inclusions mainly composed of diopside and amphibole. Quartz occurs at least as narrow fissure veins.

The distribution of the minerals is highly uneven in this rock. It is difficult to list them in order of abundance. Counted all together, the amphiboles at any rate rank first.

### Conclusions

The non-homogeneous cordierite gneiss contains narrow veins, which do not invariably run parallel to the schistosity and which contain, inter alia, hypersthene, garnet and cordierite. These veins give the impression that they do not constitute layers and that their material had not penetrated from outside any given layer but had formed by metamorphism within the layer itself and crystallized into veins.

According to Ramberg (1949), the conformable cordierite-garnet pegmatites in kinzigitic gneisses are regarded as recrystallization pegmatites and in a broader sense metasomatic-metamorphic pegmatites. According to Winkler and von Platen (1961), graywackes contain anatectic melt when the temperature rises to between 650 and 700° C. The temperature of formation of other anatectic melts is nearly in the same range or even higher (Winkler 1965).

In the extension of the peridotite lens in the exposure, there are small lenses situated parallel to the stratification, which had apparently originated by breaking off a narrow layer of basic rock. The peridotite lens might be interpreted as having formed through some sort of metamorphism from fragments of the aforementioned basic layer. Such a view might be challenged, again, by posing the question as to why the small lenses here are less metamorphosed than the large ones.

Mikkola and Sahama (1936) have described ultrabasic bodies from the granulite area in Lapland. The mode of occurrence of the peridotite here described is similar and the ultrabasic rocks mentioned also contain types corresponding to this peridotite. (See also Mikkola 1955).

#### HORNBLLENDE-PYROXENE GNEISS FROM THE OUTCROP ON THE WEST SHORE OF LAKE JUURIKKA

On the west shore of Lake Juurikka (Point 2) there is an outcrop of hornblende-pyroxene gneiss. The gneiss is black-gray. The grains measure about one millimeter in diameter. Its lineation is clear, but the schistosity plane is indeterminate. In places the rock is of coarser grain, where the orientation cannot be perceived. The gneiss is slightly banded and hornblende, in particular, has become enriched in certain layers. It is hard, to be sure, however, to observe this megascopically on the fresh surface of the outcrop. The minerals contained in the rock are plagioclase, diopside, hypersthene, hornblende, opaques, quartz, chlorite and apatite. The mineral composition of the gneiss in per cent by volume is as follows from a sample lacking any coarse-grained portions:

Plagioclase . . . . .	51.5
Pyroxenes . . . . .	31.3
Hornblende . . . . .	9.8
Apatite . . . . .	0.6
Opaques . . . . .	6.8
	Total 100.0

The composition of the plagioclase is  $An_{(45-50)}$  ( $\alpha = 1.551$ ,  $\gamma = 1.562$ ). It is twinned in accordance with very many a twinning law, and it is the most idiomorphic mineral contained in the rock. Quartz occurs in the coarse-grained portions and only to a small extent elsewhere, and its content has been included in the plagioclase classification.

The composition of the diopside includes 44 mol. per cent of the  $Fe''$ -component ( $\alpha = 1.694$ ,  $\beta = 1.703$ ,  $\gamma = 1.724$ ,  $c:\gamma = 45^\circ$ ,  $2V\gamma = 61^\circ$ ). The diopside content exceeds that of hypersthene. The hypersthene is only rather slightly pleochroic. The  $Fs$ -component ( $\alpha = 1.704$ ,  $\gamma = 1.718$ ,  $2Va = 56^\circ$ ) accounts for 43 mol. per cent of its composition. The composition of the hornblende: 50 mol. per cent ( $Fe''MnTi$ )-component ( $\alpha = 1.662 =$  very pale brown,  $\beta = 1.672 =$  greenish brown,  $\gamma = 1.684 =$  green,  $2Va = 74^\circ$ ,  $c:\gamma = 17^\circ$ ). The gneiss has a few dislocation zones, which contain hornblende of a greener color. In such spots the diopside and the plagioclase have altered to hornblende, and slight amounts of chlorite and quartz appear in association with them.

The opaques occur in many cases as inclusions in pyroxene, but minerals in this category also are present elsewhere. In some places they are ringed by a narrow hornblende border.

## THE HIGHWAY CUTS SOUTHEAST BY SOUTH OF LAKE JUURIKKA

### Introduction

Some 900 meters southeast by south from Lake Juurikka, there are a few highway cuts (Point 5). Various pyroxene- and hornblende-bearing gneisses alternate in the cuts. The layers are likely to be several meters — and even some dozens of meters — thick, though there are other layers that are quite thin, or only a few millimeters in thickness. The boundaries between the different layers are regularly razor-sharp. The following rock types can be distinguished in these layers: hypersthene-hornblende-bearing diopside gneiss, quartz-bearing amphibolite, biotite-, hypersthene- and hornblende-bearing diopside gneiss, diopside-bearing biotite amphibolite and hypersthene-bearing gneiss. Two rock types have been compared with the latter, one of which contains an abundance of quartz and the other some biotite and hornblende.

Along the western edge, the cuts border on a layer of mica gneiss.

### Hypersthene- and hornblende-bearing diopside gneiss

The hypersthene- and hornblende-bearing diopside gneiss is greenish black-brown. Its grain size is 1 mm and less. Its mineral composition is as follows in per cent by volume:

Plagioclase .....	50.1
Diopside .....	26.2
Hypersthene .....	9.5
Hornblende .....	4.8
Opagues .....	4.1
Quartz .....	3.7
Apatite .....	0.6
Other minerals .....	1.0
Total	100.0

The composition of the plagioclase is  $An_{(35-30)}$ . To some extent, it is fairly euhedral and also, among other things, twinned according to the pericline law. Table 11 presents a chemical analysis and the physical properties of the diopside. They correspond to a composition of some 37 mol. per cent of the  $Fe''$ -component. In spots it has very thin lamellae. Table 12 presents a chemical analysis and the

TABLE 11.

Chemical composition (analyst: A. Heikkinen) and physical properties of diopside of hypersthene-hornblende-bearing diopside gneiss. Point 5, Lake Juurikka, Toivaiskylä, Kiuruvesi.

Weight per cent				
SiO <sub>2</sub> . . . . .	50.86	Si . . . . .	1.95	Z = 2.00
Al <sub>2</sub> O <sub>3</sub> . . . . .	0.36	Al . . . . .	0.02	
TiO <sub>2</sub> . . . . .	0.27	Ti . . . . .	0.01	Y = 0.06
Fe <sub>2</sub> O <sub>3</sub> . . . . .	2.63	Fe <sup>3+</sup> . . . . .	0.08	
FeO . . . . .	12.30	Fe <sup>2+</sup> . . . . .	0.39	X = 1.07
MnO . . . . .	0.27	Mn . . . . .	0.01	
MgO . . . . .	11.73	Mg . . . . .	0.67	W = 0.88
CaO . . . . .	20.66	Ca . . . . .	0.85	
Na <sub>2</sub> O . . . . .	0.45	Na . . . . .	0.03	
K <sub>2</sub> O . . . . .	0.05	K . . . . .	—	
P <sub>2</sub> O <sub>5</sub> . . . . .	0.05	Physical properties:		
CO <sub>2</sub> . . . . .	0.00	a = 1.692		
H <sub>2</sub> O+ . . . . .	0.00	γ = 1.720		
H <sub>2</sub> O— . . . . .	0.02	c:γ = 45°		
Σ	99.65	D = 3.38		

TABLE 12.

Chemical composition (analyst: A. Heikkinen) and physical properties of hypersthene of hypersthene-hornblende-bearing diopside gneiss.

Weight per cent				
SiO <sub>2</sub> . . . . .	49.92	Si . . . . .	1.97	Z = 2.00
Al <sub>2</sub> O <sub>3</sub> . . . . .	0.18	Al . . . . .	0.01	
TiO <sub>2</sub> . . . . .	0.26	Ti . . . . .	0.01	Y = 0.04
Fe <sub>2</sub> O <sub>3</sub> . . . . .	1.60	Fe <sup>3+</sup> . . . . .	0.05	
FeO . . . . .	30.70	Fe <sup>2+</sup> . . . . .	1.01	X = 1.92
MnO . . . . .	0.56	Mn . . . . .	0.02	
MgO . . . . .	15.16	Mg . . . . .	0.89	W = 0.05
CaO . . . . .	1.10	Ca . . . . .	0.05	
Na <sub>2</sub> O . . . . .	0.05	Na . . . . .	—	
K <sub>2</sub> O . . . . .	0.03	Physical properties:		
P <sub>2</sub> O <sub>5</sub> . . . . .	0.07	a = 1.717		
CO <sub>2</sub> . . . . .	0.00	γ = 1.733		
H <sub>2</sub> O+ . . . . .	0.08	2Vα = 52°		
H <sub>2</sub> O— . . . . .	0.05	D = 3.60		
Σ	99.76			

physical properties of hypersthene, which has approximately 50 mol. per cent of the Fs-component. It is only slightly pleochroic. It likewise reveals the presence of very thin lamellae in spots. The lamellae in the case of both pyroxenes appear in the same way as described by Parras (1958, p. 100). The hornblende occurs in many cases as very narrow ribbons around the pyroxene and the opaques,

but also as grains about 1 mm long with, among other things, pyroxene inclusions. The following optical properties have been measured from the mineral:  $\alpha = 1.670$  = greenish yellow,  $\beta =$  greenish brown,  $\gamma = 1.691$  = brownish green,  $2V\alpha = 78^\circ$ ,  $c : \gamma = 18^\circ$ ). They correspond to a composition of 60 mol. per cent of the (Fe'' MnTi)-component. The composition of the hornblende varies. There occurs a species of the mineral whose  $c : \gamma = 24^\circ$  and whose refractive indices are below the figures given in the foregoing. The opaque minerals, including, *e.g.*, ilmenite and magnetite, are frequently observed to occur within the pyroxene as rather large grains. The quartz usually occurs as small, veinlike lenses. The rock contains a few shear zones with, *e.g.*, epidote and amphibole. Otherwise, the rock has comparatively few alteration products. The plagioclase fissures hold some hornblende. In addition, this rock contains a white, sugary accessory mineral, the specific gravity of which is over 3.8 but which has not yet been accurately identified.

### Quartz-bearing amphibolite

The quartz-bearing amphibolite is greenish black-gray. Its grain size is less than 1 mm, and it displays some narrow veins of coarser grain that have the same mineral composition as the rock itself. The structure of the amphibolite is granoblastic and mineral composition by vol. per cent is as follows:<sup>1)</sup>

Plagioclase .....	45.6
Quartz .....	1.3
Hornblende .....	49.7
Opaques .....	2.1
Other minerals .....	1.3
	Total 100.0

The composition of the plagioclase is An<sub>30</sub>. The hornblende ( $\alpha =$  pale green,  $\beta =$  green,  $\gamma =$  blue-green,  $c : \gamma = 19^\circ$ ) occurs as grain clusters and is full of small, roundish holes, in many cases stuffed with quartz. There are more holes in the middle of the grain clusters than around the margins. The hornblende is also zoned in that the marginal parts of the grain clusters are more blue-green and their double refraction is slightly greater than that of the middle portions. Quartz occurs elsewhere besides inside the hornblende. Small idiomorphic apatite grains occur in the plagioclase. In the hornblende there occur small amounts of very small, secondary grains of epidote and sphene. One occasionally sights a tiny potash feldspar grain, too.

<sup>1)</sup> The other minerals are apatite, epidote, sphene and potash feldspar. The pyroxene relicts have been included in the hornblende.

**Diopside-bearing biotite amphibolite**

The diopside-bearing biotite amphibolite resembles the quartz-bearing amphibolite, except that it is coarser of grain, and that it contains considerable diopside and biotite and very little quartz. Owing to the abundance of biotite, the foliation is more conspicuous in it than in other types.

**Hypersthene-bearing gneiss**

On the fresh surface of the outcrop, the hypersthene-bearing gneiss appears a pale greenish gray. Megascopically, its foliation is not clear, owing to the lack of flaky minerals — but in thin section it does come out. Its structure is granoblastic. The grain size of the gneiss is 1 mm and less, though some plagioclase grains of a greater magnitude do occur in it. The mineral composition of the gneiss in per cent by volume is as follows:<sup>1)</sup>

Plagioclase . . . . .	66.1
Quartz . . . . .	23.2
Hypersthene . . . . .	7.7
Apatite . . . . .	0.9
Opagues . . . . .	0.9
Other minerals . . . . .	1.2
Total	100.0

The composition of the plagioclase is  $An_{30-35}$  ( $\alpha = 1.543$ ,  $\gamma = 1.553$ ). It contains an abundance of rectangular potash feldspar splitches as antiperthite. The mineral includes a little sericite here and there as an alteration product. A few small anhedral potash feldspar grains ( $\alpha = 1.522$ ,  $\gamma = 1.526$ ) are present between other grains. These independent grains display a beautiful quadrille structure. Next to them one often finds quartz-plagioclase myrmekite. The quartz occurs as both small and large grains, the latter being mostly elongated and with an undulatory extinction.

The composition of the hypersthene is 57 mol. per cent of the Fs-component ( $\alpha = 1.718$ ,  $\gamma = 1.734$ ). Its grain size is generally about one-quarter of that of the plagioclase. The hypersthene prisms generally occur parallel to the foliation plane. The mineral is only slightly pleochroic. A few diopside grains have also been found in the rock. There is very little biotite ( $\gamma =$  dark brown). In addition, one will observe in it small amounts of secondary chlorite and amphibole.

<sup>1)</sup> The potash feldspar and the antiperthite as well as a few of the microcline grains situated in interstices have been included in the category of plagioclase. The few scattered diopside grains have been included in the hypersthene. The »other minerals» include chlorite, amphibole and sericite.

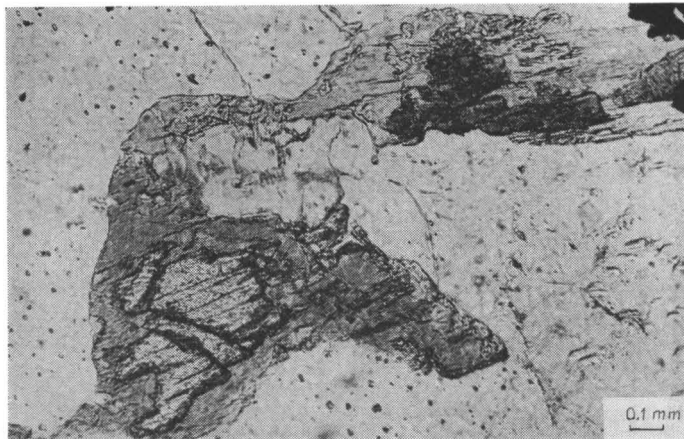


FIG. 14. Hypersthene alters to hornblende. Variety of hypersthene-bearing gneiss. 1 nic. Point 5, Lake Juurikka, Toiviaiskylä, Kiuruvesi.

A petrographical analogy might be drawn between this hypersthene-bearing gneiss and the layers of rock that contain less antiperthite and hypersthene as well as considerably more quartz than does the hypersthene-bearing gneiss. The quartz in them is quite distinctly undulatory in its extinction and occurs as grains measuring up to three millimeters in diameter. In them the hypersthene is often turning to hornblende (Fig. 14). Also around the biotite, of which there is little, one will occasionally see a ring of hornblende. A noteworthy feature of this rock is the color of the quartz — a violet watery gray, with a faint suggestion of opal. The same is shared by the quartz in the hypersthene-bearing gneiss, but it does not strike the eye so vividly on account of the tiny size of the quartz grains.

We are further able to set alongside the hypersthene-bearing gneiss certain other layers whose color is of a slightly darker greenish gray than this rock. The difference in color is due to the fact that they contain more biotite and hornblende and as much hypersthene as does the hypersthene-bearing gneiss. The hypersthene in these layers of rock is turning to hornblende. The antiperthite content in them is not striking.

### Conclusions

The aforescribed rocks might justifiably be called by different names. Some of them might be designated as granulites, some as charnockites (Holland 1900, Quensel 1951), some diorites, some quartz-diorites and some granodiorites by attaching to the label some extra qualifying term. The names given the rocks in the foregoing are strictly petrographic, for all of them are more or less gneissose.

What, then, is the origin of these rocks? In the hypersthene- and hornblende-

bearing diopside gneisses, the chemical composition of the diopside, above all, fails to fit into the compositional scheme drawn up by Deer *et al.* (1963) for the pyroxenes of magmatic rocks. On the other hand, the  $Mg/(Mg Fe'')$  of the mafic minerals of these various rocks does not always come even close to fitting the  $Mg/(Mg Fe'')$ -curves of metamorphic minerals as presented by Mueller (1961).

Again, how did the handing and the stratification in these sections evolve? Are we confronted with a product of metamorphic differentiation, or with magmatic handing? Or is it a sedimentogeneous phenomenon? or some combination of these processes?

### PYROXENE-BEARING DIORITIC AND GRANITIC GNEISSES

About one kilometer east of Lake Juurikka, Wilkman (1929) has marked down granitic gneisses and Mäkinen (1916) dioritic gneisses. These rocks have common features with the rocks described from the highway cut situated SES of Lake Juurikka (Point 5). In places they have the same texture and mineral composition, and they are apt to alternate between themselves, as is the case in the highway cut referred to. But they also occur fairly homogeneously, with only a scant content of inclusions. In spots they also exhibit features characteristic of migmatites, and these features appear largely to be the result of movements. The rocks in most cases contain pyroxene, but hypersthene is more commonly present than is diopside.

Most abundant are the occurrences of pyroxene-bearing granitic or dioritic gneisses (plagioclase ( $An_{30}$ ), quartz, potash feldspar, pyroxene (hypersthene ( $Fs_{45}$ ), biotite and/or hornblende). K-feldspar is often seen to occur as antiperthite in plagioclase. The amount of hornblende varies and is in some cases lacking in different varieties. Also the biotite is occasionally observed to be scantily represented, but there are also types in which biotite is the sole mafic mineral. The rocks are foliated or have a weak crystal lineation. Some of them are almost massive. In them occur hornblende-gneissose, dioritic and gabbroic inclusions — in some cases layers as well. Porphyritic granite types resembling augen-gneisses have also been met with in the area.

All that is needed to classify these rocks as magmatic or as metamorphic-sedimentogeneous — or both — is a favorable disposition to do so. They share many features in common with charnockites (Groves 1935, Pichamuthu 1953). However, the present author has humbly retained the old designations, for the time being.

### PORPHYRITIC GRANITE

Directly east of the area shown in Figure 1, there is an extensive tract of porphyritic granite. Wilkman (1938) has distinguished four different types of rock there:

pyroxene-quartz diorite, pyroxene granite, ordinary porphyritic granite and pyroxene granodiorite. In the view of the present writer, the order of the rocks as here listed also represents the order of their age, proceeding from the oldest to the youngest (*cf.* Wahl 1964, and Savolahti 1964).

## DISCUSSION

The somewhat similar anthophyllite-cordierite rocks of the Orijärvi area have, according to Eskola (1914), undergone extensive metasomatic changes in sediments or siliceous leptites, changes involving large-scale introductions of magnesia and iron oxides from an adjacent igneous intrusion. Eskola's view is upheld by Geijer (1917) in his study of the Falun region. As Bugge (1943) sees it, a simpler and more logical explanation may be found if we presume that the cordierite-anthophyllite-bearing rocks contained in the Kongsberg-Bamle formation had formed at a later stage during the great period of migmatization in conjunction with the advance of disperse solutions from external sources. Gavelin (1939) considers the cordierite-anthophyllite rocks as products of the internal migration and metamorphic differentiation of the rocks. He discounts the possibility of magnesium entering the rock from the outside. With regard to anthophyllite-cordierite granulites, Tilley (1937) writes that metamorphism was accomplished at the Lizard under the influence of stress combined with high temperature, »but the co-existence of andalusite and staurolite suggests, as in the case of the well-known Banffshire rocks, that high temperatures were associated also with fluctuating shearing stress.»

Sclar (1950, 1958, 1965) and Prinz and Poldervaard (1964) describe cases wherein originally homogeneous basic rocks have evolved through mylonitization and mechanical deformation into layered mylonites.

Discussing the granulites of Lapland, Scheumann, Bossdorf and Bock (1961) have suggested that a shearing or flowing deformation may be an important factor, one capable of inducing the stabilization of the homogeneous facies, straining the lattices of the minerals, and moving the mineral individuals against and into one another.

Tuominen and Mikkola (1950), discussing the cordierite-anthophyllite rocks of Orijärvi, surmise that the thick competent beds glided laterally along the relatively thin clayey beds, which were thus subjected to strong penetrating movements and to flowage toward the hinges of the folds. These investigators further submit that »under the penetrative movements the rock gradually recrystallized into minerals with sheet structure and simultaneously the constituents in excess emigrated, thus causing an enrichment in Mg and Fe within the residue.» The actual mineral composition would, accordingly, be due to later recrystallization. Eskola (1950, 1963) challenged this hypothesis on several grounds, leaving Tuominen (1951, 1957) unable to rebut all his objections.

Scheumann, Bossdorf and Bock (1961) write that great portions of the rock association in the granulite area of Lapland were formed by sedimentogeneous migmatic garnet gneisses containing more or less cordierite and that the migmatic gneisses had crystallized under conditions changing from one facies to the other. The granulites of Lapland simultaneously contain minerals or mineral combinations that usually occur either in the amphibolite facies or in the granulite facies, according to these authors.

Winkler (1965) contends that »the threshold value of about 700° C must have been surpassed under those high pressures» which operated before the granulites were formed and that »under these circumstances and at a temperature of 700° or already at a lower temperature, it is imperative that an anatectic melt would form in quartz-potassium feldspar-bearing rocks.»

The rocks of the surroundings of Lake Juurikka containing garnet, hypersthene, cordierite and/or gedrite evolved from quite different sedimentogeneous rocks, such as amphibolites, mica gneisses and quartz-feldspar schists. The mineral assemblage cited appears to be in equilibrium in them. A few types, to be sure, are lacking in gedrite, but this is apparently due to the chemical composition of the rock. The composition and the physical properties of these minerals — with the exception of gedrite — are equivalent to the composition and properties of the corresponding minerals in the granulites.

Some three kilometers east of Lake Juurikka, there begins an extensive tract of porphyritic granite, which also contains pyroxene-bearing granites. At Point 4, on the southeastern side of the lake, one finds, at the northeastern end of the plagioclase- and gedrite-bearing quartzite, generally broader zones of hypersthene-gedrite gneiss than at its southwestern end. If the porphyritic granite established itself and crystallized during the time of formation of the rocks containing garnet, hypersthene, cordierite and gedrite, then the P and the T had declined on proceeding away from the porphyritic granite. In such an event, the migration of ions had evidently also tended to take place in a direction away from the granite. But, it may be seen, for example, at Points 2 and 4 that the migration had probably taken place only within the bounds of the outcrop — and there is no evidence of long-distance migration. At Point 4, shearing movements under pressure evidently contributed considerably to the genesis of the rocks.

At Point 2, on the western side of Lake Juurikka, garnet, cordierite and hypersthene occur in narrow veins in the cordierite gneiss. This rock represents a kind of migmatite. Anatexis may have played a prominent part in the origin of the veins. Anatectic melt should have been able to form in this rock, by virtue of its chemical composition, more easily than in, for example, the rocks situated at Point 4.

At Point 3, on the eastern shore of Lake Juurikka, there is cordierite-gedrite granulite, which is massive and displays a completely intrusive character. Has anatexis proceeded farther here and the »anatectic melt» then intruded to its present situation?

In the vicinity of Lake Juurikka, the rocks cannot be described as having folded, which means that the rocks containing cordierite, hypersthene, garnet and gedrite could not have formed on top of folds. At Kalliokylä gedrite-cordierite-garnet rocks do occur on top of a fold, it is true, but also on its flanks. However, it is unnecessary for this reason alone to apply the in itself elegant hypothesis of Tuominen and Mikkola (1950) even there, especially since no facts can be produced there, either, to support the application of this hypothesis, and contradictory evidence does exist.

In the vicinity of Lake Juurikka, too, there occur two facies, one of which, the older, is the amphibolite facies and the other corresponds to the granulite facies. It was while the granulite facies prevailed that the rocks evolved which contain garnet, hypersthene, cordierite and/or gedrite. But simultaneously with the origin of these rocks, there occurred shear movements, leading to the genesis of, *e.g.*, plagioclase- and gedrite-bearing quartzite, the mineral assemblage of which does not fit in the granulite facies well and in which the minerals of this facies, such as cordierite, hypersthene and garnet, are unstable. Tectonic movements would, accordingly, have significance also as a factor producing the facies.

The author would like to take up certain theoretic-petrological problems once more after he has published his research material on the rocks of Kalliokylä and Niemisjärvi containing garnet, hypersthene, cordierite and/or gedrite.

*Acknowledgments* — The Research Council for Natural Science has given the author financial assistance to carry out this study, and for this he is duly grateful. The author owes a debt of gratitude to the Exploration Department of the Outokumpu Company for assistance received in field research work. Professor Martti Saksela deserves a vote of thanks for having read the manuscript and recommended its publication in this series.

*Manuscript received, April 14, 1966.*

#### REFERENCES

- ANDREATA, C. (1961) Die Mineralfazien polymetamorpher Gebirge. N. Jb. Miner., Abh. 96, pp. 242—243.
- BANNO, S. (1964) Alumina content of orthopyroxenes as a geologic barometer. Japanese Jour. Geol. and Geogr. 25, pp. 115—121.
- BUGGE, J. A. W. (1943) Geological and petrographical investigations in the Kongsberg—Bamble formation. Norges Geol. Unders. 160.
- COLEMAN, R. G., LEE, D. E., BEATTY, L. B., and BRANNOCK, W. W. (1965) Eclogites and eclogites: Their differences and similarities. Geol. Soc. Am. Bull. 76, pp. 483—508.
- DEER, W. A., HOWIE, R. A., and ZUSSMAN, J. (1962—1963) Rock-forming minerals. Vol. I—V. Longmans. London.
- ESKOLA, P. E. (1914) On the petrology of the Orijärvi region in southwestern Finland. Bull. Comm. géol. Finlande 40.
- (1932) On the principles of metamorphic differentiation. Bull. Comm. géol. Finlande 97, pp. 68—77.

- ESKOLA, P. E. (1933) On the differential anatexis of rocks. *Bull. Comm. géol. Finlande* 103, pp. 12—25.
- (1933 a) The term »metamorphic differentiation» first proposed by F. L. Stillwell, *Bull. Comm. géol. Finlande* 103, pp. 45—46.
- (1950) Orijärvi re-interpreted. *Bull. Comm. géol. Finlande* 150, pp. 93—102.
- (1952) On the granulites of Lapland. *Am. Jour. Sci Bowen Volume*, pp. 133—171.
- (1957) On the mineral facies of charnockites. *J. Madras Univ.*, B, 27, pp. 101—119.
- (1958) On pressure. *Proceedings of the Finnish Academy of Science and Letters*, pp. 1—17.
- (1961) Über finnische Granulite und ihren Mineralbestand. *N. Jb. Min., Abh.* 96, pp. 172—177.
- (1963) The Precambrian of Finland. *The Geologic Systems, Precambrian* 1, pp. 145—263.
- VON GAERTNER, H. R. (1962) Gedanken zur Tektonik der »Lappländischen Granulite». *Bull. Comm. géol. Finlande* 204, pp. 207—218.
- GAVELIN, S. (1939) Geology and ores of the Malånäs district Västerbotten, Sweden. *Sveriges Geol. Undersök.* 424.
- GEIJER, P. (1917) Falutraktens berggrund och malmfyndigheter. *Sveriges Geol. Undersök.* 275.
- GROVES, A. W. (1935) The charnockite series of Uganda, British East Africa. *Quart. J. Geol. Soc. London* 91.
- HOLLAND, TH. H. (1900) The charnockite series, a group of Archaean hypersthene rocks in Peninsular India. *Mem. Geol. Survey India* 28.
- HOWIE, R. A. (1963) Cell parameters of orthopyroxenes. *Miner. Soc. Am., Spec. Paper* 1, pp. 213—222.
- KRANCK, E. H. (1931) Petrologische Übersicht des Küstengebietes E von Helsingfors. *Bull. Comm. géol. Finlande* 89, pp. 67—107.
- MÄKINEN, E. (1916) Översikt av de prekambrika bildningarna i mellersta Österbotten i Finland. *Bull. Comm. géol. Finlande* 47.
- MIKKOLA, T. (1955) Origin of ultrabasics in the Orijärvi region. *Bull. Comm. géol. Finlande* 168, pp. 39—51.
- MIKKOLA, E., and SAHAMA, TH. G. (1936) The region to the south-west of the »granulite series» in Lapland and its ultrabasics. *Bull. Comm. géol. Finlande* 115, pp. 357—371.
- MUELLER, R. F. (1961) Analysis of relations among Mg, Fe, and Mn in certain metamorphic minerals. *Geochim. Cosmochim. Acta* 25, pp. 267—296.
- NICKEL, E. (1953) Texturen zwischen »magmatisch» und »metamorph». *Fortschritte der Mineralogie* 32, pp. 78—80.
- PARRAS, K. (1958) On the charnockites in the light of a highly metamorphic rock complex in south-western Finland. *Bull. Comm. géol. Finlande* 181, pp. 3—137.
- PICHAMUTHU, C. S. (1953) The charnockite problem. *Mysore Geol. Assoc. Bangalore, India*.
- PRINZ, M., and POLDERVAART, A. (1964) Layered mylonite from Beartooth Mountains, Montana. *Geol. Soc. Am. Bull.* 75, pp. 741—744.
- QUENSEL, P. (1951) The charnockite series of Varberg district on south-western coast of Sweden. *Arkiv Min. o. Geol.* 1, pp. 227—332.
- RAMBERG, H. (1949) The facies classification of rocks: A clue to the origin of quartzo-feldspathic massif and veins. *J. Geol.* 57, pp. 18—54.
- SAHLSTEIN, TH. G. (1935) Petrographie der Eklogiteinschlüsse in den Gneisen des südwestlichen Liverpool-Landes in Ost-Grönland. *Medd. om Grönland* 95, no. 5, pp. 1—43.
- SANDER, B. (1930) *Gefügekunde der Gesteine*. Springer Verlag, Wien.
- SAVOLAHTI, A. (1963) Regeln der Kristallisation, der idiomorphen und idiomorphischen Reihenfolge und ihre Anwendbarkeit in der Petrologie. *Geologie* 12, pp. 556—567.
- (1964) On the schists and associated intrusive rocks of the Vieremä—Kiuruvesi region. *Bull. Comm. géol. Finlande* 218, pp. 1—83.

- SCHEUMANN, K. H. (1961) Faziesprobleme der metamorphen Gesteine (Kolloquium am 11./12. November 1959 in Frankfurt/Main). *N. Jb. Miner., Abh.* 96, pp. 125—320.
- SCHEUMANN, K. H., BOSSDORF, R., and BOCK, TH. (1961) Versuch einer genetischen Deutung der lappländischen Granulite. *Bull. Comm. géol. Finlande* 196, pp. 327—336.
- SCHMIDT, W. (1932) *Tektonik und Verformungslehre*. Borntraeger, Berlin.
- SCHREYER, W., and YODER, H. S. (1964) The system Mg-cordierite-H<sub>2</sub>O and related rocks. *N. Jb. Miner. Abh.* 101, pp. 271—342.
- SLAR, CH. B. (1950) Origin of a layered ultramylonite from southeastern Connecticut (Abstract). *Geol. Soc. Am. Bull.* 61, p. 1501.
- »— (1958) The Preston gabbro and associated metamorphic gneisses, New London County, Connecticut. *Conn. Geol. Nat. History Survey Bull.* 88, p. 181.
- »— (1965) Layered mylonites and the processes of metamorphic differentiation. *Geol. Soc. Am. Bull.* 76, pp. 611—612.
- SEKI, Y. (1957) Petrological study of hornfelses in the central part of the median zone of Kitakami mountainland, Iwate prefecture. *Sci. Rep. Saitama Univ., Ser. B*, 2, pp. 307—362.
- STRECKEISEN, A. (1964) Zur Klassifikation der Eruptivgesteine. *N. Jb. Miner., Mh.* 7, pp. 195—222.
- TILLEY, C. E. (1937) Anthophyllite-cordierite-granulites of the Lizard. *Geological Magazine* 74, pp. 300—309.
- TRÖGER, W. E. (1959) Optische Bestimmung der gesteinsbildenden Minerale. Teil I. Bestimmungstabellen. E. Schweizerbart'sche Verlagsbuchhandlung. Stuttgart.
- TUOMINEN, H. V. (1951) Metamorphic concentration of magnesium and in the Orijärvi region: a reply. *Bull. Comm. géol. Finlande* 154, pp. 233—238.
- »— (1957) The structure of an Archea area: Orijärvi, Finland. *Bull. Comm. géol. Finlande* 177.
- TUOMINEN, H. V., and MIKKOLA, T. (1950) Metamorphic Mg-, Fe-enrichment in the Orijärvi region as related to folding. *Bull. Comm. géol. Finlande* 150, pp. 67—92.
- TURNER, F. J., and VERHOOGEN, J. (1951, 1960) *Igneous and metamorphic petrology*. McGraw—Hill Book Company, Inc. New York.
- WAHL, W. (1964) The hypersthene granites and unakites of Central Finland. *Bull. Comm. géol. Finlande* 212, pp. 84—100.
- WILKMAN, W. W. (1931) Kivilajikartan selitys. Lehti C 4, Kajaani. (With map, 1929). *General Geological Map of Finland*, 1 : 400 000.
- »— (1938) Kivilajikartan selitys. Lehti C 3, Kuopio. (With map, 1933). *General Geological Map of Finland*, 1 : 400 000.
- WINCHELL, H. (1958) The composition and physical properties of garnet. *Am. Mineralogist* 43, pp. 595—599.
- WINKLER, H. G. F. (1965) *Petrogenesis of metamorphic rocks*. Springer-Verlag. Berlin.
- »— and v. PLATEN, H. (1961) Experimentelle Gesteinsmetamorphose — IV. Bildung anatektischer Schmelzen aus metamorphosierten Grauwacken. *Geoch. Gosmoch. Acta* 24, pp. 48—69.
- YODER, H. S. (1955) Role of water in metamorphism. The crust of the earth. *Geol. Soc. Am., Special paper* 62, pp. 505—524.

## ON SYNKINEMATIC SVECOFENNIAN PLUTONISM

BY

HEIKKI V. TUOMINEN

*Department of Mining, Institute of Technology, Otaniemi, Finland*

### ABSTRACT

According to several authors the synkinematic Svecofennian plutonites form series of magmatic differentiation, which commonly range from peridotites to granodiorites. This conclusion was originally extrapolated from the Orijärvi region. Structural analysis on this region indicates, however, that the rocks described as members of such a series do not form a series at all.

### INTRODUCTION

When first discussing the characteristics of the rocks he called synkinematic and late kinematic Svecofennian granites, Eskola (1932, *cf.* Wegmann and Kranck 1931) described the Orijärvi granodiorite as the type example for the synkinematic group. He stressed that the granites of this group belong to complete series of differentiation ranging down to peridotites. This was considered as evidence for the primary magmatic origin of the series. Apart from the well known »contact metasomatic» phenomena, the regional metamorphism of the Svecofennian schists also was ascribed to the synkinematic plutonism (Eskola 1920). These views, which were in conformance with those expressed by Sederholm (1897) on his older Archean granites, have since been upheld by a number of other geologists.

Eskola (1914, 1932, 1950) considered the Orijärvi granodiorite as an »anticlinal batholith» and ascribed a similar mode of occurrence to all synkinematic Svecofennian granites. Four holes drilled (1952—1954) through the gently dipping floor of the granodiorite, however, showed that this is just a stratiform tongue of a larger pluton, as Wegmann had concluded some 25 years earlier (see Raguin 1965 p. 202). In addition, ground-magnetic survey together with study of the compositional variation of the rocks of the pluton seemed to indicate that the strata of the surrounding leptite formation continue, in a relic form, through the pluton which appears to be roughly a pseudo-phacolith (Tuominen 1961, 1966).

After this, Eskola (1963) abandoned the idea of anticlinal batholiths. He (Eskola 1961) agreed with Mikkola (1955) that the peridotites of the region are nonmagmatic but emphasized the rest of the supposed series still as evidence for the primary magmatic origin of the Orijärvi granodiorite.

It is apparent, however, that no such series exists in the Orijärvi region and that Eskola's views in this respect were based on misinterpretation<sup>1)</sup> of structural data. This matter is briefly discussed below.

### THE PLUTONIC SERIES OF ESKOLA

According to Eskola (1963) the Orijärvi granodiorite belongs to a widely differentiated pluton which ranges in composition from gabbros to granodiorites. The »pluton» thus defined is 170 km<sup>2</sup> in area and occupies the central part of the Orijärvi region; it is illustrated by the gray area in the center of Figure 1.

Describing the gabbros and diorites of the »pluton», Eskola (1914 p. 75) pointed out that in many parts of the area they would not be distinguishable from amphibolites of suppracrustal origin, if they were not associated with granitic (granodioritic) schlieren. The transition from the gabbros and diorites to granites was said to take place »by way of schlieric bands, the granitic portions growing gradually broader as they approach the granitic area». According to Eskola (*op.cit.* p. 85) »these relations hardly admit of any interpretation other than that the two series of rocks have been differentiated from the same magma».

Eskola's description of the nature of what he considered as gabbros and diorites, and of their contact relations with the granodiorites, is correct. However, I do not think that schlieren of granitoid rocks can provide as much information about the origin of their host rock as Eskola proposed. Besides, the structural relationships between the rocks concerned do not support his views.

The leptite formation is folded over axes plunging on the average gently eastwards. This folding has been accompanied and followed by deformations complying with some other common trends of deformation of the Fennoscandian shield. The most effective of these trends are represented by the major faults shown in Figures 1 and 2.<sup>2)</sup>

The deformation conforming with the transverse trends has been cross folding which culminates in imbricate-type structures with easterly dipping thrust faults. Strike-slip faults are also common, some of them having been active during the

<sup>1)</sup> Eskola worked in the Orijärvi zone and adjoining areas during the years 1908—1912, in which time he had an assistant for two months only. The task of his work was to survey an area of about 2 800 km<sup>2</sup> which meant on the average 560 km<sup>2</sup> per summer. The reinvestigations (1945—1952) comprised only 580 km<sup>2</sup> which was investigated during 8 years by a large team of geologists, geophysicists and other workers (see Tuominen 1957).

<sup>2)</sup> Of the blocks separated by these faults, the Karjalohja block represents the lowest and the Koski block the highest stratigraphic level.

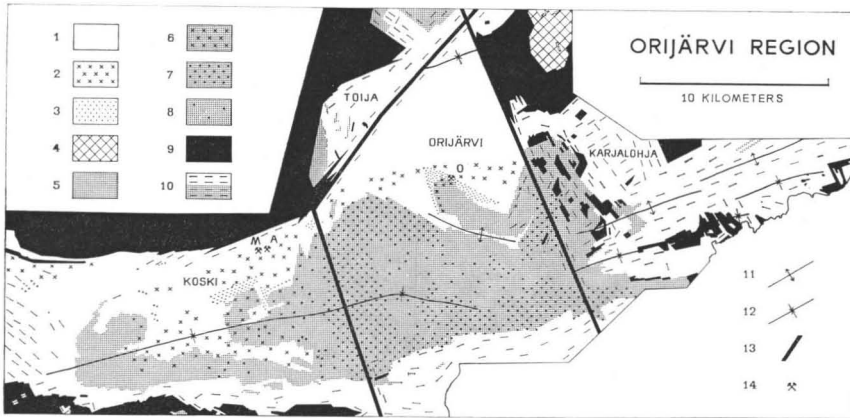


FIG. 1. Simplified geologic map of the Orijärvi region (1:400 000). 1. Rocks of leptite formation. 2. Leptite with porphyroblasts of quartz. 3. »Magnesium metasomatic» rocks. 4. Peridotite. 5. Granodiorite. 6. Granodiorite with porphyroblasts of quartz. 7. Amphibolite with »schlieren» of granodiorite. 8. Granodiorite with amphibolitic portions. 9. Microcline granite. 10. Migmatization. 11. Crests of anticlinoria. 12. Troughs of synclinoria. 13. Major thrust faults of easterly dip. 14. Mines. A — Aijala mine. M — Metsämonttu mine. O — Orijärvi mine. The Orijärvi granodiorite, as described by Eskola (1914), is the tongue of the gray area south of »Orijärvi». From Tuominen 1957.



FIG. 2. Magnetic vertical intensity ( $\Delta Z$ ) in the Orijärvi region (1:400 000) based on 500 000 ground observations. Black: > 400 gammas. Shaded: 200—400 gammas. White: < 200 gammas. The round white patch in the center is not surveyed. From Tuominen 1957.

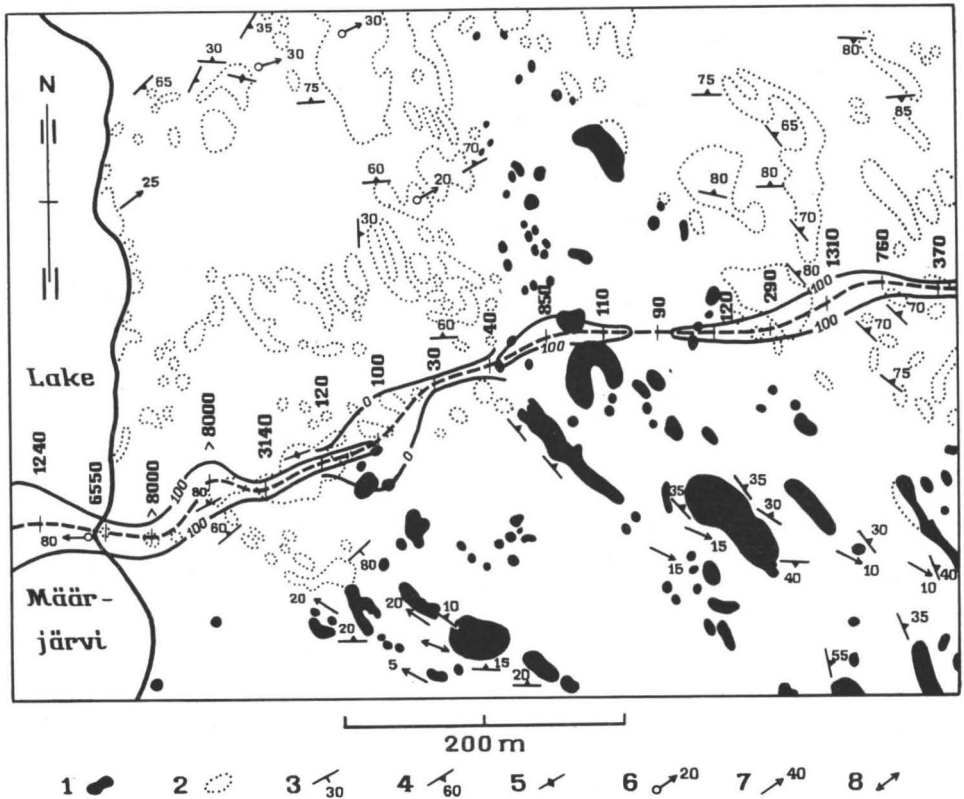


FIG 3. The Kurksaari magnetic ridge crossing the northwest wedge of the Orijärvi granodiorite, with contours for 0 and 100 gammas ( $\Delta Z$ ). The dashed line indicates the crest of the ridge. The observed crestal intensities (heavy numbers) are given at intervals of 40 meters. 1. Granodiorite. 2. Rocks of the Orijärvi »contact aureole». 3. Bedding. 4. Foliation. 5. Foliation where vertical. 6. Axis of minor fold. 7. Lination. 8. Lination where horizontal. Geological data from original outcrop map (1:2 000) by Toivo Mikkola. (By courtesy of the Finnish Prospecting Company).

folding only. An example of such faults is the western border fault of the Orijärvi granodiorite (Tuominen 1961). In many cases, however, the slip relationships are more complicated.

Observations of foliation, lination and axes of small folds show a number of frequency maxima, which correlate with the different trends of the regional deformation. Although the foliations, lineations and small folds related to the transverse deformations are found throughout the area, they are more frequent within recognizable shear zones (Tuominen 1957, Plate II).

The transverse shear zones have generally been loci of strong chemical differentiation. In many cases this has resulted in streaky gneisses consisting, for instance, of hornblenditic and granodioritic streaks.

The schlieren and the schlieric contacts described by Eskola are in most cases parallel to the transverse shear zones, while the basic host rocks represent layers that have been folded in accordance with the main folding, the latter fact being revealed by the curvature of the magnetic zones which follow the original bedding. Hence the »gabbros» and »diorites» of Eskola are mainly amphibolites of supra-crustal ancestry and partly, perhaps, stratiform intrusions from very early stages of folding. A wide time difference separates them from the granitoid schlieren.

An example which illustrates the relationships between the contacts of the granodioritic rocks and the transverse trends of deformation is seen in Figure 3, which shows the northwest point of the Orijärvi granodiorite. The strike of the bedding is indicated by the magnetic ridge, which outside the granodiorite coincides with a layer of banded magnetite ore rich in apatite (Zone III of Tuominen 1966). This layer of undoubtedly sedimentary origin, which continues for several kilometers east and west of the area shown on the map, seems to appear in a relic form in the granodiorite as well. (There is no possibility that such a sharp magnetic ridge could originate from rocks situated beneath the wedge of granodiorite.) Some of the observed foliations strike parallel to the bedding, while others show crossing strikes. The wedge of granodiorite is parallel to the eastern border fault of the Orijärvi block (see Figure 1.). This wedge, which according to Eskola (1914, 1963) represents the felsitic (chilled) contact facies of the pluton, appears to be just a blastomylonite originating from the layered rocks. In places it contains considerably cordierite and sillimanite as do the surrounding gneisses.

Altogether, there is nothing to support the assumption of the magmatic series being present in the Orijärvi region. Besides, the granodioritic rocks, which form the most part of the supposed series, seem to be products and not the source of the regional (dynamothermal) metamorphism.

In wide areas of the southern coastal zone of Finland, the synkinematic Svecofennian plutonites reveal structural relationships similar to those found at Orijärvi. This indicates that the role of the possible magmatic series can not have been as significant as Eskola and others have proposed. The field evidence in favor of such series has generally been drawn from standard reconnaissance mapping, which provides too little information about the structural evolution to show whether the rocks of the supposed series really form series or not (*cf.* Wegmann 1961, p. 125).

*Manuscript received, April 20, 1966*

## REFERENCES

- ESKOLA, P. E. (1914) On the petrology of the Orijärvi region in southwestern Finland. Bull. Comm. géol. Finlande 40; Fennia 37.
- »— (1920) Om metasomatiska omvandlingar i silikatbergarter (English summary). Norsk geologisk tidskrift 6, 89.
- »— (1932) On the origin of granitic magmas. Mineral. u. petrog. Mitt. 42, 455.
- »— (1950) Orijärvi reinterpreted. Bull. Comm. géol. Finlande 150, 93.
- »— (1961) Granitentstehung bei Orogenese und Epirogenese. Geol. Rundschau 50, 105.
- »— (1963) The Precambrian of Finland. In Rankama (editor): The Precambrian, Vol. 1, 145.
- RAGUIN, E. (1965) Geology of granite. Interscience publishers.
- SEDERHOLM, J. J. (1897) Über eine archaische Sedimentformation im südwestlichen Finnland und ihre Bedeutung für die Erklärungsweise des Grundgebirges. Bull. Comm. géol. Finlande 6.
- TUOMINEN, H. V. (1957) The structure of an Archaean area, Orijärvi, Finland. Bull. Comm. géol. Finlande 177.
- »— (1961) The structural position of the Orijärvi granodiorite and the problem of synkinematic granites. Bull. Comm. géol. Finlande 196, 499.
- »— (1966) Structural control of composition in the Orijärvi granodiorite. Bull. Comm. géol. Finlande 222, 311.
- WEGMANN, C. E. (1961) Zwei Bautypen präkambrischer Deformations- und Transformationssegmente: Kareliden und Svecofenniden. Bull. Comm. géol. Finlande 196, 123.
- »— and KRANCK, E. H. (1931) Beiträge zur Kenntnis der Svecofenniden in Finnland I. Bull. Comm. géol. Finlande 89, 1.

THE GEOLOGICAL SOCIETY OF FINLAND

Founded in 1886

Officers for 1966

VALTO VELTHEIM, President

HEIKKI TUOMINEN, Vice-President

HEIKKI IGNATIUS, Past President

OLE LINDHOLM, Councillor

PENTTI VÄHÄSARJA, Councillor

HEIKKI NIINI, Secretary

*National Board of Public Roads and Waterways,  
Water Division, Mikonkatu 2 D,  
Helsinki 10, Finland*

KAUKO MERILÄINEN, Treasurer

*Geological Survey of Finland,  
Otaniemi, Finland*



SUOMEN GEOLOGINEN SEURA  
THE GEOLOGICAL SOCIETY OF FINLAND

JÄSENLUETTELO — 30. 4. 1966 — MEMBERSHIP LIST

Kunniajäsenet — Honorary Members

Auer, Väinö, Prof.	Rakuunantie 4 B, Helsinki 33
Hausen, Hans, Prof.	Armas Lindgrens väg 5, Helsingfors 57
Laitakari, Aarne, Prof.	Geologinen tutkimuslaitos, Otaniemi
Wahl, Walter, Prof.	Bergmansg. 7 D, Helsingfors 14
Wegmann, Eugen, Prof.	43 Faubourg de l'Hôpital, Neuchâtel, Suisse

Kirjeenvaihtajajäsenet — Corresponding members

Barth, Tom F. W., Prof.	Mineralogisk-Geologisk Museum, Sarsgt. 1. NØ, Oslo, Norge
Cloos, Ernst, Dr.	The Johns Hopkins Univ., Baltimore 18, Md., USA
von Eckermann, Harry, Prof.	Edeby Gärd, Ripsa, Sverige
Flint, Richard, F., Prof.	Dept. of Geology, Yale Univ., New Haven, Conn., USA
Florin, Sten, Prof.	Geol. inst., Uppsala, Sverige
Kranck, E. H., Prof.	McGill Univ., Montreal, Canada
Lundqvist, Gösta, Prof.	Krigsstigen 21, Stocksund, Sverige
Magnusson, Nils, H., Prof.	Valhallav. 46, Stockholm Ö, Sverige
Pettijohn, F. J., Prof.	The Johns Hopkins Univ., Baltimore, Maryland— 21 218, USA
Ramdohr, Paul, Prof. Dr.	Mineralog-Petrograph. Inst. d. Univ. Heidelberg, Hauptstr. 47—51, Heidelberg, Deutschland
Sander, Bruno, Prof. Dr.	Min. Inst., Universitätsstr. 4, Innsbruck, Ös- terreich
Szádeczky-Kardoss, Elmer, Prof.	Magyar Tudományos Akadémia, Geokémiai Kutató Laboratóriuma, Budapest VIII, Múzeum körút 4/a, Magyarország.
Vendl, A., Prof.	Németvölgyiut. 70—72, Budapest, Magyarország
Wojno, Tadeusz, Prof.	Politechnica, Warszawa, Polska
Öpik, Ar., Dr.	Bureau of Mineral Resources, MLC Building, London Circuit, Canberra, Australia

## Ulkomaiset jäsenet — Foreign members

- Adamson, Olge J., Fil. Dr.  
 Armstrong, Herbert S., Prof.  
 Barbour, George B., Pres.  
 Barkey, Henri, Geolog  
 Behr, Hansjürgen, Mag.  
 Blake, Weston Jr., Dr.  
 Bloomfield, Keith, M. Sc.  
 Brognon, Georges, Ingenieur Civil des Mines  
 Brotzen, Otto, Fil. dr.  
 Bütler, H., Dr.  
 Carstens, Harald, Dr.  
 Chen, Kwan Yan, Fil. lic.  
 Clark, Alan H., Dr.  
 Collini, Bengt, Fil. lic. Laborator  
 Cooray, Gerald P., Dr.  
 Dahlström, Elis, Fil. lic., Chefgeolog  
 Dietrich, Richard V., Prof.  
 Disler, Jürg, Dr.  
 Dudék, Arnošt, Dr.  
 Du Rietz, Torsten, Fil. dr.  
 Ebert, Heinz, Prof. Dr.  
 El-Hinnawi, Essam, Dr.  
 Eriksson, Tryggve, Fil. lic., Chefgeolog  
 Felici, Maurizio, Dott.  
 Filby, Royston, M. A.  
 Franco, Rui Ribeiro, Prof.  
 Frietsch, Rudyard, Fil. dr.  
 Fromm, Erik, Fil. dr., Statsgeolog  
 Postbox 892, Oslo, Norge  
 Univ. of Alberta at Calgary, Calgary, Alberta,  
 Canada  
 Univ. of Cincinnati, Cincinnati, Ohio, USA  
 Norges geologiske undersøkelse, Trondheim,  
 Norge  
 Geol. Ins., Bergakad., Freiberg, Sachsen,  
 Deutschland  
 Geological Survey of Canada, 601 Booth Street,  
 Ottawa, Ontario, Canada  
 Geological Survey Dept., P. O. Box 27, Zomba,  
 Nyasaland  
 »Le Launoyn», route d'Evrehailles, Yvoir/Meuse,  
 Belgique  
 Min. inst. Stockholms Universitet, Stockholm Va,  
 Sverige  
 Rheinholdenstr. 105, Schaffhausen, Schweiz  
 Statens Råstofflaboratorium, Østmarknaeset,  
 Trondheim, Norge  
 Dept. of Geology, National Univ., Peking, China  
 Dept. of Geology, University College, Gower  
 Street, WC 1, London, England  
 Mineralogisk-Geologiska institutionen, Kåbo-  
 vägen 4, Uppsala 8, Sverige  
 Dept. of Mineralogy, Geological Survey of Ceylon  
 Hunupitiya Lake Road, Colombo 2, Ceylon  
 21 c/o UN/TAB Casilla 197-D, Santiago, Chile  
 Virginia Polytechnic Inst. Dept. of Geological  
 Sciences, Blacksburg, Virginia 24061, USA  
 Suite 2001, 80 Richmond Street West. Toronto 1,  
 Ont., Canada  
 Hradebni 9, Praha 1, Československo  
 Bolidens Gruv Ab., Boliden, Sverige  
 Rio Claro (Estado de S. Paulo), Faculdade de  
 Filosofia, Caixa Postal 178, Brasil  
 Mineralogische Institut, Welfengarden 1, Hanno-  
 ver 3, Deutschland  
 A. Johnson & Co, Stureplan 3, Stockholm 7,  
 Sverige  
 Via Ugo Ojetti 380, Roma, Italia  
 Mineralogisk-Geologisk Museum, Sarsgt. 1, Oslo,  
 Norge  
 Alameda Glete, 463, São Paulo, Brasil  
 Sveriges Geologiska Undersökning, Stockholm  
 50, Sverige  
 Sveriges Geologiska Undersökning, Stockholm  
 50, Sverige

- Fuster, José M., Prof.
- Føyn, Sven, Dr.
- Gaal, Gabor, Dr.  
von Gaertner, Hans Rudolf, Dr.
- Gavelin, Sven, Prof.
- Gevers, T. W., Prof.
- Gjelsvik, Tore, Dr., Direktör
- Grip, Erland, Fil. dr., Chefgeolog
- Günthert, A. W., Dr.
- Hagner, Arthur F., Dr.
- Hall, A. Jean, M. A.
- Hejtman, Bohuslaw, Dr.
- Hessland, Ivar, Prof.
- Heurtebize, Georges, Géologue
- Hietanen-Makela, Anna M., Dr.
- Hjelmqvist, Sven, Prof.
- Homma, Fujio, Prof.
- Jaanusson, Valdar Fil. lic.
- Joensuu, Oiva Fil. maist.
- Jónsson, Jón Fil. lic.
- Joplin, Germaine Anne, Dr.
- Järnefors, Björn, Fil. lic., Statsgeolog
- Kalliokoski, Jorma, Prof.
- Kautsky, Gunnar, Fil. Dr., Byråchef
- Koark, Hans Joachim, Dr.
- Krut'a, Tomáš, Dr.
- Kuonen, Ph. H., Prof.
- Kullerud, Gunnar, Dr.
- Kulling, Oscar, Docent, Statsgeolog
- Landergren, Sture, Laborator, Docent
- Laruelle, Jacques M. C., Dr.
- Labor. de Geologia, San Bernardo 51, Madrid, España
- Sørkedalsv. 93 D, Oslo, Norge
- Wien, Österreich
- Reichsamt für Bodenforschung, Wiesenstrasse 74, Hannover, Deutschland
- Stockholms Universitet, Stockholm Va., Sverige
- Geol. Dept., Univ. of Witwatersrand, Johannesburg, South Africa
- Norsk Polarinstitut, Middelthunsgate 27 B, Oslo 3, Norge
- Bolidens Gruv Ab., Boliden, Sverige
- Wasserhaus 32, Münchenstein 1, BL, Schweiz
- Dept. of Geology, Univ. of Illinois, Urbana, III, USA
- P. O. Box 709, Kitwe, Zambia
- Katedra Geologia, Albertov 6, Praha II, Československo
- Geol. Inst., Stockholms Universitet, Stockholm, Sverige
- Labor. de Géologie de la Sorbonne, 1, rue Victor Cousin, Paris 5e, France
- U. S. Geological Survey, 4 Homewood Place, Menlo Park, Calif. USA
- Geol. Inst., Lund, Sverige
- Inst. of Petrology & Geology, Imperial University Kyoto, Japan
- Paleontol. Inst., Uppsala, Sverige
- The Marine Lab. Univ. of Miami, 1 Rickenbacker Causeway, Virginia Key, Miami 49, Florida, USA
- State Electricity Authority, Geothermal Dept., Laugarveg 118, Reykjavik, Iceland
- Dept. of Geophysics, Australian National University, Canberra, A. C. T. Australia
- Sveriges Geologiska Undersökning, Stockholm 50, Sverige
- Dept. of Geology, Princeton Univ., Princeton, N. J., USA
- Sveriges Geologiska Undersökning, Stockholm 50, Sverige
- Geol. Inst., Uppsala, Sverige
- Zahradnická 9, Brno, Československo
- Geol. Inst., Melkweg 1, Groningen, Nederland
- Geophysical Laboratory, 2801 Upton St., N. W., Washington 8, D. C. 20 008, USA
- Östermalmsg. 44, Stockholm, Sverige
- Sveriges Geologiska Undersökning, Stockholm, 50, Sverige
- Geologisch Instituut, Rijksuniversiteit Gent, Rozier 6, Gent, Belgie

- Lelubre, Maurice, Prof.
- Linnman, Gunnel, Fil. mag.  
Lobjoit, William M., Dr.
- MacLeod, John M., Sc.  
Marklund, Nils, Fil. lic.  
Martna, Jüri, Fil. lic.  
Meier, Otto, Fil. Dr.  
Melcher, Geraldo, Prof.  
Mellis, Otto, Prof.
- Misař, Zdeněk, Dr.
- Moore-Lewy, G., B. Sc.
- Neumann, Henrich, Dr.  
Niemczynow, Grazyna, Mag.  
Noe-Nygaard, Arne, Prof.  
Ojakangas, Richard, M. A.
- Paulitsch, P., Prof. Dr.
- Pilava-Podgurski, N., Fil. lic.  
Preston, John, Dr.
- Robertson, Forbes S., Prof.
- Roubault, Marcel, Prof.
- Ryan, J. Donald, Dr.
- Sahlin, Anders, Ing.  
San Miguel, Alfredo, Prof.
- Sarap, Hans, Fil. lic., Statsgeolog
- Schachner, Doris, Prof. Dr.
- Schermerhorn, L. J. G., Dr.  
Shaikh, Naz Ahmed, Dr.
- Shaw, Denis M., Ph. D.
- Shuiab, S. M., Dr.
- Skålvoll, Harald, Statsgeolog
- van Straaten, L. M. J. U., Dr.  
Suisse, M., Géologue
- Laboratoire de Géologie-Pétrographie, Allées  
Jules-Guesde, Toulouse, France  
Stormästarevägen 15, Lidingö, Sverige  
Cheshire County Training College Crewe, Cheshire  
England  
23 Avalon Place, Hamilton, Ont., Canada  
Geol. Inst., Uppsala, Sverige  
Hjärnegat. 2, Stockholm K, Sverige  
Sindrevägen 8, Djursholm, Sverige  
Alameda Franca 1329, São Paulo, Brasil  
Mineral Inst., Stockholms Universitet, Stockholm,  
Sverige  
Katedra Geologia, Albertov. 6, Praha 2, Česko-  
slovensko  
Woodtown Park, Rathfarnham, Co. Dublin,  
Ireland  
Geologisk Museum, Oslo 45, Norge  
Zakopianska 8 m 1, Warszawa 33, Polska  
Østervoldgade 7, København K, Danmark  
Dept. of Geology, School of Mineral Sciences,  
Stanford University, Stanford, California, USA  
Technische Hochschule, Inst. für Mineralogie,  
Darmstadt, Deutschland  
Munkbogat. 25, Hedemora, Sverige  
Dept. of Geology, Queen's Univ., Belfast, North  
Ireland  
Department of Geology, Principia College, Elsau,  
Illinois, USA  
Univ. de Nancy, 94, Avenue de Strasbourg,  
Nancy, France  
Dept. of Geology, Lehigh Univ., Betlehem, Pa.,  
USA  
Borgmästargat. 9—12, Stockholm Sö, Sverige  
Labor. de Petrografia, Univ. de Barcelona, Bar-  
celona, España  
Sveriges Geologiska Undersökning, Stockholm  
50, Sverige  
Techn. Hochschule, Wüllnerstr. 2, Aachen,  
Deutschland  
P. C. Hoofstraat 59<sup>II</sup>, Amsterdam, Nederland  
Sveriges Geologiska Undersökning, Stockholm  
50, Sverige  
Geol. Dept., McMaster Univ., Hamilton, Ont.,  
Canada  
Mineral. Dept., Univ. of Punjab, Lahore, W.  
Pakistan  
Norges Geologiske Undersökelse, Trondheim,  
Norge  
Geol. Inst., Melkweg 1, Groningen, Nederland  
Boîte postale 210, Bouake, Cote d'Ivoire

- Sverdrup, Thor, Statsgeolog
- Tišler, Janko, Dr.  
Vera, Elpidio C., M. A.  
de Waard, Dirk., Prof. Dr.
- Wahl, William, Dr.
- Warren, Harry V., Prof.
- Watanabe, Takeo, Prof.
- Welin, Eric, Fil. dr.  
Wells, M. K., M. Sc.
- Wenk, Eduard, Dr.
- Wickman, Frans E., Prof.  
Yoder, Hatten S., Dr.
- Zeidler, Waldemar, Bergsingeniör  
Åhman, Erik, Fil. lic.
- Ödman, Olof H., Prof.
- Norges geologiske undersøkelse, Trondheim, Norge  
Maksima Gorkog. 22, Novi Sad, Jugoslavija  
Bureau of Mines, Herran St., Manila, Philippines  
Dept. of Geology, Syracuse University, Syracuse 10, N. Y., USA  
46 Owen Boulevard, R. R. 1, York Mills, Toronto, Ontario, Canada  
Dept. of Geology, Univ. of British Columbia, Vancouver 8, B. C., Canada  
Geol. Inst. Faculty of Science, Tokyo Univ., Tokyo, Japan  
Linnés väg 60, Sollentuna, Sverige  
Geol. Dept., University College, Gower Street, W. C. 1, London, England  
Mineralog-petrolog. Inst. der Universität, Basel, Schweiz  
Riksmuseet, Stockholm 50, Sverige  
Geophysical Laboratory, 2801 Upton St., N. W., Washington 8, D. C. 20008, USA  
Enrisstigen 5, Lidingö 3, Sverige  
Sveriges Geologiska Undersökning, Stockholm 50, Sverige  
Kungl. Tekn. Högskolan, Stockholm Ö, Sverige

## Kotimaiset jäsenet — Members

- Aaltonen, Seppo, Tutk. apul.  
Aario, Leo, Prof.  
Aario, Risto, Fil. toht.  
Aario, Tuula-Maija, Yliopp.  
Aarne, Eino, Kauppat. maist. FGA  
Aarne, Uuno V., Ekon., kultas.  
Ahlfors, Bruce, Dipl. ing.  
Aho, Lea, Fil. kand.  
Airas, Kari Olavi, Fil. kand.  
Alenius, P., Dipl. ins.  
Alestalo, Jouko, Fil. lis.  
Alhonen, Pentti, Fil. kand.  
Alviola, Reijo Ilmari, Luonn. kand.  
Arppe, Erkki, Yliopp.  
Arvela, A., Dipl. ins.  
Askolin, Arne, Försäljningschef.
- Aulanko, Heikki, Dipl. ins.  
Auranen, Olavi, Luonn. kand.  
Aurola, Erkki, Fil. toht.  
Autere, Ilmo, Dipl. ins.  
Backman, A. L., Fil. dr.
- Geologinen tutkimuslaitos, Otaniemi  
Yliopiston maantieteen laitos, Helsinki 10  
Haukitupa H 1, Matinkylä  
Haukitupa H 1, Matinkylä  
Pihlajatie 24 A 4, Helsinki 27.  
Et. Hesperiank. 12 A 12, Helsinki 10  
Adolf Lindforsvägen 7 A, Helsinki 40  
Geologinen tutkimuslaitos, Otaniemi  
Kirkkosalmentie 2 B 21, Helsinki 84  
Lapinkylä  
Oulun Yliopisto, Oulu  
Unionink. 6 A 3, Helsinki 13  
Caloniuksenkatu 7 A 18, Helsinki 10  
Puskantie 22, Seinäjoki  
Koroistentie 6 F, Helsinki 28  
Oy Julius Tallberg Ab, Alexandersg. 21, Helsingfors 10  
Outokumpu Oy, Outokumpu  
Humalistonkatu 15 D 99, Turku 4  
Otalaakso B 18, Otaniemi  
Tuulensuu, Outokumpu  
St. Roberstg. 25 A, Helsingfors 12

- Björklund, Alf, Nat. kand.  
 Björnberg, Fredrik, Fil. kand.  
 Blomqvist, Ralf, Yliopp.  
 Borg, Torvald, Fil. kand.  
 Boström, Rolf, Fil. mag.  
 Carlson, C. E., Dipl. ins.  
 Donner, Joakim, Prof.  
 Edelman, Nils, Prof.
- Engberg, Fjalar M. F., Stud.  
 Enkovaara, Antti, Fil. kand.  
 Erhiö, Pertti, Yliopp.  
 Ervamaa, Pentti, Fil. toht.  
 Erämetsä, Olavi, Prof.  
 Eskola, Salli, Apulaisprof.  
 Filén, Birger, Stud.  
 Forsström, Lars, Luonn. kand.  
 Fogelberg, Paul, Fil. mag.  
 Friberg, Sven, Fil. mag.  
 Gardemeister, Reijo, Fil. kand.  
 Granö, Olavi, Prof.  
 Gritzkevitsh, Boris, Kultaseppä, F G A  
 Grundström, Leo, Yliopp.  
 Grön, Toivo, Yliopp.  
 Grönros, Y., Ins.  
 Haapala, Ilmari, Fil. lis.  
 Haapala, Olavi, Dipl. ins.  
 Haapala, Paavo, Prof.  
 Hacklin, Bertel, Johtaja  
 Hagel, Maija-Leena, Stud.  
 Hakapää, Antero, Dipl. ins.  
 Halme, Erkki, Tutkimusassistent.  
 Halonen, Olli J., Yliopp.  
 Halonen, T. Olavi, Fil. kand.  
 Hannikainen, Raili, Luonn. kand.  
 Harvela, Anna-Liisa, Fil. kand.  
 Hatva, Tuomo, Luonn. kand.  
 Hautala, Pertti, Luonn. kand.  
 Havula, Toivo, Fil. kand.  
 Heikkilä, Heikki, Ins. Kultaseppä, F G A  
 Heikkinen, Aulis, Fil. lis.  
 Heiskanen, Erkki, Fil. kand.  
 Heiskanen, V. A., Prof.  
 Helkavaara, Eero K., Fil. maist.  
 Helle, Reijo, Fil. lis.  
 Heloma, Erkki, Arkkit.  
 Helovuori, Olavi, Fil. kand.  
 Hiltunen, Aimo, Luonn. kand.  
 Himmi, Reino, Fil. maist.  
 Hirvas, Heikki, Yliopp.
- Alkärrsg. 9 C 211, Helsingfors 10  
 Främlingsgatan 1 A 3, Helsingfors 14  
 Linnankatu 22 D 70, Turku  
 Hoplaksvägen 11 B 35, Helsingfors 33  
 Malmnäs, Pargas  
 Oy Kiitoketju Ab, Helsinki 70  
 Norra Kajen 12 A 3, Helsingfors 17  
 Geologiks-mineralogiska Institutet, Åbo Akademi,  
 Åbo  
 Tavastgatan 22 A 7, Åbo 2  
 Oulainen  
 Leppäsuonk. 7 A 113, Helsinki 10  
 Geologinen tutkimuslaitos, Otaniemi  
 Otakallio, Otaniemi  
 Pihlajatie 49 B 27, Helsinki 27  
 Tavastgatan 22, Åbo 2  
 Oulun yliopiston geologian laitos, Oulu  
 Flädervägen 2 A 14, Helsingfors 32  
 Varkaus 9, III  
 Postipuuntie 3 B 37, Leppävaara  
 Elinantie 3, Turku  
 Somerontie 7 A, Helsinki 55  
 Karpalotie 26, Turku 16  
 Leppäsuonk. 9 C 216, Helsinki 10  
 Vänr. Stoolink. 3 A 14, Helsinki 10  
 Geologinen tutkimuslaitos, Otaniemi  
 Outokumpu Oy, Pyhäkumpu  
 Outokumpu Oy, Helsinki 10  
 Reposaaari, Pori  
 Parsby, Pargas  
 Huovitie 1 B 48, Helsinki 40  
 Geologinen tutkimuslaitos, Otaniemi  
 P. Robertink. 4—6 N 78, Helsinki 13  
 Suomen Mineraali Oy, Paakkila  
 Neljäs linja 17—19 G, Helsinki 53  
 Kirkkokatu 24 A 9, Joensuu  
 Oulun Yliopiston Geol. laitos, Kansank. 31, Oulu  
 Nokelantie 12 A, Karjasilta, Oulu  
 Untamontie 1 C 16, Helsinki 61  
 Nordenskiöldink. 9 B 53, Helsinki 25  
 Geologinen tutkimuslaitos, Otaniemi  
 Luikonlahti, Kaavi  
 Dosentintie 3, Helsinki 33  
 Kirkkonkyläntie 3, Helsinki 70  
 Kirkkokatu 4, Oulu  
 Pajamäentie 7 C 45, Helsinki 36  
 Outokumpu Oy, Pyhäkumpu  
 Nalli 3, Raisio  
 Kirkkopuistikko 31 A 8, Vaasa  
 Huovitie 8 B 14, Helsinki 40

- Hirvonen, Yrjö, Fil. maist.  
 Hoffren, Väinö, Fil. maist.  
 Holm, Caj, Vuori-ins.  
 Hugg, Rauno, Luonn. kand.  
 Huhma, Aarto Olavi, Fil. kand.  
 Huhma, Maija, Fil. maist.  
 Huhta, Jussi, Fil. kand.  
 Hukki, Risto, Prof.  
 Huopaniemi, Pertti, Fil. kand.  
 Hyppönen, Viljami, Fil. maist.  
 Hytönen, Kai, Fil. toht.  
 Hyvärinen, Lauri, Fil. kand.  
 Hyyppä, Esa, Prof.  
 Hyyppä, Jussi, Fil. lis.  
 Häikiö, Jukka, Yliopp.  
 Häkli, Aulis, Fil. toht.  
 Hämäläinen, Pentti, Fil. kand.  
 Hämäläinen, Uljas, Ins.  
 Hämäläinen, Viljo, Fil. maist.  
 Härme, Maunu, Fil. toht.  
 Ignatius, Heikki, Fil. toht.  
 Ignatius, Vivi-Ann, Fil. maist.  
 Ikonen, Liisa, Yliopp.  
 Ikonen, Maija, Yliopp.  
 Inkinen, Osmo, Fil. kand.  
 Isokangas, Pauli, Fil. kand.  
 Jalander, Holger, Dipl. ins.  
 Johansson, Stig, Fil. mag.  
 Juurinen, Aarno, Fil. toht.  
 Jäntti, L. Olavi, A., Fil. toht.  
 Järvimäki, Paavo, Luonn. kand.  
 Järvinen, Kauko, Prof.  
 Järvinen, Matti, Fil. kand.  
 Kae, Eero, Fil. kand.  
 Kahma, Aarro, Prof.  
 Kalla, Juha, Fil. maist.  
 Kallio, Pekka, Fil. kand.  
 Kanerva, Reino, Fil. toht.  
 Kantele, Helvi, Fil. maist.  
 Karjalainen, Urpo, Luonn. kand.  
 Koskimies, Keijo, Ekon., FGA  
 Kauppinen, Heikki, Yliopp.  
 Kauranne, Kalevi, Fil. lis.  
 Kempainen, Kari, Tutk. apul.  
 Keränen, Jaakko, Prof.  
 Keto, Leijo, Fil. kand.
- Kivinen, Erkki, Prof.  
 von Knorring, Oleg, Fil. toht.  
 Koistinen, Tapio, Fil. kand.
- Finnå, Mårtensby  
 Geologinen tutkimuslaitos, Otaniemi  
 Virkkala  
 Kaarretie 4 F 8, Tuira (Oulu)  
 Outokumpu Oy, Outokumpu  
 Outokumpu Oy, Outokumpu  
 Kivikatu 20, Rovaniemi  
 Otakallio 1 A 10, Otaniemi  
 Luikonlahti  
 Tornitaso 2 A 4, Tapiola  
 Geologinen tutkimuslaitos, Otaniemi  
 Geologinen tutkimuslaitos, Otaniemi  
 Geologinen tutkimuslaitos, Otaniemi  
 Geologinen tutkimuslaitos, Otaniemi  
 Torikatu 25 A 12, Oulu  
 Outokumpu Oy, Outokumpu  
 Angervontie 4 E 50, Helsinki 32  
 Geologinen tutkimuslaitos, Otaniemi  
 Santavuorentie 7 B 31, Helsinki 40  
 Geologinen tutkimuslaitos, Otaniemi  
 Geologinen tutkimuslaitos, Otaniemi  
 Otakallio 1 B, Otaniemi  
 Otakallio 6 B 22, Otaniemi  
 Ulvila  
 Kummuntorni A 10, Outokumpu  
 Outokumpu Oy, Outokumpu  
 Koroistentie 6 b, D 23 Helsinki 28  
 Docksgatan 1 C 12, Helsingfors 15  
 Pihlajatie 50 A 5, Helsinki 27  
 Tennistie 2 G 79, Tapiola  
 Geologinen tutkimuslaitos, Otaniemi  
 Adolf Lindforsintie 11 A, Helsinki 70  
 Outokumpu Oy, Oravikoski  
 Geologinen tutkimuslaitos, Otaniemi  
 Geologinen tutkimuslaitos, Otaniemi  
 Vuolukiventie 3 B 15, Helsinki 71  
 Geologinen tutkimuslaitos, Otaniemi  
 Käpylänkuja 3 C 23, Helsinki 61  
 Vilhonk. 3 D 50, Mikkeli  
 Rautatiekatu 22, Oulu  
 Ulvilant. 29/3 F 236, Helsinki 35  
 Hämeenkatu 8 A 19, Turku 2  
 Susitie 10, Helsinki 80  
 Geologinen tutkimuslaitos, Otaniemi  
 Topeliuksenk. 1, Helsinki 26  
 Kryolitselskabet Øresund A/S, Strandboulevarden  
 84, København Ø, Danmark  
 Kauppiaank. 8 A, Helsinki 16  
 Geology Dept., The University, Leeds 2, England  
 Sinebrychoffinkatu 15 A 10, Helsinki 12

- Koivisto, Antti, Yliopp.  
 Koivisto, Marjatta, Fil. kand.  
 Kokkola, Martti, Luonn. kand.  
 Koljonen, Tapio, Fil. kand.  
 Kontas, Esko, Yliopp.  
 Kontio, Matti, Yliopp.  
 Konttinen, Lauri, Fil. kand.  
 Koponen, Olavi, Dipl. ins.  
 Korpela, Kauko, Fil. lis.  
 Korpijaakko, Erkki, Fil. kand.  
 Korsman, Kalevi, Yliopp.  
 Kortman, Caj, Fil. kand.  
 Koskela, Erkki, Dipl. ins.  
 Koskinen, Juhani, Fil. kand.  
 Kostiainen, Nils, Arkkit.  
 Kouvo, Olavi, Fil. toht.  
 Kuhmonen, Heikki, Fil. maist.  
 Kujanpää, Jorma, Fil. lis.  
 Kujansuu, Raimo, Fil. kand.  
 Kukkonen, Esa, Fil. kand.  
 Kulonpalo, Max, Fil. maist.  
 Kurki, Jaakko Antero, Fil. kand.  
 Kurppa, Reino, Dipl. ins.  
 Kurtén, Björn, Fil. dr.  
 Laajoki, Kauko V. O., Luonn. kand.  
 Laamanen, Pertti, Yliopp.  
 Laatio, Gunnar, Vuori-ins.  
 Lahermo, Pertti, Fil. kand.  
 Laitakari, Aatto, Fil. kand.  
 Laitakari, Ilkka, Fil. lis.  
 Laitakari, Lauri, Kapt., evp.  
 Laitala, Matti, Fil. kand.  
 Laiti, Ilpo, Fil. kand.  
 Lammela, Torsti, Fil. kand.  
 Lammi, Paavo, Herra  
 Lappalainen, Eino, Yliopp.  
 Lappalainen, Veikko, Fil. toht.  
 Lauerma, Raimo, Fil. toht.  
 Laurén, Lennart, Fil. mag.  
 Laurila, Matti, Fil. kand.  
 Lavikainen, Seppo, Fil. kand.  
 Lehijärvi, Mauno, Fil. toht.  
 Lehtinen, Asko, Yliopp.  
 Lehtinen, Martti, Luonn. kand.  
 Lehtovaara, Jyrki, Luonn. kand.  
 Leino, Antti, Tutkim. assist.  
 Lemmelä, Risto, Fil. kand.  
 Leskelä, Sakari Oiva, Yliopp.  
 Leskinen, Aarne, Dipl. ins.  
 Leveinen, Antero, Herra  
 Kaitalahdenkuja 4, Helsinki 84  
 Geologinen tutkimuslaitos, Otaniemi  
 Vähä-Hämeenkatu 8 a A 9, Turku 2  
 Rauhankatu 11 D 58, Helsinki 17  
 Takaluoma, Lapua  
 Länt. Papinkatu 6 A 6, Helsinki 53  
 Suurlohjank. 33 A 8, Lohja  
 Caixa Postal 1085, São Paulo, Brasil  
 Vuolukiventie 3 B 11, Helsinki 71  
 Geologinen tutkimuslaitos, Otaniemi  
 Late 1 B 1, Turku  
 Björkhemsv. 2 B 24, Helsingfors 20  
 Outokumpu Oy, Tampere  
 Outokumpu Oy, Kotolahti  
 Karhutie 32—34, Helsinki 80  
 Geologinen tutkimuslaitos, Otaniemi  
 Ikaalinen  
 Outokumpu Oy, Sauvonsaarenk. 12, Kemi  
 Geologinen tutkimuslaitos, Otaniemi  
 Läntinen Papinkatu 6 B 19, Helsinki 53  
 Geologinen tutkimuslaitos, Otaniemi  
 Liljevej 6, Hørsholm, Danmark  
 Outokumpu Oy, Pyhäkumpu  
 Djäkpevägen 24, Helsingfors 64  
 Kerttulininkatu 20 A 10, Turku  
 Takojantie 5 C, Helsinki  
 Outokumpu Oy, Lampinsaari  
 Unikkotie 5, Helsinki 72  
 Geologinen tutkimuslaitos, Otaniemi  
 Geologinen tutkimuslaitos, Otaniemi  
 Urputie 9, Savio  
 Geologinen tutkimuslaitos, Otaniemi  
 Pohjoisranta 20 C 60, Helsinki 17  
 Itsenäisyydenkatu 62, Pori  
 Harjunpää  
 Leppäsuonk. 7 A 303, Helsinki 10  
 Riistapolku 2 B 40, Tapiola  
 Geologinen tutkimuslaitos, Otaniemi  
 Geologiska institutuionen, Åbo akademi, Åbo  
 Outokumpu Oy, Outokumpu  
 Kulmakatu 1 B 3, c/o Vallinheimo, Helsinki 17  
 Geologinen tutkimuslaitos, Otaniemi  
 Itäranta 11 A 5, Tapiola  
 Rauhankatu 6 B 32, Helsinki 17  
 Tammimäki, Littoinen  
 Geologinen tutkimuslaitos, Otaniemi  
 Hyrylä  
 Leppäsuonk. 7 A 402, Helsinki 10  
 Olavintie 34 A, Savonlinna  
 Rontsa, Juuka

- Lindberg, Eric, Fil. kand.  
 Lindholm, Ole, Fil. kand.  
 Lindmark, Boris, Luonn. kand.  
 Lindroos, Hardy J., Stud.  
 Lindroos, Pentti, Luonn. kand.  
 Linna, Antti, Dipl. ins.  
 Lokka, Lauri, Prof.  
 Lonka, Anssi, Fil. lis.  
 Luho, Ville, Fil. toht.  
 Lukkarinen, Toimi, Tekn. lis.  
 Lupander, Kurt, Fil. mag.  
 Lyytikäinen, Erkki, Fil. kand.  
 Löfgren, Arvo, Fil. maist.  
 Maijala, Paavo, Dipl. ins.  
 Makkonen, Väinö, Fil. maist.  
 Markkanen, Pentti, Fil. kand.  
 Marmo, Vladi, Ylijoht., Prof.  
 Marttila, Erkki, Fil. maist.  
 Matisto, Arvo, Fil. lis.  
 Mattila, Jorma, Fil. maist.  
 Mattila, Tatu, Fil. maist.  
 Meriläinen, Kauko, Fil. toht.  
 Mielikäinen, Pekka, Luonn. kand.  
 Mikkola, Aimo, Prof.  
 Mikkola, Toini, Fil. maist.  
 Mikkola, Toivo, Fil. lis.  
 Mikkonen, Antti, Fil. kand.  
 Mustala, Jorma, Fil. kand.  
 Mäkelä, Kaarlo, Luonn. kand.  
 Mälkki, Esko, Fil. kand.  
 Mäntylä, Antti J., Luonn. kand.  
 Mäntynen, Matti, Fil. maist.  
 Mölder, Karl, Fil. toht.  
 Naukkarinen, Arvo, Luonn. kand.  
 Nenonen, Eero, Fil. kand.  
 Neuvonen, K. J., Prof.  
 Niemelä, Reijo, Tutk. apul.  
 Nieminen, Kalervo, Dipl. ins.  
 Nieminen, Veikko, Fil. maist.  
 Niini, Heikki, Fil. lis.  
 Niini, Risto, Prof.  
 Nordenswan, Einar A. O., Fil. maist.  
 Nortio, Jaakko, Fil. maist.  
 Nousiainen, Erkki, Isänn.  
 Nurmi, Aimo, Fil. maist.  
 Nuutilainen, Juhani, Fil. lis.  
 Nyberg, Harald, Labor.mäst.  
 Nyfors, Jarl, Fil. mag.  
 Nykänen, Osmo, Fil. maist.  
 Näykki, Ossi, Fil. lis.
- Geologinen tutkimuslaitos, Otaniemi  
 Otanmäki Oy., Otanmäki  
 Albatie, Matinkylä  
 Kvarnvägen 4, Karis  
 Geologinen tutkimuslaitos, Otaniemi  
 Messukylä  
 Mannerheimintie 35 A, Helsinki 25  
 Vaskivuorentie 4 X 185, Helsinki 44  
 Töölöntorink. 3 B, Helsinki 26  
 Ritokalliontie 8—10 C, Helsinki 33  
 Kapellvägen, Pl. 1339, Skövde, Sverige  
 Geologinen tutkimuslaitos, Otaniemi  
 Geologinen tutkimuslaitos, Otaniemi  
 Mäntytie 3, Helsinki 27  
 Valtak. 30 A 7, Rovaniemi  
 Harjuviita 18 A 17, Tapiola  
 Geologinen tutkimuslaitos, Otaniemi  
 Rakuunantie 55 B 39, Turku 16  
 Geologinen tutkimuslaitos, Otaniemi  
 Menninkäisentie 6, Tapiola  
 Outokumpu Oy, Lampisaari  
 Geologinen tutkimuslaitos, Otaniemi  
 Leppäsuonk. 9 C 305, Helsinki 10  
 TKK, Vuoriteollisuusosasto, Otaniemi  
 Geologinen tutkimuslaitos, Otaniemi  
 Kimmeltie 16, Tapiola  
 Kimmeltie 11 C 35, Tapiola  
 Jussarön Kaivos, Tammisaari  
 Kirkkokatu 59 as. 16, Oulu  
 Vaiveronk. 23—25 A 9, Hyvinkää  
 Matinkatu 2 B D 20, Turku  
 Heinävesi kk.  
 Kelohongantie 2 C 21, Tapiola  
 Torikatu 25 A 12, Oulu  
 Katajajarjuntie 8, as. 9, Helsinki 20  
 Multavierunk. 1 A, Turku  
 Geologinen tutkimuslaitos, Otaniemi  
 Vuorimiehenk. 23 b A 9, Helsinki 10  
 Kauppak. 29 B 21 Kajaani  
 TVH, vesistöosasto, Mikonkatu 2 D, Helsinki 10  
 Karstulantie 2 A, Helsinki 55  
 Runebergink. 17 A, Helsinki 10  
 Lassintie 1 B 13, Oulu-Tuira  
 Ruskealan Marmor Oy, Louhi  
 Geologinen tutkimuslaitos, Otaniemi  
 Kansankatu 2, Rovaniemi  
 Karstulavägen 2 A 34, Helsingfors 55  
 Kukonkarinkatu 20, Rauma  
 Geologinen tutkimuslaitos, Otaniemi  
 Pihlajatie 43 A 5, Helsinki 27

- Ohenoja, Vilho, Luonn. kand.  
 Ohlson, Birger, Prof.  
 Oivanen, Paunu, Fil. kand.  
 Ojala, Tauno I., Yliopp.  
 Ojanperä, Pentti, Fil. maist.  
 Okko, Marjatta, Fil. toht.  
 Okko, Veikko, Prof.  
 Oksanen, E. V., Johtaja  
 Otava, Seppo, Yliopp.  
 Paakkola, Juhani, Fil. kand.  
 Paarma, Heikki, Fil. maist.  
 Paavilainen, Eero, Maat. metsät. toht.  
 Palin, Urpo, Fil. kand.  
 Palomäki, Antti, Dipl. ins.  
 Palosuo, Erkki, Fil. toht.  
 Papunen, Heikki, Fil. kand.  
 Paronen, Tauno, Johtaja  
 Parras, Kauko, Fil. toht.  
 Partio, Esko, Luonn. kand.  
 Patrikainen, Pekka, Luonn. kand.  
 Pehkonen, Eero, Fil. kand.  
 Pehrman, Gunnar, Prof.  
 Pekkarinen, Jouni, Fil. kand.  
 Pelkonen, Kalevi, Luonn. kand.  
 Peltola, Esko, Fil. toht.  
 Peltonen, Pietari, Dipl. ins.  
 Penttilä, Aarne K., Fil. kand.  
 Penttilä, Esko, Fil. lis.  
 Perttunen, Vesa, Fil. kand.  
 Pesola, Pentti, Dipl. ins.  
 Peura, Heikki, Luonn. kand.  
 Piirainen, Tauno, A., Fil. kand.  
 Piirola, Jouko  
 Piispanen, Risto, Fil. kand.  
 Pipping, Fredrik, Fil. lic.  
 Pipping, Gisela, Fil. mag.  
 Pohjanlehto, V. O., Herra  
 Pohjolainen, Jussi, Yliopp.  
 Pokki, Eero, Fil. kand.  
 Pouttu, Topi, Luonn. kand.  
 Punakivi, Kalevi, Fil. kand.  
 Puranen, Maunu, Prof.  
 Purokoski, Paavo, Prof.  
 Puustinen, Kauko, Luonn. kand.  
 Pääkkönen, Veikko, Fil. lis.  
 Pönkkä, Lauri, Yliopp.  
 Raatikainen, Esko, Yliopp.  
 Rainio, Heikki, Fil. kand.  
 Alppitie 5 B 60, Tuira—Oulu  
 Maantieteen laitos, Turun Yliopisto, Turku  
 Geologinen tutkimuslaitos, Otaniemi  
 It. Rantakatu 48 B 25, Turku 5  
 Geologinen tutkimuslaitos, Otaniemi  
 Geologinen tutkimuslaitos, Otaniemi  
 Lahnaruohont. 3 B, Helsinki 20  
 Laivastok. 4 B 12, Helsinki 16  
 Södrick, Tuomarila  
 Jäälinkylä, Oulu  
 Veitikantie 33 A 10, Rovaniemi  
 Parkano kk  
 Kanneltie 4 A, Helsinki 42  
 Oy Tampella Ab, Tampere  
 Merentutkimuslaitos, Tähtitornink. 2, Helsinki 14  
 Kerttulink. 3 A 13, Turku 2  
 Pikalähetintie 14 E, Helsinki 62  
 Tytyrink. 3, Lohja  
 Huopalahdentie 15 C 41, Helsinki 33  
 Oulun yliop. geol. laitos, Kansank. 31, Oulu  
 Tornitie 2, Pyhäkumpu  
 V. Strandg. 17., Åbo  
 Geologinen tutkimuslaitos, Otaniemi  
 Leppäsuonk. 9 C 407, Helsinki 10  
 Outokumpu Oy, Outokumpu  
 Ulvilantie 11 b, E 126, Helsinki 35  
 Valtak. 60 A, Lappeenranta  
 Viestitie 1, Helsinki 37  
 Geologinen tutkimuslaitos, Otaniemi  
 Muijala  
 Horo, Teuva  
 Oulun yliopiston geol. laitos, Kansank. 31, Oulu  
 Taivaanvuohentie 8 A 17, Helsinki 20  
 Hoikantie 14—22 E 34, Oulu—Hintta  
 Geological Survey Department, P. O. Box R. W.  
 135, Ridgeway, Lusaka, Zambia  
 Geological Survey Department, P. O. Box R. W.  
 135, Ridgeway, Lusaka, Zambia  
 Harjunpää, Pori  
 Saariniemenk. 1 B 37, Helsinki 53  
 Keijukaistenpolku 6 A 13, Helsinki 82  
 Isokylä  
 Nordvägen 2 C 66, Hagalund  
 Geologinen tutkimuslaitos, Otaniemi  
 Rapakivenkuja 1 D 55, Helsinki 71  
 Uudenkaupungintie 8 B 9, Helsinki 35  
 Geologinen tutkimuslaitos, Otaniemi  
 Kolmas linja 3 A 3, Helsinki 53  
 Isokatu 45 as. 6, Oulu  
 Mannerheimintie 100 A 28, Helsinki 25

- Raja-Halli, Heikki, Dipl. ins.  
 Rancken, Ragnar, Fil. dr.  
 Rankama, Kalervo, Prof.  
 Rantala, Erkki, Fil. kand.  
 Rastas, Pentti, Luonn. kand.  
 Rauhamäki, Eero, Luonn. kand.  
 Renvall, Åge, Fil. mag.  
 Repo, Reino, Fil. toht.  
 Ristiluoma, Sinikka, Yliopp.  
 Ristola, Veikko, Ins.  
 Rosblom, Heikki, Fil. kand.  
 Rosenlund, K. Olof, Stud.  
 Rosenqvist, Harry A., Stud.  
 Rouhunkoski, Pentti, Fil. lis.  
 Runolinna, Urmas, Prof.  
 Räsänen, Veikko, Fil. kand.  
 Saari, Esko, Fil. kand.  
 Saarinen, Vilho, Tutk. ass.  
 Saastamoinen, Jukka, Yliopp.  
 Saastamoinen, Jyry, Fil. kand.  
 Sahama, Th. G., Prof.
- Saikkonen, Reijo, Fil. kand.  
 Sakko, Matti, Fil. maist.  
 Saksela, Martti, Prof.  
 Salli, Ilmari, Fil. toht.  
 Sallinen, Kalevi, Fil. maist.  
 Salmi, Martti, Fil. toht.  
 Salmi, Martti, H., Fil. maist.  
 Salminen, Kyllikki, Fil. lis.  
 Salo, Urpo J., Dipl. ins.
- Saltikoff, Boris, Luonn. kand.  
 Sandbacka, Rolf E. R., Stud.  
 Saraste, Ahti, Geologi  
 Sarikkola, Risto, Fil. kand.  
 Savolahti, Antti, Fil. tri.  
 Savolainen, E., Prof.  
 Seitsaari, Juhani, Prof.  
 Siikarla, Toivo, Dipl. ins.  
 Siivola, Jaakko, Fil. kand.  
 Silvennoinen, Ahti, Luonn. kand.  
 Similä, Pentti, Dipl. ins., Fil. maist.  
 Simola, Kaarlo, Kaivosmittaaja  
 Simola, Liisa, Fil. lis.  
 Simonen, Ahti, Prof.  
 Sipilä, Esko, Fil. kand.  
 Sippola, Martti, Fil. kand.  
 Sirén, Arne, Fil. dr.  
 Soveri, Jouko, Yliopp.
- Otakallio 1, Otaniemi  
 Gamlasvägen 8 F, Helsingfors 42  
 Yliop. geol. laitos, Snellmanink. 5, Helsinki 17  
 Haapajärvi  
 Geologinen tutkimuslaitos, Otaniemi  
 Mäntyviita 4 A 48, Tapiola  
 Ikaalinen  
 Geologinen tutkimuslaitos, Otaniemi  
 Kristianinkatu 16 A 7, Helsinki 17  
 Geologinen tutkimuslaitos, Otaniemi  
 Pilpala, Hunsala  
 Tegelslagaregatan 5 B 40, Åbo 5  
 Österlånggatan 28, 11, Åbo 6  
 Puistotie 1 A, Lampinsaari  
 Oulun Yliopisto, Oulu  
 Geologinen tutkimuslaitos, Otaniemi  
 Koskitie 28 D 10, Oulu  
 Geologinen tutkimuslaitos, Otaniemi  
 Luoteisväylä 26 A 5, Helsinki 20  
 Outokumpu Oy, Outokumpu  
 Yliopiston geoloian laitos, Snellmanink. 5, Helsinki 17  
 Tytyrinkatu 3, as. 17, Lohja  
 Geologinen tutkimuslaitos, Otaniemi  
 Temppeleik. 21, Helsinki 10  
 Geologinen tutkimuslaitos, Otaniemi  
 Pietarinkatu 5 A 4, Helsinki 14  
 Bulevardi 9 A, Helsinki 12  
 Pietarink. 9 B 23, Helsinki 14  
 Geologinen tutkimuslaitos, Otaniemi  
 Kauppa- ja teollisuusministeriön kaivostoimisto,  
 Hallituskatu 4, Helsinki 17  
 Etupellontie 9, Helsinki 66  
 Biskopsgatan 10 B 90, Åbo 2  
 Topeliuksenk. 37 A 11, Helsinki 25  
 Kaivoskatu 10/9 Lampinsaari  
 Jääkäriink. 10 A 12, Helsinki 15  
 Geologinen tutkimuslaitos, Otaniemi  
 Raharinnantie 43, Oulu  
 Geologinen tutkimuslaitos, Otaniemi  
 Geologinen tutkimuslaitos, Otaniemi  
 Pakkahuoneenkatu 23 B 4, Oulu  
 Virkkala  
 Outokumpu  
 Ritarikatu 9 B 15, Helsinki 17  
 Geologinen tutkimuslaitos, Otaniemi  
 Malminetsijä Oy, Jyväskylä  
 Fredrikink. 30 B 19, Helsinki 12  
 Mecheling. 26 B 23, Helsingfors 10  
 Rauhankatu 6 A 25, Helsinki 17

- Soveri, Urpu, Prof.  
 Stenberg, Aarne, Fil. maist.  
 Stigzelius, Erik, Stud.  
 Stigzelius, Herman, Tekn. dr.  
 Stolpe, Tor Björn, Fil. kand.  
 Stranström, Gerg, Fil. kand.  
 Suomalainen, Mikko, Fil. maist.  
 Suomalainen, Tellervo, Fil. maist.  
 Suominen, Eero, Fil. maist.  
 Suominen, Paavo, Fil. kand.  
 Suominen, Veli O., Yliopp.  
 Suvenmaa, L., Herra  
 Såde, Railo K., Kultaseppä  
 Säynäjärvi, Klaus, Fil. maist.  
 Söderholm, Bengt, Natv. kand.  
 Talvitie, Jouko, Fil. lis.  
 Tanner, Heikki, Vuori-ins.  
 Tanskanen, Heikki, Luonn. kand.  
 Tapaninen, Kristo, Yliopp.  
 Tavela, Matti, Fil. lis.
- Tillander, Herbert, Pääkonsuli  
 von Timroth, Michael, Dipl. ins.  
 Toivonen, A. V. P., Fil. maist.  
 Tolonen, Kimmo, Fil. maist.  
 Torssonen, Markus, Lab. apul.  
 Tuittila, Helmer, Luonn. kand.  
 Tuominen, Heikki, Fil. toht.  
 Turkka, Seppo, Fil. kand.
- Tyni, Matti, Fil. kand.  
 Tynni, Risto, Fil. toht.  
 Tyrväinen, Aimo, Fil. kand.  
 Uussaari, Ester, Fil. maist.  
 Vaasjoki, Oke, Fil. toht.  
 Vaasjoki, Pirjo, rouva  
 Waldén, Olavi, Fil. maist.  
 Valovirta, Veikko, Fil. toht.  
 Vanhala, Risto, Fil. kand.  
 Varma, Arno, Fil. kand.  
 Vartiainen, Heikki, Fil. kand.  
 Vasari, Yrjö, Fil. toht.  
 Wecksell, Juhani, Luonn. kand.  
 Veijola, Erkki, Fil. kand.  
 Veltheim, Valto, Fil. toht.  
 Wennervirta, Heikki, Fil. kand.  
 Ventin, Kurt, Natv. kand.  
 Wessman, Curt, Fil. mag.  
 Westerlund, Keijo, Tutk. assist.  
 Viento, Aimo, Johtaja
- Hiidenkiventie 1 B, Tapiola  
 Aijala  
 Bulevarden 11 A 10, Helsingfors 12  
 Bulevarden 11 A 10, Helsingfors 12  
 Carpelansv. 1, Ekenäs  
 Skådesspelarv. 22 G 82, Helsingfors 40  
 Kaarelantie 97 E 53, Helsinki 42  
 Geologinen tutkimuslaitos, Otaniemi  
 Östanskog, Kauniainen  
 Suvantokatu 3 B, Karjasilta  
 Sepänkatu 6 A 12, Turku 6  
 Somero  
 Tallbergin puistotie 6 A, Helsinki 20  
 Laivastok. 8—10 C 27, Helsinki 16  
 Mannerheimvägen 114 A 19, Helsingfors 25  
 Kairatie 3 A 2, Rovaniemi  
 Outokumpu Oy, Helsinki 10  
 Elontie 22, Helsinki 66  
 Yo-talo C 225, Turku 2  
 Room 1031, Div. of Mines and Geology, Ferry  
 Building, San Francisco 11, Calif. USA  
 Aleksanterinkatu 48 A, Helsinki 10  
 Virkkala  
 Geologinen tutkimuslaitos, Otaniemi  
 Unionink. 44, Helsinki 17  
 Geologinen tutkimuslaitos, Otaniemi  
 Hoikantie 14—22 D 29, Oulu  
 Haukiharju A 4, Matinkylä  
 Kryolitselskabet Øresund A/S, Strandboulevarden  
 84, København Ø, Danmark
- Luikonlahti  
 Geologinen tutkimuslaitos, Otaniemi  
 Geologinen tutkimuslaitos, Otaniemi  
 Geologinen tutkimuslaitos, Otaniemi  
 Otsolahdentie 20 A 3, Tapiola  
 Otsolahdentie 20 A 3, Tapiola  
 Outokumpu Oy, Lampinsaari  
 Geologinen tutkimuslaitos, Otaniemi  
 Maaseudun Keskusrakennuststo Oy, Oulu  
 Aijala  
 Torikatu 40, Oulu  
 Oulun yliopiston kasvit. laitos, Oulu  
 Oulun yliopiston geologinen laitos, Oulu  
 Kokkola  
 Geologinen tutkimuslaitos, Otaniemi  
 Kallelan alue, Outokumpu  
 Universitetsgatan 10 A 7, Åbo  
 Elinantie 8 as. 128, Turku 3  
 Geologinen tutkimuslaitos, Otaniemi  
 Pellervontie 23 as. 3, Helsinki 61

Wihuri, Heikki, Fil. maist.  
Wiik, Hugo, Birger, Fil. dr.

Willman, Jussi, Autoilija  
Viluksela, Erkki, Fil. kand.  
Winterhalter, Boris, Fil. kand.  
Virkkala, Kalevi, Fil. toht.  
Virkkunen, Marjatta, Fil. maist.  
von Volborth, A., Fil. toht.  
Vorma, Atso, Fil. toht.  
Vormisto, Kauno, Fil. maist.  
Vornanen, Erkki, Fil. kand.  
Vuorelainen, Yrjö, Herra  
Vuorio, Kari, Tutk. apul.  
Vuorjoki, Aarre, Fil. maist.  
Vähäsarja, Pentti, Fil. kand.  
Vähätalo, Veikko, Fil. toht.  
Väisänen, Seppo, Yliopp.  
Väänänen, Paavo, Fil. maist.  
Väänänen, Pauli, Luonn. kand.  
Yletyinen, Veijo, Fil. maist.  
Ylinen, Mauno, Fil. kand.  
Åberg, Ragnar, Fil. mag.  
Äyräs, Matti, Luonn. kand.  
Öhman, Börje, Fil. mag.  
Österman, Hans, Yliopp.

Kampinkatu 4 A 12, Helsinki 10  
Department of Chemistry, Arizona State University,  
Tempe, Arizona, USA  
Vesanto kk.  
Outokumpu Oy, Outokumpu  
Stenbäckink. 6 B 39, Helsinki 25  
Geologinen tutkimuslaitos, Otaniemi  
Geologinen tutkimuslaitos, Otaniemi  
Box 8003, University Station, Reno, Nevada, USA  
Geologinen tutkimuslaitos, Otaniemi  
Outokumpu Oy, Kivikatu 6, Rovaniemi  
Otanmäki Oy, Otanmäki  
Outokumpu Oy, Outokumpu  
Geologinen tutkimuslaitos, Otaniemi  
Kotipolku 16, Helsinki 60  
Mäntykallio F 56, Matinkylä  
Outokumpu Oy, Outokumpu  
Leppäsuonkatu 9 C 211, Helsinki 10  
Geologinen tutkimuslaitos, Otaniemi  
Huovitie 1 B 36, Helsinki 40  
Geologinen tutkimuslaitos, Otaniemi  
Hoikantie 14—22 E 38, Oulu  
Pargas Kalkberg, Lappeenranta  
Yo-talo B 186, Turku 2  
Skräbböle, Pargas  
Itätuulentie 7, Helsinki 85

## MEMBERSHIP

Membership is open to any Finnish national interested in geoscience. Foreign membership is open to any foreign geologist on the recommendation of two Finnish members.

Members receive the following publications: »Snomen Geologisen Seuran Julkaisuja» (Comptes Rendus de la Société géologique de Finlande), founded in 1929, one issue per year, containing scientific articles; »Geologi», founded in 1949, 10 issues per year, containing short articles in Finnish or Swedish on geoscientific subjects, book reviews, membership news, etc.

The annual membership fee is 10 Finnish marks. Lifetime membership fee 150 Finnish marks.

